



BRNO UNIVERSITY OF TECHNOLOGY

VYSOKÉ UČENÍ TECHNICKÉ V BRNĚ

FACULTY OF MECHANICAL ENGINEERING

FAKULTA STROJNÍHO INŽENÝRSTVÍ

INSTITUTE OF MACHINE AND INDUSTRIAL DESIGN

ÚSTAV KONSTRUOVÁNÍ

**FRICITION AND LUBRICATION OF HIP
AND KNEE JOINT REPLACEMENTS**

TŘENÍ A MAZÁNÍ KYČELNÍCH A KOLENNÍCH KLOUBNÍCH NÁHRAD

HABILITATION THESIS

HABILITAČNÍ PRÁCE

AUTHOR

AUTOR

Ing. David NEČAS, Ph.D.

BRNO 2021

To my beloved wife Lucie, for her endless support...

“The reason why we have dreams is to make them come true...”

ACKNOWLEDGMENT

It is a pleasure for me to thank the following people who helped me to achieve this important milestone.

I wish to thank the head of our institute Prof. Martin Hartl and the head of the Department of tribology Prof. Ivan Křupka for their ongoing support and encouragement to the research throughout my whole career.

Special thanks must go to all the Biotribology research group members for the great job we did over the past years.

Furthermore, I would like to thank Prof. Yoshinori Sawae from Kyushu University, who invaluabley influenced my research career. I feel honoured that I had an opportunity to spend nearly one year in your laboratory, and I am looking forward to future research challenges.

Last but not least, I would like to thank my wife, my parents, and my brother for their support and patience...

Friction and lubrication of hip and knee joint replacements

ABSTRACT

Total hip and knee replacements represent the most effective way of returning patients suffering from severe joint diseases to their everyday lives. However, despite the development achieved in the last sixty years, the limited durability of the implants persists. Most of the failures are wear-associated. However, wear is a consequence of friction and lubrication processes. Therefore, the present thesis aims at the investigation of friction and lubrication of hip and knee joint replacements. The respective chapters of the thesis provide an insight into each area accompanied by the detailed literature review, followed by the author's contribution in the field. Overall, twelve papers are attached, while ten of these were published in the journals with an impact factor in the Web of Science database. The rest two were issued in the journals with CiteScore in Scopus. Achieved results suggest that the extensive experimental investigation supported by numerical modelling may substantially contribute to further development towards theoretically infinite longevity of implants.

KEYWORDS: Biotribology; Total hip replacement; Total knee replacement; Friction; Lubrication; In situ observation; Adsorption; Optical methods, Numerical modelling

Tření a mazání kyčelních a kolenních kloubních náhrad

ABSTRAKT

Totální náhrada kyčelního a kolenního kloubu je nejúčinnějším prostředkem, který umožňuje pacientům s vážným kloubním onemocněním návrat k běžnému životu. Navzdory pokroku v uplynulých šedesáti letech je však přetrvávajícím problémem omezená životnost náhrad. Většina selhání souvisí s procesy opotřebení. Opotřebení je však pouhým důsledkem procesů tření a mazání. Tato práce se proto zaměřuje na problematiku tření a mazání kyčelních a kolenních kloubních náhrad. Jednotlivé kapitoly práce poskytují vhled do problematiky, následovaný detailním přehledem současné literatury a vlastním příspěvkem autora k dané oblasti. Celkem bylo publikováno dvanáct prací, přičemž deset z nich vyšlo v časopisech s impakt faktorem v databázi Web of Science. Zbývající dva články byly vydány v časopisech s indikátorem CiteScore v databázi Scopus. Dosažené výsledky naznačují, že rozsáhlý experimentální výzkum podpořený numerickým modelováním, může zásadním způsobem přispět k dalšímu vývoji směrem k teoreticky neomezené životnosti implantátů.

KLÍČOVÁ SLOVA: Biotribologie; Náhrada kyčelního kloubu; Náhrada kolenního kloubu; Tření; Mazání; In situ pozorování; Adsorpce; Optické metody, Numerické modelování

CONTENTS

1. INTRODUCTION.....	11
2. FRICTION OF JOINT REPLACEMENTS	15
2.1 Unidirectional and reciprocating experimental investigations.....	16
2.2 Swinging and multidirectional experimental investigations	22
2.3 Surface texturing towards reduced friction.....	28
2.4 Author’s contribution to the field	31
2.4.1 The Influence of Proteins and Speed on Friction and Adsorption of Metal/UHMWPE Contact Pair	32
2.4.2 The effect of kinematic conditions and synovial fluid composition on the frictional behaviour of materials for artificial joints.....	34
2.4.3 Running-in friction of hip joint replacements can be significantly reduced: The effect of surface-textured acetabular cup.....	35
2.5 Attachments of Chapter 2	39
3. LUBRICATION OF HIP JOINT REPLACEMENTS.....	77
3.1 Numerical investigations.....	78
3.2 Experimental investigations.....	82
3.3 Author’s contribution to the field	89
3.3.1 In situ observation of lubricant film formation in THR considering real conformity: The effect of diameter, clearance and material.....	91
3.3.2 In situ observation of lubricant film formation in THR considering real conformity: The Effect of Model Synovial Fluid Composition	92
3.3.3 On the observation of lubrication mechanisms within hip joint replacements. Part I: Hard-on-soft bearing pairs	94
3.3.4 On the observation of lubrication mechanisms within hip joint replacements. Part II: Hard-on-hard bearing pairs.....	96
3.3.5 Towards the Direct Validation of Computational Lubrication Modelling of Hip Replacements.....	97
3.4 Attachments of Chapter 3	99
4. LUBRICATION OF KNEE JOINT REPLACEMENTS.....	155
4.1 Numerical investigations.....	156
4.2 Experimental investigations.....	157

4.3 Author's contribution to the field	158
4.3.1 Observation of lubrication mechanisms in knee replacement: A pilot study	159
4.3.2 The Effect of Albumin and γ -globulin on Synovial Fluid Lubrication: Implication for Knee Joint Replacements.....	161
4.3.3 Towards the Understanding of Lubrication Mechanisms in Total Knee Replacements – Part I: Experimental Investigations.....	162
4.3.4 Towards the Understanding of Lubrication Mechanisms in Total Knee Replacements – Part II: Numerical Modeling.....	163
4.4 Attachments of Chapter 4	165
5. CONCLUSIONS AND IMPLICATIONS FOR FURTHER RESEARCH	209
6. REFERENCES	213
LIST OF FIGURES	227
LIST OF TABLES.....	230
LIST OF ABBREVIATIONS	231

INTRODUCTION

Natural human synovial joints represent a unique tribological system. Thanks to the properties of articular cartilage, the well-lubricated biphasic structure, the friction level in the joints may be even lower than that of ice skate gliding on ice. However, it should be noted that once the cartilage is damaged, it has a minimal healing ability [1], which is very dangerous especially for patients suffering from osteoarthritis (OA). Assuming that the length of human life continuously increases, and an increasing occurrence of obesity within the population leading to a higher load of the joints, the number of people affected by OA grew considerably within the last decades. OA is usually associated with painful motion and overall stiffness [2]. Recently, viscosupplementation (VS) of the affected joint by hyaluronic acid- (HA) based viscous solutions was introduced as a non-invasive way of treatment [3]. Nevertheless, it is well reported that the treatment efficiency considerably varies for each patient, being affected by a couple of factors. Therefore, once VS is no more effective, the only chance how to return the patient to everyday life is to replace the natural joint with an artificial one.

Although any joint in the human body may be affected by OA, some locations are more susceptible. Hips and knees belong to the joints exhibiting a higher incidence of OA [4]. Assuming the direct impact on motion ability, total hip, and knee replacements (THR, TKR; see Fig. 1) represent the majority of artificial joints worldwide. According to Health at Glance 2019 report, 182 hip and 135 knee surgeries per 100,000 population on average were conducted in OECD countries in 2017 [5]. Concerning the above numbers and minimal associated risks, total hip and knee arthroplasties (THA, TKA) are recognised to be the most successful and most applied surgeries of modern medicine, allowing millions of people to return to normal life [6],[7].

Even though the number of replaced joints exhibits continuous growth, implants' limited service life represents a persisting challenge for scientists and producers. Following retrospective analyses, it is estimated that the average implant survives from 15 to 25 years at the maximum [8],[9]. While this may seem to be enough for the elderly, less active people, the durability is insufficient for active young patients. The implant failure harms an individual in terms of both physical and mental health. While the physical site is associated with very limited or even disabled mobility, the psyche is affected mainly by the necessity of revision surgery. Economic aspects should also be taken into account. It is estimated that the costs associated with revision are two to three times higher than those of primary surgery. The growth of the expenses is related to removing the failed implant, increased invasiveness, and associated complications such as implant fixation in the surrounding degraded tissue. Therefore, the "unlimited" durability of the

joint replacements needs to be achieved towards patients' improved lives and substantial economic savings.

When searching for the main reason leading to implant failure, aseptic loosening as a consequence of osteolysis plays a major role for both THRs [10],[11] and TKRs [12],[13]. Osteolysis is a degenerative process of bone tissue related to inflammation due to the presence of wear particles released during joint articulation [14],[15]. However, it should be noted that wear is only a consequence of rubbing of two opposing surfaces. Thus, implants' longevity is directly influenced by the overall tribological performance, including contact mechanics, friction, and lubrication. While the wear rate of implants focusing on various factors has been extensively studied using the joint simulators, e.g. [16]-[21], less attention was previously paid to understanding interfacial friction and lubrication processes. Most of the studies have thus been published over the last two decades. The explanation is that the wear rate analysis may be conducted with the use of various commercial devices. On the contrary, investigations of friction and lubrication require the development of advanced experimental approaches. The applied methods and experimental configurations employed to understand the friction and lubrication processes are described in detail in the three following chapters.

Apparently, the tribological behaviour of the contact is influenced by multiple factors. While various aspects such as implant geometry, surface roughness, lubricant composition, kinematic conditions, or load need to be taken into account, the chosen material combination is fundamental. In general, hard-on-soft and hard-on-hard pairs may be distinguished for THRs. The contact couple may be composed of a metal or ceramic femoral head combined with metal, ceramic, or polyethylene (PE) acetabular cup [22]. Regarding PE, ultra-high molecular weight PE (UHMWPE), or highly cross-linked PE (HXLPE) may be used. In the case of TKRs, current implants are mostly of hard-on-soft configuration where the metal femoral part articulates with the PE tibial insert fixed in a metal tibial part [23]. Each material combination exhibits some pros and cons. For example, hard-on-soft metal-on-PE (MoP) and ceramic-on-PE (CoP) pairs lead to more favourable contact conditions; however, the cumulative wear rate may be considerably higher than that of hard-on-hard couples. On the contrary, hard-on-hard pairs, such as metal-on-metal (MoM) or ceramic-on-ceramic (CoC) exhibit a lower wear rate, but the contact pressures are much higher. Besides, metal particles are toxic to some extent leading to the minimisation or complete ban of using metal implants in some countries. Furthermore, a squeaking phenomenon may occur [25], which is even more pronounced for CoC combination [26],[27]. Besides, while metals are elastic, the ceramic is brittle while sudden fracture under impact load may occur, which is severe and painful for the patient.

The main aim of the thesis is to provide an insight into the current state of the art regarding the friction and lubrication processes of THRs and TKRs and to demonstrate the author's contribution to the research field. Thus, the three following chapters represent the central part of the thesis. Chapter no. 2 focuses on investigating the friction of joint replacements using various experimental approaches when revealing the role of several influencing factors. Since the analyses are often conducted in simplified geometrical configurations, many data may be transferred to both THRs and TKRs. Chapter no. 3 aims at the lubrication mechanisms of THRs.

Different experimental methods are introduced, showing a substantial development in the field over the last two decades. Chapter no. 4 deals with the lubrication of TKRs. Each of these three chapters includes an overview of the leading research findings, followed by short comments on the papers published by the author of the thesis. In addition to the literature provided, each article involves a more detailed background, highlighting the research gap to clearly show the contribution and novelty of each presented study.

In total, the thesis is built on twelve co-authored journal papers. All studies were published in peer-reviewed journals. Chapter 2 involves three papers, chapter 3 includes five articles, and the rest four documents are described in Chapter 4. Ten of the studies were published in journals with impact factor (IF) being issued in the Web of Science (WoS) database. The rest two articles were published in the journals having CiteScore indexed in the Scopus database. These two papers were published as extensions of contributions presented at international conferences in the respective special issues. Focusing on the papers with IF, five documents were published in journals in the first quartile (Q1), and the rest five belong to the second quartile (Q2). The highest IF = 5.29, while this specific journal belongs to the first decile (top 10% of the journals in the given category). The scientometric data of all journals are stated in the corresponding chapters. The citations' information, including citing articles, is listed in the document "Autoevaluation criteria of the applicant for habilitation".

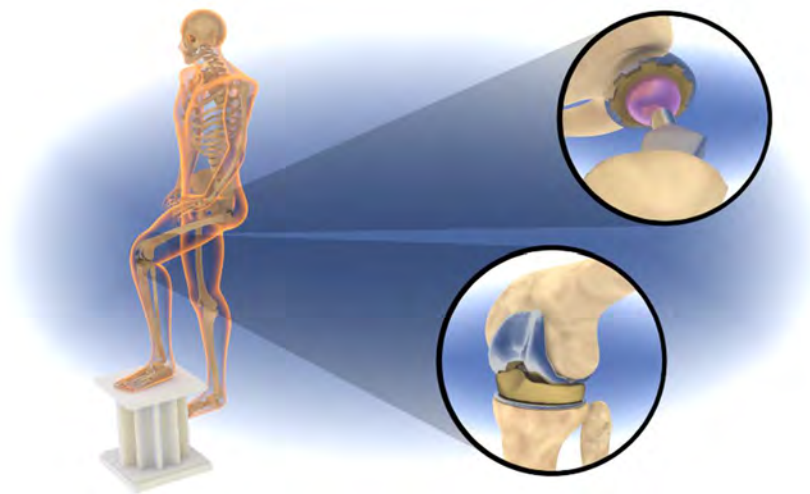


Figure 1: The detail of total hip and total knee joint replacement.

2

FRICITION OF JOINT REPLACEMENTS

Friction as a passive resistance to motion substantially impacts the resulting wear rate, considerably affecting the implant service life. While friction monitoring is generally a routine engineering technique, several factors need to be considered regarding joint replacements. Firstly, in contrast to many technical applications, the experiments may be hardly realised directly in the human body (in vivo). Up to date, only two studies of in vivo friction measurement introduced by a single research group were carried out according to the author's knowledge [28],[29]. Therefore, laboratory investigations need to be employed to understand the frictional behaviour of joint implants better. Secondly, the synovial fluid (SF) differs considerably from patient to patient while the concentrations of individual constituents, its mutual ratio, or dynamic viscosity may vary by an order of magnitude [30]. Thirdly, both THRs and TKRs represent highly conformal contacts, i.e. the implant components are in geometric compliance. This fact is quite limiting, especially for TKRs, where the geometry is very complicated. Finally, the joints operate under transient kinematic and loading conditions, making the friction evaluation even more complicated. Following the above points, most of the investigations are realised in simplified configurations.

Experimental evaluation of the friction of joint replacements usually adopts a couple of simplifications. These simplifications are mostly in (i) geometry, (ii) lubricating fluid, and (iii) applied operating conditions. Regarding geometry, pin-on-disc, pin-on-plate, ball-on-disc, or ball-on-plate arrangements are often employed. Considering the lubricants, human SF is usually substituted by a model SF of various degrees of complexity. Reference lubricants such as phosphate-buffered saline (PBS) solution, carboxymethyl cellulose (CMC), Ringer's solution (RS), or Hanks' balanced salt solution (HBSS) may be used as well, enabling a more straightforward comparison of findings across various methodologies. Concerning the operating conditions, the ISO kinematic and loading cycles recommended for THR [31], and TKR [32] testing are usually replaced by simplified reciprocating motion or unidirectional rotation. It should be noted that the above standards are set for testing of long-term wear rate, mimicking typical activities such as walking, running, or stair climbing. Friction tests mostly focus on a general comparison of materials, applied coatings, surface texturing, or effects such as load and speed rather than on the comprehensive prediction under realistic conditions. Furthermore, the suggested frequency by the standards is 1 Hz while all the parameters change relatively fast, which would most likely lead to inaccuracies in friction measurements. Therefore, a substitution

of the complex cycles by simplified conditions seems to be reasonable for understanding the friction fundamentals.

2.1 Unidirectional and reciprocating experimental investigations

Monitoring of friction in the contact of two rubbing bodies using rotational pin-on-disc and ball-on-disc or translational pin-on-plate and ball-on-plate tribometers became a well-established approach. Focusing on the role of materials of hip and knee implants, one of the pilot studies was introduced by Sawae et al. [33] in 1998. The authors focused on SF constituents' effect on friction and wear of UHMWPE pin sliding against rotating metal and alumina ceramic disc specimens. The contact was lubricated by bovine serum (BS) as a referential lubricant, while saline solutions containing albumin and HA were used to elucidate the effect of these specific components. Albumin was found to have a negligible impact on wear and a negative impact on friction. In contrast, HA could effectively reduce both the monitored parameters. It was pointed out that further investigation of other constituents should be of interest to clarify the frictional behaviour of the materials for implants.

The following study, given by Yao et al. [34], provided a more profound insight regarding the lubricant role. Specifically, deionised (DI) water, undiluted and diluted bovine calf serum (BCS), and human periprosthetic SF were applied to the contact of UHMWPE pin and CoCr disc. Although the measured viscosity of BCS was similar to that of DI water, the results confirmed that the proteins lead to higher friction, in general. Another important conclusion of the study is that BCS does not mimic human SF despite nearly identical viscosity. Surprisingly, the lowest friction was measured for periprosthetic SF. Individual viscosities of all the applied lubricants together with the corresponding friction coefficients are shown in Fig. 2. The authors further considered the effect of irradiation, finding no statistical difference in friction compared to non-irradiated samples.

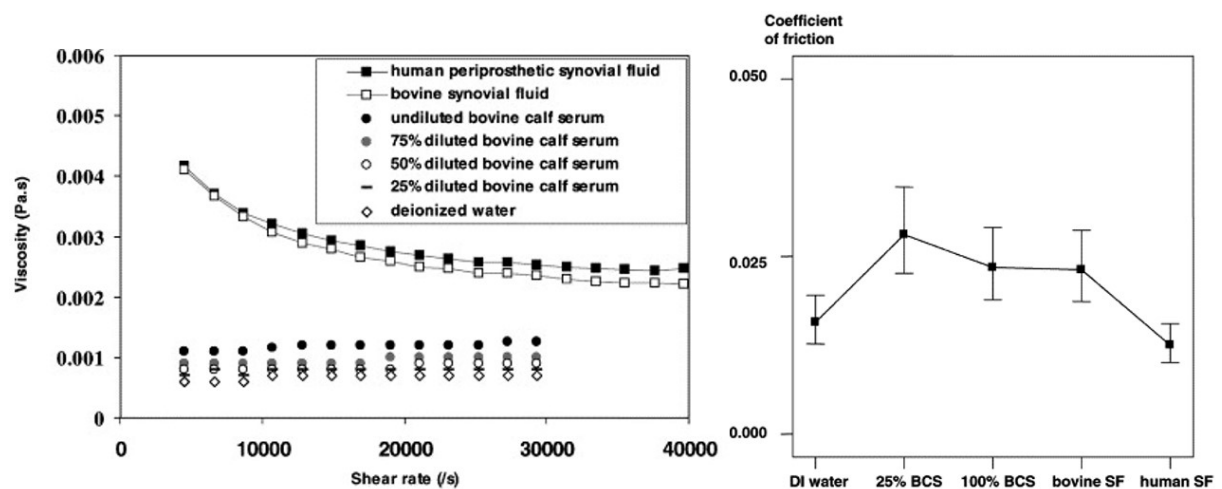


Figure 2: Viscosities of various lubricants (left) and corresponding friction coefficients in UHMWPE-on-CoCr configuration (right). The figure was partially modified and reprinted based on [34].

Further studies concentrated on the biochemical processes occurring within the contact in more detail. The effect of adsorbed film on a polymer surface was examined by Widmer et al. [35]. In this reference, the surface nature of UHMWPE was modified using oxygen-plasma treatment. Subsequent friction tests showed that the modified surface supports the adsorption of human serum albumin (HSA) film, promoting boundary lubrication, which led to a substantial reduction of both dynamic and static friction. However, the authors mentioned that even better conditions were achieved when the surface became more hydrophilic, which contrasts with the above papers. Therefore, a further investigation focused on the potential effect of conformational changes of the protein on the adsorption behaviour [36]. The same configuration consisting of the UHMWPE pin and the ceramic disc was tested while attention was paid to analysing the proteins' structure. The authors concluded that the denatured proteins rather adsorb onto hydrophobic surfaces. Instead, the modified hydrophilic surface supports the adsorption of the proteins in their native form, forming a thicker and denser film lowering the friction. A protein-boundary molecular model summarising the presented findings is shown in Fig. 3.

Yang et al. [37] presented a similar investigation, performed however in the pin-on-plate configuration under reciprocating motion. The authors conducted the experiments in two different formats considering hydrophobic UHMWPE and hydrophilic cartilage sliding against a stainless steel plate to reveal the surface wettability influence. The load effect was also involved, being expressed by four different applied levels of compressive displacement. The observations agreed with the previous paper to some extent. Unfolded (denatured) albumin formed a compact adsorbed layer under higher load, resulting in increased hydrophobic polymer friction. However, under lower compression, the effect was the opposite. This finding indicates that the level of protein denaturation has a substantial impact on frictional behaviour. The model showing the adsorption on UHMWPE surface considering native and unfolded albumin is presented and compared with the model introduced by Heuberger et al. [36] in Fig. 3.

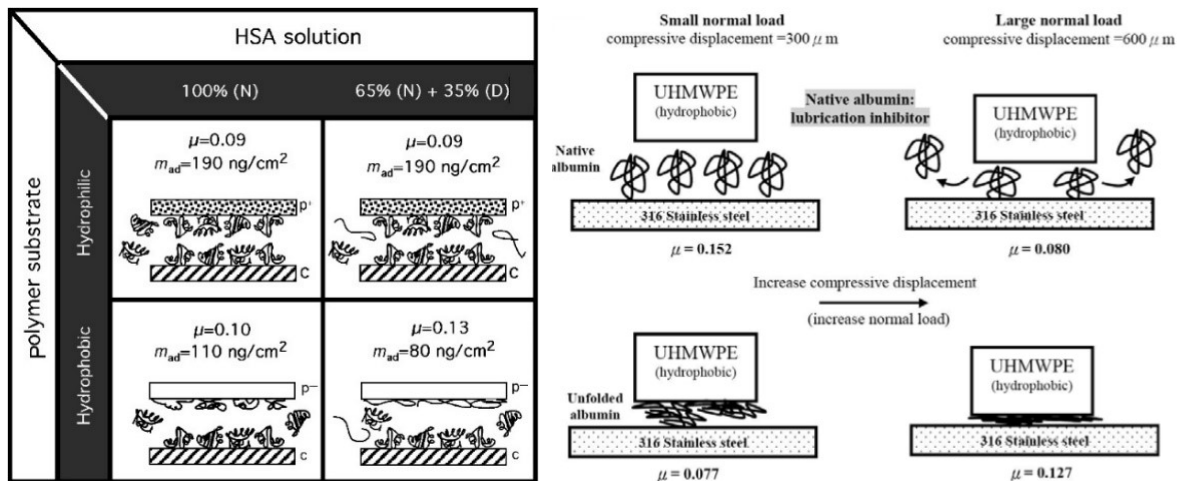


Figure 3: Left: A molecular model of boundary protein film for various natures of polymer surfaces. (N) – native protein structure, (D) – a form of the irreversibly denatured protein, μ – coefficient of friction [36]. Right: A hypothesis adsorption model of folded and unfolded albumin onto hydrophobic polymer surface [37].

A combined effect of albumin adsorption was later observed by Gispert et al. [38]. The authors investigated stainless steel/CoCrMo/ceramic-UHMWPE pairs lubricated by HBSS, which was subsequently doped by HA, BSA, and a mixture of HA and BSA. Focusing on the role of HA, the initial positive effect on friction was minimised with increasing time (sliding distance). The addition of BSA led to contradictive findings. While BSA led to stabilisation and lower friction for the metal pins, an increase of friction was observed for the ceramic pin. It is assumed that the adsorbed BSA film on the hydrophobic metal surface is more stable in contrast to the adsorption layer on the hydrophilic ceramic. When protein-free lubricant was used, the transfer of UHMWPE film to the metal surface was more pronounced than that for ceramics. Protein addition suppressed the transfer of UHMWPE film to metal but did not so for the ceramic. To conclude, the authors provided important insights and underlined issues related to biochemical processes occurring due to articulation. The load effect in terms of contact pressure was also presented, finding that the load influence depends on the applied lubricant type. A further clarification of the adsorption process was introduced in [39]. The experiments realised using X-ray photoelectron spectroscopy, radiolabelling, and atomic force microscopy (AFM) confirmed that the protection of metallic surfaces by the adsorbed film is more efficient compared to ceramic. The protection against UHMWPE film transfer leads to improved tribological performance accompanied by lower friction.

Previous findings were followed by Crockett et al. [40], who adopted fluorescent observation of the transferred polymer film for the first time. Contact of UHMWPE and CoCrMo in pin-on-disc configuration was lubricated by PBS, BSA, and bovine SF (BSF). The authors pointed to the fundamental importance of considering more complex lubricants when investigating SF friction and lubrication. Specifically, while there was no substantial difference between the friction coefficients for PBS and BSF, much higher friction was reported for BSA lubricant. The importance of other constituents in SF interacting together and substantially influencing the frictional behaviour is thus highlighted. Based on the deposited film observations, it is concluded that the transfer of UHMWPE correlates with the friction results. In particular, decreased friction was reported when the polymer film transfer to the metal surface was minor. Vice versa, a higher density of the transferred film was associated with higher friction, as can be seen in Fig. 4.

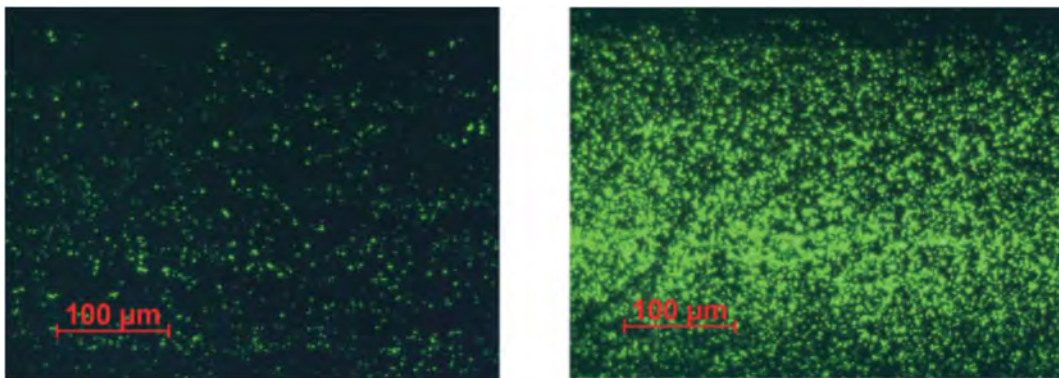


Figure 4: Fluorescent images of transferred UHMWPE film on CoCrMo surface after friction test. Coefficient of friction corresponding to the left and right image was 0.06 and 0.11, respectively [40].

These findings comply with the previous work [39]. Concerning another study [36], it is necessary to distinguish the transfer of polymer particles and the adsorption of albumin molecules. Assuming that CoCrMo surface generally supports adsorption, and following the findings that denatured proteins rather adsorb onto hydrophobic surfaces (e.g. CoCrMo), both surface properties and structure of the proteins need to be taken into account. Moreover, some discrepancies may also come from changing the load or speed.

Even more comprehensive description of the role of albumin concerning the implant material was given by Mishima and Kojima [41]. The authors investigated pin-on-disc contact in four material combinations; CoCrMo-on-UHMWPE, alumina ceramic Al_2O_3 -on-UHMWPE, Al_2O_3 -on- Al_2O_3 , and CoCrMo-on-CoCrMo, respectively. The experimental device scheme and respective values of friction coefficient for individual combinations lubricated by albumin solution and PBS are shown in Fig. 5. The differences in the friction coefficients were extensively discussed concerning protein adsorption and conformational changes. Results of the previous study were confirmed to some extent, showing that the adsorbed proteins on hydrophobic surfaces (metal, UHMWPE) led to the lowering of friction and wear. In ceramic-on-ceramic contact, the proteins did not adsorb on hydrophilic surfaces; thus, the effect on friction was negligible. It is pointed out that the conformational changes of the proteins due to thermal and mechanical action may considerably affect the adsorption, and thus the friction.

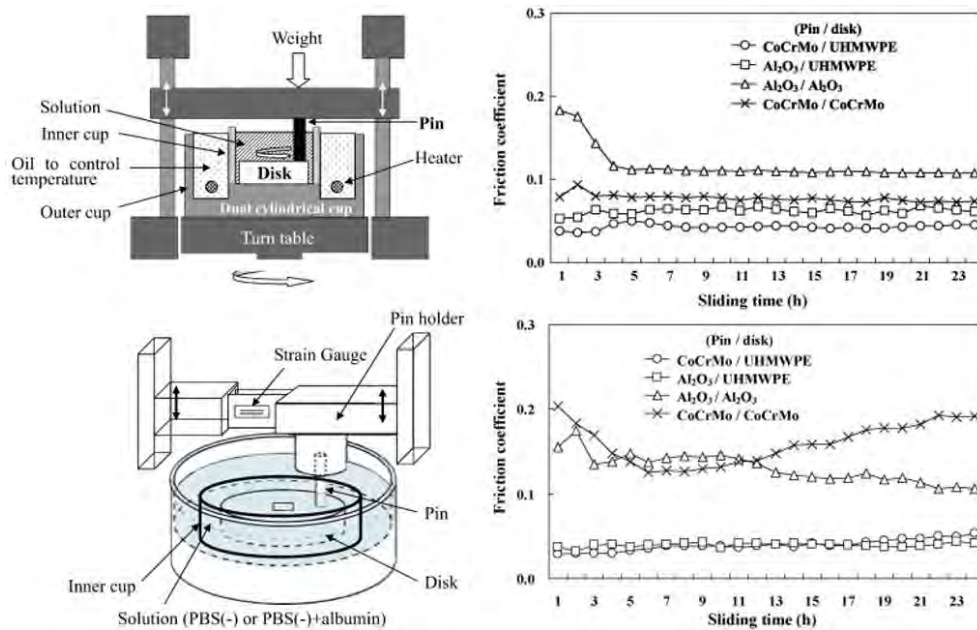


Figure 5: A scheme of pin-on-disc tribometer (left); results of friction coefficient for various material combinations lubricated by albumin solution (right top) and PBS (right bottom).

The figure was partially modified and reprinted based on [41].

Although based on the reciprocating pin-on-plate test, a similar investigation was performed by Chen et al. [42]. To better understand the interaction of the surfaces dependently on the configuration, the authors made both the pins and plates from the same materials. They focused on the following combinations (pin-on-plate order): UHMWPE-on-CoCrMo, UHMWPE-on-

Al₂O₃, CoCrMo-on-UHMWPE, and Al₂O₃-on-UHMWPE. Dry conditions were compared with those under lubrication by DI water, BCS, and denatured BCS. A general protective function of the adsorbed layer was observed while the CoCrMo substrate led to the strongest adhesion. Focussing on the specific material combinations, the combination of UHMWPE pins with metal or ceramic plates resulted in a considerable lowering of friction under BCS lubrication compared to DI water. The friction was comparable for both metal and ceramic counterfaces, attributed to the similar adsorbed albumin film. In the reversed arrangement (metal/ceramic pin with UHMWPE plate), the friction rapidly increased for BCS (see Fig. 6). The authors pointed at the potential role of contact stress, suggesting the necessity of further investigations.

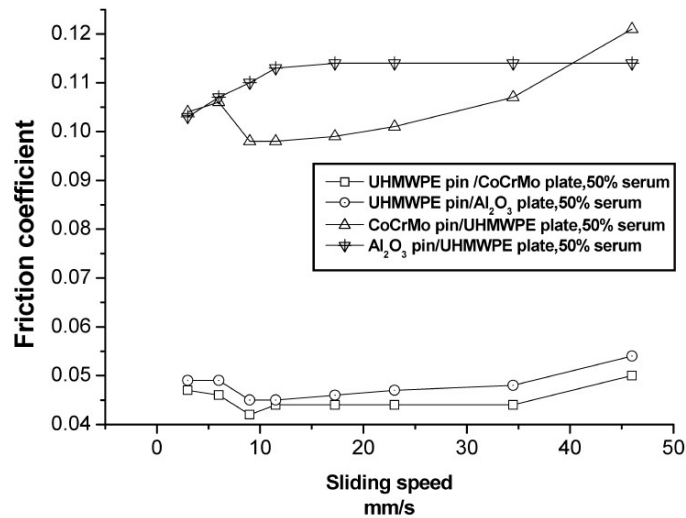


Figure 6: Frictional behaviour of various material combinations under lubrication by BCS as a function of sliding speed [42].

An insight into the influence of polymer crystallinity on the friction of ceramic Si₃N₄-on-UHMWPE pair was investigated in micro- and nanoscale by Kanaga Karuppiah et al. [43]. Microtribometer in a ball-on-flat configuration in combination with AFM was employed. Friction tests were realised under dry conditions without the presence of a lubricant. Different crystallinity levels were achieved by heating the polymer specimens above the melting temperature with varying hold times and subsequent controlled cooling. Crystallinity degree was then evaluated using differential scanning calorimetry. The results showed that a higher degree of crystallinity led to lower friction and wear resistance attributed to increased hardness and elastic modulus. However, omitting the lubricating medium might have a particular impact. Although this study is not directly related to other researches performed and described, all the aspects possibly affecting implants' friction should be presented in the author's opinion.

A comprehensive investigation of friction in ball-on-disc (steel-on-steel) configuration was introduced by Mavraki and Cann [44]. Apparently, most of the above papers concentrated on albumin protein. Therefore, following the implications of some studies regarding the importance of more complex model fluids, the authors prepared mixtures of albumin and γ -globulin dissolved in two different buffers (Tris and PBS). Two ratios were considered, 1:2 and 2:1, respectively. Furthermore, BS in various concentrations was also applied. The experiments were realised under

high sliding conditions and the constant load of 5 N, resulting in contact pressure of 0.34 GPa. The coefficient of friction was studied as a function of mean speed. It was found that both BS and protein solutions lead to lower friction at lower mean speeds. Buffer selection was found to be a key factor substantially influencing friction. The authors also employed the optical interferometry measurement method to evaluate the quantitative film thickness in the steel-on-glass configuration for the first time. This paper is therefore discussed also in terms of lubrication in the following Chapter 3. To conclude, since the friction and the film thickness seemed to be time/sliding distance-related, the importance of the deposited film was highlighted. The friction test device scheme and results for the two protein solutions in different buffers are presented in Fig. 7. The influence of albumin and γ -globulin concentration was also investigated in a microscale. Duong et al. [45] used AFM to obtain the friction coefficient in the contact of silicon AFM tip and CoCr samples of retrieved hip implants. The study showed that the concentration of both constituents has a clear impact on friction. In particular, γ -globulin exhibited the lowest friction within the physiological levels. Focusing on albumin, an initial increase in concentration had a positive effect; however, there was a particular maximum concentration, above which the reduction in friction was no more statistically significant.

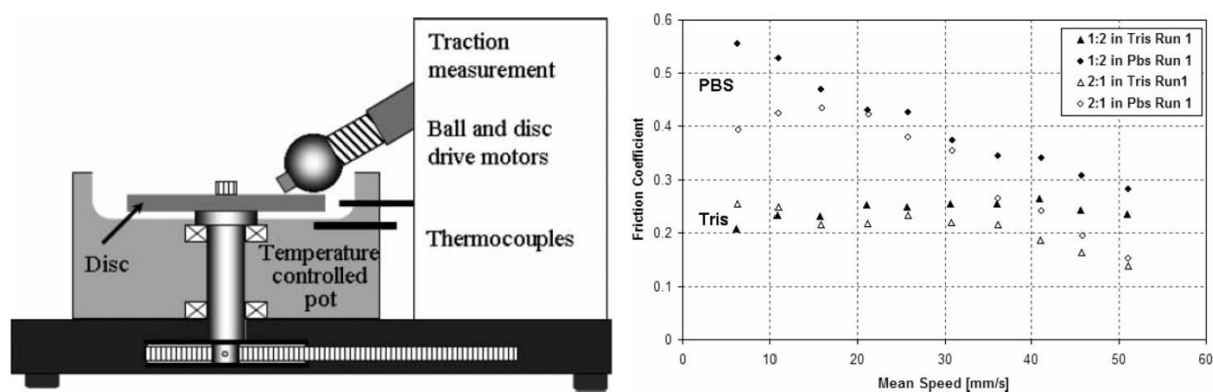


Figure 7: Ball-on-disc test device for friction measurements (left); results of friction coefficients in steel-on-steel configuration considering protein solutions in different buffers (right).

The figure was partially modified and reprinted based on [44].

In the introduction part of the thesis, the VS procedure helping to prolong the function of diseased joints was briefly mentioned. While the process is currently used exclusively for natural joints, some studies indicate that a similar approach might also improve the durability of artificial joints [46]. Nowadays, most of the solutions used for intra-articular injection are based on HA. Therefore, Guezmill et al. [47] investigated the friction and wear of UHMWPE rubbing against stainless steel in pin-on-disc arrangement considering various bio-lubricants that might improve the tribological performance. Specifically, saline solution, sesame oil, and *Nigella sativa* oil were tested. The experiment was also carried out under dry conditions. All the tested fluids led to friction decrease. The lowest values were achieved when the contact was lubricated by the oils, while the difference between them was negligible. The ability to keep a very low friction level is attributed to the adsorption of fatty acids on the steel surface. The authors later enhanced the study, replacing stainless steel with the conventional CoCrMo alloy used for implants [48].

Additionally, the contact of UHMWPE with titanium alloy TiAl₆V₄ was investigated. Titanium alloys are not used for articulating parts of THRs and TKRs; however, they may be used for tibial stem or replacements of small joints, among others. In this reference, saline solution, sesame oil, Nigella sativa oil, and Hyalgan[®] (HA-based substance for VS of diseased joints) were used as the test lubricants. Focusing on CoCrMo alloy, the saline solution led to quantitatively the same friction as Hyalgan[®]. When the natural oils were used, the friction dropped to half. In the case of titanium alloy, the oils also had a positive effect; however, the change was not as substantial.

2.2 Swinging and multidirectional experimental investigations

All the above papers concerning the frictional behaviour of the materials used for THRs and TKRs employed simplified geometrical configurations. While such an approach might be beneficial when revealing fundamentals (e.g. investigation of adsorption phenomenon or revealing some general effects such as load or speed), more advanced techniques based on the use of joint simulators, enable to bring a more in-depth knowledge. Following is an overview of studies dealing with friction evaluation considering realistic joint geometry. Due to the very complex TKR design, most of the below papers focus on describing the frictional behaviour of hip implants.

Substantial contribution to the field is attributed to Unsworth, Scholes and co-authors. One of the first papers was published in 1994 [49], employing a commercial hip joint simulator to compare the frictional response of original and explanted implants. The experiments were carried out under dry and lubricated conditions, finding that lubrication led to considerable friction reduction, as expected. Based on the investigation of 54 retrieved implants, it was found that while most of them operated under friction comparable to the new implants, a significant portion of the samples exhibited higher friction coefficient compared to the average value. Furthermore, only a weak correlation between friction and penetration depth was found. It means that the elevated wear depth is not affected only by the friction during articulation, highlighting the importance of overall tribological performance.

The following two papers, given by Scholes et al. [50],[51], focused on the prediction and experimental verification of the behaviour of hip implants made from different materials, having a nominal diameter of 28 mm. The experiments were carried out using the same simulator as in the previous article. Three material pairs were tested, CoCrMo-on-CoCrMo, alumina-on-alumina, and CoCrMo-on-UHMWPE, respectively. The contact was lubricated by CMC, silicone fluid, SF, and BS of variable concentrations. The typical lubrication regimes for each pair are discussed based on the detailed analysis. When analysing the friction data, higher clinical relevance comes from the experiments conducted with biological lubricants. Under lubrication by SF, the metal pair exhibited the highest friction, followed by ceramic-on-ceramic and metal-on-UHMWPE. While there was only a negligible difference between the latter two combinations, metal-on-metal showed three to fourfold higher friction. Very similar behaviour was also observed for BS; however, the ceramic pair showed even lower friction than the metal/polymer combination. The concentration of BS was found to have only a limited effect.

In the following paper, the authors employed the same methodology, including more material pairs and focusing on the role of clearance, among others [52]. Implants of three various diameters were involved in the study. The following couples were studied: stainless steel-on-UHMWPE, zirconia ceramic-on-UHMWPE, and DLC coated stainless steel-on-UHMWPE (all 22 mm), alumina-on-alumina (28 mm) and CoCrMo-on-CoCrMo (32 mm). CMC, BS, and SF were used for lubrication. Due to variable diameters and clearances, it is a bit difficult to summarise the findings. The bio-lubricants' data agreed with the previous paper, i.e. the friction of CoCrMo pair was substantially higher than that of the rest combinations. Regarding clearance, there was no clear effect on friction in terms of increasing or decreasing clearance for neither pair. Each pair had a specific value of the diametric gap, which seemed to be optimum; however, the friction results were not dramatically influenced considering the biological fluids.

Ash et al. [53] published one of the pilot studies aiming at the more complex assessment of friction of knee replacements. The improved version of the simulator employed before, enabling to investigate both hip and knee implants, was used. The authors aimed at friction analysis of the femoral metal component in contact with the compliant PE and polyurethane (PU) tibial parts under the presence of third body bone cement particles. Bone cement was mixed with distilled water to avoid the combined effect of the particles with SF constituents. The results showed that the added particles led to a substantial increase in friction, which further grew with a higher concentration of the particles. However, the measured friction torque continuously decreased with time, indicating that the number of particles was squeezed out of the contact due to the motion of the components. This phenomenon was even more pronounced in the case of PE. Concerning the general behaviour of both materials, PE exhibited much higher friction which can be seen from the Stribeck plots provided (see Fig. 8). Substantially lower friction of PU compared to UHMWPE was also observed for hip implants [54]; however, the previous study pointed out that PU was susceptible to creep, which may negatively impact durability [55].

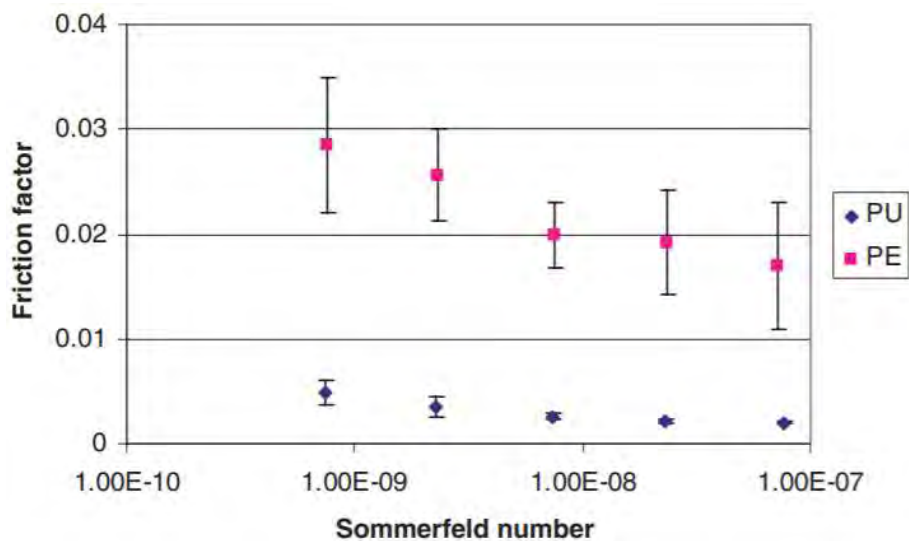


Figure 8: Stribeck curves for PU and PE knee tibial component articulating with CoCrMo femoral part lubricated by a mixture of water and bone cement particles [53].

The extension of the above hip investigations was published by Scholes and Unsworth [56], while the same hip pairs as used in [50] and [51] were tested. This time, Stribeck curves for individual couples lubricated by BS were provided additionally to the previous papers. It is concluded that the proteins contained in BS have a substantial impact on frictional behaviour. While generally a positive effect of adsorbed proteins in terms of wear is expected, the implication regarding friction is ambiguous; i.e. friction may exhibit both drop and growth dependently on the thickness and composition of the adsorbed boundary layer. Based on the data, the authors suggest developing new model lubricants, which would better fit human SF. Besides the hip joints, unicondylar knee replacement was also investigated, showing that BS led to increased friction in both the lateral and medial compartment, which is in agreement with hips. The observations were then extended, finding that sufficient lubrication is fundamental to keep low friction and minimised wear [57]. However, it should be noted that unicondylar knee implants represent only a minor portion of knee replacements.

Flannery et al. [58] thus provided an analysis of TKR friction. CoCr-on-UHMWPE combination was investigated using the simulator developed based on the devices applied before. The contact was lubricated by CMC and BCS. The friction was measured at the beginning of the test, after one million, and after two million cycles. Nevertheless, the effect of the test stage on friction was found to be insignificant for CMC. In the case of BCS, the combined effect depending on the tested set was revealed (see Fig. 9). The study further pointed at the vital role of BCS constituents. In compliance with previous observations, BCS led to higher friction than CMC. However, increasing protein concentration did not have a substantial effect. Besides, the positive impact of adding HA was underlined, as can be seen in Fig. 9.

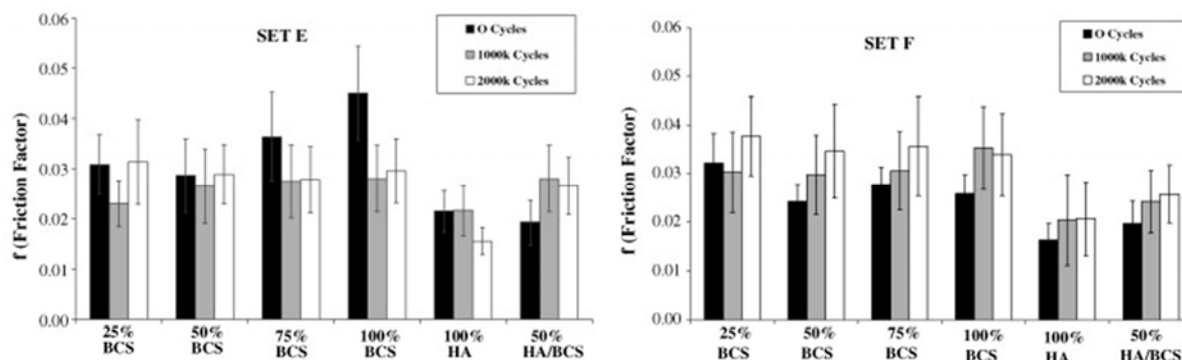


Figure 9: Resulting friction coefficients in various experiment stages for two tested pairs lubricated by different solutions. The figure was partially modified and reprinted based on [58].

Rest of the studies focused exclusively on THR testing. Brockett et al. [59] provided a systematic comparison of various THR pairs, focusing on the effect of lubricant and load. An overview of the tested combinations, including further details regarding clearance and surface roughness, is provided in Tab. 1. The implants were lubricated by water and BS of two different concentrations. The experiments were performed considering the transient operating conditions while the friction was evaluated at peak load and peak velocity of the cycle in both forward and backward directions. The results confirmed some of the previous findings that MoM combination

exhibits the highest friction. For the rest of the combinations, the friction factors were found to be comparable. Surprisingly, MoM showed lower friction when lubricated by BS solution compared to water. Regarding the load, all the tested combinations exhibited increasing friction with higher load. The authors later focused on the effect of clearance [25]. The study was limited to MoM pair of larger surface replacements (54.6 mm in diameter). Three various clearances were considered, finding no clue in the size of the gap between the surfaces. While the lowest friction occurred for the medium clearance at lower serum concentration, a positive minimum clearance effect was observed for undissolved BS. Thus, the role of constituents is essential.

Head	Cup	Bearing Combination	No. of Samples	Mean Radial Clearance (mm)	Head Ra (μm)	Cup Ra (μm)
CoCrMo	CoCrMo	MoM	6	0.029	0.011	0.009
CoCrMo	UHMWPE	MoP	4	0.132	0.010	0.752
Alumina	UHMWPE	CoP	4	0.123	0.004	0.752
Zirconia-toughened alumina	CoCrMo	CoM	4	0.034	0.003	0.009
Alumina	Alumina	CoC	4	0.030	0.004	0.005

Table 1: Detailed description of the tested THR pairs [59].

The following study was given by Bishop et al. [60]. A custom hip simulator enabling the application of physiological conditions was developed. The simulator scheme, the applied load, and the associated deflection angle are shown in Fig. 10. The authors investigated MoM, MoP, CoC, and MoC combinations. The implants were of various diameters and clearances to get a comprehensive set of data. In general, the findings correlate with previous studies. MoM exhibited the highest friction, followed by MoP, while the values for ceramic cups were found to be the lowest. As in [59], water led to higher friction in MoM pairs. The influence of conditions was also discussed, highlighting that the friction may be reduced by increasing the loading frequency. The effect of the swing phase load and the rest period between the cycles were found to have little impact.

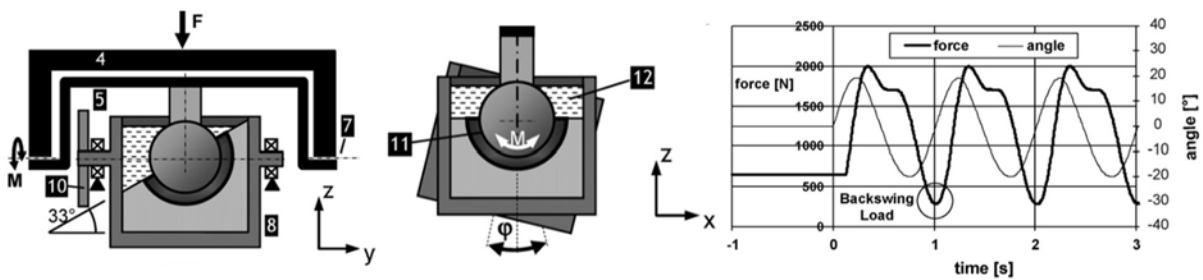


Figure 10: Scheme of the simulator central part (left, middle); applied conditions (right).

The figure was partially modified and reprinted based on [60].

In 2015, Vrbka et al. [61] introduced an alternative approach for investigating THR friction using the simulator based on the principle of pendulum [62]. The author of this habilitation thesis co-authored this paper; however, the article is not considered as the own author's contribution. The reason is that the document is written in the Czech language, which might be confusing if the foreign reviewer(s) would be invited. In this study, the implants of two nominal diameters

(28 mm and 36 mm) provided by two producers were evaluated. Attention was paid to MoP, CoP, and CoC pairs. The contact was lubricated by BS. At the beginning of the test, the swinging pendulum arm with the attached femoral head was deflected to a maximum and released. The friction coefficient was then evaluated based on the pendulum damping response. In the case of pairs containing a ceramic femoral head, an increase in diameter led to lower friction for both producers. A similar effect was later observed by Choudhury et al. [63], who applied the same simulator. In the case of MoP combination, the impact of implant size on friction was negligible, which also applies for MoM pair [63]. To sum up, MoP showed the highest friction, followed by CoP and CoC [61].

Previous studies applied simplified operating conditions focusing on flexion-extension (FE) motion while neglecting internal-external (IE) and abduction-adduction (AA) rotations. The first attempt to monitor friction under complex transient conditions was presented by Kaddick et al. [64]. In this pilot study, the authors focused on 28 mm and 48 mm implants in CoC and CoP configurations. The approach was initially validated, employing a simplified swinging cycle and comparing the obtained data with previous references. Subsequently, simulated walking conditions were applied. Very high precision of the testing was achieved. Under walking conditions, highly dynamic frictional moments, increasing with implant diameter, were measured. The authors highlighted the necessity of further investigations towards validation of the experimental setup.

Even more comprehensive study was provided a year later by Haider et al. [65]. The authors implemented the 6-degree-of-freedom (DOF) load cell below the sample in a hip joint simulator (see Fig. 11). MoP, CoP, and MoM couples were investigated. Diluted BS of constant concentration was used as the lubricant in all the experiments. The test procedure of Test 1 consisted of three phases. In phase one, a standard test lasting 5 million cycles with clean lubricant was carried out. In step two, crashed poly(methyl methacrylate) (PMMA) particles were added to the lubricant, simulating third body abrasive particles. In phase three, the metal femoral head was intentionally scratched to increase the wear rate, allowing for evaluation of polymers' resistance under severe rubbing conditions. Within this experiment, CoCrMo-on-UHMWPE (conventional), CoCrMo-on-HXLPE, and CoCrMo-on-Vitamin E HXLPE material combinations were assessed. Subsequent Test 2 was based on standard testing described above, comparing the frictional behaviour of MoP (UHMWPE), MoP (HXLPE), MoM (standard), MoM (TiN-coated), MoM (standard resurfacing), MoM (resurfacing with small lubricant pocket) and CoP (UHMWPE). Regarding the results of Test 1, the lowest friction was reported for the standard UHMWPE cup, followed by HXLPE and Vitamin E HXLPE in phases one and two. Step three with the scratched head led to a rapid increase of standard UHMWPE friction, indicating its lower resistance to more severe contact conditions. For Test 2, the lowest friction was that for MoP (UHMWPE), while the highest for MoM (TiN-coated). The detailed results may be seen in Fig. 11.

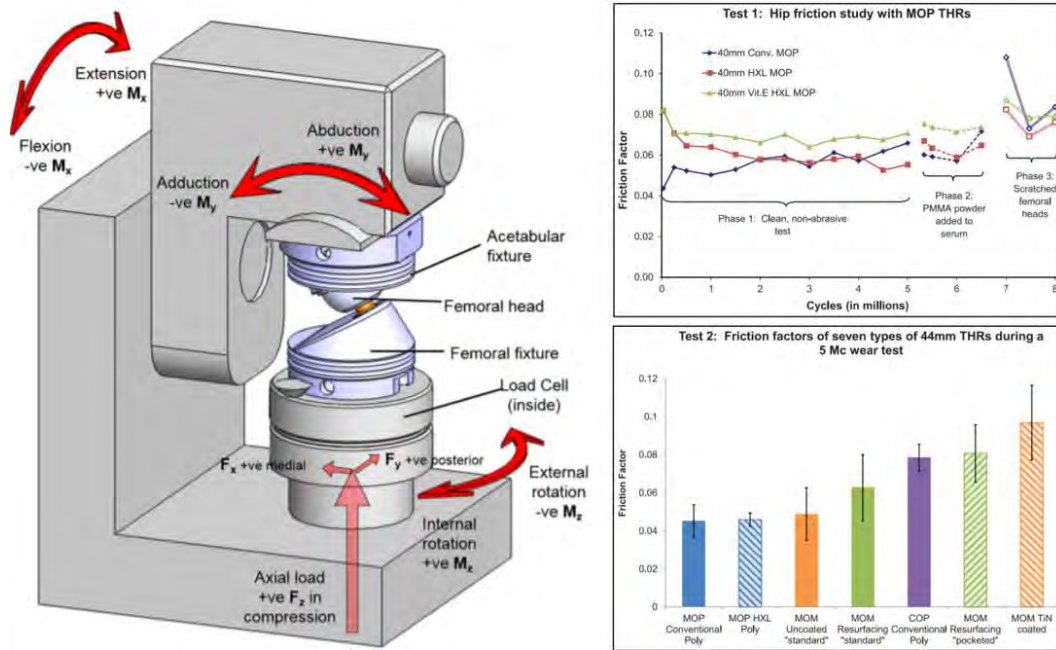


Figure 11: Hip joint simulator with a 6-DOF load cell (left); results of friction coefficient – Test 1 (right top); results of friction coefficient – Test 2 (right bottom).
The figure was partially modified and reprinted based on [65].

The latest paper dealing with THR friction measurement using the simulator was introduced by Sonntag et al. [66]. The authors employed two different approaches, while the first one was based on the modification of the hip simulator, allowing for three-dimensional friction evaluation. The second was based on the physical pendulum (similar to [61]) for system validation. The authors followed the pilot work of Kaddick et al. [64], focusing on CoP hip pairs of three various diameters, 28 mm, 36 mm, and 40 mm, respectively. Water and BCS were used for contact lubrication. As reported before, increasing the implant diameter led to increasing frictional torque. The authors suggested that similar experimental approaches are beneficial to understand the overall performance of hip implants better. The simulator model, together with the frictional torque results for the tested implants, is shown in Fig. 12.

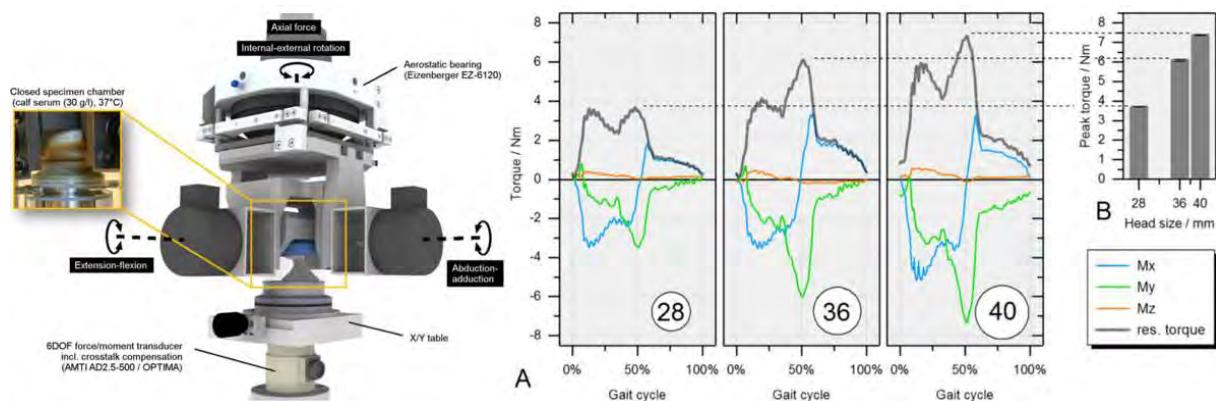


Figure 12: Model of the hip joint simulator (left); frictional torque moments for individual pairs (right A); peak resulting moments (right B). The figure was partially modified and reprinted based on [66].

2.3 Surface texturing towards reduced friction

The above subchapters summarised friction studies of hip and knee replacements relevant for the present thesis. A targeted surface modification represents a specific feature that needs to be considered towards further development of implants. The following is an overview of the papers dealing with the possibility of surface texturing of implants.

One of the first papers in the field was given by Nishimura et al. [67]. A pin-on-disc tribometer was applied, focusing on friction and wear under low load and high load conditions. The authors used a photochemical etching technique to fabricate the dimples on stainless steel pins and UHMWPE discs. The contact was lubricated by saline solution. Substantial improvement of tribological behaviour was observed independently of the applied load for the modified surfaces. The authors introduced optimal texture parameters, suggesting the dimples to be the lubricant reservoirs, enhancing lubrication performance. However, due to the production technique employed, the dimples' diameters were somewhat larger than recommended in later studies. The pin-on-disc test was carried out also by Young et al. [68]. The effect of texturing on friction and wear of UHMWPE specimens in contact with a standard CoCrMo pin under BS lubrication was studied. The dimples having a diameter of 0.16 mm and the depth of 0.32 mm were produced by computer numerical control (CNC) machining. The reciprocating test lasted for three hours at a relatively high speed (110 mm/s). The resulting friction of the modified samples was reduced by 42%. In contrast to the previous study, the authors did not observe wear reduction, which is mainly attributed to the type of applied lubricant.

Ball-on-plate reciprocating tests exploring the effect of UHMWPE surface modification on friction were performed by Kustandi et al. [69]. The study presents a nanoimprint lithography technique for making the texture on polymer plates fixed on the glass substrate. Silicon nitride ball was used as the counterface. Despite the substantial friction reduction reported (ranging from 8% to 35%), it needs to be pointed out that the study was carried out in a microscale under very low loads and dry conditions. Therefore, the implication regarding implants of real dimensions lubricated by biological fluids is somewhat limited.

A comprehensive investigation focusing on finding the optimal parameters of the structure made on the metal surface was performed by Cho and Choi [70]. Nanosecond pulse laser was used for dimple production in a variety of patterns. Microscopic images of the dimples are shown in Fig. 13. The authors reported sleeves around the edges of the dimples, which had to be removed by polishing. The diameter of the dimples was set to 75 μm , while the mesh density ranged from 5% to 25% and the pore depth was from 20 μm to 75 μm . Pin-on-disc tests were realised using the UHMWPE virgin pins. Both dry and lubricated (synthetic oil) conditions were considered. Regardless of the texture pattern, the friction was always lower for the modified metal surface. Based on the data, pore depth equal to 20 μm and an area density of 25% were recommended as the optimal structure pattern parameters. However, it needs to be noted that these parameters may be valid under specific considered conditions such as the fixed pore diameter or lubrication by oil (not by biological lubricant).

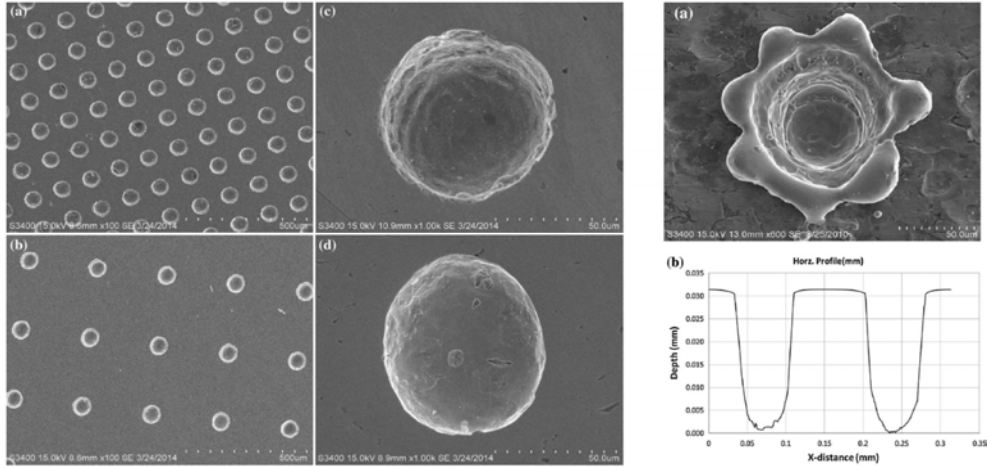


Figure 13: Left: various area densities (a, b) and various depths of the pores (c, d).
 Right: the sleeve around the dimple edge (a), dimple profile after polishing (b).
 The figure was partially modified and reprinted based on [70].

The first application of surface texturing on ceramic surfaces used for hip implants was presented by Roy et al. [71]. A rectangular array of circular dimples on the flat ceramic surface was fabricated by CNC micro-drilling. The experiments were conducted in the pin-on-disc configuration under BS lubrication. The authors fixed the dimple depth ($30\ \mu\text{m}$) and tested the effect of dimple diameter ($300\ \mu\text{m}$ vs $400\ \mu\text{m}$) and dimple density (5%, 10%, 15%). The experiments were realised at a variety of loads and speeds. The maximum friction reduction (22%) was achieved for dimples of $400\ \mu\text{m}$ in diameter at the coverage density of 15%. The latest pin-on-disc study was given by Borjali et al. [72] in 2018. With the use of laser surface texturing (LST), concave dimples were created on smooth flat CoCrMo discs. The pins made of UHMWPE and HXLPE were used for testing. The BS was adopted as the lubricant. The authors designed five various microstructure patterns, as is shown in Fig. 14. The sixth disc remained unmodified as the reference. The parameters of the patterns significantly influenced the friction response. In general, a positive effect of texturing on frictional behaviour was observed. The results for HXLPE pin are shown in Fig. 14.

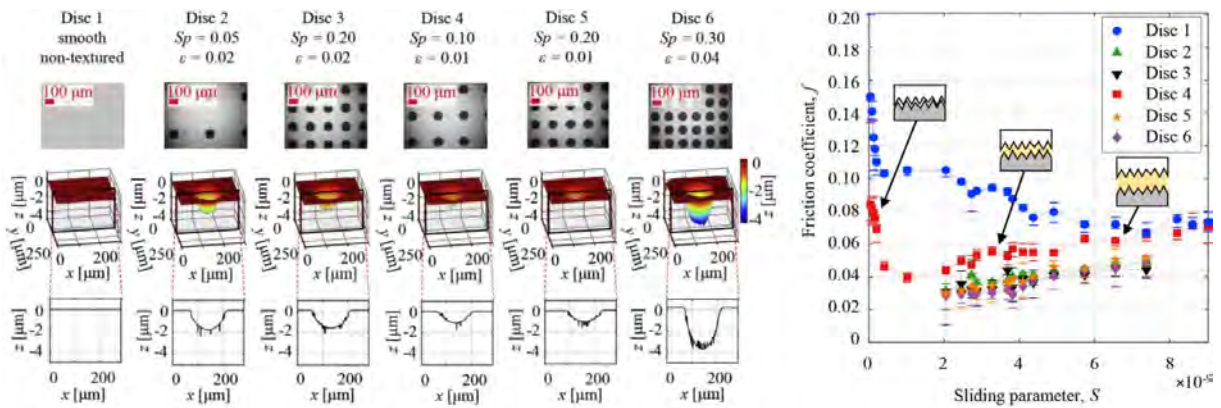


Figure 14. The designed patterns of surface texturing and the dimple profiles (left); respective friction coefficients for HXLPE pin (right). The figure was partially modified and reprinted based on [72].

Previous references considered the effect of texturing upon employing simplified geometrical configurations. The pilot study focused on surface modification adopting a joint simulator was provided by Ito et al. [16] at the beginning of the millennium. The authors applied a pattern of dimples to CoCr femoral head using an electrical discharge etching method. The diameter and depth of the dimples were 0.5 mm and 0.1 mm, respectively. The authors applied water for contact lubrication. The friction test lasted for 20 hours. The use of a patterned implant led to considerable friction reduction. The following simulator study was introduced by Chyr et al. [73], who reported an increased load-carrying capacity of the textured CoCr surface. The experimental configuration consisted of CoCr cylinder and UHMWPE concave channel-like sample to achieve the compliance of bodies. The cylinder undergoes a reciprocating rotation under the frequency of 1 Hz, simulating the FE motion of the hip implant. Four patterns of dimples derived based on a simple numerical model were applied to the cylinder surface using LST. The dimple diameter was 50 μm , while the depth and coverage ratio varied. The contact was lubricated by BS, while the applied maximum contact pressure was a little over 1 MPa. As for most of the above papers, a friction reduction was achieved for the dimpled surface compared to the reference smooth sample under most conditions. However, at the highest contact pressure, the effect was rather negative. The tested patterns, together with the resulting friction coefficients for various contact pressures, are summarised in Fig. 15.

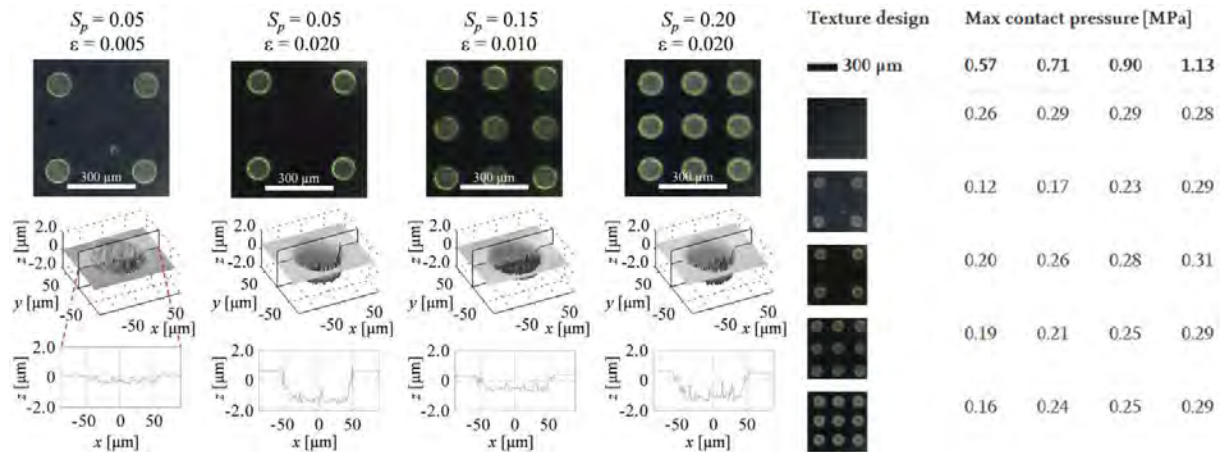


Figure 15. Designed parameters and patterns of the textures (left); respective friction coefficients for various patterns and loads (right). The figure was partially modified and reprinted based on [73].

The effect of surface texture considering various shapes of the dimples using the pendulum hip joint simulator was investigated by Choudhury et al. [63]. The authors textured the metal femoral head, designing three different arrays of dimples (square, triangle, and circular). The friction in MoM and MoP was investigated. While two of the patterns led to lower friction for the metal pair, an adverse effect was observed when the polymer acetabular cup was used. Despite the findings presented in the latest study, surface texturing has a great potential to reduce the friction of materials used for the joint prosthesis. However, it is noted that further investigation in the field is essential since reduced friction does not necessarily lead to a lower wear rate. Based on the reciprocating pin-on-plate test, Zhou et al. [74] reported that independently of the applied

texture on the metal counterface, the wear of UHMWPE increased, which contrasts with some of the above observations. Therefore, long-term wear tests need to be carried out to assess the role of texturing in a broader context. Since wear studies are time- and cost-consuming, friction tests play an essential role in suggesting suitable dimensions and patterns of the textures that might be beneficial in a longer period.

2.4 Author's contribution to the field

Based on the above references, it may be seen that there is a broad spectrum of studies focusing on the friction of hip and knee implants. Several papers dealt with the fundamental research of adsorbed boundary layer. However, most of the articles concentrated on albumin behaviour. Although this protein is dominant in SF, other constituents may dramatically influence the adsorption process. Moreover, even though many authors consider adsorption to have a positive protective function, some studies suggested that the adsorbed layer might also cause an increase in friction considering both micro [75] and macro [76] scales. Besides, the importance of SF constituents was confirmed not only for traditional materials of implants. Lower friction for BCS was reported even for various alumina ceramic nanocomposites, which might be used for implants in the future [77]. In contrast to the investigations of fundamentals, simulator studies benefit from higher relevance for clinical practice.

Therefore, the author of the thesis published three papers focused on different fields. The first study (i) deals with the analysis of MoP pair in pin-on-plate reciprocating configuration while applying protein solutions, focusing on measuring the friction and adsorbed film thickness. The layer structure is further investigated using Fourier-transform infrared spectroscopy (FTIR). The second study (ii) provides a comprehensive overview of the frictional response of MoM, MoP, CoP, and CoC material combinations in the established ball-on-disc configuration. Various mixtures of proteins were used for lubrication, while the effect of kinematic conditions was investigated as well. The third study (iii) deals with friction measurements using the pendulum simulator, focusing on the impact of PE cup texturing. Four various femoral head materials are considered, while PBS and mimicked SF are used for lubrication.

All the papers were published in peer-reviewed journals (one is published in Scopus database and the rest two are published in journals with IF in WoS). The list of the included papers is as follows:



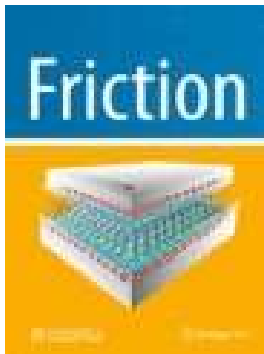
[78] Nečas, D., Sawae, Y., Fujisawa, T., Nakashima, K., Morita, T., Yamaguchi, T., Vrbka, M., Křupka, I., Hartl, M., 2017. The Influence of Proteins and Speed on Friction and Adsorption of Metal/UHMWPE Contact Pair. *Biotribology* 11, 51-59.

Author's contribution (BUT):	= 85%
Journal metrics (CiteScore ₂₀₁₇):	= 2.10
Citations (Google Scholar):	= 11 (excl. self-citations)



[79] Nečas, D., Vrbka, M., Křupka, I., Hartl, M., 2018. The Effect of Kinematic Conditions and Synovial Fluid Composition on the Frictional Behaviour of Materials for Artificial Joints. *Materials* 11.

Author's contribution: = 70%
Journal metrics (IF₂₀₁₈): = 2.97
Citations (Google Scholar): = 4 (excl. self-citations)



[80] Nečas, D., Usami, H., Niimi, T., Sawae, Y., Křupka, I., Hartl, M., 2020. Running-in friction of hip joint replacements can be significantly reduced: The effect of surface-textured acetabular cup. *Friction* 8, 1137-1152.

Author's contribution (BUT): = 90%
Journal metrics (IF₂₀₁₉): = 5.29 (IF₂₀₂₀ is not yet available)
Citations (Google Scholar): = 1 (excl. self-citations)

2.4.1 The Influence of Proteins and Speed on Friction and Adsorption of Metal/UHMWPE Contact Pair

The first paper demonstrating the author's contribution to the field was focused on evaluating the friction and the detailed analysis of the adsorbed protein layer. The experiments were conducted in the pin-on-plate reciprocating configuration using HEIDON Tribo Gear TYPE:38 tribometer. CoCrMo pin having the radius of curvature of 100 mm was fixed against a sliding medical-grade UHMWPE plate of 2 mm thickness.

The experiments were performed with protein-free PBS, simple solutions of albumin and γ -globulin, and the mixture of both proteins. Three different constituents' concentrations were considered when focusing on simple solutions, 0.4 wt%, 0.7 wt%, and 1.4wt%, respectively. In the case of the mixture, the content was the same for both (0.7 wt%). The measurements were repeated under two sliding speeds (10 mm/s and 50 mm/s) simulating normal walking and fast running. It needs to be noted that the speeds within the joints are higher compared to the overall motion speed. The stroke length was 25 mm, while the overall sliding distance, regardless of the applied rate, was 90 m. The normal load was 4.9 N, resulting in the contact pressure of 6.3 MPa. After the friction test, the samples were gently washed and air-dried. The adsorbed layer thickness was subsequently determined using the spectroscopic ellipsometry (HORIBA UVISEL LT) optical method. Subsequent structure analysis of the adsorbed layer was carried out using FTIR.

The results showed that proteins added to the serum rapidly increase the friction coefficient. Both concentration and the sliding speed were found to be significant regarding the frictional response. The effect of speed was even more pronounced at lower concentrations (see Fig. 16).

When analysing the thickness of the adsorbed layer, albumin formed a thicker film under most conditions. However, at the highest concentration, the thickness was similar (higher speed) or lower than that of γ -globulin (lower speed), see Fig. 16. The comparison of friction and adsorbed thickness showed nearly linear dependence. Nevertheless, while the friction increased with thickness at a lower speed, the behaviour was opposite at a higher rate. The difference was subsequently explained utilising FTIR analysis. While mostly denatured proteins were identified after the test realised at 10 mm/s, the higher speed allowed a portion of the proteins to keep their native structure. A simplified illustrative sketch of the protein layer adsorbed on UHMWPE surface was proposed based on the results. It is concluded that the state of proteins has a decisive impact on friction and lubrication performance. The overall research scheme of the study is shown in Fig. 17.

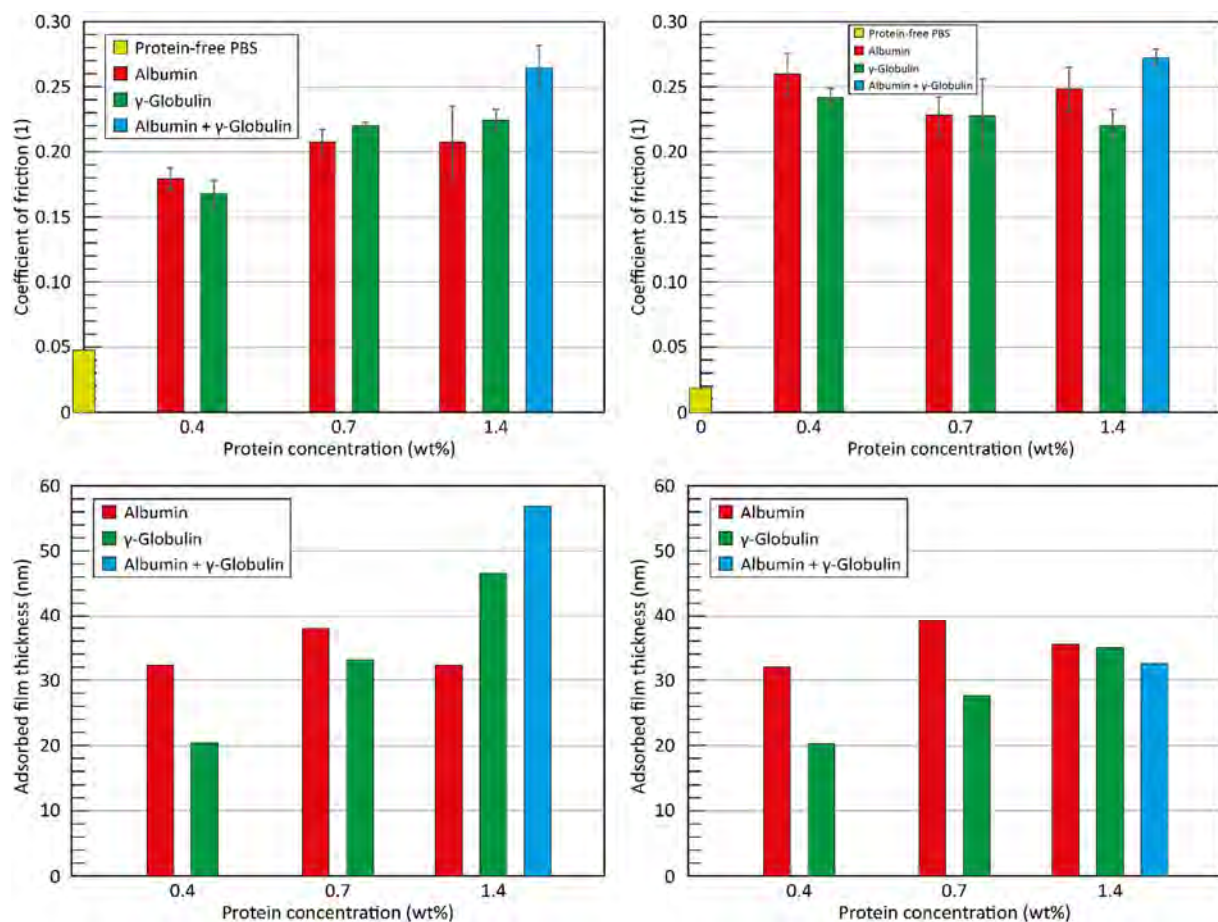


Figure 16: Results of friction coefficient (top) and adsorbed film thickness (bottom) for various protein solutions in the reciprocating pin-on-plate test under lower (left) and higher (right) sliding speed.

The figure was partially modified and reprinted based on [78].

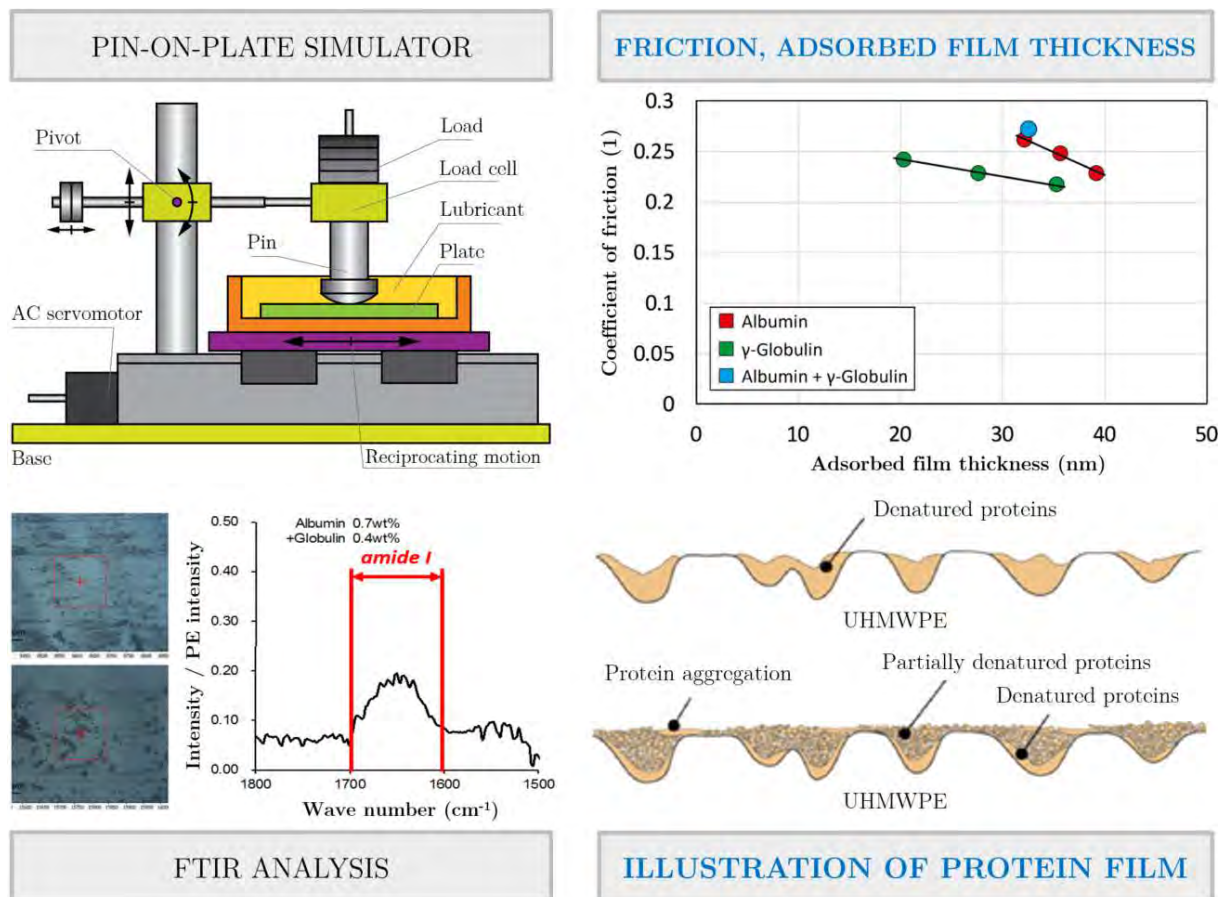


Figure 17: Research scheme of the study [78].

2.4.2 The effect of kinematic conditions and synovial fluid composition on the frictional behaviour of materials for artificial joints

The following study aimed at the detailed understanding of protein frictional behaviour, focusing on the effect of material combination, speed, and slide-to-roll ratio (SRR), which may bring some implications for TKR, where a slip changes throughout the cycle. The measurements were realised in ball-on-disc tribometer using Mini Traction Machine test device. Four material combinations were tested, MoM, CoC, MoP, and CoP, respectively.

Similar protein solutions and PBS, as in the previous paper, were used initially for lubrication. A subsequent set of measurements was carried out with the protein mixtures, while the ratio of albumin to γ -globulin changed to approach the physiological composition. To better understand the protein interactions, the ratio was also flipped. The experiments with simple solutions were performed at a single speed; protein mixtures were investigated under two different rates. Furthermore, two SRRs were considered, mimicking relatively severe sliding conditions. Specifically, SRR equal $\pm 150\%$ was applied. The normal load was 0.5 N for the metal ball and 0.4 N for the ceramic one. The resulting contact pressures for individual combinations were 265 MPa (MoM), 9.9 MPa (MoP), 280 MPa (CoC), and 9.5 MPa (CoP). The contact pressure is generally higher than that in real implants due to non-conformity of the contact.

Concerning the effect of material, the highest friction was always exhibited by MoM combination, followed by CoC, MoP, and CoP. This behaviour was observed for both speeds and both SRRs. However, the positivity/negativity of SRR considerably affected the results when investigating the effect of fluid composition for individual pairs. Regarding the lubricant influence, hard couples (i.e. MoM, CoC) showed lower friction for protein solutions compared to PBS. In the case of MoP pair, the proteins had a somewhat negative impact; however, the results were strongly dependent on the applied lubricant type under negative sliding (the ball rotates faster than the disc). Under positive sliding, the lubricant impact was even more complicated. Very similar behaviour was also observed for CoP. To sum up, this study provided a comprehensive set of data about the friction of implant materials, focusing on the detailed effect of material combination, lubricant composition, and kinematic conditions. The overall research scheme of the study is shown in Fig. 18.

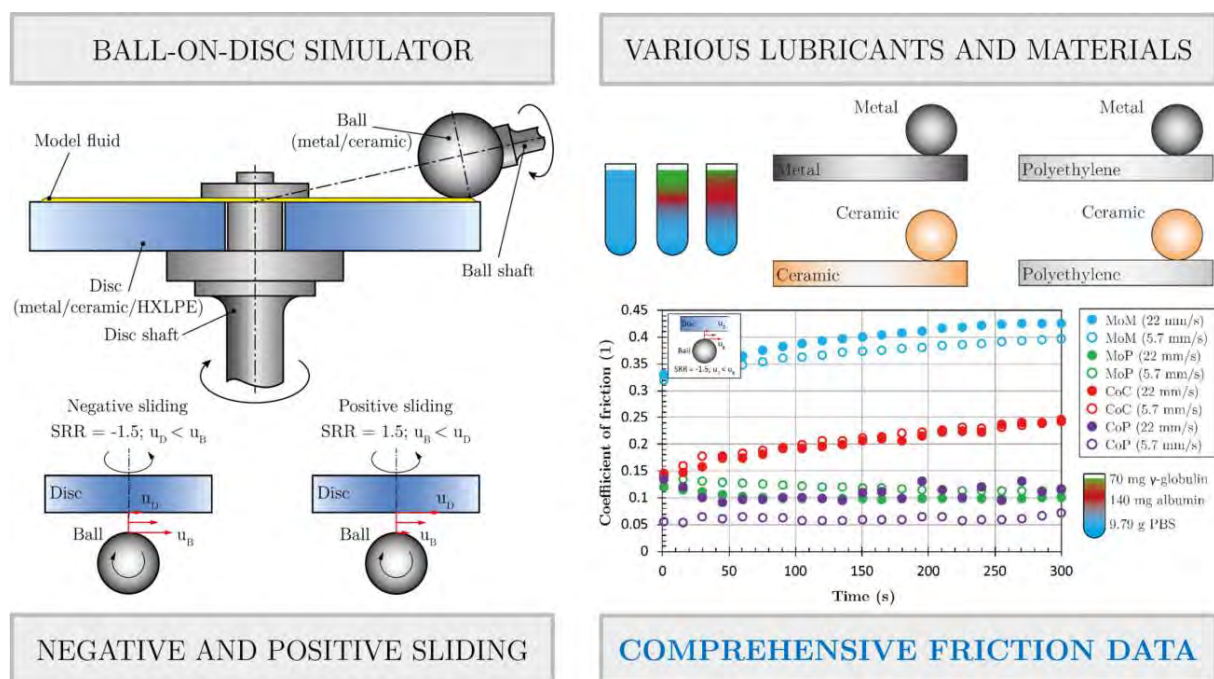


Figure 18: Research scheme of the study [79].

2.4.3 Running-in friction of hip joint replacements can be significantly reduced: The effect of surface-textured acetabular cup

The last author's paper in this field deals with the effect of surface texturing. Pendulum hip joint simulator was employed for friction evaluation comparing non-textured and textured UHMWPE acetabular cups. As described above, the measurement using the pendulum is relatively simple in terms of methodology. The acetabular cup is securely fixed in the base frame. The pendulum arm with the femoral head is deflected and released while the motion is damped due to joint articulation. Pendulum response (angular velocity) is then transferred to the friction coefficient. A unique tilling technology was applied for manufacturing tiny dimples of precise dimensions on the cup surface. The production method is based on CNC micromachining using

the end mill with a cutting edge. One of the benefits of this approach is that the occurrence of sleeves, often reported when using lasers is avoided, and there is no thermal-affected zone near the dimples. Therefore, there is no risk of thermal influence of the base material. Following the previous feasibility study and experiences of the research team, the dimples had a diameter of 300 μm , while the depth was only 5 μm . In this study, the surface coverage ratio was 15%. Four femoral heads were involved in order to reveal the combined effect of surface modification and material. Specifically, CoCrMo, alumina ceramic, zirconia-toughened ceramic, and Oxinium (an elastic metal implant with modified surface properties mimicking ceramic) implants were used. The nominal diameter of the implants was 32 mm, while comparable clearance was considered for both non-textured and textured cup.

The contact was lubricated by PBS and model fluid mimicking human SF. The concentration of specific constituents was as follows: albumin = 20 mg/ml, γ -globulin = 3.6 mg/ml, HA = 2.5 mg/ml, PLs = 0.15 mg/ml. A series of eight consequent swinging tests were performed, twice with each head and cup combination to get statistically relevant data. The applied load was 532 N, resulting in contact pressure ranging from 2.9 MPa to 4 MPa, dependently on the test couple.

The model SF constituents caused a substantial increase in friction compared to PBS for all the tested femoral heads, confirming the previous investigations of hard-on-soft pairs. Concerning the effect of the dimples, the friction was reduced regardless of the head material or the lubricant. For the metal and both ceramic heads, the friction reduction was more pronounced under SF lubrication. Oxinium exhibited relatively unstable behaviour with a limited contribution of texturing. Focusing on the results with SF which have a higher relevance for clinical practice, the friction for metal, alumina, zirconia-toughened, and Oxinium head dropped by 25.5%, 40%, 38.8%, and 9.9%, respectively (see Fig. 19). It is well reported that the polymer surface of the implant is worn over time. However, the wear rate is the most progressive in the so-called running-in phase. Thus, it is suggested that the dimples made on the polymer cup may reduce running-in friction, potentially slowing down the process of mechanical wear, extending the life of the implant eventually. Furthermore, the tiling technique may be used for texturing both soft and hard materials. Therefore, it is expected that there is excellent potential regarding further development of implants. The research scheme of the study is shown in Fig. 20.

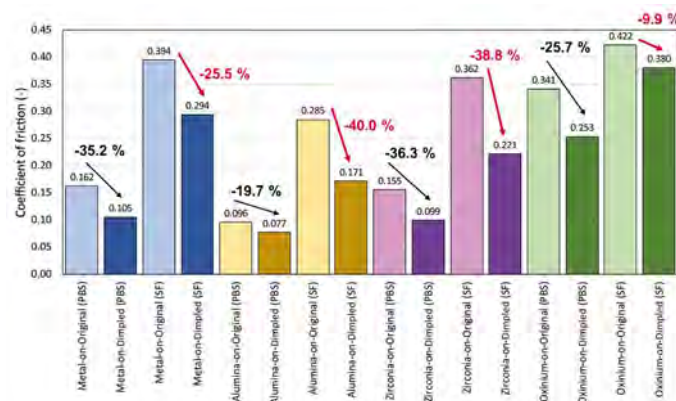


Figure 19: Results of friction coefficients for various material combinations lubricated by PBS and model SF. The figure was partially modified and reprinted based on [80].

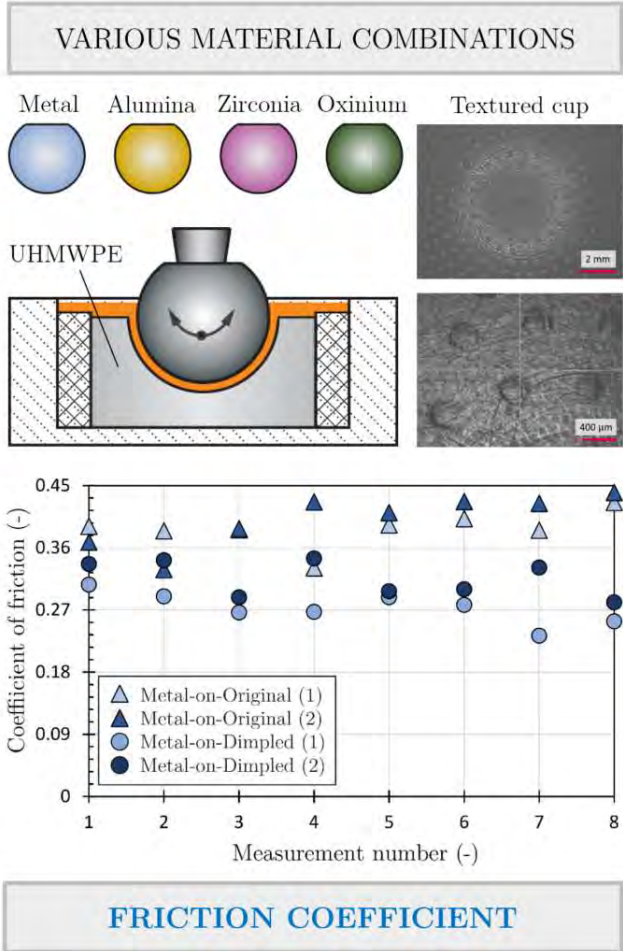
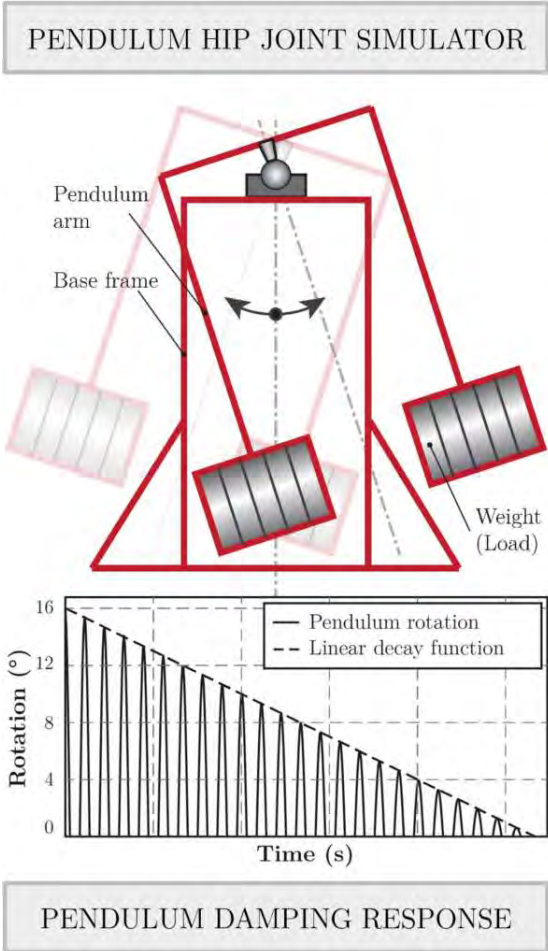


Figure 20: Research scheme of the study [80].



The Influence of Proteins and Speed on Friction and Adsorption of Metal/UHMWPE Contact Pair



D. Nečas^{a,*}, Y. Sawae^{b,c}, T. Fujisawa^b, K. Nakashima^b, T. Morita^{b,c}, T. Yamaguchi^{b,c}, M. Vrbka^a, I. Křupka^a, M. Hartl^a

^a Faculty of Mechanical Engineering, Brno University of Technology, Czech Republic

^b Faculty of Engineering, Kyushu University, Japan

^c International Institute for Carbon-Neutral Energy Research, Kyushu University, Japan

ARTICLE INFO

Keywords:

Joint prosthesis
Proteins
Friction
UHMWPE
Adsorption

ABSTRACT

It was reported in several studies that friction and wear of joint prosthesis are apparently influenced by the proteins contained in the synovial fluid. However, detailed mechanisms of these tribological processes have not been clarified yet. The present study aims on the effect of adsorbed protein film on frictional behaviour of metal/polyethylene contact pair. Reciprocating pin-on-plate test was conducted, while the CoCrMo pin was sliding against UHMWPE plate. The contact was lubricated by various solutions of albumin and γ -globulin solved in PBS. After the friction test, the thickness of adsorbed film was evaluated using spectroscopic ellipsometry. Structure of the adsorbed proteins was later examined by FT-IR. The results showed that at low sliding speed equal to 10 mm/s, there was a linear correlation between the friction coefficient and the thickness of the adsorbed protein film. An increase of friction was thus accompanied by the evolution of protein film. In that case, both proteins undergone substantial conformational changes, losing their original structure. On the contrary, proteins could sustain their secondary structure to some extent at higher sliding speed (50 mm/s), when different behaviour of the both proteins could be observed. This phenomenon was attributed to different structure of albumin and γ -globulin in its native state. It might be concluded that friction coefficient of metal-on-polyethylene joint prosthesis is influenced by protein content, as well as kinematic conditions, since the sliding conditions have a certain effect on both the adsorbed film formation and structure of the adsorbed molecules.

1. Introduction

One of the crucial task in the area of hip replacements is still the durability of the implants. The main reason of the failure seems to be aseptic loosening as a consequence of wear of rubbing surfaces [1]. In meaning of the implants materials, the combination of metal/ceramic head with ultra-high molecular weight polyethylene (UHMWPE) cup is well-established and most popular contact pair world widely nowadays [2]. It is estimated that the longevity of such replacements can reach up to 15 years [3]. In an effort to improve the service life of implanted components, the understanding of tribological processes and lubrication mechanisms within the hip joints under various operating conditions is necessary [4].

Several investigators focused on *in vitro* testing of UHMWPE in terms of wear. It was reported by Wang et al. [4] that adding just a small amount of proteins into a water as a base lubricant led to rapid increase of wear. It was found that the maximum wear occurs while the

protein concentration is around 30 mg/ml. Further increase of concentration led to a slight decrease of wear rate. The authors concluded that soluble proteins are not effective lubricants for UHMWPE joints. The study was extended by Wang et al. [5] who pointed out that not just the protein concentration but also the ratio of albumin and γ -globulin has to be taken into account. It was recommended that the total protein concentration for *in vitro* testing should be maintained between 20 and 30 mg/ml while the ratio of albumin/ γ -globulin should be kept in the range from 1 to 1.5. Similar results were published by Saikko [6] who highlighted that the protein concentration smaller than 20 mg/ml is not suitable for *in vitro* wear tests, since the results for lower concentrations were not representative in meaning of clinical wear. Therefore, the authors recommended to apply higher protein concentration when using wear simulators.

Considering wear processes, an important information can also come from the analysis of real cups retrieved from the patients during revising operations. Ranuša et al. [7] developed an optical method

* Corresponding author.

E-mail address: david.necas@vut.cz (D. Nečas).

based on 3D optical scanning when analysing 13 explanted cups. The authors proved very high accuracy of the experimental approach simultaneously with the minimization of the measurement time. The introduced technique seems to be a very powerful tool for future analysis, while the evaluated wear rate can be identified regarding to the particular patients according to their age, sex, BMI, implant orientation in the body or its duration.

Widmer et al. [8] explored the effect of surface treatment of UHMWPE on tribological behaviour of UHMWPE-ceramic sliding pair. It was found that oxygen-plasma treatment led to a higher hydrophobicity ensuring faster protein adsorption onto rubbing surfaces. Significant reduction of both dynamic and static friction was observed. As the static friction is believed to be a major wear contributor, it is expected that the surface treatment has a great potential regarding to durability of joint implants. This study was later followed by Heuberger et al. [9] who extended the knowledge investigating the impact of bovine serum albumin (BSA) conformational state on its adsorption in relation to surface wettability. The authors found that hydrophilic surfaces rather attract proteins in a native state, forming thicker and denser films that lead to a reduction of friction between the surfaces. However, it should be highlighted that UHMWPE-ceramic results can differ compared to that of UHMWPE-metal. Serro et al. [10] focused on the adsorption of (BSA) on rubbing surfaces, employing metal/ceramic pins sliding against UHMWPE discs. It was clearly evidenced that the adsorption behaviour regarding to particular contact couples is different, while more extensive adsorption could be observed when metal pins were used as counterfaces.

Sawae et al. [11,12] focused on the effect of hyaluronic acid and lipids. Using the unidirectional pin-on-disc test device, the authors found that adding the hyaluronic acid into a saline solution led to a reduction of both friction and wear of UHMWPE [11]. In later study, three-station multidirectional sliding pin-on-plate apparatus was used for the evaluation of the effect of protein and lipid concentration on wear rate of UHMWPE sample. Several test lubricants with various protein concentrations from very low level up to a physiological concentration were used. The lipid concentration was kept in physiological concentration from 0.005 to 0.02 wt%. From the results, it can be assumed that under low protein concentration, an increasing amount of lipids led to a decrease of wear. However, the opposite effect was observed when the protein concentration reached physiological level [12].

Crockett et al. [13] studied the friction coefficient in UHMWPE-CoCrMo pair using fluorescent microscopy method. Three various lubricants were employed; Phosphate Buffered Saline (PBS), BSA and bovine synovial fluid (BSF). As quenching phenomenon [14] was not observed in the case of PE-metal contact, the authors focused, among others, on the correlation between friction and transfer of PE particles during sliding test. It was found that low friction is accompanied by low amount of transferred particles. In terms of friction, just very low differences were observed when PBS and BSF were applied; however, BSA exhibited substantially higher friction.

Frictional properties of different implant materials were tested in a more detail by Vrbka et al. [15] using the pendulum hip joint simulator. As the test lubricant, 25% BS solution was applied. In the case of UHMWPE cup, the coefficient of friction (CoF) varied in the range from 0.11 to 0.19 dependently on femoral head material and its nominal diameter. In general, higher diameter led to decrease of friction. It was also pointed out that the friction characteristics can be significantly influenced by the size of the diametric clearance.

One of the key factors influencing the friction and wear is the thickness of lubricating film. Although several studies investigating the film thickness between the components of artificial joints have been published recently; so far, there is no a study considering the UHMWPE as one of the counterfaces. This comes from the limitation of experimental methods. It is well known that UHMWPE has a poor conductivity; therefore, it is not possible to apply the methods based on the

change of electrical capacitance described previously [16,17]. Optical interferometry, which seems to be a well-established approach for studying the lubricant film in the area of biotribology [18,19,20,21], cannot be applied, as the reflectivity of UHMWPE is insufficient. However, in the future study, the optical method based on the principle of fluorescence [14,22] seems to be applicable even for non-reflective bodies.

Due to above information, it is particularly complicated to evaluate the lubricant film *in situ* considering the pairs containing UHMWPE as one of the counterfaces. However, adsorbed protein film, which can be determined after the experiment, can provide the fundamental information about the proteins behaviour under various operating conditions. It was reported several times that the protein adsorption must be taken into account when trying to assess the lubrication processes within hip joint replacements [23–26].

From the literature review, it is apparent that the main attention is paid to *in vitro* testing of friction and wear of UHMWPE in combination with metal/ceramic counterfaces. However, little is yet known about the influence of protein content, protein ratio and sliding speed on adsorbed protein film. Therefore, the aim of the present study is to evaluate the adsorbed protein film thickness and to assess the role of particular proteins on lubricating processes. For this purpose, a reciprocating pin-on-plate tests with various model fluids under different kinematic conditions were realized. After the experiment, the thickness of adsorbed protein film on UHMWPE was evaluated using spectroscopic ellipsometry. Moreover, the structure of adsorbed proteins on the polyethylene plate was checked by FT-IR. The CoF was evaluated in an effort to better describe the lubricating mechanisms.

2. Materials and Methods

The friction tests were carried out using pin-on-plate reciprocating simulator (HEIDON Tribo Gear TYPE:38). The contact was realized between CoCrMo pin of the radius of curvature equal to 110 mm and UHMWPE plate of the thickness of 2 mm. Medical grade cast CoCrMo alloy (ASTM-F75) was used as the pin specimen. Its surface was polished using diamond slurry to a surface roughness R_a of $0.01 \pm 0.005 \mu\text{m}$. The plate specimen was prepared from GUR1050 bar stock. Plate surfaces were polished as well, leading to resulting surface roughness R_a of $0.1 \pm 0.02 \mu\text{m}$. Plate specimens used in this study did not experience any sterilization prior the experiments. Before the friction test, all specimens were washed in an ultrasonic cleaner in a detergent (polyoxyethylene *p*-*t*-octylphenyl ether) for 30 min and subsequently in distilled water for additional 30 min. Finally, the samples were washed ultrasonically in ethanol for 15 min. After the cleaning process, the specimens were dried at 60°C for 30 min at vacuum drying chamber.

The pin was fixed in the holder on the lever which can rotate around the pivot on the console. The plate was placed in the PDMS dish and was fixed by the attachments to ensure stable position during the test. Load was applied by the weight placed above the pin and the reciprocating motion with constant speed was applied by AC servomotor. The CoF between the metal pin and the polyethylene plate is calculated from the frictional force measured by the load cell. The schematic of the experimental apparatus is displayed in Fig. 1.

As the test lubricant, protein-free PBS and several protein solutions were applied. The proteins were dissolved naturally in PBS. BSA (Sigma Aldrich A7030) and bovine serum γ -globulin (BSG, Sigma Aldrich G5009) were used, while the effect of various concentrations was investigated. The concentrations in the case of both proteins were 0.4, 0.7 and 1.4 wt%, respectively. Moreover, to check the effect of proteins combination, mixture consisting of 0.7 wt% BSA and 0.7 wt% BSG was also applied. The total amount of the lubricant used in each experiment was 15 ml and the tests were realized under fully flooded conditions. The applied lubricants are summarized in Table 1. The concentrations of proteins are lower compared to that in human synovial fluid. It was

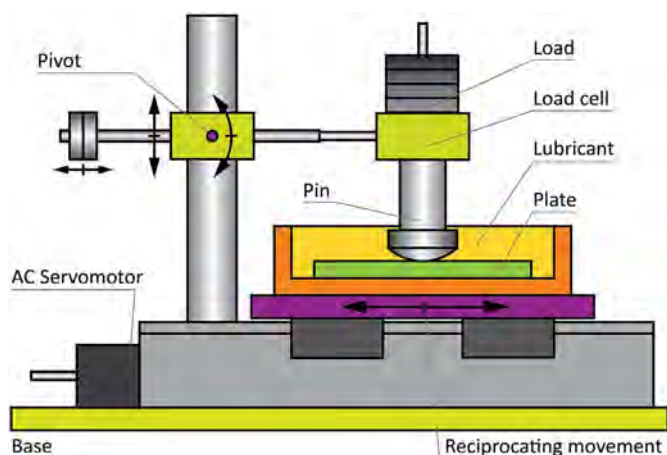


Fig. 1. Scheme of the pin-on-plate friction tester.

Table 1
Summary of the tested protein solutions.

Lubricant number	Protein	Protein concentration (wt%)
1	PBS	0
2	Albumin	0.4
3	Albumin	0.7
4	Albumin	1.4
5	γ -globulin	0.4
6	γ -globulin	0.7
7	γ -globulin	1.4
8	Albumin + γ -globulin	0.7 + 0.7

reported by Galandáková et al. [27] that the average concentration of albumin and γ -globulin is around 28 mg/ml and 10 mg/ml, respectively. However, the employed lubricants were prepared following the previous findings given by Nakashima et al. [28], while the applied concentrations should ensure optimal level of friction.

In all the experiments, the applied load was 4.9 N resulting to a maximum contact pressure of 6.3 MPa. Two different sliding speeds were applied, 10 and 50 mm/s, respectively. The stroke length was 25 mm, while the total sliding distance was 90 m. All the tests were carried out under controlled ambient temperature of 25 °C. After the test, the specimens were stored in desiccator in the same room to avoid any thermal influence of the adsorbed layer. Because of the repeatability, the experiments were conducted three times under each conditions with all the lubricants.

After the sliding test, UHMWPE plate specimen was carefully rinsed by running pure water to remove the residual lubricant and to avoid a contamination by the precipitation of unadsorbed protein molecules. After the air-dry, the formation of adsorbed protein film on the UHMWPE surface was analysed using two different optical methods.

Spectroscopic ellipsometry (HORIBA UVISEL LT) was employed to estimate the thickness of adsorbed protein film. Ellipsometry is a well-established optical technique for determining the thickness of thin films ranged from angstroms to several microns. If polarized light is emitted to the sample surface, the polarization state of light is affected upon the reflection on the surface. Therefore, the optical condition of the interested surface can be characterized by capturing reflected light with a detector thus analysing the polarization state of light by calculating the amplitude ratio ψ and phase difference Δ between p-polarized and s-polarized fractions of the light. In this study, the optical condition of polyethylene surface was examined before and after the experiment. Then, the protein film thickness, elaborated during the sliding test, can be evaluated from the change of ψ and Δ values. It should be highlighted that the thickness of adsorbed protein layer is not a representative of the lubricant film thickness inside the contact during the relative motion. During sliding conditions, the film is enhanced by the introduction of the lubricant into the contact, while it is generally known that the adsorbed layer is thinner compared to film thickness under dynamic (rolling/sliding) conditions [29].

The UHMWPE plate surface was also analysed using Fourier Transform Infrared (FT-IR) microscope (ThermoScientific Nicolet iN10 MX FT-IR) equipped with germanium attenuated total reflectance (ATR) objective to characterise the secondary structure of adsorbed protein molecules. FT-IR spectrum with the wavenumber ranged from 1200 cm^{-1} to 2000 cm^{-1} and the resolution of 4 cm^{-1} was obtained from 3 to 5 points in the central area of sliding path formed on the polyethylene surface. For all measurements, the aperture size and the cumulative number was set to 150 $\mu\text{m} \times 150 \mu\text{m}$ and 64, respectively.

3. Results

3.1. Coefficient of Friction

Initially, CoF was evaluated employing the reciprocating test described above. Fig. 2 shows the results of friction measurements for 0.7 wt% albumin solution. The transition of CoF during the three following cycles since 1 000th cycle is displayed in Fig. 2a. For each reciprocating cycle, several data points were extracted from the steady region of both forward and reverse strokes and the average CoF was calculated. The average CoF against time is plotted in Fig. 2b. As can be seen in Fig. 2b, at the beginning of the experiment, a certain running-in period was observed and CoF varies for the three iterated tests. After few hundreds of cycles, friction is stabilized and is kept almost constant until the end of the experiment. The difference among three experiments became small after the stabilization of friction coefficient. For the purposes of latter analyses, CoF was averaged between the strokes 600 and 1800. As is apparent from the both figures that very good reproducibility of the data could be obtained.

Fig. 3a shows the friction results of all the tested model fluids at lower speed equal to 10 mm/s. As can be seen, protein-free PBS exhibits

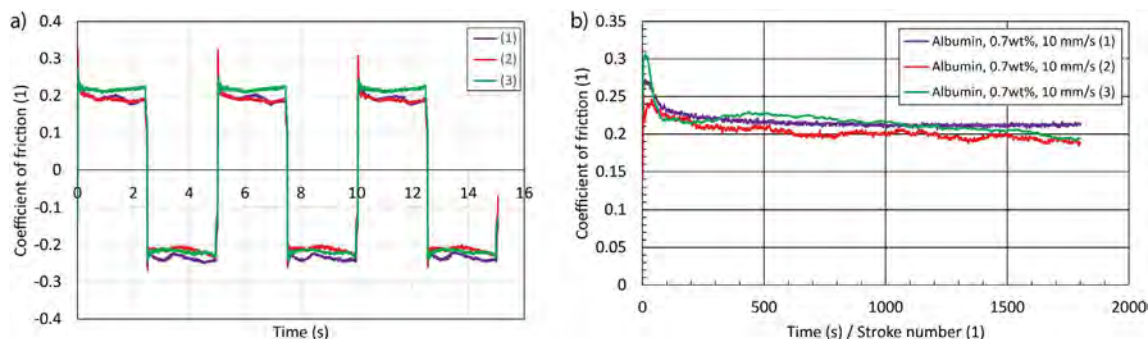


Fig. 2. a) The transition of CoF during the three following cycles since 1 000th cycle of three iterated tests for 0.7 wt% albumin solution. b) Time Evolution of average CoF calculated from steady region of both forward and reverse strokes.

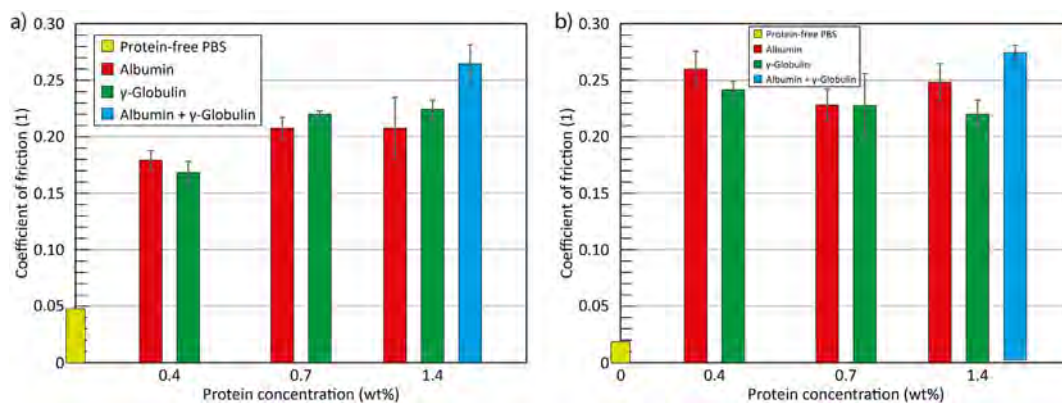


Fig. 3. The results of CoF plotted against protein concentration for all the tested protein solutions at sliding speeds equal to 10 mm/s (a) and 50 mm/s (b). Each bar indicates the average value of three iterated experiments and the error bar indicates standard deviation.

very low friction, which is less than 0.05. Considering the protein solutions, adding the proteins led to a rapid increase of friction. In terms of individual proteins, CoF seems to slightly increase with the protein concentration, especially in the case of γ -globulin. At higher concentrations, γ -globulin exhibits bit higher friction compared to albumin. Independently of the employed lubricant and protein concentration, friction is kept between 0.17 and 0.23 without any significant variance. The mixture of the proteins showed the highest friction reaching up to 0.27.

An increase of sliding speed to 50 mm/s led to an increase of CoF, in general, as can be seen in Fig. 3b. Protein concentration as well as the type of the protein seems to be not so substantial in this case, while the friction varies from 0.22 for 1.4 wt% γ -globulin solution to 0.26 for 0.4 wt% albumin solution. What is in a good correlation with the lower speed is that very low friction (around 0.02) could be observed for pure PBS. Mixture of the proteins exhibits the highest friction again; however, it should be noted that the difference against the simple protein solutions is not so substantial. Moreover, an increase of speed did not cause any CoF change for the mixed lubricant, it was still around 0.27.

3.2. Adsorbed Film Thickness

After the friction test, adsorbed protein film thickness was evaluated using ellipsometry method. It is evident from Fig. 4a that at low sliding speed, the thickness of albumin adsorbed layer is not dependent on the total protein concentration. The film thickness reaches around 32 to 38 nm. However, different behaviour is exhibited by γ -globulin, the layer of which continuously increased with concentration from 20 to 47 nm. The thickest layer was formed when the mixture of the both proteins was investigated. In that case, the film reached almost 60 nm.

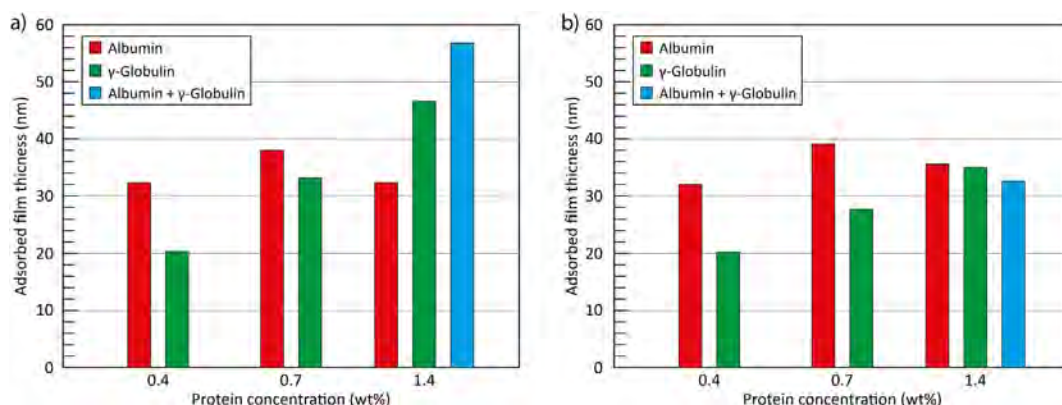


Fig. 4. The results of adsorbed film thickness plotted against protein concentration for all the tested protein solutions at sliding speeds equal to 10 mm/s (a) and 50 mm/s (b).

When comparing the two sliding speeds it can be concluded that the impact of kinematic conditions on adsorbed albumin film thickness is limited, see Fig. 4a vs. Fig. 4b, since the results at 50 mm/s very well correspond to those at 10 mm/s. Considering the γ -globulin solution, an increasing tendency can be identified; however, compared to lower speed, the thickness for 0.7 and 1.4 wt% protein concentrations decreased to 27 and 35 nm, respectively. What is in discrepancy with the lower speed results is the fact that the mixed solution does not exhibit the thickest film; actually, it is very similar to simple protein solutions of the corresponding concentration.

3.3. Relationship Between Evolution of Adsorbed Protein Film and Friction Coefficient

Finally, we plotted the results of CoF against the adsorbed film thickness. It can be seen from Fig. 5a that at lower sliding speed, there is a linear correlation between CoF and layer thickness for both albumin and γ -globulin protein solutions. In that case, albumin and γ -globulin showed the similar behaviour so all the results were on the identical regression line. Therefore, it can be assumed that the evolution of adsorbed film is associated with the increase of friction between the surfaces. Despite the limited amount of data, statistical evaluation of the CoF-adsorbed thickness dependence was performed as well. Statistical parameters for all protein solutions were as follows: $R\text{-squared}_{10} = 0.845$, $p\text{-value}_{10} = 0.054$. Considering the significance level $\alpha = 0.1$, it can be concluded that the correlation is statistically significant at low speed conditions. At higher speed (Fig. 5b) the behaviour is completely opposite, showing that an increase of the protein film is accompanied by the decrease of friction. In addition, albumin and γ -globulin showed different tendency and a different regression line was fitted to each protein. This indicates that the

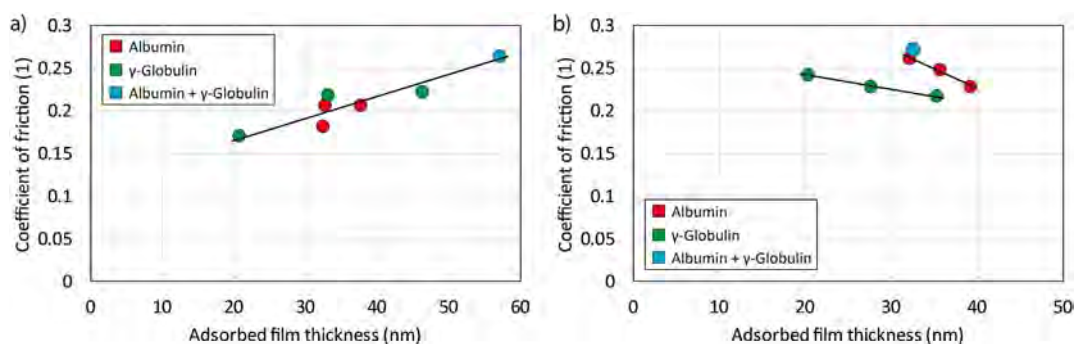


Fig. 5. The results of CoF plotted against adsorbed film thickness for all the tested protein solutions at sliding speeds equal to 10 mm/s (a) and 50 mm/s (b).

kinematic conditions play a key role in film forming process, possibly due to conformational changes of the proteins. Under 50 mm/s, following statistical descriptors were obtained: $R\text{-squared}_{\text{alb50}} = 0.993$, $p\text{-value}_{\text{alb50}} = 0.053$, $R\text{-squared}_{\text{glob50}} = 0.996$, $p\text{-value}_{\text{glob50}} = 0.038$. Comparing the p -values with the significance level α , it can be seen that the regressions for both the protein solutions are statistically significant.

3.4. FT-IR Analysis

Representative surface images obtained by the FT-IR microscope prior to the IR measurement are shown in Fig. 6. The red square in the centre of images indicates the aperture from which the IR spectrum was obtained. The morphological characteristics of polyethylene surface in the sliding path depended on both the type of the lubricant and the sliding speed. Under the low sliding speed, polyethylene surfaces exhibited clear tracks in the direction of sliding for all the lubricants (Fig. 6a, b and c). The tracks clearly evidence limited lubricating film formation between the pin and the plate. Only in the case of γ -globulin solution, there are visible aggregations of protein molecules attached on the polyethylene surface and elongated in the sliding direction (Fig. 6b). At higher sliding speed of 50 mm/s, abrasive

tracks on the polyethylene surface became unclear, see Fig. 6d, e and f. Instead, small and particulate protein aggregates adsorbed on UHMWPE appeared in the surface image for all the test lubricants. Clear difference in the size of protein aggregations can be found between albumin and γ -globulin: γ -globulin left larger protein aggregates compared to albumin.

FT-IR spectra obtained from the sliding tracks formed on the plate surfaces are compared in Fig. 7. For all the spectra, IR intensity was normalized by the peak intensity at 1460 cm^{-1} attributed to C–H bending vibration of polyethylene chain. In this figure, the attention is focused on the IR spectrum ranged from 1500 cm^{-1} to 1800 cm^{-1} including amide I band (1600 cm^{-1} to 1700 cm^{-1}). Amide I band of IR spectra is sensitive to secondary structure of proteins and has been widely used to examine folding and unfolding of protein molecules [30–36]. It contains IR peaks corresponding to representative secondary structures of proteins, such as α -helices (1654 cm^{-1}) and β -sheet ($1633\text{--}1639\text{ cm}^{-1}$) [30,31,34,36].

Sliding tracks lubricated with the albumin solution and the mixture of albumin and γ -globulin showed similar results of the IR measurement. Under the low sliding speed, the intensity of IR spectra within amide I band was quite weak, irrespective of protein concentration and only a broad peak centered at 1650 cm^{-1} could be recognized (Fig. 7a,

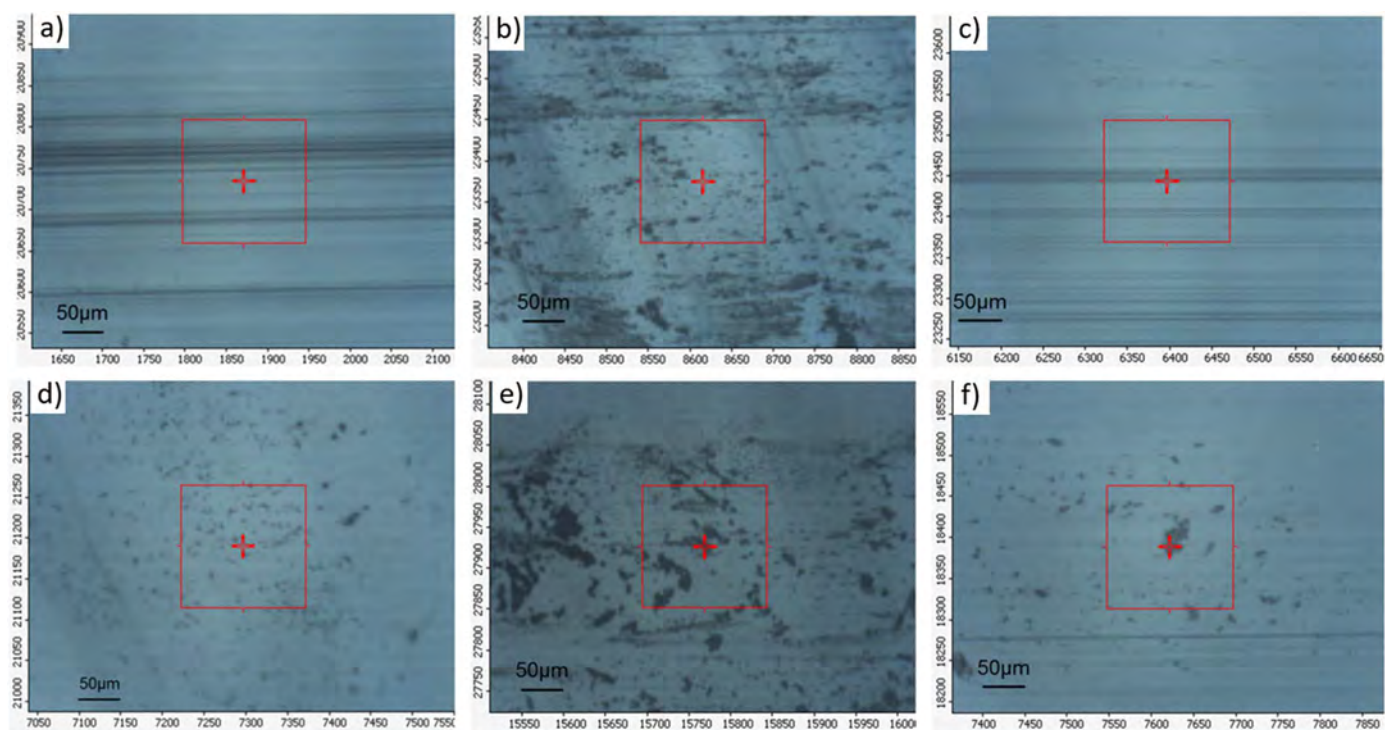


Fig. 6. FT-IR images of the contact drag on UHMWPE surface for the tested lubricants with the protein concentration of 1.4 wt%. a) albumin, 10 mm/s, b) γ -globulin, 10 mm/s, c) albumin + γ -globulin, 10 mm/s, d) albumin, 50 mm/s, e) γ -globulin, 50 mm/s, f) albumin + γ -globulin, 50 mm/s.

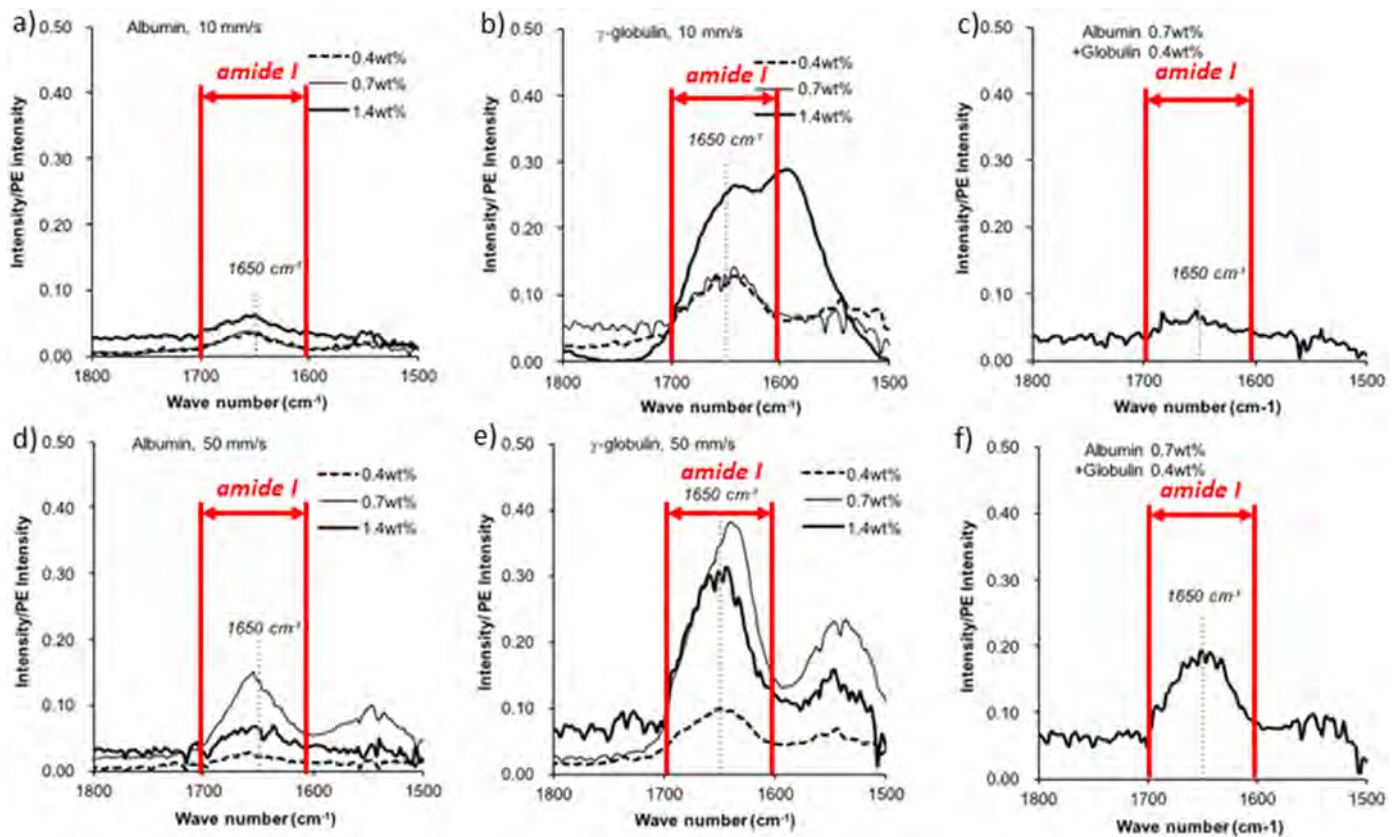


Fig. 7. FT-IR spectra corresponding to the images displayed in Fig. 6. a) albumin, 10 mm/s, b) γ -globulin, 10 mm/s, c) albumin + γ -globulin, 10 mm/s, d) albumin, 50 mm/s, e) γ -globulin, 50 mm/s, f) albumin + γ -globulin, 50 mm/s.

c). As the sliding speed increased, the peak in amide I band became significant. The peak intensity varied with the protein concentration and the center of peak slightly shifted to higher wave number in the case of albumin 0.7 wt% solution (Fig. 7d, f). IR spectra for γ -globulin have relatively clear amide I peak regardless of the sliding speed (Fig. 7b, e). They also have a broadened amide I peak around 1650 cm^{-1} under low sliding speed. However, the peak was severely distorted and another peak appeared at lower wave number if the γ -globulin concentration increased to 1.4 wt% (Fig. 7b). Under the high sliding speed, amide I peak became sharp by increasing the γ -globulin concentration and the centre of peak shifted to lower wave number (Fig. 7e).

4. Discussion

Since the wear debris-induced osteolysis was recognized as a major risk factor limiting service life of joint prostheses, a large number of studies have been conducted to gain the knowledge about the *in vivo* wear mechanisms of UHMWPE used in artificial joints [4–7,11,12,37]. Among these studies, several researchers have pointed out that the biological macromolecules contained in synovial fluid should be playing a critical role deciding *in vivo* friction and wear behaviour. Some *ex vivo* studies suggested that there were certain interactions between implanted UHMWPE and synovial constituents, such as proteins and lipids [37–40]. Especially, well-organized surface analyses of retrieved UHMWPE acetabular cups revealed that the polyethylene surface was fully covered with adsorbed proteins during implantation [39,40]. Effects of proteins were experimentally confirmed by a number of researches for wear of UHMWPE [4–6,11,12] and friction between metal/UHMWPE [11,41] or ceramic/UHMWPE [9,11,41]. However, there are still some uncertainties about how proteins behave between sliding surfaces and how do they affect friction and wear.

In this study, we just focused on the friction exerted between UHMWPE and CoCrMo alloy and examined the effect of two different types of serum proteins, albumin and γ -globulin, added to the lubricant applying the reciprocating sliding test. After the sliding test, details of adsorbed protein film formed on the polyethylene surface were analysed by using spectroscopic ellipsometry and FT-IR, since the former method was frequently used to evaluate the thickness of adsorbed protein film [42,43] and the latter one is known as a preferable tool for examining secondary structure changes of proteins [30–36]. We intended to use these data to understand how proteins affect the friction.

Our experimental results indicate that proteins contained in synovial fluid substantially increase friction between metal and UHMWPE components of joint prosthesis. CoF in all protein solutions was significantly higher than that in protein-free PBS, while the results for saline solution are in a good correlation with the data published elsewhere [44,45]. A rapid increase of friction when considering albumin solution compared to PBS was introduced also by Crockett et al. [13]. The effect of proteins depended not only on the type and concentration of the proteins contained in the test lubricant but also on the relative speed between the CoCrMo pin and UHMWPE plate.

In the present study, it was observed that the CoF slightly increased with increasing sliding speed, while similar behaviour was already reported by Chen et al. [46]. The sliding speed is one of the predominant factors determining the lubricating film formation between relatively moving surfaces and the fluid film thickness is limited at low sliding speed. Larger fraction of the load is supported by the solid contact, as the contribution of fluid film decreases, thus causing the contact conditions in the real contact area to be more severe.

Under such low sliding speed conditions, a clear correlation could be found between friction coefficient and the thickness of the adsorbed protein film formed on UHMWPE plate. It means that proteins adsorbed

on polyethylene surface have a predominant effect on the friction between UHMWPE and CoCrMo considering these sliding conditions. IR spectra obtained from adsorbed proteins had a broad peak centered at 1650 cm^{-1} in amide I region regardless of the type and concentration of the proteins. Non-denatured albumin and γ -globulin have a characteristic secondary structure, α -helix for albumin and β -sheet for γ -globulin, and show a corresponding IR peak in amide I region near to 1654 cm^{-1} and 1638 cm^{-1} , respectively [31,35,36]. Sagner et al. [35,36] demonstrated that the intensity of these peaks decreased gradually as proteins are denatured and finally both albumin and γ -globulin show a broad peak around 1650 cm^{-1} . Barth [34] also pointed out that the featureless amide I band centered at 1650 cm^{-1} is a characteristics of IR spectra obtained from unfolded proteins. Therefore, results of our IR measurements are indicating that protein molecules adsorbed on the polyethylene surface were denatured and lost their original secondary structures under the low sliding speed conditions. The denaturation of albumin, caused by the sliding between CoCrMo and UHMWPE, was also reported by Mishina and Kojima [41]. As suggested by Heuberger et al. [9], denatured and unfolded proteins preferentially adsorb on hydrophobic polyethylene surface and increase friction between the sliding surfaces. Protein film thickness obtained by the ellipsometry ranged from 20 to 60 nm under sliding speed of 10 mm/s. These values are still much smaller than the initial surface roughness of UHMWPE plate (around 100 nm). Also, the spot size of ellipsometry was relatively large, 3 mm in diameter. Therefore, actual protein adsorption would be inhomogeneous in the spot area and the obtained value is the average within it. The adsorbed proteins might fill the gap between polyethylene asperities like schematically indicated in Fig. 8a. The larger fraction of real contact area was therefore covered by denatured proteins as amount of adsorbed proteins increased. Consequently, the friction exerted between the surfaces linearly increased with the measured thickness of adsorbed protein film. In this case, albumin and γ -globulin already lost their characteristic secondary structures and showed almost identical results.

As the sliding speed increased, the fluid film formation was enhanced and more protein molecules might be entrained into the contact zone with buffer solution. At the same time, the shear conditions between the two surfaces would become milder with mitigated solid-solid contact. In this case, the peak in amide I band of albumin slightly shifted to higher wave number (Fig. 7d). It is probably because a fraction of α -helices, those corresponding IR peak appears at 1654 cm^{-1} , still remains in albumin molecules. Similarly, the amide I peak of γ -globulin shifted to lower wave number as they kept some β -sheet structure, those corresponding IR peak position was at $1633\text{--}1639\text{ cm}^{-1}$. From these results, the adsorbed protein film formed under the high sliding speed conditions presumably consisted of both highly denatured proteins and partially or non-denatured proteins, as schematically indicated in Fig. 8b. If protein molecules sustained their secondary structure to some extent, the adsorption to the polyethylene surface was relatively weak compared to highly denatured proteins and certain fraction of adsorbed proteins might be washed out during rinsing the plate by the running water. As a result, the adsorbed protein film thickness evaluated by the ellipsometry became thinner compared to low sliding speed conditions and lost its correlation with the measured CoF. Also, two types of serum proteins exhibited different relationships between CoF and adsorbed protein film thickness since they still have different secondary structure (Fig. 5b). Even the proteins

kept their secondary structure, the friction between UHMWPE and CoCrMo alloy increased due to protein molecules entraining the contact zone.

The results of adsorbed film thickness were compared with the theoretical prediction of film thickness given by Hooke [47]. Nevertheless, it must be noted that the predicted values are strongly dependent on the applied lubricant viscosity. As the viscosity was not measured, it was considered as 0.002 Pa·s which should correspond to 25% bovine serum often used as the model of synovial fluid [48]. Calculated film thickness is approximately 29 nm in the case of 10 mm/s and around 76 nm at higher speed of 50 mm/s. Confronting the theoretical and experimental data, it is apparent that the action of fluid film is limited at lower sliding speed. However, an increase of speed substantially enhances fluid film. The conformational changes and molecules interaction may play an important role as well.

Obviously, the authors admit some limitations of the performed study. First of all, the employed test lubricants do not entirely correspond to human synovial fluid which contains other constituents like hyaluronic acid and phospholipids [27]. Similarly, the applied concentration is bit smaller compared to physiological state. As it is expected that hyaluronic acid and phospholipids can substantially influence the lubrication mechanisms [11,12], deeper investigation considering more complex model fluids is necessary. However, the present paper profits from the finding the interaction between tribological performance and the structure of the molecules.

Another limitation would be the temperature setting of the sliding test. All the tests were carried out under ambient temperature of $25\text{ }^{\circ}\text{C}$ which is apparently lower than that in human body. However, the difference between the ambient and body temperature is just around $12\text{ }^{\circ}\text{C}$. This difference is too small to influence the conformational changes. Sagner et al. [36] reported that the denaturation of proteins starts to be evident at $40\text{ }^{\circ}\text{C}$. Moreover, it was proved in literature that there is no effect of elevated temperature on protein film formation [18].

Our protein film analyses exhibit also certain limitations. UHMWPE plates were rinsed with running pure water and air-dried before the measurement of protein film thickness and FT-IR analysis. In this case, only protein molecules firmly adsorbed on the polyethylene surface were taken into account and contribution of loosely adsorbed molecules might be excluded from the measured film thickness and obtained IR spectra. In addition, there should be some effects of drying on the data. The results of experiments at high sliding speed might be more susceptible to these limitations. FT-IR analyses indicated that certain fraction of adsorbed proteins still kept their original structure and their adsorption to the polyethylene surface was relatively weak compared to significantly denatured proteins under low sliding speed. The spatial resolution in the case of ellipsometry and FT-IR would be another limitation of our analyses. The film thickness data and IR spectra were obtained from the circular area of the diameter of 3 mm and the $150\text{ }\mu\text{m} \times 150\text{ }\mu\text{m}$ square area, respectively. Those aperture sizes might be too large to identify the spatial variation of adsorbed protein film in micron scale, for example due to formation of protein aggregates. Consequently, some significant changes captured by the optical microscopy could not be recognized in results of the ellipsometry and FT-IR analysis.

The main drawback of the experimental setup might be that the non-conformal pin-on-plate contact was studied; however, human

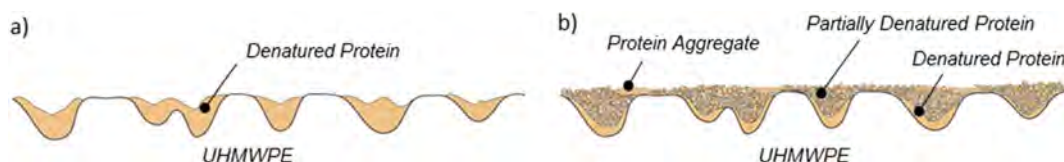


Fig. 8. Schematic illustration of the real contact area consisted of polyethylene asperities and adsorbed proteins. At low sliding speed, most of the proteins were denatured (a). At high sliding speed, some fraction of adsorbed proteins still keep their secondary structure and some proteins form aggregates (b).

joints are highly conformal. It was recently proved in our previous papers that the conformity influences the formation of lubricant film in hard-on-hard bearing pairs [21,48]. Therefore, it is expected that the tribological processes might be affected even in the case of hard-on-soft couples, which were investigated in the present paper.

5. Conclusion

The present study dealt with the evaluation of CoF between CoCrMo pin and UHMWPE plate, while the effects of kinematic conditions and proteins contained in the test lubricants were examined. Moreover, the adsorbed protein film thickness on the plate surface was evaluated. To be able to better explain the lubrication mechanisms, FT-IR spectroscopy was employed as well. The findings coming from the performed analysis can be summarized into the following points:

- Protein-free PBS exhibits the lowest friction, while adding the proteins causes a rapid increase of friction indicating the importance of proteins regarding to lubrication mechanisms of metal/UHMWPE sliding pair.
- CoF is dependent on both, protein concentration as well as the kinematic conditions.
- FT-IR results indicate that there is a certain effect of the kinematic conditions on the structure of the protein molecules adsorbed on the UHMWPE surface, apparently influencing the frictional behaviour of the contact couple.
- At low sliding speed of 10 mm/s, the adsorbed proteins denature, losing their original structure; therefore, the friction is substantially influenced by the total protein concentration and adsorbed film thickness.
- At high sliding speed of 50 mm/s, the adsorbed molecules keep their native structure, indicating that the frictional behaviour is influenced by the type of the protein and its concentration.

Acknowledgement

The research was supported by the project no. FSI-S-14-2336 with the financial support from the Ministry of Education, Youth and Sports of the Czech Republic. The part of this study was also supported by Grant-in-Aid for Specially Promoted Research (23000011) and Grant-in-Aid for Scientific Research (B) of Japan Society for the Promotion of Science (23360076). Authors would like to thank S. Onitsuka for supporting our FT-IR measurement.

References

- [1] A.B. Joshi, M.L. Porter, I.A. Trail, L.P. Hunt, J.C. Murphy, K. Hardinge, Long-term results of Charnley low-friction arthroplasty in young patients, *J. Bone Joint Surg. Br. Vol. 75 (4)* (1993) 616–623.
- [2] D. Dowson, New joints for the Millennium: wear control in total replacement hip joints, *Proc. Inst. Mech. Eng. H J. Eng. Med.* 215 (2001) 335–358.
- [3] A. Unsworth, Recent developments in the tribology of artificial joints, *Tribol. Int.* 28 (1995) 485–495.
- [4] A. Wang, A. Essner, V.K. Polineni, C. Stark, J.H. Dumbleton, Lubrication and wear of ultra-high molecular weight polyethylene in total joint replacements, *Tribol. Int.* 31 (1998) 17–33.
- [5] A. Wang, A. Essner, G. Schmidig, The effects of lubricant composition on in vitro wear testing of polymeric acetabular components, *J. Biomed. Mater. Res.* 68B (2004) 45–52.
- [6] V. Saikko, Effect of lubricant protein concentration on the wear of ultra-high molecular weight polyethylene sliding against a CoCr counterface, *J. Tribol.* 125 (2003) 638–642.
- [7] M. Ranuša, J. Gallo, M. Vrbka, M. Hobza, D. Paloušek, I. Křupka, M. Hartl, Wear analysis of extracted polyethylene acetabular cups using a 3D optical scanner, *Tribol. Trans.* (2016) 1–11.
- [8] M.R. Widmer, M. Heuberger, J. Vörös, N.D. Spencer, Influence of polymer surface chemistry on frictional properties under protein-lubrication conditions: implications for hip-implant design, *Tribol. Lett.* 10 (2001) 111–116.
- [9] M.P. Heuberger, M.R. Widmer, E. Zobeley, R. Glockshuber, N.D. Spencer, Protein-mediated boundary lubrication in arthroplasty, *Biomaterials* 26 (2005) 1165–1173.
- [10] A.P. Serro, M.P. Gispert, M.C.L. Martins, P. Brogueira, R. Colaço, B. Saramago, Adsorption of albumin on prosthetic materials: implication for tribological behavior, *J. Biomed. Mater. Res. A* 78A (2006) 581–589.
- [11] Y. Sawae, T. Murakami, J. Chen, Effect of synovia constituents on friction and wear of ultra-high molecular weight polyethylene sliding against prosthetic joint materials, *Wear* 216 (1998) 213–219.
- [12] Y. Sawae, A. Yamamoto, T. Murakami, Influence of protein and lipid concentration of the test lubricant on the wear of ultra high molecular weight polyethylene, *Tribol. Int.* 41 (2008) 648–656.
- [13] R. Crockett, M. Roba, M. Naka, B. Gasser, D. Delfosse, V. Frauchiger, et al., Friction, lubrication, and polymer transfer between UHMWPE and CoCrMo hip-implant materials: a fluorescence microscopy study, *J. Biomed. Mater. Res. A* 89A (2009) 1011–1018.
- [14] D. Nečas, M. Vrbka, F. Urban, I. Křupka, M. Hartl, The effect of lubricant constituents on lubrication mechanisms in hip joint replacements, *J. Mech. Behav. Biomed. Mater.* 55 (2016) 295–307.
- [15] M. Vrbka, D. Nečas, J. Bartošik, M. Hartl, I. Křupka, A. Galandáková, J. Gallo, Determination of a friction coefficient for THA bearing couples, *Acta Chir. Orthop. Traumatol. Českoslov.* 82 (2015) 341–347.
- [16] D. Dowson, C.M. McNie, A.A.J. Goldsmith, Direct experimental evidence of lubrication in a metal-on-metal total hip replacement tested in a joint simulator, *Proc. Inst. Mech. Eng. C J. Mech. Eng. Sci.* 214 (2000) 75–86.
- [17] S.L. Smith, D. Dowson, A.A.J. Goldsmith, R. Valizadeh, J.S. Colligon, Direct evidence of lubrication in ceramic-on-ceramic total hip replacements, *Proc. Inst. Mech. Eng. Part C* 215 (2001-1-1) 265–268.
- [18] A. Mavraki, P.M. Cann, Lubricating film thickness measurements with bovine serum, *Tribol. Int.* 44 (2011) 550–556.
- [19] M. Vrbka, T. Navrat, I. Krupka, M. Hartl, P. Sperka, J. Gallo, Study of film formation in bovine serum lubricated contacts under rolling/sliding conditions, *Proc. Inst. Mech. Eng. Part J* 227 (2013) 459–475.
- [20] M. Vrbka, I. Krupka, M. Hartl, T. Navrat, J. Gallo, A. Galandakova, In situ measurements of thin films in bovine serum lubricated contacts using optical interferometry, *Proc. Inst. Mech. Eng. H J. Eng. Med.* 228 (2014) 149–158.
- [21] M. Vrbka, D. Nečas, M. Hartl, I. Křupka, F. Urban, J. Gallo, Visualization of lubricating films between artificial head and cup with respect to real geometry, *Biotribology* 1–2 (2015) 61–65.
- [22] D. Nečas, M. Vrbka, I. Křupka, M. Hartl, A. Galandáková, Lubrication within hip replacements – implication for ceramic-on-hard bearing couples, *J. Mech. Behav. Biomed. Mater.* 61 (2016) 371–383.
- [23] M. Parkes, C. Myant, P.M. Cann, J.S.S. Wong, The effect of buffer solution choice on protein adsorption and lubrication, *Tribol. Int.* 72 (2014) 108–117.
- [24] M. Parkes, C. Myant, P.M. Cann, J.S.S. Wong, Synovial fluid lubrication: the effect of protein interactions on adsorbed and lubricating films, *Biotribology* 1-2 (2015) 51–60.
- [25] S.C. Scholes, A. Unsworth, The effects of proteins on the friction and lubrication of artificial joints, *Proc. Inst. Mech. Eng. Part H* 220 (2006) 687–693.
- [26] C. Myant, R. Underwood, J. Fan, P.M. Cann, Lubrication of metal-on-metal hip joints: the effect of protein content and load on film formation and wear, *J. Mech. Behav. Biomed. Mater.* 6 (2012) 30–40.
- [27] A. Galandáková, J. Ulrichová, K. Langová, A. Hanáková, M. Vrbka, M. Hartl, et al., Characteristics of synovial fluid required for optimization of lubrication fluid for biotribological experiments, *J. Biomed. Mater. Res. Part B* (2016).
- [28] K. Nakashima, Y. Sawae, T. Murakami, Effect of conformational changes and differences of proteins on frictional properties of poly(vinyl alcohol) hydrogel, *Tribol. Int.* 40 (2007) 1423–1427.
- [29] J. Fan, C.W. Myant, R. Underwood, P.M. Cann, A. Hart, Inlet protein aggregation: a new mechanism for lubricating film formation with model synovial fluids, *Proc. Inst. Mech. Eng. Part H* 225 (2011) 696–709.
- [30] D.M. Byler, H. Susi, Examination of the secondary structure of proteins by deconvolved FTIR spectra, *Biopolymers* 25 (1986) 469–487.
- [31] F.M. Wasacz, J.M. Olinger, R.J. Jakobsens, Fourier Transform infrared studies of proteins using nonaqueous solvents. Effects of methanol and ethylene glycol on albumin and immunoglobulin G, *Biochemistry* 26 (1987) 1464–1470.
- [32] A. Barth, C. Zscherp, What vibrations tell us about proteins, *Q. Rev. Biophys.* 35 (2002) 369–430.
- [33] K. Murayama, M. Tomida, Heat-induced secondary structure and conformation change of bovine serum albumin investigated by Fourier Transform Infrared Spectroscopy, *Biochemistry* 43 (2004) 11526–11532.
- [34] A. Barth, Infrared spectroscopy of proteins, *Biochim. Biophys. Acta* 1767 (2007) 1073–1101.
- [35] E. Saguier, P. Alvarez, A.A. Ismail, Heat-induced denaturation/aggregation of porcine plasma and its fractions studied by FTIR spectroscopy, *Food Hydrocoll.* 27 (2012) 208–219.
- [36] E. Saguier, P.A. Alvarez, J. Sedman, A.A. Ismail, Study of the denaturation/aggregation behaviour of whole porcine plasma and its protein fractions during heating under acidic pH by variable-temperature FTIR spectroscopy, *Food Hydrocoll.* 33 (2013) 402–414.
- [37] L. Ambrosio, G. Carotenuto, G. Marletta, L. Nicolais, A. Scandurra, Wear effects in retrieved acetabular UHMW-PE cups, *J. Mater. Sci. Mater. Med.* 7 (1996) 723–729.
- [38] P. Eyerer, Y.C. Ke, Property changes of UHMW polyethylene hip cup endoprostheses during implantation, *J. Biomed. Mater. Res.* 18 (1984) 1137–1151.
- [39] S.P. James, S. Blazka, E.W. Merrill, M. Jasty, K.R. Lee, G.R. Bragdon, Challenge to the concept that UHMWPE acetabular components oxidize in vivo, *Biomaterials* 14 (1993) 643–647.
- [40] L. Costa, M.P. Luda, L. Trossarelli, E.M. Brach del Prever, M. Crova, P. Gallinaro, In vivo UHMWPE biodegradation of retrieved prosthesis, *Biomaterials* 19 (1998) 1371–1385.

- [41] H. Mishina, M. Kojima, Changes in human serum albumin on arthroplasty frictional surfaces, *Wear* 265 (2008) 655–663.
- [42] H. Elwing, Protein absorption and ellipsometry in biomaterial research, *Biomaterials* 19 (1998) 397–406.
- [43] A.P. Carapeto, A.P. Serro, B.M.F. Nunes, M.C.L. Martins, S. Todorovic, M.T. Duarte, V. André, R. Colaço, B. Saramago, Characterization of two DLC coatings for joint prosthesis: the role of albumin on the tribological behaviour, *Surf. Coat. Technol.* 204 (2010) 3451–3458.
- [44] M.P. Gispert, A.P. Serro, R. Colaço, B. Saramago, Friction and wear mechanisms in hip prosthesis: comparison of joint materials behaviour in several lubricants, *Wear* 260 (2006) 149–158.
- [45] M. Guezmil, W. Bensalah, S. Mezlini, Tribological behavior of UHMWPE against TiAl6V4 and CoCr28Mo alloys under dry and lubricated conditions, *J. Mech. Behav. Biomed. Mater.* 63 (2016) 375–385.
- [46] X.M. Chen, Z.M. Jin, J. Fisher, Effect of albumin adsorption on friction between artificial joint materials, *Proc. Inst. Mech. Eng. Part J* 222 (2008-5-1) 513–521.
- [47] C.J. Hooke, The elastohydrodynamic lubrication of heavily loaded point contacts, *J. Mech. Eng. Sci.* 22 (4) (1980) 183–187.
- [48] D. Nečas, M. Vrbka, F. Urban, J. Gallo, I. Křupka, M. Hartl, In situ observation of lubricant film formation in THR considering real conformity: the effect of diameter, clearance and material, *J. Mech. Behav. Biomed. Mater.* 69 (2017) 66–74.

Article

The Effect of Kinematic Conditions and Synovial Fluid Composition on the Frictional Behaviour of Materials for Artificial Joints

David Nečas * , Martin Vrbka, Ivan Křupka and Martin Hartl

Faculty of Mechanical Engineering, Institute of Machine and Industrial Design, Brno University of Technology, Technická 2896/2, 616 69 Brno, Czech Republic; martin.vrbka@vut.cz (M.V.); krupka@fme.vutbr.cz (I.K.); martin.hartl@vut.cz (M.H.)

* Correspondence: david.necas@vut.cz; Tel.: +420-541-143-239

Received: 23 April 2018; Accepted: 8 May 2018; Published: 10 May 2018



Abstract: The paper introduces an experimental investigation of frictional behaviour of materials used for joint replacements. The measurements were performed using a ball-on-disc tribometer, while four material combinations were tested; metal-on-metal, ceramic-on-ceramic, metal-on-polyethylene, and ceramic-on-polyethylene, respectively. The contact was lubricated by pure saline and various protein solutions. The experiments were realized at two mean speeds equal to 5.7 mm/s and 22 mm/s and two slide-to-roll ratios, -150% and 150% . It was found that the implant material is the fundamental parameter affecting friction. In general, the metal pair exhibited approximately two times higher friction compared to the ceramic. In particular, the friction in the case of the metal varied between 0.3 and 0.6 while the ceramic pair exhibited friction within the range from 0.15 to 0.3 at the end of the test. The lowest friction was observed for polyethylene while it decreased to 0.05 under some conditions. It can be also concluded that adding proteins to the lubricant has a positive impact on friction in the case of hard-on-hard pairs. For hard-on-soft pairs, no substantial influence of proteins was observed. The effect of kinematic conditions was found to be negligible in most cases.

Keywords: joint replacement; friction; material; proteins; kinematic conditions

1. Introduction

Total joint arthroplasty is an efficient and well-established surgical procedure improving the life of patients suffering from joint diseases. According to the Health at a Glance 2015 report [1], 161 operations per 100,000 inhabitants were performed in Organisation for Economic Co-operation and Development (OECD) countries in 2013. However, despite the rapid improvement of the implanted materials in the last few decades [2], limited longevity is still recognized as the main drawback of the replacements. It should be highlighted that failure of the implant is accompanied by the need for a revising operation, which is an economic burden and substantially deteriorates the comfort of the patient. As the number of young active people with artificial joints still increases [3], it is necessary to ensure a sufficient service-life of implants to avoid any inconvenience associated with its improper function. Since the main cause of the failure is osteolysis [4] followed by aseptic loosening, the tribological performance of implants has to be understood in the context of the further development of replacements.

Several aspects have to be taken into account considering tribological processes within artificial joint contact. Mavraki and Cann [5] employed a ball-on-disc configuration when evaluating the coefficient of friction (CoF) as a function of mean speed. Metal-on-metal contact was investigated, while several test lubricants were tested. In general, CoF was kept between 0.1 and 0.4 while the test

fluid had a significant impact on results. It was found that bovine serum (BS) and simple protein solutions lead to a reduction of friction in a slow-speed regime. It was also highlighted that the choice of buffer solution affects the lubrication conditions. Finally, it was concluded that friction as well as lubricating film thickness are time and sliding-distance dependent, indicating the importance of the adsorbed protein layer on the surfaces.

One of the first studies which was focused on the influence of lubricant composition on friction between polymer and metal surface was undertaken by Yao et al. [6]. A pin-on-disk tribometer was used for the evaluation of CoF, while various test fluids were used as the lubricants; particularly deionized water, diluted (25%, 50%, 75%) and undiluted bovine calf serum (BCS), bovine synovial fluid (SF) and human periprosthetic SF. A significant variance of CoF results was observed, attributed mainly to the substantial changes of protein concentrations and rheological properties of the fluids. The lowest friction (≈ 0.013) was exhibited by human SF followed by deionized water. Remarkably, higher friction was detected for bovine SF and undiluted BCS (≈ 0.024). The highest CoF was detected for 25% BCS, which was around 0.028. Scholes and Unsworth [7] demonstrated the importance of lubricant composition in relation to the material combination of the implants. The authors tested various model fluids finding that the highest friction can be detected in the case of metal-metal implants. No significant difference between the ceramic-ceramic and metal-polyethylene pair was observed. Although there was a rapid influence of the model fluid on the CoF, the effect of proteins could not be generalized, since both decrease and increase of friction could be observed dependent on implant material. The role of individual constituents contained in SF was demonstrated by Sawae et al. [8]. The contact between an ultra-high molecular weight polyethylene (UHMWPE) pin sliding against metal/ceramic disc was studied, while a clear positive effect of hyaluronic acid added to saline solution on friction was detected.

Moreover, it was well reported that the frictional behaviour of the contact pair is substantially influenced by the surface conditions. Widmer et al. [9], investigated the ceramic-polyethylene sliding pair, finding that the oxygen-plasma based treatment of polyethylene (PE) led to improved abilities of protein adsorption onto rubbing surfaces, thus reducing both static and dynamic friction. Subsequently, it was pointed out that conformational changes have to be taken into account [10]. The authors showed that hydrophilic nature of the surfaces supports adsorption of the proteins in a native state, forming thicker lubricating film leading to lower friction between the components. An extensive investigation of the effect of model fluid composition on CoF dependent on kinematic conditions was provided in our previous study [11]. Reciprocating pin-on-plate (metal-UHMWPE) test was conducted, showing that the kinematic conditions have a crucial impact on the conformational changes of proteins, thus influencing frictional behaviour of the contact pair. At a slow speed regime (10 mm/s), a very slight increase of friction with increasing protein concentration was observed for both albumin and γ -globulin solution. The highest friction occurred when a mixture of the mentioned proteins was used as the test lubricant. An increase of sliding speed to 50 mm/s caused just a negligible change of friction. Independent of sliding speed, CoF was substantially higher when comparing protein solutions (≈ 0.17 – 0.27) with phosphate-buffered saline (PBS) without any constituents. In that case, friction was lower than 0.05. These results are in good agreement with the observation provided previously [12,13]. In the study mentioned, the effect of albumin undergoing conformational changes on the friction between the UHMWPE pin and stainless steel plate was evaluated. A substantial effect of the applied load on the results was observed; while at low loads, post-friction degraded albumin added to PBS led to a decrease of friction compared to fresh protein. The opposite behaviour occurred at higher loads. Based on the above references [11,12], it can be concluded that friction between the rubbing surfaces is affected by both kinematic and loading conditions.

The effect of replacement geometry has to be taken into account as well. Dowson et al. [14] conducted a predictive numerical analysis of friction and wear for metal-metal implant, finding that the frictional torque increases with increasing nominal diameter; however, it is affected just a little by the initial clearance between the surfaces. An experimental study of the effect of diametric clearance

together with the role of model fluid was undertaken by Brockett et al. [15]. Nominal diameter of the implant was 54.6 mm, while three different clearances were considered; 53 μm , 94 μm , and 194 μm , respectively. The lowest friction factor was detected for the medium size of the clearance. Lowering the clearance led to a negligible increase of friction; however, in the case of the highest clearance, a substantial increase of friction to almost double was detected. Regarding the model fluid, 25% and 100% BS were tested, with the finding that lower friction could be reached in the case of higher protein concentration, in general, which is in a good agreement with one of the previous studies [6]. Finally, an experimental investigation of the friction coefficient using a pendulum hip joint simulator focusing on the effect of implant material and diameter was conducted by Vrbka et al. [16]. This applied 25% BS of a total protein concentration of 22.4 mg/mL, testing 28 mm and 36 mm metal-UHMWPE, ceramic-UHMWPE and ceramic-ceramic pairs. The highest CoF (≈ 0.16) was detected in the case of the metal-UHMWPE pair with no clear effect of nominal diameter. Ceramic-UHMWPE exhibited lower friction (≈ 0.14), while a larger diameter led to a further decrease (≈ 0.13). The lowest friction (0.12) was detected in the ceramic-ceramic pair with the same effect of diameter as in the previous case.

Based on the above references, it is apparent that the tribological behaviour of artificial joints is influenced by several aspects, such as composition of the model SF, implant material, geometry, kinematic and loading conditions. However, most of the authors focused on one particular material combination or specific composition of the test lubricant. Therefore, the aim of the present paper is to provide a detailed analysis of frictional behaviour considering various implant materials, kinematic conditions, and the composition of model synovial fluid. According to the authors' best knowledge, such an extensive investigation has not been performed before.

2. Materials and Methods

The measurements of the CoF were conducted utilizing a commercial ball-on-disc test device Mini Traction Machine (MTM, PCS Instruments, London, United Kingdom). Both the components, the ball and the disc, could be driven independently, thus enabling the application of various kinematic conditions. The mean dynamic (sometimes also called kinetic or sliding) friction coefficient [17] is evaluated based on the ratio of friction and normal force measured by the load cell. CoF was evaluated with the acquisition frequency of 0.1 Hz. A contact pair consisted of metal (cobalt-chromium-molybdenum—CoCrMo) and alumina ceramic balls of diameter 19.05 mm sliding against 46 mm-diameter discs of metal, ceramic, and highly-crosslinked PE (HXPE), respectively. The thickness of the discs was 6 mm. A schematic illustration of the measurement configuration is displayed in Figure 1. Initial surface topography of the test specimens was checked using the phase-shifting interferometry method (Contour GT-X8, Bruker, Billerica, MA, USA). Five points which were expected to be in the contact drag of each sample were measured, while the surface roughness results are shown in Table 1.

To clarify the effect of kinematic conditions, the experiments were realized under two different mean speeds, 5.7 mm/s and 22 mm/s. Mean speed represents the average value of the ball and the disc speed under various rolling/sliding conditions. In the following text, the terms positive and negative sliding are used. In the case of negative sliding, the ball rotates faster than the disc. By contrast, under positive sliding the disc is faster. The course of the speeds of the individual components considering negative and positive sliding is demonstrated using the red arrows in the bottom part of Figure 1. Regarding the human body, it can be assumed that the hip joint operates under pure negative sliding conditions, which means that the cup is stationary, while the head rotates. Considering the ball-on-disc configuration, pure sliding represents bit severe conditions and so significant wear of the samples apparently influencing the results of CoF could be expected. Therefore, the experiments were realized under partial sliding of 150%. To avoid inaccuracies coming from the slippage of the components, the tests were realized under both positive (150%) and negative (−150%) sliding. The slide-to-roll ratio (SRR) which determines the level of slip, can be easily determined following the equation $SRR = 2(u_D - u_B)/(u_D + u_B)$, where u_d is the speed of the disc and u_b is the speed of the ball. Combined rolling/sliding conditions normally occur in the knee joint; however, it should be highlighted that the

present study is not focused on one particular joint type, but on the general assessment of frictional behaviour of materials used for joint implants. Applied load was 0.5 N in the case of the metal and 0.4 in the case of the ceramic balls, leading to the following contact pressures: metal-on-metal (264.7 MPa), metal-HXPE (9.9 MPa), ceramic-ceramic (280.5 MPa), ceramic-HXPE (9.5 MPa).

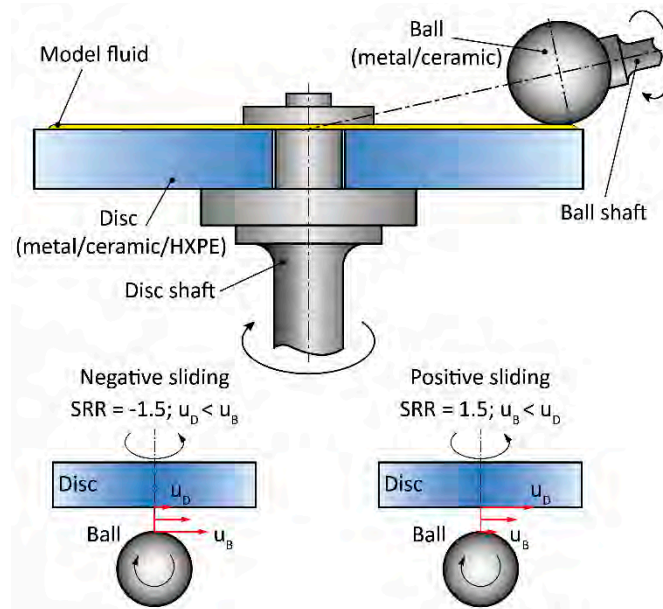


Figure 1. Schematic illustration of the measurement configuration.

Table 1. Surface topography parameters of the test samples.

Parameter	Ball		Disc		
	Metal	Ceramic	Metal	Ceramic	HXPE
Average surface roughness Ra (μm)	0.087	0.035	0.008	0.998	0.841
Standard deviation SD (μm)	± 0.00587	± 0.00414	± 0.00039	± 0.10707	± 0.13631

The main interest of the current study was in the effect of the composition of model fluid. Therefore, five test lubricants were prepared while the results were compared with those for pure PBS. The model fluids contained the dominant proteins of SF; albumin and γ -globulin, respectively. Lubricants were prepared 24 h prior to the tests and were stored in a refrigerator to enable a complete solution of the proteins in PBS. Bovine serum albumin (9048-46-8, Biomol GmbH, Hamburg, Germany) and γ -globulin from human blood (G4386, Sigma Aldrich, Darmstadt, Germany) were added to PBS in various concentrations, while the simple protein solutions were investigated as well. A summary of the test fluids is provided in Table 2. Despite the ability of the test device to control the temperature of the pot, the experiments were realized under ambient laboratory temperature of 22 °C, since it was previously referenced in literature that the increase to body temperature does not influence the results substantially [18]. The experiments were conducted under fully flooded conditions to avoid any effects coming from starvation of the contact. Eighty experiments were realized in total, while Table 3 provides the complete overview of the performed tests for better orientation. The detailed information about the speeds of the ball and the disc during various tests is given in Table 4. Random tests were conducted three times to check the repeatability of the results. Since there was excellent data agreement in terms of both the trends and the absolute values of CoF (standard deviation not larger than 0.04), the rest of the experiments were performed only once.

Table 2. Summary of the applied model fluids.

Model Synovial Fluid (MSF)	Volume (mL)	Protein Content (mg/mL)		Total Protein Concentration (mg/mL)
-	-	Albumin	γ -globulin	-
Alb70+Glob35	10	7	3.5	10.5
Alb35+Glob70	10	3.5	7	10.5
Alb140+Glob70	10	14	7	21
Albumin70	10	7	-	7
γ -globulin35	10	-	3.5	3.5
PBS	10	-	-	-

Table 3. Overview of the performed experiments.

Experiment Set	Material Combination	Mean Speed (mm/s)	Slide-To-Roll Ratio (%)	Model Synovial Fluid
1	Metal-on-Metal (MoM)	5.7; 22	150; -150	Alb70+Glob35; Alb35+Glob70; Alb140+Glob70; PBS
2	Metal-on-highly crosslinked polyethylene (HXPE) (MoP)	5.7; 22	150; -150	Alb70+Glob35; Alb35+Glob70; Alb140+Glob70; PBS
3	Ceramic-on-Ceramic (CoC)	5.7; 22	150; -150	Alb70+Glob35; Alb35+Glob70; Alb140+Glob70; PBS
4	Ceramic-on-HXPE (CoP)	5.7; 22	150; -150	Alb70+Glob35; Alb35+Glob70; Alb140+Glob70; PBS
5	MoM	22	150; -150	Albumin70; γ -globulin35
6	MoP	22	150; -150	Albumin70; γ -globulin35
7	CoC	22	150; -150	Albumin70; γ -globulin35
8	CoP	22	150; -150	Albumin70; γ -globulin35

Table 4. A detailed overview of the kinematic conditions.

Slide-To-Roll Ratio (%)	Mean Speed (mm/s)	Ball Speed (mm/s)	Disc Speed (mm/s)
-150	5.7	9.975	1.425
-150	22	38.5	5.5
150	5.7	1.425	9.975
150	22	5.5	38.5

3. Results and Discussion

3.1. The Effect of Material and Kinematic Conditions

Initially, the experiments were performed with pure PBS for all the material combinations, considering both positive and negative sliding at lower (5.7 mm/s) and higher (22 mm/s) speed. The results showed that independent of kinematic conditions, the MoM combination exhibits the highest friction; however, this effect was significant mainly under negative sliding, when the friction at the end of the experiment reached almost 0.6. By contrast, the lowest friction was detected for MoP and CoP, while in the case of CoP, the friction level was less than 0.1, particularly around 0.05 for the dominant period of the experiments, which is in a good correlation with previous observations [11,19,20]. CoC frictional behaviour was found to be somewhere between, while the friction reached about 0.25. Nevertheless, it should be taken into account that the surface roughness of

the employed ceramic disc was an order of magnitude higher than the surface of the ball, which could affect the results. Based on the previous findings, it might be expected that if realistic roughness of the disc could be achieved, the friction coefficient would be lower. However, without the experimental results, the potential level of CoF reduction can be only estimated. Nevertheless, it should be emphasized that the present study is rather comparative, not predicting the friction within real implants. With the exception of MoM under positive sliding conditions, there was not a substantial effect of speed. Considering the effect of time, only in the case of MoM was the development of friction with time observed. For the rest of the material combinations, CoF was stable without any fluctuations over the entire experiment. All the results can be seen in Figure 2. It should be noted that even the acquisition frequency was 0.1 Hz; for better clarity of the results, the plotted dots represent average CoF in particular time steps (1 s, 15 s, 30 s . . . 300 s). The inset figures are shown to illustrate the kinematic conditions. The red arrows represent the speed course.

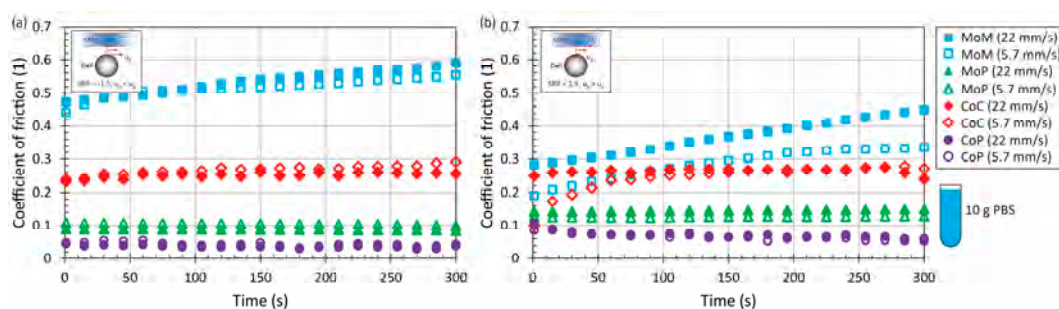


Figure 2. Development of coefficient of friction (CoF) as a function of time for four material combinations at lower and higher mean speed under negative (a) and positive (b) sliding conditions. Contact is lubricated by phosphate-buffered saline (PBS).

Adding the proteins into the saline solution in relatively low concentration (10.5 mg/mL in total) led to a slight change of CoF evolution, see Figures 3 and 4. Compared to the pure PBS results, time-dependent behaviour was observed for MoM and also for CoC contact pairs, while the maximum at the end of the test was from 0.3 to 0.4 for metal. For ceramic, the friction level was about 0.2, while the very same behaviour was observed in literature, where the contact of a ceramic ball sliding against a ceramic plate lubricated by BS was analyzed [21]. To determine the influence of fluid composition, it can be seen that even if the concentration of albumin and γ -globulin was switched, see Figure 3 vs. Figure 4, almost the same results could be obtained for most of the materials and kinematic conditions. Only in the case of MoP did higher content of γ -globulin lead to a decrease of friction, as can be seen in Figure 4a.

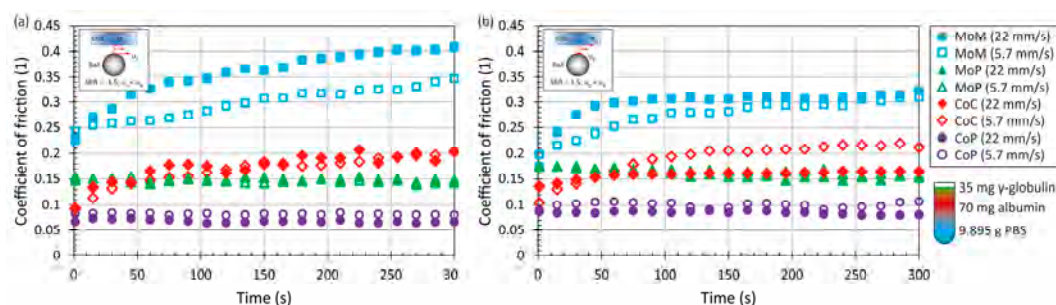


Figure 3. Development of CoF as a function of time for four material combinations at lower and higher mean speed under negative (a) and positive (b) sliding conditions. Contact is lubricated by model fluid Alb70+Glob35.

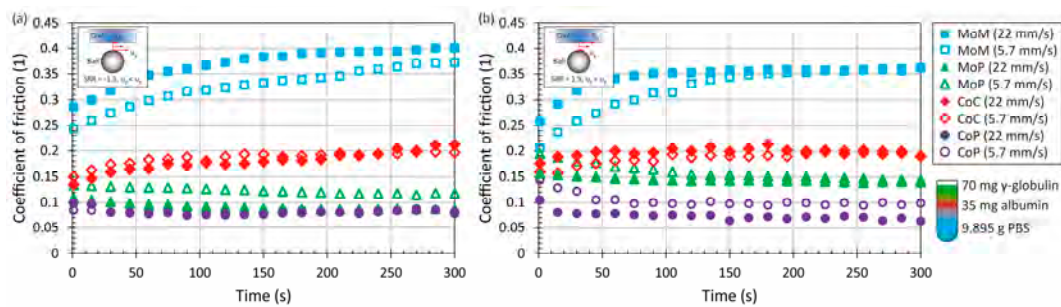


Figure 4. Development of CoF as a function of time for four material combinations at lower and higher mean speed under negative (a) and positive (b) sliding conditions. Contact is lubricated by model fluid Alb35+Glob70.

An increase of protein concentration to 21 mg/mL led to a very slight increase of friction for ceramic and metal pairs. In the case of MoP and CoP, the friction remained the same or decreased a little bit. However, since the change is negligible, see Figures 3 and 4 vs. Figure 5, it can be concluded that the protein content does not play an important role regarding these so-called hard-on-soft bearing pairs. Finally, focusing on the particular material combinations, it can be seen that the behaviour corresponds well to the pure PBS results, while the highest friction is exhibited by MoM, followed by CoC, MoP and CoP (Figures 2–5). The highest friction in the case of metal-metal contact was reported also by Scholes and Unsworth [7]. Nevertheless, it should be noted that the results do not completely correspond to observations provided by Vrbka et al. [16], who determined the friction coefficient for various implant pairs. In the reference, the authors measured the lowest friction when considering a ceramic head sliding against a ceramic cup. However, it must be noted that different experimental conditions were employed; in particular, BS was employed as the test lubricant, and the experiments were realized in different geometrical configurations. Moreover, as mentioned above, the roughness of ceramic discs used in the present study was an order of magnitude higher than is the roughness of real acetabular cups, which can also play a significant role.

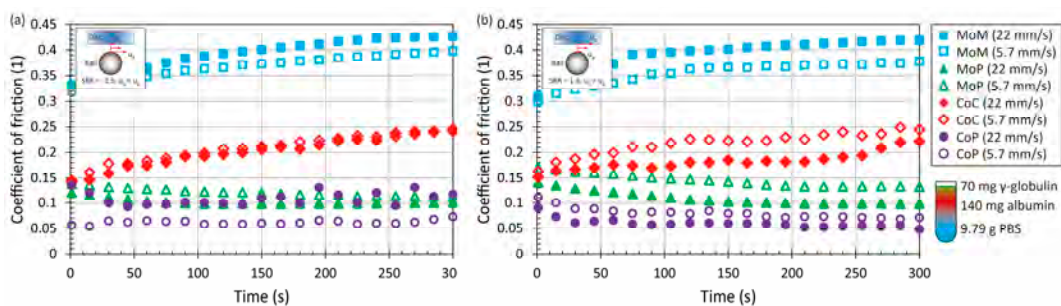


Figure 5. Development of CoF as a function of time for four material combinations at lower and higher mean speed under negative (a) and positive (b) sliding conditions. Contact is lubricated by model fluid Alb140+Glob70.

3.2. The Effect of Model Synovial Fluid Composition

To clearly identify the effect of model SF composition on frictional behaviour, the additional tests were performed at higher speed considering the simple protein solutions of albumin and γ -globulin as well. The results for individual material combinations are displayed in Figures 6–9, respectively. For MoM contact, it can be seen that the results for pure PBS are influenced by the positivity/negativity of sliding. Under negative sliding, the level of friction is considerably higher (around 0.6 at maximum) for PBS compared to protein solution (around 0.4). In terms of individual fluids, albumin-containing lubricant exhibited the lowest friction, approximately 0.37. For the rest of the lubricants, there is

no clear impact on lubrication, while the friction is kept between 0.4 and 0.43 at the end of the test, see Figure 6a. Considering the positive sliding conditions, the CoF development is slightly different. The highest friction over the dominant part of the experiment was exhibited by the solution with relatively high protein content. However, after 75 s, the friction was stabilized at about 0.4 without any further time-dependent change. The course of friction for saline solution is linearly increasing (the same behaviour as under negative sliding), reaching 0.45 at the end. For the other protein solutions, the behaviour is almost the same, with the exception of lubricant containing 70 mg/mL of albumin and 35 mg/mL of γ -globulin, which exhibits the lowest friction. This can be attributed to the action of the protein film. It was observed in literature that, considering the same model fluid as in the case of the present study, a metal head formed much thicker protein film under positive sliding, which can lead to a decrease of friction between the surfaces [22].

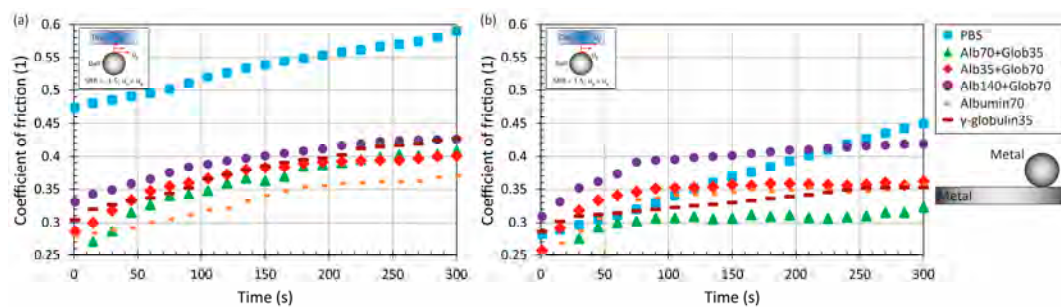


Figure 6. Development of CoF as a function of time for metal-on-metal pair at higher mean speed under negative (a) and positive (b) sliding conditions for various model fluids.

It is apparent that the MoM combination exhibits an increasing tendency of friction, in general. By contrast, when the disc is of polyethylene, friction is decreasing or constant, as is shown in Figure 7. In that case, the friction level is associated with the kinematic conditions. When the ball rotates faster than the disc, the lowest friction was exhibited by PBS, and the lubricant with the higher content of γ -globulin. The highest friction was observed for lubricant with lower protein concentration (10.5 mg/mL) and the dominant presence of albumin. The tendency was also quite unstable in that case. Nevertheless, it has to be taken into account that the difference between minimum and maximum friction is just 0.05; therefore, it might be assumed that the effect of the lubricant is negligible. When the disc was faster, the lowest friction was reached, once the lubricant with higher protein content (21 mg/mL) was employed. In addition, both the simple solution exhibited relatively low friction of around 0.11. What is in correlation with previous findings is the friction level for saline solution. In a recent study [23], a polyethylene disc conducted reciprocating motion against a metal pin (pure positive sliding), while the friction was from 0.12 to 0.16, which corresponds to the present results, see Figure 7b.

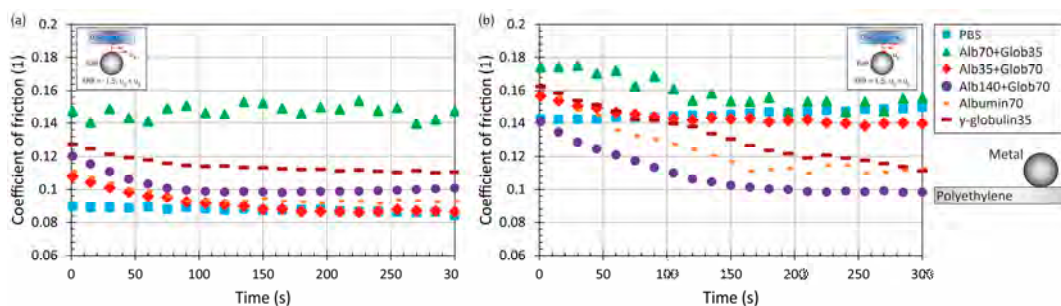


Figure 7. Development of CoF as a function of time for metal-on-polyethylene pair at higher mean speed under negative (a) and positive (b) sliding conditions for various model fluids.

Considering the ceramic-ceramic contact, the friction is increasing under negative sliding as in the case of the metal-metal pair. Moreover, there is a good correlation of the effect of proteins, while adding the proteins to the saline solution led to a decrease of friction, especially during the first part of the test, see Figure 8a. The same behaviour can be observed even for positive sliding, while the effect of the lubricant is more substantial; anyway, the variance in friction is still limited. In this particular case, the friction is relatively stable for all the test fluids, as is displayed in Figure 8b. Similar friction with film thickness development can be found, as mentioned for the metal sliding pair. Using the fluorescent microscopy technique, we evaluated the central film thickness in ceramic-on-glass contact, while it was found that the lubricant layer for alumina ceramic under positive sliding was much thicker compared to negative sliding [24].

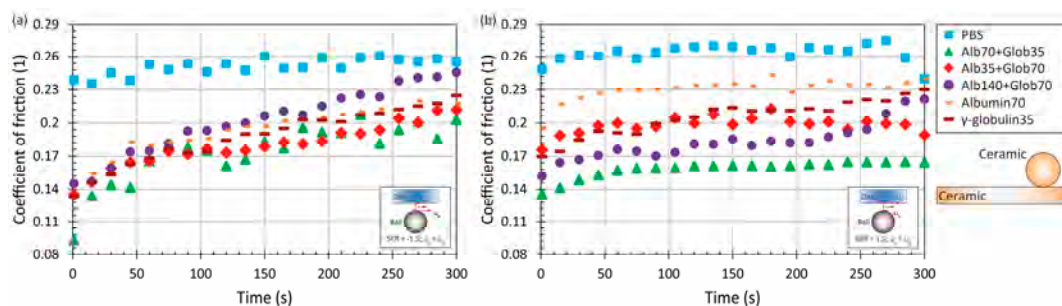


Figure 8. Development of CoF as a function of time for ceramic-on-ceramic pair at higher mean speed under negative (a) and positive (b) sliding conditions for various model fluids.

Finally, the experiments were realized with a ceramic ball and polyethylene disc. The effect of the lubricant was again very limited, as for the MoP pair. In particular under positive sliding, the role of fluid is unimportant, since the difference between minimum and maximum friction is just about 0.04, see Figure 9b. Therefore, it is not suitable to identify which lubricant leads to the lowest and the highest friction, respectively. The only noticeable finding is that in the case of negative sliding, slightly higher friction (around 0.12) was exhibited by simple γ -globulin solution and by the solution with a higher content of protein.

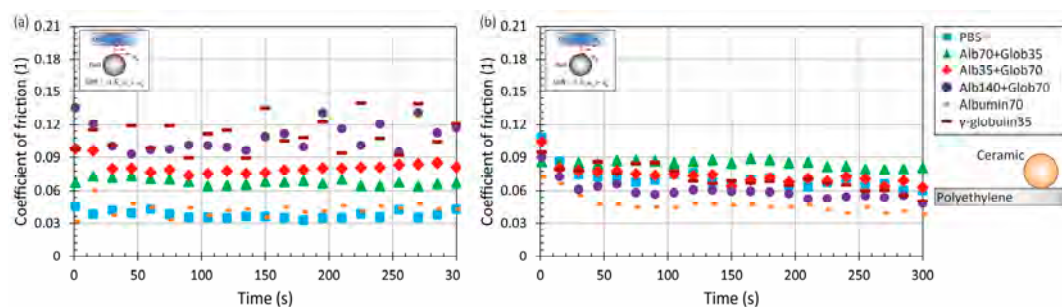


Figure 9. Development of CoF as a function of time for ceramic-on-polyethylene pair at higher mean speed under negative (a) and positive (b) sliding conditions for various model fluids.

As could be expected based on the previous findings, the present results clearly prove that the most important factor influencing the frictional behaviour of implants is the material of the components. What is quite surprising is the limited influence of model fluid composition, mainly in the case of MoP and CoP pairs. Nevertheless, it should be taken into account that in hard-on-soft pairs significantly lower contact pressure occurs; therefore, this may be an explanation for relatively low sensitivity of friction to test fluid. Anyway, since the previous observations focusing on the assessment of film thickness in hip replacements explored whether the effect of fluid composition

may be fundamental [25–28], deeper investigation of lubrication mechanisms seems to be a crucial challenge for biotribologists.

Obviously, the authors realize several limitations to the performed study. The most important point might be the geometrical arrangement. Previously, most of the tribological studies dealing with friction and film thickness evaluation were conducted considering simplified ball-on-disc (pin-on-plate) test configuration. However, our recent observations clearly indicate that the lubrication is apparently influenced by the contact conformity [29]. However, it should be noted that the main purpose of the present study was to provide a comprehensive comparison of frictional behaviour regarding implant material, the composition of model synovial fluid, and kinematic conditions. Therefore, the main findings can be generalized irrespective of the contact geometry. A similar approach was presented before in literature [5]. A later limiting point is the composition of the employed test lubricants. As discussed above, the protein content and its ratio may not be as substantial as previously expected. Although several experimental investigations focused on *in vitro* wear, the testing of implants could provide satisfactory wear data compared to clinical observations; it should be taken into account that our recent study [28] clearly indicates that the lubrication mechanisms are affected dominantly by the presence of hyaluronic acid and phospholipids. These findings are in a good agreement with the data published elsewhere [8,30]. The last point arising could be the effect of temperature on frictional behaviour. However, an increase of temperature of around 15 °C should not cause any change in terms of lubrication performance [18], and also conformational changes potentially influencing the results [11] are not expected. Considering the aforementioned limitations, the motivation for future study should be the necessity of applying complex model fluids containing all the synovial constituents together with attention to the real conformity of rubbing surfaces.

4. Conclusions

The performed study focused on the evaluation of the friction coefficient within the contact of materials used for joint replacements. The contact was lubricated by various model synovial fluids while the study was aimed at assessment of the effect of implant material and kinematic conditions in terms of speed and slide-to-roll ratio. The findings can be summarized as follows:

Based on the results obtained, it seems that the dominant factor influencing the frictional performance of joint replacements is the implant material. The effect of kinematic conditions as well as the composition of model synovial fluid was found to be much less important.

The highest friction is exhibited by metal-metal contact. For the ceramic-ceramic pair, the friction was approximately half compared to the metal pair. This behaviour was observed independent of the applied test fluid.

If the polyethylene disc was used as the counterpart, the friction was very low, less than 0.05 in some cases. Generally, the lowest friction was detected for the ceramic-polyethylene pair.

Considering the trend of friction for various fluids regarding individual material combinations, it was found that the friction has an increasing tendency in the case of hard-on-hard pairs (MoM, CoC); however, the tendency is decreasing or constant for hard-on-soft implants (MoP, CoP).

Proteins added to saline solution lead to a decrease of friction for the metal-metal pair, while for the other combinations there are no significant differences when comparing PBS results with protein solutions.

In the case of a hard-on-soft bearing pair in particular, the role of fluid compositions was found to be negligible, as the differences between minimum and maximum values at the end of the experiments are less than 0.08.

Author Contributions: Conceptualization, M.H. and D.N.; Methodology, D.N. and I.K.; Validation, D.N. and M.V.; Formal Analysis, D.N.; Investigation, D.N. and M.V.; Resources, M.H. and D.N.; Data Curation, D.N. and M.V.; Writing-Original Draft Preparation, D.N.; Writing-Review & Editing, D.N. and I.K.; Supervision, M.H. and I.K.; Project Administration, M.H.; Funding Acquisition, M.H., and I.K.

Funding: This research was funded by the Ministry of Education, Youth and Sports of the Czech Republic, grant number LTAUSA17150.

Acknowledgments: The authors express their thanks to T. Tkadlec for his help with the friction tests.

Conflicts of Interest: The authors declare no conflict of interest.

References

1. The Organisation for Economic Co-operation and Development (OECD). *Health at a Glance 2015: OECD Indicators*; OECD: Paris, France, 2015.
2. Pramanik, S.; Agarwal, A.K.; Rai, K.N. Chronology of total hip joint replacement and materials development. *Trends Biomater. Artif. Organs* **2005**, *19*, 15–26.
3. Huch, K.; Müller, K.A.C.; Stürmer, T.; Brenner, H.; Puhl, W.; Günther, K.-P. Efficacy of prednisone 1–4 mg/day in patients with rheumatoid arthritis: A randomised, double-blind, placebo controlled withdrawal clinical trial. *Ann. Rheum. Dis.* **2005**, *64*, 1715–1720. [[CrossRef](#)] [[PubMed](#)]
4. Joshi, A.B.; Porter, M.L.; Trail, I.A.; Hunt, L.P.; Murphy, J.C.; Hardinge, K. Long-term results of Charnley low-friction arthroplasty in young patients. *Bone Jt. J.* **1993**, *75*, 616–623. [[CrossRef](#)]
5. Mavraki, A.; Cann, P.M. Friction and lubricant film thickness measurements on simulated synovial fluids. *Proc. Inst. Mech. Eng. Part J J. Eng. Tribol.* **2009**, *223*, 325–335. [[CrossRef](#)]
6. Yao, J.Q.; Laurent, M.P.; Johnson, T.S.; Blanchard, C.R.; Crowninshield, R.D. The influences of lubricant and material on polymer/CoCr sliding friction. *Wear* **2003**, *255*, 780–784. [[CrossRef](#)]
7. Scholes, S.C.; Unsworth, A. The Effects of Proteins on the Friction and Lubrication of Artificial Joints. *Proc. Inst. Mech. Eng. Part H J. Eng. Med.* **2006**, *220*, 687–693. [[CrossRef](#)] [[PubMed](#)]
8. Sawae, Y.; Murakami, T.; Chen, J. Effect of synovia constituents on friction and wear of ultra-high molecular weight polyethylene sliding against prosthetic joint materials. *Wear* **1997**, *216*, 213–219. [[CrossRef](#)]
9. Widmer, M.R.; Heuberger, M.; Vörös, J.; Spencer, N.D. Influence of polymer surface chemistry on frictional properties under protein-lubrication conditions: implications for hip-implant design. *Tribol. Lett.* **2001**, *10*, 111–116. [[CrossRef](#)]
10. Heuberger, M.P.; Widmer, M.R.; Zobeley, E.; Glockshuber, R.; Spencer, N.D. Protein-mediated boundary lubrication in arthroplasty. *Biomaterials* **2005**, *26*, 1165–1173. [[CrossRef](#)] [[PubMed](#)]
11. Nečas, D.; Sawae, Y.; Fujisawa, T.; Nakashima, K.; Morita, T.; Yamaguchi, T.; Vrbka, M.; Křupka, I.; Hartl, M. The Influence of Proteins and Speed on Friction and Adsorption of Metal/UHMWPE Contact Pair. *Biotribology* **2017**, *11*, 51–59. [[CrossRef](#)]
12. Yang, C.B.; Fang, H.W.; Liu, H.L.; Chang, C.-H.; Hsieh, M.-C.; Lee, W.-M.; Huang, H.-T. Frictional characteristics of the tribological unfolding albumin for polyethylene and cartilage. *Chem. Phys. Lett.* **2006**, *431*, 380–384. [[CrossRef](#)]
13. Wang, A.; Essner, A.; Polineni, V.K.; Stark, C.; Dumbleton, J.H. Lubrication and wear of ultra-high molecular weight polyethylene in total joint replacements. *Tribol. Int.* **1998**, *31*, 17–33. [[CrossRef](#)]
14. Dowson, D.; Wang, F.C.; Wang, W.Z.; Jin, Z.M. A predictive analysis of long-term friction and wear characteristics of metal-on-metal total hip replacement. *Proc. Inst. Mech. Eng. Part J J. Eng. Tribol.* **2007**, *221*, 367–378. [[CrossRef](#)]
15. Brockett, C.L.; Harper, P.; Williams, S.; Isaac, G.H.; Dwyer-Joyce, R.S.; Jin, Z.; Fisher, J. The influence of clearance on friction, lubrication and squeaking in large diameter metal-on-metal hip replacements. *J. Mater. Sci. Mater. Med.* **2008**, *19*, 1575–1579. [[CrossRef](#)] [[PubMed](#)]
16. Vrbka, M.; Nečas, D.; Bartošik, J.; Hartl, M.; Křupka, I.; Galandáková, A.; Gallo, J. Determination of a Friction Coefficient for THA Bearing Couples. *Acta Chirurgiae Orthopaedicae et Traumatologiae Cechoslovaca* **2015**, *82*, 341–347. [[PubMed](#)]
17. Brostow, W.; Hagg Lobland, H.E. *Materials: Introduction and Applications*; John Wiley & Sons: Hoboken, NJ, USA, 2017.
18. Mavraki, A.; Cann, P.M. Lubricating film thickness measurements with bovine serum. *Tribol. Int.* **2011**, *44*, 550–556. [[CrossRef](#)]
19. Gispert, M.P.; Serro, A.P.; Colaço, R.; Saramago, B. Friction and wear mechanisms in hip prosthesis: Comparison of joint materials behaviour in several lubricants. *Wear* **2006**, *260*, 149–158. [[CrossRef](#)]

20. Guezmil, M.; Bensalah, W.; Mezlini, S. Tribological behavior of UHMWPE against TiAl6V4 and CoCr28Mo alloys under dry and lubricated conditions. *J. Mech. Behav. Biomed. Mater.* **2016**, *63*, 375–385. [[CrossRef](#)] [[PubMed](#)]
21. Morillo, C.; Sawae, Y.; Murakami, T. Effect of bovine serum constituents on the surface of the tribological pair alumina/alumina nanocomposites for total hip replacement. *Tribol. Int.* **2010**, *43*, 1158–1162. [[CrossRef](#)]
22. Nečas, D.; Vrbka, M.; Urban, F. The effect of lubricant constituents on lubrication mechanisms in hip joint replacements. *J. Mech. Behav. Biomed. Mater.* **2016**, *55*, 295–307. [[CrossRef](#)] [[PubMed](#)]
23. Guezmil, M.; Bensalah, W.; Mezlini, S. Effect of bio-lubrication on the tribological behavior of UHMWPE against M30NW stainless steel. *Tribol. Int.* **2016**, *94*, 550–559. [[CrossRef](#)]
24. Nečas, D.; Vrbka, M.; Křupka, I.; Hartl, M.; Galandáková, A. Lubrication within hip replacements—Implication for ceramic-on-hard bearing couples. *J. Mech. Behav. Biomed. Mater.* **2016**, *61*, 371–383. [[CrossRef](#)] [[PubMed](#)]
25. Fan, J.; Myant, C.W.; Underwood, R.; Hart, A. Inlet protein aggregation: A new mechanism for lubricating film formation with model synovial fluids. *Proc. Inst. Mech. Eng. Part H J. Eng. Med.* **2011**, *225*, 696–709. [[CrossRef](#)] [[PubMed](#)]
26. Myant, C.; Underwood, R.; Fan, J. Lubrication of metal-on-metal hip joints: The effect of protein content and load on film formation and wear. *J. Mech. Behav. Biomed. Mater.* **2012**, *6*, 30–40. [[CrossRef](#)] [[PubMed](#)]
27. Parkes, M.; Myant, C.; Cann, P.M.; Wong, J.S.S. The effect of buffer solution choice on protein adsorption and lubrication. *Tribol. Int.* **2014**, *72*, 108–117. [[CrossRef](#)]
28. Nečas, D.; Vrbka, M.; Rebenda, D.; Gallo, J.; Galandáková, A.; Wolfová, L.; Křupka, I.; Hartl, M. In situ observation of lubricant film formation in THR considering real conformity: The effect of model synovial fluid composition. *Tribol. Int.* **2018**, *117*, 206–216. [[CrossRef](#)]
29. Nečas, D.; Vrbka, M.; Urban, F.; Gallo, J.; Křupka, I.; Hartl, M. In situ observation of lubricant film formation in THR considering real conformity: The effect of diameter, clearance and material. *J. Mech. Behav. Biomed. Mater.* **2017**, *69*, 66–74. [[CrossRef](#)] [[PubMed](#)]
30. Sawae, Y.; Yamamoto, A.; Murakami, T. Influence of protein and lipid concentration of the test lubricant on the wear of ultra high molecular weight polyethylene. *Tribol. Int.* **2008**, *41*, 648–656. [[CrossRef](#)]



© 2018 by the authors. Licensee MDPI, Basel, Switzerland. This article is an open access article distributed under the terms and conditions of the Creative Commons Attribution (CC BY) license (<http://creativecommons.org/licenses/by/4.0/>).

Running-in friction of hip joint replacements can be significantly reduced: The effect of surface-textured acetabular cup

David NEČAS^{1,*}, Hatsuhiko USAMI², Tatsuya NIIMI³, Yoshinori SAWAE⁴, Ivan KŘUPKA¹, Martin HARTL¹

¹ Faculty of Mechanical Engineering, Brno University of Technology, Brno 61669, Czech Republic

² Faculty of Science and Technology, Meijo University, Nagoya 468-8502, Japan

³ Kanefusa Corporation, Nagoya 480-0192, Japan

⁴ Faculty of Engineering, Kyushu University, Fukuoka 819-0395, Japan

Received: 13 August 2019 / Revised: 17 October 2019 / Accepted: 05 December 2019

© The author(s) 2019.

Abstract: Hip joint replacements represent the most effective way of treatment for patients suffering from joint diseases. Despite the rapid improvement of implant materials over the last few decades, limited longevity associated with wear-related complications persists as the main drawback. Therefore, improved tribological performance is required in order to extend the service life of replacements. The effect of surface texturing of ultra-high molecular weight polyethylene (UHMWPE) acetabular cup was investigated in the present study. Unique tilling method was utilized for manufacturing the dimples with controlled diameter and depths on the contact surface of the cup. The experiments with four commercial femoral components and two model lubricants were realized. The main attention was paid to a coefficient of friction considering the differences between the original and the dimpled cups. Results showed remarkable lowering of friction, in general. Focusing on the simulated human synovial fluid, friction was reduced by 40% (alumina ceramic), 38.8% (zirconia toughened ceramic), 25.5% (metal), and 9.9% (oxinium). In addition, the dimples helped to keep the friction stable without fluctuations. To conclude, the paper brings a new insight into frictional behaviour of the hip replacements during running-in phase which is essential for overall implant lifespan. It is believed that proper surface texturing may rapidly improve the life quality of millions of patients and may lead to considerable financial savings.

Keywords: hip joint replacement; friction; texturing; dimple; longevity

1 Introduction

It is often reported in literature that human joint replacements suffer from limited longevity which is usually associated with aseptic loosening due to osteolysis [1, 2]. Osteolysis is a wear-related problem indicating the importance of tribological performance of the implants [3, 4]. Therefore, correlation between lubrication, friction, and wear has to be well understood when aiming on the improved durability of the replacements. Regarding wear, it was shown that wear rate is significantly higher during running-in phase [5, 6].

It is assumed that wear is a consequence of elevated friction associated within sufficient lubrication. Recently, number of papers dealt with lubrication analysis using optical methods [7, 8]. Various effects such as kinematic conditions [9], material and geometry [10], or the role of synovial fluid (SF) constituents [11, 12] were clarified. However, in an effort to lengthen the implant lifespan, fundamental analyses have to be supported by suggestions. The aim is to enhance lubrication performance, thus decreasing friction during running-in to slow down the wear process. From the engineering point of view, surface texturing

* Corresponding author: David NEČAS, E-mail: David.Necas@vut.cz

seems to be very effective solution [13–15].

Considering the application of surface textures on artificial joints, most of the previous studies were focused on wear rate evaluation. Pilot study was provided by Ito et al. [16]. The authors applied concave dimples on the surface of metal femoral head, finding significant reduction of counter polyethylene (PE) surface wear. The positive effect was attributed to reduction of abrasive wear by reservoirs for released particles and improved lubricity due to continuous supply of the lubricant stored in the dimples. The same material combination was later tested in pin-on-plate configuration while the results confirmed reduction of wear rate. It was pronounced that suitable shape of the textures may extend longevity of implants by more than two times compared to smooth sliding surfaces [17]. The study was extended by Borjali et al. [18], who examined effect of the dimple pattern made on metal polished surface sliding against PE specimen. Three PE based materials used for prosthetic joints were investigated; UHMWPE, highly cross-linked PE (HXPE), and vitamin E highly cross-linked PE (VEXPE), respectively. In general, the lowest wear rate was observed for VEXPE. Nevertheless, the effect of surface texturing was the most apparent in the case of conventional UHMWPE. Recent paper introduced by Langhorn et al. [19] confirmed previous findings about metal-PE contact pair. The authors observed reduction of wear rate by more than 50% when textured metal surface was employed.

Frictional behaviour of metal-PE contact was studied by Cho and Choi [20]. Pin-on-disc sliding tests were conducted while the contact surface of the disc was modified. Various depths and surface coverage densities were investigated. Lowering of friction was observed regardless the texturing parameters. For the given conditions, 25% surface coverage with the dimples having the depth 25 μm were found to be optimal. The effect of micro texturing on friction and wear of ceramic materials was discussed by Roy et al. [21]. Pin-on-disc tests were performed under loading conditions corresponding to normal gait of a hip joint. Both friction and wear were reduced significantly, specifically by 22% and 53%. It is apparent that pin-on-disc does not correspond to the real joint arrangement. Since it was shown that contact conformity plays an important role, Choudhury et al. [22] focused on the

effect of the dimples made on the femoral heads on a friction coefficient. The measurements were realized using pendulum hip simulator in order to ensure real contact geometry [23]. The effect of material combination and the diameter was studied. Focusing on the role of surface texturing, metal-on-metal (MoM) and metal-on-PE (MoP) contacts were analysed while three dimple arrays (square, triangle, and circular) were designed. Surprisingly, in the case of MoP contact, the effect of the dimples was found to be negative independently of an array. For MoM, triangular and square arrays led to decreased friction while circular arrangement caused friction increase [22]. A phenomenon of elevated friction in some cases was attributed mainly to the larger diameter and the depth of the dimples made by laser texturing. Size of the dimples probably led to starved lubrication conditions eventually. Therefore, an issue of texture geometry was emphasized among others.

Several authors also aimed on the effect of texturing on lubrication performance. Initial numerical study was presented in Ref. [24]. MoM model of the hip implant was developed. Simple cylindrical dimples were modelled considering steady state and walking conditions. The results indicated that texturing of the contact surfaces may have positive effect on the reduction of asperity contact ratio, thus improving the lubrication conditions. The study was later extended, focusing on the lubrication of a knee implant [25]. In such case, the contact of metal femoral and PE tibial components was considered. Combined effect of texturing was observed. Although it was shown that a lateral condyle benefits from the introduced dimples, opposite behaviour was observed for a medial compartment. In Ref. [26], lubrication model of the hip implant was developed aiming on the development of an optimal design of microtextures. It was found that the textures increase load-carrying capacity and the film thickness, together with lowering the contact pressure. The results were supported by experimental investigation of friction with the designed structure pattern. Metal cylinder with the dimpled contact surface rotated against stationary PE specimen while friction decreased by nearly 50%.

It is well known in biotribology that numerical models often suffer from specific limitations such as

adsorption or agglomeration of proteins which can be hardly simulated. Therefore, an experimental investigation takes place in order to provide relevant information about the lubrication mechanisms. A unique study, combining the direct film thickness measurement together with assessment of the effect of surface texturing, was presented by Choudhury et al. [27]. Contact of metal dimpled ball and glass acetabular cup was observed while the effect of triangular, ellipse, and square dimples on the film thickness development was assessed. Non-dimpled head was considered as a reference while the film thickness was always higher for the textured heads, independently of the dimple shape. In particular, especially in the case of square and triangular dimples, substantial increase of lubricant film was observed.

Based on the above references, it is apparent that surface texturing affects friction, lubrication, and wear which influence the service-life of the joint implants. Various studies were performed, aiming on the various aspects of texturing while positive effect on the tribological performance was observed in the most cases. Nevertheless, it should be emphasized that the authors always considered hard (metal, ceramic) surface to be dimpled. This may lead to negative effect in a long-term point of view. Once the dimples are filled by wear particles, abrasive wear may increase. Therefore, a motivation for the present

study is to examine the effect of the dimples made on UHMWPE cup surface in order to lower running-in friction coefficient thus preventing excessive wear. It is suggested that decreased friction at the beginning of operation leads to longer running-in phase, thus ensuring more favourable contact conditions. Eventually, durability of the implants may be extended due to slower wear progression.

2 Materials and methods

The experiments were realized using a pendulum hip joint simulator presented in the previous studies [8, 23, 28]. The acetabular cup is fixed by a resin in a stainless steel pot which is mounted to a base frame. The head is attached to a swinging arm using a cone. At the beginning of the experiment, the pendulum arm is deflected to initial position and is released. Spontaneous swinging is then damped due to friction between the ball and the cup. Instantaneous deflection of the pendulum is recorded via an angular velocity sensor. Subsequently, the signal is processed enabling to obtain the friction coefficient. Evaluation is based on a linear model of damping. It should be emphasized that the employed materials exhibit linear decay. Exponential response occurs when viscoelastic materials such as cartilage or hydrogel are introduced. Illustration of the simulator together with the representative decay signal record is shown in Fig. 1.

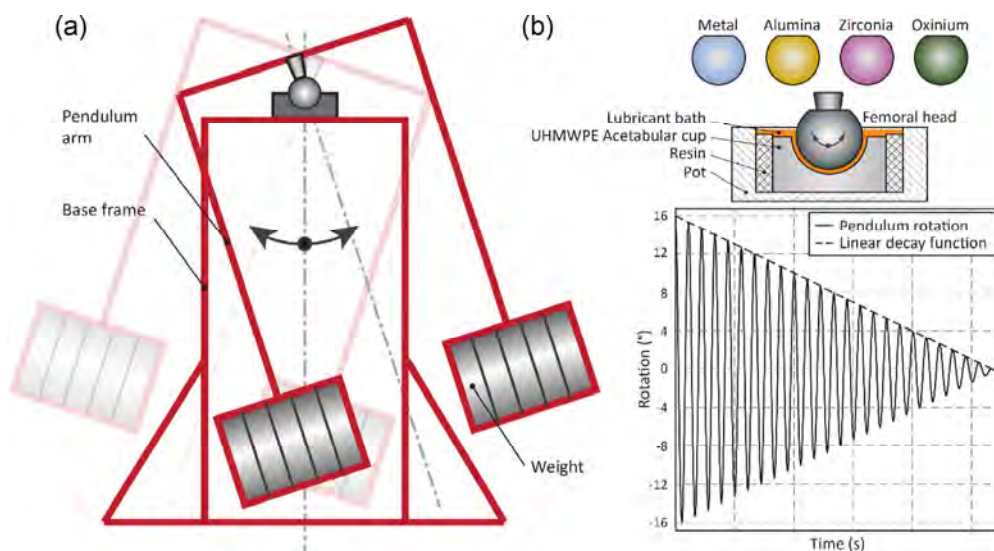


Fig. 1 (a) A schematic illustration of the pendulum hip joint simulator. (b) Overview of the tested femoral components, detail of the contact couple, and representative linear decay signal.

In the present study, various material combinations were tested. Four commercially available balls were used; metal, alumina ceramic, zirconia toughened ceramic, and oxinium, in particular. Two cups made of UHMWPE (GUR 1050) were tested. The first, reference cup was original without surface texturing. The second cup was fabricated from PE stock with the defined dimensions and the surface roughness corresponding to the original component. Circular dimples were subsequently made on the contact surface. Various approaches may be used for surface texturing. One of the ways is to use a micro drilling. However, the technology suffers from limited accuracy. Another option is to use a laser. Nevertheless, in such case, the diameter and the depth of the dimples cannot be precisely controlled. In addition, the sleeves around the dimples occurring due to elevated temperature leading to increased wear are often observed. Therefore, so-called “tilling” technology, previously successfully applied when texturing aluminium alloy [15], was employed in the present study. The dimples were made by fixing the fabricated UHMWPE cup to a chuck of CNC machining centre. One by one, the dimples were manufactured by removing the material by interrupted micro cutting using an end mill with a cutting edge. It should be emphasized that the process is fully automated and thus very fast. The dimple production rate is about 100 per second. The overall texturing process takes around one minute, dependently on the cup size and dimple pattern design. Therefore, the introduced method is very effective for routine use in large series.

Array and the dimensions of the dimples were designed based on the previous experience of the research team. The diameter and the depth of the dimples were set to 300 and 5 μm , respectively. The designed coverage ratio was 15%. The shape and the pattern of the dimples could be precisely controlled by adjusting tool path, rotation speed, and feed rate. A macroscopic image of the textured surface, the detail of the group of the dimples, and one random dimple are shown in Fig. 2. Topography map of the bottom of the dented cup is shown in Fig. 3. A nominal diameter of the tested implants was 32 mm. Before the experiments, the surface properties and the actual diameters of all the specimens were carefully checked using a 3D optical profiler and an optical scanning

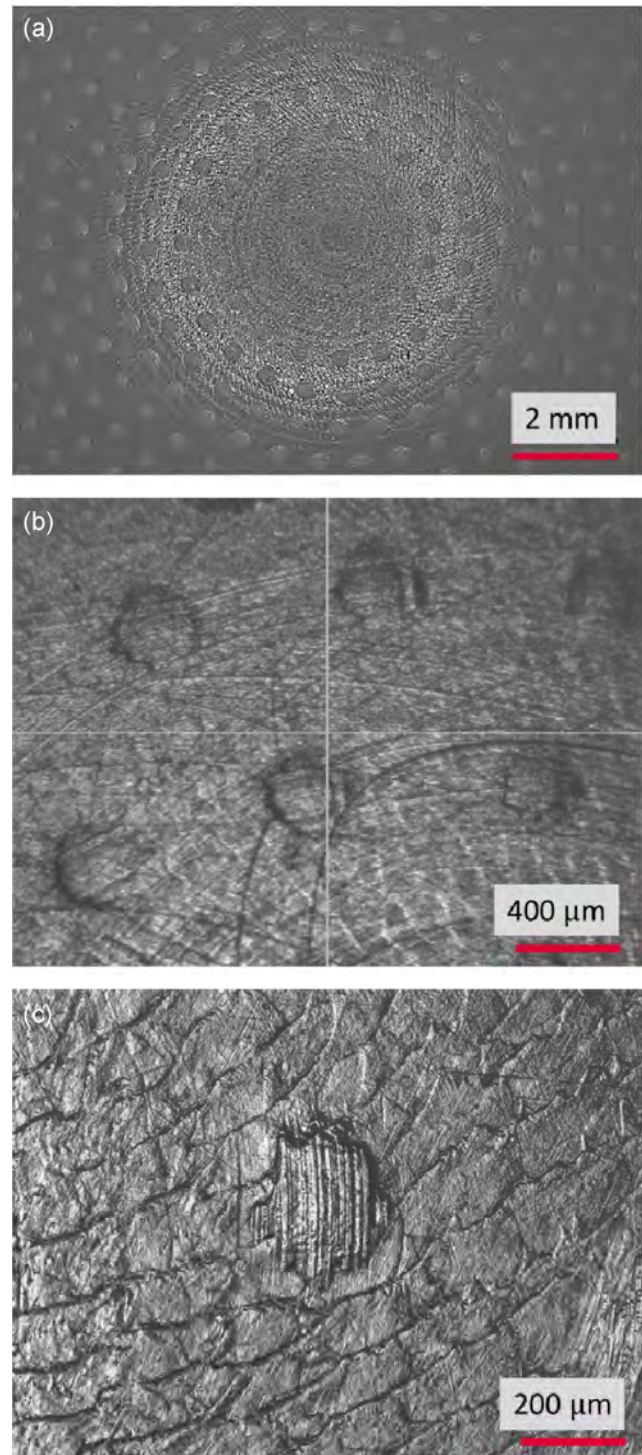


Fig. 2 Macroscopic image of (a) the dimpled cup and (b) group of the dimples taken by laser microscope. (c) Detail of the dimple taken by confocal microscope.

method [29]. Summary of the test samples together with the information about surface roughness, material properties, and contact conditions are presented in Table 1. Although a diametric clearance considering

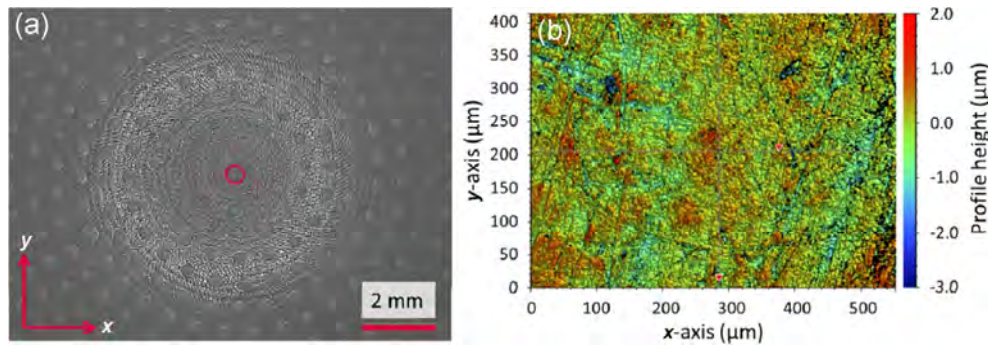


Fig. 3 (a) Macroscopic image of the dimpled cup with the indicated circle area. (b) Topography map within the area.

Table 1 Overview of the test samples and contact conditions.

Sample	Actual diameter (mm)	Surface roughness (nm)	Elastic modulus (GPa)	Poisson's ratio
Metal head	31.96	12.05	230	0.29
Alumina head	31.97	9.03	340	0.28
Zirconia toughened head	31.97	12.01	320	0.28
Oxinium head	31.90	57.63	98	0.3
Original UHMWPE cup	32.24	573	0.8	0.37
Dimpled UHMWPE cup	32.35	625	0.8	0.37

Contact couple	Diametric clearance (μm)	Contact pressure (MPa)	Contact diameter (mm)
Metal-on-original metal-on-dimpled	280 390	3 3.7	18.5 16.6
Alumina-on-original alumina-on-dimpled	270 380	2.9 3.6	18.7 16.8
Zirconia-on-original zirconia-on-dimpled	270 380	2.9 3.6	18.7 16.8
Oxinium-on-original oxinium-on-dimpled	340 450	3.4 4	17.4 15.9

the dimpled cup is larger, the value is within the tolerances measured for the original commercial UHMWPE cups.

All the experiments were realized under fully flooded conditions. Before the test, the cup was filled by a lubricant. Two various model fluids were employed. Initially, a phosphate buffered saline (PBS) was used as a reference. Subsequently, the contact was lubricated by the designed model SF. It is well

known that the proteins significantly influence frictional behaviour of metal/ceramic-on-PE pair [30, 31]. Composition of simulated SF was as follows: albumin = 20 mg/ml, γ -globulin = 3.6 mg/ml, hyaluronic acid (HA) = 2.5 mg/ml, phospholipids (PH) = 0.15 mg/ml; which fits to a physiological SF composition. To avoid results influence due to adsorption of the SF constituents, a strict cleaning procedure was followed. Both the ball and the cup were firstly cleaned by a sodium dodecyl sulphate solution. Subsequently, the components were rinsed by a pure water and dried by a pressed air. Finally, the specimens were washed in an isopropyl alcohol. The attention was also paid to storage conditions. While PBS was stored in a fridge, the SF was deeply frozen to $-22\text{ }^{\circ}\text{C}$ and was stored in a freezer to avoid protein degradation. Prior to the experiments, the lubricants were removed from the freezer/fridge to heat up naturally to an ambient temperature. The experiments were realized under controlled laboratory temperature ($22 \pm 1\text{ }^{\circ}\text{C}$) as it was shown that an elevated temperature to body level does not affect the lubrication conditions [32].

Based on the previous research of lubrication mechanisms within the hip replacements, a load was set to 532 N for all the tests. Such load level is basically lower compared to physiological conditions. However, it should be emphasized that during the gait cycle, the load is transient with short-term high-load peaks. In the case of the pendulum, the mean load value throughout the cycle corresponds to the mean level of physiological loading. Therefore, it is assumed that the overall load effect is comparable. Resulting contact stresses and the diameters of the contact zones for various couples are stated in Table 1.

Initial deflection of the pendulum was 16° and was controlled by a digital angle gauge. In order to provide statistically relevant data, the swinging test was carried out 8 times in a sequence. Once the motion stopped, the pendulum was deflected and released again. In addition, the complete series of the tests were repeated once more another day. All the series of eight swinging tests were performed without the lubricant change or additional supply. It should be noted that the swinging time was from two to four minutes dependently on the contact couple and the applied lubricant. Therefore, the whole series did not last longer than forty minutes. It is expected that the lubricant does not degrade within that time. When the contact couple was changed, fresh lubricant was applied.

3 Results

The results for the metal head are shown in Fig. 4. The friction coefficient for the contact lubricated by PBS is plotted on Fig. 4(a). As can be seen, independently of the tested cup, friction is very stable over the measurement series. In particular, for the original cup, friction is around 0.16 while for the dimpled cup it decreased to around 0.1. In the case of PBS, no fluctuations were observed and the data showed only a little variance. Figure 4(b) shows the data under lubrication by model SF. It is apparent that friction significantly increased compared to PBS. This indicates clear role of the proteins aggregating and adsorbing on the surfaces, thus causing sudden jumps in the results. Focusing on the effect of surface texturing, the dimples led to a substantial lowering of friction from near 0.4 to 0.3.

Following experiments were conducted with alumina ceramic femoral head. The results are shown in Fig. 5. As in the previous case, PBS results exhibited stable behaviour (Fig. 5(a)). Compared to the metal, friction is much lower. Moreover, the dimples contributed to a further decrease from 0.1 to 0.08. As is shown in Fig. 5(b), introduction of SF led to relatively scattered results when the original acetabular cup was used. An average value of friction was around 0.29. The dimples on the cup caused that the behaviour was stabilized and the friction coefficient remarkably dropped to approximately 0.17.

In the present study, two generations of the ceramic materials were investigated. In the next series of the tests, zirconia toughened ceramic head was employed while the results of friction are plotted in Fig. 6. Contrary to previous experiments, especially during the first round of testing, PBS led to slightly fluctuating results. Average friction for PBS was around 0.16. Notwithstanding, the positive effect of the dimples could be observed, causing a drop to less than 0.1. Moreover, as is apparent from the graph, friction tendency was stabilized. In the case of SF, continuously increasing friction with each following swinging test was observed for the non-textured cup. The dimples contributed to maintain significantly lower and steady friction (Fig. 6(b)) which was reduced from around 0.36 to 0.22.

Oxinium is recognized as an advanced material for the joint prostheses combining an advantage of tough elastic core and wear resistive contact surface. The results of the friction coefficient are displayed in Fig. 7. Against expectations, oxinium head exhibited the highest friction from all the tested materials, independently of the applied lubricant. Possible causes of higher friction are discussed below. Focusing on the general effect of surface texturing, the behaviour is similar to previous observations. Friction dropped from 0.34 to 0.25 for PBS and from 0.42 to 0.38 for model SF. Assuming that the most important results regarding potential clinical application are those for simulated SF, the effect of the dimples is not as considerable in the case of oxinium. Although friction is quite high, it was reduced by less than 10% (Fig. 7(b)).

Figures 4–7 showed development of the friction coefficient for various femoral heads and lubricants. To provide a clear comparison of results, Fig. 8 and Table 2 containing evaluation summary are presented. As is clear from Fig. 8, the dimples on the cup surface led to friction reduction for all the head materials whether the contact was lubricated by PBS or SF. Focusing on the specific results for PBS solution, the dimples helped to decrease friction by 36.3% (maximum–zirconia toughened ceramic) to 19.7% (minimum–alumina ceramic). Summarizing the data for simulated SF, maximum reduction of friction was around 40% in the case of zirconia toughened ceramic. Considering the alumina ceramic and the metal, friction dropped by 38.8% and 25.5%, respectively.

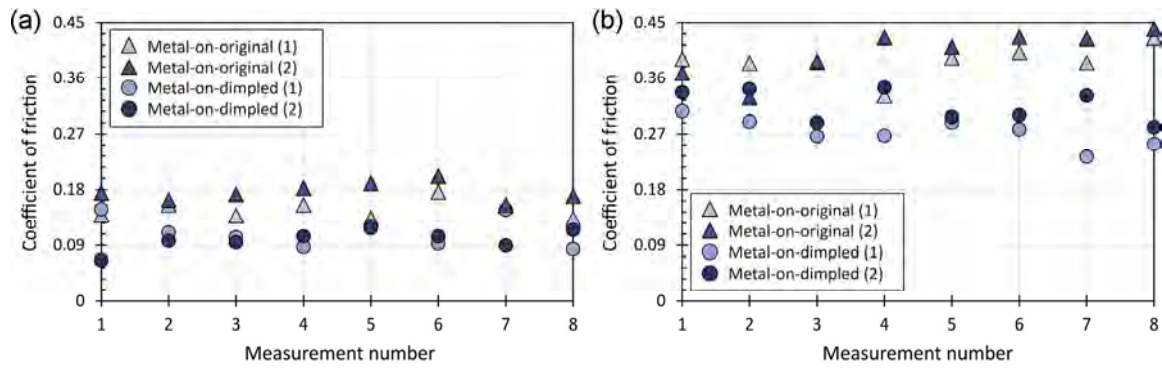


Fig. 4 Results of friction coefficient for metal femoral head using (a) PBS and (b) model SF.

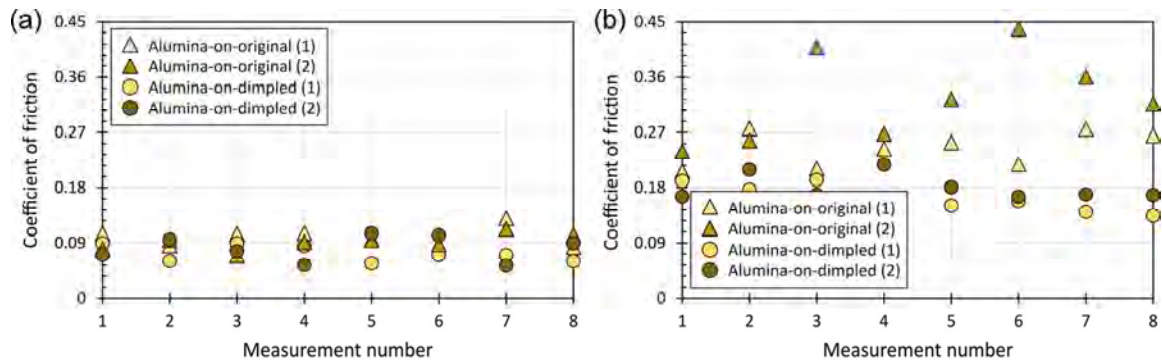


Fig. 5 Results of friction coefficient for alumina ceramic femoral head using (a) PBS and (b) model SF.

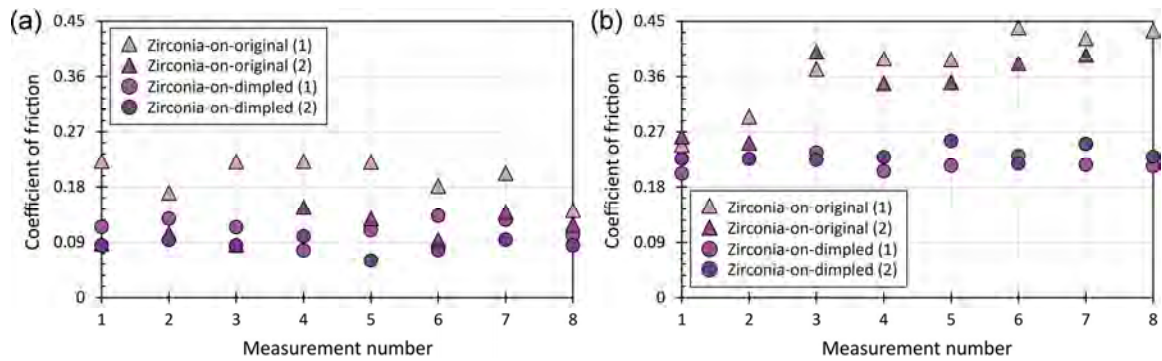


Fig. 6 Results of friction coefficient for zirconia toughened ceramic femoral head using (a) PBS and (b) model SF.

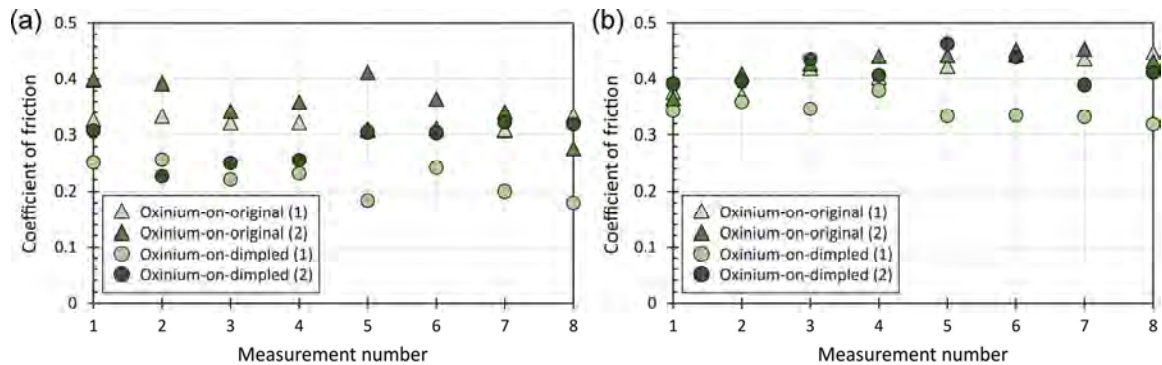


Fig. 7 Results of friction coefficient for oxinium femoral head using (a) PBS and (b) model SF.

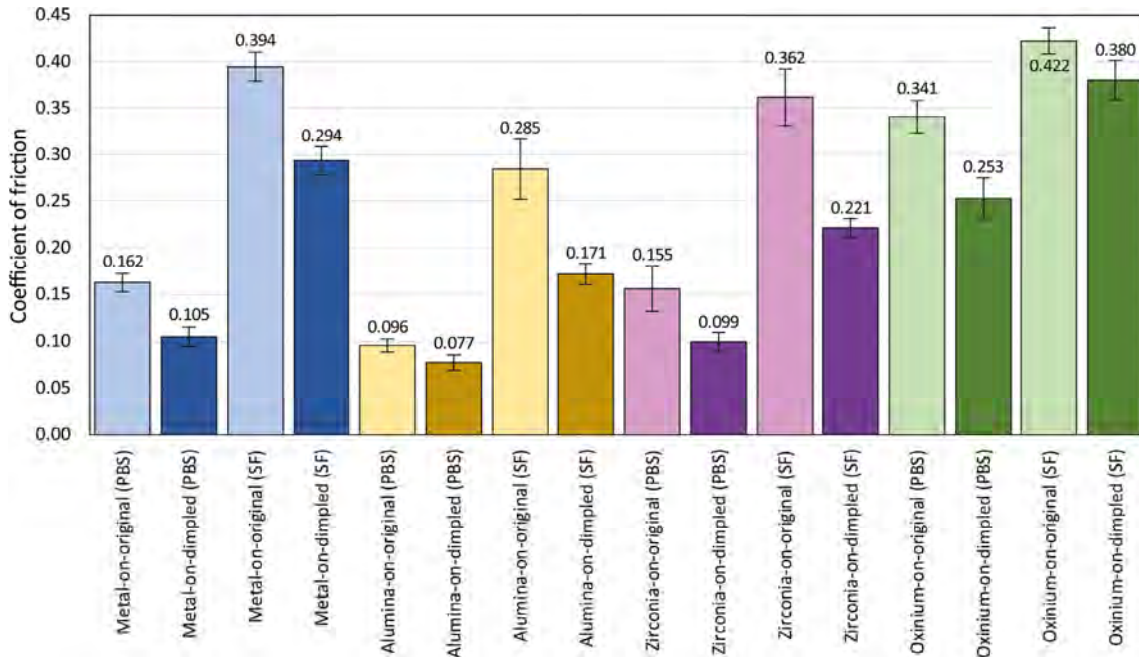


Fig. 8 Results summary (the number above each bar indicates mean coefficient of friction).

Table 2 Results summary: n = number of measurements; CoF = coefficient of friction; SD = standard deviation; % Diff. = percentage difference, i.e., decrease of friction for the dimpled cup (for mean value).

Cup	Metal femoral head							
	PBS solution (n = 16)				Synovial fluid (n = 16)			
	Median CoF	Mean CoF	SD	% Diff.	Median CoF	Mean CoF	SD	% Diff.
Original	0.159	0.162	±0.020		0.392	0.394	±0.031	
Dimpled	0.104	0.105	±0.021	-35.2%	0.289	0.294	±0.031	-25.5%
Cup	Alumina ceramic femoral head							
	PBS solution (n = 16)				Synovial fluid (n = 16)			
	Median CoF	Mean CoF	SD	% Diff.	Median CoF	Mean CoF	SD	% Diff.
Original	0.095	0.096	±0.014		0.266	0.285	±0.066	
Dimpled	0.074	0.077	±0.017	-19.7%	0.168	0.171	±0.022	-40.0%
Cup	Zirconia toughened ceramic femoral head							
	PBS solution (n = 16)				Synovial fluid (n = 16)			
	Median CoF	Mean CoF	SD	% Diff.	Median CoF	Mean CoF	SD	% Diff.
Original	0.144	0.155	±0.049		0.385	0.362	±0.062	
Dimpled	0.097	0.099	±0.020	-36.3%	0.225	0.221	±0.020	-38.8%
Cup	Oxinium femoral head							
	PBS solution (n = 16)				Synovial fluid (n = 16)			
	Median CoF	Mean CoF	SD	% Diff.	Median CoF	Mean CoF	SD	% Diff.
Original	0.334	0.341	±0.035		0.430	0.422	±0.028	
Dimpled	0.251	0.253	±0.045	-25.7%	0.385	0.380	±0.043	-9.9%

4 Discussion

Within the last few decades, lifespan of the joint replacements became a subject of many debates throughout engineering and medical disciplines [4, 33–35]. Most of the implants fail due to wear-related causes highlighting the necessity of the improved tribological performance [1, 2, 36]. Some of the studies concentrate on the development of new materials or coatings [37–40]. The limitation is that it takes a long time to bring the new materials to practice. In particular, it is necessary to consider risks associated with biocompatibility [41], long-term and complicated process of clinical testing [39], or unexpected behaviour (e.g. delamination in the case of coated implants) [42, 43]. Assuming an expected rapid increase of the joint replacements by 2030 [44], it is highly topical to find a solution which will be easy and fast to implement (a), will not endanger patients (b), and will bring a clear improvement leading to a longer implant survival (c). It is apparent that the development of material, design, or coating application is a long-term process. In order to fulfil three above requirements in a reasonable time frame, together with adequate expenditures, surface modification of the existing implants seems to be an opportunity.

The present study was aimed on evaluation of the friction coefficient of the hip joint replacements. Four commercial femoral heads and two lubricants were tested while the measurements were realized with the original and the dimpled UHMWPE acetabular cup. The research was carried out using the pendulum hip joint simulator enabling to simulate steady-state flexion-extension conditions. The dimples on the cup were fabricated using tilling manufacturing technology. The swinging tests were repeated eight times in order to get statistically relevant data. In addition, the series of experiments for both PBS and SF were repeated another day. Under most conditions, very satisfactory reproducibility of the data was observed. Small differences between the series are attributed mainly to the fact that the same (original/dented) cup was used while its position in the pendulum frame could be slightly different due to twist of the cup.

In order to show a significance of the obtained data, statistical analysis was performed. In total, 256 experiments were conducted (16 measurements for

4 head materials, 2 cups, and 2 lubricants). The data analysis showed that for most of the head-on-cup combinations, the results exhibit normal (Gauss) distribution. However, in some specific cases (alumina-on-original (SF), zirconia-on-original (PBS), and zirconia-on-original (SF), see Fig. 8) apparent data deviation was observed. This variance may be clearly seen in Figs. 5(b) and 6 for the original cup. Therefore, the relevance of these three data sets may be limited. Even though, introduction of the dimpled cup led to friction stabilization which is accompanied by a rapid decrease of a standard deviation (Table 2). Moreover, it should be emphasized that Fig. 8 displays the results of both the measurement series being analysed together. When focusing on individual sets of eight swinging tests, the repeatability and thus the statistical evidence were even better.

Focusing on the effect of the implant material, the lowest friction was observed for ceramic, followed by metal and oxinium. This is in a compliance with previous observations [22, 23, 45]. Regarding two generations of ceramic, lower friction was detected for alumina which also corresponds to literature [4]. Bit surprising is elevated friction in the case of oxinium. Oxinium head is basically metal substrate with contact surface transformed by oxygen diffusion (zirconium – 2.5% niobium alloy) from metallic to a low-friction ceramic nature [46]. Worse frictional behaviour reported in this paper is attributed to a significantly higher surface roughness resulting to the contact of surface asperities, thus leading to a transition from mixed to boundary lubrication regime [47]. In addition, diameter of the oxinium head is smaller compared to metal or ceramic. Therefore, it is suggested that the larger diametric clearance also contributes to higher friction due to insufficient lubrication conditions [10].

The difference in size of the diametric clearance considering the original and the dimpled cup needs to be clarified as well. As stated in Table 1, the difference in clearance is 110 μm while the dimpled cup exhibits generally larger clearance. In order to confirm the effect of the dimples, it is referred to previously published study using the same simulator and following the same experimental procedure [23]. In that case, the implants of nominal diameters of 28 and 36 mm supplied by two various producers were investigated. It should be noted that the difference in clearance

for both metal-on-PE and ceramic-on-PE pairs was always higher than that in the present study. Nevertheless, despite a significant clearance difference, variance in friction was very limited for most of the tested couples. In addition, larger clearance usually led to higher friction. Thus, it is assumed that the lower friction observed for the dimpled cups (having larger clearance) in the present paper may be attributed mainly to the dimple effect.

Behaviour of the joint replacements is indisputably influenced by the properties of the lubricant. Human synovial joints are lubricated by SF. Ability of film formation and viscosity of SF are driven especially by content and ratio of the included constituents [48, 49]. An issue of optimal model fluid for laboratory tests, suitably mimicking human body conditions, is often discussed. The authors commonly employ bovine serum (BS) solution with given overall protein content [50]. However, the content of specific constituents is rarely declared in the case of BS. Moreover, the composition may vary producer to producer as well as series to series. Therefore, it is suggested that despite the number of studies employing BS, it might be not an optimal equivalent lubricant mimicking the behaviour of human SF [51, 52]. Following this implication, the model SF was designed while the detailed composition is stated above. The concentration of the constituents is based on evaluation of the samples of human SF extracted from the patients during surgeries [53]. The designed fluid composition corresponds to a physiological level. Other sets of the tests were performed with PBS to get a reference. Independently of the head material, PBS exhibited lower friction compared to simulated SF. This confirms previous findings that the proteins cause a rapid increase of friction considering the metal/ceramic-on-PE contact pair [30, 54–56].

Focusing on the particular values of friction, the data seem to be higher than usually reported. However, it must be emphasized that the most of the studies describing very low friction factors often deal with a simplified configuration (e.g., pin-on-disc) considering low loads at low speeds. Therefore, comparable results come from the experiments performed using the hip simulator employing real ball-on-cup model [22, 23, 45]. In all the mentioned studies, 25% BS was used as the test lubricant. When comparing the results for

metal and ceramic heads, friction observed in Refs. [22, 23] was nearly double compared to that presented in Ref. [45].

Generally higher friction coefficient is attributed mainly to the increased concentration of SF constituents which is indisputably higher than in the case of 25% BS. In addition, it is assumed that higher concentration of albumin (20 mg/ml) is responsible for elevated friction as previously shown [54]. The level of applied load may contribute as well. As is stated in materials and methods section, the applied load was designed in order to mimic average physiological load effect throughout the walking cycle. However, the lower load causes the phenomenon of slippage at the moment of pendulum reversal. According to our previous experience, when higher load is applied, slippage during reversal is mitigated, thus leading to lower friction. Finally, it should be emphasized that the arrangement of the ball and the cup is in inversed position to enable the contact to be fully flooded which may also play a role. Therefore, it is assumed that higher friction is due to a combination of higher protein concentration (a), substantially higher content of albumin (b), lower level of load (c), and inversed geometrical arrangement (d). However, when investigating the behaviour of the joint replacements, it should be emphasized that the specific value of friction/wear rate/film thickness is not as decisive. The importance comes from the general comparison of the effect of various inputs on the observed parameter. Therefore, the main outcome of the introduced paper is the percentage difference in friction considering the original and the dimpled cup.

Regarding the potential implication for practice, the important findings are related to model SF behaviour (Table 2, Figs. 4(b), 5(b), 6(b), and 7(b)). Independently of the head material, friction was significantly reduced by introducing the dimples. The highest reduction rate was observed for alumina ceramic (40%) followed by zirconia toughened ceramic (38.8%), metal (25.5%), and oxinium (9.9%). As can be seen, the lower initial friction, the larger friction reduction for simulated SF. Moreover, it is assumed that reduction of wear would be even higher than reduction of friction. As was shown by Roy et al. [21], who studied pin-on-disc contact of ceramic counterfaces, surface texturing led to 22% friction reduction, resulting in

53% wear rate reduction. Thus, it is expected that even in the case of oxinium, exhibiting relatively insignificant friction reduction, wear rate might be lowered substantially.

Another benefit of the dimples can be observed especially in the case of the ceramic heads. Introduction of the dimples led to evident stabilization of the friction coefficient, indicating more favourable contact conditions (Figs. 5(b) and 6(b)). When thinking about the mechanism of friction reduction, it is suggested that there are two essential factors. Enhanced lubricant film formation due to storage of the fluid within the cavities is considered to be the first factor [16]. The second point is the reduced contact asperity ratio eventually contributing to improved lubrication conditions [24]. The second statement is supported by the results of oxinium head having higher surface roughness, thus resulting to limited dimple effect.

Positive role of the dimples was already pronounced in both experimental [16–22] and numerical [24–26] studies. However, the previous papers considered hard (metal/ceramic) surfaces to be textured. An explanation for such motivation seems to be logical. At first, it is much easier to make the texture on the hard convex shape. Moreover, it is suggested that the dimples on a soft matter material (such as PE) might be removed after some time due to articulation of surfaces. Nevertheless, this might be a key. As mentioned in introduction part, wear is progressive especially during running-in phase. Subsequently, the process is stabilized with slowly and continuously increasing wear rate [5, 6]. Although there is a substantial contribution of PE creep during running-in [6, 57, 58], friction doubtlessly plays a role as well. Therefore, it is concluded that the dimples made on UHMWPE cup are able to diminish running-in friction and wear. After some time, the surface of the cup is polished due to articulation having positive effect on surface roughness. This leads to a reduction of the contact asperity ratio, enabling the implant to operate smoothly for longer time.

The amount of wear particles released during running-in period can be hardly estimated. Nevertheless, it is expected that wear rate might be lowered significantly, since it was shown that wear reduction well correlates to friction reduction [59]. The authors feel a strong motivation for further investigation. The

present results are fundamental. Nevertheless, there is a lot of aspects which need to be clarified in future research. The main attention should be paid to finding the optimal parameters of the dimples in terms of the geometry and the surface coverage ratio in order to maximize friction reduction.

The authors admit the limitations of the pendulum simulator. However, it should be emphasized that the pendulum has been representing well-established tool for friction investigation of the joint replacements for decades. It has been used not only by the scientists, it can be found in laboratories of producers of the implants as well. Assuming the importance of surface conformity, number of studies using multi-directional test stations when measuring friction is very limited so far [60–62]. Moreover, the pendulum is sometimes used in order to validate the multi-axial measurements [63]. Therefore, the authors are convinced that despite the simplified loading and kinematic conditions, the pendulum provides valuable data regarding further development of the implants. Positive role of the dimples should be confirmed also in terms of wear using multi-directional hip simulators with transient kinematic and loading conditions to better mimic *in vivo* situation. Simultaneous monitoring of wear and friction represents a challenging task for further studies. The effect of the combination of the textured cup and the textured head should be clarified as well.

A further shortcoming of the present paper is the use of limited number of the cups. It should be noted that only one dimpled cup was available for this study. After the manufacturing, the shape and the dimensions were carefully checked while the dimples were fabricated subsequently. Regarding the original cup, detailed shape, surface, and dimension analysis of three commercial implants was conducted with the use of 3D optical scanning [29] and optical profiler. Based on the analysis, the cup exhibiting minimum sphericity deviation together with the required roughness and the actual diameter was used. In order to prevent results influence due to wear of the cups, a sequence of the experiments with the given fluids was kept the same (firstly PBS, then SF). Also an order of the heads was the same (metal, alumina, zirconia, and oxinium). Nevertheless, it should be noted that despite the number of the experiments, there was almost no wear. The imaging using laser

microscope showed that the number of scratches was very limited. Therefore, it is assumed that the results should not be affected by the fact that only two cups (one original and one dimpled) were used.

Focusing on the limitations of the present paper, the performed study was purely experimental. In order to confirm the observed phenomena, numerical solution would be helpful. The research team has been involved in the development of numerical model for the determination of lubricant film thickness within the hip implant. It is suggested that in future, this model should be further developed in order to enable estimation of the coefficient of friction. Then, the effect of the textured geometry could be easily verified by means of numerical simulation.

5 Conclusions

According to author's best knowledge, the present study introduces the first experimental investigation of frictional behaviour of the hip joint replacements using the surface-textured UHMWPE acetabular cup. The main findings can be summarized in the following points.

1) The tilling technology enables to manufacture very precise dimples on the shaped soft-matter surfaces without undesirable sleeves occurring due to thermal influence of the surface in the case of laser texturing.

2) Under lubrication by model SF, the dimples on the cup surface led to a significant reduction of friction independently of the head material. In addition, the textured cup exhibited stabilized frictional behaviour without sudden fluctuations.

3) The texturing of PE acetabular cups represents an easy, time and cost undemanding, and apparently effective way to lower running-in friction of the joint replacements. Moreover, since conventional, well-established materials may be used, there is no threat for the patients associated with clinical testing of new materials or coating layers.

4) It is deeply believed that lower friction during running-in phase substantially reduces running-in wear. This may slow down the overall wear process which eventually leads to extended service life of the implants. If this assumption would be confirmed by long-term wear test and clinical study, introduction

of surface texturing would improve the life quality of millions of patients and would save an amount of financial costs associated with the revising operations.

Acknowledgements

The research was carried out under the project JSPS/OF280, PE17046 with financial support from the Japan Society for the Promotion of Science. This research was also supported by the project FSI-S-17-4415 with financial support from the Ministry of Education, Youth and Sports of the Czech Republic (MEYS). The study was also supported by the project LTAUSA17150 with financial support from MEYS. The authors would like to thank Kanefusa Corporation for dimple manufacturing and M. Černohlávek for his help with the experiments.

Open Access This article is licensed under a Creative Commons Attribution 4.0 International License, which permits use, sharing, adaptation, distribution and reproduction in any medium or format, as long as you give appropriate credit to the original author(s) and the source, provide a link to the Creative Commons licence, and indicate if changes were made.

The images or other third party material in this article are included in the article's Creative Commons licence, unless indicated otherwise in a credit line to the material. If material is not included in the article's Creative Commons licence and your intended use is not permitted by statutory regulation or exceeds the permitted use, you will need to obtain permission directly from the copyright holder.

To view a copy of this licence, visit <http://creativecommons.org/licenses/by/4.0/>.

References

- [1] Gallo J, Goodman S B, Kontinen Y T, Wimmer M A, Holinka M. Osteolysis around total knee arthroplasty: A review of pathogenetic mechanisms. *Acta Biomater* **9**(9): 8046–8058 (2013)
- [2] Gallo J, Vaculova J, Goodman S B, Kontinen Y T, Thyssen J P. Contributions of human tissue analysis to understanding the mechanisms of loosening and osteolysis in total hip replacement. *Acta Biomater* **10**(6): 2354–2366 (2014)

- [3] Tandon P N, Jaggi S. Wear and lubrication in an artificial knee joint replacement. *Int J Mech Sci* **23**(7): 413–422 (1981)
- [4] Rieker C B. Tribology of total hip arthroplasty prostheses: What an orthopaedic surgeon should know. *EFORT Open Rev* **1**(2): 52–57 (2016)
- [5] Penmetsa J R, Laz P J, Petrella A J, Rullkoetter P J. Influence of polyethylene creep behavior on wear in total hip arthroplasty. *J Orthop Res* **24**(3): 422–427 (2006)
- [6] Zeman J, Ranuša M, Vrbka M, Gallo J, Křupka I, Hartl M. UHMWPE acetabular cup creep deformation during the run-in phase of THA's life cycle. *J Mech Behav Biomed Mater* **87**: 30–39 (2018)
- [7] Myant C, Cann P. On the matter of synovial fluid lubrication: Implications for Metal-on-Metal hip tribology. *J Mech Behav Biomed Mater* **34**: 338–348 (2014)
- [8] Vrbka M, Nečas D, Hartl M, Křupka I, Urban F, Gallo J. Visualization of lubricating films between artificial head and cup with respect to real geometry. *Biotribology* **1–2**: 61–65 (2015)
- [9] Myant C W, Cann P. The effect of transient conditions on synovial fluid protein aggregation lubrication. *J Mech Behav Biomed Mater* **34**: 349–357 (2014)
- [10] Nečas D, Vrbka M, Urban F, Gallo J, Křupka I, Hartl M. In situ observation of lubricant film formation in THR considering real conformity: The effect of diameter, clearance and material. *J Mech Behav Biomed Mater* **69**: 66–74 (2017)
- [11] Nečas D, Vrbka M, Galandáková A, Křupka I, Hartl M. On the observation of lubrication mechanisms within hip joint replacements. Part I: Hard-on-soft bearing pairs. *J Mech Behav Biomed Mater* **89**: 237–248 (2019)
- [12] Nečas D, Vrbka M, Rebenda D, Gallo J, Galandáková A, Wolfová L, Křupka I, Hartl M. In situ observation of lubricant film formation in THR considering real conformity: The effect of model synovial fluid composition. *Tribol Int* **117**: 206–216 (2018)
- [13] Ali F, Křupka I, Hartl M. Reducing the friction of lubricated nonconformal point contacts by transverse shallow microgrooves. *Proc Inst Mech Eng Part J J Eng Tribol* **229**(4): 420–428 (2015)
- [14] Gachot C, Rosenkranz A, Hsu S M, Costa H L. A critical assessment of surface texturing for friction and wear improvement. *Wear* **372–373**: 21–41 (2017)
- [15] Usami H, Sato T, Kanda Y, Nishio S. Applicability of Interrupted Micro Cutting Process “Tilling” as Surface Texturing. *Key Eng Mater* **749**: 241–245 (2017)
- [16] Ito H, Kaneda K, Yuhta T, Nishimura I, Yasuda K, Matsuno T. Reduction of polyethylene wear by concave dimples on the frictional surface in artificial hip joints. *J Arthroplasty* **15**(3): 332–338 (2000)
- [17] Sawano H, Warisawa S, Ishihara S. Study on long life of artificial joints by investigating optimal sliding surface geometry for improvement in wear resistance. *Precis Eng* **33**(4): 492–498 (2009)
- [18] Borjali A, Langhorn J, Monson K, Raeymaekers B. Using a patterned microtexture to reduce polyethylene wear in metal-on-polyethylene prosthetic bearing couples. *Wear* **392–393**: 77–83 (2017)
- [19] Langhorn J, Borjali A, Hippensteel E, Nelson W, Raeymaekers B. Microtextured CoCrMo alloy for use in metal-on-polyethylene prosthetic joint bearings: Multi-directional wear and corrosion measurements. *Tribol Int* **124**: 178–183 (2018)
- [20] Cho M, Choi H J. Optimization of surface texturing for contact between steel and ultrahigh molecular weight polyethylene under boundary lubrication. *Tribol Lett* **56**(3): 409–422 (2014)
- [21] Roy T, Choudhury D, Ghosh S, Mamat A B, Pingguan-Murphy B. Improved friction and wear performance of micro dimpled ceramic-on-ceramic interface for hip joint arthroplasty. *Ceram Int* **41**(1): 681–690 (2015)
- [22] Choudhury D, Vrbka M, Mamat A B, Stavness I, Roy C K, Mootanah R, Krupka I. The impact of surface and geometry on coefficient of friction of artificial hip joints. *J Mech Behav Biomed Mater* **72**: 192–199 (2017)
- [23] Vrbka M, Nečas D, Bartošík J, Hartl M, Křupka I, Galandáková A, Gallo J. Determination of a Friction Coefficient for THA Bearing Couples. *Acta Chir Orthop Traumatol Čech* **82**(5): 341–347 (2015)
- [24] Gao L M, Yang P R, Dymond I, Fisher J, Jin Z M. Effect of surface texturing on the elastohydrodynamic lubrication analysis of metal-on-metal hip implants. *Tribol Int* **43**(10): 1851–1860 (2010)
- [25] Gao L M, Hua Z K, Hewson R, Andersen M S, Jin Z M. Elastohydrodynamic lubrication and wear modelling of the knee joint replacements with surface topography. *Biosurf Biotribol* **4**(1): 18–23 (2018)
- [26] Chyr A, Qiu M F, Speltz J W, Jacobsen R L, Sanders A P, Raeymaekers B. A patterned microtexture to reduce friction and increase longevity of prosthetic hip joints. *Wear* **315**(1–2): 51–57 (2014)
- [27] Choudhury D, Rebenda D, Sasaki S, Hekrle P, Vrbka M, Zou M. Enhanced lubricant film formation through micro-dimpled hard-on-hard artificial hip joint: An *in-situ* observation of dimple shape effects. *J Mech Behav Biomed Mater* **81**: 120–129 (2018)
- [28] Stanton T E. Boundary lubrication in engineering practice. *Engineer* **29**: 678–680 (1923)
- [29] Ranuša M, Gallo J, Vrbka M, Hobza M, Paloušek D,

- Křupka I, Hartl M. Wear analysis of extracted polyethylene acetabular cups using a 3D optical scanner. *Tribol Trans* **60**(3): 437–447 (2017)
- [30] Nečas D, Sawae Y, Fujisawa T, Nakashima K, Morita T, Yamaguchi T, Vrbka M, Křupka I, Hartl M. The Influence of proteins and speed on friction and adsorption of metal/UHMWPE contact pair. *Biotribology* **11**: 51–59 (2017)
- [31] Sawae Y, Murakami T, Chen J. Effect of synovia constituents on friction and wear of ultra-high molecular weight polyethylene sliding against prosthetic joint materials. *Wear* **216**(2): 213–219 (1998)
- [32] Mavraki A, Cann P M. Lubricating film thickness measurements with bovine serum. *Tribol Int* **44**(5): 550–556 (2011)
- [33] Evans J T, Walker R W, Evans J P, Blom A W, Sayers A, Whitehouse M R. How long does a knee replacement last? A systematic review and meta-analysis of case series and national registry reports with more than 15 years of follow-up. *Lancet* **393**(10172): 655–663 (2019)
- [34] di Puccio F, Mattei L. Biotribology of artificial hip joints. *World J Orthop* **6**(1): 77–94 (2015)
- [35] Isaac G H. Life cycle aspects of total replacement hip joints. *Tribol Interface Eng Ser* **48**: 147–160 (2005)
- [36] Rao A J, Gibon E, Ma T, Yao Z Y, Smith R L, Goodman S B. Revision joint replacement, wear particles, and macrophage polarization. *Acta Biomater* **8**(7): 2815–2823 (2012)
- [37] Lappalainen R, Santavirta S S. Potential of coatings in total hip replacement. *Clin Orthop Relat Res* **430**: 72–79 (2005)
- [38] Choudhury D, Lackner J M, Major L, Morita T, Sawae Y, Mamat A B, Stavness I, Roy C K, Krupka I. Improved wear resistance of functional diamond like carbon coated Ti–6Al–4V alloys in an edge loading conditions. *J Mech Behav Biomed Mater* **59**: 586–595 (2016)
- [39] Haider H, Weisenburger J N, Namavar F, Garvin K L. Why coating technologies for hip replacement systems, and the importance of testing them in vitro. *Oper Tech Orthop* **27**(3): 152–160 (2017)
- [40] Balla V K, Banerjee S, Bose S, Bandyopadhyay A. Direct laser processing of a tantalum coating on titanium for bone replacement structures. *Acta Biomater* **6**(6): 2329–2334 (2010)
- [41] Goodman S B, Gómez Barrena E, Takagi M, Kontinen Y T. Biocompatibility of total joint replacements: A review. *J Biomed Mater Res A* **90A**(2): 603–618 (2009)
- [42] Rahaman M N, Huang T, Bal B S, Li Y. In vitro testing of Al₂O₃–Nb composite for femoral head applications in total hip arthroplasty. *Acta Biomater* **6**(2): 708–714 (2010)
- [43] Łapaj Ł, Markuszewski J, Wendland J, Mróz A, Wierusz-Kozłowska M. Massive failure of TiNbN coating in surface engineered metal-on-metal hip arthroplasty: Retrieval analysis. *J Biomed Mater Res B Appl Biomater* **104**(5): 1043–1049 (2016)
- [44] Kurtz S, Ong K, Lau E, Mowat F, Halpern M. Projections of primary and revision hip and knee arthroplasty in the United States from 2005 to 2030. *J Bone Joint Surg Am* **89**(4): 780–785 (2007)
- [45] Brockett C, Williams S, Jin Z M, Isaac G, Fisher J. Friction of total hip replacements with different bearings and loading conditions. *J Biomed Mater Res B Appl Biomater* **81B**(2): 508–515 (2007)
- [46] Ozden V E, Saglam N, Dikmen G, Tozun I R. Oxidized zirconium on ceramic; Catastrophic coupling. *Orthop Traumatol Surg Res* **103**(1): 137–140 (2017)
- [47] Sagbas B. Biotribology of artificial hip joints. In *Advances in Tribology*. Darji P H, Ed. Croatia: InTechOpen, 2016.
- [48] Park J B, Duong C T, Chang H G, Sharma A R, Thompson M S, Park S, Kwak B C, Kim T Y, Lee S S, Park S. Role of hyaluronic acid and phospholipid in the lubrication of a cobalt–chromium head for total hip arthroplasty. *Biointerphases* **9**(3): 031007 (2014)
- [49] Smith A M, Fleming L, Wudebwe U, Bowen J, Grover L M. Development of a synovial fluid analogue with bio-relevant rheology for wear testing of orthopaedic implants. *J Mech Behav Biomed Mater* **32**: 177–184 (2014)
- [50] Essner A, Schmidig G, Wang A G. The clinical relevance of hip joint simulator testing: In vitro and in vivo comparisons. *Wear* **259**(7–12): 882–886 (2005)
- [51] Parkes M, Myant C, Cann P M, Wong J S S. Synovial fluid lubrication: The effect of protein interactions on adsorbed and lubricating films. *Biotribology* **1–2**: 51–60 (2015)
- [52] Mazzucco D, McKinley G, Scott R D, Spector M. Rheology of joint fluid in total knee arthroplasty patients. *J Orthop Res* **20**(6): 1157–1163 (2002)
- [53] Galandáková A, Ulrichová J, Langová K, Hanáková A, Vrbka M, Hartl M, Gallo J. Characteristics of synovial fluid required for optimization of lubrication fluid for biotribological experiments. *J Biomed Mater Res B Appl Biomater* **105**(6): 1422–1431 (2017)
- [54] Crockett R, Roba M, Naka M, Gasser B, Delfosse D, Frauchiger V, Spencer N D. Friction, lubrication, and polymer transfer between UHMWPE and CoCrMo hip-implant materials: A fluorescence microscopy study. *J Biomed Mater Res A* **89A**(4): 1011–1018 (2009)
- [55] Gispert M P, Serro A P, Colaço R, Saramago B. Friction and wear mechanisms in hip prosthesis: Comparison of joint materials behaviour in several lubricants. *Wear* **260**(1–2): 149–158 (2006)
- [56] Guezmil M, Bensalah W, Mezlini S. Tribological behavior of UHMWPE against TiAl₆V₄ and CoCr₂₈Mo alloys under

- dry and lubricated conditions. *J Mech Behav Biomed Mater* **63**: 375–385 (2016)
- [57] Engh C A Jr, Stepniewski A S, Ginn S D, Beykirch S E, Sychterz-Terefenko C J, Hopper R H Jr, Engh C A. A randomized prospective evaluation of outcomes after total hip arthroplasty using cross-linked marathon and non-cross-linked enduron polyethylene liners. *J Arthroplasty* **21**(6): 17–25 (2006)
- [58] Higuchi Y, Seki T, Morita D, Komatsu D, Takegami Y, Ishiguro N. Comparison of wear rate between ceramic-on-ceramic, metal on highly cross-linked polyethylene, and metal-on-metal bearings. *Rev Bras Ortop* **54**(3): 295–302 (2019)
- [59] Wang A, Essner A, Klein R. Effect of contact stress on friction and wear of ultra-high molecular weight polyethylene in total hip replacement. *Proc Inst Mech Eng H J Eng Med* **215**(2): 133–139 (2001)
- [60] Damm P, Dymke J, Ackermann R, Bender A, Graichen F, Halder A, Beier A, Bergmann G. Friction in total hip joint prosthesis measured *in vivo* during walking. *PLoS One* **8**(11): e78373 (2013)
- [61] Kaddick C, Malczan M, Buechele C, Hintner M, Wimmer M A. On the measurement of three-dimensional taper moments due to friction and contact load in total hip replacement. In *Modularity and Tapers in Total Joint Replacement Devices*. Greenwald A, Kurtz S, Lemons J, Mihalko W, Eds. West Conshohocken, PA: ASTM International, 2015.
- [62] Haider H, Weisenburger J N, Garvin K L. Simultaneous measurement of friction and wear in hip simulators. *Proc Inst Mech Eng H J Eng Med* **230**(5): 373–388 (2016)
- [63] Sonntag R, Braun S, Al-Salehi L, Reinders J, Mueller U, Kretzer J P. Three-dimensional friction measurement during hip simulation. *PLoS One* **12**(9): e0184043 (2017)



David NEČAS. He received his B.S., M.S., and Ph.D. degrees in mechanical engineering from Brno University of Technology, Czech Republic, in 2010, 2012, and 2016, respectively. His current position is an assistant professor and member of

Biotribology Research Group at Institute of Machine and Industrial Design, Faculty of Mechanical Engineering, Brno University of Technology. His research areas cover friction and lubrication of joint replacements, tribological performance of articular cartilage, and soft EHL lubrication.



Hatsuhiko USAMI. He received his B.S. degree from Meijo University, and M.S. and Ph.D. degrees in mechanical engineering from Nagoya Institute of Technology, Japan. From 1995, he has been working for

Mechanical Engineering Department of Meijo University. His current position is a professor and a member of Materials Science and Engineering Department. His research areas focus on material design including surface modification and texturing for tribological application.



Tatsuya NIIMI. He received his B.S. degree in electrical and electronic engineering from Gifu University, Japan, in 2010. His current

position is an engineer of Kanefusa Corporation. His research areas cover effects of surface texture fabricated by interrupted micro cutting on tribological properties.



Yoshinori SAWAE. He received his B.S., M.S., and Dr. Eng. degrees in mechanical engineering from Kyushu University, Japan, in 1991, 1993, and 1997, respectively. He joined Department of Mechanical Engineering, Faculty of Engineering,

Kyushu University as a lecturer in 1996 and became a professor of Machine Elements and Design Engineering Laboratory in 2011. His primal research area is biotribology, especially working on the *in vivo* wear mechanism of prosthetic joint materials and the lubrication mechanism of natural synovial joint.



Ivan KŘUPKA. He received his M.S. and Ph.D. degrees in mechanical engineering from Brno University of Technology, Czech Republic, in 1990 and 1997, respectively. His current position is a professor and

head of Tribology Group, Institute of Machine and Industrial Design, Faculty of Mechanical Engineering, Brno University of Technology. His research areas cover the mixed and elastohydrodynamic lubrication, surface texturing effect, and lubricant rheology.



Martin HARTL. He received his M.S. and Ph.D. degrees in mechanical engineering from Brno University of Technology, Czech Republic, in 1990 and 1997, respectively. His current position is a professor and

head of Institute of Machine and Industrial Design, Faculty of Mechanical Engineering, Brno University of Technology. His research areas cover the boundary, mixed and elastohydrodynamic lubrication, roughness effect, and biotribology.

3

LUBRICATION OF HIP JOINT REPLACEMENTS

The previous chapter summarised the findings regarding the friction of the joint prosthesis. However, the resulting friction is indisputably associated with lubrication processes. As highlighted in the introduction, natural cartilage provides an outstanding lubrication performance, while several studies aimed at understanding the cartilage lubrication mechanisms. Various lubrication regimes such as weeping, squeeze film, boosted lubrication, hydration lubrication, or biphasic lubrication were introduced [81]-[84]. Instead, artificial hip joints are supposed to operate mainly in a boundary or mixed and rarely in the fluid film regime [51],[85]. Nevertheless, the particular importance of lubrication of artificial joints needs to be considered towards the prolonged durability of implants [86],[87]. Natural cartilage may be inspiring for further development; however, the detailed understanding of the lubrication processes of the implants is essential.

Film thickness, lubricant flow, protein adsorption, and the behaviour of specific SF constituents represent the main concerns of lubrication studies. As in the case of friction, *in vivo* investigations of lubrication may be hardly realised. Therefore, alternative approaches need to be employed while both numerical and experimental studies have been proposed. Apparently, both ways exhibit some advantages and disadvantages.

A relatively simple implementation of realistic ball-in-socket geometry represents one of the main benefits of numerical modelling. A further advantage of modelling is in the ability to easily modify input parameters such as materials, lubricant properties, or operating conditions. Nevertheless, even numerical approaches often suffer from several limitations such as the consideration of simplified geometry (see Fig. 21), simplified dynamics, non-realistic characteristics of the lubricant, or even the full absence of the lubricant. Moreover, the protein adsorption extensively discussed in the previous chapter may be only hardly simulated. Some studies dealt with adsorption in a microscale, but typical numerical papers exploring the behaviour of implants neglect this phenomenon. Concerning the experimental investigations, approaching realistic conditions may be even more challenging. Standard materials of implants are non-transparent, disabling the direct contact observation. Furthermore, except MoM pairs, the materials are non-conductive, limiting the approaches based on the measurement of electrical quantities. The application of realistic kinematic and loading conditions may also be hardly simulated using simplified testers, i.e. pin-on-disc (-plate) or ball-on-disc (-plate). Therefore, particular assumptions are often adopted in experimental studies, as is described below.

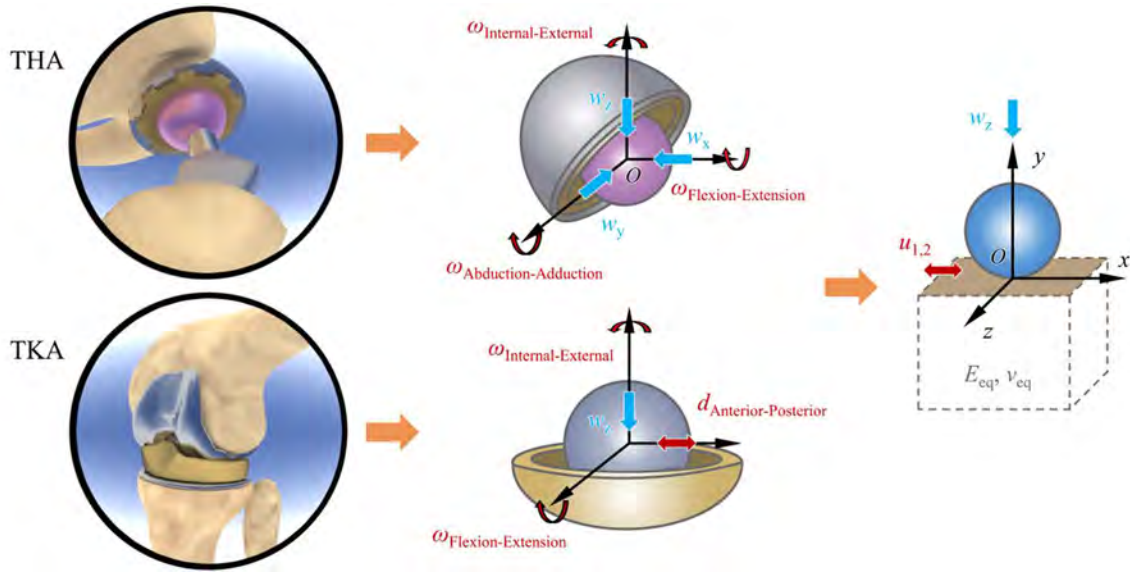


Figure 21: Simplification of the geometry of THR and TKR often adopted in numerical simulations.

3.1 Numerical investigations

It should be noted that the author of the habilitation thesis is interested mostly in experimental investigations. However, two papers proving the author's contribution (one in Chapter 3 and another in Chapter 4) are based on the application of numerical modelling. Therefore, a general overview of the articles focused on the modelling of THRs, without paying specific attention to the detailed description, is provided below.

Numerical studies often aim at the prediction of film thickness, indicating the prevalent lubrication regime. Jin et al. [88] predicted the minimum film thickness in MoM, CoC, and MoP implants, adopting traditional proximity equations based on elastohydrodynamic lubrication (EHL) theory. Isoviscous Newtonian nature of the lubricant and elastic deformations of the contacting bodies were considered. Using a simplified equivalent ball-on-plane model, the authors suggested that hard pairs may operate in the fluid film regime when the very low surface roughness is achieved, and the radial clearance is small. Otherwise, a mixed regime is typical for MoM and CoC pairs. MoP couplings mostly operate in the boundary regime. The authors further highlighted the importance of contact mechanics, finding a clear correlation of contact width and the film thickness. Jin and Dowson [89] extended the study, implementing a full numerical solution based on the Reynolds equation in spherical coordinates for hard pairs. The authors considered three-dimensional load and speed variations mimicking steady walking. The combined effect of squeeze film and entraining action is predicted based on the solution, allowing to develop a certain film during the cycle. The importance of implant design in terms of geometry and clearance was also underlined. The contribution of a smaller clearance towards the transition from mixed to fluid film regime for MoM pairs under realistic walking conditions was subsequently confirmed by the analysis performed by Udofia and Jin [90].

Ball-in-socket model of MoP pair was studied by Jagatia et al. [91]. The authors implemented a simultaneous solution of the Reynolds equation using Newton-Raphson (N-R)

method and elasticity equation based on the finite element method (FEM) and constrained column model to predict UHMWPE cup deformation. The calculated film thickness was compared with a simple analytical solution [92], finding a good correlation between both approaches. The authors analysed the important influencing parameters, highlighting the implant geometry, cup thickness, and elastic modulus of the polymer surface. The same procedure was subsequently adopted also for MoM pair [93]. The predicted minimum film thickness based on the numerical solution was very similar to that calculated for the simplified ball-on-plane model proposed earlier by Hamrock and Dowson [94], which was later confirmed by Jalali-Vahid et al. [95], who performed isoviscous EHL analysis of point contact. Therefore, a simple ball-on-plane model was later considered when investigating the effect of dynamic load and speed, indicating the importance of the swing phase [96]. The role of start-up motion on the predicted film thickness was also investigated, finding a negligible impact. The film was built right after the simulation started, which is vital for short-term laboratory testing [97]. However, the simplified geometrical configuration was found to be insufficient for hard-on-soft pairs, where it led to an overestimation of the predicted film thickness [98].

The comparison of estimated film thickness in the natural and artificial hip joint was carried out by Jalali-Vahid et al. [99]. The authors compared ball-on-plane and full ball-in-socket models, finding that the predicted film thickness in the natural joint is fivefold higher than that of the artificial MoP pair. The study was extended, revealing that a thicker lubricating film may be achieved for larger femoral heads, combined with smaller clearance, increased cup thickness, and the lower elastic modulus of the cup (see Fig. 22) [100]. Nevertheless, it is assumed that the typical film thickness in hip implants is in the range of surface roughness, indicating the prevalence of the mixed lubrication regime.

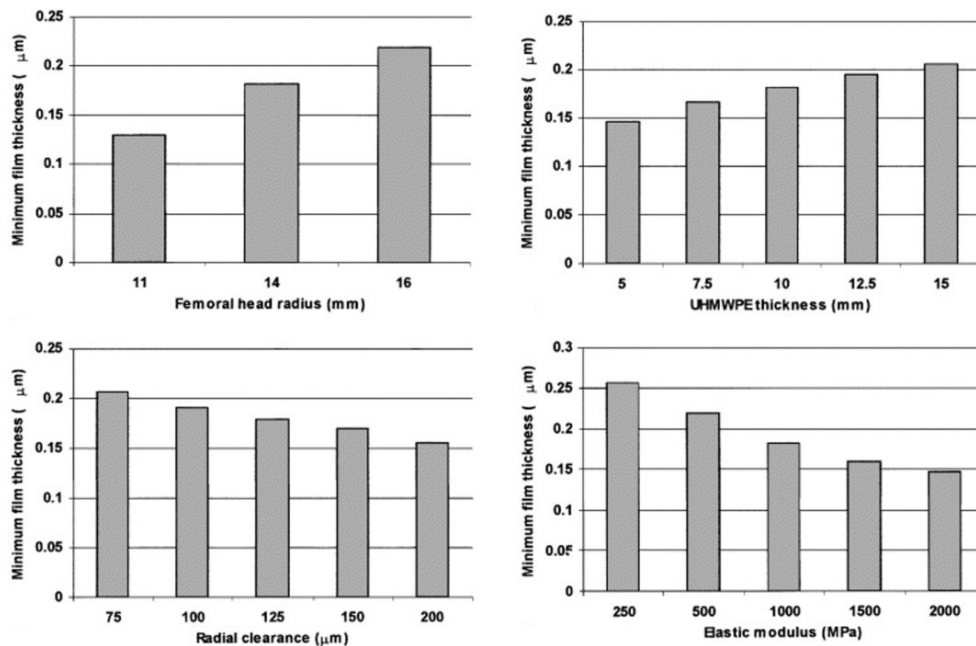


Figure 22: The effect of femoral head radius, radial clearance, UHMWPE cup thickness, and UHMWPE cup elastic modulus on predicted minimum film thickness using the ball-in-socket model.

The figure was partially modified and reprinted based on [100].

The authors subsequently conducted a time-transient analysis of MoP and CoP pairs using the above-developed models [101]. Regardless of considerable changes of both the angular velocity and the load, the predicted minimum film thickness remained constant. It is suggested that the lubrication behaviour is given by a combined action of entraining and squeeze film action, which corresponds to the previous work [89]. It is further shown that the values of film thickness based on transient analysis are in good agreement with the prediction based on EHL calculation under quasi-static conditions using averaged speed and load [102].

Later, Wang and Jin [103] adopted the above model [101], solving the Reynolds equation by N-R method with finite-difference discretization. The deformation of the metal head and either polymer or metal cup was solved by spherical fast Fourier transformation (SFFT) approach. The calculated parameters corresponded to those obtained using FEM. The introduced system thus allowed for getting relevant data at substantially reduced computational times. It is suggested that the technique is suitable for analysing hip implants considering transient conditions and realistic surface topography. The authors also provided an important implication for experimental studies, referring to the importance of various aspects related to THR function. Specifically, it was found that both the inclination angle and IE rotation have a negligible effect on the predicted film thickness, while a particular role of FE motion was highlighted [104]. The introduced SFFT method was subsequently adopted also for hard pairs, allowing for optimized efficiency of the calculations considering the dynamic loading and kinematic parameters [105]. Under transient conditions, the squeeze film effect considerably contributed to the resulting film thickness. The contribution was evident mainly at the reversal point, where the speed is equal to zero for a short moment. As for hard-on-soft pairs, the inclination angle of the cup was found to have a limited impact on lubrication.

Further improvement of accuracy and numerical stability of the computations was enabled by using a multigrid (MG) method instead of N-R [106]. The impact of transient three-dimensional physiological loading and kinematic conditions on film formation using the MG approach was carried out by Gao et al. [107]. The simulations suggested considerable time- and location-dependent variation of the film thickness distribution. The reported values were considerably different from those for unidirectional load and motion, as shown in Fig. 23.

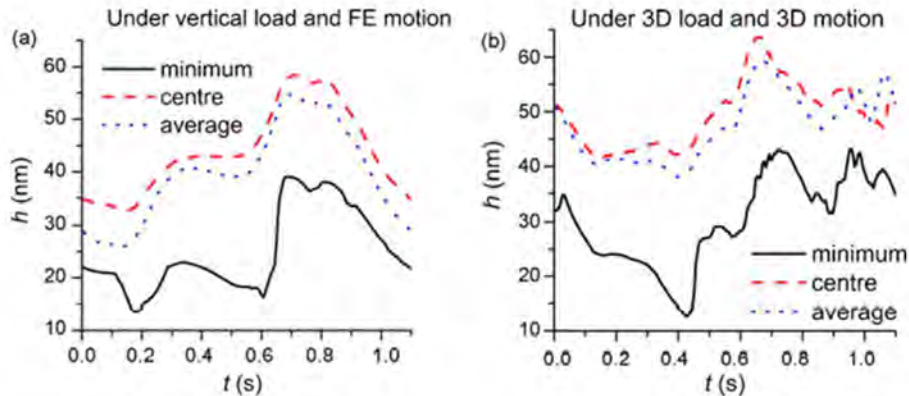


Figure 23: The variation of minimum, central, and average film thickness under the walking cycle; vertical load and FE motion (left); 3D load and motion (right) [107].

A further development in EHL problems led to introducing a multi-level multi-integration (MLMI) method [108]. The technique was adopted to calculate elastic deformations in ball-on-plane [106] and ball-in-socket [109] configurations. Gao et al. [110] presented a substantial impact of various walking patterns on film formation in MoM pair, using the advanced numerical model. The authors pointed at the important role of the squeeze film effect, which enabled the formation of a stable separating film even during short breaks of motion. The impact of metal implant non-sphericity was investigated by Meng et al. [111]. The authors investigated Alpharabola femoral head and cup, comparing the film thickness results with standard spherical implants. Even though the behaviour of non-spherical component was very complex due to variable clearance, the film thickness was generally much higher. At the same time, the pressure substantially dropped. The film increase was attributed mainly to the enhanced squeeze film action. MLMI method was subsequently adopted for the analysis of CoM pairings [112]. Dried and lubricated conditions were investigated, finding that CoM exhibits behaviour typical for hard (MoM, CoC) pairs. Specifically, it was shown that increased head diameter, together with smaller clearance lead to enhanced lubrication conditions. Concerning the film thickness, CoM exhibited a thicker layer than CoC, but thinner compared to MoM. However, it is assumed that the pairs with the ceramic femoral head are more likely to operate in the fluid film regime. The results summary is displayed in Fig. 24.

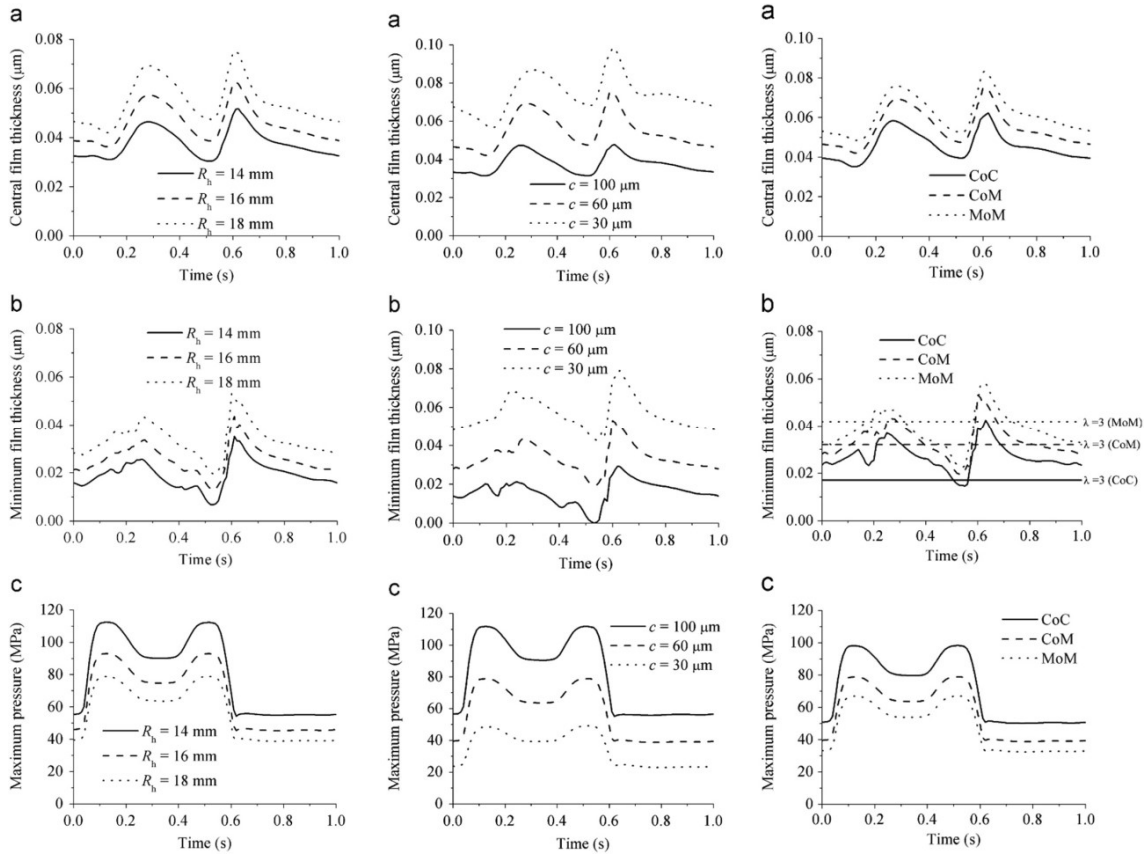


Figure 24: Central (a), minimum (b) film thickness and pressure distribution (c) for CoM pair considering the effect of the head radius (left) and radial clearance (middle); prediction of the parameters for CoC, CoM, and MoM pairs (right). The figure was partially modified and reprinted based on [112].

Most of the previous studies considered simple fluids assuming isoviscous Newtonian behaviour. The effect of lubricant rheology on the performance of MoM THR was introduced by Wang et al. [113]. The parameters provided previously in the literature [34],[114] were considered, aiming at the lubricant film thickness and pressure distribution. The results showed that under typical operating conditions, the non-Newtonian effect is minimal, indicating that the shear-thinning behaviour of SF may be neglected. However, Gao et al. [115] conducted a transient MG MLMI-based EHL analysis considering a shear-thinning Cross model, finding a strong impact of non-Newtonian lubricant on the contact conditions. Under physiological operating conditions, the film thickness was considerably enhanced due to higher viscosity at low shear rates. Variable viscosity further led to a decisive squeeze film action, maintaining a thicker film throughout the cycle. As in some previous papers, the thicker lubricating film was predicted for decreasing the radial clearance. The analysis further revealed that MoM replacement operates in the fluid film regime during the swing phase. In contrast, the stance phase is more likely to be accompanied by mixed and boundary conditions.

Recent investigations dealt with the numerical modelling of the effect of surface modifications on the lubrication of hard-on-soft pairs. Lubricant film thickness in the soft-EHL model considering the modified rigid surface combined with a deformable member mimicking PE was studied. The papers focused on the role of texture density, coverage ratio [116], and optimal floor profile of the texture [117] on the lubrication conditions. The simulations were carried out for Newtonian lubricant while the optimal parameters of the textures were suggested to optimize the lubrication performance. However, the authors admit that further lubricant aspects, such as the contribution of proteins, shear-thinning behaviour, or improved mass-converging cavitation modelling, would have a particular impact on the obtained results.

3.2 Experimental investigations

The previous subchapter suggests that the application of numerical modelling has excellent potential in the preliminary assessment of the tribological performance of newly designed THRs. However, following the findings given by Gao et al. [115] and the statement introduced by Scholes et al. [50] that calculations using simple non-biological lubricants suffer from certain limitations, the development of joint replacements needs to be supported by experimental investigations taking real biological fluids into account.

Several experimental methods for the investigation of lubrication characteristics have been introduced in tribology over the past 60 years. Concerning the analysis of film thickness, electrical, optical, or acoustic methods may be used, in general [118]. In the field of hip implants, the use of an electrical resistance method, optical interferometry, fluorescent microscopy, and acoustic ultrasonic reflection method was proposed. Each of the methods requires consideration of some simplifications. The electrical technique requires sufficient conductivity of the tested materials, which disqualifies non-conductive polymers and ceramics. The method also suffers from lower accuracy and sensitivity, which may be crucial upon an investigation of thin lubricating films. Optical methods require at least one of the contact bodies to be transparent,

leading to the necessity of substituting real implants by transparent members. The acoustic method has not been widely used as it has a low spatial resolution, enabling to obtain only an averaged value of the film thickness. Regardless of the applied approach, certain simplifications are associated with laboratory investigations. Specifically, the aspects of (i) geometry, (ii) material, (iii) lubricant, or (iv) test conditions may be mentioned.

A pilot study adopting the electrical resistance method for the investigation of film thickness in MoM THR was published by Dowson et al. [119] at the beginning of the millennium. Realistic ball-in-socket configuration was considered, while the separation of the surfaces throughout the walking cycle was evaluated. The contribution of proteins contained in the lubricating serum was found to be essential. In particular, the thicker lubricating film was achieved for more concentrated serum. The data showed the implant to operate in a mixed lubrication regime. The method was subsequently adopted also for CoC hip pair [120]. However, due to insufficient conductivity, the ceramic bodies were coated by a thin titanium nitride layer. It is noted that the coating might influence the results to some extent. Considerable voltage fluctuations attributed to partial coating detachment combined with the contact of surface asperities were observed, disabling to achieve a clear dependence between the cycle phase and the corresponding surface separation.

Therefore, the authors remained concentrated on MoM pairs, focusing on the effect of implant geometry. Concerning the impact of nominal THR diameter, nearly zero surface separation was observed for the 16 mm and 22 mm femoral heads, indicating the prevalence of a boundary regime, which may negatively influence a wear rate [18]. An increase in diameter to 28 mm led to the partial formation of the serum film, suggesting mixed lubrication. The largest 36 mm implant exhibited sufficient surface separation by a protective lubricating film over a considerable portion of the cycle. A further investigation aimed at the role of diametric clearance [121]. In accordance with the above numerical studies, a smaller clearance enhanced lubricant film formation. The effect of simplified and physiological motion and loading cycle was also explored, finding that physiological conditions lead to worse lubrication conditions. Thus, based on the investigations adopting the electrical resistivity measurement method, it may be concluded that larger implants with smaller clearance benefit from the best lubrication performance. At the same time, laboratory testing should be carried out under physiological conditions. The positive contribution of smaller clearance was generally supported by Brockett et al. [25], who used the ultrasonic reflection acoustic method to measure film thickness in MoM implant. However, when the clearance was too small, the film was substantially reduced together with an increase in friction and elevated incidence of implant squeaking. Therefore, it is assumed that the implant dimensions need to be balanced to provide optimal performance.

Further development in the field is associated with the use of optical methods. Although there is a need to substitute one of the contact bodies by a transparent sample, direct observation of the contact substantially contributes to a better understanding of the lubrication mechanisms. The first application of optical interferometry method for measuring protein solution and BS film thickness was introduced by Mavraki and Cann [44] in 2009. Albumin and γ -globulin were dissolved in two concentrations in different buffers, PBS and Tris, respectively. The study was

mainly focused on friction investigation, which is described in subchapter 2.1. Ball-on-disc tribometer was used for optical observation, while the contact between the stainless steel ball and the disc made from the optical glass was studied. Film thickness was evaluated as a function of speed under pure rolling conditions. The measured thicknesses did not exceed 100 nm. Concerning BS, a continuous increase of the film was observed with an increase and subsequent decrease of speed. Protein solutions exhibited relatively stable behaviour, while the buffer effect was substantial. Specifically, PBS led to the formation of a much thicker film than Tris. The results are summarized in Fig. 25. At the end of the test, a thin adsorbed layer of proteins on the surfaces was detected. The role of buffer solution in terms of pH level on both static adsorbed and dynamic protein films was later confirmed by Parkes et al. [122].

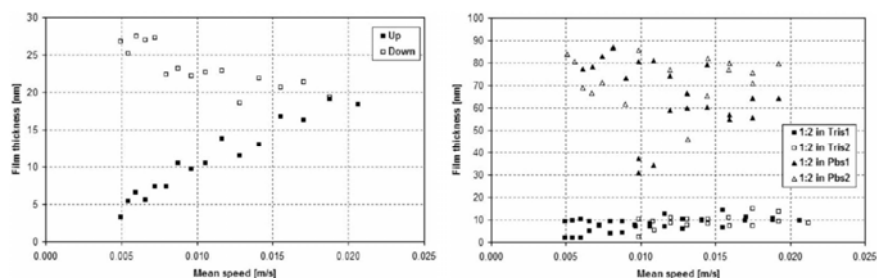


Figure 25: Results of the film thickness of BS (left) and protein solutions in various buffers (right) in ball-on-disc configuration measured by optical interferometry. The figure was partially modified and reprinted based on [44].

The following study given by the same authors employed the developed methodology for investigating the effect of kinematic conditions, load, and temperature [123]. Pure sliding conditions, when the ball rotated against the stationary disc, were taken into account in addition to pure rolling. In contrast to rolling, severe sliding conditions led to a dramatic decrease in the film thickness and limited adsorption ability. The load effect was also found to be significant. The metal ball was substituted by metal-coated convex glass lens (see Fig. 26) while the experiments were carried out under positive sliding conditions (the disc rotates against the fixed lens). The lower contact pressure contributed to the thicker BS film, especially when the speeds were lower. This finding needs to be considered when discussing concentrated ball-on-disc results where the pressure is considerably higher compared to conformal THR. The study is thus the

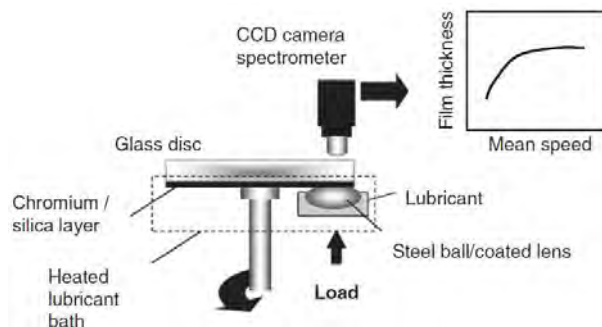


Figure 26: The scheme of modified ball-on-disc tribometer for direct observation of the contact lubricated by BS using optical interferometry method [123].

first experimental implication regarding the role of surface conformity in the lubrication process. However, some differences may also be in the character of slip, i.e. the influence of slip positivity/negativity needs to be considered. The impact of temperature was negligible as the elevation from laboratory to body temperature did not affect the results substantially. Since the experimental values of film thickness were considerably higher than those predicted based on EHL theory, the essential role of the BS constituents was highlighted.

Fan et al. [124] replaced the stainless steel ball by a real CoCrMo femoral head in the consequent paper. The experiments were realised with the fixed head (positive sliding conditions) focusing on the effect of speed and lubricant composition. Regardless of the applied lubricant, a thin adhered layer was formed quickly, while a further increase in the film was augmented by the hydrodynamic effect, especially at lower speeds. Concerning the effect of fluid composition, no remarkable differences were observed, while the film was mostly kept within the range of tens of nanometres. Formation of a boundary phase composed of protein molecules aggregated by a shear flow in the contact inlet was detected using optical imaging. The observations were enhanced by Myant et al. [125]. An initial set of experiments was conducted with simple albumin and γ -globulin solutions, focusing on the adsorption capability. The test was based on a repeated loading and unloading the contact without any relative motion. It was found that independently of concentration, albumin hardly adsorbs onto surfaces. In contrast, γ -globulin formed a relatively stable thicker film, which increased with each following loading step. Subsequent time test carried out at 10 mm/s showed qualitatively similar behaviour. While the albumin film was not thicker than 50 nm, γ -globulin layer was more than 200 nm thick. Load effect was further investigated, confirming that higher load is mostly associated with the decreased lubricating film. Protein agglomerations of high viscosity reported previously [124] were responsible for an instantaneous increase of the film while randomly passing through the contact. This gel-like phase of proteins was subsequently described in detail, finding that the longitudinal length of this inlet phase correlates with the development of film thickness (see Fig. 27) [126]. The authors of this study further pointed at the fundamental aspect of the application of natural lubricants. In particular, an apparent shear-thinning behaviour was observed, which implies the importance of the non-Newtonian description of the fluids in numerical simulations.

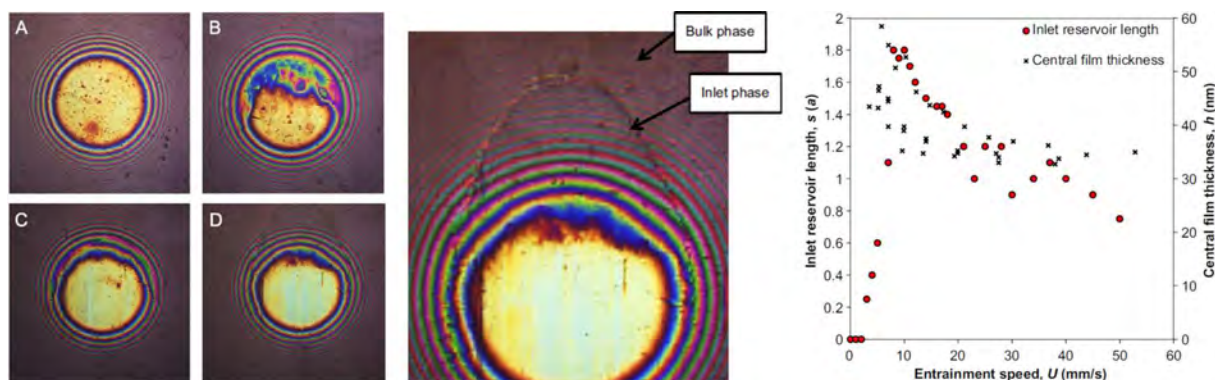


Figure 27: Images of the contact zones at various speeds (left); detail of the aggregated inlet phase of proteins (middle); dependence of inlet phase length and the film thickness (right).

The figure was partially modified and reprinted based on [126].

The experiments presented in the above references were realised under simplified unidirectional motion. However, it was shown in the previous parts of the thesis that the tribological behaviour is supposed to be influenced by the applied kinematics. To elucidate this effect in the ball-on-disc arrangement, Myant and Cann [127] performed the tests under three different motions; unidirectional motion at a constant speed, unidirectional motion with sinusoidal speed, and the reversal motion better mimicking joint function, respectively. While the first two settings led to comparable film thickness, reversing led to a considerable decrease in the film. The achieved knowledge regarding protein lubrication was summarised by Myant and Cann [128] in the paper where a novel protein aggregation lubrication (PAL) regime was defined. Various aspects were discussed in the study, while the main differences against traditional EHL theory were assessed.

The previous investigations focused exclusively on metal THR components. Comparison of metal and ceramic femoral head lubrication behaviour was given by Vrbka et al. [129]. The contact was lubricated by BS, while the authors focused on the effect of speed and SRR. In general, the metal head formed a thicker lubricating film under most conditions. A typical sequence of images showing the passage of the proteins through the contact is shown in Fig. 28. Under pure rolling, the film thickness continuously increased for both the investigated materials. Introduction of slip led to a remarkable change in film formation. The film initially dramatically increased at positive sliding, while then it dropped to deficient levels without any further development. In contrast, under negative sliding, the film was negligible throughout the test, confirming limited adsorption under severe rubbing. Adsorption of proteins was further studied by Parkes et al. [130]. The authors compared simple albumin and γ -globulin with the mixture of these constituents. Both static and dynamic tests were carried out, finding that simple γ -globulin better adsorbs onto rubbing surfaces. When mixed with albumin, the adsorption ability was substantially reduced. The results revealed that the absolute film thickness depends somewhat on the ratio of the proteins, rather than on the overall concentration. The latter finding supports the importance of using the model SFs instead of BS of unknown detailed composition.

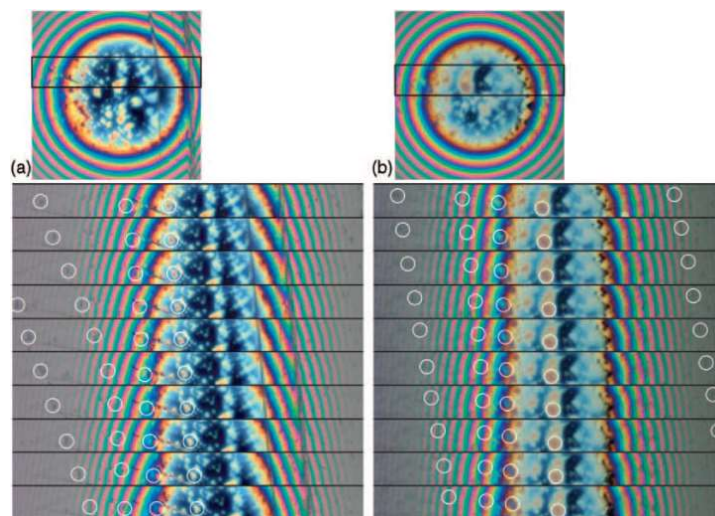


Figure 28: A set of the interferograms illustrating the passage of the protein film through the contact for metal (a) and ceramic (b) femoral head under positive sliding conditions [129].

Considering the evident role of contact pressure and surface conformity, Vrbka et al. [131] modified the ball-on-disc tribometer to a more conformal ball-on-concave lens arrangement (see Fig. 29). The configuration allowed only for the application of pure negative sliding, where the ball rotates against the fixed lens. These conditions better reflect the real THR function anyway. In the previous ball-on-disc observation [129], negative sliding led to a negligible protein film. However, more conformal contact showed an immediate increase followed by continuous drop and stabilisation at levels higher than surface roughness, ensuring sufficient lubrication protection of the surfaces.

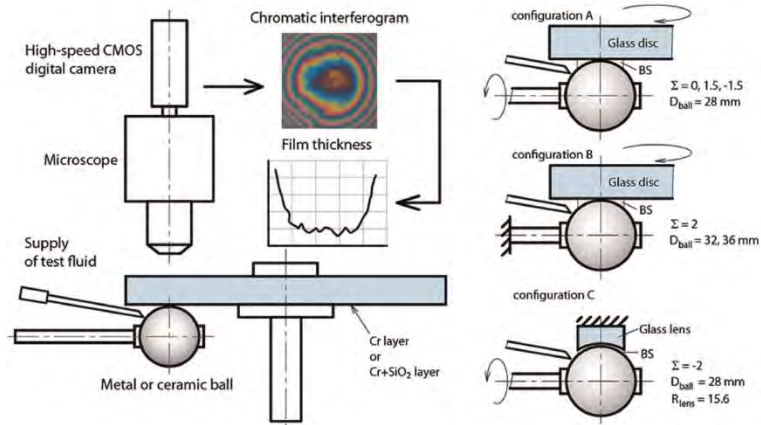


Figure 29: Modification of ball-on-disc tribometer towards improved compliance of the contact conditions mimicking THR [131].

With respect to the previous study, the logical step was to achieve full contact conformity towards approaching the realistic geometry of the THR model. Therefore, the pendulum hip joint simulator described above [61] was further modified (see section 3.3.1). The author of the thesis was involved in this study. However, the published paper was a part of his PhD topic, so this study is not directly considered the author's contribution to the habilitation thesis. The modification of the simulator was in the use of a transparent glass acetabular cup, fabricated based on the dimensions of a real UHMWPE socket. The simulator was equipped with an optical interferometry module, allowing for direct in situ contact observation in the actual ball-in-socket configuration. Such an experiment has not been carried out before. The film thickness was evaluated under swinging FE motion, finding that the better conformity supports the formation of the thicker and more stable lubricating film.

The simulator was later used by Choudhury et al. [133], who observed the formation of film thickness considering the effect of femoral head surface texturing. Various textures in the shape of square, triangle, elliptical-minor, and elliptical-major were made on the metal heads using a picosecond laser and comparing the film thickness with the non-textured implant. Regardless of the texture shape, the film thickness was enhanced, while the maximum values were approximately 3.5 higher than that of the original head (see Fig. 30). The study combined with the author's own contribution to surface texturing [80] is very promising towards further development of THRs and TKRs.

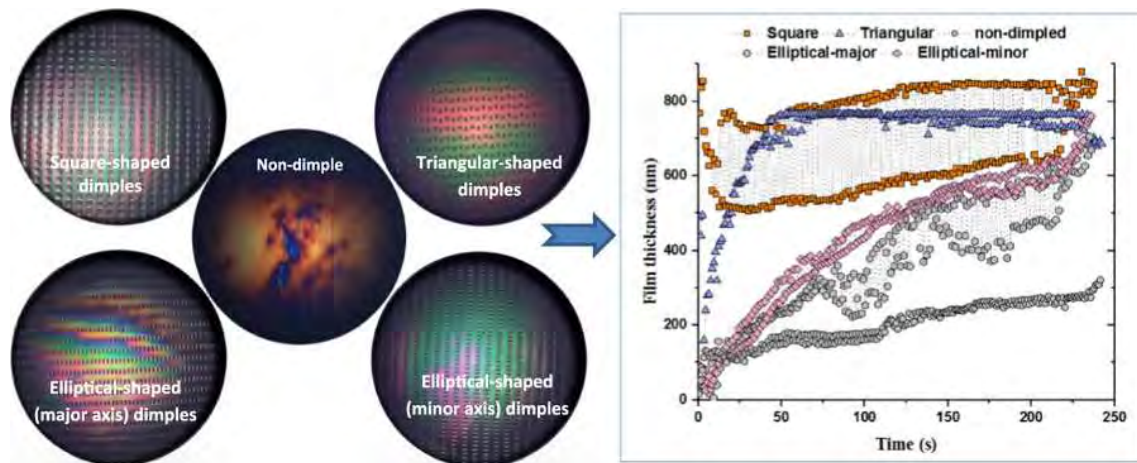


Figure 30: Various shapes of textures made on the metal femoral heads (left); respective film thickness measured by optical interferometry (right) [133].

It may be seen that optical interferometry became well-established measurement method when analysing protein film thickness. However, due to the principle of the technique, the main output is in the quantitative thickness, while there is no detailed information about the behaviour of individual synovial fluid constituents. Since the investigations of simple solutions may not clarify the interactions of the ingredients of SF, an alternative approach had to be developed, allowing for a deeper understanding.

This task was the main goal of the author's PhD thesis; therefore, the respective papers are not included in the author's contribution within the habilitation thesis as in the previous case [132]. Fluorescent microscopy method, formerly used for the observation of film flow and film thickness in engineering applications was adopted, while the methodology based on fluorescently stained constituents was proposed [134],[135]. The first study [134] dealt with methodology development. A little step back was made in terms of the experimental setup. As it was necessary to understand the fundamentals of the novel approach first, the investigation was carried out in ball-on-disc configuration. The contact of the metal femoral head and the glass disc was studied, while optical interferometry and fluorescent microscopy were combined. A mixture of albumin and γ -globulin was used as the test lubricant. Two different speeds and three SRRs were applied to get a comprehensive data set under various kinematic conditions. Initially, the film thickness was measured quantitatively using the interferometry technique. Subsequently, the tests were repeated with one of the constituents fluorescently stained, while the qualitative dimensionless film thickness was evaluated (see Fig. 31). Finally, the fluorescently labelled component was switched. This approach enabled the identification of each protein contribution to the lubricating film while mixed with another protein. The overall trends corresponded to previous observations [129], while the data obtained using fluorescent microscopy perfectly matched with those from interferometry. By simple scaling of the data, the role of albumin and γ -globulin in lubricant film formation mechanisms could be revealed. The approach was later adopted also for alumina and zirconia-toughened ceramic heads [135].

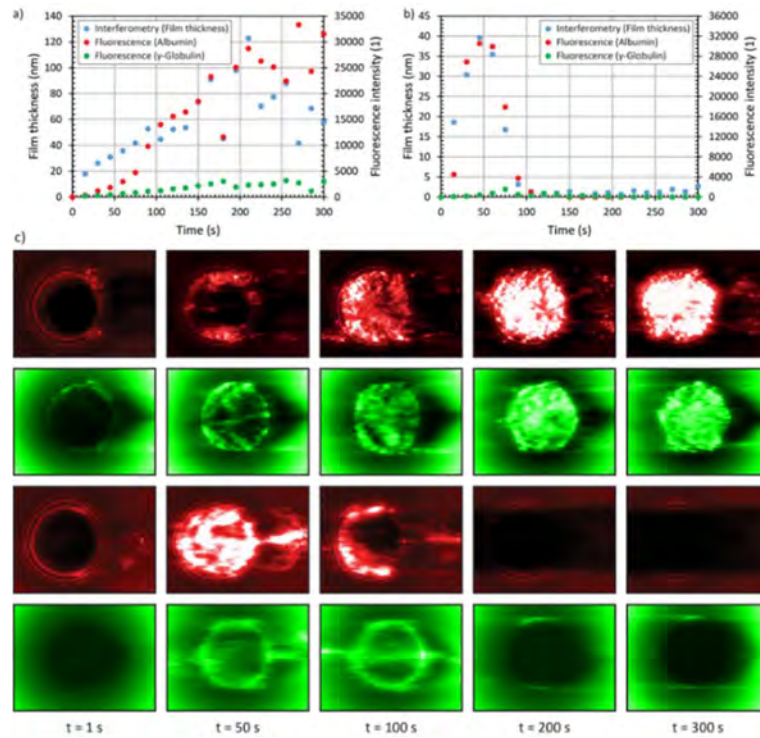


Figure 31: Time-dependence of film thickness for the metal femoral head at lower (a) and higher (b) speed under positive sliding conditions in ball-on-disc configuration; fluorescent images of the contact zone (c). The figure was partially modified and reprinted based on [134].

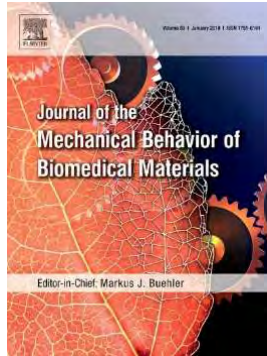
3.3 Author's contribution to the field

The overview of both numerical and experimental methods for lubrication analysis of THR provides a clear insight into the development in the field over the last twenty years. However, it is also shown that a number of numerical papers suffer from neglecting the real properties of biological lubricants, and most of the experimental studies were carried out in simplified configurations. Furthermore, all the empirical studies focused on hard-on-hard bearing pairs, while the current data from national registries clearly show that hard-on-soft couples are dominant all over the world [136],[137],[138]. Following the suggestions arising based on previous research [44],[50],[115],[132],[134], further development of theoretical models and experimental approaches is fundamental towards improved performance of implants.

Therefore, the author of the thesis published five papers focused on different topics, contributing mainly to experimental investigations. The first study (i) is focused on the effect of head material, diameter and clearance on lubrication performance using the real ball-in-socket model in the pendulum simulator. Three different femoral heads were used while static adsorption was studied among others. The second study (ii) enhances the recent observations in terms of the SF composition influence, comparing the behaviour of two different model SFs with BS. The effect of load on the adsorbed film is also investigated. The third investigation (iii) adopted the methodology based on fluorescent microscopy, studying ball-in-socket hard-on-soft implant for the first time. The UHMWPE acetabular cup was substituted by the cup made of PMMA having comparable mechanical and physical properties. The fourth paper (iv) concentrates on the

hard-on-hard pairs, focusing on the kinematic conditions and highlighting some main differences against hard-on-soft couples. The last article (v) proposes a direct comparison of experimental and numerical data regarding THR lubrication, introducing a new effective viscosity equation, which enables advanced modelling of the protein solution behaviour.

All the papers were published in peer-reviewed journals with IF in WoS. The list of the included papers is as follows:



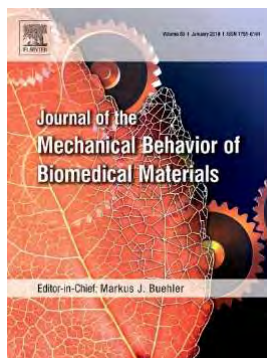
[139] Nečas, D., Vrbka, M., Urban, F., Gallo, J., Křupka, I., Hartl, M., 2017. In situ observation of lubricant film formation in THR considering real conformity: The effect of diameter, clearance and material. Journal of the Mechanical Behavior of Biomedical Materials 69, 66-74.

Author's contribution (BUT): = 55%
 Journal metrics (IF₂₀₁₇): = 3.24
 Citations (Google Scholar): = 8 (excl. self-citations)



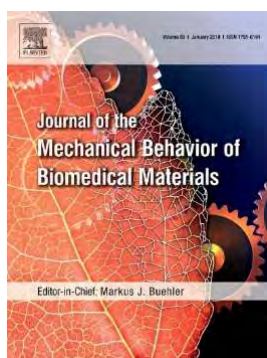
[140] Nečas, D., Vrbka, M., Rebenda, D., Gallo, J., Galandáková, A., Wolfová, L., Křupka, I., Hartl, M., 2018. In situ observation of lubricant film formation in THR considering real conformity: The effect of model synovial fluid composition. Tribology International 117, 206-216.

Author's contribution (BUT): = 40%
 Journal metrics (IF₂₀₁₈): = 3.52
 Citations (Google Scholar): = 12 (excl. self-citations)



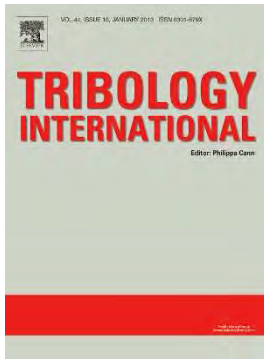
[141] Nečas, D., Vrbka, M., Galandáková, A., Křupka, I., Hartl, M., 2019. On the observation of lubrication mechanisms within hip joint replacements. Part I: Hard-on-soft bearing pairs. Journal of the Mechanical Behavior of Biomedical Materials 89, 237-248.

Author's contribution (BUT): = 75%
 Journal metrics (IF₂₀₁₉): = 3.37
 Citations (Google Scholar): = 8 (excl. self-citations)



[142] Nečas, D., Vrbka, M., Gallo, J., Křupka, I., Hartl, M., 2019. On the observation of lubrication mechanisms within hip joint replacements. Part II: Hard-on-hard bearing pairs. Journal of the Mechanical Behavior of Biomedical Materials 89, 249-259.

Author's contribution (BUT): = 60%
 Journal metrics (IF₂₀₁₉): = 3.37
 Citations (Google Scholar): = 8 (excl. self-citations)



[143] Lu, X., Nečas, D., Meng, Q., Rebenda, D., Vrbka, M., Hartl, M., Jin, Z., 2020. Towards the direct validation of computational lubrication modelling of hip replacements. *Tribology International* 146, 106240.

Author's contribution (BUT): = 45%
Journal metrics (IF₂₀₁₉): = 4.27 (IF₂₀₂₀ is not yet available)
Citations (Google Scholar): = 0

3.3.1 In situ observation of lubricant film formation in THR considering real conformity: The effect of diameter, clearance and material

The first study in this section was focused on the effect of hip implant material and dimensions on lubrication behaviour. The experiments were realised with the pendulum, which was further modified to apply continuous FE motion via electromotors. The 28 mm metal, alumina ceramic (BIOLOX[®]forte) and zirconia-toughened ceramic (BIOLOX[®]delta) femoral heads were articulated with an acetabular glass cup, enabling to assess the effect of the implant material. The experiments focused on the geometry effect were realised with metal heads of two nominal diameters (28 mm vs 36 mm), and two different clearances (smaller and larger).

Before starting the test, the cup was entirely flooded with the BS to ensure sufficient lubrication. The applied load (515 N) resulted in contact pressures from 16.6 MPa to 70.4 MPa, dependently on the contact couple. Initially, protein adsorption was studied by application of simple loading-unloading (15 s vs 45 s) sequence without relative motion. Twenty such tests were performed in total. Subsequently, a swinging FE test was performed, while the overall test duration was 200 s. After that, the motors were stopped, and the motion was damped naturally.

Adsorption tests showed that the metal head supports a more stable adhered layer. In the case of the ceramic implants, the film fluctuated pointing at weaker bonds, being accompanied by repetitive adsorption and desorption of the molecules. Nevertheless, despite the different behaviour, the resulting adsorbed film after twenty cycles was around 150 nm, independently of the head material. The dynamic FE experiments showed improved lubrication when the metal head was used. The film continuously increased, reaching the maximum detectable value (approx. 900 nm) in less than two minutes of swinging. In contrast, both ceramic materials exhibited thinner, but relatively stable films, thick enough to protect the surfaces. Concerning the role of geometry, a positive impact of diametric clearance was observed. For both nominal diameters, the smaller clearance led to increasing lubricating film. In contrast, the larger clearance disabled the film to be fully developed while constant values were measured throughout the whole test. In the perspective of clearance, the results for ceramic heads may be skewed a little, as the clearance of ceramic-on-glass pairs was nearly double compared to the metal-on-glass couple (see Tab. 2). Finally, the measured film thickness was always considerably higher than that predicted by EHL theory for isoviscous fluid. The overall research scheme of the study is shown in Fig. 32.

Ball material	Ball diameter (mm)	Cup diameter (mm)	Diametric clearance (μm)	Hertzian contact pressure (MPa)	Hertzian contact zone diameter (mm)	Test type
Metal	27.97	28.01	40	16.6	7.69	Dynamic
Metal	27.97	28.288	318	65.8	3.87	Dynamic
Metal	35.95	36.093	143	27.8	5.95	Static/Dynamic
Metal	35.95	36.535	585	70.4	3.74	Dynamic
BIOLOX ^{forte}	27.97	28.067	93	29.1	5.81	Dynamic
BIOLOX ^{forte}	35.96	36.087	124	25.2	6.24	Static
BIOLOX ^{delta}	27.97	28.067	97	31.8	5.56	Dynamic
BIOLOX ^{delta}	35.98	36.087	109	23.2	6.52	Static

Table 2. Summary of the tested THR couples [139].

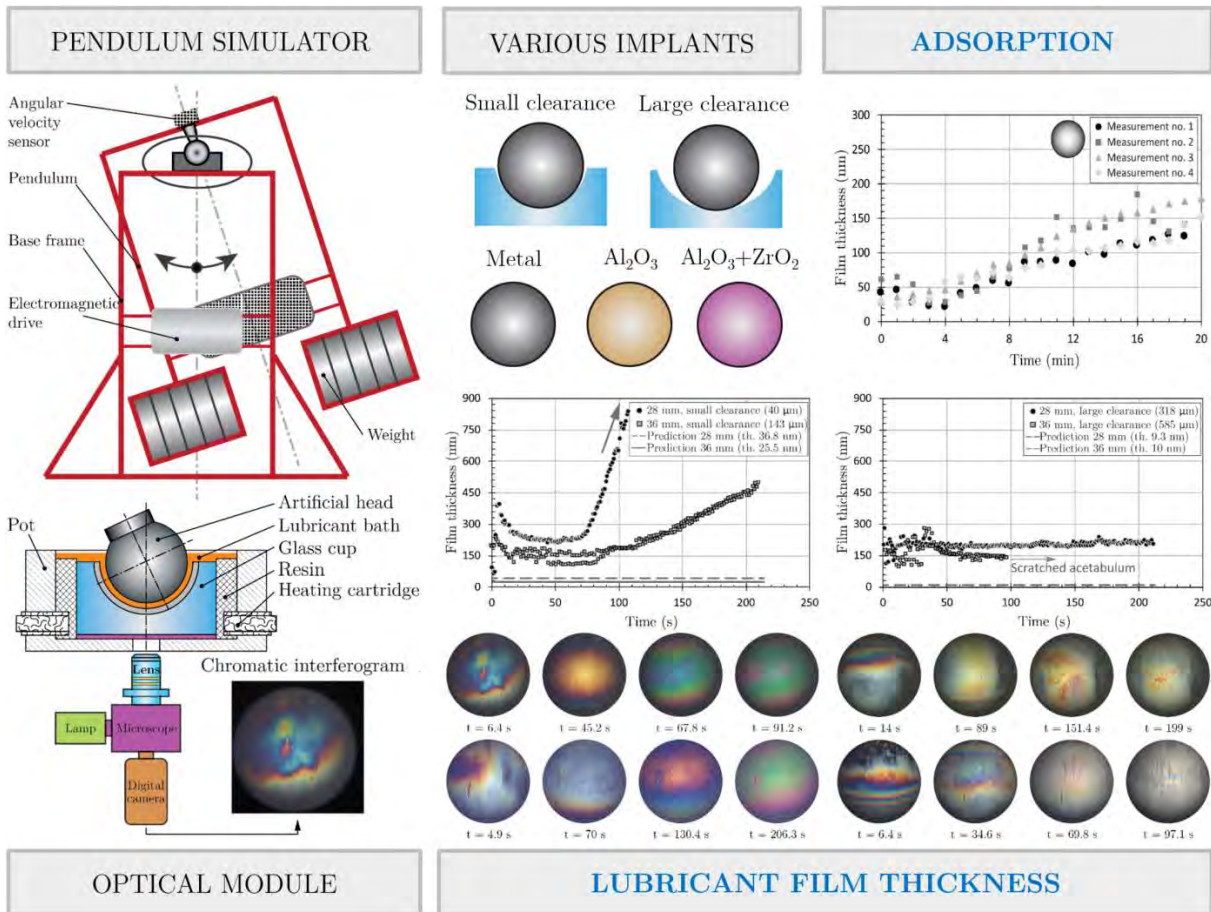


Figure 32: Research scheme of the study [139].

3.3.2 In situ observation of lubricant film formation in THR considering real conformity: The Effect of Model Synovial Fluid Composition

The following paper was based on the same methodology (pendulum simulator + optical interferometry). Attention was paid to the effect of lubricant composition and the behaviour of individual constituents. The same materials of femoral heads were employed. Concerning the suggestions regarding the importance of all the constituents, two different model SFs were prepared. The specific compositions followed SFs of patients with and without THR. Summary of the applied lubricants is provided in Tab. 3. At first, the static adsorption test was carried out, followed by investigating the load effect. Subsequent swinging tests were performed with all the model fluids. The experiments conducted are summarised in Tab. 4.

Test fluid	Albumin (mg/ml)	γ -globulin (mg/ml)	HA (mg/ml)	Phospholipids (mg/ml)	Total concentration (mg/ml)	Volume (ml)
25% BS	Unknown	Unknown	-	-	22.4	12
Model SF1	28	11	1.1	0.17	40.27	
Model SF2	28	9.4	1.9	0.31	39.61	
Albumin	28	-	-	-	28	
γ -globulin	-	11	-	-	11	
HA1	-	-	5	-	5	
HA2	-	-	20	-	20	

Table 3: The summary of the applied test lubricants [140].

Experiment set	Contact couple	Test lubricant	Test type	Load
1	Metal/Glass	BS, SF1, SF2	Static	532 N
2	Metal/Glass	BS, SF1, SF2, albumin, γ -globulin, HA1, HA2	Dynamic	532 N
3	BIOLOX [®] forte/Glass	BS, SF1, SF2	Static	532 N
4	BIOLOX [®] delta/Glass	BS, SF1, SF2	Static	532 N
5	BIOLOX [®] delta/Glass	BS	Static/Load effect	532 N; 857 N; 1157 N; 1457 N; 1757 N

Table 4: The summary of the performed experiments [140].

The lubricant composition effect was found to have a remarkable impact on the formation of film thickness. Referring to the static adsorption test, BS formed the thickest adhered layer for all the femoral heads despite the lower overall protein content. Since the content of albumin and γ -globulin in model SFs was comparable, the attention was focused on HA and PLs. Surprisingly, the higher content of these constituents led to the thinnest adsorbed film in the case of the metal head. For the ceramics, the mimicked SFs exhibited very similar thicknesses.

Concerning the load effect, it was found that the adsorbed layer continuously decreases with increasing load. The swinging FE test showed that HA and PLs substantially influence film formation. While the SF having the lower content of these constituents hardly formed a sufficient lubricating film, the increased concentration led to a rapid improvement of lubrication conditions, resulting in a remarkably thicker layer. BS results were somewhere between the model fluids. Thus, it is suggested that protein concentration is less important than the content of HA and PLs, which play a role of film enhancers (see Fig. 33). However, the experiments conducted with simple solutions of proteins and HA of two different molecular weights showed that a single HA could not form a sufficient film. Thus, a fundamental aspect of the interaction of the constituents was underlined (see Fig. 34).

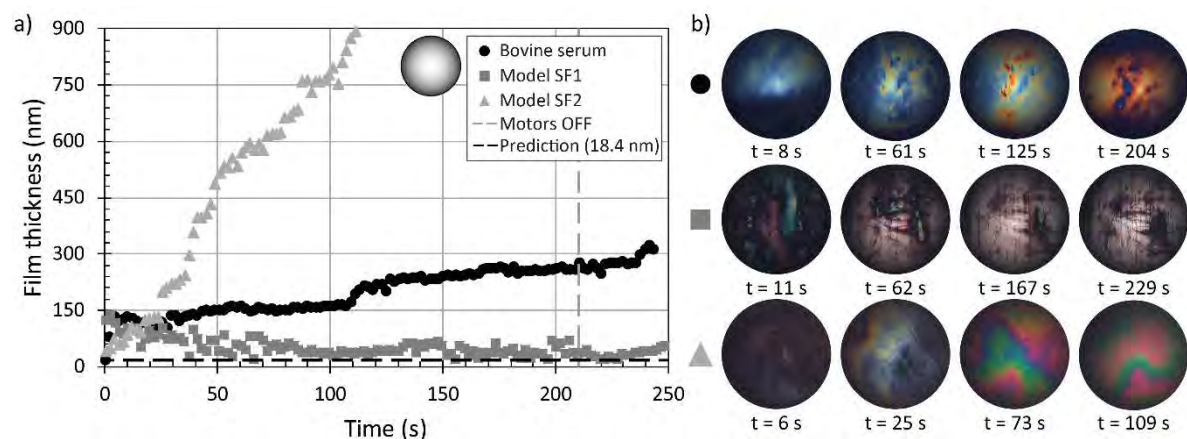


Figure 33: Development of film thickness for various model lubricants (a); respective contact images (b) [140].

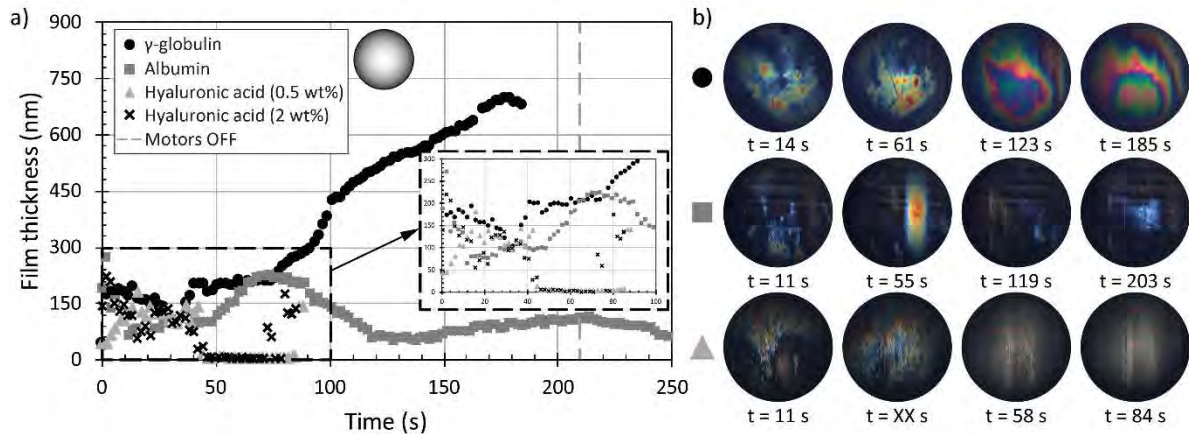


Figure 34: Development of film thickness for simple solutions of albumin, γ -globulin, and HA (a); respective contact images (b) [140].

3.3.3 On the observation of lubrication mechanisms within hip joint replacements. Part I: Hard-on-soft bearing pairs

The following two papers were published in sequence as a two-part study. The first part adopts the previously introduced fluorescent microscopy, which was implemented in the pendulum simulator instead of optical interferometry. For the first time, an actual-shaped acetabular cup made from transparent PMMA was used to reveal the lubrication mechanisms in the hard-on-soft THR. As a counterface, the metal femoral head was used while the implant nominal diameter was 28 mm. The lubricant had to be fluorescently stained to enable in situ observation.

In this study, a complex model SF was applied, containing all the essential constituents, i.e. albumin, γ -globulin, HA, and PHs. As the content of PHs is the lowest, attention was paid to the rest three constituents. The procedure based on repeating the tests under the same conditions using various mixtures with always one of the constituents to be labelled was applied. Finally, so-called master fluid was used, where all the three main components were labelled. A detailed overview of the applied test lubricants, showing the specific combinations of fluorescently stained and non-stained constituents is provided in Tab. 5.

Two types of tests were carried out. The first dynamic test was based on three-minutes lasting FE swinging. The second test was more complex, simulating repetitive loading and unloading of the joint with a subsequent short one-minute swinging phase mimicking a couple of walking steps. It should be noted that previous numerical simulations showed that the film in THR is developed very quickly, so even the dynamic part of the second test was shorter, the findings related to the load effect are useful. An overview of the test conditions is provided in the research scheme (see Fig. 35). The applied load was 532 N, resulting in the contact pressure of 5.1 MPa.

The results of the dynamic tests showed that simple albumin forms a thin lubricating film. However, when mixed with other constituents, the lubrication ability is considerably enhanced. A mixture of γ -globulin and albumin led to the thickest layer, while HA and PHs led to a decrease in the film. However, substantial stabilisation of the film was observed. As presented in the previous study, simple HA is not able to produce a sufficient film. The statement was confirmed

in this study. Although the layer thickness was very low, regardless of the composition, the thickest HA-based film was detected when HA was mixed with all the rest constituents, highlighting the importance of interactions between the ingredients. Since the master curve behaviour confirmed the tendency observed for individual solutions, the mechanism of film formation was revealed. It was found that HA combined with PHs has a strong stabilising impact on the formation of boundary γ -globulin film, which allows for layering of albumin, increasing the overall film thickness. Concerning the combined static/dynamic test, the global tendencies corresponded with the above dynamic results. Excellent repeatability of the experiments was achieved for both tests, which is also presented in the paper. It may be concluded that the approach based on the use of fluorescent microscopy is useful for investigations of hard-on-soft bearing couples. The overall research scheme of the study is shown in Fig. 35.

Lubricant no.	Labelled constituent(s) (concentration)	Non-labelled constituent(s) (concentration)	Total concentration	Base fluid (total amount)
1	Albumin (24.9 mg/ml)	–	24.9 mg/ml	PBS (4 ml)
2	Albumin (24.9 mg/ml)	γ -globulin (6.1 mg/ml)	31 mg/ml	PBS (4 ml)
3	Albumin (24.9 mg/ml)	γ -globulin (6.1 mg/ml)	32.49 mg/ml	PBS (4 ml)
4	Albumin (24.9 mg/ml)	HA (1.49 mg/ml) γ -globulin (6.1 mg/ml) HA (1.49 mg/ml) PHs (0.34 mg/ml)	32.83 mg/ml	PBS (4 ml)
5	γ -globulin (6.1 mg/ml)	–	6.1 mg/ml	PBS (4 ml)
6	γ -globulin (6.1 mg/ml)	Albumin (24.9 mg/ml)	31 mg/ml	PBS (4 ml)
7	γ -globulin (6.1 mg/ml)	Albumin (24.9 mg/ml)	32.49 mg/ml	PBS (4 ml)
8	γ -globulin (6.1 mg/ml)	HA (1.49 mg/ml) Albumin (24.9 mg/ml) HA (1.49 mg/ml) PHs (0.34 mg/ml)	32.83 mg/ml	PBS (4 ml)
9	HA (1.49 mg/ml)	PHs (0.34 mg/ml)	1.83 mg/ml	PBS (4 ml)
10	HA (1.49 mg/ml)	PHs (0.34 mg/ml)	26.73 mg/ml	PBS (4 ml)
11	HA (1.49 mg/ml)	Albumin (24.9 mg/ml) PHs (0.34 mg/ml)	7.93 mg/ml	PBS (4 ml)
12	HA (1.49 mg/ml)	γ -globulin (6.1 mg/ml) Albumin (24.9 mg/ml) γ -globulin (6.1 mg/ml) PHs (0.34 mg/ml)	32.83 mg/ml	PBS (4 ml)
13	Albumin (24.9 mg/ml) γ -globulin (6.1 mg/ml) HA (1.49 mg/ml)	PHs (0.34 mg/ml)	32.83 mg/ml	PBS (4 ml)

Table 5: The summary of the applied test lubricants showing the combinations of labelled and non-labelled constituents [141].

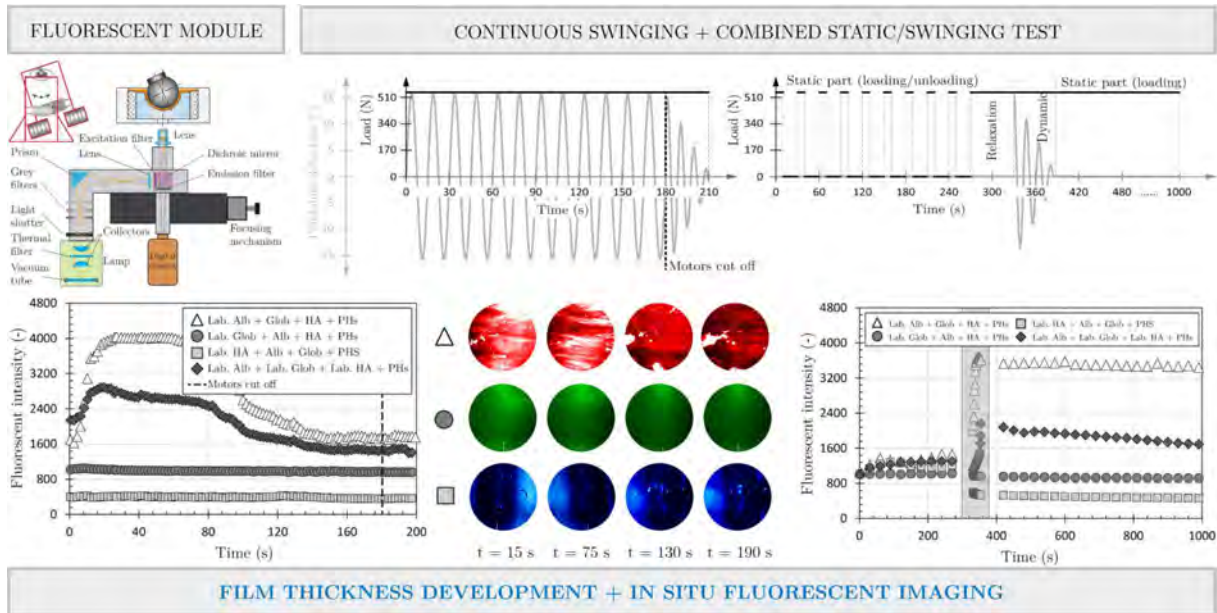


Figure 35: Research scheme of the study [141].

3.3.4 On the observation of lubrication mechanisms within hip joint replacements. Part II: Hard-on-hard bearing pairs

The second part of the study focused on hard-on-hard pairs, conducting the above-described combined static/swinging tests to compare the two groups of implants, among others. The comparison of fundamental geometrical and material properties is summarised in Tab. 6. Model fluids of the same compositions were applied, allowing for a direct description of the effects and interactions of individual constituents. Besides, two more model SFs were involved to assess the role of protein concentration. Since previous investigations of hard pairs exhibited some repeatability issues, the detailed analysis of the data and several repetitions of the selected tests were later performed.

Parameter	Hard-on-soft pair	Hard-on-hard pair
Ball diameter	27.9714 ± 0.0007 mm	27.9714 ± 0.0007 mm
Cup diameter	28.1105 ± 0.0005 mm	28.0504 ± 0.0004 mm
Diametric clearance	0.13 mm	0.080 mm
Ball elastic modulus	230 GPa	230 GPa
Ball Poisson's ratios	0.28	0.28
Cup elastic modulus	3 GPa	85 GPa
Cup Poisson's ratios	0.37	0.209
Load	532 N	532 N
Contact pressure	5.1 MPa	26.4 MPa
Contact zone diameter	14.1 mm	6.2 mm
Observed zone diameter	1.5 mm	1.5 mm
Ball surface roughness	7.81 ± 1.24 nm	7.81 ± 1.24 nm
Cup surface roughness	4.8 ± 0.7 nm	< 1 nm
Ball wetting angle	78 ± 0.5° (ball sample)	78 ± 0.5° (ball sample)
Cup wetting angle	81 ± 0.7° (flat sample)	92 ± 1.1° (flat sample)

Table 6: Comparison of hard-on-soft and hard-on-hard bearing couples [142].

The results of hard pairs showed that HA generally enhances the film thickness; however, the contribution is strongly influenced by the protein content. The essential effect of contact mechanics was revealed based on comparing results for hard-on-hard and hard-on-soft pairs. The differences were more pronounced especially under swinging motion. While the film had a decreasing tendency for the hard couple, the use of the polymer cup led to improved lubrication conditions. The findings are in agreement with previous suggestions regarding the effect of contact pressure on SF film. However, despite the enhanced film thickness, the soft THR pair exhibited higher friction, as the motion attenuation after the motors stopped was faster than that of the hard couple. Thus, the importance of internal lubricant friction is suggested. The repeatability results of hard pairs showed satisfactory compliance of the data for all the three tested SFs (see Fig. 36).

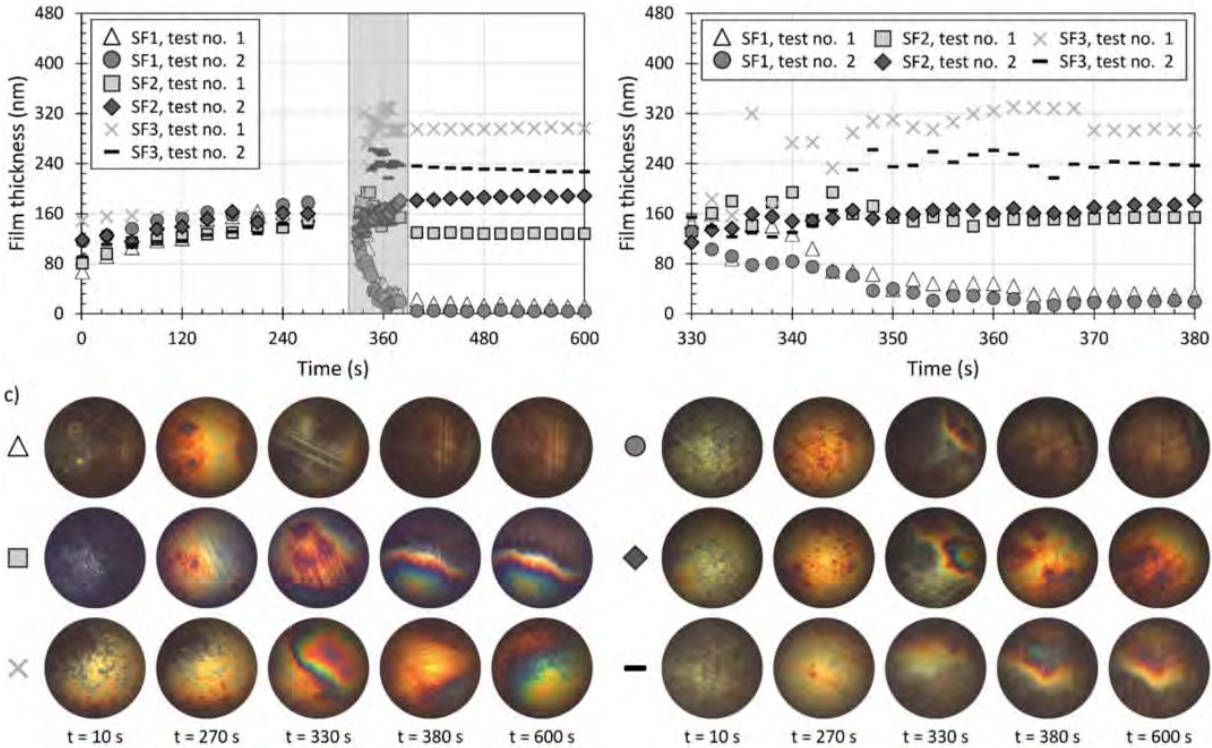


Figure 36: Repeatability test performed with three SFs of different composition.

The figure was partially modified and reprinted based on [142].

3.3.5 Towards the Direct Validation of Computational Lubrication Modelling of Hip Replacements

The last paper in this section dealt with the direct comparison of experimental investigation and numerical modelling of THR lubrication. The importance of a combination of numerics and experiments is often discussed. However, according to the author’s best knowledge, such a comprehensive comparison has not been proposed before in the area of THR lubrication. The numerical analysis of the hip joint in ball-in-socket configuration was performed based upon MG and MLMI model. The data were compared with those from the pendulum simulator. The contact

of CoCrMo femoral head and glass cup was considered. For the model validation, low-viscosity mineral oil of known rheological properties was used. The oil was subsequently replaced by BS to capture the role of biological liquid.

The experimental results of oil film thickness complied with the values predicted by the model. However, a substantial difference was observed under BS lubrication. Therefore, a novel velocity-effective viscosity relation was derived based on the experiments and was implemented to the calculation. For this purpose, the modified Cross rheological model was adopted. The modification led to the achievement of an excellent agreement between the predicted and measured data (see Fig. 37). Thus, the importance of an appropriate fluid rheology description together with shear-thinning effect was underlined.

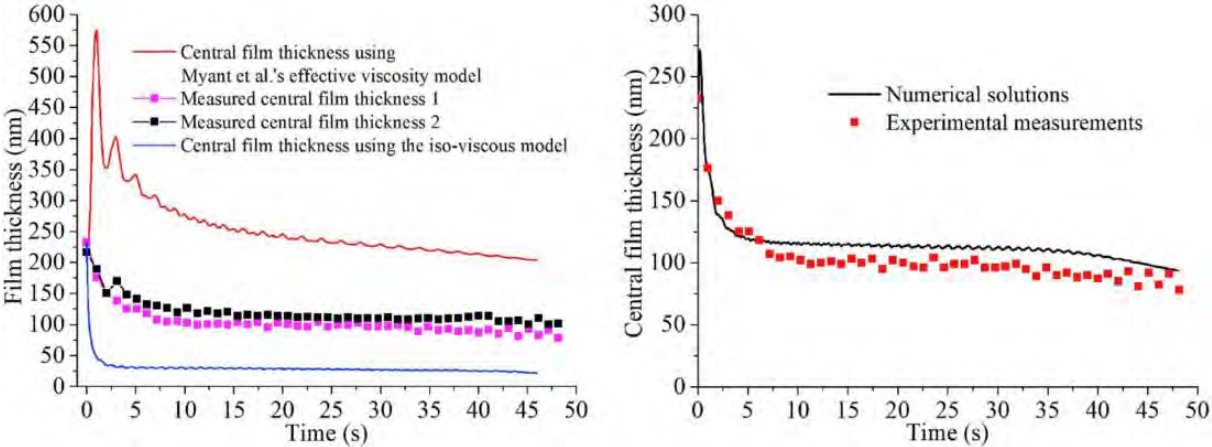


Figure 37: Comparison of the central film thickness based on the experimental measurement and predictive numerical model. Isoviscous and literature-based effective viscosity model (left); the novel velocity-effective viscosity equation (right). The figure was partially modified and reprinted based on [143].



In situ observation of lubricant film formation in THR considering real conformity: The effect of diameter, clearance and material

D. Nečas^{a,*}, M. Vrbka^a, F. Urban^a, J. Gallo^b, I. Křupka^a, M. Hartl^a

^a Faculty of Mechanical Engineering, Brno University of Technology, Czechia

^b Department of Orthopaedics, Faculty of Medicine and Dentistry, Palacky University Olomouc, University Hospital Olomouc, Czechia

ARTICLE INFO

Keywords:

Hip joint replacement
Head and cup diameter
Diametric clearance
Lubrication
Film thickness
Optical interferometry

ABSTRACT

The aim of the present study is to provide an analysis of protein film formation in hip joint replacements considering real conformity based on in situ observation of the contact zone. The main attention is focused on the effect of implant nominal diameter, diametric clearance and material. For this purpose, a pendulum hip joint simulator equipped with electromagnetic motors enabling to apply continuous swinging flexion–extension motion was employed. The experimental configuration consists of femoral component (CoCrMo, BIOLOX[®]forte, BIOLOX[®]delta) and acetabular cup from optical glass fabricated according to the dimensions of real cups. Two nominal diameters were studied, 28 and 36 mm, respectively, while different diametric clearances were considered. Initially, a static test focused on the protein adsorption onto rubbing surfaces was performed with 36 mm implants. It was found that the development of adsorbed layer is much more stable in the case of metal head, indicating that the adsorption forces are stronger compared to ceramic. A consequential swinging test revealed that the fundamental parameter influencing the protein film formation is diametric clearance. Independently of implant diameter, film was much thicker when a smaller clearance was considered. An increase of implant size from 28 mm to 36 mm did not cause a substantial difference in film formation; however, the total film thickness was higher for smaller implant. In terms of material, metal heads formed a thicker film, while this fact can be, among others, also attributed to clearance, which is more than two times higher in the case of ceramic implant.

1. Introduction

Total hip arthroplasty is recognized as one of the most applied surgical procedure of modern medicine. Hip replacements lead to an increase of life quality of patients whose natural joints need to be restored due to injury or disease. Despite a substantial development in the area of hip implants the replacements still suffer from limited longevity, which is estimated to be between 10–20 years. Considering the factors leading to the implant failure, the main cause is aseptic loosening as a consequence of osteolysis (Joshi et al., 1993). This process is strongly affected by particles released from the rubbing surfaces during joint articulation. Therefore, it is apparent that better understanding of biotribology of hip replacements is essential for further improvement of implant service-life.

As it is evident that the tribological processes significantly affect the performance of hip replacements, there are extensive discussions about a suitable implant size and material in relation to lubrication and wear (Cross et al., 2012; Di Puccio and Mattei, 2015; Gandhe and Grover, 2008; Girard, 2015). Gandhe and Grover (2008) focused on the effect

of head size on wear and implant stability. It was concluded that it is necessary to consider the risk of dislocation against the wear rate, while, especially in the case of elderly patients, dislocation is a more considerable problem than wear, so the large head size allowing a larger range of motion is a proper way to follow. However, the increasing head size leads to more wear particles possibly endangering the replacement durability in the case of young active people.

Experimental investigation of the effect of replacement diameter was conducted by Brockett et al. (2007) who analysed friction and friction torque in metal-on-metal (MoM) implants by a hip joint simulator. Two different configurations were compared; conventional replacement with nominal diameter equal to 28 mm and hip resurfacing of a diameter of 55 mm. As a test lubricant, 25% and 100% bovine serum (BS) was applied finding that independently of operating conditions, the configuration with the larger diameter had a lower friction factor. Dowson et al. (2004) conducted extensive research with the aim to determine the effect of MoM implant diameter and the size of diametric clearance on wear of rubbing surfaces. Five different diameters were investigated; 16 mm, 22 mm, 28 mm, 36 mm, and

* Corresponding author.

E-mail address: necas@fme.vutbr.cz (D. Nečas).

54.5 mm, respectively. It was suggested that the lubrication regime has an essential effect on volumetric wear. The authors thought that 16 mm and 22 mm implants operated under a boundary lubrication regime, and in this regime, the increase of size led to the increase of wear with the number of cycles. However, further enlargement of head diameter was associated with lower wear and this was attributed to a transition from boundary to mixed lubrication. As it was shown that wear also decreased with decreasing clearance, it was concluded that the implants should be as large as possible with the diametric clearance as low as practicable. The importance of diametric clearance was highlighted by Brockett et al. (2008) who investigated the lubricant film thickness inside the contact by using ultrasonic measurement method. It was shown that the largest clearance exhibited the thinnest lubricating film and the highest coefficient of friction. Moreover, the largest clearance was associated with the highest incidence of squeaking. A very thin film was observed even in the case of smallest clearance, however, there was no such a clear impact on friction.

A lubrication analysis in MoM replacements focused on the effect of diametric clearance was performed by Smith et al. (2001a). The authors employed the electrical resistivity technique to detect the surface separation between the head and the cup during a physiological and simplified walking cycle. The clearance varied between 130 and 170 μm , concluding that the lubricant film thickness was enhanced by a decrease of clearance. In the case of the largest clearance, there was no surface separation independently of gait cycle. The study was extended by considering the effect of head diameter on lubrication by the same authors (Smith et al., 2001b). The diameters from 16 to 36 mm were considered in the analysis. Moreover, wear rate was analysed by a simple gravimetric method based on the comparison of the components weight before and after 2 million cycles. The contact was lubricated by 25% BS. The joints were subjected to dynamic motion and loading in an effort to simulate the walking conditions. Electrical resistance measurements were used to assess surface separation. The study showed that in the case of 16 mm and 22.225 mm there was no surface separation over the gait cycle suggesting that joints operate in boundary lubrication regime. An increase to 28 mm led to some surface separation suggesting that the transition to the mixed regime occurred. Further increase to 36 mm caused separation of the surfaces during a considerable part of the cycle; therefore, it was evident that the surfaces were sufficiently protected by some sort of lubricating film. In terms of wear, similar trends as in the case of Dowson et al. (2004) were observed.

A numerical analysis focused on the effect of head diameter, clearance and cup wall thickness in MoM prosthesis on lubrication

was conducted by Liu et al. (2006). The first and second generation of MoM hip resurfacing of nominal diameter of 50 mm was compared with 28 mm total replacement, finding that 50 mm hip resurfacing exhibited a higher central film thickness compared to total replacement independently of the viscosity of lubricant. The results in the case of diametric clearance were not clearly conclusive, since there was a combined effect of clearance and head and cup wall thickness. However, resurfacing with smaller clearance showed a thicker film for both, the first and the second generation of replacement. According to Jalali-Vahid et al. (2001), similar behaviour can be observed even when the cup is made from ultra-high molecular weight polyethylene (UHMWPE). The authors performed a numerical simulation of film thickness according to the implant diameter, clearance, thickness of the cup and cup elastic modulus. It was shown that the predicted film thickness increases with increasing head diameter and decreasing diametric clearance.

Investigation of lubricant film formation can substantially help to better understand the processes occurring inside the contact of artificial joint. The initial study observing the contact in situ, while measuring the film thickness by optical interferometry method, was given by Mavraki and Cann (2009). A model ball-on-disc configuration was used while the effect of mean speed and model fluid was studied. The knowledge was extended by Myant and Cann (2013) who observed the aggregations of proteins in front of the contact zone passing through the contact in time intervals, apparently increasing the lubricant film thickness. As the human synovial fluid (SF) exhibits a non-newtonian shear thinning behaviour (Mavraki and Cann, 2011) and the adsorption of proteins on rubbing surfaces also significantly influences the protein film formation (Parkes et al., 2014), it is evident that the protein lubrication mechanisms do not correspond to classical elastohydrodynamic lubrication. The main differences were described by Myant and Cann (2014a).

Considering the function of human natural and artificial joints, several facts should be taken into account. The first point is that the contact is highly conformal, so it is particularly complicated to attribute the results obtained on the ball-on-disc test device (non-conformal contact) to real joints. The effect of surface conformity on lubricant film formation was firstly mentioned by Vrbka et al. (2013). Later, the same authors changed the configuration to ball-on-lens configuration to approach better conformity of surfaces (Vrbka et al., 2014). As there was a considerable difference against previously published ball-on-disc results, we developed a methodology enabling to measure lubricant film thickness under real conformity of rubbing surfaces (Vrbka et al., 2015b). The experiments were realized in pendulum hip joint simulator

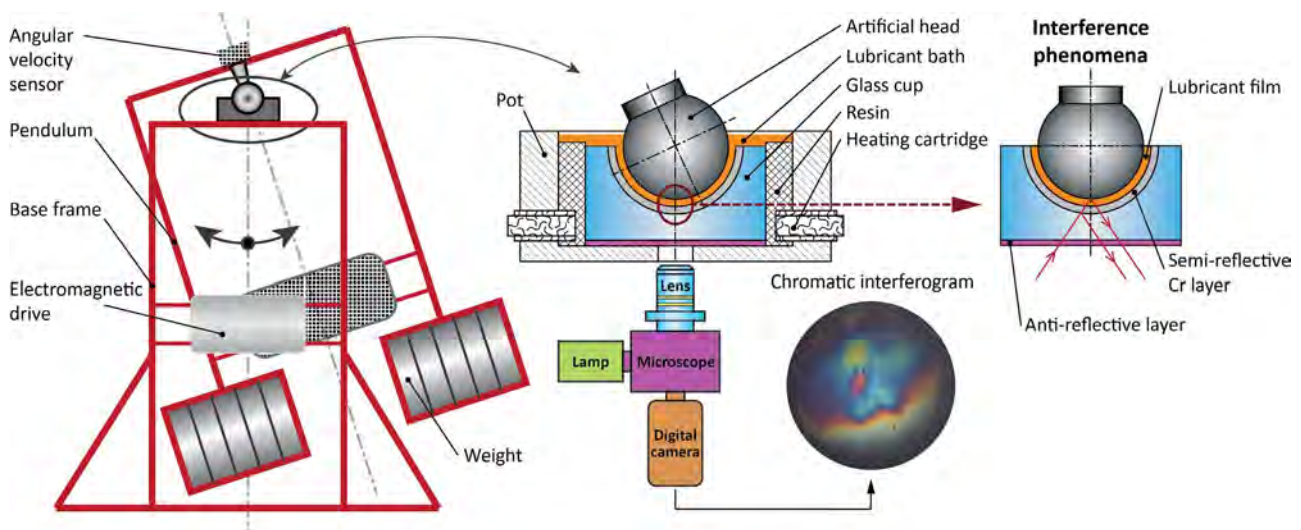


Fig. 1. Scheme of the applied experimental approach.

while considering flexion–extension motion in the range from -16° to 16° . The importance of complex motion was introduced by Myant and Cann (2014b) who measured film thickness under unidirectional and reversing motion. It was revealed that the change of kinematics caused the reduction of lubricant film by approximately 70%.

From the literature review, it is clear that the diameter of hip replacement, as well as the diametric clearance, have a direct impact on the tribological performance of implant. However, so far there has been a lack of experimental studies focusing on in situ observation of protein film formation considering the real conformity of components. Therefore, the aim of the present study is to employ the methodological approach developed in our previous study (Vrbka et al., 2015b) and to measure lubricant film thickness while considering various diameters and clearances. Moreover, the effect of implant material will also be investigated.

2. Materials and methods

The test device used for film thickness measurement consists of hip joint simulator based on the principles of pendulum and optical imaging system. The simulator is composed of base frame with the acetabular cup and the swinging pendulum with the femoral head. Electromagnetic motors are employed to drive the pendulum allowing a continuous motion in the flexion–extension plane. The optical system is composed of illuminator, episcopic microscope, complementary metal-oxide-semiconductor (CMOS) high-speed camera (Phantom v710) and PC. The scheme of the experimental apparatus is shown in Fig. 1.

For the evaluation of film thickness, an optical method based on colorimetric interferometry was employed (Hartl et al., 2001). Optical interference is a physical phenomenon occurring when two light beams reflected from nearby interfaces are composed together. In the case of ball-on-cup configuration, the first interface is between the thin chromium layer deposited on the glass cup and the film of model fluid. The second interface is between the film and the femoral head. The principle of this method can be seen in Fig. 1 (right). It was previously proved by Hartl et al. (2001) that the method enables very accurate measurement of lubricant film with the resolution down to 1 nm. The maximum detectable film thickness is around 900 nm. The evaluation procedure is based on the three following steps.

1. The image of lightly loaded static contact is captured, while the calibration curves based on the shape of the contact zone can be obtained. Therefore, the dependence between the colour and the corresponding film thickness is known.
2. Capturing of the fully loaded contact zone during the swinging test via digital camera.
3. Matching of the captured interferograms with calibration curves; determining of the film thickness in arbitrary pixels of the images.

In the present study, the femoral components made from CoCr alloy were mainly studied. Moreover, to be able to determine the effect of

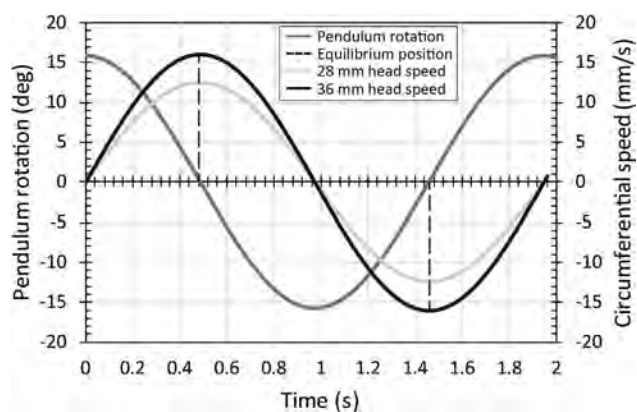


Fig. 2. Kinematics of the performed swinging tests per one cycle.

material, ceramic implants (BIOLOX^{forte} – Al₂O₃; BIOLOX^{delta} – 75% Al₂O₃, 24% ZrO₂, Cr₂O₃) were also considered. The heads were of two different nominal diameters; 28 and 36 mm, respectively. As a counterface, a custom-made acetabular cup from optical glass (BK7) was used and it was manufactured according to the dimensions of real cups to be able to assess the role of diametric clearance. The individual cups were measured using the optical scanning method (GOM ATOS Triple Scan). To ensure a sufficient interference of light, the contact convex surface of the cup was coated with a semi-reflective chromium layer. A detailed summary of the tested implants including the information about the size of clearances is provided in Table 1. The material properties of the tested samples are as follows: metal ($E = 230$ GPa, $\nu = 0.3$), ceramic ($E = 340$ GPa, $\nu = 0.28$), optical glass ($E = 85$ GPa, $\nu = 0.209$).

As a model SF, 25% bovine serum (B9433 Sigma Aldrich) with the protein content equal to 22.4 mg/ml was applied. The total amount of lubricant was 12 ml and it was deeply frozen to -22°C immediately after preparation. The solution was taken out from the freezer 2 h prior to testing to avoid any temperature shock during thawing. The simulator controls the temperature of the lubricant in the cup pot using heating cartridges, so the experiments were carried out under body temperature of $37 \pm 1^\circ\text{C}$. All the contact components were cleaned in 1% sodium dodecyl sulphate solution, subsequently rinsed in distilled water, dried by pressed air, and finally washed in isopropyl alcohol.

Two types of tests were carried in the present study. Initially, a static test was conducted with the aim to understand the protein adsorption process onto rubbing surfaces. It consisted of 15 s of loading and subsequent unloading lasting 45 s. Therefore, the duration of one cycle was 1 min, while 20 cycles were performed in total. After the static test, a dynamic swinging test was performed, while the film thickness as a function of time was evaluated. Duration of the dynamic test was not constant since it was affected by the contact behaviour disabling the film thickness evaluation due to several phenomena discussed below. However, the maximum time of the test was set to

Table 1
Summary of the test samples.

Ball material	Ball diameter (mm)	Cup diameter (mm)	Diametric clearance (μm)	Hertzian contact pressure (MPa)	Hertzian contact zone diameter (mm)	Test type
Metal	27.97	28.01	40	16.6	7.69	Dynamic
Metal	27.97	28.288	318	65.8	3.87	Dynamic
Metal	35.95	36.093	143	27.8	5.95	Static/Dynamic
Metal	35.95	36.535	585	70.4	3.74	Dynamic
BIOLOX ^{forte}	27.97	28.067	93	29.1	5.81	Dynamic
BIOLOX ^{forte}	35.96	36.087	124	25.2	6.24	Static
BIOLOX ^{delta}	27.97	28.067	97	31.8	5.56	Dynamic
BIOLOX ^{delta}	35.98	36.087	109	23.2	6.52	Static

210 s. The range of the flexion–extension motion was -16° to $+16^\circ$, while the film thickness was evaluated in the equilibrium position of the pendulum (deflection is 0°). The film thickness is an average value inside a circle with the radius of $200\ \mu\text{m}$. The load in the case of all tests was $515\ \text{N}$; corresponding contact pressures and the contact zone diameters are listed in Table 1. The kinematics of the experiment cycle including a circumferential speed for both nominal diameters is displayed in a greater detail in Fig. 2.

3. Results

3.1. Static test

A static test allowing to study adsorption of proteins on rubbing surfaces was conducted with all the tested materials, while the nominal diameter of heads was $36\ \text{mm}$ and small diametrical clearances were considered. Due to repeatability, the experiment was conducted four times. The results are shown in Figs. 3–5. As can be seen, in the case of metal head (Fig. 3), the results are clearly conclusive with very satisfactory repeatability. Initially, the film is relatively thin and stable around $50\ \text{nm}$. From the fourth cycle, the film thickness gradually increases until the end of the test, while the maximum film is approximately $150\ \text{nm}$. The increasing tendency of protein film can be also observed on the interferograms, see Fig. 3b.

In the case of BIOLOX[®]forte ceramic (Fig. 4), there is a substantial

variance of results especially during the first loading cycles. After 8 min (8 cycles), the film is relatively stable and is kept between 100 and $200\ \text{nm}$ according to particular replications. The fluctuations of film thickness can be seen on the obtained interferograms captured at different time intervals (Fig. 4b). A different character of protein film development was observed in the case of BIOLOX[®]delta ceramic (Fig. 5). With the exception of the measurement number four, the film thickness is almost constant between the third and seventh minute; it is about $100\ \text{nm}$. After that, the results become more scattered and the film varies between 50 and $250\ \text{nm}$. As can be seen, during the measurement number one, the adsorbed layer continuously increased, as is also evident from the images of the contact zone (Fig. 5b).

3.2. Dynamic test – the effect of head diameter and diametric clearance

Since it is evident that human joints operate under complex kinematic conditions, swinging experiments were performed to acquire information about the film formation during flexion–extension movement. As can be seen in Figs. 6 and 7, the effect of nominal diameter on protein film development is substantial, especially with a smaller diametric clearance being considered, see Fig. 6. In the case of $28\ \text{mm}$ head, the film initially increases rapidly reaching up to $430\ \text{nm}$. After a short time, it decreases while being kept constant between the twentieth and seventieth second. This phase is followed by

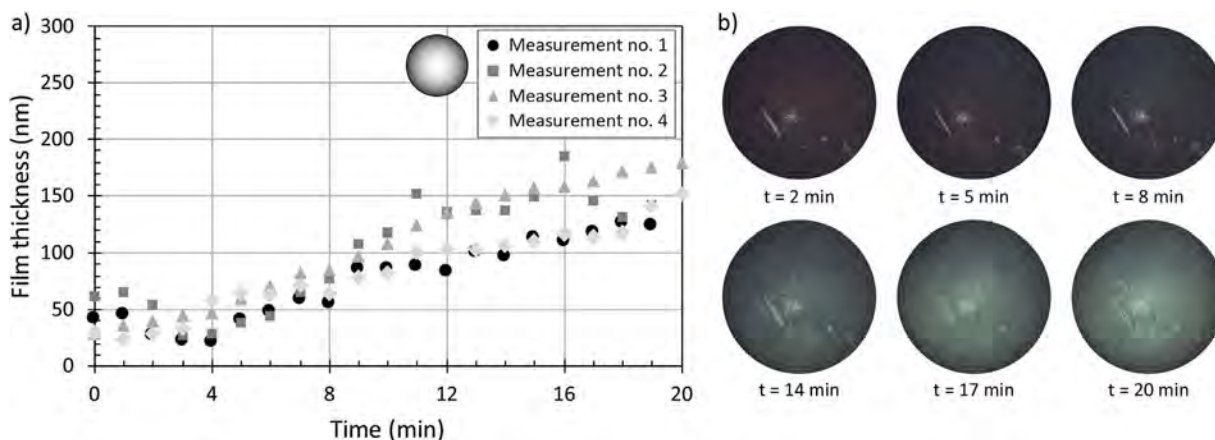


Fig. 3. a) Static test - film thickness as a function of time for metal head: nominal diameter $36\ \mu\text{m}$, diametric clearance $143\ \mu\text{m}$. b) Chromatic interferograms taken during the first measurement.

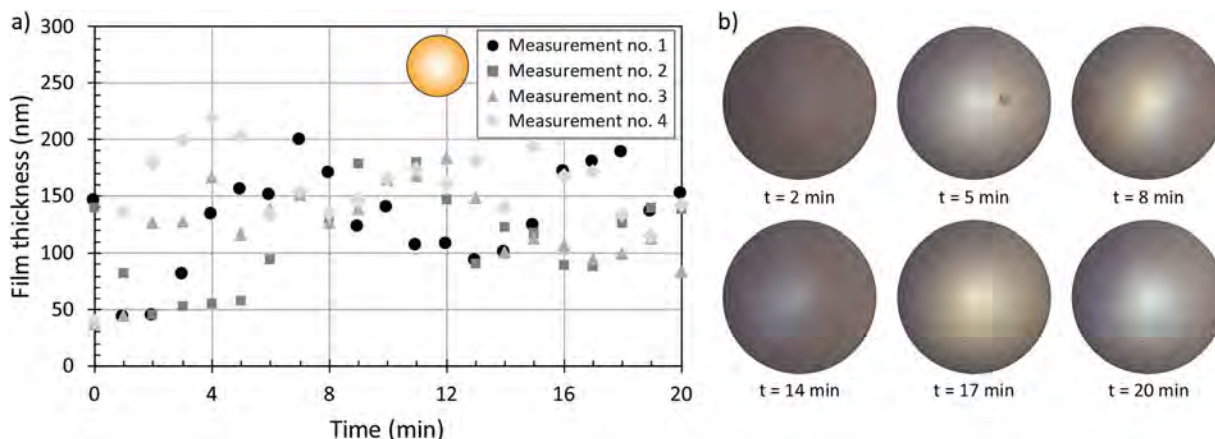


Fig. 4. a) Static test - film thickness as a function of time for BIOLOX[®]forte head: nominal diameter $36\ \mu\text{m}$, diametric clearance $124\ \mu\text{m}$. b) Chromatic interferograms taken during the first measurement.

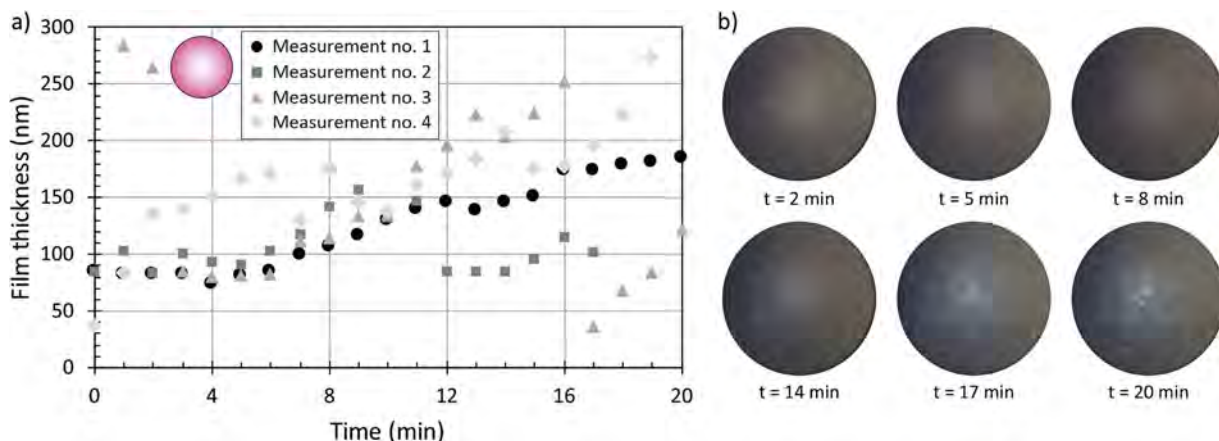


Fig. 5. a) Static test - film thickness as a function of time for BIOLOX*delta head: nominal diameter 36 mm, diametric clearance 109 μm . b) Chromatic interferograms taken during the first measurement.

gradual increment of lubricating film up to a measurable level. Although the evaluation is not possible due to the limits of this method (around 900 nm), it is expected that the film continuously increases, thus sufficiently protecting the surfaces against the mutual contact which can positively affect wear of rubbing surfaces. For the larger diameter, the film formation is similar during the first eighty seconds; however, the film thickness is smaller, around 150 nm. Consequently, the film starts to slightly increase for the rest of the experiment, while the final maximum is slightly less than 500 nm.

For larger clearance, the influence of head size on film thickness is not so significant, as is shown in Fig. 7. The 28 mm head shows almost a constant course of lubricating film which is around 220 nm. In the case of larger diameter, the film is stabilized after approximately 40 s;

reaching 150 nm. However, as can be seen from the chromatic interferograms, in the case of 36 mm head, the chromium layer on the acetabular cup was gradually removed due to articulation within the first 100 s of the experiment, indicating that the wear rate might be much higher compared to that of a smaller head. When there is no chromium layer on the surface, the evaluation process fails; therefore, it is not possible to determine the film thickness anymore.

From the graphs in Fig. 6, Fig. 7, it can be clearly concluded that the most important geometrical parameter influencing the protein film formation is diametric clearance. The comparison of results is displayed in Fig. 8 while it is apparent that lowering the clearance between the surfaces has a very positive impact on the thickness of the lubricant film.

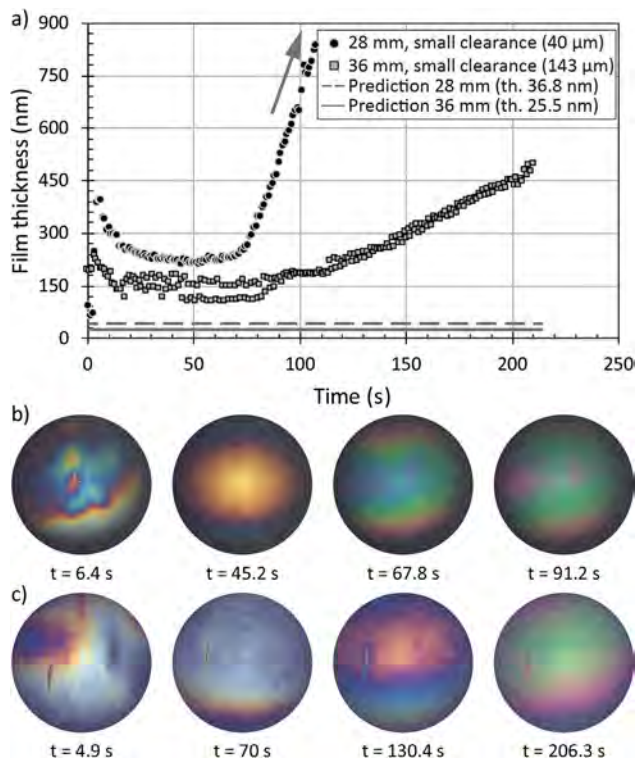


Fig. 6. a) Film thickness development as a function of time for 28 and 36 mm pairs with smaller clearances. Predictions are from conventional elastohydrodynamic theory as explained in the Discussion section. Bottom: Chromatic interferograms of the contact zone captured at time intervals during the experiment; b) 28 mm, c) 36 mm. Inlet/outlet is on the top/bottom of the images.

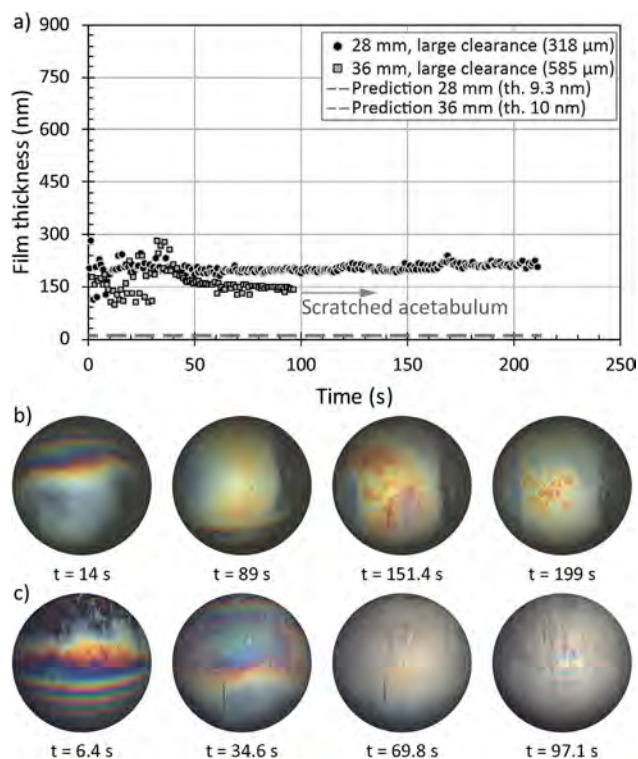


Fig. 7. a) Film thickness development as a function of time for 28 and 36 mm pairs with larger clearances. Predictions are from conventional elastohydrodynamic theory as explained in the Discussion section. Bottom: Chromatic interferograms of the contact zone captured at time intervals during the experiment; b) 28 mm, c) 36 mm. Inlet/outlet is on the top/bottom of the images.

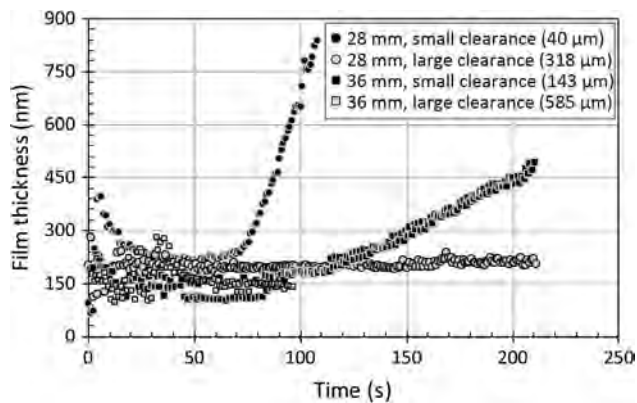


Fig. 8. Film thickness development as a function of time for different head diameters and diametric clearances.

3.3. Dynamic test – the effect of material

To be able to assess the role of material in relation to protein film formation, a dynamic test was also conducted with ceramic heads of nominal diameter of 28 mm, while the clearances for BIOLOX[®]forte and BIOLOX[®]delta ceramic were 93 and 97 μm, respectively. The results are shown in Fig. 9. The thickest film was formed when the metal head was investigated. As was mentioned above, the maximum film thickness was more than 800 nm. In the case of BIOLOX[®]forte

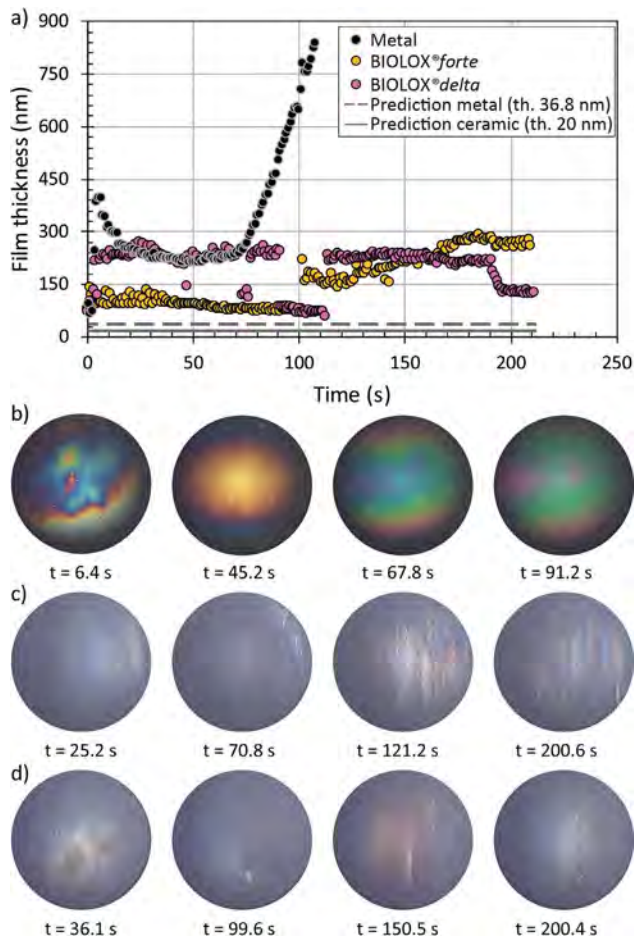


Fig. 9. a) Film thickness development as a function of time for different materials of nominal diameter of 28 mm. Predictions are from conventional elastohydrodynamic theory as explained in the Discussion section. Bottom: Chromatic interferograms of the contact zone captured at time intervals during the experiment; b) metal, c) BIOLOX[®]forte, d) BIOLOX[®]delta. Inlet/outlet is on the top/bottom of the images.

ceramic, the film thickness was not substantially changed within the first 100 s; during this time the layer thickness was around 100 nm. Then there was a sudden skip of film to approximately 160 nm, while it slightly increased for the rest of the experiment. An opposite behaviour was observed for BIOLOX[®]delta. The initial stable film in the range between 210 and 270 nm was followed by a substantial drop to about 70 nm between the ninetieth and one hundred fifteenth second. Then the film skipped back to 230 nm and during the last 20 s it again decreased. The instabilities of the film thickness in the case of ceramic materials can be explained in terms of protein agglomerations moving through the contact zone as a consequence of joint articulation.

4. Discussion

Recently, extensive research was conducted to clarify the lubrication processes inside the total hip replacement. For this purpose, the optical interferometry method in combination with ball-on-disc tribometers was successfully employed for film thickness measurement along with investigations of several factors such as mean speed (Mavraki and Cann, 2009, 2011); model fluid composition (Fan et al., 2011; Myant and Cann, 2013); load (Myant et al., 2012); time; rolling/sliding distance; implant material (Vrbka et al., 2013, 2014); motion character (Myant and Cann, 2014b); or surface wettability and surface conformity (Vrbka et al., 2014) influencing protein film formation. Later, Vrbka et al. (2015b) developed a methodological approach allowing for determination of lubricant film thickness considering the real conformity of rubbing surfaces. As there were significant differences between the results obtained for non-conformal and conformal contacts, it was recommended to focus on the real shape bodies approaching the conditions inside the joint. From the literature review, it is apparent that the implant diameter as well as diametric clearance have a substantial effect on lubrication and wear of rubbing surfaces (Brockett et al., 2007; 2008, Dowson et al., 2004, Smith et al., 2001a; 2001b). Therefore, an experimental investigation based on in situ observation of contact zone was conducted, aiming to define the optimal implant combination ensuring sufficient lubrication of rubbing surfaces.

The initial static test was carried out allowing for evaluation of the protein adsorption onto rubbing surfaces. It can be seen from Figs. 3–5 that, according to the implant material, the adsorbed film thickness after several loading cycles is in the range from 100 to more than 200 nm. A similar test was conducted by Myant et al. (2012). The authors focused on metal femoral component and the experiments were conducted on ball-on-disc device where the contact pressure was considerably higher. In the case of bovine serum as a test lubricant, the adsorbed protein layer was only around 10 nm. The present results indicate that the contact pressure has a substantial effect on protein film emphasizing the importance of real conformity consideration. When focusing on particular materials, it can be seen in Fig. 3 that in the case of metal component the film thickness continuously increases with loading cycles. This indicates that the adsorption forces are strong enough to avoid protein desorption from the surfaces due to repeated loading and unloading. In the case of ceramic heads (Figs. 4 and 5), the results are not so clear. In general, the film thickness was higher; however, significant fluctuations of results were observed referring to repeating adsorption and desorption of the proteins onto the contact bodies. The higher thickness is attributed to protein agglomerations entrapped within the contact during the loading phase, which could be observed on the images of the contact zone. Nevertheless, the adsorption forces are not enough strong to maintain the proteins on the surfaces; therefore, the proteins repeatedly desorb when the contact is unloaded, eventually leading to unstable protein film development.

The main goal of the present study was to assess the role of implant geometry and material on protein film formation during flexion–extension motion. For this purpose, a dynamic swinging test was performed giving the following results. The main parameter influencing

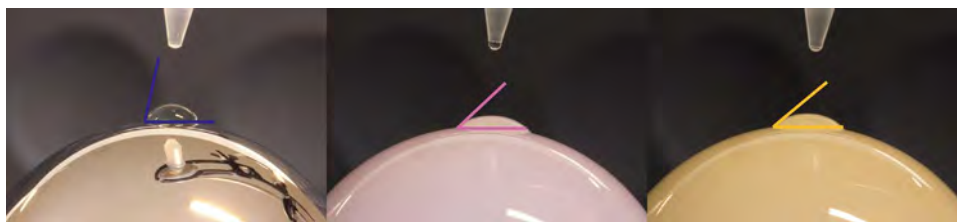


Fig. 10. Comparison of the contact angles representing the surface wettability. From the left: metal, BIOLOX®delta, BIOLOX®forte.

the protein film was found to be the diametric clearance. It was previously discussed in the literature that clearance has a substantial effect on surface separation during articulation (Smith et al.; 2001a). From Fig. 8, it is clear that lowering the diametric clearance led to a rapid change of film formation for tested diameters, 28 and 36 mm, respectively. It is expected that lowering the clearance between the surfaces can lead to a more stable arrangement with a lower level of slippage of the components, which can potentially lead to removal of the proteins from the contact. A gradual increase is caused by swinging motion while the amount of proteins between the surfaces increases with each following cycle; the proteins are passing through the contact being entrapped in the central zone. However, in the case of larger clearance the femoral head slips against the cup; therefore, the film is repeatedly disrupted and cannot be fully developed, so the surfaces are not sufficiently separated by lubricant film, which can negatively influence the wear rate (Fig. 7c) and hence eventually the service life of implant. Slippage phenomena can be clearly observed when the pendulum is deflected to a maximum angle ($-16/+16$) and the direction of movement is changed. It means that during the swing cycle, the head is continuously approaching the maximum deflection. Suddenly, when the maximum deflection is reached and; therefore, the speed is equal to zero, a slight slipping of the head in the cup can be identified. This is, in author's opinion, associated with the size of the diametric clearance. If the radius of the cup would be the same as the radius of the ball, the ball could not move within the cup (it could just rotate) as its position would be restricted by the cup shape. On the contrary, when the clearance between the surfaces increases, the ball can perform both, rotation and slight motion in the cup leading to the slippage phenomena at the extreme position of the pendulum arm. From the experiment records, it is evident that the slippage is more considerable for implants with larger clearances.

It is particularly complicated to compare the results with previously published ball-on-disc data as it was already discussed that the approaches are completely different, which leads to a different character of film formation. In our previous study introducing the methodological approach for film thickness determination under real conformity, we measured the film thickness between the 28 mm metal head and glass cup, while the diametric clearance was $92\ \mu\text{m}$ (Vrbka et al., 2015b). The clearance was considered to be relatively small indicating that the results could be comparable with the current study. In the previous paper, the film thickness reached almost 240 nm immediately after the beginning of the experiment, while it continuously decreased for the rest of the test. This behaviour does not correspond to the present results; however, it should be noted that previously (Vrbka et al., 2015b) the pendulum was not driven by the motors; deflection was naturally damped due to friction between the components. Therefore, it can be concluded that a continuous motion helps to improve lubrication conditions.

In terms of material, it is shown in Fig. 9 that, in general, the metal head forms a thicker film compared to the ceramic one. A similar behaviour in protein film formation was also observed for ball-on-disc arrangement (Vrbka et al., 2013). This can be mainly attributed to surface wettability. It was shown by Vrbka et al. (2014) that a hydrophobic nature of surface supports protein film formation. Moreover, it was discussed by Malmsten (1998) that both dominant

constituents contained in BS (albumin and γ -globulin) adsorb better onto hydrophobic surfaces. Although all the tested materials are hydrophobic, hydrophobicity of metal head is higher, leading to a thicker protein film. Wettability of all the three tested materials was checked using a droplet test. The tests were realized with BS, while it was showed in literature that the difference in wettability considering water and BS is negligible (Salehi et al., 2006). Drop of BS was putted on the top of the heads and the contact angle was investigated by image processing. The highest wettability was exhibited by metal, followed by BIOLOX®delta and BIOLOX®forte. The particular values of contact angles were as follows: 77.7° , 43° , and 39.6° , respectively. The contact angles for particular femoral heads are depicted in Fig. 10. Similar investigation was introduced by Wusylko et al. (2014), who compared the wettability of new and retrieved femoral heads. The authors obtained qualitatively the same results for the new implants.

The substantial drops and jumps of protein film in the case of ceramic heads support our statement that the film formation is substantially influenced by the nature of the head material. As was discussed above, stronger protein agglomerations were observed in the case of ceramic heads potentially causing an increase of film thickness during the static adsorption test. However, the film fluctuated significantly due to repeating protein desorption from the surfaces. Although the film was more stable in the case of dynamic test, the adsorption forces are not enough strong to maintain the proteins on the ceramic surfaces; therefore, the film was removed due to joint articulation, leading to sudden drops of the protein film. Within few following cycles, the film is adsorbed onto rubbing surfaces again, leading to a sudden increase of film thickness. This effect could be clearly observed on the records of the experiments. While in the case of metal, adsorbed protein film moved with the moving head, in the case of ceramic, protein agglomerations rolled between the surfaces occasionally adsorbing onto the surfaces.

In addition, it must be taken into account that the diametric clearance in the case of ceramic heads was more than twice that of the metal head (BIOLOX®forte: $93\ \mu\text{m}$; BIOLOX®delta: $97\ \mu\text{m}$; metal: $40\ \mu\text{m}$), proving the importance of the surface geometry. It should be pointed out that the manufacturing process of tailor made acetabular cups is particularly complicated. Although all the cups were fabricated in the range of defined tolerances, some differences between the individual cups could be detected. Nevertheless, $93\ \mu\text{m}$ and $97\ \mu\text{m}$ is still considered to be small diametric clearances. It is expected that further decrease of clearance would lead to thicker protein film; however, it would be still thinner compared to metal due to different wettability.

From the results displayed in Fig. 6, Figs. 7 and 9, it is apparent that the proteins play an important role in terms of lubrication, since all the measured thicknesses are higher compared to theoretical predictions based on the equation given by Hooke (1980), see Eq. (1). This equation was previously employed several times when predicting the film thickness in the contact lubricated by the model synovial fluid, as is widely reported in literature (Fan et al., 2011; Mavraki and Cann, 2011; Myant et al., 2012; Myant and Cann, 2013, 2014a, 2014b; Vrbka et al., 2013). Especially in the case of metal heads, lubricant film is substantially thicker independently of diameter and the size of the diametric clearance. The prediction of film thickness

varied from 9.3 nm (28 mm metal head, large diametric clearance) to 36.8 nm (28 mm metal head, small diametric clearance), while the measured data ranged between 100 nm and 850 nm.

$$h = 4.18 \frac{(U\eta)^{0.6} R'^{-0.67}}{W^{0.13} E^{-0.47}}, \quad (1)$$

where U is the entrainment speed (6.12 mm/s for 28 mm head, and 7.85 mm/s for 36 mm head, respectively), η is a dynamic viscosity of the test lubricant (for 25% BS it is considered as $\eta = 0.00213$ Pa·s based on Mavraki and Cann, (2011)), R' is the reduced radius calculated as $1/R' = (1/R_{bx} + 1/R_{by}) - (1/R_{cx} + 1/R_{cy})$, where R_{bx} , R_{by} and R_{cx} , R_{cy} denote the radii of the ball and the cup in x and y direction, W is the applied load ($W=515$ N) and E' is reduced Young's modulus defined as $2/E' = (1-\nu_b^2)/E_b + (1-\nu_c^2)/E_c$, while ν_b , ν_c , E_b , E_c are the Poisson's ratios and Young's moduli of the ball and the cup, respectively.

Obviously, the authors realize that the present study suffer from several limitations. First of all, the material of acetabular cup should be mentioned. It is evident that one of the counterparts has to be reflective to enable the in situ observation of the contact. The elastic modulus of the optical glass is approximately 85 GPa. For CoCr alloys and ceramic materials, it is about 230 GPa and 340 GPa, respectively; so the glass cup is three to five times softer in comparison with hard implant materials. On the other hand, the elastic modulus of ultra-high molecular weight polyethylene (UHMWPE), which is often used as a cup material, is only in the range of units of GPa. Therefore, the results rather correspond to hard-on-hard implants than to hard-on-soft combination. This statement is also supported in terms of the size of diametric clearances. It was published in our previous study (Vrbka et al., 2015a) that the clearances in the case of metal-on-polyethylene and ceramic-on-polyethylene implants are generally higher compared to those of metal-on-metal or ceramic-on-ceramic.

Secondly, as discussed above, the dynamic tests were conducted considering the swinging motion in only flexion-extension plane under the constant load. According to the conditions such as walking, running, stance phase, etc., it is apparent that the motion character of synovial joints is multidirectional and, in addition, the load is changed over the cycle. The currently used simulator did not allow to change the load abruptly as the load is applied by putting the weights on the arms of the pendulum. For this purpose, a new loading system which could be completely controlled by the software has to be developed.

Finally, human SF contains many constituents such as proteins, lipids or hyaluronic acid (Sawae et al., 2008). To be able to better simulate in vivo conditions, a more complex model fluid should be considered in future studies. It is also desirable to assess the behaviour of individual proteins contained in the model fluid. For this purpose, different methodological approaches have to be applied. The measurement method employed in the present study allows for evaluation of the surface separation with very high accuracy. However, it does not enable to distinguish the particular parts of the lubricant. This can be solved by the optical method based on fluorescent microscopy, since it was already proved that it can be used for detection of protein film intensity for both metal (Nečas et al., 2015) and ceramic (Nečas et al., 2016) materials.

5. Conclusion

The results of the present study can be concluded into following points:

- The static test showed that the adsorption forces are generally stronger in the case of metal heads where the film thickness development was very stable without significant fluctuations. However, even ceramic heads exhibited a relatively thick adsorbed

layer, suggesting the importance of the proteins contained in BS.

- Based on the swinging test, it is evident that the most important geometrical parameter influencing the tribological performance of hip replacement is the diametric clearance. Lowering the clearance from 318 to 40 μm of 28 mm implant led to a substantial increase of lubricant film potentially protecting the rubbing surfaces.
- The increase of implant nominal size from 28 to 36 mm did not cause a substantial change of film formation. Although the total film thickness was higher for 28 mm implant, it is apparent that the nominal diameter is not as critical parameter as diametric clearance when considering 28 mm and 36 mm implants.
- It was shown that during articulation the metal heads form a thicker film compared to the ceramic heads. Nevertheless, it must be taken into account that the diametric clearance in the case of ceramic heads was more than two times higher compared to the metal one. Moreover, ceramic materials generally exhibit lower friction (Vrbka et al., 2015a), indicating that the surfaces can be suitably protected against wear even if the film thickness is smaller.
- Considering the prediction formula for film thickness estimation, it is apparent that the measured film thicknesses are considerably higher. The film thickness is substantially affected by the behaviour of the model synovial fluid. The first point is that the fluid exhibits shear thinning behaviour. Moreover, it is particularly complicated to involve the role of proteins, contained in the model fluid, to the theoretical prediction. Both, protein adsorption on rubbing surfaces, as well as protein aggregation substantially influence the film thickness, enhancing the lubricant layer, in general, indicating that the theoretical predictions might not be a suitable tool in implant design process.

Further study should involve a more complex model fluid, as well as a transient character of loading, with the aim to approach the conditions inside the synovial joints, while the main attention should be paid to the role of particular fluid constituents.

Acknowledgement

This research was carried out under the project NETME CENTRE PLUS (LO1202) with financial support from the Ministry of Education, Youth and Sports under the National Sustainability Programme I. The research was also supported by the project no. FSI-S-14-2336 with the financial support from the Ministry of Education, Youth and Sports of the Czech Republic. The authors express their thanks to D. Rebenda, who participated in film thickness measurements as well as in data evaluation and their analysis.

References

- Brockett, C.L., Williams, S., Jin, Z.M., et al., 2007. A comparison of friction in 28 mm conventional and 55 mm resurfacing metal-on-metal hip replacements. *Proc. Inst. Mech. Eng. Part J: J. Eng. Tribol.* 221 (3), 391–398.
- Brockett, C.L., Harper, P., Williams, S., et al., 2008. The influence of clearance on friction, lubrication and squeaking in large diameter metal-on-metal hip replacements. *J. Mater. Sci.: Mater. Med.* 19 (4), 1575–1579.
- Cross, M.B., Nam, D., Mayman, D.J., 2012. Ideal femoral head size in total hip arthroplasty balances stability and volumetric wear. *HSS J.* 8 (3), 270–274.
- Dowson, D., Hardaker, C., Flett, M., et al., 2004. A hip joint simulator study of the performance of metal-on-metal joints: part II: design. *J. Arthroplast.* 19 (8), 124–130.
- Di Puccio, F., Mattei, L., 2015. Biotribology of artificial hip joints. *World J. Orthop.* 6 (1), 77–94.
- Fan, J., Myant, C.W., Underwood, R., et al., 2011. Inlet protein aggregation: a new mechanism for lubricating film formation with model synovial fluids. *Proc. Inst. Mech. Eng. Part H: J. Eng. Med.* 225 (7), 696–709.
- Gandhe, A., Grover, M., 2008. (i) Head size, does it matter? *Curr. Orthop.* 22 (3), 155–164.
- Girard, J., 2015. Femoral head diameter considerations for primary total hip arthroplasty. *Orthop. Traumatol.: Surg. Res.* 101 (1), 25–29.
- Hartl, M., Křupka, I., Poliščuk, R., et al., 2001. Thin film colorimetric interferometry. *Tribol. Trans.* 44 (2), 270–276.

- Hooke, C.J., 1980. The elastohydrodynamic lubrication of heavily loaded point contacts. *J. Mech. Eng. Sci.* 22 (4), 183–187.
- Jalali-Vahid, D., Jagatia, M., Jin, Z.M., et al., 2001. Prediction of lubricating film thickness in UHMWPE hip joint replacements. *J. Biomech.* 34 (2), 261–266.
- Joshi, A.B., Porter, M.L., Trail, I.A., et al., 1993. Long-term results of Charnley low-friction arthroplasty in young patients. *J. Bone Jt. Surg. Br.* 75 (4), 616–623.
- Liu, F., Jin, Z., Roberts, P., et al., 2006. Importance of head diameter, clearance, and cup wall thickness in elastohydrodynamic lubrication analysis of metal-on-metal hip resurfacing prostheses. *Proc. Inst. Mech. Eng. Part H: J. Eng. Med.* 220 (6), 695–704.
- Malmsten, M., 1998. Formation of adsorbed protein layers. *J. Colloid Interface Sci.* 207 (2), 186–199.
- Mavraki, A., Cann, P.M., 2009. Friction and lubricant film thickness measurements on simulated synovial fluids. *Proc. Inst. Mech. Eng. Part J: J. Eng. Tribol.* 223 (3), 325–335.
- Mavraki, A., Cann, P.M., 2011. Lubricating film thickness measurements with bovine serum. *Tribol. Int.* 44 (5), 550–556.
- Myant, C., Cann, P., 2013. In contact observation of model synovial fluid lubricating mechanisms. *Tribol. Int.* 63, 97–104.
- Myant, C., Cann, P., 2014a. On the matter of synovial fluid lubrication: implications for metal-on-metal hip tribology. *J. Mech. Behav. Biomed. Mater.* 34, 338–348.
- Myant, C., Cann, P., 2014b. The effect of transient conditions on synovial fluid protein aggregation lubrication. *J. Mech. Behav. Biomed. Mater.* 34, 349–357.
- Myant, C., Underwood, R., Fan, J., et al., 2012. Lubrication of metal-on-metal hip joints: the effect of protein content and load on film formation and wear. *J. Mech. Behav. Biomed. Mater.* 6, 30–40.
- Nečas, D., Vrbka, M., Urban, F., et al., 2015. The effect of lubricant constituents on lubrication mechanisms in hip joint replacements. *J. Mech. Behav. Biomed. Mater.* 55, 295–307.
- Nečas, D., Vrbka, M., Krupka, I., et al., 2016. Lubrication within hip replacements—implication for ceramic-on-hard bearing couples. *J. Mech. Behav. Biomed. Mater.* 61, 371–383.
- Parkes, M., Myant, C., Cann, P.M., et al., 2014. The effect of buffer solution choice on protein adsorption and lubrication. *Tribol. Int.* 72, 108–117.
- Salehi, A., Tsai, S., Pawar, V., et al., 2006. Wettability analysis of orthopaedic materials using optical contact angle methods. *Key Eng. Mater.* 309, 1199–1202.
- Sawae, Y., Yamamoto, A., Murakami, T., 2008. Influence of protein and lipid concentration of the test lubricant on the wear of ultra high molecular weight polyethylene. *Tribol. Int.* 41 (7), 648–656.
- Smith, S.L., Dowson, D., Goldsmith, A.A.J., 2001a. The effect of diametral clearance, motion and loading cycles upon lubrication of metal-on-metal total hip replacements. *Proc. Inst. Mech. Eng. Part C: J. Mech. Eng. Sci.* 215 (1), 1–5.
- Smith, S.L., Dowson, D., Goldsmith, A.A.J., 2001b. The effect of femoral head diameter upon lubrication and wear of metal-on-metal total hip replacements. *Proc. Inst. Mech. Eng. Part H: J. Eng. Med.* 215 (2), 161–170.
- Vrbka, M., Návrat, T., Krupka, I., et al., 2013. Study of film formation in bovine serum lubricated contacts under rolling/sliding conditions. *Proc. Inst. Mech. Eng. Part J: J. Eng. Tribol.* 227 (5), 459–475.
- Vrbka, M., Krupka, I., Hartl, M., et al., 2014. In situ measurements of thin films in bovine serum lubricated contacts using optical interferometry. *Proc. Inst. Mech. Eng. Part H: J. Eng. Med.* 228 (2), 149–158.
- Vrbka, M., Nečas, D., Bartošik, J., et al., 2015a. Determination of a friction coefficient for THA bearing couples. *Acta Chir. Orthop. Traumatol. Cechoslov.* 82 (5), 341–347.
- Vrbka, M., Nečas, D., Hartl, M., et al., 2015b. Visualization of lubricating films between artificial head and cup with respect to real geometry. *Biotribology* 1–2, 61–65.
- Wusylko, A., Freed, R., Brandt, J. M., et al., 2014. Comparison Between Surface Roughness and Wettability on Retrieved Metal and Ceramic Femoral Heads. In: *Society for Biomaterials Annual Meeting and Exposition 2014: Transactions Proceedings of the 38th Annual Meeting, Society For Biomaterials, USA*, s. 277. ISBN 978-1-63266-236-1. ISSN 1526-7547.



In situ observation of lubricant film formation in THR considering real conformity: The effect of model synovial fluid composition



D. Nečas^{a,*}, M. Vrbka^{a,e}, D. Rebenda^a, J. Gallo^b, A. Galandáková^c, L. Wolfová^d, I. Křupka^{a,e}, M. Hartl^a

^a Faculty of Mechanical Engineering, Brno University of Technology, Czech Republic

^b Department of Orthopaedics, Faculty of Medicine and Dentistry, Palacky University Olomouc, University Hospital Olomouc, Czech Republic

^c Faculty of Medicine and Dentistry, Palacky University Olomouc, Czech Republic

^d Contipro a.s., Czech Republic

^e CEITEC - Central European Institute of Technology, Brno University of Technology, Czech Republic

ARTICLE INFO

Keywords:

Total hip arthroplasty
Lubricant film
Synovial fluid
Hyaluronic acid

ABSTRACT

The present paper explores the effect of synovial fluid composition on lubricant film formation in hip replacements. The measurements were realized utilizing pendulum hip joint simulator, while the film thickness was evaluated using optical interferometry. Contact couples consisted of metal and ceramic femoral heads articulating with glass acetabular cups. As the test lubricants, various model fluids were employed. Initially, static tests, aimed on the effect of material and load on adsorption, were conducted. It was found that adsorbed film thickness increases independently of the head material. Consequently, swinging flexion-extension experiments were realized, revealing that the film formation is substantially affected by composition of model fluid. The thickest film was observed when higher concentration of hyaluronic acid and phospholipids was applied.

1. Introduction

Hip joint arthroplasty is known to be well-established surgery, substantially improving the life quality of millions of patients [1]. Nevertheless, as the number of young active patients with joint replacements gradually increases [2], it is necessary to ensure sufficient service-life of implants to avoid its failure. Since the most common cause limiting the replacement durability is aseptic loosening [3], an extensive attention of researchers is paid to clarify both wear and lubrication processes inside the artificial joints. For this purpose, various types of commercial, as well as tailor-made simulators have been employed, while it is indicated that the key factor, apparently influencing lubricant film formation and subsequent wear rate, is the composition of model synovial fluid (SF) [4].

Although bovine serum (BS) is widely used as the substitution of human SF for *in vitro* investigations [5], it must be taken into account that the composition of BS and SF is different. While BS is composed of proteins (albumin, γ -globulin) and lipids (cholesterol, triglycerides), SF contains albumin, γ -globulin, phospholipids and hyaluronic acid (HA). Especially HA substantially affects the rheology [6] and; moreover, it has a great impact on lubrication properties of the fluid [7]. However, it was shown by Galandáková et al. [8] that the composition and properties of

human SF differ significantly according to factors such as age, body mass index (BMI), or joint condition. Therefore, it is desired to carefully consider the composition of model SF when studying the tribological performance of joint replacements.

Typically, biotribological analysis of hip joints can be divided into two groups. The first group deals with *in vitro* evaluation of wear rate under various operating conditions, and the second one aims on the description of lubrication mechanisms inside the contact. Especially the lubrication processes have not been fully clarified yet. However, such a knowledge can help to understand the interaction of human body with the replacements, leading to the further extension of implant durability eventually. Since numerical analyses suffer from several attributes, such as the shear thinning behaviour of SF [9], or protein adsorption [10], whose simulation is particularly complicated, the main attention is focused on experimental investigations.

The influence of various model fluids on lubricant film formation was introduced by Fan et al. [11]. The authors employed simplified ball-on-disc geometrical configuration, while the contact between the glass disc sliding against the stationary CoCrMo femoral head was observed through microscope. Film thickness was evaluated using optical interferometry method. The experiments were performed in the range of

* Corresponding author.

E-mail address: David.Necas@vut.cz (D. Nečas).

speeds from 2 to 60 mm/s and the results obtained for protein solutions were compared with those of BS. Although the protein content was higher in the case of BS, protein solutions formed thicker protein film, in general. When comparing the particular solutions, it was observed that despite lower concentration, the model fluid containing γ -globulin exhibited higher film thickness. Adsorbed protein film at the end of the experiment was examined as well. In that case, the adsorbed layer varied from 20 to 60 nm, while the thinnest film was detected for 25% BS and thickest for the mixture of albumin and γ -globulin in a ratio 2:1.

The study was later followed by Myant et al. [4] who also utilized ball-on-disc device and performed three types of experiments; static adsorption test, pure sliding time test, and pure sliding speed test. As the test lubricants, albumin (10 mg/ml; 20 mg/ml; 30 mg/ml), γ -globulin (6 mg/ml), and 25% BS solution (13 mg/ml) were used. The results of static test at zero speed revealed that the adsorbed protein layer was the thickest (around 30 nm) for γ -globulin solution. On the contrary, independently of protein concentration, adsorbed film was less than 5 nm in the case of albumin solutions. BS film reached approximately 10 nm. The results of consequence time test were in a good qualitative correlation with results of static test, while γ -globulin layer was between 200 and 250 nm compared to 30–40 nm for albumin and BS solutions. Finally, speed test exhibited very complex behaviour of the lubricants with no clear conclusions in relation to particular fluids.

Qualitatively similar results were presented by Parkes et al. [12] for rolling contact. The authors compared solution of albumin (10 mg/ml), γ -globulin (2.4 mg/ml) and protein mixtures of concentrations of 10 mg/ml and 2.4 mg/ml, respectively. The measurements were performed in the same experimental configurations as in the case of previous studies, whilst the applied load (5 N) resulted to a contact pressure of 200 MPa. Rolling speed was set to 10 mm/s and the measurements were realized under ambient temperature. The effect of lubricant pH was examined as well. The measurements were reproduced three times, while it was found that albumin solution formed the thinnest film, which was dependent on pH of the solution. Film thickness for the solution of lower pH (7.4) was relatively unstable and was kept between 5 and 40 nm. An increase of pH to 8.1 caused stabilization of the film; however, the thickness dropped to less than 10 nm. In contrast, γ -globulin exhibited similar behaviour at both pH, while the maximum film was around 350 nm and 250 nm, respectively. In the case of protein mixtures, similar formation as for albumin solution could be observed, while the film varied from 10 to 80 nm at lower, and from 10 to 40 nm at higher pH.

From the above references, it is apparent that the dominant protein leading to increase of film thickness is γ -globulin. However, these implication is based on the observations of simple protein solutions. The authors were not able to distinguish the individual constituents of model SF due to the limitation of the employed measurement method (optical interferometry), which provides just the information about the thickness of the layer between the contact bodies [13]. In our previous studies, we employed the fluorescent microscopy method allowing to separate particular proteins of the model fluid, concluding that under most conditions, the dominant protein responsible for film thickness development is albumin. These findings were revealed for metal [14], as well as for ceramic material of the femoral head [15]. Therefore, it is apparent that the proteins interact and both of them contribute to the film formation, indicating that it is desirable to investigate complex model fluids.

As was mentioned, SF contains not only proteins (albumin, γ -globulin), but also HA and phospholipids. The interaction of individual SF constituents is still a subject of many debates. When investigating the role of individual fluid components, most of the authors focused on the determination of friction of synovial joint cartilage, which is able to operate for many tens of years, exhibiting extremely low friction coefficient [16–18]. Forsey et al. [19] examined friction level in cartilage-cartilage contact focusing on the influence of HA and phospholipids, finding that both the constituents lead to reduction of friction. Moreover, when both the components were combined, further rapid decrease of friction could be observed. Even the specific role of the

constituents could be hardly fully explain, the authors suggest that HA targets on chondrocytes promoting the synthesis of new HA molecules. The ability of HA to reduce friction between the cartilage surfaces was later confirmed by Schmidt et al. [20]. Interaction of HA with proteins contained in synovial fluid in relation to friction within cartilage-glass contact was examined by Murakami et al. [21]. The authors confirmed positive effect of HA, while this effect was enhanced when γ -globulin was added into HA solution. In contrast, adding of albumin into HA led to higher friction in all the performed tests. An extensive study clarifying the role of individual constituents and their mixtures on friction in cartilage-glass contact was pronounced in the consequent study [16]. Various test fluids were employed, while the coefficient of friction was studied as a function of sliding distance. Both intact and damaged cartilage were investigated. Focusing on the intact sample and simple solutions of individual constituents, it was found that the lowest friction is exhibited by phospholipids, followed by HA, albumin, and γ -globulin. Almost negligible difference was observed when phospholipids were mixed with albumin and γ -globulin, respectively. Nevertheless, both the proteins led to decrease of friction. Finally, the tests performed with complex fluids revealed that the protein content plays an important role as well. Considering the composition consisting of HA, phospholipids and albumin, it was shown that the friction is substantially lower with increasing protein concentration. The fluid containing 1.4 wt% of albumin exhibited the maximum level of friction equal to approximately 0.01; however, when the content of the protein decreased to 0.7 wt%, the friction increased to around 0.1 at maximum. Very low friction was observed even in the case of HA mixed with phospholipids (≈ 0.02) and also in the case of HA with phospholipids doped by γ -globulin (≈ 0.03). As some differences could be observed when focusing on damaged cartilage, the authors concluded that the role of the individual fluid constituents depends not only on the interaction of the molecules, but also on the condition of the cartilage tissue. This was later confirmed by Park et al. [22] who focused on friction measurements considering normal cartilage as well cartilage corresponding to early-stage and advanced-stage of osteoarthritis (OA). Positive effect of γ -globulin and HA on friction was confirmed in the case of advanced OA; however, only a little influence was observed in the case of normal and early-stage OA cartilage.

A detailed insight into an interaction of the individual fluid constituents on friction was given by Seror et al. [17]. The authors concluded that a single constituent is not able to ensure extremely low friction level which can be down to 0.001. It was pronounced that each the molecule has a different role; however, due to mutual interaction, very low friction can be maintained even at very high contact pressures. Particularly, it was explained that HA is anchored to the surface of the cartilage via molecules of lubricin, creating a complex layer together with phospholipids, thus providing extremely low friction. The importance of so-called boundary layer and the interaction of molecules was recently highlighted by Jahn et al. [18]. The authors pointed out that better understanding of the mechanisms occurring inside the joint, ensuring operation under low level of friction, should be of a greater interest, since it may be an implication for many areas, including treatment of OA, preventing the necessity of joint replacements.

Considering the investigation of lubrication within hip replacements, it must be taken into account that ball-on-disc model configuration, which was employed several times in the above references, does not correspond to the real geometrical configuration of the joint, where the contact is highly conformal. The first step on the way to approach higher degree of conformity was conducted by Vrbka et al. [23] who substituted the glass disc by the convex glass lens, thus obtaining completely different results compared to previously investigated ball-on-disc arrangement [24]. Addressing the implication of the importance of contact geometry, we developed a simulator based on the principle of pendulum to be able to investigate the film thickness under real geometrical configuration [25]. Recently, our effort was focused on the clarification of the influence of head diameter, diametric clearance and head material on film formation; finding that thicker film is formed when

metal head is employed, while this fact was attributed to higher surface hydrophobicity, among others. In terms of geometry, it was proved that the crucial parameter affecting the formation of lubricating film is the size of the clearance between the surfaces, which should be as low as possible to ensure sufficient separation of rubbing surfaces by the lubricant [26]. The findings about the importance of the size of the diametric clearance are supported by some previous observations given by other authors. Using the electrical resistivity technique, Smith et al. [27] determined the surface separation of the hip implant components as a function of the diametric clearance, while it was found that the film thickness increased with decreasing clearance. Positive impact of lowering the clearance on enhancing the lubrication conditions was later demonstrated also with the use of full numerical simulation [28]. Brockett et al. [29] investigated the effect of clearance on lubrication, friction, and squeaking of metal-on-metal (MoM) implants, confirming that the lower clearance leads to higher film thickness, together with lower friction and decreasing incidence of squeaking.

The issue of clearance was also discussed in relation to the viscosity of the lubricating fluid. Hu et al. [30] examined frictional torque in MoM joints considering both physiological and pathological SF. It was found that in the case of the smallest clearance (20 μm), friction was relatively high due to limited ability of the lubricant to enter the contact of the surfaces. For larger clearances, (100 μm and 200 μm), frictional torque was substantially influenced by the lubricant viscosity. Lower clearance led to lower friction when less viscous lubricant was employed and, vice versa, reduction of friction was observed for the larger clearance when the fluid of higher viscosity was introduced. This indicates that the implants of larger clearance allow better fluid recovery during the unloaded phase, which might be necessary especially in the case of highly viscous fluids. Finally, it was also shown that the smaller size of the clearance is advantageous in terms of wear rate [31]. The authors investigated MoM implants of five different nominal diameters with various clearances, concluding that wear rate decreases with increasing diameter and decreasing clearance, suggesting that the transition of lubrication regime from boundary to mixed lubrication occurs. Therefore, it was pointed out that the implants should be as large as possible, while the size of the clearance should be minimized. Nevertheless, it must be taken into account that too small clearance may lead to equatorial contact of the ball and the cup [32]. This is related to so-called edge loading effect, which represents a substantial risk factor in the case of MoM implants, while the service-life may be significantly shortened [33].

Based on the literature, it might be summarized that the lubrication processes inside the artificial joints are of a great importance in relation to durability of implants. Optical methods have been extensively employed to investigate film formation *in situ*, giving the opportunity to understand the mechanisms of film formation, potentially leading to further development of the replacements. However, it was found that the investigation of simple protein solutions cannot be generalized in meaning of SF lubrication, since the constituents in model fluid mutually interact. Later, the importance of real surface geometry was highlighted and it was discussed that BS is not sufficient representative of SF. Finally, it was revealed in the study given by Galandáková et al. [8] that the composition of SF substantially differs patient to patient. Therefore, the aim of the present study is to examine the effect of proteins (albumin, γ -globulin), HA, and phospholipids on the development of lubricant film thickness in artificial hip joints. According to author's knowledge, so far, such a study has not been performed. Even there are some clear indications, especially about the importance of HA and phospholipids in relation to friction and wear of materials used for joint implants [7, 34–36], these statements have not been supported in terms of lubrication mechanisms inside the contact yet. If the essential role of the mentioned constituents will be confirmed by *in situ* observations, it can lead to further development of hip implants. Moreover, it might be an important indication for orthopaedic practice as well, as the treatment of the joints (i.e. viscosupplementation) might be introduced even in the case of hip

2. Materials and methods

The experiments were performed using pendulum hip joint simulator, while the contact was realized between the femoral head and tailor-made acetabular cup from optical glass (BK7), the diameter of which respects the dimensions of real cups used in clinical practice. Film thickness was investigated as a function of time, while the data were evaluated utilizing thin film colorimetric interferometry method [37]. A detailed description of the test device and measurement method is provided in our previous studies [25,26]. Schematic illustration of the simulator is displayed in Fig. 1.

The main attention was paid to the effect of the composition of model SF. Initially, the measurements were realized with 25% BS, which is often being employed as the substitution of SF. Subsequently, two model SFs based on the investigation of composition of extracted SFs were prepared. The composition of the model fluids corresponded to the composition of SFs representing various groups of patients. Galandáková et al. [8] performed an extensive study focused on the evaluation of SF fluid composition, focusing on the concentration of albumin, γ -globulin, HA and phospholipids. Patients, from which the SF was extracted, were divided into four following groups, while the average composition of the fluids is provided in Table 1.

- Group 1: Patients with aseptic loosening of total joint replacement (TJR).
- Group 2: Patients with TJR without any signs of periprosthetic osteolysis.
- Group 3: Patients without TJR with end state of osteoarthritis (patients before surgery).
- Group 4: Patients without TJR, without osteoarthritis, with non-inflammatory SF.

As can be seen in Table 1, composition of the fluids of the patients with and without TJR is relatively similar. Therefore, for the purpose of the present study, two model SFs fluids were prepared, having the composition similar to average composition of the groups 1 and 2 (in the following text, the fluid is assigned as model SF1) and the groups 3 and 4 (in the following text, the fluid is assigned as model SF2).

To compare the behaviour of complex fluids with simple protein solutions, additional tests were performed with albumin and γ -globulin solutions. BS and model SFs were prepared and deeply frozen to $-22\text{ }^{\circ}\text{C}$. One and half hour before the tests, the substances were removed from the freezer to allow natural thawing process. Simple protein solutions were prepared and stored in a refrigerator overnight enabling the proteins to be completely dissolved. These solutions were used within 24 h after preparation. Moreover, HA of two different concentrations was investigated as well. Hyaluronan (sodium hyaluronate/hyaluronic acid/HA) is a natural, unbranched polysaccharide. In nature, the molecular weight (MW) range of HA is from 1 kDa to more than 2 MDa. Solutions of HA are commonly used for viscosupplementation of osteoarthritic joints. High molecular weight HA ($\geq 1\text{ MDa}$) is typically used for this therapy [38,39]. HA (Contipro a.s.) with average molecular weight (M_w) of 1.02 MDa and polydispersity equal to 1.2 was used for the purpose of this study. The composition of all the model fluids is specified in Table 2. Prior to tests, the cup pot was pre-heated to $37 \pm 1\text{ }^{\circ}\text{C}$ to mimic body temperature.

Three different materials of femoral heads were investigated in the present paper; metal (CoCrMo) alloy, BIOLOX[®] forte (Al_2O_3) and BIOLOX[®] delta (75% Al_2O_3 , 24% ZrO_2 , Cr_2O_3), respectively. The nominal diameters of the heads were 28 mm and 36 mm. Real dimensions of the heads and the cups were obtained using optical scanning method (GOM ATOS Triple Scan). Description of the investigated contact couples is provided in Table 3. The material properties of the test samples as well as the overview of the performed experiments are summarized in Table 4. Prior and after each performed test, the samples were thoroughly cleaned to avoid any results influence coming from the contamination by impurities or proteins adsorbed during the previous test. Initially, the both

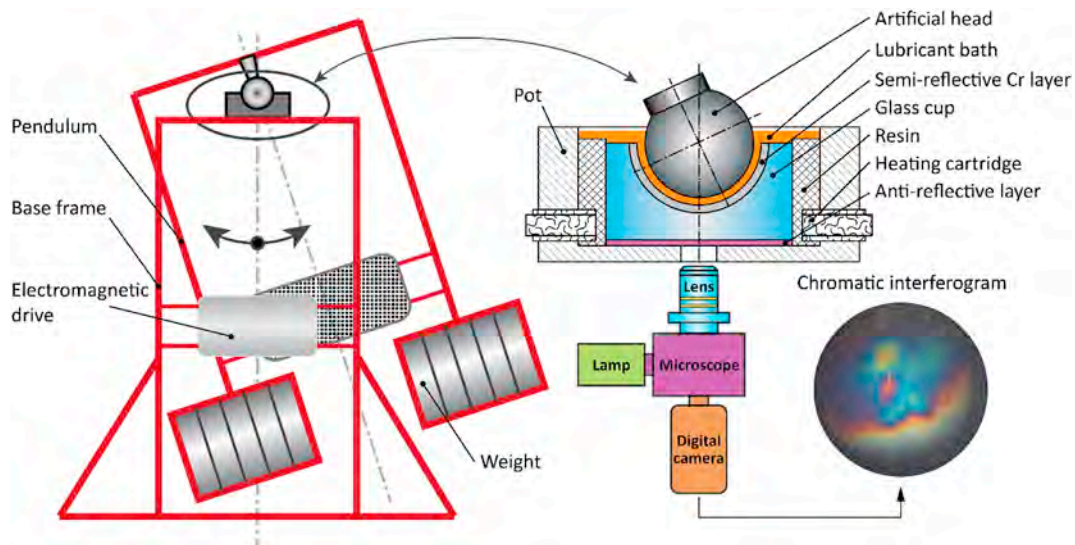


Fig. 1. Scheme of the pendulum hip joint simulator.

Table 1
Composition of the SFs belonging to various groups of patients [8].

	Albumin (mg/ml)	γ -globulin (mg/ml)	HA (mg/ml)	Phospholipids (mg/ml)
Group 1	28.2	11.5	1.4	0.154
Group 2	27.9	10.5	0.8	0.175
Group 3	26.7	8.7	1.9	0.305
Group 4	29.1	10.2	2.0	0.312

contact samples were cleaned in 1% sodium dodecyl sulphate solution. Subsequently, they were rinsed by pure deionized water and were dried by pressed air. Finally, the samples were washed in isopropyl alcohol.

Initially, static adsorption tests were realized with all the materials, while BS, model SF1, and model SF2 were used as the test lubricants. The heads of nominal diameters of 36 mm were employed in this case. To avoid any inaccuracies coming from sudden protein agglomerations reported in our previous study [26], all the experiments were repeated two (the effect of load) to four times (the effect of model fluid on adsorbed film). The results provided below represent average values of the performed tests. Each test consisted of 20 cycles combining 15 s lasting loading phase and 45 s lasting unloading phase; therefore, the length of

one cycle was 1 min. Moreover, the effect of load on adsorbed BS film was examined for BIOLOX[®] delta head, while the load was changed from 532 N (reference load) to 857 N, 1157 N, 1457 N, and 1757 N, respectively. Since the experiments consist of simple loading and unloading, without relative motion of the components, only one femoral component for each investigated material (metal, BIOLOX[®] forte, and BIOLOX[®] delta) was employed, because no wear or scratches of the rubbing surfaces could be observed.

Subsequently, dynamic swinging tests were realized with metal femoral head, while the effect of lubricant was of the main interest. The range of flexion-extension swinging was from -16° to $+16^\circ$, while the electromagnetic motors ensured continuous swinging motion. Time of the test was set to 210 s. Then, the motors were turned off and the motion was naturally damped as a consequence of friction between the rubbing surfaces. In some cases, the time of the experiment was shorter, since the chromium layer on the cup was removed due to articulation; disabling further evaluation of film thickness. Therefore, the experiment was stopped to avoid a severe damage of the glass cup. To avoid any influence of the results by the change of surface topography due to wear of rubbing surfaces, four new metal heads were used during the experiments. After each test, the topography of the femoral head in five defined locations was checked using 3D optical profilometer. Once some scratches could be

Table 2
Composition of the applied test lubricants.

Test fluid	Albumin (mg/ml)	γ -globulin (mg/ml)	HA (mg/ml)	Phospholipids (mg/ml)	Total concentration (mg/ml)	Volume (ml)
25% BS	Unknown	Unknown	–	–	22.4	12
Model SF1	28	11	1.1	0.17	40.27	
Model SF2	28	9.4	1.9	0.31	39.61	
Albumin	28	–	–	–	28	
γ -globulin	–	11	–	–	11	
HA1	–	–	5	–	5	
HA2	–	–	20	–	20	

Table 3
Summary of the contact couples.

Ball material	Nominal diameter (mm)	Diametric clearance (μ m)	Max. Hertzian contact pressure (MPa)	Hertzian contact zone diameter (mm)	Test type
Metal	36	137	26.8	6.06	Static
Metal	28	93.2–107.3	29.3–32.2	5.62–5.89	Dynamic
BIOLOX [®] forte	36	137.2	28.4	5.89	Static
BIOLOX [®] delta	36	136.4	28.3	5.90	Static
BIOLOX [®] delta	36	136.4	28.3	5.90	Static/Load effect

Table 4
Material properties of the employed test samples and the summary of the performed experiments.

Material	Elastic modulus	Poisson's ratio
Metal	230 GPa	0.3
BIOLOX [®] forte	340 GPa	0.28
BIOLOX [®] delta	340 GPa	0.28
Glass	85 GPa	0.209

Experiment set	Contact couple	Test lubricant	Test type	Load
1	Metal/Glass	BS, SF1, SF2	Static	532 N
2	Metal/Glass	BS, SF1, SF2, albumin, γ -globulin, HA1, HA2	Dynamic	532 N
3	BIOLOX [®] forte/Glass	BS, SF1, SF2	Static	532 N
4	BIOLOX [®] delta/Glass	BS, SF1, SF2	Static	532 N
5	BIOLOX [®] delta/Glass	BS	Static/Load effect	532 N; 857 N; 1157 N; 1457 N; 1757 N

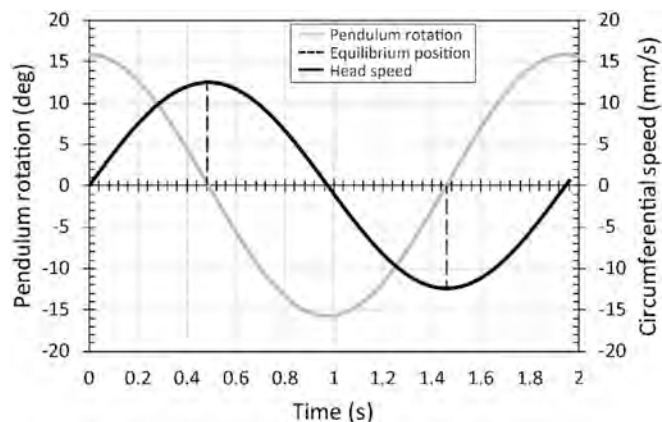


Fig. 2. Kinematic analysis of the one swinging cycle.

observed, the head was excluded and was substituted by the new one. It should be noted that the film thickness was evaluated in the equilibrium position of the pendulum, where the deflection of swinging arm is 0°. Kinematic analysis of the pendulum rotation and the circumferential speed of the 28 mm head over one swinging cycle is shown in Fig. 2. Applied load was 532 N resulting to various contact pressures specified in Table 3. To evaluate the importance of proteins in relation to film formation process, the results of swinging tests were compared with the theoretical prediction of central film thickness h_c (eq. (1)) based on equation given by Hamrock [40], previously successfully employed by Medley et al. [41]:

$$h_c = 5.083 \cdot \frac{(\eta \cdot u)^{0.660} \cdot R^{0.767}}{E^{0.447} \cdot F^{0.213}} \quad (1)$$

where η is a dynamic viscosity (estimated as $\eta = 0.00213$ Pa s), u is the entrainment speed ($u_1 = 6.1$ mm/s), R' is the reduced radius given as $1/R' = (R_c \cdot R_b)/(R_c + R_b)$, where R_c and R_b denote the radii of the cup and the ball, F is the applied load ($W = 532$ N) and E' is reduced Young's modulus defined as $2/E' = (1 - \mu_b^2)/E_b + (1 - \mu_c^2)/E_c$, while μ_b , μ_c , E_b , E_c are the Poisson's ratios and Young's moduli of the ball and the cup.

3. Results

3.1. Static test

In the case of static adsorption test, film thickness gradually increased with each following cycle for metal femoral head. It can be seen in Fig. 3 that the thickest film was formed by BS, followed by model SF1 and model SF2, respectively. During the first 2–3 cycles, the adsorbed layer was quite similar for all the lubricants, it varied between 20 and 40 nm. Slight decrease of the thickness can be observed for model SF2 between the second and the fifth cycle; nevertheless, then it starts to increase as in the case of the other two lubricants. Total film thickness of BS at the end of the test is more than two times higher compared to model SF2, while the film for model SF1 is approximately in the middle.

The effect of model fluid on adsorbed film was found to be significant also for ceramic materials. In the case of BIOLOX[®]forte head (Fig. 4), combined increasing/decreasing tendency could be observed for BS and model SF1. The thickest film considering BS was detected after 10 loading cycles, when the film reached around 150 nm. At the same time,

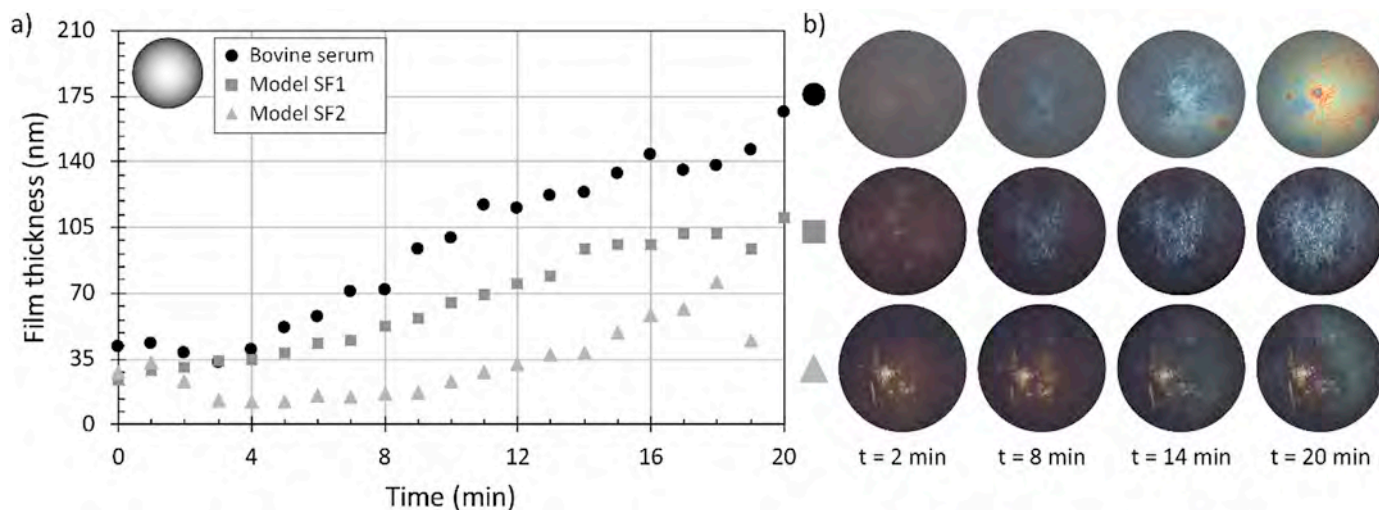


Fig. 3. a) Static test - film thickness of adsorbed film as a function of time for 36 mm metal head and various model fluids. b) Chromatic interferograms taken during the experiment; from the top: BS, model SF1, model SF2. 1 min corresponds to 1 cycle.

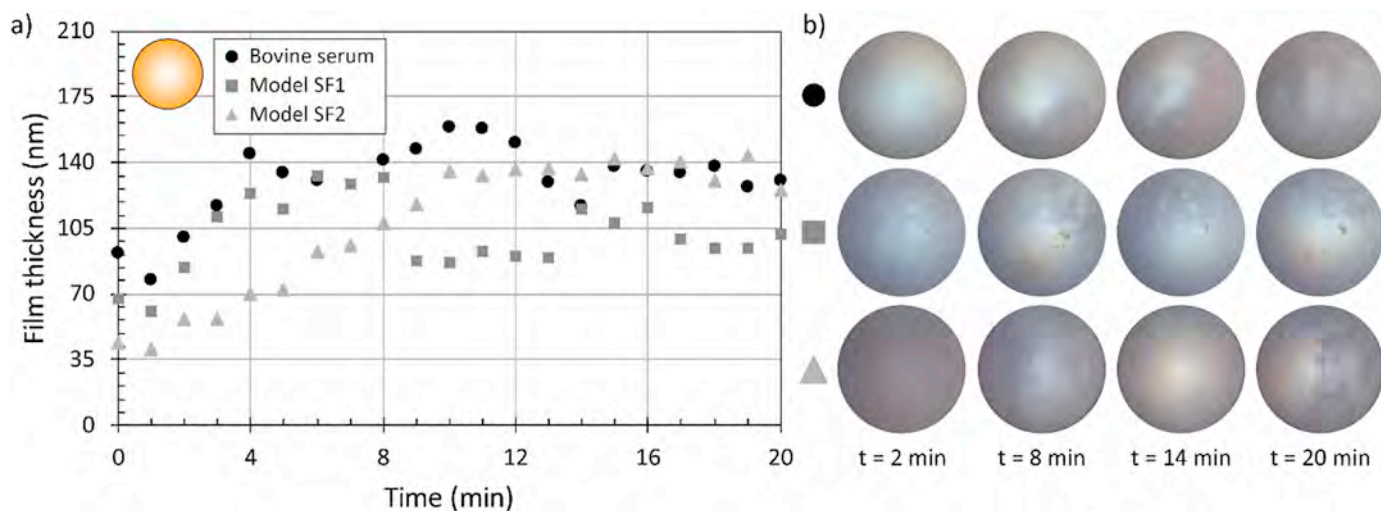


Fig. 4. a) Static test - film thickness of adsorbed film as a function of time for BIOLOX[®]forte 36 mm head and various model fluids. b) Chromatic interferograms taken during the experiment; from the top: BS, model SF1, model SF2. 1 min corresponds to 1 cycle.

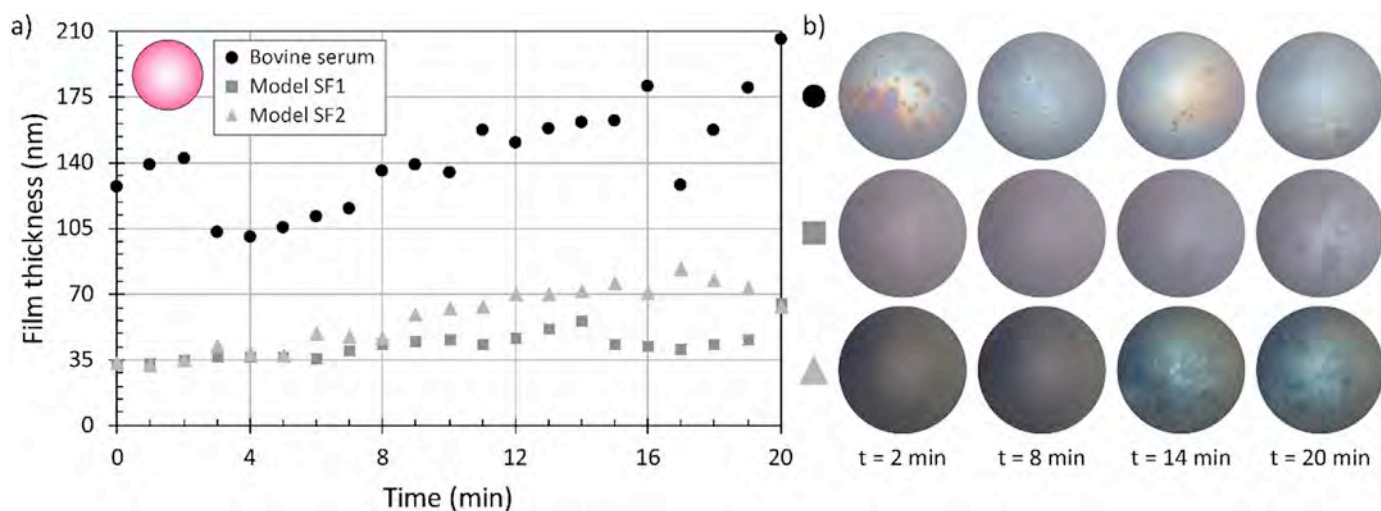


Fig. 5. a) Static test - film thickness of adsorbed film as a function of time for BIOLOX[®]delta 36 mm head and various model fluids. b) Chromatic interferograms taken during the experiment; from the top: BS, model SF1, model SF2. 1 min corresponds to 1 cycle.

substantial drop of the layer was observed for model SF1 reaching approximately 90 nm. Focusing on the model SF2, the film increased during the first 10 cycles being stabilized at around 140 nm with no significant fluctuations. The most substantial influence of the applied lubricant on lubricating film was observed in the case of BIOLOX[®]delta (Fig. 5). Both model fluids exhibited relatively similar behaviour with a slight increasing tendency of the adsorbed layer, while the thickness after twenty cycles was little bit less than 70 nm. On the contrary, the layer was much thicker for BS, while the maximum thickness reached almost 210 nm.

To clarify the effect of contact pressure on adsorbed film, additional experiments were performed with BIOLOX[®]delta under five different levels of load. As a test lubricant, BS was used, while the results revealed that with the exception of the first 5 cycles, there was no significant effect of load increasing from 532 N to 1157 N. However, further increase to 1457 N and 1757 N caused a reduction of the film between fifth and seventeenth cycle. In general, the thinnest film was detected for the highest load, while the thickness was half compared to the lowest load (110 vs. 210 nm), see Fig. 6.

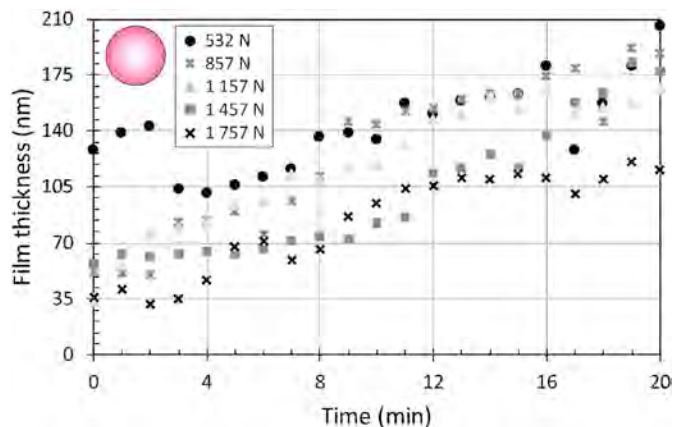


Fig. 6. Static test - film thickness of adsorbed film as a function of time and load for BIOLOX[®]delta. 36 mm head. 1 min corresponds to 1 cycle.

3.2. Dynamic test

To mimic flexion-extension motion, swinging tests were performed with 28 mm head to evaluate the effect of model fluid on film formation. As can be seen in Fig. 7, both BS and model SF2 form gradually increasing lubricating film potentially protecting rubbing surfaces against mutual contact minimizing wear rate. Especially model SF2 exhibits gradual steep increase during the first 50 s reaching around 500 nm. Then, the slope of the tendency is changed; however, the film still increases and exceeds a measurable level (900 nm) within approximately 110 s. On the contrary, model SF1 forms much thinner film over the entire experiment. Thickness is just between 50 and 70 nm without any significant fluctuations.

To determine the effect of individual constituents of model fluids on film thickness development, the experiments were later performed with simple solutions of albumin, γ -globulin and HA, respectively. Fig. 8 shows that γ -globulin layer increases with time reaching approximately 700 nm at maximum. Albumin layer is of similar thickness as γ -globulin during the first 80 s; then it drops to around 50–100 nm and is stabilized until the end of the experiment. Both solutions of HA exhibit scattered results with the film thickness varying between 30 and 200 nm during the first 40 s. After that, the film dropped to a negligible level with just

occasional skips caused by the entrapment of HA molecules between the surfaces during joint articulation. Nevertheless, it is apparent that HA as itself is not effective lubricant.

4. Discussion

As the number of young active patients with hip joint replacement continuously increases, it is desirable to ensure sufficient longevity of implants preventing the need of revising operations. One of the main goals of the researchers is to understand the tribological processes inside the joint to minimize wear of rubbing surfaces leading to osteolysis and aseptic loosening eventually. Although quantification of wear rate has been widely reported; so far, the lubrication mechanisms within the contact have not been fully clarified. In an effort to investigate the formation of lubricating film, optical methods such as optical interferometry [4,9,11,23–25] or fluorescent microscopy [14,15] are usually employed.

Since it was indicated that the conformity of rubbing surfaces apparently affects film formation [23], we developed a simulator in ball-on-cup configuration allowing to observe the contact of femoral component and glass acetabular cup considering real dimensions of implants including diametric clearance. In our previous paper, we investigated the effect of head size and the size of the clearance on lubricating

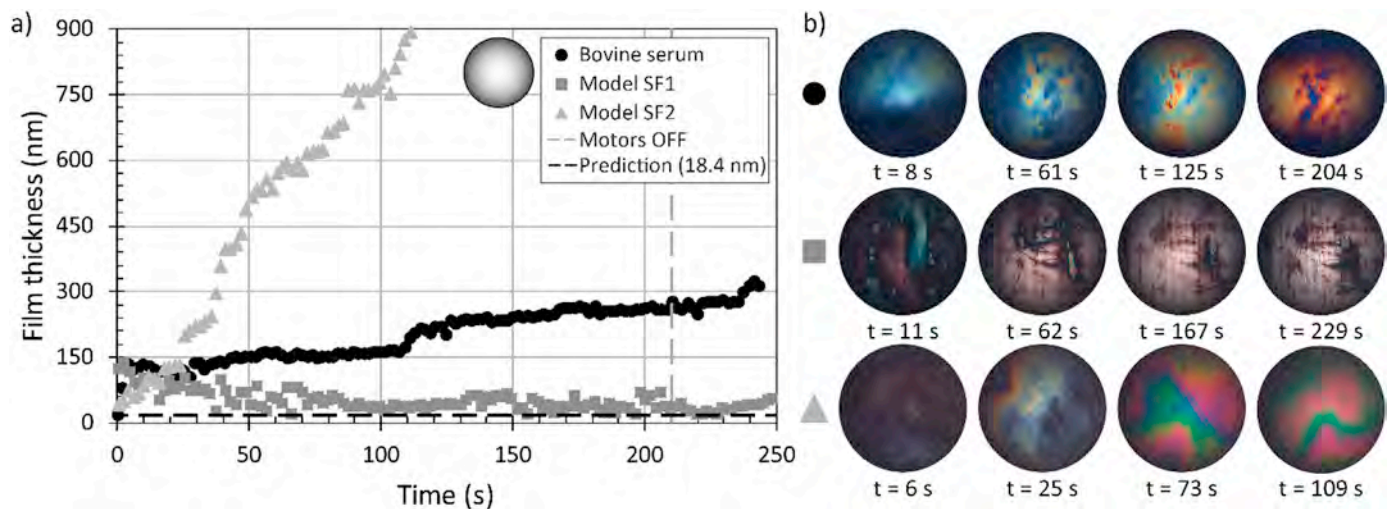


Fig. 7. a) Film thickness development as a function of time for 28 mm metal head and various model fluids. b) Chromatic interferograms taken during the experiment; from the top: BS, model SF1, model SF2. Inlet/outlet is on the top/bottom of each image.

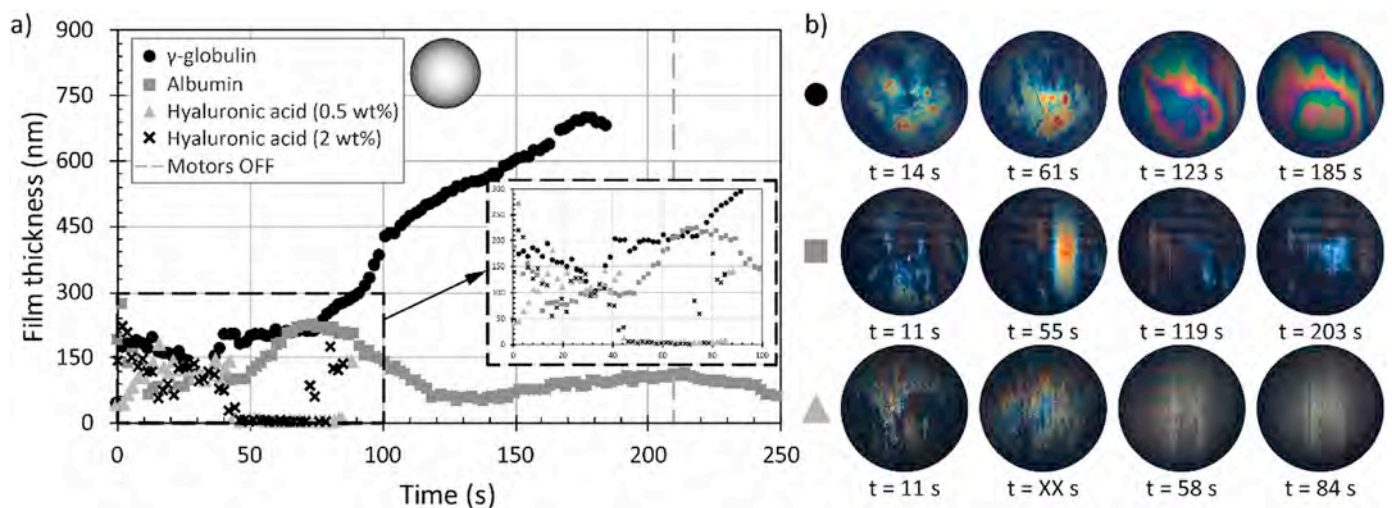


Fig. 8. a) Film thickness development as a function of time for 28 mm metal head and various model fluids. b) Chromatic interferograms taken during the experiment; from the top: γ -globulin, albumin, 0.5 wt% HA. Inlet/outlet is on the top/bottom of each image.

film, while it was found that the substantial parameter affecting the lubricating film is the diametric clearance, the lowering of which leads to a rapid increase of film thickness [26]. This is in a good agreement with previous observations [27–29]. As the positive effect of lowering the clearance was proved also in terms of wear rate [31], it might be concluded that the hip replacements should be fabricated with the clearance as small as applicable. Nevertheless, in the case of very low clearances, edge loading effect may occur, which may drastically shorten the longevity of implants [32,33]. The dynamic experiments in the present study were conducted with the contact pairs having the diametric clearance between 93 μm and 107 μm . This value is a representative for commonly used bearing pairs. However, in some cases, substantially smaller clearances have been reported, while it can be less than 20 μm in the case of MoM pairs. Therefore, we performed some additional tests considering the clearance equal to 40 μm , see Fig. 9b. Even the clearance was less than half compared to other test couples, lubrication performance was still very satisfactory. As can be seen in the figure, film thickness continuously increased with time. Moreover, it should be highlighted that in this case BS was employed, which is apparently not the best lubricant (see Fig. 7), to suppress the positive impact of HA and phospholipids. It is particularly complicated to predict how would be the effect of further decrease of the clearance. Nevertheless, following the literature review, it is expected that there is some critical value, below which the lubrication performance is limited, while lubricant film breakdown may occur due to edge loading phenomenon [33]. This leads to increase of friction and wear; thus shortening the service-life of implant. The critical size of the clearance cannot be generally defined, since it was shown by Hu et al. [30] that the friction of rubbing surfaces is substantially influenced by the viscosity of the lubricating fluid. Therefore, it is expected that the size of the clearance should reflect the composition of the SF of the patients, while the patients with less viscous SF should receive the replacements with smaller clearance compared to those with more viscous SF. Following these findings, it is evident that the lubrication performance of the implants is associated with the conditions inside the joint, while the composition of SF seems to be the crucial factor.

Galandáková et al. [8] performed an extensive study identifying the composition of SF related to various groups of patients, finding significant differences, especially when talking about the concentration of HA and phospholipids. Therefore, in the present paper, we utilized the previously developed simulator in combination with optical interferometry to evaluate the effect of model SF composition on lubricant film formation. Moreover, simple solutions of proteins and HA were investigated as well to show that the interaction of constituents may play an important role.

Initially, static adsorption test at zero speed was conducted with metal and ceramic heads. Metal head exhibited a gradual increase of

lubricant film for all the tested lubricants. The thickest layer was formed by BS, thinnest film was detected for model SF2 with higher content of HA and phospholipids (Fig. 3). It was discussed in our previous paper [26] that metal head exhibits higher hydrophobicity; therefore, the adsorption forces are strong enough to maintain the proteins on rubbing surfaces even during unloading phase. What is surprising is that the BS, which has a smaller total protein concentration, forms thicker film. This means that HA and phospholipids have a negative effect on adsorption process, since with the increasing concentration of the mentioned constituents, the film decreases. In the case of ceramic heads, protein adsorption is strongly influenced by the type of the ceramic. Alumina ceramic (BIOLOX[®] forte) did not show any clear dependence between the type of the lubricant and film thickness. On the contrary, zirconia toughened alumina ceramic (BIOLOX[®] delta) showed that BS formed the thickest adsorbed layer, as in the case of metal head. Focusing on the model SFs, it can be concluded that there is no significant difference between the results dependently on fluid composition, proving that the concentration of individual constituents is less important. As can be seen in Fig. 5, BS film is unstable and sudden drops of the film can be observed. This fact is attributed to lower wettability of ceramic compared to metal. Although the film is relatively thick, during unloading phase, the proteins desorb from the surfaces due to weak adsorption forces. This phenomenon is not observed in the case of model SFs, where the film is much thinner; however, the layer is stable without significant fluctuations. This supports our findings from the previous studies [24,26], showing that the hydrophobicity of contact surfaces has a strong impact on the protein formation.

Regarding to the applied test lubricants, it should be noted that BS does not mimic the behaviour of model SF1 nor SF2. However, it should be taken into account that BS is very often used as the test fluid when examining the lubrication mechanisms within hip replacements [4,9,23–26,42–44]. Therefore, it can be concluded that the results of the performed study clearly confirm the idea that the use of BS is not suitable and complex solutions respecting the composition of human SFs should be preferably used when dealing with replacements lubrication [6,12,45].

The effect of load on lubricant film was previously observed by Myant and Cann [42], who concluded that lowering the contact pressure has a positive effect on the protein film. As is shown in Fig. 6, in the case of present study, doubling the initial load did not lead to a substantial change of the film thickness. However, further increase caused a drop of the film, which corresponds to the above-mentioned study. Although it is apparent that in the range of the considered levels of load (532 N–1757 N), the reduction of the adsorbed film thickness is not substantial, it must be taken into account that the resulting force in the joint of adult people can reach up to 3000 N. Therefore, physiological load level will apparently lead to thinner lubricating film compared to

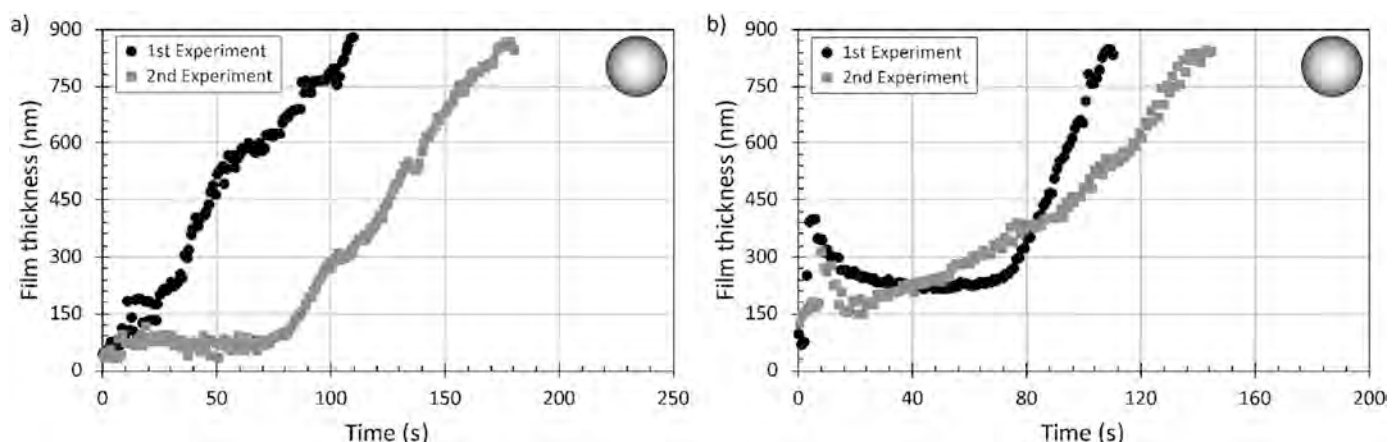


Fig. 9. a) Results repeatability for metal head and model SF2. b) Results repeatability for metal head and BS considering small diametric clearance of 40 μm .

results obtained in the performed experimental study.

After the evaluation of adsorbed film, swinging flexion-extension tests were carried out with the metal head considering various lubricants. As can be seen in Fig. 7, model SF with lower concentration of HA and phospholipids formed thin and stable film in the range from 30 to 70 nm during the experiment. An increase of concentration of the mentioned constituents led to a completely different character of film formation, causing a continuous increase of the film reaching a maximum measurable value of 900 nm within approximately 110 s. These results clearly prove the importance of HA and phospholipids in relation to lubrication processes. It is expected that HA and phospholipids create a boundary lubrication layer [17,18], which is able to adsorb on the surfaces, leading to thicker lubricating film. Nevertheless, when focusing on the results of static tests, it is apparent that the influence of higher concentration of HA and phospholipids is very limited. Therefore, the ability of the fluid to form the lubricating film is substantially affected by the hydrodynamic action due to joint articulation. BS forms continuously increasing stable film, the thickness of which is little bit higher than 300 nm at maximum. As the exact composition of BS is not provided by the producer, it is not possible to explain the increase of the film in terms of the role of particular constituents.

To be able to assess the film formation in relation to individual constituents, additional experiments were conducted (Fig. 8). It was found that simple γ -globulin solution formed much thicker film compared to albumin solution (680 nm vs. 120 nm). This is in agreement with the previously published studies, showing that despite the higher protein concentration, albumin film is always considerably thinner than that formed by γ -globulin [4,12]. The last set of measurements was conducted with two various solutions of HA. Independently of concentration, the film exhibits significant variance during the first 40 s of the test caused by strong agglomerations of the HA molecules. After some time, the film drops to a negligible level. Therefore, it is evident that simple HA solution is not an effective lubricant. This corresponds to previous observations [17]. It was indicated that the individual SF constituents are not able to ensure operation under low friction, which is associated with higher film thickness due to transition from boundary to mixed lubrication regime [31]. However, the interaction of the molecules seems to be crucial phenomenon in relation to film formation process, as is apparent from Fig. 7. The presented results clearly support the findings about the necessity of HA and phospholipids, which can substantially improve the lubrication conditions inside the joints, as was reported in relation to friction and wear of joint replacements [35,36], viscosupplementation of diseased joints [34] as well as frictional behaviour of synovial joint cartilage [16–22].

To illustrate the importance of proteins, the results are compared with theoretical prediction introduced by Hamrock [40] in Fig. 7. The theoretical thickness of proteins film is approximately 18.4 nm; however, it should be highlighted that the exact viscosity of model SFs was not evaluated. Surprisingly, the measured thickness well corresponds to the theory in the case of model SF1. Nevertheless, BS and model SF2 exhibited substantially thicker film, confirming that it is necessary to perform experimental analysis when investigating the lubrication processes within hip implants instead of numerical predictions, since theory cannot cover phenomena such as proteins agglomeration or adsorption onto rubbing surfaces.

Obviously, the authors admit some limitations of the performed study. First of all, repeatability of the measurements has to be mentioned. Repeatability of results considering SF lubrication is still a subject of many debates. SF constituents can exhibit very unstable behaviour and; therefore, strict respecting of the consequence steps during the experiment is necessary. The authors would like to highlight that the overall time duration of each conducted experiment is relatively high. It can take up to 8 h from the samples preparation, over film thickness calibration, measurement, to data evaluation. Moreover, the costs associated with one experiment are very high since the manufacturing technology of the glass cups and its covering by chromium layer is extremely precise

process. Due to above reasons, we were not able to repeat all the swinging tests multiple times. Nevertheless, some additional experiments were realized to give a prove about the data relevance, while the results are displayed in Fig. 9. As can be seen, very satisfactory agreement of the data could be obtained. In the case of the test with model SF2, the same increasing tendency was observed, the only difference was that it took a longer time since the film started to increase continuously (Fig. 9a). The second repeatability test was performed with BS. As the cup used originally could not be employed again due to damage of the chromium layer, new cup of a smaller diameter had to be used, while the configuration exhibited less than half diametric clearance, particularly 40 μm . As it is apparent from Fig. 9b, the behaviour of the lubricating film is almost the same. The results of additional experiments support our previous findings indicating that the smaller diametric clearance substantially contributes to thicker lubricating film [26]. Considering our long-term experience with the measurements of film thickness inside the artificial joints, consequently with very strict compliance with laboratory protocol and the clear prove of repeatability for two different geometries and two different model fluids, the authors are convinced that the presented data are relevant and give a clear insight to lubrication mechanisms in hip replacements dependently on the composition of SF.

Further, kinematics of the motion over the experiment should be mentioned. The substantial impact of kinematic conditions on SF lubrication was highlighted by Myant and Cann [43]. The pendulum hip simulator, employed in the present paper, allows to simulate flexion-extension motion in a specific range. The real joints operate under much more complex conditions, while abduction-adduction as well as joint rotation are not considered in the submitted study. Nevertheless, based on the extensive literature review, it is apparent that so far, there is no commercial nor laboratory designed simulator, which would enable to perform *in situ* observation of lubricant film formation in real geometrical arrangement considering complex kinematics according to ISO standards. The available test devices enabling to apply real kinematic conditions are being used exclusively for long-term wear tests.

Another limitation is related to loading conditions. In the case of the pendulum simulator, the load is constant over the test as it is applied by the dead weight on the pendulum arm. In real situation, the load varies over the walking cycle reaching from several hundreds of N up to 2.7 kN. To avoid damage of the glass cup, the maximum load during the dynamic experiments could not exceed approximately 532 N. However, the static tests revealed that even tripling the load did not affect the character of protein film formation, it just led to decrease of total film thickness. This indicates that the film thickness under physiological load would be lower compared to the measured values, but it is expected that the character of film development is similar to that at lower load.

As the next point, the composition of the SF should be discussed. In the present study, the fluid consists of proteins (albumin, γ -globulin), HA, and phospholipids. Concentration of all the constituents comes from the study performed by Galandáková et al. [8], in an effort to simulate the fluid of patients with and without joint replacement. Although the real SF contains some other constituents (e.g. lubricin), it should be noted that the other parts are presented just in a trace amount and are often neglected when preparing model SFs. As the base media, phosphate-buffered saline solution was used, which is a satisfactory representative of interstitial fluid from blood plasma. Therefore, it is assumed that the used lubricants can suitably mimic the behaviour of real SF.

Further limitation is the arrangement of the test samples. In the human body, the cup is on the top and the whole joint is encapsulated, so the SF surrounds the space around the joint. Apparently, we had to employ inverted arrangement, since if the physiological position would be applied, all the lubricant would leak away from the contact. It can be doubt if the lubrication conditions adequately correspond to the human joint; nevertheless, the main goal of this study was to assess the relation between the fluid composition and lubrication performance of the artificial joint. As all the experiments were performed in the same

configuration, it is assumed that the obtained data are relevant.

Although the performed experimental configuration is metal/ceramic on glass, it should be noted that this arrangement rather mimics so called hard-on-hard pairs such as metal-on-metal, metal-on-ceramic or ceramic-on-ceramic. This can be explained in terms of material properties as well as in consideration about the size of diametric clearance. Modulus of elasticity of hard implants is between 200 and 350 GPa. For the optical glass, it is around 85 GPa. However, in the case of hard-on-soft contact couples the cup is made from polyethylene (PE), the modulus of which is just in the range of units of GPa. Therefore, the glass better mimics metal or ceramic than PE. In terms of geometry, hard-on-soft pairs exhibit higher diametric clearance than hard-on-hard couples, in general [44]. As the clearances of all the tested pairs varied from 93 to 137 μm , it rather corresponds to metal-on-metal or ceramic-on-ceramic couples.

The current study showed that the character of film formation is considerably affected by the composition of model SF. It was found that in the case of static test, the adsorbed film is thicker when ceramic heads were investigated, while the same behaviour was observed even in the previous paper [26]. The major findings come from the performed swinging test, which showed that the model SF with higher concentration of HA and phospholipids leads to thicker film, preventing the surfaces against mutual contact, lowering the wear rate eventually. Moreover, as the results for BS do not correspond to those of model SFs, it should be highlighted that the BS is not a suitable substitution of SF for the purposes of tribological tests of hip replacements, as reported previously [12]. This statement was discussed also by Mazzucco et al. [45], who compared the viscosity of SF extracted from patients with viscosity of BS which was at least an order of magnitude less viscous than SF.

5. Conclusion

The aim of the present paper was to determine the effect of model SF composition on lubrication mechanisms within hip replacements considering real geometry of rubbing surfaces. The main novelty of the study comes from finding the clear relation between the composition of SF and lubrication performance of the contact couple, while the contact representing hard-on-hard joint bearing pair was observed *in situ*. Such a study has not been performed before. Although some findings follow previous laboratory observations, this is the first paper investigating the development of film thickness within the hip joint during flexion-extension motion for various model fluids, the composition of which corresponds to SFs belonging to various groups of patients. Static adsorption and dynamic swinging tests were performed, while the results can be summarized into the following concluding points.

- The results showed that the composition of synovial fluid has a substantial effect on lubrication mechanisms inside the contact of hip replacements, apparently influencing the tribological performance of the rubbing pair, thus affecting the service-life of implant.
- Independently of model fluid, adsorbed film continuously increases in the case of metal head, while higher concentration of HA and phospholipids causes the reduction of the film thickness.
- In general, alumina ceramic exhibits thicker adsorbed film compared to zirconia toughened alumina ceramic or metal. This fact is attributed to strong protein agglomerations. However, due to lower wettability [26] the adsorption is not as strong, so the proteins desorb from the surfaces during unloading phase causing a substantial instabilities of the lubricating film. No dependence between the model fluid and film thickness was observed.
- The results of zirconia toughened alumina ceramic showed that the thickest film was formed by BS, while sudden drops attributed to proteins desorption could be observed, as well as in the case of alumina. Both model SFs led to a remarkably lower film compared to BS; however, the film was stable without fluctuations.
- An increase of load can affect the adsorbed layer. Nevertheless, doubling of the initial load did not cause any change of the thickness;

therefore, there is no clear correlation between the level of load and film thickness.

- The results from swinging test clearly evidenced the importance of HA and phospholipids. The model SF2 with higher concentration of the mentioned constituents exhibited the thickest film which reached the maximum measurable level within few tens of seconds. BS results were somewhere between the two model SFs.
- Simple protein solutions formed thinner film than model SF2. Moreover, HA solutions exhibited a negligible film thickness, proving that the interaction of all the constituents must be considered and; therefore, the tests with simple solutions are not valid in an effort to understand the lubrication mechanisms within hip replacements.
- The presented results give a clear insight into the lubrication performance of hip replacements. The importance of the composition on SF, especially in terms of the content of HA and phospholipids, might be one of the most important implications for orthopaedic practice, while greater attention should be paid to individualized approach (e.g. composition of SF of particular patients).

The performed study utilized the contact of the metal/ceramic heads sliding against glass acetabular cups approaching the contact conditions in hard-on-hard hip implants. To mimic also hard-on-soft bearing pairs, the cup will be made from transparent poly(methyl methacrylate) in the following study. As the role of the individual constituents in relation to film thickness development cannot be clarified using optical interferometry method, fluorescent microscopy will be employed, since it was introduced in our previous papers that this technique enables to observe lubricant film formation considering both metal and ceramic femoral heads [14,15].

Acknowledgement

This research was carried out under the project CEITEC 2020 (LQ1601) with financial support from the Ministry of Education, Youth and Sports of the Czech Republic under the National Sustainability Programme II. The research was also supported by the project no. FSI-S-14-2336 with the financial support from the Ministry of Education, Youth and Sports of the Czech Republic. Further, the research was supported by the project NETME Centre TechUp - CZ.1.05/2.1.00/19.0397. The authors express their thanks to F. Urban, who participated in film thickness measurements as well as in data evaluation and their analysis.

References

- [1] Holzwarth U, Cotogno G. Total hip arthroplasty: state of the art, challenges and prospects. Luxembourg: European Commission. Publications Office of the European Union. ISBN: 978-92-79-25280-8.
- [2] Huch K. Sports activities 5 years after total knee or hip arthroplasty: the Ulm Osteoarthritis Study. *Ann Rheumatic Dis* 2005;64:1715–20.
- [3] Bedard NA, Callaghan JJ, Steff MD, Liu SS. Systematic review of literature of cemented femoral components: what is the durability at minimum 20 Years followup? *Clin Orthop Relat Res* 2015;473:563–71.
- [4] Myant C, Underwood R, Fan J, Cann PM. Lubrication of metal-on-metal hip joints: the effect of protein content and load on film formation and wear. *J Mech Behav Biomed Mater* 2012;6:30–40.
- [5] Essner A, Schmidig G, Wang A. The clinical relevance of hip joint simulator testing: in vitro and in vivo comparisons. *Wear* 2005;259:882–6.
- [6] Smith AM, Fleming L, Wudebwe U, Bowen J, Grover LM. Development of a synovial fluid analogue with bio-relevant rheology for wear testing of orthopaedic implants. *J Mech Behav Biomed Mater* 2014;32:177–84.
- [7] Park JB, Duong CT, Chang HG, Sharma AR, Thompson MS, Park S, et al. Role of hyaluronic acid and phospholipid in the lubrication of a cobalt–chromium head for total hip arthroplasty. *Biointerphases* 2014;9:031007.
- [8] Galandáková A, Ulrichová J, Langová K, Hanáková A, Vrbka M, Hartl M, et al. Characteristics of synovial fluid required for optimization of lubrication fluid for biotribological experiments. *J Biomed Mater Res Part B Appl Biomaterials* 2016. <http://dx.doi.org/10.1002/jbm.b.33663>.
- [9] Mavraki A, Cann PM. Lubricating film thickness measurements with bovine serum. *Tribol Int* 2011;44:550–6.
- [10] Parkes M, Myant C, Cann PM, Wong JSS. The effect of buffer solution choice on protein adsorption and lubrication. *Tribol Int* 2014;72:108–17.

- [11] Fan J, Myant CW, Underwood R, Cann PM, Hart A. Inlet protein aggregation: a new mechanism for lubricating film formation with model synovial fluids. *Proc Inst Mech Eng Part H J Eng Med* 2011;225:696–709.
- [12] Parkes M, Myant C, Cann PM, Wong JSS. Synovial fluid lubrication: the effect of protein interactions on adsorbed and lubricating films. *Biotribology* 2015;1–2: 51–60.
- [13] Reddyhoff T, Choo JH, Spikes HA, Glovnea RP. Lubricant flow in an elastohydrodynamic contact using fluorescence. *Tribol Lett* 2010;38:207–15.
- [14] Nečas D, Vrbka M, Urban F, Krupka I, Hartl M. The effect of lubricant constituents on lubrication mechanisms in hip joint replacements. *J Mech Behav Biomed Mater* 2016;55:295–307.
- [15] Nečas D, Vrbka M, Krupka I, Hartl M, Galandáková A. Lubrication within hip replacements – implication for ceramic-on-hard bearing couples. *J Mech Behav Biomed Mater* 2016;61:371–83.
- [16] Murakami T, Yarimitsu S, Nakashima K, Sawae Y, Sakai N. Erratum to: influence of synovia constituents on tribological behaviors of articular cartilage. *Friction* 2014; 2:391.
- [17] Seror J, Zhu L, Goldberg R, Day AJ, Klein J. Supramolecular synergy in the boundary lubrication of synovial joints. *Nat Commun* 2015;3-10;6. 6497.
- [18] Jahn S, Seror J, Klein J. Lubrication of articular cartilage. *Annu Rev Biomed Eng* 2016;18:235–58.
- [19] Forsey R, Fisher J, Thompson J, Stone M, Bell C, Ingham E. The effect of hyaluronic acid and phospholipid based lubricants on friction within a human cartilage damage model. *Biomaterials* 2006;27:4581–90.
- [20] Schmidt TA, Gastelum NS, Nguyen QT, Schumacher BL, Sah RL. Boundary lubrication of articular cartilage: role of synovial fluid constituents. *Arthritis & Rheum* 2007;56:882–91.
- [21] Murakami T, Nakashima K, Yarimitsu S, Sawae Y, Sakai N. Effectiveness of adsorbed film and gel layer in hydration lubrication as adaptive multimode lubrication mechanism for articular cartilage. *Proc Inst Mech Eng Part J J Eng Tribol* 2011;225:1174–85.
- [22] Park J-Y, Duong C-T, Sharma AR, Son K-M, Thompson MS, Park S, et al. Effects of hyaluronic acid and γ -globulin concentrations on the frictional response of human osteoarthritic articular cartilage. *PLoS One* 2014;9. e112684.
- [23] Vrbka M, Krupka I, Hartl M, Návrat T, Gallo J, Galandáková A. In situ measurements of thin films in bovine serum lubricated contacts using optical interferometry. *Proc Inst Mech Eng Part H J Eng Med* 2014;228:149–58.
- [24] Vrbka M, Návrat T, Krupka I, Hartl M, Sperka P, Gallo J. Study of film formation in bovine serum lubricated contacts under rolling/sliding conditions. *Proc Inst Mech Eng Part J J Eng Tribol* 2013;227:459–75.
- [25] Vrbka M, Nečas D, Hartl M, Krupka I, Urban F, Gallo J. Visualization of lubricating films between artificial head and cup with respect to real geometry. *Biotribology* 2015;1–2:61–5.
- [26] Nečas D, Vrbka M, Urban F, Gallo J, Krupka I, Hartl M. In situ observation of lubricant film formation in THR considering real conformity: the effect of diameter, clearance and material. *J Mech Behav Biomed Mater* 2017;69:66–74.
- [27] Smith SL, Dowson D, Goldsmith AAJ. The effect of diametral clearance, motion and loading cycles upon lubrication of metal-on-metal total hip replacements. *Proc Inst Mech Eng Part C J Mech Eng Sci* 2006;215:1–5.
- [28] Meng Q, Liu F, Fisher J, Jin Z. Contact mechanics and lubrication analyses of ceramic-on-metal total hip replacements. *Tribol Int* 2013;63:51–60.
- [29] Brockett CL, Harper P, Williams S, Isaac GH, Dwyer-Joyce RS, Jin Z, et al. The influence of clearance on friction, lubrication and squeaking in large diameter metal-on-metal hip replacements. *J Mater Sci Mater Med* 2008;19:1575–9.
- [30] Hu XQ, Wood RJK, Taylor A, Tuke MA. The tribological behaviour of different clearance MOM hip joints with lubricants of physiological viscosities. *Proc Inst Mech Eng Part H J Eng Med* 2011;225:1061–9.
- [31] Dowson D, Hardaker C, Flett M, Isaac GH. A hip joint simulator study of the performance of metal-on-metal joints. *J Arthroplasty* 2004;19:124–30.
- [32] Dowson D. Tribological principles in metal-on-metal hip joint design. *Proc Inst Mech Eng Part H J Eng Med* 2006;220:161–71.
- [33] Underwood RJ, Zografos A, Sayles RS, Hart A, Cann P. Edge loading in metal-on-metal hips: low clearance is a new risk factor. *Proc Inst Mech Eng Part H J Eng Med* 2011;226:217–26.
- [34] Cherniakova YM, Pinchuk LS. Tribological aspects of joint intraarticular therapy. *Acta Bioeng Biomech* 2011;13:57–63.
- [35] Sawae Y, Murakami T, Chen J. Effect of synovia constituents on friction and wear of ultra-high molecular weight polyethylene sliding against prosthetic joint materials. *Wear* 1998;216:213–9.
- [36] Sawae Y, Yamamoto A, Murakami T. Influence of protein and lipid concentration of the test lubricant on the wear of ultra high molecular weight polyethylene. *Tribol Int* 2008;41:648–56.
- [37] Hartl M, Krupka I, Poliscuk R, Liska M, Molimard J, Querry M, et al. Thin film colorimetric interferometry. *Tribol Trans* 2001;44:270–6.
- [38] Gaffney J, Matou-Nasri S, Grau-Olivares M, Slevin M. Therapeutic applications of hyaluronan. *Mol Biosyst* 2010;6:437–43.
- [39] Henrotin Y, Raman R, Richette P, Bard H, Jerosch J, Conrozier T, et al. Consensus statement on viscosupplementation with hyaluronic acid for the management of osteoarthritis. *Semin Arthritis Rheum* 2015;45:140–9.
- [40] Hamrock BJ. *Fundamentals of fluid film lubrication*. New York: McGraw-Hill c; 1994.
- [41] Medley JB, Krygier JJ, Bobyn JD, Chan FW, Lippincott A, Tanzer M. Kinematics of the MATCO™ hip simulator and issues related to wear testing of metal-metal implants. *Proc Inst Mech Eng Part H J Eng Med* 1997;1-1;211:89–99.
- [42] Myant C, Cann P. On the matter of synovial fluid lubrication: implications for Metal-on-Metal hip tribology. *J Mech Behav Biomed Mater* 2014;34:338–48.
- [43] Myant CW, Cann P. The effect of transient conditions on synovial fluid protein aggregation lubrication. *J Mech Behav Biomed Mater* 2014;34:349–57.
- [44] Vrbka M, Nečas D, Bartošík J, Hartl M, Krupka I, Galandáková A, et al. Determination of a friction coefficient for THA bearing couples. *Acta Chir Orthop Traumatologiae Cechoslov* 2015;82:341–7.
- [45] Mazzucco D, McKinley G, Scott RD, Spector M. Rheology of joint fluid in total knee arthroplasty patients. *J Orthop Res* 2002;20:1157–63.



On the observation of lubrication mechanisms within hip joint replacements. Part I: Hard-on-soft bearing pairs



D. Nečas^{a,*}, M. Vrbka^a, A. Galandáková^b, I. Křupka^a, M. Hartl^a

^a Faculty of Mechanical Engineering, Brno University of Technology, Czech Republic

^b Faculty of Medicine and Dentistry, Palacky University Olomouc, Czech Republic

ARTICLE INFO

Keywords:

Hip joint replacements
Hard-on-soft pairs
Lubrication
Fluorescent microscopy
Synovial fluid

ABSTRACT

The present study describes the lubrication mechanisms within artificial hip joints considering real conformity of rubbing surfaces. Part I is focused on hard-on-soft material combination, introducing the fundamentals of lubrication performance. These pairs have not been explored in terms of in situ observation before. The contact of metal femoral component articulating with transparent polymer acetabular cup was studied using a hip joint simulator. The film formation was evaluated by fluorescent microscopy method. Various model synovial fluids were employed while the key constituents, i.e. albumin, γ -globulin, and hyaluronic acid were fluorescently stained to determine its role in film formation process. Two types of the tests were performed. The first dynamic test aimed on the development of film thickness under constant load during motor driven swinging motion mimicking flexion-extension. Subsequently, a combined test was designed consisting of the three phases; static part with loading/unloading phase (1), pendulum swinging till spontaneous damping of the motion due to friction (2), and static observation under the constant load (3). The results clearly confirmed that the interaction of constituents of synovial fluid plays a dominant role and substantially influences the lubrication conditions. In particular, the main finding coming from the present study is that γ -globulin together with hyaluronic acid form relatively thin stable boundary layer enabling the enhanced adsorption of albumin, thus increasing the lubricant film. Part II of the present study is focused on hard-on-hard pairs while the main differences in film formation process are highlighted among others.

1. Introduction

Total joint arthroplasty has become a routine surgical technique for patients suffering from joint diseases. With respect to the statistics, it is apparent that the replacements of hips and knees are dominant. Currently, various materials have been used. In general, joint implants can be divided into two groups. The first group, representing a major portion of implanted pairs, is known as hard-on-soft. In such a case, hard femoral head or knee femoral component made of metal or ceramic articulates with polyethylene (PE) acetabular cup or knee tibial plateau. These pairs are investigated within the Part I of the present study. Part II is focused on the second material combination known as hard-on-hard where both the implant components are made of metal or ceramic (Nečas et al., 2018a).

Although the amount of joint surgeries continuously increases, limited longevity of replacements persists as the main drawback. The implant is expected to fulfil its function for approximately 8–15 years which is limiting especially in the case of younger active patients

(Huch, 2005; Unsworth, 1995). It must be taken into account that revision surgeries are more complicated and the associated costs are substantially higher. Implant failure is often accompanied by aseptic loosening as a consequence of osteolysis (Holzwarth and Cotogno, 2012); the process related to the interaction of hard and soft tissues with wear particles released during joint articulation. Indisputably, wear rate is associated with implant material. It was reported that the highest wear occurs in the case of metal-on-PE material combination while the amount of PE debris is of several orders of magnitude higher compared to metal-on-metal or ceramic-on-ceramic (Heisel et al., 2003).

Previously, an extensive research was carried out focusing on the determination of wear rate considering not only the implant material but also on its size (Goldsmith et al., 2006; Smith et al., 2001) or the size of the clearance between the rubbing surfaces (Brockett et al., 2008; Dowson et al., 2004). Focusing on hard-on-soft pairs, several in vitro studies were introduced, bringing an insight into wear mechanisms respecting the influence of synovial fluid. It was found that even a

* Corresponding author.

E-mail address: David.Necas@vut.cz (D. Nečas).

<https://doi.org/10.1016/j.jmbbm.2018.09.022>

Received 13 July 2018; Received in revised form 14 September 2018; Accepted 17 September 2018

Available online 19 September 2018

1751-6161/ © 2018 Elsevier Ltd. All rights reserved.

small amount of proteins leads to rapid increase of PE wear (Wang et al., 1998). The authors later reported that not only the total content of proteins in synovial fluid but also its ratio affects wear progression (Wang et al., 2004). The role of lipids in terms of wear of PE was later described by Sawae et al. (2008), who found that the effect of lipids is influenced by the total concentration of proteins. Considering low concentration, an increased amount of lipids led to a decrease of wear rate; however, opposite behaviour was observed when physiological protein concentration was considered. Assuming that wear is strongly affected by the overall tribological performance of the contact couple, friction and lubrication should be also taken into account when identifying the factors limiting the durability of implants (Wang et al., 1998).

Vrbka et al. (2015a) employed real implant components when determining the friction coefficient considering various material combinations. Using 25% bovine serum (BS) it was found that the friction between the head and the cup varies from 0.1 to 0.2 dependently on the head material. The effect of implant diameter was observed as well. Our previous paper was aimed on the deeper clarification of the effect of proteins on friction of metal-PE sliding pair, finding that simple saline solution ensures the lowest level of friction (Nečas et al., 2017a). Proteins added to the base lubricant led to immediate increase of friction which corresponds to elevated wear published elsewhere (Wang et al., 1998). It was also pointed out that the frictional behaviour is considerably influenced by the kinematic conditions while different film formation mechanisms could be observed under lower and higher sliding speed. Although the proteins are dominant components of synovial fluid (Galandáková et al., 2016), hyaluronic acid (HA) has to be also taken into account as it was previously shown that it leads to lowering of both the friction and wear (Sawae et al., 1998).

Frictional behaviour of the contact is also influenced by the surface conditions. Widmer et al. (2001) focused on the ceramic-PE sliding pair concluding that oxygen-plasma treatment of PE caused enhanced adsorption ability of proteins, resulting to reduction of static and dynamic friction, thus affecting service-life of implants. The following paper aimed on the effect of conformational changes of BS albumin (BSA) on adsorption abilities (Heuberger et al., 2005). The authors concluded that the hydrophilic surfaces support the adsorption of proteins in a native state, forming thicker and denser film leading to reduced friction. Nevertheless, it should be pointed out that the surface properties of ceramic and metal are different (Nečas et al., 2017b) indicating that these findings should not be generalized. This statement is supported by later experimental observation focused on the adsorption of BSA (Serro et al., 2006). The results of pin-on-disc tests clearly showed that more pronounced adsorption occurred in the case of hydrophobic metal pin.

The above papers focused on the friction and wear providing a limited knowledge about lubrication. As the lubricating film apparently affects the joint conditions, a deeper understanding of lubrication mechanisms in hard-on-soft pairs should be of a greater interest. At this point, some limitations related to these bearing pairs should be highlighted. The fundamental point is the issue of material. Considering hard-on-hard pairs, optical glass is usually used as a substitution of one of the rubbing surfaces, allowing direct observation while keeping the rigid nature of the contact (Mavraki and Cann, 2011; Vrbka et al., 2014, 2015b). The authors often employed optical interferometry technique for film thickness investigation (Hartl et al., 2001). However, in the case of hard-on-soft pairs, mimicking the contact mechanics is much more complicated and the routine techniques usually fail. One of the pilot studies focused on the observation of lubrication mechanisms was given by Crockett et al. (2009) who enhanced the friction data by *ex situ* fluorescent observation of PE particles released during the sliding test. It was found that low friction is basically accompanied by relatively low amount of transferred wear particles. The authors also compared the effect of model fluid, finding that there was no significant difference considering saline solution and BS; however, BSA exhibited substantially higher friction.

Summarizing the literature review about the tribological behaviour of hard-on-soft bearing pairs, it can be concluded that some clear results have been published in relation to wear and friction mechanisms during the last three decades. However, so far, there is not a study examining the lubricant film formation based on in situ observation. The main reason is complicated modelling of contact mechanics together with limitations of the routine techniques used for film formation investigation. Therefore, the aim of the Part I of the present study is to clarify the lubrication mechanisms within hard-on-soft pairs with the use of direct contact observation. The main attention is paid to the effect of model synovial fluid composition, focusing on the determination of the mutual interaction of the constituents of model SF in relation to lubricant film formation. For this purpose, the fluorescent technique is a suitable tool since it is not dependent on the surface reflectivity nor conductivity (Myant et al., 2010; Fowell et al., 2014; Necas et al., 2018b). The technique was previously successfully employed when examining the lubrication considering both ceramic-on-glass (Nečas et al., 2016a) and metal-on-glass (Nečas et al., 2016b) material combinations; however, its use for soft-based joint replacements is presented for the first time. To be able to observe the contact in situ, the acetabular cup is made of transparent poly(methyl) methacrylate (PMMA) which exhibits similar mechanical properties like conventionally used PE.

2. Materials and methods

The measurements were realized utilizing pendulum hip joint simulator originally designed by Stanton (1923). Real geometrical ball-on-cup contact, mimicking the artificial hip joint is considered while the continuous swinging in flexion-extension plane may be applied. The range of swinging motion was set according to the standards together with the respect to actual motion range of hip joint published in literature. ISO 14242 provides the loading and displacement parameters for testing of hip implants, defining the range of flexion/extension from $+25^\circ$ to -18° . However, it was found by Roaas and Andersson (2009) that actual extension angle is smaller; $-9.5^\circ \pm 5.2^\circ$ in particular. Additionally, it should be emphasized that the pendulum does not allow to apply asymmetric swinging; the maximum deflection has to be the same considering both ways (flexion vs. extension). Therefore, the conservative range of motion from $+16^\circ$ to -16° was applied.

The acetabular cup is fixed in the stainless steel pot using the resin and is mounted to the stationary frame of the simulator. The femoral head is attached to the cone and is inserted into the swinging pendulum arm. Some simulators exhibit the limitation associated with centring of the femoral component in the cup; however, in the case of pendulum, the contact is centred spontaneously as the swinging arm is released and the ball fits into the socket. The arm is then powered by electromagnetic motors while its bottom part flange moves within the rolling guide. Therefore, any undesirable rotation or deflection of the pendulum in transverse plane do not occur. The reverse arrangement of the contact allows direct observation using the imaging system (Vrbka et al., 2015b). For the first time, the use of fluorescent microscopy together with pendulum simulator is introduced in the present study. For this purpose, a tailor-developed optical module was implemented. The contact is illuminated by mercury lamp while the light passes through the assembly of optical filters. High speed scientific complementary metal-oxide semiconductor camera Andor Neo 5.5 is employed for data recording. A schematic sketch of the experimental methodology is displayed in Fig. 1.

The optical method based on the principle of fluorescence was used for the investigation of lubricant film formation. The fluorescence phenomenon is known to be a consequence of the following steps (Haugland et al., 1996; Lakowicz, 2006):

- **Excitation:** A photon is excited by the external light source being absorbed by the fluorophore contained in the lubricant.

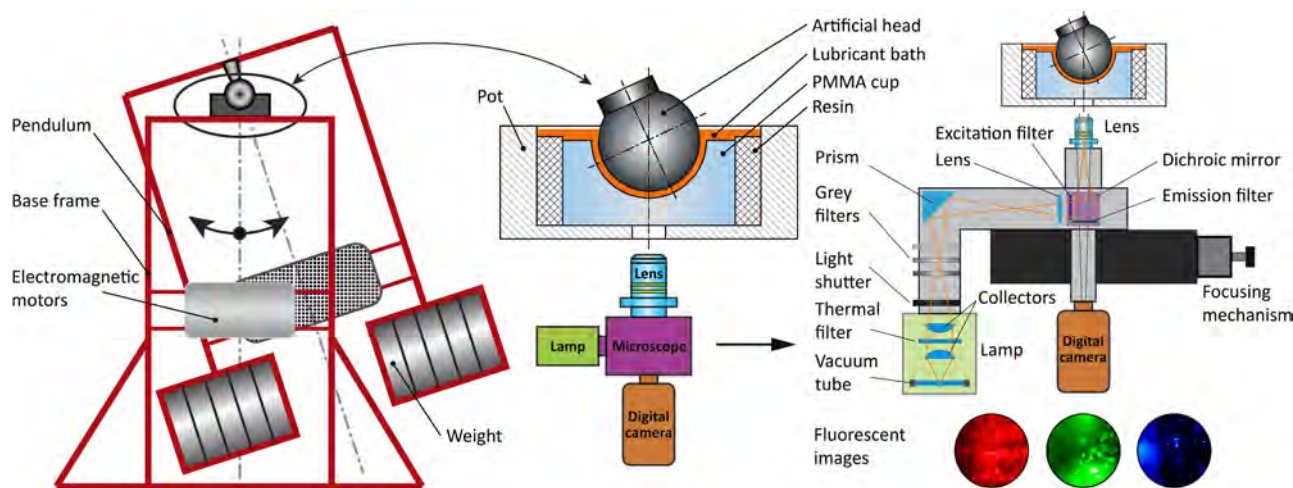


Fig. 1. A schematic illustration of the measurement methodology.

- **Excited-state period:** This period lasts for a very short time, usually between 1 and 10 ns. During this phase, partial energy dissipation occurs, so fluorescent emission arises.
- **Emission:** As a consequence of energy dissipation during excited-state period, the emitted photon exhibits lower energy accompanied by emission of radiation at higher wavelength. The difference in excitation and emission is known as Stokes shift, which actually enables to separate the excitation and emission; therefore, the fluorescent yield can be determined.

The main advantage of fluorescent method is that it is very powerful compared to other conventional methods introduced for film formation investigation. This is due to the measurement principle, since the method evaluates the actual amount of lubricant presented between the two surfaces (Spikes, 1999). This enables to use PMMA component which surface is poorly reflective; therefore, optical interferometry desiring high reflectivity cannot be employed. Moreover, polymers are usually non-conducting that disables the use of the methods based on the change of electrical quantity (Albahrani et al., 2015). In addition, fluorescent microscopy allows to separate particular constituents of SF so its role in lubrication process can be clarified.

However, some limitations of the method were identified as well. Namely, the film thickness could not be evaluated quantitatively, since undesired interference fringes occurred, disabling to obtain a calibration curve. Unfortunately, the contrast of the fringes was poor, so the use of optical interferometry was not possible. Similar limitation was reported previously in literature (Sugimura et al., 2000). Another point is fluorescence quenching phenomenon occurring due to the presence of chromium (Jie et al., 1998) in the femoral head. Since the quenching effect is not linear and is dependent on many factors, e.g. type of fluorescent dye and its concentration, or level of chromium, this limitation cannot be easily issued. Due to above limitations, the film thickness was evaluated as function of time in a qualitative manner. It means that the main attention was paid to the trends of film development and mutual influence of the synovial fluid components. The fluorescent intensity detected by the camera expresses the dimensionless film thickness, since it was showed that the film thickness is proportional to fluorescent intensity (Azushima, 2006).

According to the settings of external light source, microscope filters, and dependently on the used fluorescent marker and its amount, the initial fluorescent intensity varies measurement to measurement. To be able to compare the results within one scale, all the obtained data were normalized. The normalization is based on a simple division. Firstly, the initial intensity was determined analysing the data at the beginning of the test. Subsequently, it was decided to normalize the data to obtain

initial value equal to 1 000; therefore, the constant of division was obtained. Finally, all the data from the particular experiment were divided by this constant. This approach enables to compare the data even if there is various fluorescent intensity at the beginning of the test. This approach was already introduced and validated successfully within our previous studies (Nečas et al., 2016a, 2016b).

The contact consisted of original metal femoral component of the nominal diameter of 28 mm (actual diameter 27.97 mm) and the PMMA cup. The cup was fabricated according to the dimensions of real highly cross-linked PE acetabular cup, while its diameter was 28.11 mm. The dimension was checked using the optical scanning method (Ranuša et al., 2017). The initial surface topography was evaluated using 3D optical profiler, finding that the surface roughness of the ball varies between 6 and 9 nm. The surface roughness of the cup was around 5 nm. Fine polishing was applied to ensure sufficient optical properties of the cup. The elastic moduli and Poisson's ratios of the test samples are as follows: $E_{\text{ball}} = 230 \text{ GPa}$, $\nu_{\text{ball}} = 0.28$; $E_{\text{cup}} = 3 \text{ GPa}$, $\nu_{\text{cup}} = 0.37$.

The contact was lubricated by model synovial fluids prepared in collaboration with faculty hospital. Based on the extensive analysis of synovial fluid composition (Galandáková et al., 2016) and based on our previous findings (Nečas et al., 2017b, 2018c), a model fluid of the following composition was designed: albumin = 24.9 mg/ml, γ -globulin = 6.1 mg/ml, HA = 1.49 mg/ml, phospholipids (PHs) = 0.34 mg/ml. Various test fluids were prepared to identify the role of the individual constituents. The attention was also paid to the mutual interaction of the components contained in SF. Therefore, the measurements were initially performed with simple solutions of albumin, γ -globulin, and solution of HA with PHs as these were identified as the main driving constituents affecting the lubrication conditions. Simple solutions of HA and PHs were not considered since their concentration is very low and; moreover, it is expected based on some previous observations that their lubricity without interaction with other constituents is limited. Subsequently, other constituents were added to the solutions; therefore, we could clearly identify, how each individual constituent affects the film formation process.

To be able to distinguish the selected constituent (albumin, γ -globulin, and HA) in the fluid containing more than one constituent, fluorescent markers were used. When using the fluorescent microscope and appropriate filters, it is possible to focus on one particular constituent while the action of other components of the fluid is still considered. It means that the development of film thickness is influenced by all the contained ingredients; however, the observation is focused on one specific constituent. Therefore, the experiments had to be repeated multiple times while always we focused on one of the above-mentioned components. During the first phase, albumin was fluorescently stained

Table 1
Summary of the test lubricants.

Lubricant no.	Labelled constituent(s) (concentration)	Non-labelled constituent(s) (concentration)	Total concentration	Base fluid (total amount)	Corresponding results
1	Albumin (24.9 mg/ml)	–	24.9 mg/ml	PBS (4 ml)	Fig. 3, Fig. 6, Fig. 11
2	Albumin (24.9 mg/ml)	γ -globulin (6.1 mg/ml)	31 mg/ml	PBS (4 ml)	Fig. 3, Fig. 6
3	Albumin (24.9 mg/ml)	γ -globulin (6.1 mg/ml) HA (1.49 mg/ml)	32.49 mg/ml	PBS (4 ml)	Fig. 3, Fig. 6
4	Albumin (24.9 mg/ml)	γ -globulin (6.1 mg/ml) HA (1.49 mg/ml) PHs (0.34 mg/ml)	32.83 mg/ml	PBS (4 ml)	Fig. 3, Fig. 6, Fig. 9, Fig. 10
5	γ -globulin (6.1 mg/ml)	–	6.1 mg/ml	PBS (4 ml)	Fig. 4, Fig. 7, Fig. 12
6	γ -globulin (6.1 mg/ml)	Albumin (24.9 mg/ml)	31 mg/ml	PBS (4 ml)	Fig. 4, Fig. 7
7	γ -globulin (6.1 mg/ml)	Albumin (24.9 mg/ml) HA (1.49 mg/ml)	32.49 mg/ml	PBS (4 ml)	Fig. 4, Fig. 7
8	γ -globulin (6.1 mg/ml)	Albumin (24.9 mg/ml) HA (1.49 mg/ml) PHs (0.34 mg/ml)	32.83 mg/ml	PBS (4 ml)	Fig. 4, Fig. 7, Fig. 9, Fig. 10
9	HA (1.49 mg/ml)	PHs (0.34 mg/ml)	1.83 mg/ml	PBS (4 ml)	Fig. 5, Fig. 8
10	HA (1.49 mg/ml)	PHs (0.34 mg/ml)	26.73 mg/ml	PBS (4 ml)	Fig. 5, Fig. 8
11	HA (1.49 mg/ml)	Albumin (24.9 mg/ml) PHs (0.34 mg/ml)	7.93 mg/ml	PBS (4 ml)	Fig. 5, Fig. 8
12	HA (1.49 mg/ml)	γ -globulin (6.1 mg/ml) Albumin (24.9 mg/ml) γ -globulin (6.1 mg/ml) PHs (0.34 mg/ml)	32.83 mg/ml	PBS (4 ml)	Fig. 5, Fig. 8, Fig. 9, Fig. 10
13	Albumin (24.9 mg/ml) γ -globulin (6.1 mg/ml) HA (1.49 mg/ml)	PHs (0.34 mg/ml)	32.83 mg/ml	PBS (4 ml)	Fig. 9, Fig. 10

while other constituents were non-stained. Subsequently, γ -globulin was stained with other non-stained, and finally the same with stained HA and the rest non-stained. Once these partial experiments were finished, the overall intensity of the lubricating film was identified. For this purpose, the lubricant containing stained albumin, stained γ -globulin, stained HA and non-stained PHs was used. This approach enabled to identify the mechanism of lubricant film formation between the surfaces.

Albumin and HA were doped by Rhodamine-B-isothiocyanate (283924, Sigma-Aldrich) and γ -globulin was doped by Fluorescein-isothiocyanate (F7250, Sigma-Aldrich). The constituents were solved in phosphate-buffered saline (PBS) solution, while the total amount of lubricant per one experiment was 4 ml. For better clarity, the overview of the applied test lubricants is specified in a detail in Table 1. Before the experiment, both the ball and the cup were rinsed in water and cleaned by 1% solution of sodium dodecyl sulphate. Subsequently they were rinsed in pure water, dried by pressed air and finally washed in isopropyl alcohol. The same process was repeated also immediately after the experiment to avoid any influence of the results of the following test by the residual film.

Two types of the tests were realized to assess the film formation

within the replacement during various activities of daily life. The aim of the first experiment was to simulate three-minutes steady-state walking. For this purpose, forced continuous swinging of the pendulum within the range from $+16^\circ$ to -16° was kept for 180 s. After that, the electromotors were stopped and the motion was damped naturally. Consequently, combined test was designed to cover more complex body action. At the beginning, several transitions from sitting to stance were simulated, followed by short walk, and subsequent ten-minutes still standing. In particular, the course of the test was as follows. Initially, 9 cycles lasting 30 s in total, composed of 10-s loading phase and 20-s unloading phase were repeated. After the static part, 1-min relaxation under full load was applied. Then, the pendulum was deflected to a maximum and was let to swing freely without the external driving. Once the motion completely stopped, the contact was kept loaded for additional 10 min.

It should be noted that an attention was paid to minimize inaccuracies coming from the loss of fluorescent intensity due to excitation by external light source (Ford and Foord, 1978). Therefore, during the static part, the single images were taken each loading cycle while the light excitation was avoided during the rest of the loading and unloading phases. Then, the record of the dynamic part of the test was

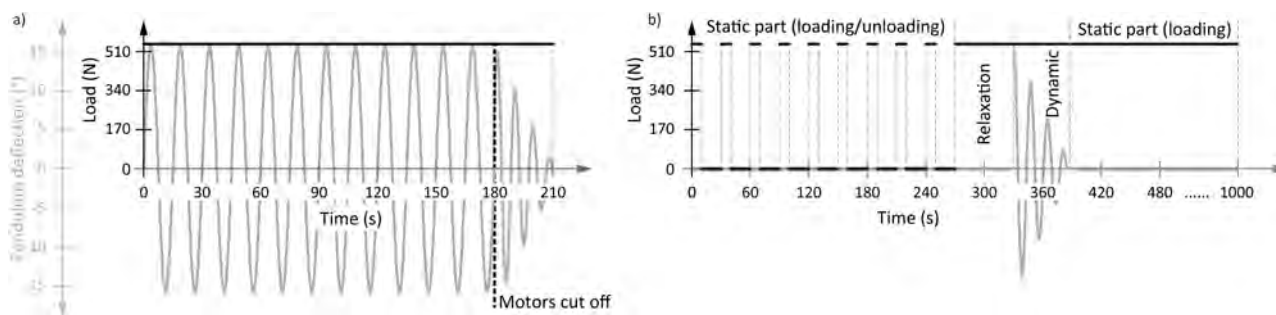


Fig. 2. Kinematics and load of the performed tests. a) Dynamic test; b) Combined test.

taken under continuous excitation. Finally, during the relaxation time, single images under discontinuous contact illumination were taken each 30 s. Both the tests are schematically illustrated in Fig. 2. Considering the dynamic part of the combined test, the film intensity was evaluated in the equilibrium position (pendulum deflection = 0°).

The load applied by the weight on the pendulum arm was 532 N. Corresponding contact pressure between the ball and the cup was 5.1 MPa and the total contact area diameter was equal to 14.1 mm. The applied load is based on the numerical simulations focused on the determination of maximum contact pressure in metal-on-polyethylene hip replacement (Enab and Bondok, 2014; Hua et al., 2014). Using the fluorescent microscope, the zone equal to 1.5 mm in a diameter was observed. The evaluated non-dimensionless film thickness in Fig. 3 to Fig. 12 corresponds to the average value of the fluorescent intensity throughout the observed zone. The measurements were conducted under ambient laboratory temperature of 22 °C, since it was shown previously that elevated temperature to body level does not cause any change in film formation considering synovial fluid lubrication (Mavraki and Cann, 2011). Moreover, protein conformational changes do not take place under these relatively low temperature changes.

3. Results

3.1. Dynamic tests

Initially, dynamic tests with labelled albumin were performed while the results are shown in Fig. 3. As can be seen, simple albumin solution forms the thinnest layer. The images of the contact zone displayed in Fig. 3b show that the film is relatively uniform. Adding γ -globulin caused a rapid increase of the film thickness which was three to four times higher. After reaching the maximum, quite a substantial drop of the film could be observed while the thickness at the end of the measurement was double compared to simple albumin. On the contact images, it can be seen that when albumin and γ -globulin are mixed together, substantial protein aggregations can be observed, causing an increase of the lubricant film. Further step was addition of HA. The results show similar trend like the mixture of the proteins, while the thickness is somewhere between the simple solution and mixed protein solution in the first part. At the end, the intensity values are almost the same like in the case of albumin. Focusing on the details of the contact zone, the visual information corresponds to the results, since the film in the case of albumin mixed with γ -globulin and HA is not as uniform; however, nor localized aggregations can be observed. The thickest film

thickness could be detected when complex fluid containing all the constituents including PHs was applied. Nevertheless, as in the previous case, the film could not be maintained over the whole test. It exhibited decreasing tendency during the second half. The images prove that complex fluid forms the thickest layer. Independently of the test fluid, switching off the electromotors did not cause any change of the film, as can be seen in the right part of the graph (Fig. 3a).

The second set of the experiments was conducted with labelled γ -globulin. The results are displayed in Fig. 4. As in the previous case, the thinnest film was detected when simple solution was used. Moreover, the behaviour is almost the same while initial increase of intensity is followed by continuous decrease. The film is stabilized after approximately 100 s. By contrast to previous observation, the thickest film was formed when the proteins were mixed together (without HA nor PHs). Moreover, the film formed by protein mixture exhibited very stable behaviour without decreasing tendency. Addition of HA and HA with PHs did not cause any further improvement of the lubricating film. Nevertheless, both the mentioned constituents led to a stable film formation without any fluctuations. The data about fluorescent intensity are supplemented by the images of the contact zone in Fig. 4b. As can be seen, simple solution and solution of proteins containing HA and HA with PHs form very uniform film. However, second row of the images corresponding to protein mixture declares that the film was enhanced considerably. As in the case of the measurements realized with stained albumin, the film at the end of the test was not influenced by stopping the swinging motion.

Further, the experiments were performed with stained HA (Fig. 5). Initially, HA was mixed with PHs. At that time, gradually decreasing tendency was detected during the first 50 s. Then, the film was stabilized while sudden drop attributed to removal of the film from the cup surface could be observed in the last third of the test. Adding albumin or γ -globulin did not cause any difference in film formation. As is shown in the graph in Fig. 5a, the film decreased to very low level being stabilized after 40 s with no further fluctuations. The thickest film was detected for complex model fluid. Nevertheless, the intensities of the film are much lower compared to that observed above, which is discussed in a detail in the following chapter. Focusing on the contact images on Fig. 5b, it can be seen that HA with PHs form random agglomerations leading to apparently thicker film. However, the adsorbed layer is very thin, not different from the mixtures containing the individual proteins. Only in the case of complex fluid, more uniform film formation was observed.

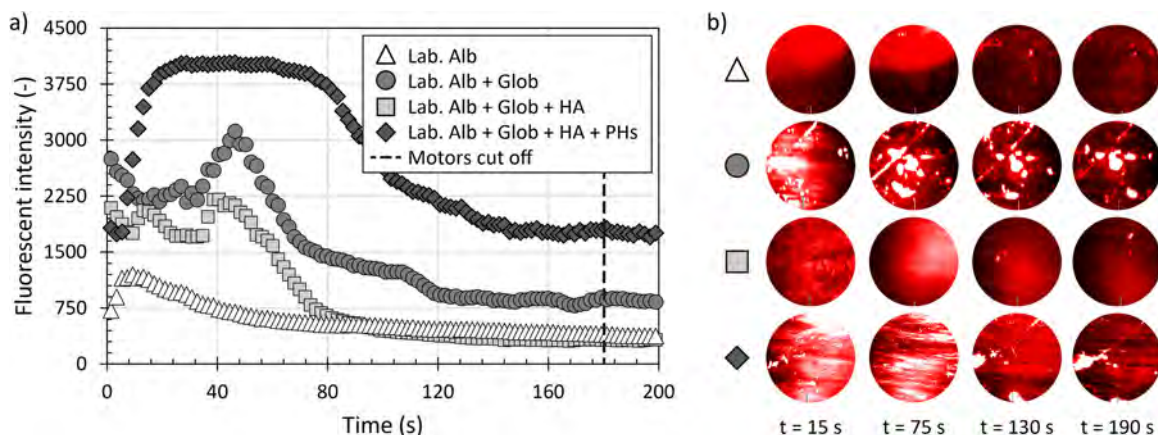


Fig. 3. a) Development of fluorescent intensity (dimensionless film thickness) of various model fluids containing fluorescently labelled albumin as a function of time over the dynamic test; b) Images of the contact zone (inlet/outlet is on the left/right).

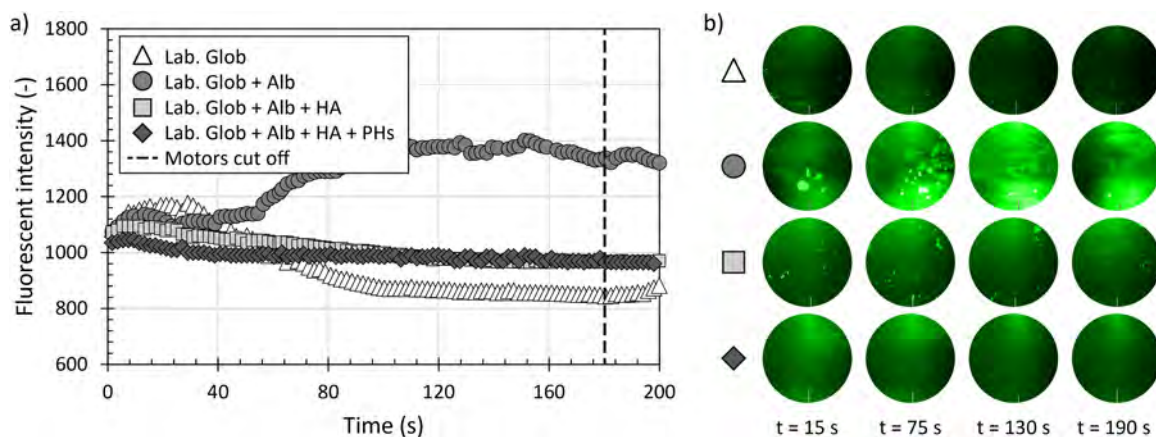


Fig. 4. a) Development of fluorescent intensity (dimensionless film thickness) of various model fluids containing fluorescently labelled γ -globulin as a function of time over the dynamic test; b) Images of the contact zone (inlet/outlet is on the left/right).

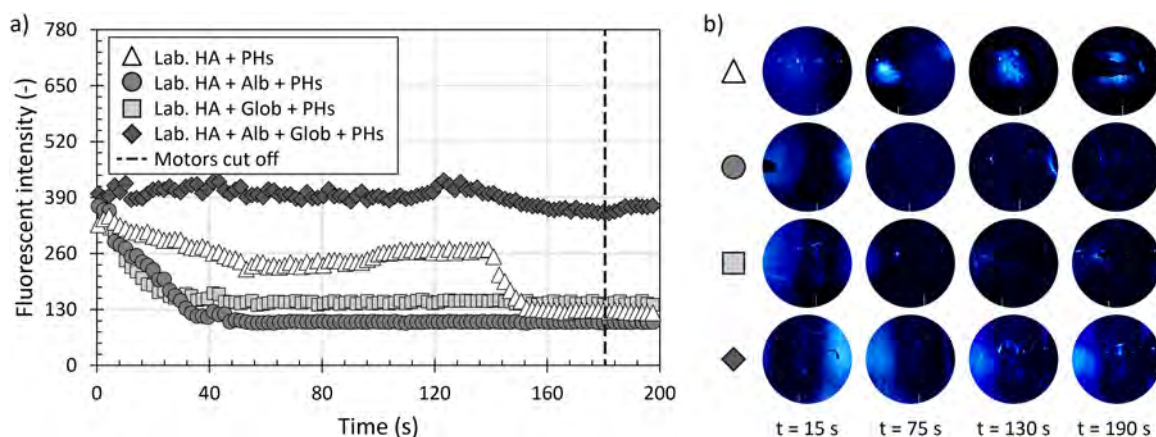


Fig. 5. a) Development of fluorescent intensity (dimensionless film thickness) of various model fluids containing fluorescently labelled hyaluronic acid as a function of time over the dynamic test; b) Images of the contact zone (inlet/outlet is on the left/right).

3.2. Combined tests

After the swinging dynamic test, the combined test was realized. The results for the fluids with labelled albumin are displayed in Fig. 6. Fig. 6a shows the course of the film intensity over the entire test lasting 1 000 s in total. As the swinging part (highlighted grey part of Fig. 6a) is quite short, the corresponding data are plotted in Fig. 6b. During the first part of the experiment, a continuous increase of film layer could be observed independently of the test fluid. As there is no pendulum motion, this film is attributed to adsorption on the surfaces. Focusing on the swinging part, the results are in a good agreement with the dynamic tests (Fig. 3a). As can be seen in Fig. 6b, simple albumin forms the thinnest layer while only a negligible increase can be observed. Combination of albumin with γ -globulin led to rapid enhancement of the film, while the same effect was observed when complex fluid containing all the constituents was used. When the proteins were mixed only with HA without PHs, the increase of the film was not as substantial. During the subsequent static part, simple albumin and complex fluid exhibited very stable behaviour. However, in the case of proteins mixture and proteins mixed with HA, a slight decrease of the film occurs, as can be seen in the right part of Fig. 6a. It should be noted that during the last period, the contact was permanently loaded. Therefore, the decreasing tendency indicates that the adsorption forces are not strong enough to maintain the constituents on the surfaces. By contrast, albumin and complex fluid exhibit stronger adsorption as the film remains.

In the case of labelled γ -globulin solutions, the adsorption at the

beginning of the experiment was limited, as is shown in Fig. 7a. Considering the swinging period (Fig. 7b), different behaviour can be observed compared to dynamic tests (Fig. 4a). In particular, even in the case of simple γ -globulin, the film continuously increases for approximately 50%. Combination of the proteins exhibits qualitatively similar results, while the increment of film thickness is more rapid during the first few swinging cycles. Then, the layer is stabilized. Both the protein solutions containing HA and HA with PHs do not show any development of the film. Independently of the applied lubricant, the film intensity continuously decreases over the last 10 min of permanent loading. As can be seen, the drop of the film is the most apparent for simple γ -globulin. On the contrary, the lubricants containing HA and HA with PHs do not undergo such a rapid decrease; however, it should be pointed out that the lubricant film was very thin compared to adsorbed layer of albumin in Fig. 6a.

The results for lubricants containing stained HA are plotted in Fig. 8. During the static part of the test, HA with PHs and the fluid containing albumin did not exhibit any substantial development of the adsorbed layer. The other two fluids led to some fluctuations; nevertheless, the data are not clear compared to albumin (Fig. 6) and γ -globulin (Fig. 7) solutions. During the pendulum swinging, the initial layer was almost completely removed, while no enhancement of the film due to hydrodynamic action was observed. Based on the Fig. 8b, it seems that the film is constant. However, the intensity values are very low, so the film is extremely thin. The results basically correspond to dynamic tests (Fig. 5), showing that HA can only hardly form a uniform lubricating film.

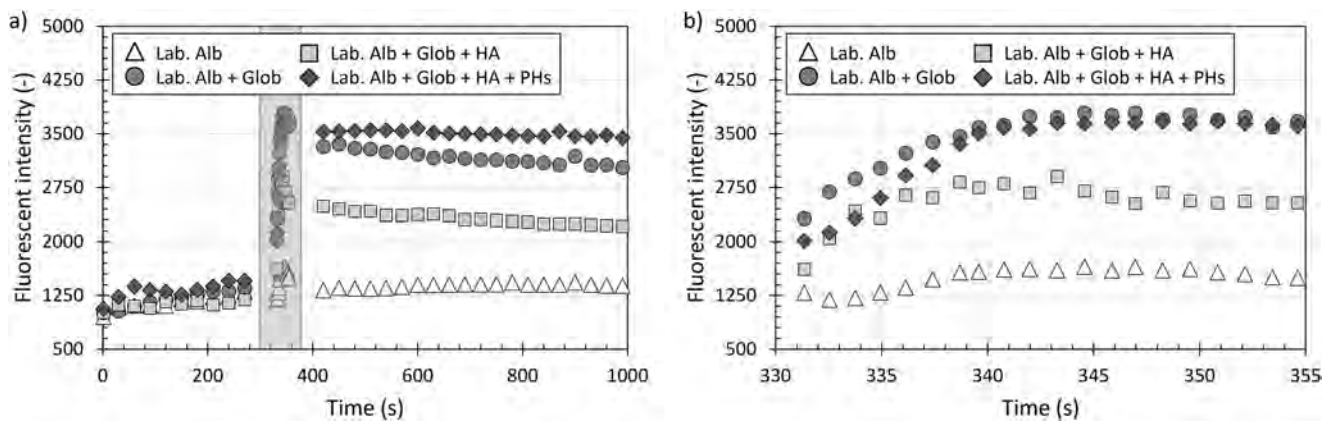


Fig. 6. a) Development of fluorescent intensity (dimensionless film thickness) of various model fluids containing fluorescently labelled albumin as a function of time over the combined test; b) Detail of the dynamic part of the experiment – highlighted part in graph (a).

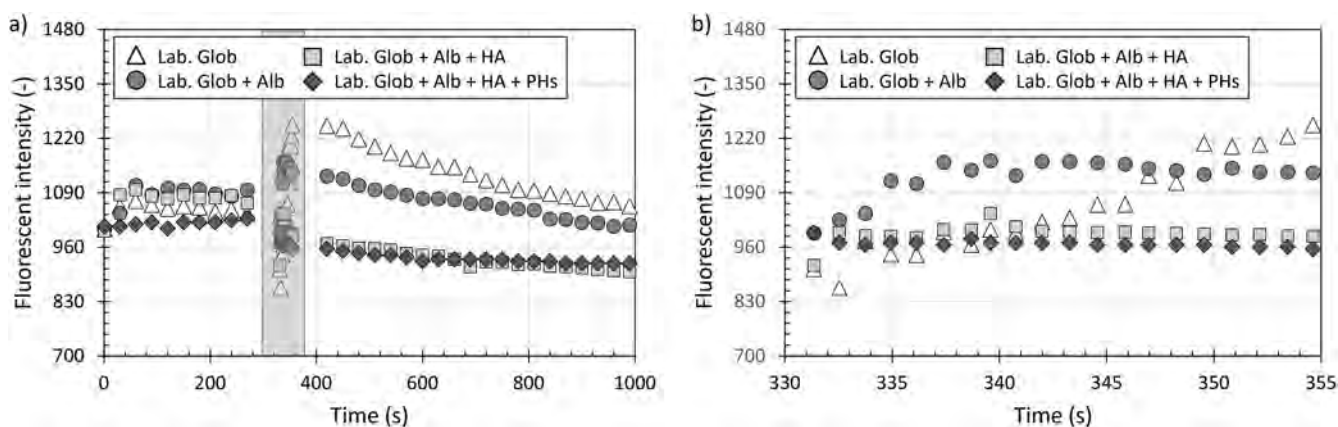


Fig. 7. a) Development of fluorescent intensity (dimensionless film thickness) of various model fluids containing fluorescently labelled γ -globulin as a function of time over the combined test; b) Detail of the dynamic part of the experiment – highlighted part in graph (a).

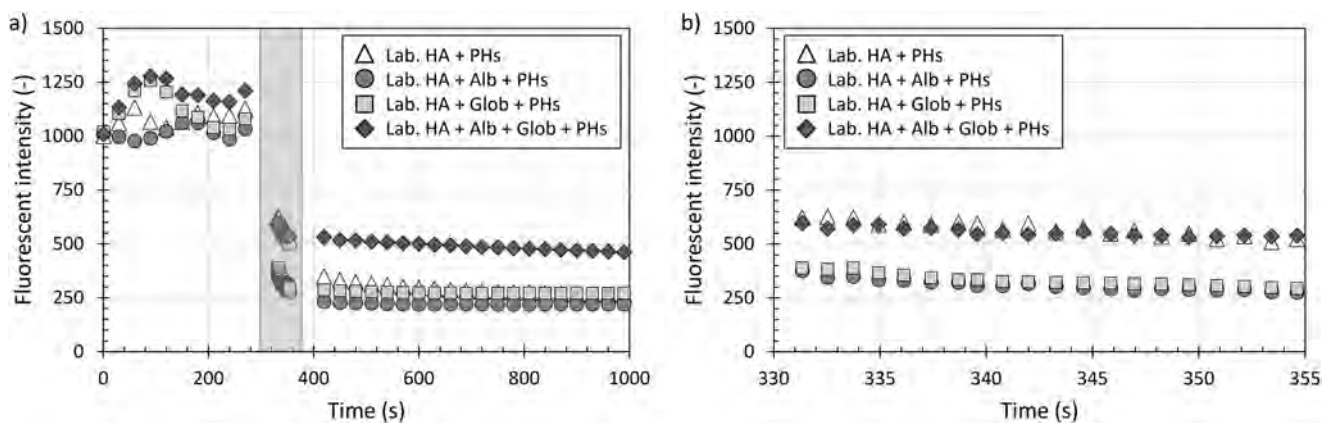


Fig. 8. a) Development of fluorescent intensity (dimensionless film thickness) of various model fluids containing fluorescently labelled hyaluronic acid as a function of time over the combined test; b) Detail of the dynamic part of the experiment – highlighted part in graph (a).

3.3. Comparison of complex fluids

Finally, the results considering complex fluids with various labelled constituents were compared. Additionally, the experiments with the fluid containing all the three aforementioned fluorescently stained constituents were performed to show the overall behaviour of the complex film. The results of the dynamic tests are summarized in Fig. 9. These data are fundamental, since it allows to understand the mechanism of lubricant film formation in hard-on-soft pairs. As can be

seen, labelled HA in complex fluid forms the thinnest layer. Considering γ -globulin, the film thickness is about two times higher; however, still quite thin and constant without any fluctuations. By contrast, the thickest film is formed by stained albumin, while the maximum film thickness is almost five times higher compared to γ -globulin. After some time, the film starts to gradually decrease being stabilized after 150 s. The results indicate that γ -globulin with HA form thin stable boundary layer while further development can be attributed to the increase of albumin film.

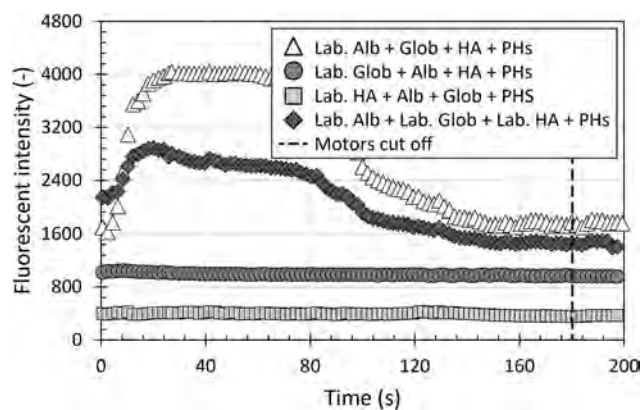


Fig. 9. a) Development of fluorescent intensity (dimensionless film thickness) of various complex model fluids containing various fluorescently labelled constituents as a function of time over the dynamic test.

It should be noted that when only single constituent is stained, it does not provide the information about the overall film thickness development. Only the behaviour of one particular component, influenced by the other constituents, can be determined. However, the above information about film formation mechanism is clearly supported by the behaviour of the model fluid containing labelled albumin, labelled γ -globulin, and labelled HA. As can be seen in Fig. 9, the tendency is almost the same exhibiting initial increase, followed by decrease and stabilization. Apparently, the question is, why the intensity of complexly labelled fluid is lower compared to intensity of solution containing stained albumin. Assuming that complex fluid contains higher amount of fluorescent dye in total, it might be expected that higher fluorescent intensity should be observed. This decrease is caused by mutual interaction of the fluorescent markers, which was described in the literature (Hidrovic and Hart, 2001) and is discussed in a detail in the following chapter.

The described mechanism of lubricant film formation was confirmed also in the case of combined static/dynamic test (Fig. 10). During the initial phase, the lubricant film increased gradually, while the most significant enhancement of the adsorbed layer was observed for stained albumin and the fluid containing all the three main constituents labelled. Subsequent dynamic part of the experiment led to relatively rapid increase of the albumin layer, followed by gradual intensity increase of the complexly labelled fluid. Other two fluids did not show any development during the swinging motion (Fig. 10b). Focusing on the last static part, most of the fluids showed very stable behaviour with the exception of complexly labelled lubricant the thickness of which continuously decreased. As in the case of the dynamic test, this

decrease is attributed to the interaction of the fluorescent markers discussed below.

4. Discussion

In an effort to avoid a failure of joint replacements, the producers aim on the extension of the service-life of implants. A new generation replacements have been introduced in literature, such as the implants with diamond-like carbon (DLC) coating (Choudhury et al., 2015b) or oxinium implants (McCalden et al., 2011). Although these modern replacements have been already involved to clinical testing, so far the survivorship of the implants could not be extended sufficiently. Therefore, the deeper understanding of tribological performance is required. Previously, in vitro wear laboratory tests were extensively performed (Goldsmith et al., 2006; Smith et al., 2001). However, only a little attention was paid to the clarification of lubrication mechanisms. The preliminary studies raised around year 2010 (Mavraki and Cann, 2009, 2011). Nevertheless, all of the previous investigations were conducted using glass component as one of the counterfaces. Since the elastic modulus is high, such an arrangement better corresponds to hard-on-hard joint replacements. Therefore, the present study introduces the use of polymer acetabular component in an effort to mimic PE cups which are dominant nowadays.

Initially, dynamic tests focused on the development of lubricant film thickness under continuous swinging were carried out. To identify the role of individual constituents of SF, various lubricants were prepared. The first set of experiments was performed with fluorescently stained albumin (Fig. 3). The results showed that simple albumin solution does not provide sufficient lubricity. It means that very thin lubricant film was formed. This is in a good agreement with some previous observations (Myant et al., 2012; Nečas et al., 2018c). Addition of γ -globulin led to a substantial increase of film thickness, indicating that the co-existence of proteins improves the lubrication performance. Further, HA was added into the solution, surprisingly leading to a decrease of the film. Finally, the lubricant was additionally doped by PHS exhibiting the highest film thickness which maximum was almost two times higher compared to protein solution (without HA and PHS).

Subsequently, γ -globulin was fluorescently stained (Fig. 4). It was reported in the literature (Myant et al., 2012; Nečas et al., 2018c) that γ -globulin forms the thickest layer considering simple solutions. However, in the case of the present study, the lubrication ability of simple γ -globulin was limited. This indicates some differences in film formation considering hard-on-hard and hard-on-soft bearing pairs. In particular, it should be taken into account that usage of PMMA leads to a substantial lowering of the contact pressure. Previously, it was described that lower load should have a positive effect on SF lubrication (Myant and Cann, 2014). However, the finding seems to be limited for γ -

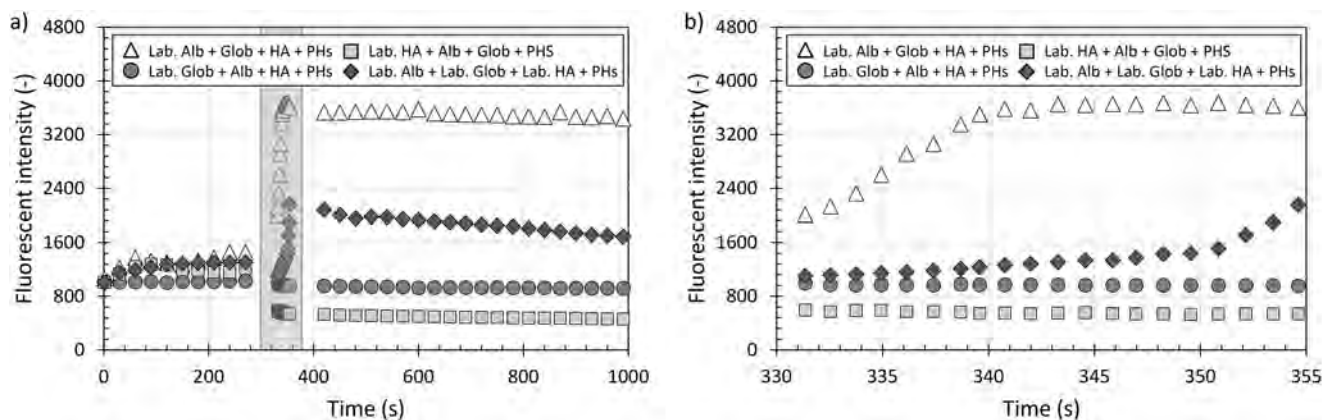


Fig. 10. a) Development of fluorescent intensity (dimensionless film thickness) of various complex model fluids containing various fluorescently labelled constituents as a function of time over the combined test; b) Detail of the dynamic part of the experiment – highlighted part in graph (a).

globulin which is able to form relatively thick layer even under high concentrated loads (Myant et al., 2012). The thickest film was observed for the mixture of the proteins. Addition of HA and HA with PHs showed rather negative effect.

The experiments were later repeated with fluorescently labelled HA (Fig. 5). As it was shown in our previous study, simple HA does not provide sufficient lubricity (Nečas et al., 2018c). Moreover, following the results obtained for albumin-stained and γ -globulin-stained solutions, the HA was not used as a simple solution. One of the points is the protection of PMMA surface. Assuming the poor lubricity of simple HA, the cup would be scratched quite quickly. Therefore, HA was mixed with PHs initially, forming stable film which suddenly dropped after some time due to removal of the attached agglomerations from the cup surface. Addition of the proteins did not cause any improvement of lubrication. However, when the fluid was complex composition of all the constituents, the film was the thickest. Therefore, it can be concluded that the interaction of the components of SF is fundamental in film formation process. This is highlighted also in the Part II for hard-on-hard pairs (Nečas et al., 2018a) and it supports our previous conclusions that simple solutions cannot mimic the behaviour of the complex fluids.

Subsequent combined tests showed that the adsorption ability of albumin during simple loading/unloading (without the presence of swinging motion) is comparative independently of other constituents (Fig. 6). Focusing on the dynamic part, the behaviour well corresponded to the dynamic tests with the exception of the mixture of the albumin with γ -globulin. It exhibited similar development like complex fluid. This indicates that the initial protein adsorption on the surfaces may enhance the film thickness during the subsequent swinging phase. Last static part of the test enabled to detect the sensitivity of the formed layer on load. In that case, simple albumin and complex fluid exhibited constant behaviour. On the other hand, mixture of the proteins and mixture doped by HA showed a slight drop, indicating that the film is continuously squeezed out from the contact.

More complex behaviour was observed for the fluids with stained γ -globulin (Fig. 7). Initially, the adsorbed film immediately increased for all the fluids with the exception of complex liquid. Subsequent swinging phase caused significant increase of simple solution and gradual increase of protein solution with no effect of HA or HA with PHs. The latest part of the experiment led to continuous decrease of the film for all the tested fluids. The negative effect of HA which caused that γ -globulin film could not be fully developed should be emphasized. This is an important finding indicating that the HA reinforces albumin layer, which is originally of α -helix structure (Howard and Smales, 2005). However, it does not improve aggregation of γ -globulin, which is in β -sheet form (Dev et al., 1988).

Focusing on the solutions containing fluorescently labelled HA (Fig. 8), initial phase led to bit chaotic adsorption for most of the lubricants. The combined increasing/decreasing tendency says that the adsorption forces are weak and the aggregations of HA molecules are being repeatedly attached and detached to and from the contact surfaces. The swinging part of the test did not lead to further development of the film which became very stable. When focusing on the last static period, the behaviour of HA with PHs should be highlighted. It can be observed that its thickness dropped within just one minute after the motion stopped. This is related to squeezing the film out of the contact.

When summarizing the data, it should be emphasized that the partial results displayed in Fig. 3 to Fig. 8 do not give the information about the overall film thickness behaviour. It just provides the knowledge about the layer of individual constituent affected by other constituents. Therefore, the concluding tests were carried out while the stained albumin, stained γ -globulin, and stained HA were mixed together. The main motivation for these experiments was to find out if the overall film development can be assessed in terms of the formation of individual constituents. This approach was previously successfully applied in our study focused on film formation considering simplified ball-

on-disc model for both metal and ceramic femoral components (Nečas et al., 2016a, 2016b). However, in the given reference, only a mixture of albumin and γ -globulin was investigated. The results of dynamic tests are shown in Fig. 9. As can be seen, the behaviour of complexly stained fluid very well corresponds to the development of the complex fluid with stained albumin. By contrast, in the given scale, it is apparent that HA forms stable, but very thin layer. γ -globulin is also almost constant while its thickness is about two times higher compared to HA. Based on these results, it can be concluded that the base layer of the film is formed by γ -globulin, HA, and PHs while the subsequent development is driven mainly by albumin.

As mentioned above, it might be expected that when three constituents are fluorescently stained, the intensity should be the highest due to increased total amount of fluorescent marker. The explanation of lower intensity of the complexly stained fluid is related to emission reabsorption (Hidrovic and Hart, 2001). This phenomenon occurs when emission wavelength of one dye is similar to excitation wavelength of another dye. In that case, the emitted light is partially consumed for further excitation of another dye. As a result, the total emitted intensity is lower than it could be if this phenomenon would not occur.

The mechanism of film formation is supported also by the results for combined test (Fig. 10). The difference in the development of lubricant with stained albumin and complexly stained lubricant during the dynamic part of the test is also attributed to emission reabsorption. The process can be well distinguished especially during the last static part. As can be seen in Fig. 10a, only the complexly stained film decreases. Because the fluids are completely the same in terms of the composition, there is no other explanation than consumption of the emission by other fluorescent agents.

In biotribology, the issue of repeatability is always discussed. It should be noted that when focusing on lubrication of hip joints, the measurement methodology is very complicated and the analyses require strict respecting of the experimental protocol. Considering the time requirements, together with the costs related to the experiments with biological agents, it is particularly complicated to repeat all the experiments multiple times to avoid any doubts. It should be emphasized that significant variance of results was previously reported several times; however, always in the case of simplified ball-on-disc configuration. Nevertheless, using the real conformity, quite good repeatability could be observed in our previous study considering metal-on-glass contact (Fig. 9 in Nečas et al., 2018a). In order to get a general imagination about the data validity for hard-on-soft pairs, two independent repeatability tests were made. The dynamic test was repeated with simple stained albumin while the combined test was conducted two times with labelled γ -globulin. The tests were realized in different days with fresh lubricants. Very satisfactory repeatability was achieved as can be seen in Fig. 11 and Fig. 12. In the case of the dynamic test, the difference is negligible. For the combined test, very little deviation was observed; however, the data are still in a very good agreement.

In addition, it should be emphasized that the methodology based on the fluorescent observation was previously successfully validated when investigating the point contact (Nečas et al., 2016a, 2016b). In that case, the qualitative trends of albumin and γ -globulin film between the metal/ceramic ball and the glass disc were validated by quantitative measurements of film thickness using optical interferometry. Since it was shown that the trends were almost identical, the credibility of the methodology approach was proved. Considering the presented repeatability and mainly following the clear correlation between the results of partially stained fluids and complexly stained fluid, it is assumed that the provided data are highly representative.

The issue of data evaluation should be discussed as well. Light conditions might differ test to test due to excitation light intensity, amount of fluorescent dye, or settings of the microscope filters. In addition, two fluorescent markers were used while each provides different yield of fluorescent emission. To avoid any inaccuracies, the data were normalized to the same initial level equal to fluorescent intensity of

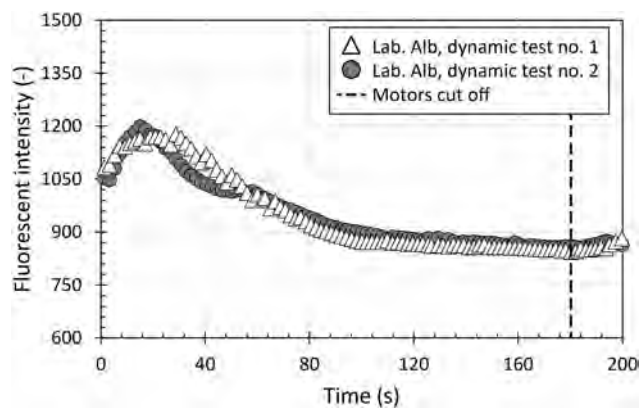


Fig. 11. Repeatability of the dynamic experiment with fluorescently labelled albumin.

1000 at the beginning of the test, as mentioned above. It is necessary to highlight that the normalization procedure (i.e. the division constant for the given test) was based on the first few images taken within around one tenth of second. The experiments started when the position of the pendulum was maximally deflected (16°). However, the above presented data correspond to equilibrium position when the pendulum deflection is equal to 0° . Therefore, when focusing on the graph of dynamic tests, it can be seen that in the case of albumin, the initial values are not the same for the individual lubricants (Fig. 3). This means that during the first half swing of the pendulum (from the deflected to equilibrium position) the film changed. By contrast, γ -globulin layer exhibited almost no change at the beginning of the test (Fig. 4). Finally, HA layer dropped to about one third immediately after the pendulum release (Fig. 5). This approach based on the normalization at the early beginning of the experiment enables to better capture the initial changes which might significantly influence the rest of the experiment. Moreover, the same approach was applied in previous ball-on-disc studies (Nečas et al., 2016a, 2016b).

The potential contribution of the performed study needs to be highlighted in terms of further development of joint replacements. It is indisputable that preclinical testing of implants provides a clear feedback to the designers (Trommer and Maru, 2017). However, to the author's best knowledge, most of the currently used commercial as well as tailor-made simulators have been used for evaluation of wear rate or/and coefficient of friction. Nevertheless, these tribological processes coexist and are substantially influenced by lubrication. Therefore, the film formation ability of the implant should be involved in the testing during the development of replacements as well. If the implant will ensure the formation of stable lubricant film of sufficient thickness,

wear may be substantially reduced, thus leading to enhanced durability. One of the great advantages of the methodology is that it can provide the initial information about the lubrication performance very quickly. There is no need to perform hundreds of thousands of cycles. The ability of film formation may be obtained within several hours including experiment preparation, measurement, and data evaluation. Moreover, due to measurement principle, it is not limited in terms of head materials. Therefore, even unconventional implants (e.g. oxinium, DLC) may be studied. In addition, PMMA cup can be machined quite easily which enables fast evaluation of some newly proposed approaches, such as surface texturing.

The present study provides a complex overview about the lubrication mechanisms in hard-on-soft hip implants. The authors were not able to involve fluorescently stained PHs, since the methodology of labelling of these is bit specific compared to proteins or HA. Moreover, it was reported that there is no significant effect of PHs on friction of metal-PE sliding pair (Mazzucco and Spector, 2004). In addition, considering very low concentration, it is expected that PHs do not form sufficient lubricating layer as itself. Its role is rather related to enhancement of the interaction of other constituents leading to thicker lubricating film (Fig. 3, Fig. 5). Further, the composition of the fluid does not perfectly fit to those in human body, since lubricin is not involved. However, its concentration is substantially lower compared to other constituents. In addition, its contribution to lubrication performance was confirmed only in the case of cartilage lubrication (Swann et al., 1985). For metal-PE pair, the effect of lubricin was not confirmed (Mazzucco and Spector, 2004).

Considering the partial limitations of the performed study, the roughness of PMMA cup should be also mentioned. To achieve optimal optical conditions, the contact surfaces of the cups were fine polished while the roughness is lower compared to real PE cups (Vrbka et al., 2015a). It is expected that this leads to enhanced lubrication conditions since it is well reported that during the running-in phase of the implant operation, wear rate is substantially higher. It means that after the surface is smoothed due to initial phase joint articulation, wear progress decreases. Therefore, it might be assumed that the present results correspond to the situation when the running-in period is over.

Finally, the motivation for future study should be mentioned. On the way to the extension of implant durability, some new approaches have been discussed recently. One of the very innovative approach might be the modification of the contact surfaces. The initial tests are promising in terms of enhanced lubrication performance (Choudhury et al., 2015a, 2018). Nevertheless, more analyses have to be done before these innovative techniques become routine and clinical testing will be allowed. For this purpose, the introduced methodology represents a suitable way for further investigation of commonly used hard-on-soft bearing pairs in an effort to contribute to further development of implants.

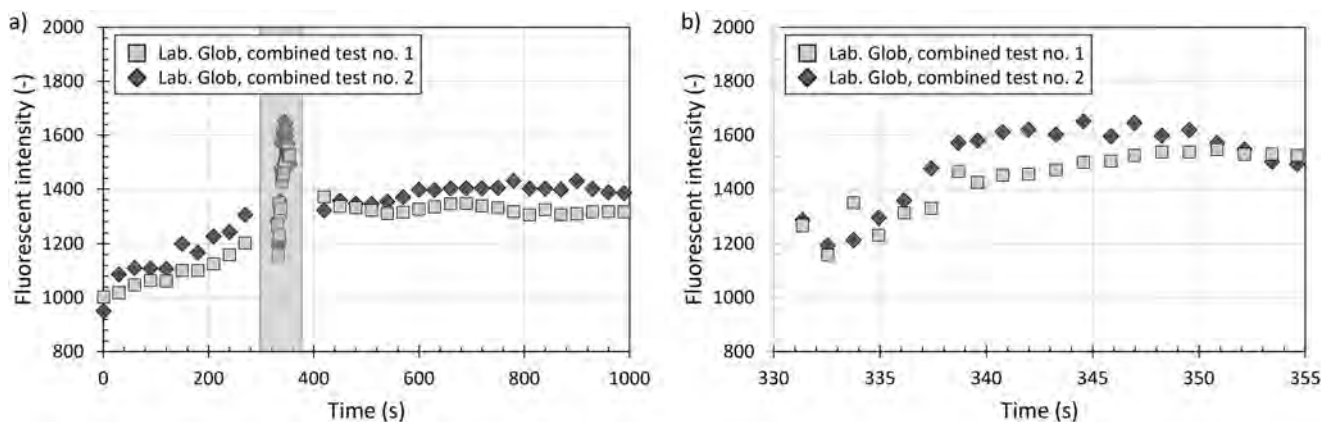


Fig. 12. Repeatability of the combined experiment with fluorescently labelled γ -globulin. b) Detail of the dynamic part of the experiment – highlighted part in graph (a).

5. Conclusion

The present paper introduces the fundamentals of lubrication mechanisms of hard-on-soft hip implants. According to author's best knowledge, in situ observation of the lubricant film formation considering these bearing pairs was performed for the very first time. An optical method based on the fluorescent microscopy was implemented to the hip joint simulator while the contact was lubricated by various model fluids containing various fluorescently stained constituents. Two types of the tests were performed simulating various daily activities. The main findings can be summarized as follows:

- Fluorescent optical method represents a powerful tool for real time in situ observation of the lubricant film formation within the conformal hard-on-soft contact of hip joint replacements.
- The introduced methodology can be suitably implemented within preclinical validation of the new replacements. It enables to understand the lubrication ability which affects overall tribological performance, thus affecting the service-life of implant. Moreover, the initial information about lubrication ability can be obtained in a short time.
- Usage of various model fluids with various fluorescently stained constituents provided a clear information about the lubrication mechanisms. Moreover, since the methodology enables to separate individual constituents of SF, its role can be clearly determined.
- The results confirmed some previous findings related to hard-on-hard bearing pairs that simple HA is not able to form sufficient lubricating film. Moreover, in some cases, simple HA led to decrease of film thickness. Focusing on PHs, it can be concluded that it has a positive effect on albumin and HA film. However, no impact on γ -globulin layer was observed. Both the mentioned constituents (HA together with PHs) have a supportive function enhancing the interaction of molecules, thus contributing to better lubrication performance.
- Regarding the development of the lubricant film, the results showed that γ -globulin together with HA form relatively thin but very stable and uniform boundary layer. Subsequent development of the film thickness is attributed exclusively to increasing/decreasing layer of albumin. This behaviour is supported by the film formation of complexly stained lubricant which exhibits almost the same behaviour in a qualitative manner.
- By contrast to some previous investigations of lubrication mechanisms within hip replacements, hard-on-soft pairs exhibit very satisfactory level of repeatability.

Acknowledgement

This research was carried out under the project LTAUSA17150 with financial support from the Ministry of Education, Youth and Sports of the Czech Republic. The authors express their thanks to T. Tkadlec for his help with the experiments.

References

Albahrani, S.M.B., Philippon, D., Vergne, P., Bluet, J.M., 2015. A review of in situ methodologies for studying elastohydrodynamic lubrication. *Proc. Inst. Mech. Eng. Part J: J. Eng. Tribol.* 230, 86–110.

Azushima, A., 2006. In situ 3D measurement of lubrication behavior at interface between tool and workpiece by direct fluorescence observation technique. *Wear* 260, 243–248.

Brockett, C.L., Harper, P., Williams, S., Isaac, G.H., Dwyer-Joyce, R.S., Jin, Z., Fisher, J., 2008. The influence of clearance on friction, lubrication and squeaking in large diameter metal-on-metal hip replacements. *J. Mater. Sci.: Mater. Med.* 19, 1575–1579.

Choudhury, D., Ay Ching, H., Mamat, A.B., Cizek, J., Abu Osman, N.A., Vrbka, M., Hartl, M., Krupka, I., 2015a. Fabrication and characterization of DLC coated microdimples on hip prosthesis heads. *J. Biomed. Mater. Res. Part B: Appl. Biomater.* 103, 1002–1012.

Choudhury, D., Urban, F., Vrbka, M., Hartl, M., Krupka, I., 2015b. A novel tribological

study on DLC-coated micro-dimpled orthopedics implant interface. *J. Mech. Behav. Biomed. Mater.* 45, 121–131.

Choudhury, D., Rebenda, D., Sasaki, S., Hekrlé, P., Vrbka, M., Zou, M., 2018. Enhanced lubricant film formation through micro-dimpled hard-on-hard artificial hip joint: an in-situ observation of dimple shape effects. *J. Mech. Behav. Biomed. Mater.* 81, 120–129.

Crockett, R., Roba, M., Naka, M., Gasser, B., Delfosse, D., Frauchiger, V., Spencer, N.D., 2009. Friction, lubrication, and polymer transfer between UHMWPE and CoCrMo hip-implant materials: a fluorescence microscopy study. *J. Biomed. Mater. Res. Part A* 89A, 1011–1018.

Dev, S.B., Keller, J.T., Rha, C.K., 1988. Secondary structure of 11 S globulin in aqueous solution investigated by FT-IR derivative spectroscopy. *Biochim. Biophys. Acta (BBA) – Protein Struct. Mol. Enzymol.* 957, 272–280.

Dowson, D., Hardaker, C., Flett, M., Isaac, G.H., 2004. A hip joint simulator study of the performance of metal-on-metal joints. *J. Arthroplast.* 19, 124–130.

Enab, T.A., Bondok, N.E., 2014. Effect of femoral head size on contact pressure and wear in total hip arthroplasty. *Int. J. Innov. Res. Sci. Eng. Technol.* 3, 14214–14223.

Ford, R.A.J., Foord, C.A., 1978. Laser-based fluorescence techniques for measuring thin liquid films. *Wear* 51, 289–297.

Fowell, M.T., Myant, C., Spikes, H.A., Kadiric, A., 2014. A study of lubricant film thickness in compliant contacts of elastomeric seal materials using a laser induced fluorescence technique. *Tribology Int.* 80, 76–89.

Galandáková, A., Ulrichová, J., Langová, K., Hanáková, A., Vrbka, M., Hartl, M., Gallo, J., 2016. Characteristics of synovial fluid required for optimization of lubrication fluid for biotribological experiments. *J. Biomed. Mater. Res. Part B: Appl. Biomater.* 105, 1422–1431.

Goldsmith, A.A.J., Dowson, D., Isaac, G.H., Lancaster, J.G., 2006. A comparative joint simulator study of the wear of metal-on-metal and alternative material combinations in hip replacements. *Proc. Inst. Mech. Eng. Part H: J. Eng. Med.* 214, 39–47.

Hua, X., Li, J., Wang, L., Jin, Z., Wilcox, R., Fisher, J., 2014. Contact mechanics of modular metal-on-polyethylene total hip replacement under adverse edge loading conditions. *J. Biomech.* 47, 3303–3309.

Hartl, M., Krupka, I., Poliscuk, R., Liska, M., Molimard, J., Querry, M., Vergne, P., 2001. Thin film colorimetric interferometry. *Tribol. Trans.* 44, 270–276.

Haugland, R.P., Spence, M.T., Johnson, I.D., 1996. *Handbook of Fluorescent Probes and Research Chemicals*, 6th ed. Molecular Probes, Eugene, OR, USA (4849 Pitchford Ave., Eugene 97402).

Heisel, C., Silva, M., Schmalzried, T.P., 2003. Bearing surface options for total hip replacement in young patients. *J. Bone Jt. Surg.* 85, 1366–1379.

Heuberger, M.P., Widmer, M.R., Zobeley, E., Glockshuber, R., Spencer, N.D., 2005. Protein-mediated boundary lubrication in arthroplasty. *Biomaterials* 26, 1165–1173.

Hidrovó, C.H., Hart, D.P., 2001. Emission reabsorption laser induced fluorescence (ERLIF) film thickness measurement. *Meas. Sci. Technol.* 12, 467–477.

Howard, M.J., Smales, C.M., 2005. NMR analysis of synthetic human serum albumin α -helix 28 identifies structural distortion upon amadori modification. *J. Biol. Chem.* 280, 22582–22589.

Huch, K., 2005. Sports activities 5 years after total knee or hip arthroplasty: the Ulm Osteoarthritis Study. *Ann. Rheum. Dis.* 64, 1715–1720.

Holzwarth, U., Cotogno, G., 2012. *Total Hip Arthroplasty: State of the Art, Challenges and Prospects*. 2012 European Commission. Publications Office of the European Union, Luxembourg.

Jie, N., Zhang, Q., Yang, J., Huang, X., 1998. Determination of chromium in waste-water and cast iron samples by fluorescence quenching of rhodamine 6G. *Talanta* 46, 215–219.

Lakowicz, J.R., 2006. *Principles of Fluorescence Spectroscopy*, 3rd ed. Springer, New York.

Mavradi, A., Cann, P.M., 2009. Friction and lubricant film thickness measurements on simulated synovial fluids. *Proc. Inst. Mech. Eng. Part J: J. Eng. Tribology* 223, 325–335.

Mavradi, A., Cann, P.M., 2011. Lubricating film thickness measurements with bovine serum. *Tribol. Int.* 44, 550–556.

Mazzucco, D., Spector, M., 2004. The John Charnley Award paper: the role of joint fluid in the tribology of total joint arthroplasty. *Clin. Orthop. Relat. Res.* 429, 17–32.

McCalden, R.W., Charron, K.D., Davidson, R.D., Teeter, M.G., Holdsworth, D.W., 2011. Damage of an Oxinium femoral head and polyethylene liner following 'routine' total hip replacement. *J. Bone Jt. Surg. Br. Vol. 93-B* 409–413.

Myant, C., Reddyhoff, T., Spikes, H.A., 2010. Laser-induced fluorescence for film thickness mapping in pure sliding lubricated, compliant, contacts. *Tribol. Int.* 43, 1960–1969.

Myant, C., Underwood, R., Fan, J., Cann, P.M., 2012. Lubrication of metal-on-metal hip joints: the effect of protein content and load on film formation and wear. *J. Mech. Behav. Biomed. Mater.* 6, 30–40.

Myant, C., Cann, P., 2014. On the matter of synovial fluid lubrication: implications for metal-on-metal hip tribology. *J. Mech. Behav. Biomed. Mater.* 34, 338–348.

Nečas, D., Vrbka, M., Křupka, I., Hartl, M., Galandáková, A., 2016a. Lubrication within hip replacements – implication for ceramic-on-hard bearing couples. *J. Mech. Behav. Biomed. Mater.* 61, 371–383.

Nečas, D., Vrbka, M., Urban, F., Křupka, I., Hartl, M., 2016b. The effect of lubricant constituents on lubrication mechanisms in hip joint replacements. *J. Mech. Behav. Biomed. Mater.* 55, 295–307.

Nečas, D., Sawae, Y., Fujisawa, T., Nakashima, K., Morita, T., Yamaguchi, T., Vrbka, M., Křupka, I., Hartl, M., 2017a. The influence of proteins and speed on friction and adsorption of metal/UHMWPE contact pair. *Biotribology* 11, 51–59.

Nečas, D., Vrbka, M., Urban, F., Gallo, J., Křupka, I., Hartl, M., 2017b. In situ observation of lubricant film formation in the considering real conformity: the effect of diameter, clearance and material. *J. Mech. Behav. Biomed. Mater.* 69, 66–74.

- Nečas, D., Vrbka, M., Gallo, J., Křupka, I., Hartl, M., 2018a. On the observation of lubrication mechanisms within hip joint replacements. Part II: Hard-on-hard bearing pairs. *J. Mech. Behav. Biomed. Mater.* (XX, X-X).
- Nečas, D., Jaroš, T., Dockal, K., Šperka, P., Vrbka, M., Krupka, I., Hartl, M., 2018b. The effect of kinematic conditions on film thickness in compliant lubricated contact. *J. Tribol.* **140**, 051501. <https://doi.org/10.1115/1.4039529>.
- Nečas, D., Vrbka, M., Rebenda, D., Gallo, J., Galandáková, A., Wolfová, L., Křupka, I., Hartl, M., 2018c. In situ observation of lubricant film formation in the considering real conformity: the effect of model synovial fluid composition. *Tribol. Int.* **117**, 206–216.
- Ranuša, M., Gallo, J., Vrbka, M., Hobza, M., Paloušek, D., Křupka, I., Hartl, M., 2017. Wear analysis of extracted polyethylene acetabular cups using a 3D optical scanner. *Tribol. Trans.* **60**, 437–447.
- Roaas, A., Andersson, G.B.J., 2009. Normal range of motion of the hip, knee and ankle joints in male subjects, 30–40 years of age. *Acta Orthop. Scand.* **53**, 205–208.
- Sawae, Y., Murakami, T., Chen, J., 1998. Effect of synovia constituents on friction and wear of ultra-high molecular weight polyethylene sliding against prosthetic joint materials. *Wear* **216**, 213–219.
- Sawae, Y., Yamamoto, A., Murakami, T., 2008. Influence of protein and lipid concentration of the test lubricant on the wear of ultra high molecular weight polyethylene. *Tribol. Int.* **41**, 648–656.
- Serro, A.P., Gispert, M.P., Martins, M.C.L., Brogueira, P., Colaço, R., Saramago, B., 2006. Adsorption of albumin on prosthetic materials: implication for tribological behavior. *J. Biomed. Mater. Res. Part A* **78A**, 581–589.
- Smith, S.L., Dowson, D., Goldsmith, A.A.J., 2001. The effect of femoral head diameter upon lubrication and wear of metal-on-metal total hip replacements. *Proc. Inst. Mech. Eng. Part H: J. Eng. Med.* **215**, 161–170.
- Spikes, H.A., 1999. Thin films in elastohydrodynamic lubrication: the contribution of experiment. *Proc. Inst. Mech. Eng. Part J: J. Eng. Tribol.* **213**, 335–352.
- Stanton, T.E., 1923. Boundary lubrication in engineering practice. *Engineer* **135**, 678–680.
- Sugimura, J., Hashimoto, M., Yamamoto, Y., 2000. Study of elastohydrodynamic contacts with fluorescence microscope, In: *Thinning Films And Tribological Interfaces, Proceedings of the 26Th Leeds-Lyon Symposium On Tribology, Tribology Series, Elsevier*, pp. 609–617.
- Swann, D.A., Silver, F.H., Slayter, H.S., Stafford, W., Shore, E., 1985. The molecular structure and lubricating activity of lubricin isolated from bovine and human synovial fluids. *Biochem. J.* **225**, 195–201.
- Trommer, R.M., Maru, M.M., 2017. Importance of preclinical evaluation of wear in hip implant designs using simulator machines. *Rev. Bras. Ortop. (Engl. Ed.)* **52**, 251–259.
- Unsworth, A., 1995. Recent developments in the tribology of artificial joints. *Tribol. Int.* **28**, 485–495.
- Vrbka, M., Křupka, I., Hartl, M., Návrát, T., Gallo, J., Galandáková, A., 2014. In situ measurements of thin films in bovine serum lubricated contacts using optical interferometry. *Proc. Inst. Mech. Eng. Part H: J. Eng. Med.* **228**, 149–158.
- Vrbka, M., Nečas, D., Bartošik, J., Hartl, M., Křupka, I., Galandáková, A., Gallo, J., 2015a. Determination of a friction coefficient for THA bearing couples. *Acta Chir. Orthop. Traumatol. Cechoslov.* **82**, 341–347.
- Vrbka, M., Nečas, D., Hartl, M., Křupka, I., Urban, F., Gallo, J., 2015b. Visualization of lubricating films between artificial head and cup with respect to real geometry. *Biotribology* **1–2**, 61–65.
- Wang, A., Essner, A., Polineni, V.K., Stark, C., Dumbleton, J.H., 1998. Lubrication and wear of ultra-high molecular weight polyethylene in total joint replacements. *Tribol. Int.* **31**, 17–33.
- Wang, A., Essner, A., Schmidig, G., 2004. The effects of lubricant composition on in vitro wear testing of polymeric acetabular components. *J. Biomed. Mater. Res.* **68B**, 45–52.
- Widmer, M.R., Heuberger, M., Vörös, J., Spencer, N.D., 2001. Influence of polymer surface chemistry on frictional properties under protein-lubrication conditions: implications for hip-implant design. *Tribol. Lett.* **10**, 111–116.



Contents lists available at ScienceDirect

Journal of the Mechanical Behavior of Biomedical Materials

journal homepage: www.elsevier.com/locate/jmbbm

On the observation of lubrication mechanisms within hip joint replacements. Part II: Hard-on-hard bearing pairs

D. Nečas^{a,*}, M. Vrbka^a, J. Gallo^b, I. Křupka^a, M. Hartl^a^a Faculty of Mechanical Engineering, Brno University of Technology, Czech Republic^b Department of Orthopaedics, Faculty of Medicine and Dentistry, Palacky University Olomouc, University Hospital Olomouc, Czech Republic

ARTICLE INFO

Keywords:

Hip joint replacements
Hard-on-hard pairs
Lubrication
Optical interferometry
Synovial fluid

ABSTRACT

The present paper represents Part II of the extensive study focused on the lubrication of hip joint replacements. The main goal is to assess the fundamentals of lubrication considering both hard-on-soft (Part I) and hard-on-hard (Part II) bearing pairs. In addition, the effect of individual constituents contained in the model fluid is clarified. For this purpose, multiple model fluids of various composition were employed. In this part of the study, metal-on-glass contact representing hard bearing pairs was observed *in situ* using pendulum hip joint simulator in combination with thin film colorimetric interferometry method. The designed test consists of initial static loading/unloading phase for the determination of adsorption of molecules on rubbing surfaces. This period is followed by swinging of the pendulum and latest static part under constant load. Three groups of measurements were carried out while fourteen different lubricants were tested. Initially, the experiments were performed with albumin-based model fluid. In that case a substantial positive effect of hyaluronic acid was identified. In contrast, the fluids with γ -globulin as a base constituent showed improved lubrication conditions when phospholipids were added to the solution. Finally, considering the complex fluid, a combined effect of hyaluronic acid and phospholipids caused a better endurance of the lubricant film. The latest part of the paper aims on the comparison of film formation considering hard and soft pairs, highlighting some clear differences. In general, hard pairs exhibit clear decreasing tendency of the film during swinging motion while opposite behaviour was observed for soft pairs.

1. Introduction

Hard-on-soft bearing pairs which are investigated in the part I (Nečas et al., 2018a) of the present study represent a most common combination for hip replacements nowadays (Dowson, 2001). However, in some specific cases, hard-on-hard pairs can take place as well. In particular, by early 2000, a potential usage of metal-on-metal implants for young more active patients was pronounced. Although wear rate of these implants was substantially lower compared to conventional metal/ceramic-on-polyethylene, the metallic debris and ions led to adverse reaction of the body in some cases (Hutchings, 2016); therefore, metal-on-metal pairs have been subjected to many debates especially in medical community (Howard, 2016). As an alternative combination, ceramic-on-ceramic has been used. Nevertheless, despite excellent wear resistivity, the squeaking effect has been reported, occurring occasionally in 25% cases (Jin et al., 2016). Despite the aforementioned drawbacks of hard-on-hard pairs, these still represent around 20% of hip implants (NJR Editorial Board, 2017). As the

prevalent cause of implant failure is aseptic loosening, the understanding of tribological processes persists as one of the challenges for implant designers.

In contrast to hard-on-soft implants, several findings were already presented regarding lubrication mechanisms for hard-on-hard material combination. This knowledge was reached employing glass counterface enabling *in situ* observation of the contact zone. Initially, the authors focused on the fundamentals of synovial fluid lubrication using simplified ball-on-disc configuration introduced originally by Gohar and Cameron (1963). The first paper given by Mavraki and Cann (2009) aimed on the evaluation of friction coefficient of the contact lubricated by various protein solutions and bovine serum (BS) as a potential model of synovial fluid (SF). The additional experiments focused on the film thickness measurements were conducted under pure rolling; revealing that the lubricant film continuously increases with increasing speed. At the end of the experiment, the authors could detect the residual layer, highlighting the importance of protein adsorption onto rubbing surfaces which was later studied in a detail by Parkes et al. (2014).

* Corresponding author.

E-mail address: David.Necas@vut.cz (D. Nečas).<https://doi.org/10.1016/j.jmbbm.2018.09.026>

Received 13 July 2018; Received in revised form 14 September 2018; Accepted 17 September 2018

Available online 19 September 2018

1751-6161/ © 2018 Elsevier Ltd. All rights reserved.

Consequent study provided an extended results focused on the effect of kinematic and loading conditions on film thickness development (Mavraki and Cann, 2011). The speed-dependent tests confirmed previous observations, since the film thickness increased with speed under pure rolling. However, under pure sliding with stationary glass disc, the film was substantially reduced for around seventy percent. The authors later compared the influence of high and low contact pressure considering ball-on-disc and lens-on-disc configuration, finding that lower contact pressure enhances the lubrication performance, especially at lower speeds. A considerable scatter of results was also reported which was attributed to inherent nature of the applied BS. It was pointed out that SF as well as its models exhibit non-Newtonian shear thinning behaviour (Myant and Cann, 2013).

The detailed investigation of the effect of albumin and γ -globulin contained in the model SF was introduced by Fan et al. (2011), who employed real femoral CoCrMo component for the first time (previous studies employed stainless steel balls). The results showed that protein-containing solutions form thicker film compared to BS. Thickness of the lubricant layer was enhanced by hydrodynamic effect which was more obvious at lower speeds. Based on the observations, the authors concluded that the proteins form high-viscosity agglomerations at the contact inlet, periodically passing through the contact, thus increasing the lubricant layer. This gel-like phase of aggregated proteins was later defined as an inlet phase by Myant and Cann (2013). In the given reference, the authors found a clear correlation between the length of the phase in longitudinal direction and the film thickness. In addition, the lubrication mechanism was explained in a detail. It was confirmed that the adsorbed thin boundary layer is augmented by hydrodynamic effect.

Myant et al. (2012) employed various simple solutions of albumin and γ -globulin and confronted the results with BS conducting static and dynamic experiments. Considering the static test under zero speed which aimed on the adsorption ability, it was found that γ -globulin forms the thickest layer. In contrast, albumin adsorption was limited independently of concentration. BS adsorbed layer was somewhere between albumin and γ -globulin. The subsequent time test at relatively low speed led to qualitatively similar results in terms of protein film behaviour. The study also confirmed that the lubrication performance is limited when higher load is applied, as published elsewhere (Mavraki and Cann, 2011). Finally, speed-dependent test was conducted while significant variance of results occurred. Nevertheless, the authors pointed out that the effect of proteins on lubrication performance is obvious. The role of albumin and γ -globulin in a complex solution was presented in one of our previous studies. Ball-on-disc measurements were realized with the use of metal and ceramic femoral components while the results showed that albumin plays a dominant role in film formation process under most conditions (Nečas et al., 2016a; 2016b). The role of individual constituents considering complex fluid could be revealed developing quite unique approach. Previously, the researchers employed optical interferometry for film thickness measurements (Hartl et al., 2001). The method provides the information about the gap between the opposing surfaces (Fowell et al., 2014); however, the behaviour of individual fluid constituents cannot be determined. This was issued establishing the method based on mercury lamp induced fluorescence (Lakowicz, 2006; Nečas et al., 2018b). As the results differed significantly compared to that of simple protein solutions, it was highlighted that complex fluids should be considered when examining lubrication processes within hip replacements.

The effect of implant material was originally introduced by Vrbka et al. (2013) who employed the same ball-on-disc based experimental approach; however, the measurements were performed with both metal and alumina ceramic femoral components. The authors investigated the effect of various slide-to-roll ratio as well. The contact was lubricated by BS while the results showed that metal formed thicker film independently of kinematic conditions. Under pure rolling, the film exhibited increasing tendency. Considering rolling/sliding conditions, the

film formation was strongly affected by the speed of the individual components. Thus, it was shown that the film thickness development is substantially influenced by the kinematic conditions. This was later supported by Myant and Cann (2014b) who measured film thickness under various types of motions. Regarding the hip joints, it undergoes complex multidirectional motion with transient loading during various motion activities. Nevertheless, the above discussed ball-on-disc studies considered simple unidirectional motion. Myant and Cann (2014b) found that changing the conditions from unidirectional to reversal caused a substantial decrease of the lubricating film.

The above references led to many findings highlighting that SF lubrication exhibits several specific issues. Regarding the nature of the applied test fluids, together with the apparent effect of proteins, Myant and Cann (2014a) defined protein aggregation lubrication (PAL) regime providing some general comparison with conventional elastohydrodynamic (EHL) and boundary lubrication theories. In particular, while reduction of contact pressure has always a positive effect on lubrication, the effect of increasing sliding speed seemed to be rather negative in the case of PAL. Additionally, surface chemistry as well as fluid chemistry are more important compared to EHL. In contrast, bulk viscosity of the lubricant seems to be less important.

All the above references considered non-conformal ball-on-disc (lens-on-disc) experimental configuration investigating the fundamentals of SF lubrication mechanisms. However, it should be noted that such a configuration represents substantial simplification, since artificial joint is of ball-on-socket arrangement while much larger contact area leads to substantially lower contact pressure. Following the implications about the effect of contact pressure on protein film (Mavraki and Cann, 2011; Myant et al., 2012), Vrbka et al. (2014) substituted the disc by concave glass lens to approach better conformity of rubbing surfaces. As the results of film formation were completely different compared to ball-on-disc, the issue of conformity was doubtlessly confirmed, motivating us for establishing *in situ* based observation with respect to real geometry of rubbing surfaces (Vrbka et al., 2015b). The developed methodology was based on the use of simple pendulum simulator while the contact is observed in an inverted arrangement. The observation of the contact is enabled using transparent acetabular cup made from optical glass fabricated precisely according to the dimensions of the real cups. Two above mentioned limitations were issued by this approach; real conformity is considered (1) and swinging reversing motion mimicking flexion-extension may be applied (2).

The methodology was recently employed when performing a comprehensive analysis of the effect of implant material, geometry, and model SF composition on film formation (Nečas et al., 2017; 2018c). It was found that metal forms thicker lubricating film, in general which confirmed previous ball-on-disc results (Vrbka et al., 2014). Regarding the implant geometry, the nominal diameter was found to be much less important than the diametric clearance which should be as small as possible to ensure improved lubrication conditions (Nečas et al., 2017). However, it has to be emphasized that too small clearance can lead to edge loading effect which should be avoided (Liu et al., 2018; Underwood et al., 2011). The further study focused on the effect of model SF showed that hyaluronic acid (HA) and phospholipids (PHs) represent a dominant constituents responsible for film formation process. It was pointed out that simple HA has a poor lubricity; therefore, the interaction of molecules of SF is essential (Nečas et al., 2018c). This confirmed the previous observation that simple solutions are not able to mimic complex SF.

Based on the above references, it might be concluded that the research of hard-on-hard bearing pairs has been exhibiting an outstanding progress over the last decade. In particular, a methodology based on *in situ* observation with the respect to real conformity of rubbing surfaces was introduced which led to several unique findings clarifying the fundamentals of hip implants lubrication. Moreover, it was pointed out that complex fluids should be considered since the mutual interaction of proteins, HA, and PHs has a substantial impact on the lubrication

performance. The present paper aims on the deeper understanding of lubricant film formation in hard-on-hard bearing pairs while the main attention is paid to the effect of SF composition. Moreover, the experiments were performed with the same fluids and under the same kinematic conditions as in the Part I of the present study (Nečas et al., 2018a); therefore, the differences in film formation compared to hard-on-soft bearing pairs are highlighted. According to author’s best knowledge, such a comprehensive comparison has not been presented so far.

2. Materials and methods

The experiments were carried out using pendulum hip joint simulator described in a detail in Part I (Nečas et al., 2018a). The only difference is the used optical module, since optical interferometry is used for film thickness evaluation. The optical system consists of the light source, episcopic microscope, CMOS digital camera (Phantom v710), and PC. The system is mounted in an inverted position. Based on the findings arising from the first part of the study focused on hard-on-soft pairs, the measurements were realized considering combined static/dynamic test. The test consists of initial 9 loading/unloading cycles (full load for 10 s followed by 20 s relaxation) which enables to determine the adsorption of the molecules on rubbing surfaces. Subsequently, the pendulum is deflected to a maximum and is released while it oscillates freely till the motion is damped due to the friction

between the surfaces. Finally, the contact is exposed to static load for additional 3 min to observe the strength of the residual adsorbed film (in Part I, 10 min’ static phase was considered due to investigation of fluorescence quenching phenomenon; for adsorption observation, three minutes provides sufficient information). The applied methodology is shown in Fig. 1.

Film thickness was studied as a function of time in an equilibrium position of the pendulum (deflection of the pendulum arm is equal to zero). Thin film colorimetric interferometry method was applied. It provides very precise information about the thickness of the lubricant layer with the resolution down to 1 nm (Hartl et al., 2001). The maximum measurable film thickness is around 900 nm; nevertheless, our previous observations showed that the measurement range is sufficient for artificial hip joints in the most cases. The evaluation procedure is based on the consequence of the following phases:

- **Calibration:** A calibration curve is obtained based on the chromatic and monochromatic image of a lightly loaded static contact. The obtained chromatic interferogram is matched with the measured profile of the contact (ball surface) using CIELAB colour algorithm, giving the dependence between particular colour and the corresponding film thickness.
- **Measurement:** The interferograms of fully loaded contact under given conditions are obtained while the settings of the light and microscope filters has to be maintained.

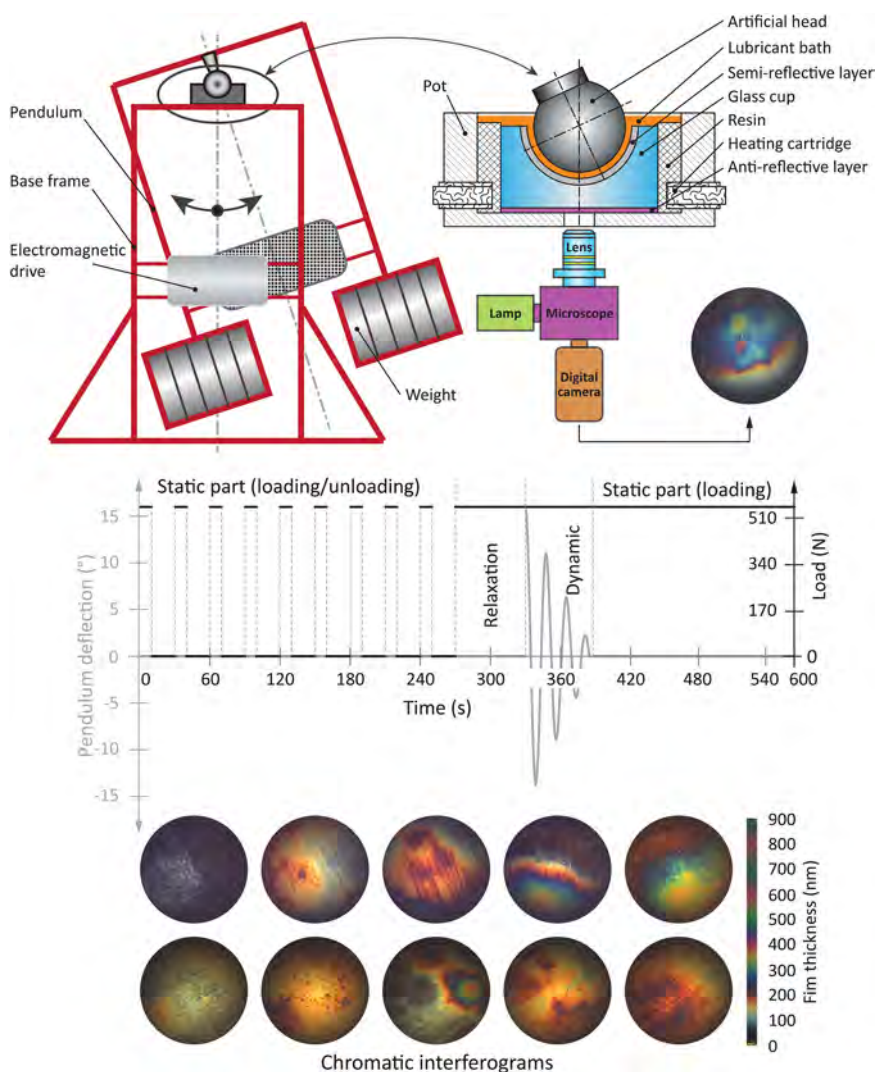


Fig. 1. A schematic illustration of the measurement methodology.

Table 1
Summary of the test lubricants.

Lubricant no.	Constituent(s) (concentration)	Total concentration	Base fluid (total amount)	Corresponding results
1	Albumin (24.9 mg/ml)	24.9 mg/ml	PBS (4 ml)	Fig. 2, Fig. 5
2	Albumin (24.9 mg/ml) HA (1.49 mg/ml)	26.39 mg/ml	PBS (4 ml)	Fig. 2
3	Albumin (24.9 mg/ml) PHs (0.34 mg/ml)	25.24 mg/ml	PBS (4 ml)	Fig. 2
4	Albumin (24.9 mg/ml) HA (1.49 mg/ml) PHs (0.34 mg/ml)	26.73 mg/ml	PBS (4 ml)	Fig. 2
5	γ -globulin (6.1 mg/ml)	6.1 mg/ml	PBS (4 ml)	Fig. 3, Fig. 5
6	γ -globulin (6.1 mg/ml) HA (1.49 mg/ml)	7.59 mg/ml	PBS (4 ml)	Fig. 3
7	γ -globulin (6.1 mg/ml) PHs (0.34 mg/ml)	6.44 mg/ml	PBS (4 ml)	Fig. 3
8	γ -globulin (6.1 mg/ml) HA (1.49 mg/ml) PHs (0.34 mg/ml)	7.93 mg/ml	PBS (4 ml)	Fig. 3
9	Albumin (24.9 mg/ml) γ -globulin (6.1 mg/ml)	31 mg/ml	PBS (4 ml)	Fig. 4
10	Albumin (24.9 mg/ml) γ -globulin (6.1 mg/ml) HA (1.49 mg/ml)	32.49 mg/ml	PBS (4 ml)	Fig. 4
11	Albumin (24.9 mg/ml) γ -globulin (6.1 mg/ml) PHs (0.34 mg/ml)	31.34 mg/ml	PBS (4 ml)	Fig. 4
12	Albumin (24.9 mg/ml) γ -globulin (6.1 mg/ml) HA (1.49 mg/ml) PHs (0.34 mg/ml)	32.83 mg/ml (repeatability test – SF1)	PBS (4 ml)	Fig. 4, Fig. 5, Fig. 6
13	Albumin (26.3 mg/ml) γ -globulin (8.2 mg/ml) HA (0.87 mg/ml) PHs (0.35 mg/ml)	35.72 mg/ml (repeatability test – SF2)	PBS (4 ml)	Fig. 6
14	Albumin (20 mg/ml) γ -globulin (3.6 mg/ml) HA (2.5 mg/ml) PHs (0.15 mg/ml)	26.25 mg/ml (repeatability test – SF3)	PBS (4 ml)	Fig. 6

– **Film thickness evaluation:** The obtained images of the contact are linked with the calibration curve; therefore, the film thickness in any location of the contact can be assessed.

The contact pair consists of original metal CoCrMo alloy femoral head and the glass acetabular cup. The diametric clearance between the rubbing surfaces was 80 μ m while the diameters of the ball and the cup were 27.97 mm and 28.05 mm, respectively. The clearance was set as an average clearance value of several original hard-on-hard pairs while the dimensions were determined using optical scanning based on 3D active fringe projection (Ranuša et al., 2017). The surface roughness of the ball is in the range of units of nm while the cup surface is optically smooth. The specific values are stated in Table 2. To enhance the contrast of interference fringes, the contact surface of the glass cup is covered by thin chromium layer. This leads, in addition, to better simulation of the contact mechanics considering metal-on-metal contact. The elastic moduli and Poisson's ratios of the test samples are: $E_{ball} = 230$ GPa, $\nu_{ball} = 0.28$; $E_{cup} = 85$ GPa, $\nu_{cup} = 0.209$. The authors admit that following the above material properties, metal-on-glass combination does not fully represent hard-on-hard assignment which is usually used in tribology considering metal-on-metal, ceramic-on-ceramic, or ceramic-on-metal combination. Nevertheless, the glass elastic modulus is still comparably higher than that of polymer. Therefore, hard-on-hard assignment is adopted throughout the manuscript for the clarity, indicating that hard bearing pairs are rather mimicked using this metal-on-glass material combination.

The test load was equal to 532 N leading to a contact pressure of 26.4 MPa. The corresponding contact area diameter is 6.2 mm. The

authors observed the zone equal to 1.5 mm. The experiments were performed under ambient temperature, since the effect of elevated body temperature should be negligible, as discussed elsewhere (Mavraki and Cann, 2011). A strict compliance of the measurement protocol was desired. The attention was also paid to the cleaning procedure to avoid any influence of the results coming from residual film from the previous test. The details about cleaning the samples are stated in Part I (Nečas et al., 2018a).

As emphasized above, simple solutions do not behave like complex model fluids. Nevertheless, in an effort to understand the interaction of SF constituents, the experiments were performed using various test fluids with various level of complexity. The present study is not focused on the determination of the influence of concentration of SF constituents, nor its mutual ratio. This was partially issued in the previous paper (Nečas et al., 2018c). The present study is mainly aimed on the understanding of interaction of the molecules and on the understanding the differences in film formation process considering hard-on-hard and hard-on-soft bearing pairs. For this purpose, one particular composition of model SF, based on the extensive investigation of real SF of patients (Galandáková et al., 2016), was designed. The overall composition of the fluid is as follows: albumin = 24.9 mg/ml, γ -globulin = 6.1 mg/ml, HA = 1.49 mg/ml, PHs = 0.34 mg/ml. Only for the demonstration of the measurement repeatability, another two fluids with different content of the constituents representing various stages of osteoarthritis were employed. The constituents were always dissolved in a phosphate-buffered saline (PBS) solution. The list of the applied fluids is given in Table 1.

3. Results

3.1. Albumin-based model fluids

The experiments were initially realized with model fluids based on albumin solution. The results are shown in Fig. 2. As can be seen, there is no substantial difference considering addition of HA or PHs to base solution in terms of adsorbed film thickness during the first phase of the experiment. The maximum is around 150 nm after 9 loading/unloading cycles. Nevertheless, a combination of the base solution with both HA and PHs led to quite rapid decrease of the adsorbed layer to a half level. During the swinging phase (Fig. 2b), the adsorbed film was more or less removed for all the fluids; however, albumin with HA formed the thickest film, in general. Albumin with PHs dropped after around 20 s of swinging while simple albumin and albumin combined with HA and PHs exhibited almost the same behaviour with immediate removal of the adsorbed film after the start of swinging. Under subsequent static load, the film thickness was very thin just in the range of units or tens of nm for all the tested fluids indicating very low adsorption ability.

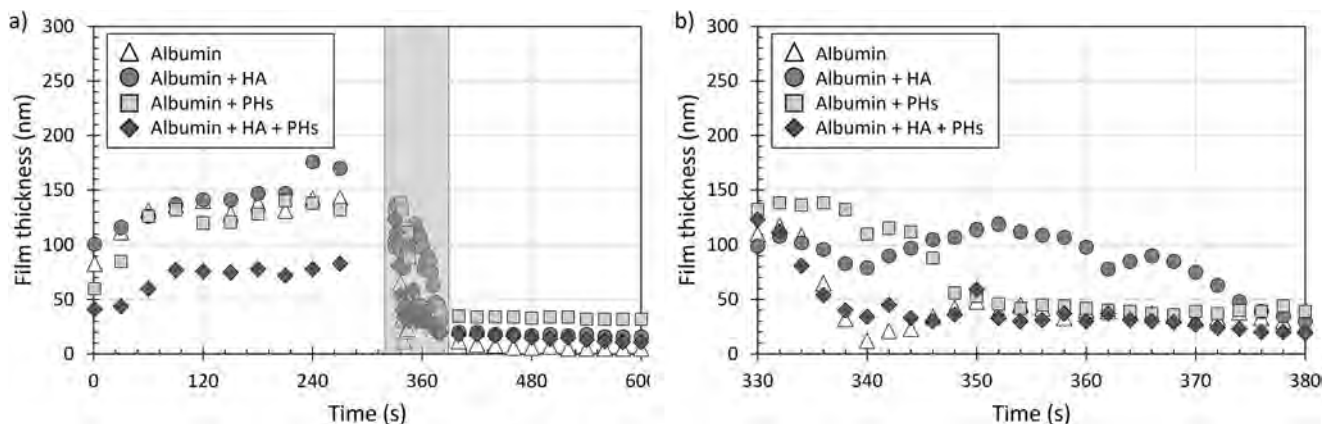


Fig. 2. a) Development of film thickness of various albumin-based model fluids as a function of time over the combined test; b) Detail of the dynamic part of the experiment – highlighted part in graph (a).

3.2. γ -globulin-based model fluids

Second series of the experiments was conducted with the fluids the base of which was γ -globulin. The initial static part of the test confirmed some previous observations indicating better adsorption ability of γ -globulin compared to albumin. As can be seen in Fig. 3a, even if the simple solution is used, the adsorbed film gradually increases up to

nearly 300 nm which is two times higher than for simple albumin. Addition of HA and PHs led to some reduction of the film while the maximum varied between 150 nm and 210 nm. During the swinging motion, simple γ -globulin exhibited sudden drop to around 150 nm with subsequent gradual decrease lasting for approximately 35 s of swinging (Fig. 3b). At that time, the film dropped to zero level with no further development. Similar behaviour was observed for γ -globulin doped by HA and PHs with the difference in lasting effect, as the film disappeared just within 15 s. Considering γ -globulin with HA, the film started to decrease; however, a sudden jump occurred after some time due to strong agglomeration of the molecules passing through the contact. Then, the layer continuously decreased till the end of the swinging phase. Very stable behaviour was observed for γ -globulin mixed with PHs. At that time, only a slight increase could be detected when swinging started while for the rest of the experiment, the film was very stable; reaching around 120–140 nm. Moreover, this layer was kept even under the static load, as can be seen in the right part of Fig. 3a.

3.3. Protein-based model fluids

As aforementioned, simple solutions of proteins are not able to mimic the behaviour of complex model fluids since the interaction of the molecules plays an important role. Therefore, the measurements were later conducted with the fluids based on the mixture of albumin and γ -globulin (Fig. 4). The adsorption behaviour of these fluids was

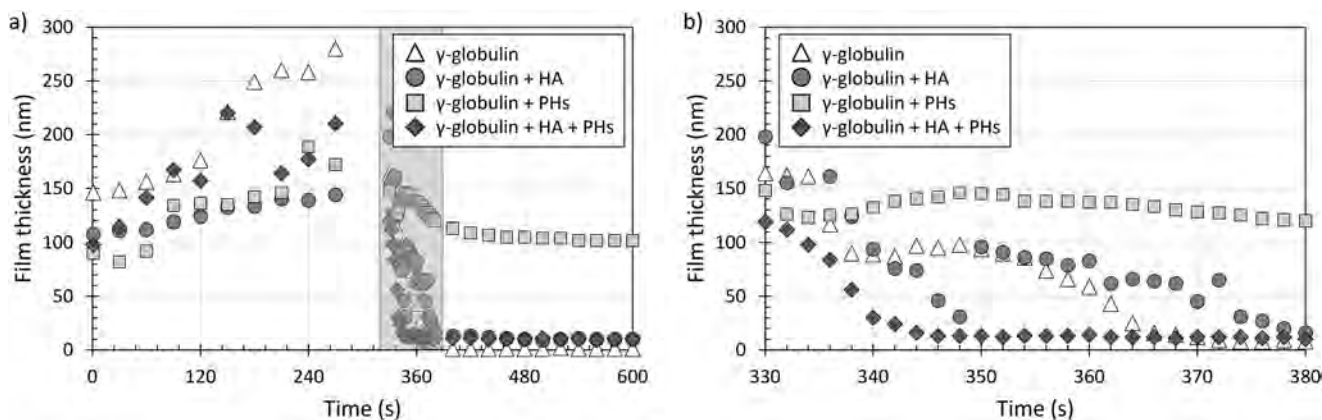


Fig. 3. a) Development of film thickness of various γ -globulin-based model fluids as a function of time over the combined test; b) Detail of the dynamic part of the experiment – highlighted part in graph (a).

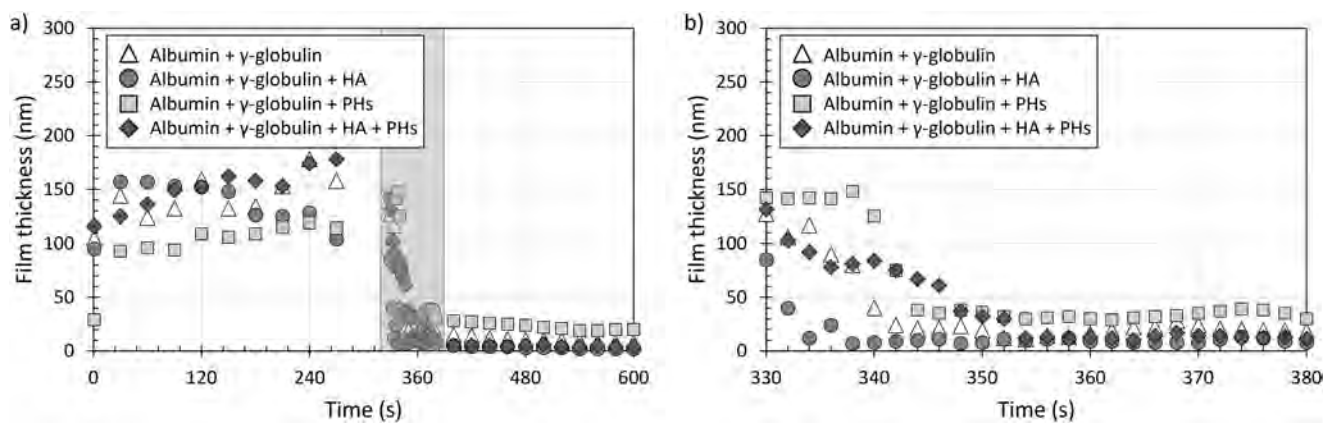


Fig. 4. a) Development of film thickness of various protein-based model fluids as a function of time over the combined test; b) Detail of the dynamic part of the experiment – highlighted part in graph (a).

quite similar; nevertheless, the film was generally thicker for protein solution and complex fluid doped by HA and PHs. When only HA or PHs were added, the adsorption ability was diminished while the film reached just around 100 nm compared to 150–170 nm for other two solutions. Focusing on the dynamic part of the experiment displayed in Fig. 4b, it can be concluded that the film thickness continuously decreases independently of the applied test lubricant. Only in the case when the proteins were doped by PHs, the layer was kept stable for some time; however, after 10 s it started to drop quite rapidly. Nevertheless, a combined positive effect of HA and PHs could be observed, leading to the fact that the film decrease is not as steep as in other cases. The residual film during the last period of the experiment was very thin, less than 30 nm for all the tested lubricants in particular.

3.4. Hard-on-hard vs. hard-on-soft pairs

Finally, the evaluated data for metal-on-glass contact were confronted with those of metal-on-PMMA presented in Part I of the present study (Nečas et al., 2018a). For the purpose of the comparison, three different lubricants were chosen; pure albumin solution, pure γ -globulin solution, and complex model fluid. It should be emphasized that the scales are just set to fit into one graph for visual comparison of the trends. The specific fluorescent intensities on minor vertical axes in graphs in Fig. 5 do not correspond to the particular film thicknesses shown on the major vertical axes. Based on the Fig. 5a, it can be seen that the adsorption behaviour differs for both the considered material combinations, especially when simple γ -globulin and complex fluid is applied. In particular, for hard-on-hard pairs, γ -globulin exhibits quite rapid increase while for hard-on-soft pairs, its layer is almost constant. In contrast, behaviour of albumin is very similar for both the investigated material combinations. Complex fluid shows similar increasing tendency, while in the case of hard-on-hard pair, the increase is more steep. Completely different results were obtained during the swinging phase of the experiment. The first fundamental point is that the pendulum swinging lasted two times longer in the case of hard-on-hard pair, see Fig. 5b. Focusing on the particular solutions, it can be seen that the results are not in agreement. While the lubricant layer always decreased in the case of hard-on-hard pair, the lubrication was enhanced when soft cup was employed. The film thickness development during the swinging part also determines the behaviour under static loading at the end of the experiment (right part of Fig. 5a). In that case, the film is negligible for all the fluids for hard pair while in the case of hard-on-soft material combination, it slightly increases (albumin) or decreases (γ -globulin, complex lubricant).

Focusing on the no-data period between 354th and 380th second for hard-on-soft pair in Fig. 5b, it should be highlighted that once the swinging motion stopped, the external light source was avoided to

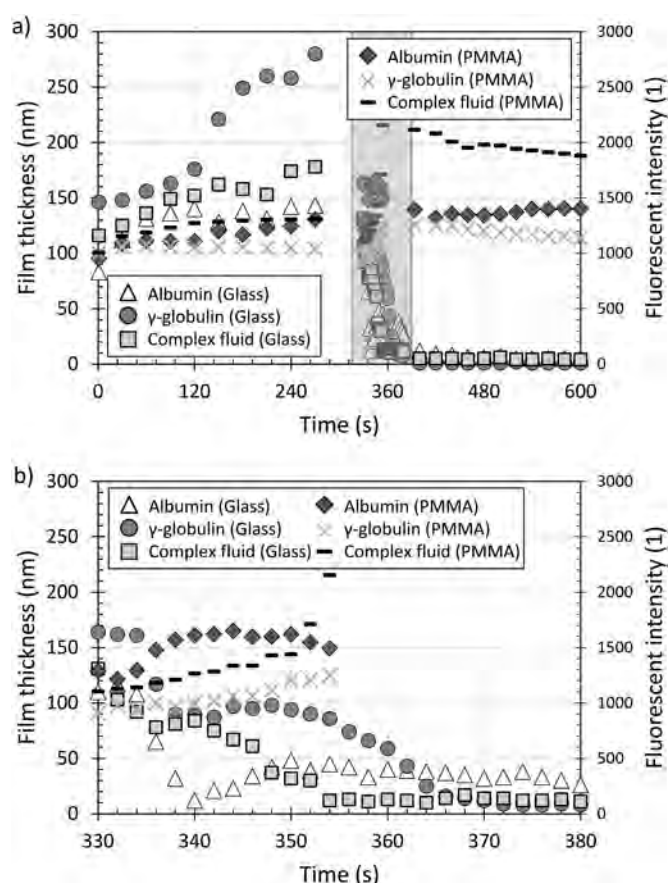


Fig. 5. a) Development of film thickness of various model fluids as a function of time over the combined test for glass and PMMA acetabular cup (Nečas et al., 2018a); b) Detail of the dynamic part of the experiment – highlighted part in graph (a).

minimize loss of fluorescence intensity, as is discussed in a detail in Part I (Nečas et al., 2018a). First consequent evaluated point is at 380th second which already represents static loading period. Therefore, the results at this time are not displayed on a minor vertical axis in Fig. 5b since this graph shows only the dynamic part of the experiment as is stated in the caption. Nevertheless, it can be clearly seen that the first evaluated data in the static loading part are almost the same as the last data during the dynamic part for hard-on-soft pair (see Fig. 5a); therefore, it can be assumed that only a negligible change occurred during non-evaluated period.

4. Discussion

Lubrication mechanisms of hard-on-hard hip replacements have been relatively widely investigated in recent years. Initially, a model approach based on the combination of ball-on-disc tribometer with optical interferometry was introduced (Mavraki and Cann, 2009). The same methodology was subsequently successfully employed revealing various effects on lubricant film formation. In particular, kinematic (Mavraki and Cann, 2011), loading conditions (Myant et al., 2012), the role of material (Vrbka et al., 2013), or the behaviour of various models of SF (Fan et al., 2011) were studied. The findings were summarized by Myant and Cann (2014a) who defined PAL regime giving a comprehensive implication for metal-on-metal hip tribology. Subsequently, a fluorescent microscopy enabling to determine the role of albumin and γ -globulin was established (Nečas et al., 2016b). Nevertheless, it was pointed out by Vrbka et al. (2014) that non-conformal contact in the case of ball-on-disc configuration can significantly affect the lubrication mechanisms. Therefore, the disc was substituted by glass lens to approach higher degree of contact conformity. As the results differed compared to ball-on-disc arrangement, we developed a hip joint simulator based on the principle of pendulum while we applied glass acetabular cup fabricated according to the dimensions of the real cups to be able to observe the contact *in situ* under real geometrical configuration (Vrbka et al., 2015b). Using the developed methodology, the influence of implant geometry, material (Nečas et al., 2017), and the effect of SF composition (Nečas et al., 2018c) was examined. The present study follows our previous findings while newly designed model SF, inspired by an extensive analysis of samples of real SF (Galandáková et al., 2016) was applied as the test lubricant. Moreover, partial models of the fluid were also prepared to better understand the interaction of the individual molecules. Previously, we investigated adsorption of SF molecules under static loading and film formation under dynamic conditions separately. Currently, the combined test was designed composing of loading/unloading static phase (simulating the transition from sitting to stance), followed by dynamic swinging representing short walking, with the final static loading phase simulating still standing. In addition, the experiments were also performed with hard-on-soft material combination mimicking the most common type of implant pairs while the results are described in a detail in Part I of the present study (Nečas et al., 2018a).

Considering hard-on-hard pairs, the first series of the experiments was conducted with the use of four model fluids the base of which was albumin protein (Fig. 2). Focusing on the albumin adsorption, there was no positive effect of HA nor PHs. Surprisingly, when both the components were added together, the adsorbed layer decreased substantially. During the swinging part of the experiment, HA led to improved lubrication. The effect of PHs was rather positive as well. Nevertheless, mixture of HA and PHs did not lead to thicker film; the behaviour was very similar to simple albumin solution. This indicates that albumin can hardly form sufficient lubricating film without the support of γ -globulin even if HA and PHs are added. Similar behaviour was observed before for hard bearing pairs (Myant et al., 2012). This is related to limited adsorption ability of albumin which was reported by Nakashima et al. (2007). Anyway, based on the results during the last static part under the constant load, it is apparent that the adsorption is enhanced by the presence of PHs which formed bit thicker layer compared to the rest of the lubricants.

The subsequent experiments were performed with the fluids based on γ -globulin, see Fig. 3. In this case, initial adsorbed layer of simple solution was the thickest. This supports the assumption about better adsorption ability of γ -globulin. Both HA and PHs caused a decrease of the adsorbed film thickness, in general. Under pendulum swinging, the lubricant containing γ -globulin and PHs formed relatively thick constant layer which was approximately double compared to simple solution and solution doped by HA. Fluid containing both HA and PHs did not show a good lubrication performance; the film decreased within the

first few swings to almost zero thickness. Focusing on the contact images, relatively large agglomerations of SF constituents could be observed for γ -globulin with HA. This effect can be clearly seen on Fig. 3b where the film suddenly increases around 350th and 375th second. As in the case of albumin-based fluids, PHs led to more stable adsorbed film during the final static loading part of the experiment. The film thickness is around 100 nm which is considerably higher than for other lubricants.

Finally, the measurements were performed with the fluid containing both the aforementioned proteins which represent the dominant part of the SF (Fig. 4). In terms of adsorption during loading/unloading phase, there is no substantial effect of lubricant; nevertheless, protein mixture doped by PHs exhibits the thinnest film. In contrast, this fluid is able to keep the film stable for some time under dynamic conditions as the only one (Fig. 4b). The other fluids exhibited decreasing tendency while the decrease of complex fluid containing HA and PHs is the most relaxed. Considering the last part of the test, the results are very similar to that for albumin-based lubricants. When comparing Fig. 2, Fig. 3 and Fig. 4, it can be seen that the mixture of the proteins behaves very similarly as simple albumin solution does. This is quite important finding which can be attributed to substantially higher concentration of albumin. Focusing on the dynamic part of the experiments, it seems that albumin suppresses the ability of γ -globulin film formation. Moreover, this behaviour seems to be independent of contact pressure since very similar results were presented by Parkes et al. (2015) who suggests that the adsorbed layer in the case of combination of albumin and γ -globulin consists mainly of albumin. It should be noted that the present paper does not consider solution of HA and PHs (without proteins) when examining the lubrication performance of hard-on-hard pairs. This comes from the limited lubricity of simple HA which was already proven in our previous observation (Nečas et al., 2018c) and very low concentration of PHs.

One of the main goals of the present experimental investigation was to describe the differences in film formation considering hard-on-hard and hard-on-soft bearing couples. Fig. 5 shows the comparison of simple albumin solution, γ -globulin solution, and complex fluid containing all the considered constituents including HA and PHs. As was emphasized above, it is necessary to take into account that the lubricant layer is expressed by quantitative film thickness (major vertical axis) in the case of hard-on-hard pairs while for hard-on-soft pairs, the film is evaluated qualitatively in terms of fluorescent intensity which represents dimensionless film thickness (minor vertical axis). Therefore, it is not possible to quantify specific film thickness in the case of hard-on-soft implants; the major and minor vertical axes are just set to fit into one graph. The difficulties disabling direct film thickness measurement in the case of hard-on-soft configuration are discussed in a detail in Part I (Nečas et al., 2018a).

As can be seen, hard pairs exhibit rather increasing tendency of adsorbed layer independently of the applied test lubricant (Fig. 5a). In contrast, the adsorbed film is relatively stable when soft couple is investigated. Completely different behaviour was observed during the dynamic swinging conditions (Fig. 5b). At that time, hard pair exhibited drop of the lubricant film for all the tested fluids. On the contrary, soft pair led to enhanced film thickness while the effect is the most apparent especially when complex fluid containing proteins, HA, and PHs is applied. However, despite the decreasing film thickness, hard pair exhibited almost two times longer swinging period than soft one. This fact may be attributed to the lubrication regime and corresponding friction coefficient. As the contact zone is quite large in the case of hard-on-soft pair and due to the nature of PMMA surface, it is assumed that the soft contact operates under mixed lubrication regime leading to elevated friction thus causing faster pendulum damping. To confirm higher friction in the case of hard-on-soft bearing pair, pendulum response was analysed using Stanton's model (Stanton, 1923) which enables to determine the coefficient of friction based on the damping characteristics of the pendulum. Nevertheless, since friction coefficient is not of a main

interest of the present study, it was evaluated only for the fluids considered in Fig. 5, i.e. for pure albumin, pure γ -globulin, and complex fluid. Both the tested pairs showed linear decay, in general. In the case of hard-on-hard pair, the resulting friction was around 0.13 which correlates to previous experimental investigation considering ceramic-on-ceramic pair (Vrbka et al., 2015a). In the case of the present paper, only a little influence by the applied fluid was observed. As expected, substantially higher friction was detected when PMMA cup was used. At that time, the friction increased up to 0.25 while the lowest value (0.21) was observed for the complex fluid. Although these values are quite high, there is not a substantial difference compared to friction of metal-on-UHMWPE pair reported elsewhere where the friction coefficient reached 0.18 (Vrbka et al., 2015a).

Another cause of the shorter pendulum swinging in the case of hard-on-soft pair might be a smaller clearance between metal head and glass cup which results in more stable swinging without sudden light slips in extreme deflection positions (transition in swinging direction). In addition, larger clearance between the ball and the cup also leads to higher friction as was shown by Brockett et al. (2008). Another point is much larger contact area in the case of soft couple. Small scratches of the acetabulum could be observed while the released wear particles increased friction between the surfaces leading to faster pendulum damping. Focusing on the static loading, it might be seen in Fig. 5a that while hard pair shows almost zero film thickness, this is kept relatively stable in the case of soft pair. As the intensities of the film are the same compared to those during swinging period, it can be concluded that the film remains relatively thick. This is associated not only to adsorption forces but also to substantially larger contact zone (reduced contact pressure) causing that the film is not squeezed out from the contact as quickly. The most important finding is that the film formation process under relative motion of the hip joint components shows a clear difference. It was pointed out by Dowson et al. (2004) that individual SF constituents cannot provide joint operation under low friction accompanied by thick lubricant film due to transition from boundary to mixed lubrication regime. The performed study confirms this statement, suggesting that the mutual interaction and influence of the SF molecules represents a dominant factor affecting lubricant film formation between the articulating surfaces; thus determining an overall tribological performance of hip replacements. Apparently, the role of particular constituents of SF might be clarified using the fluorescent technique introduced in Part I (Nečas et al., 2018a). However, the glass acetabular cup is covered by a semi-reflective chromium layer to ensure sufficient contrast of interference fringes for precise film thickness evaluation (a) and to provide better compliance in terms of contact mechanics considering metal-on-metal contact (b). Even though the chromium layer is very thin, the high content of chromium causes substantial loss of fluorescent emission totally disabling the observation of film formation in the case of some low-emitting lubricants. Following the previous experience with the investigation of hard-on-hard pairs using the interferometry method and considering the above-discussed limitations, the authors decided to compare two experimental approaches based on the two different optical methods.

To conclude, the differences in the substantial parameters, describing the investigated pairs, should be summarized. For this purpose, Table 2 containing both geometrical and material parameters of the contact couples was designed. As is shown, the contact pressure in the case of soft pairs is more than five times lower which has a positive effect on film formation under swinging motion as well as on the residual adsorbed film. In contrast, the larger clearance together with elevated wear of PMMA, accompanied by amount of visible scratches and transition to mixed lubrication regime leads to higher friction, thus shortening the swinging period length. Finally, considering the surface nature, there should be no substantial influence of film formation. The metal head was the same for both cases. Further, even though optical glass is naturally hydrophilic, the chromium layer coating causes that the surface becomes hydrophobic. The wetting angle of the flat optical

Table 2

Comparison of geometrical, material, and contact parameters of the investigated pairs.

Parameter	Hard-on-soft pair	Hard-on-hard pair
Ball diameter	27.9714 ± 0.0007 mm	27.9714 ± 0.0007 mm
Cup diameter	28.1105 ± 0.0005 mm	28.0504 ± 0.0004 mm
Diametric clearance	0.13 mm	0.080 mm
Ball elastic modulus	230 GPa	230 GPa
Ball Poisson's ratios	0.28	0.28
Cup elastic modulus	3 GPa	85 GPa
Cup Poisson's ratios	0.37	0.209
Load	532 N	532 N
Contact pressure	5.1 MPa	26.4 MPa
Contact zone diameter	14.1 mm	6.2 mm
Observed zone diameter	1.5 mm	1.5 mm
Ball surface roughness	7.81 ± 1.24 nm	7.81 ± 1.24 nm
Cup surface roughness	4.8 ± 0.7 nm	< 1 nm
Ball wetting angle	78 ± 0.5° (ball sample)	78 ± 0.5° (ball sample)
Cup wetting angle	81 ± 0.7° (flat sample)	92 ± 1.1° (flat sample)

glass surface coated by chromium layer was measured finding the value is approximately 92°. Considering the flat PMMA surface, wetting angle was found to be 81° which means that PMMA is rather hydrophilic; however, the difference in wetting angles is not so significant. It was discussed previously that both albumin and γ -globulin better adsorb on hydrophobic surfaces (Malmsten, 1998; Serro et al., 2006). Since there is some difference in surface wettability, the lubrication performance can be influenced by the used material to some extent. Nevertheless, it is expected that the film formation is driven mainly by the processes associated with contact mechanics.

As discussed in Part I, biotribological analyses focusing on lubrication are sometimes exposed to debates due to repeatability. Especially, considering simplified ball-on-disc configuration, significant variance of results was reported several times (Mavraki and Cann, 2011; Myant et al., 2012). This seems to be successfully issued using the real conformity. Especially for hard-on-soft pairs, we could obtain excellent repeatability considering two types of the tests and two various lubricant solutions (Nečas et al., 2018a). In this Part II, we present the data for three different fluids while the experiments were repeated two times for all of them. The SF1 is the same fluid as is the complex fluid used within the combined tests. The results are shown in Fig. 6. As can be seen, very good correlation of film thickness was found especially for SF1 an SF2. In the case of SF3, some small difference during the dynamic part occurred (Fig. 6b); however, the tendency is almost the same suggesting the overall validity of the measured data. It should be pointed out that the particular measured film thickness is not decisive. In real joints, several aspects have to be taken into account such as impact loading, multidirectional transient uneven motion, or reverse arrangement of the components compared to model pendulum configuration. The main goal of the experimental observations is the examination of general effects as well as the assessment of the tendencies of lubricant film development. Considering some theoretical predictions, it should be noted that the pendulum undergone only spontaneous oscillation without external driving in the case of the present paper. Therefore, the predicted film decreases with each following cycle since the speed of the ball decreases from initial 12 mm/s to zero. Considering the maximum speed, the predicted film thickness should be around 17 nm. The estimation is based on Hamrock's (1994) formula which was previously presented by Medley et al. (2005). As can be seen in Fig. 2 to Fig. 4, the film thickness at the beginning of the swinging tests was always several times higher, confirming the importance of SF constituents in film formation process. Nevertheless, it should be emphasized that the film was also enhanced by initial adsorption phase. The chromatic interferograms obtained in specific time steps for the selected experiments are shown in Fig. 6c. Times equal to 330th s and 380th s correspond to the begin and end of the swinging phase. As can

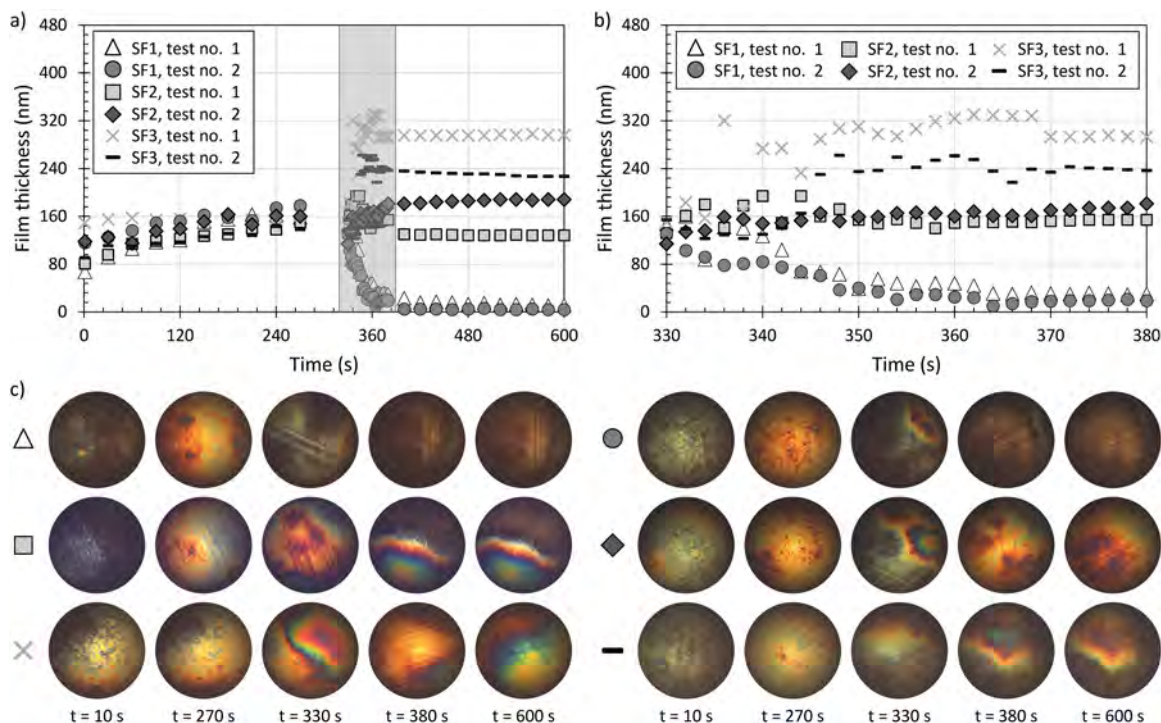


Fig. 6. Repeatability of the combined experiment for various complex fluids. b) Detail of the dynamic part of the experiment – highlighted part in graph (a). c) Chromatic interferograms taken during the experiments; inlet/outlet is on the top/bottom of each image.

be seen, strong aggregations are apparent on these images, especially for SF2 and SF3.

The measurements shown in Fig. 6 additionally supplemented our previous research focused on the effect of model SF composition (Nečas et al., 2018c). In the case of previous study, dynamic swinging tests considering external driving were conducted while the main finding was that the lubricant film thickness is substantially affected by the content of HA and PHs. It was also stated that the concentration of proteins seems to be of a less importance. This is partially confirmed by the current results especially for SF3. In that case, even there is very low protein content, the film is the thickest, attributed to the action of HA. However, focusing on the composition of SF1 and SF2 in Table 1, it can be seen that SF2 has lower content of HA while forming thicker film. In author's opinion, this is partially caused by higher content of albumin. As is shown in Fig. 2b and Fig. 3b, HA has a substantial positive effect on albumin and slightly positive on γ -globulin film. Therefore, it is expected that higher protein content can lead to enhancement of lubricant film which goes against the previous study (Nečas et al., 2018c). Nevertheless, in that case, the content of albumin was the same for the two tested fluids, while content of γ -globulin varied only a little. Therefore, up-to-date observations can be concluded as follows. Considering simple solutions of proteins, the content does not have a significant effect on lubricity. However, when the proteins are doped by HA, both the protein content as well as the content of HA plays a very important role. Assuming the composition of SF3, the content of PHs is not as important; however, without PHs, HA action is weakened. This only confirms the necessity of molecules interaction. Regarding the potential role of lubricin, which is not considered in the model fluids, its effect is more obvious in cartilage-cartilage contact, as was pointed out in literature (Swann et al., 1985). The positive effect on friction considering materials for hip implants was not confirmed (Mazzucco and Spector, 2004).

During the last few years, a rapid improvement of knowledge regarding the lubrication of hip replacements has been reported.

Considering the motivation for future research, it should be noted that despite the progress of the used materials, fabrication techniques, or design, the service-life of implants has not been extended sufficiently to avoid implant failure after some time so far. Therefore, the researchers should take into account some indications related to innovative approaches such as the new bearing materials like DLC coating (Choudhury et al., 2015a; 2015b) and potential new design of bearing surfaces. One of the ways is the use of microtextures, the positive influence of which was already proved in the area of EHL. Regarding the hip implants, the effect of microtextures was studied both numerically (Gao et al., 2010) and experimentally (Choudhury et al., 2018), indicating some very promising results.

5. Conclusion

The present study extends the knowledge in the area of lubrication mechanisms considering hard-on-hard hip joint replacements. A detailed observation of lubricant film thickness was performed while the main attention was paid to the interaction of individual constituents contained in SF. Pendulum hip joint simulator in combination with thin film colorimetric interferometry were employed while this methodology was successfully established within our previous studies. This paper represents Part II of the extensive analysis of lubrication mechanisms of artificial joints, aiming on the deeper understanding of the differences considering hard-on-soft and hard-on-hard bearing pairs. For this purpose, a combined static/dynamic test was designed and model SF was prepared following the analysis of samples of real SF. The main conclusions are summarized in the following points:

- Mutual interaction of the constituents of SF plays a dominant role in film formation process while the effect of individual components cannot be generalized. It is necessary to take into account the complex composition as the impact of various constituents differs with the respect to the content of the others. In particular, it was found that

HA supports formation of thicker lubricating film with increasing concentration; however, this effect may be weakened by lower protein content. The content of PHs was found to be less important; nevertheless, PHs are essential due to interaction with HA.

- Albumin-based solutions showed enhanced lubrication when the solution was doped by HA. Similar positive effect was observed also for PHs, but the film dropped after some time. The effect of both HA and PHs was rather negative while the film thickness development corresponded to pure albumin solution during the dynamic part of the experiment.
- γ -globulin formed thicker lubricating film, in general. Considering the swinging period, addition of PHs led to sufficient stable lubricant film which remained over time under subsequent static loading. As in the case of albumin, when doped by HA together with PHs, the film formation was very limited.
- Mixture of the proteins showed quite similar results for all the tested fluids. However, when complex lubricant containing all the constituents was used, the film under dynamic conditions exhibited continuous decrease compared to other fluids. Moreover, when used together, albumin suppressed γ -globulin lubrication ability as the behaviour of the solution was similar to albumin-based solutions.
- Considering the comparison of hard-on-soft and hard-on-hard pairs, it can be concluded that the film formation is different, especially under swinging motion. While the film decreases more or less rapidly in the case of hard pairs, in soft contact, the film is enhanced. This indicates the importance of SF behaviour under loading. Reduced contact pressure in soft contact enables better entrance of the fluid into the contact, thus increasing the lubricant layer eventually.
- In contrast, soft pairs exhibit higher friction since the spontaneous swinging of the pendulum lasted for significantly shorter time than in the case of hard pair. This is attributed to transition to mixed lubrication regime and to larger clearance between the head and PMMA cup as well as to more obvious wear of the cup surface in terms of small scratches.

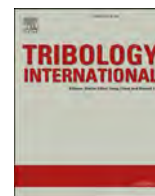
Acknowledgement

This research was carried out under the project LTAUSA17150 with financial support from the Ministry of Education, Youth and Sports of the Czech Republic. The authors express their thanks to P. Hekrl for his help with the experiments.

References

- Brockett, C.L., Harper, P., Williams, S., Isaac, G.H., Dwyer-Joyce, R.S., Jin, Z., Fisher, J., 2008. The influence of clearance on friction, lubrication and squeaking in large diameter metal-on-metal hip replacements. *J. Mater. Sci.: Mater. Med.* 19, 1575–1579.
- Choudhury, D., Urban, F., Vrbka, M., Hartl, M., Krupka, I., 2015b. A novel tribological study on DLC-coated micro-dimpled orthopedics implant interface. *J. Mech. Behav. Biomed. Mater.* 45, 121–131.
- Choudhury, D., Ay Ching, H., Mamat, A.B., Cizek, J., Abu Osman, N.A., Vrbka, M., Hartl, M., Krupka, I., 2015a. Fabrication and characterization of DLC coated microdimples on hip prosthesis heads. *J. Biomed. Mater. Res. Part B: Appl. Biomater.* 103, 1002–1012.
- Choudhury, D., Rebenda, D., Sasaki, S., Hekrl, P., Vrbka, M., Zou, M., 2018. Enhanced lubricant film formation through micro-dimpled hard-on-hard artificial hip joint: an in-situ observation of dimple shape effects. *J. Mech. Behav. Biomed. Mater.* 81, 120–129.
- Dowson, D., 2001. New joints for the millennium: wear control in total replacement hip joints. *Proc. Inst. Mech. Eng. Part H: J. Eng. Med.* 215, 335–358.
- Dowson, D., Hardaker, C., Flett, M., Isaac, G.H., 2004. A hip joint simulator study of the performance of metal-on-metal joints. *J. Arthroplast.* 19, 124–130.
- Fan, J., Myant, C.W., Underwood, R., Cann, P.M., Hart, A., 2011. Inlet protein aggregation: a new mechanism for lubricating film formation with model synovial fluids. *Proc. Inst. Mech. Eng. Part H: J. Eng. Med.* 225, 696–709.
- Fowell, M.T., Myant, C., Spikes, H.A., Kadiric, A., 2014. A study of lubricant film thickness in compliant contacts of elastomeric seal materials using a laser induced fluorescence technique. *Tribol. Int.* 80, 76–89.
- Galandáková, A., Ulrichová, J., Langová, K., Hanáková, A., Vrbka, M., Hartl, M., Gallo, J., 2016. Characteristics of synovial fluid required for optimization of lubrication fluid for biotribological experiments. *J. Biomed. Mater. Res. Part B: Appl. Biomater.* 105, 1422–1431.
- Gao, L., Yang, P., Dymond, I., Fisher, J., Jin, Z., 2010. Effect of surface texturing on the elasto-hydrodynamic lubrication analysis of metal-on-metal hip implants. *Tribol. Int.* 43, 1851–1860.
- Gohar, R., Cameron, A., 1963. Optical measurement of oil film thickness under elasto-hydrodynamic lubrication. *Nature* 200, 458–459.
- Hamrock, B.J., 1994. *Fundamentals of Fluid Film Lubrication*. McGraw-Hill, New York.
- Hartl, M., Krupka, I., Poliscuk, R., Liska, M., Molimard, J., Querry, M., Vergne, P., 2001. Thin film colorimetric interferometry. *Tribol. Trans.* 44, 270–276.
- Howard, J., 2016. Balancing innovation and medical device regulation: the case of modern metal-on-metal hip replacements. *Med. Device.: Evid. Res.* 9, 267–275.
- Hutchings, I., 2016. Fifty years of tribology. *Ingenia R. Acad. Eng. Mag.* (66).
- Jin, Z.M., Zheng, J., Li, W., Zhou, Z.R., 2016. Tribology of medical devices. *Biosurf. Biotribol.* 2, 173–192.
- Lakowicz, J.R., 2006. *Principles of Fluorescence Spectroscopy*, 3rd ed. Springer, New York, pp. c.
- Liu, F., Feng, L., Wang, J., 2018. A computational parametric study on edge loading in ceramic-on-ceramic total hip joint replacements. *J. Mech. Behav. Biomed. Mater.* 83, 135–142.
- Malmsten, M., 1998. Formation of adsorbed protein layers. *J. Colloid Interface Sci.* 207, 186–199.
- Mavraki, A., Cann, P.M., 2009. Friction and lubricant film thickness measurements on simulated synovial fluids. *Proc. Inst. Mech. Eng. Part J: J. Eng. Tribol.* 223, 325–335.
- Mavraki, A., Cann, P.M., 2011. Lubricating film thickness measurements with bovine serum. *Tribol. Int.* 44, 550–556.
- Mazzucco, D., Spector, M., 2004. The John Charnley Award paper: the role of joint fluid in the tribology of total joint arthroplasty. *Clin. Orthop. Relat. Res.* 429, 17–32.
- Medley, J.B., Krygier, J.J., Bobyn, J.D., Chan, F.W., Lippincott, A., Tanzer, M., 2005. Kinematics of the MATCO™ hip simulator and issues related to wear testing of metal-metal implants. *Proc. Inst. Mech. Eng. Part H: J. Eng. Med.* 211, 89–99.
- Myant, C., Cann, P., 2013. In contact observation of model synovial fluid lubricating mechanisms. *Tribol. Int.* 63, 97–104.
- Myant, C., Cann, P., 2014a. On the matter of synovial fluid lubrication: implications for metal-on-metal hip tribology. *J. Mech. Behav. Biomed. Mater.* 34, 338–348.
- Myant, C., Cann, P., 2014b. The effect of transient conditions on synovial fluid protein aggregation lubrication. *J. Mech. Behav. Biomed. Mater.* 34, 349–357.
- Myant, C., Underwood, R., Fan, J., Cann, P.M., 2012. Lubrication of metal-on-metal hip joints: the effect of protein content and load on film formation and wear. *J. Mech. Behav. Biomed. Mater.* 6, 30–40.
- Nakashima, K., Sawae, Y., Murakami, T., 2007. Effect of conformational changes and differences of proteins on frictional properties of poly(vinyl alcohol) hydrogel. *Tribol. Int.* 40, 1423–1427.
- National Joint Registry for England, Wales, Northern Ireland and the Isle of Man, 2017. 14th Annual Report. ISSN 2054-1821 (print).
- Necas, D., Jaroš, T., Dockal, K., Šperka, P., Vrbka, M., Krupka, I., Hartl, M., 2018b. The effect of kinematic conditions on film thickness in compliant lubricated contact. *J. Tribol.* 140, 051501. <https://doi.org/10.1115/1.4039529>.
- Nečas, D., Vrbka, M., Křupka, I., Hartl, M., Galandáková, A., 2016a. Lubrication within hip replacements – implication for ceramic-on-hard bearing couples. *J. Mech. Behav. Biomed. Mater.* 61, 371–383.
- Nečas, D., Vrbka, M., Urban, F., Křupka, I., Hartl, M., 2016b. The effect of lubricant constituents on lubrication mechanisms in hip joint replacements. *J. Mech. Behav. Biomed. Mater.* 55, 295–307.
- Nečas, D., Vrbka, M., Urban, F., Gallo, J., Křupka, I., Hartl, M., 2017. In situ observation of lubricant film formation in the considering real conformity: the effect of diameter, clearance and material. *J. Mech. Behav. Biomed. Mater.* 69, 66–74.
- Nečas, D., Vrbka, M., Galandáková, A., Křupka, I., Hartl, M., 2018a. On the observation of lubrication mechanisms within hip joint replacements. Part I: hard-on-soft bearing pairs. *J. Mech. Behav. Biomed. Mater.* XX (X-X).
- Nečas, D., Vrbka, M., Rebenda, D., Gallo, J., Galandáková, A., Wolfová, L., Křupka, I., Hartl, M., 2018b. In situ observation of lubricant film formation in THR considering real conformity: the effect of model synovial fluid composition. *Tribol. Int.* 117, 206–216.
- Parkes, M., Myant, C., Cann, P.M., Wong, J.S.S., 2014. The effect of buffer solution choice on protein adsorption and lubrication. *Tribol. Int.* 72, 108–117.
- Parkes, M., Myant, C., Cann, P.M., Wong, J.S.S., 2015. Synovial fluid lubrication: the effect of protein interactions on adsorbed and lubricating films. *Biotribology* 1–2, 51–60.
- Ranuša, M., Gallo, J., Vrbka, M., Hobza, M., Paloušek, D., Křupka, I., Hartl, M., 2017. Wear analysis of extracted polyethylene Acetabular Cups using a 3D optical scanner. *Tribology Trans.* 60, 437–447.
- Serro, A.P., Gispert, M.P., Martins, M.C.L., Brogueira, P., Colaço, R., Saramago, B., 2006. Adsorption of albumin on prosthetic materials: implication for tribological behavior. *J. Biomed. Mater. Res. Part A* 78A, 581–589.
- Stanton, T.E., 1923. Boundary lubrication in engineering practice. *Engineer* 135, 678–680.
- Swann, D.A., Silver, F.H., Slayter, H.S., Stafford, W., Shore, E., 1985. The molecular structure and lubricating activity of lubricin isolated from bovine and human synovial fluids. *Biochem. J.* 225, 195–201.

- Underwood, R.J., Zografos, A., Sayles, R.S., Hart, A., Cann, P., 2011. Edge loading in metal-on-metal hips: low clearance is a new risk factor. *Proc. Inst. Mech. Eng. Part H: J. Eng. Med.* 226, 217–226.
- Vrbka, M., Návrát, T., Křupka, I., Hartl, M., Šperka, P., Gallo, J., 2013. Study of film formation in bovine serum lubricated contacts under rolling/sliding conditions. *Proc. Inst. Mech. Eng. Part J: J. Eng. Tribol.* 227, 459–475.
- Vrbka, M., Křupka, I., Hartl, M., Návrát, T., Gallo, J., Galandáková, A., 2014. In situ measurements of thin films in bovine serum lubricated contacts using optical interferometry. *Proc. Inst. Mech. Eng. Part H: J. Eng. Med.* 228, 149–158.
- Vrbka, M., Nečas, D., Bartošik, J., Hartl, M., Křupka, I., Galandáková, A., Gallo, J., 2015a. Determination of a friction coefficient for THA bearing couples. *Acta Chir. Orthop. Traumatol. Cechoslov.* 82, 341–347.
- Vrbka, M., Nečas, D., Hartl, M., Křupka, I., Urban, F., Gallo, J., 2015b. Visualization of lubricating films between artificial head and cup with respect to real geometry. *Biotribology* 1–2, 61–65.



Towards the direct validation of computational lubrication modelling of hip replacements

Xianjiu Lu^{a,b}, David Nečas^b, Qingen Meng^{c,*}, David Rebenda^b, Martin Vrbka^b, Martin Hartl^b, Zhongmin Jin^{a,c,d,**}

^a State Key Laboratory for Manufacturing Systems Engineering, Xi'an Jiaotong University, 710054, Xi'an, Shanxi, China

^b Institute of Machine and Industrial Design, Faculty of Mechanical Engineering, Brno University of Technology, Technická 2896/2, 616 69, Brno, Czech Republic

^c School of Mechanical Engineering, University of Leeds, LS2 9JT, UK

^d Tribology Research Institute, School of Mechanical Engineering, Southwest Jiaotong University, Chengdu, 610031, Sichuan, China

ARTICLE INFO

Keywords:

Artificial hip joint
Lubrication
Computational modelling
Validation

ABSTRACT

This study attempted to provide insights into validating computational lubrication modelling of hip replacements. Direct comparisons between experimental measurements and numerical simulations were conducted for the central film thickness in a CoCr-on-glass hip bearing pair. A low-viscosity mineral oil and a 25% bovine serum were used as lubricants, respectively. Results indicated that for the low-viscosity lubricant case, the film thicknesses predicted by the computational model were comparable to the experimental measurements. For the bovine serum case, the computational results did not agree with those measured by experiments due to the viscosity model adopted in the computational models. A new effective viscosity equation was proposed to accurately predict the lubrication performance of hip replacements for protein-containing lubricants under transient conditions.

1. Introduction

Hip replacements have been considered as one of the most successful surgical treatments of hip joint diseases, such as osteoarthritis, rheumatoid arthritis, and osteonecrosis [1]. The wear particles produced in hip replacements are a potential risk of adverse biological reactions [2]. An effective lubricant film can prevent the bearing surfaces from the direct asperity contact and significantly minimize the amount of wear debris. Therefore, understanding the lubrication performance of hip replacements is extremely important. Because the *in-vivo* measurement of the lubricant film thickness in hip replacements is very difficult (if not impossible) to achieve at present, computational modelling has played a significant role in investigating the lubrication performance of hip replacements.

Indeed, computational lubrication modelling has provided important information for the design and adoption of hip replacements. For instance, Dowson et al. [3] pointed out that metal-on-metal hip replacements operate in the mixed-lubrication regime and ceramic-on-ceramic hip replacements are more likely to achieve full

fluid film lubrication due to their smooth bearing surfaces. Jin et al. [4–8] found that a smaller clearance and a larger size are beneficial for the lubrication performance of hip replacements. Furthermore, Liu et al. [8] and Meng et al. [9] found that the underneath soft structure of hip replacements and aspherical bearing surfaces are helpful for improving the lubrication performance, respectively.

The full numerical solutions mentioned above have been well verified by mesh convergence studies [10] and comparing with dry contact mechanics analyses [5,9,10]. Moreover, some of the conclusions were indirectly validated by wear test results. For instance, Dowson et al. [11] confirmed that larger head diameters and smaller clearances produced lower wear rate, which indirectly validated the previous theoretical lubrication analyses [4–8]. The direct comparison of the lubrication performance of hip replacements under the same operating conditions between computational modelling and experiments can provide confidence for both approaches. For instance, such a comparison can validate the governing equations and related assumptions of the computational model and provide more reliable theoretical supports for experiments. However, due to the difficulties in the full numerical solution and the

* Corresponding author. School of Mechanical Engineering, University of Leeds, LS2 9JT, UK.

** Corresponding author. State Key Laboratory for Manufacturing Systems Engineering, Xi'an Jiaotong University, 710054, Xi'an, Shanxi, China.

E-mail addresses: Q.Meng@leeds.ac.uk (Q. Meng), zmjin@mail.xjtu.edu.cn (Z. Jin).

experimental tests of the lubrication performance of hip replacements, no direct comparison between the full numerical models and the experiments under the same operating conditions has been conducted for the lubrication performance of hip replacements.

Experimental techniques to measure the lubricant film thickness of hip replacements have been substantially developed in the last decade. Notably, the optical interferometry method has been employed to study the lubricant film thickness of artificial hip joints [12–19]. The early-stage studies investigated the effects of protein-solution lubricants on the film thickness of hip replacements with the optical interferometry method, employing a non-conformal ball-on-disc configuration to represent the conformal contact between the femoral head and the acetabular cup of hip replacements [14–17,20,21]. Recently, Vrbka et al. [22] developed the experimental technique to measure the lubricant film thickness between a CoCr head and a glass cup, which made measuring the film thickness of hip replacements with the realistic geometric representation feasible. Based on this optical interferometry technique, the effects of lubricant constituents, diameter, clearance and materials on the lubricant film formation of hip replacements were examined [23,24]. This experimental technique has made the validation of the computational lubrication models of hip replacements possible, especially when the realistic conditions of hip replacements (e.g., geometry, loading and motion, and rheology of lubricants) are all taken into consideration.

Therefore, this paper intended to provide insights into the direct validation of the current full numerical lubrication model by directly comparing it with experimental measurements. For this purpose, the lubrication film thicknesses between a CoCr femoral head and a glass acetabular cup, lubricated by a low-viscosity mineral oil and a bovine serum solution, respectively, were numerically solved using a computational lubrication model and experimentally measured using the optical interferometry method.

2. Materials and methods

2.1. Materials

The lubricated contact between a CoCr femoral head and a glass acetabular cup was studied in this study. Glass acetabular cups are not used in modern realistic hip replacements. The reason for using a glass acetabular cup was that the optical interferometry method, in which the acetabular cup has to be transparent to observe the film formation inside the contact, was employed to measure the film thickness. The radius of the femoral head was 13.985 mm and the radial clearance between the cup and the head was 40 μm . The outside radius of the cup was 24.025 mm, resulting in a cup thickness of 10 mm. The maximum pressure that the contact surfaces of the CoCr head and glass acetabular cup were subjected to in this study was about 30 MPa, which was much smaller than the yielding stresses of the CoCr alloy and the compressive strength of glass. Therefore, both the CoCr head and glass acetabular cup were assumed linear elastic. The material properties and geometry of the metallic head and the glass cup are summarized in Table 1.

Two types of lubricants were used in this study. First, a low-viscosity mineral oil (SN100) was adopted to exclude the protein aggregation and adsorption effects in synovial fluids and the bovine serum solution. The second type lubricant was a 25% bovine serum solution. This lubricant

was chosen because the bovine serum solution is widely used in wear and lubrication experiments to represent the synovial fluid [20,25].

2.2. Loading and motion conditions

The configuration of the pendulum hip joint simulator (Fig. 1) was considered in the present study. The outer surface of the cup was fixed. The head was positioned at the centre of the cup with an applied vertical load of 532 N. The head rotated around the z-axis in Fig. 1 with an angular speed of ω_z to simulate the flexion-extension motion of the hip joint.

Two types of motions were adopted as the inputs of the lubrication systems of this study. The analogous sinusoidal angular velocity shown in Fig. 2a was used for the SN 100 oil case. The maximum amplitude of the oscillation was around 1 rad/s, with a frequency of 0.5 Hz. The start-up and shut-down processes of the pendulum were both considered in the numerical analyses and experiments (Fig. 2a). To compare the computational results with the published experimental results [22], the amplitude-decayed sinusoidal angular velocities (Fig. 2b) were adopted for the 25% bovine serum case. In this case, the amplitude of the maximum angular velocity decayed from 0.45 rad/s to zero, with a frequency of 0.5 Hz (Fig. 2b).

2.3. Computational methods

2.3.1. Viscous properties of the lubricants

The viscosities of the mineral oil (SN100) under different pressures (varying from 0.0 to 40.1 MPa) were measured at 25 °C. The measured viscosity values were subsequently curve-fitted to the Roelands' viscosity-pressure equation [26].

$$\eta = \eta_0 \exp\{(\ln \eta_0 + 9.67)[(1 + 5.1 \times 10^{-9} p)^z - 1]\} \quad (1)$$

The fitted values for η_0 and z were 0.033 Pa s and 0.703, respectively (Fig. 3a). The error in the viscosity between the values obtained from the fitted relation and the measured values was 0.35%.

To provide more insights into the direct validation of the computational lubrication models of hip replacements, two types of viscous models were used for the 25% bovine serum. As demonstrated in the previous studies [20,27], the viscosity of the 25% bovine serum solution is constant when the shear rate is above 1000 s^{-1} . The shear rates in most of the contact area of the hip replacement are above 1000 s^{-1} , and the lower shear rates only exist at the boundaries of the contact area,

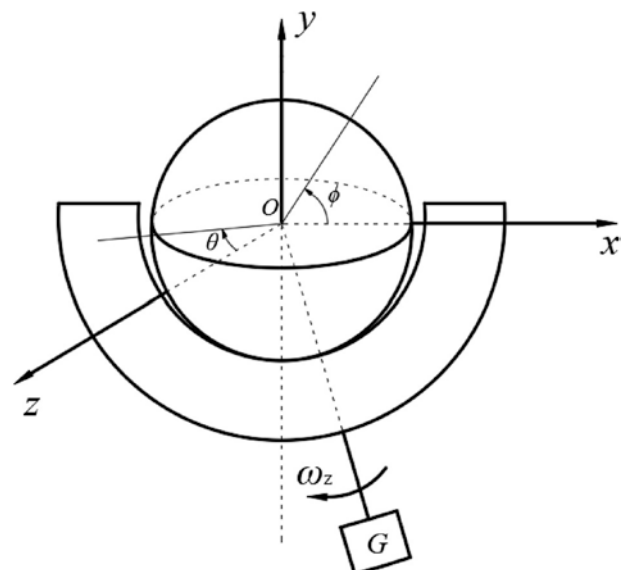


Fig. 1. A ball-in-socket lubrication model of the pendulum hip joint simulator.

Table 1

Material and geometrical parameters adopted in this study.

Radius of CoCr femoral head, R_H	13.985 mm
Radial clearance, c	40 μm
Thickness of glass cup	10 mm
Elastic modulus of CoCr	230 GPa
Elastic modulus of glass	85 GPa
Poisson's ratio of CoCr	0.3
Poisson's ratio of glass	0.209

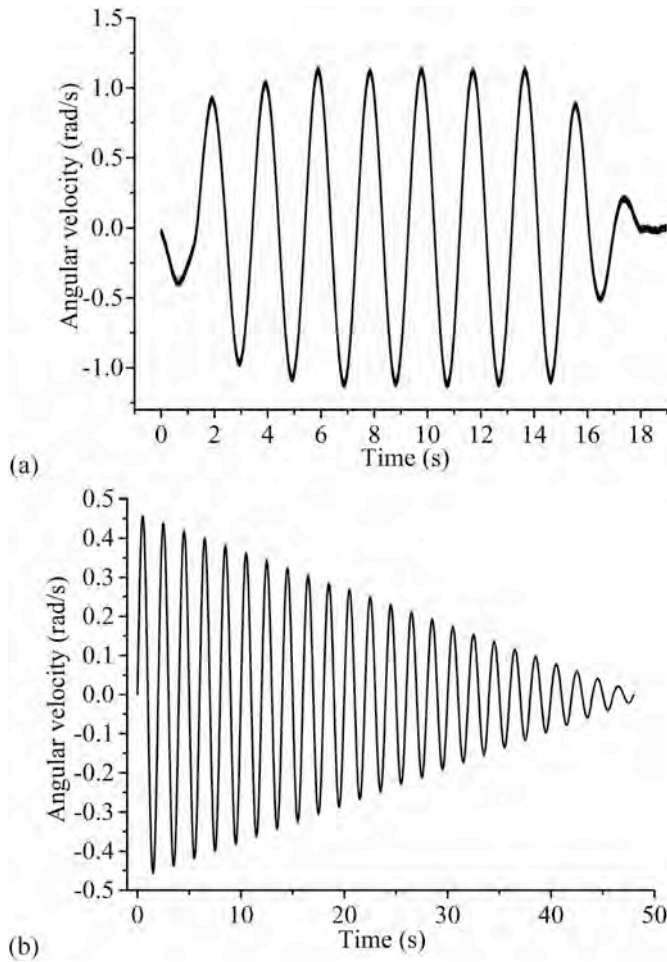


Fig. 2. (a) The analogous sinusoidal angular velocity used for the SN 100 oil case (b) The amplitude-decayed sinusoidal angular velocities adopted for the 25% bovine serum case.

which have little influence on the overall film thickness distribution. Therefore, it was a common and reasonable method to adopt a constant viscosity value (0.0009–0.0025 Pa s) for the 25% bovine serum in the computational lubrication studies of hip replacements [8,11,28]. This study examined this constant-viscosity model by adopting a value of 0.002 Pa s for the 25% bovine serum solution.

Moreover, Myant et al. [15] found that under steady-state conditions, the boundary layer formed on the surfaces was augmented by the high viscosity fluid film generated by the hydrodynamic effect. The lubricant film thickness was thicker for low-speed cases, and an effective velocity-viscosity relation was proposed for the bovine serum to consider the protein aggregation effect. Therefore, this velocity-viscosity relation (equation (2)) [15] was also used to model the viscosity of the bovine serum solution in the numerical lubrication model.

$$\eta = k_1 U z_1 \quad (2)$$

where U is the entrainment speed, and the values of the coefficients ($k_1 = 3.422$ and $z_1 = -1.248$) were obtained by fitting the viscosity-velocity data presented in literature [15] to equation (2) (Fig. 3b).

2.3.2. Governing equations

The governing equations for a transient computational lubrication model included the Reynolds, the film thickness, the deformation, and the load balance equations. The time-dependent Reynolds equation in spherical coordinates for the ball-in-socket model was [29].

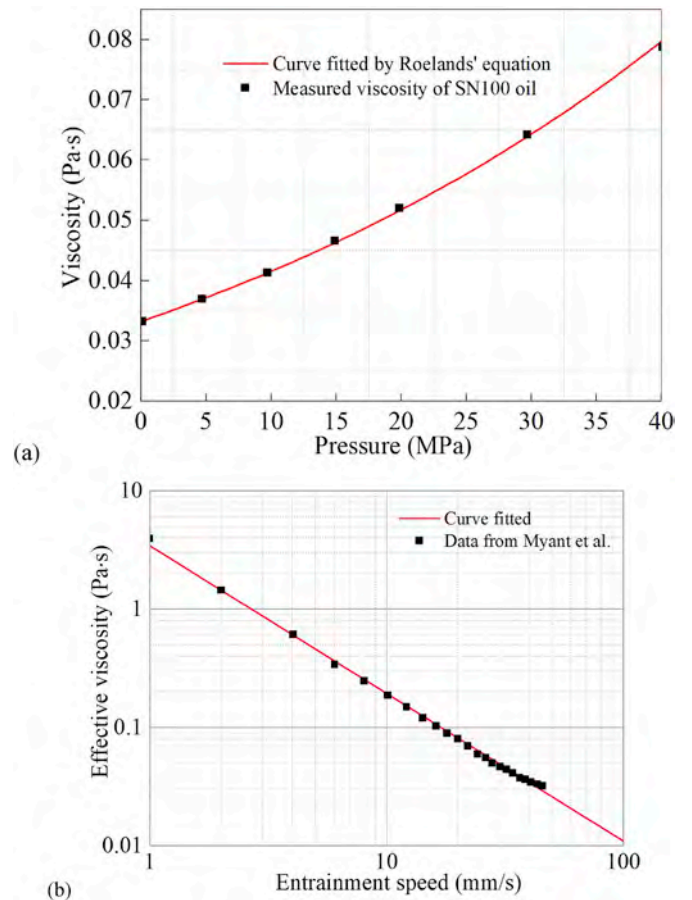


Fig. 3. (a) The measured and curve-fitted Roelands' viscosity-pressure relationship for the SN100 oil (b) The entrainment velocity-effective viscosity relation proposed by Myant et al. [15] for the 25% bovine serum solution.

$$\sin \theta \frac{\partial}{\partial \theta} \left(\frac{h^3}{\eta} \sin \theta \frac{\partial p}{\partial \theta} \right) + \frac{\partial}{\partial \varphi} \left(\frac{h^3}{\eta} \frac{\partial p}{\partial \varphi} \right) = 6R^2 \sin^2 \theta \left(\omega(t) \frac{\partial h}{\partial \varphi} + 2 \frac{\partial h}{\partial t} \right) \quad (3)$$

where p is the hydrodynamic pressure; h is the film thickness; η is the viscosity of the lubricants, which was described in section 2.3.1 for the mineral oil and bovine serum cases; t is time; ω is the angular velocity of the femoral head; and φ and θ are the spherical coordinates. The boundary conditions of the Reynolds equation at each time instant were

$$p(0, \theta) = p(\pi, \theta) = p(\varphi, 0) = p(\varphi, \pi) = 0$$

$$\frac{\partial p}{\partial \varphi} = \frac{\partial p}{\partial \theta} = 0, \quad 0 < \varphi < \pi, \quad 0 < \theta < \pi$$

The cavitation boundary condition was achieved by setting the obtained negative pressure as zero during the relaxation process in the entire calculation domain.

The film thickness equation contained both the undeformed gap between the spherical bearing surfaces of hip replacements and the elastic deformation of the bearing surfaces due to the hydrodynamic pressure [30].

$$h(\varphi, \theta) = c - e_x \sin \theta \cos \varphi - e_y \sin \theta \sin \varphi + \delta(\varphi, \theta) \quad (4)$$

where c represents the radial clearance between the cup and the head; e_x and e_y are the eccentricity components of the centre of the head with respect to the cup in the φ and θ direction, respectively. $\delta(\varphi, \theta)$ is the elastic deformation of the bearing surfaces.

The external load components were balanced by the integration of the hydrodynamic pressure [30].

$$\begin{aligned}
f_x &= R_C^2 \int_0^\pi \int_0^\pi p \sin^2 \theta \cos \varphi d\theta d\varphi = 0 \\
f_y &= R_C^2 \int_0^\pi \int_0^\pi p \sin^2 \theta \sin \varphi d\theta d\varphi = w_y \\
f_z &= R_C^2 \int_0^\pi \int_0^\pi p \sin \theta \cos \theta d\theta d\varphi = 0
\end{aligned} \quad (5)$$

2.3.3. Numerical methods

To facilitate the calculation process and improve the stability of numerical analysis, all the governing equations were non-dimensionalised [31]. Each oscillating cycle was divided into 50 instants. At each instant, the Reynolds equation was solved using a multi-grid technique [31] and the deformation was calculated using a Fast Fourier Transform method [32]. Three levels of grids were adopted for the multi-grid method. On different levels, the calculation domains of the spherical hip bearing surfaces (from 0 to π for both φ and θ) were discretised into different numbers of nodes. The number of nodes on the finest level was 257 in both the φ and θ directions [28]. The load balance equation was solved by iteratively adjusting the eccentricities in the φ and θ direction according to the difference between the integration of the hydrodynamic pressure and the applied load [31]. To be consistent with the experiments, at the first time instant (when $t = 0$), the head and the cup were assumed in contact and the pressure was set as zero. Then these film thicknesses and pressure values were used as the initial values for the next time instant.

At each instant of the transient lubrication analysis, the deformation was calculated using the following equation [30].

$$\delta_{i,j} = \sum_k \sum_l C_{i,j,k,l} p_{k,l} \quad (6)$$

where $C_{i,j,k,l}$ is the displacement coefficients matrix, defined by the average displacement at node (i, j) caused by a unit pressure distribution at node (k, l) . The displacement coefficients were calculated using the method developed by Wang and Jin [32]. Finite element models were constructed for the head and cup first. Then a unit pressure was applied to the element at the centre of the articulating surface of the head and the cup, respectively. The normal elastic deformations of the head and the cup along a longitudinal line were obtained through finite element analyses. These displacements were used to curve fit a displacement influence function of the spherical distance. Finally, the deformation coefficients were calculated for all the nodes on the articulating surfaces of the head and the cup using the fitted function.

Because three levels of grids were used for the multi-grid method, the deformation coefficients were calculated for different numbers of nodes (i.e., 65×65 , 129×129 , and 257×257). The accuracy of the elastic deformation coefficients was examined by calculating the deformation caused by a given pressure distribution (using equation (6)) and then comparing it with the deformation obtained from a finite element analysis. To achieve this, a parabolic pressure distribution with the maximum pressure of 10 MPa and a half contact angle of 30° was applied to the central region of the bearing surface of the cup and head [32]. In this study, the largest oscillating angle of the pendulum was 32° and the contact between the head and the cup was within the central region of the cup (i.e., not close to the rim of the cup). Therefore, the position of the parabolic pressure distribution would not affect the calculated deformation [32].

2.4. Experiment methods

The pendulum hip joint simulator and the optical imaging system [22,24,33,34] were employed to measure the film thickness of the hip replacement. In the pendulum hip simulator, the glass acetabular cup was fixed in a base frame and the femoral head was connected to a swinging pendulum by a pendulum arm. The swinging motion of the pendulum was in the flexion-extension plane because the major velocity

component of hip implants is in the flexion/extension direction [22]. The pendulum was driven manually, allowing a continuous motion in the flexion-extension plane. The thin film colorimetric interferometry method [33] was employed to evaluate the film thickness. The resolution of this technique could reach 1 nm [33]. The maximum detectable film thickness is around 900 nm. The contact was captured by a complementary metal-oxide-semiconductor (CMOS) high-speed camera (Phantom V710). The details of the test devices and measurement method can be found in the literature [22,24,34]. In general, three basic steps were involved. First, the calibration curves, which gave the relationship between the colors of the interferograms and the values of the film thickness, was obtained based on a lightly loaded static contact. Second, using the high-speed camera, the interferograms of the lubricant film were captured for the load and motion conditions in Section 2.2. Finally, the film thickness within the contact area was evaluated by comparing the captured interferograms with the calibrated curves.

The contact area continuously changed within the cup over the oscillation. However, only the central film thickness when the pendulum arm reached the vertical (equilibrium) position was measured because the high-speed camera was fixed underneath the central contact position of the cup. At each instant, the measured central film thickness was the average value of the film thicknesses within a circular area of 40 pixels (diameter of around 0.2 mm) [24]. When the cross-sectional central film thicknesses in the entraining and side leakage directions were compared with the numerical solutions, the film thickness values along one pixel in the side leakage or entraining direction and 421 pixels in the perpendicular direction were extracted from the interferograms.

2.5. A new entrainment velocity-effective viscosity relation

Based on the assumption that the iso-viscous viscosity and the effective viscosity model (equation (2)) could not produce accurate film thicknesses for the bovine serum case, a new entrainment velocity-effective viscosity relation was proposed. The experimentally measured central film thicknesses [22] were used as the target values in a numerical fitting process. At each instant, an initial viscosity was given to the model and the governing equations were solved using the given viscosity. Then the obtained central film thickness was compared with the target values. The viscosity was subsequently updated based on the difference in the central film thickness until the relative difference between the numerical and experimental values was less than a given criterion (10^{-3}). After the effective viscosity values were obtained for each instant of the first 3 s of the amplitude-decayed sinusoidal oscillation, the effective viscosities were curve fitted to equation (7) to obtain the relationship between the effective viscosity and the entrainment velocity (Fig. 8).

$$\eta = \eta_\infty + \frac{\eta_0 - \eta_\infty}{1 + (u/c)^{p_1}} \quad (7)$$

where η_0 is the effective viscosity when the entrainment speed is zero; η_∞ is the effective viscosity when the entrainment speed is infinity; u is the entrainment speed; c and p_1 are curve fitted constants. This equation was close to the Cross rheological model [35], which describes the relationship between the shear rate and viscosity. The Cross rheological model has been used in the previous study [20] to represent the bovine serum solution and showed good consistency. Enlightened by these previous studies, the relationship between the effective viscosity and the entrainment velocity (equation (7)) followed a similar form. However, for the convenience of the application in numerical analyses, the shear rate in the Cross rheological model was replaced by the entrainment velocity.

After the parameters in equation (7) were obtained from the fitting process, the fitted entrainment velocity-effective viscosity relation was used to solve the governing equations in the numerical analyses for the whole oscillation process (48 s) and the results were compared with the

experiments. Since only the effective viscosities of the first 3 s of the amplitude-decayed sinusoidal oscillation were used when the constants of equation (7) were derived, the comparison of the film thickness at other instants (from 3 s to 48 s) between the numerical analyses and the experimental measurements can validate the proposed new entrainment velocity-effective viscosity relation.

3. Results

Accurate elastic deformation of the CoCr head and the glass cup was predicted from the displacement coefficients matrix (Fig. 4). The deformations of the CoCr head and the glass cup calculated from the deformation coefficients was very close to those solved from the FEA (Fig. 4). The differences in the predicted deformation between the deformation coefficients and the FEA were less than 1.5%.

For the SN100 oil case, the central film thickness at the vertical position of the pendulum arm predicted by the computational model agreed well with the average central film thickness measured by the experiment (Fig. 5). When the oscillation was relatively steady (after 6.0 s), the central film thickness in the equilibrium position predicted by the numerical simulation was around 250 nm and the value measured by the experiment was about 260 nm. Moreover, after the oscillation was steady, the predicted maximum pressure oscillated around 27.5 MPa with a small amplitude of 2.5 MPa. To compare, the maximum Hertz pressure of the system was 26.5 MPa. Moreover, during the oscillation, the maximum angular velocities and the maximum central film thicknesses of the numerical simulation and experiment did not occur at the same instants (Fig. 5). The cross-sectional film profiles in the entraining direction and the side leakage direction predicted by the numerical solutions were very close to those measured by the experiments, although the experimentally measured cross-sectional film thickness fluctuated at all the three instants investigated in this study (Fig. 6). The maximum fluctuation amplitude of the experimentally measured film thickness was around 50 nm (Fig. 6).

The central film thicknesses predicted by the iso-viscous model and the effective viscosity model did not agree well with the experimental measurements (Fig. 7). The variation in the central film thickness predicted by the iso-viscous model decreased during the first a few seconds and reached a constant value. This trend was quite similar to the experimental measurements. However, the steady central film thickness predicted by the iso-viscous model was approximately five times smaller than the experimental measurements. The effective viscosity model

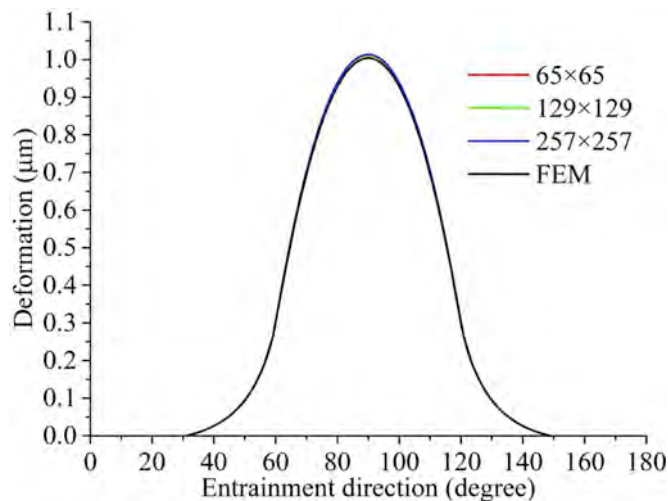


Fig. 4. The elastic deformation of the CoCr head and the glass acetabular cup in the latitude direction caused by a parabolic pressure distribution, calculated from the elastic deformation coefficients of the three levels of grid and the finite element method.

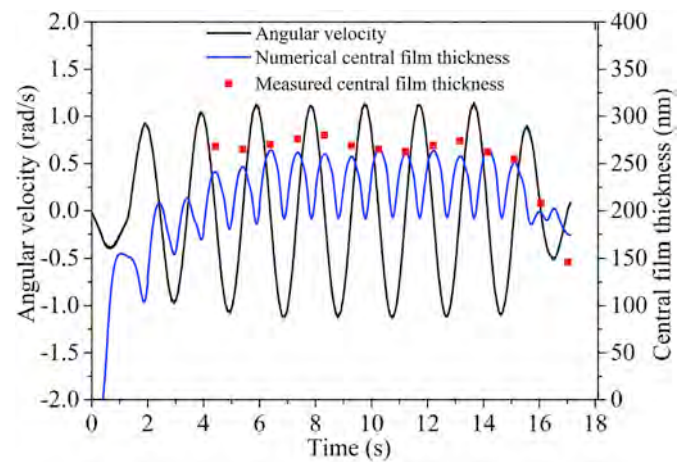


Fig. 5. The comparison of the central film thickness between the experimental measurements and the numerical analyses for the low-viscosity mineral oil case (SN100, $\eta_0 = 0.0332$ Pa s).

proposed in Ref. [15] predicted a gradually decreasing trend for the central film thickness. However, during the whole cycle of the oscillation, the effective viscosity significantly overestimated the central film thickness (more than the double of the experimental measurement, Fig. 7).

The following values were obtained for the variables of equation (7): $\eta_\infty = 0.038$ Pa s, $\eta_0 = 0.352$ Pa s, $c = 0.175$ mm/s and $p_1 = 1.668$ (Fig. 8). Compared with the original viscosities derived from the experiments, the residual sum of squares of the fitted entrainment velocity-effective viscosity relation was 0.017. Even if only the effective viscosities of the first 3 s of the amplitude-decayed sinusoidal oscillation were used to derive the constants of equation (7), the central film thickness calculated using the new entrainment velocity-effective viscosity equation agreed very well with the experimental measurements during the whole oscillation process (Fig. 9). For the period from 3 s to 48 s, the average relative error in the central film thicknesses calculated from the new entrainment velocity-effective viscosity equation was about 14%.

To provide more insights into the lubrication mechanism of hip replacements, the central film thicknesses and shear rates of an oscillation cycle produced by the three viscosity models (i.e., the iso-viscous, the effective viscosity model proposed by Myant et al., and the effective viscosity model proposed in this study) were plotted against the velocity in Fig. 10 (a). Generally, apart from a few instants when the entraining velocity was nearly zero, the shear rates calculated from the three viscosity models were all greater than 10^3 s⁻¹ during the whole cycle. Moreover, because the film thickness only varied very slightly during one cycle, the variations of the shear rates of the three viscosity models were all determined by that of the velocity (Fig. 10 (a)). The variations in the entraining velocity, the shear rate, and the effective viscosity within one cycle were investigated for the effective viscosity models proposed by Myant et al. and this study (Fig. 10 (b) and (c), respectively). Clearly, the shear rates produced by these two effective viscosity models were at the same order of magnitude. However, the effective viscosities of Myant et al.'s model (equation (2)) varied from 1.07 Pa s to an extremely large value (theoretically, infinity), while those of the new viscosity model proposed in this study varied from 0.10 to 0.35 Pa s.

4. Discussion

Understanding the lubrication performance of hip replacements is very important because an effective lubricant film can prevent the bearing surfaces from the direct asperity contact and significantly minimize the amount of wear debris. The *in vivo* measurement of the lubricant film thickness of hip replacements is still very difficult.

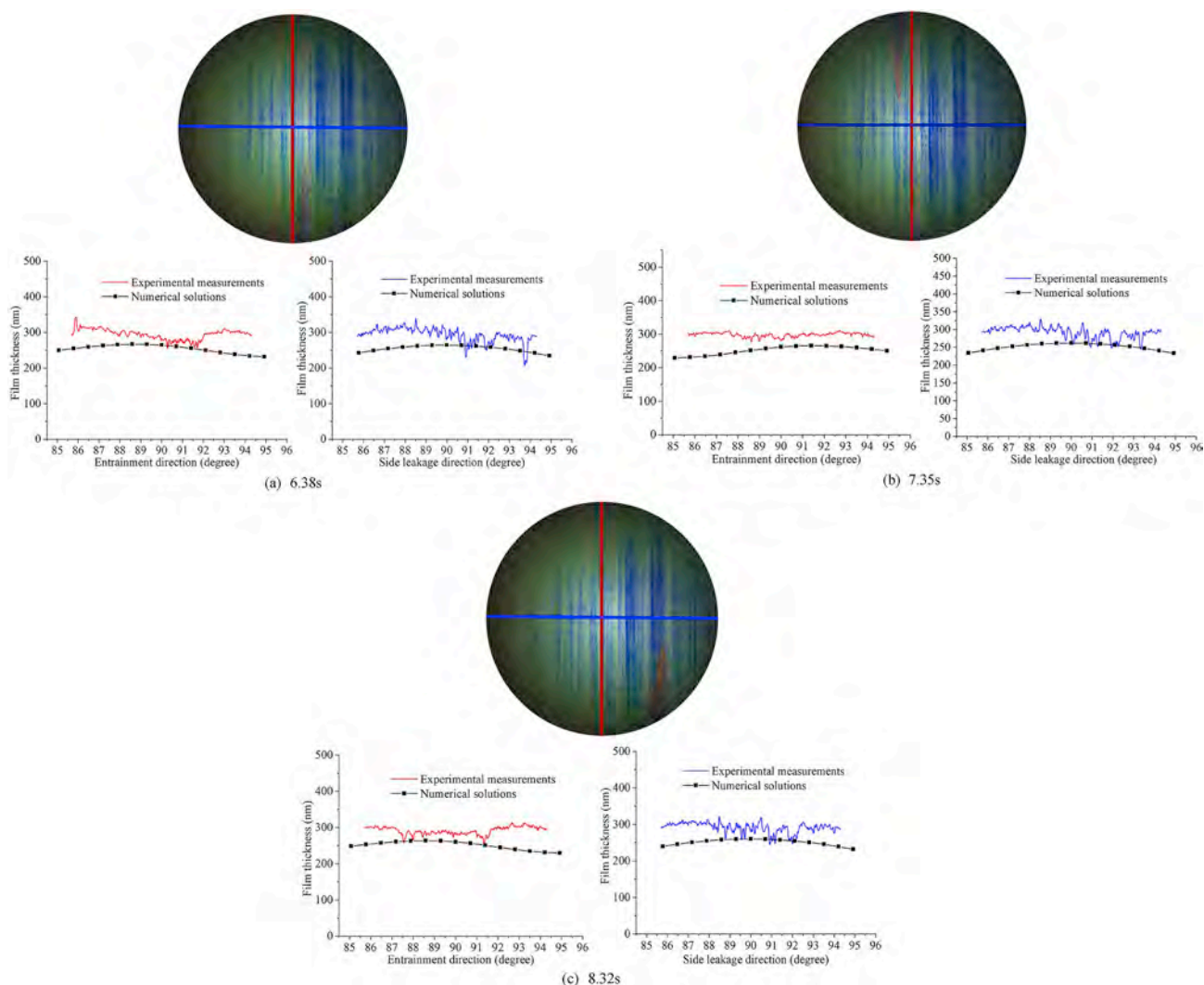


Fig. 6. The comparison of the cross-sectional film profiles in the entraining and side leakage directions between the experimental measurements and the numerical analyses at three time instants ((a) 6.38s, (b) 7.35 s, and (c) 8.32 s) for the SN100 mineral oil case.

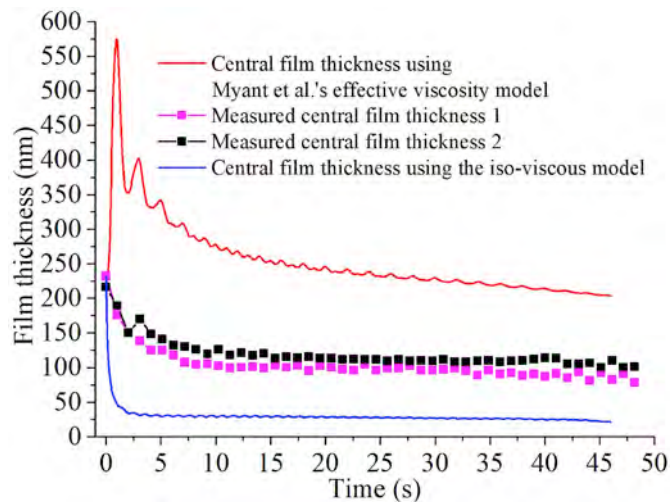


Fig. 7. The comparisons between the experimentally measured and numerically calculated central film thicknesses at the equilibrium position of the pendulum. The central film thicknesses predicted by both the iso-viscous model and the effective viscosity model did not agree well with the experimental measurements for the 25% bovine serum solution case.

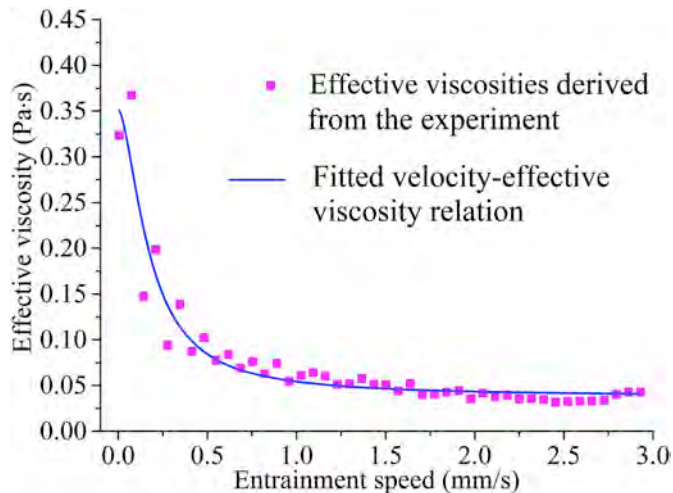


Fig. 8. The effective viscosities derived from the film thicknesses measured by experiments and the full numerical solutions, and the fitted entrainment velocity-effective viscosity curve.

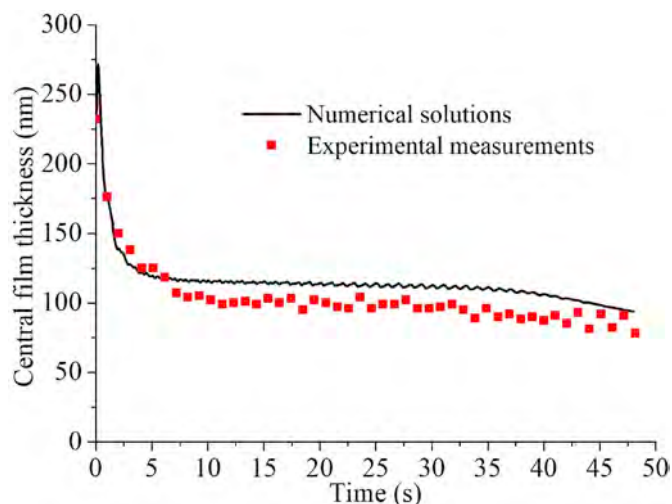


Fig. 9. The comparison of the central film thickness between the experimental measurements and the numerical solutions solved using the new entrainment velocity-effective viscosity equation.

Therefore, computational modelling has played a significant role in investigating the lubrication performance of hip replacements. Previous full numerical solutions for the lubrication performance of hip replacements have been well verified by mesh convergence studies [10] and comparing with dry contact mechanics analyses [5,9,10], and indirectly validated by wear test results [11]. However, due to the difficulties in the full numerical solution and experimental measurements of the film thickness of hip replacements, the direct validation of the full numerical computational model has not been conducted, especially when considering the realistic ball-in-socket geometry of the hip replacements. A validated computational model can provide more reliable results, which may be difficult or even impossible to obtain from the direct experimental observation. Therefore, this study intended to compare the lubricant film thickness of a CoCr-glass replacement calculated from full numerical analyses with that measured by experiments, thus providing insights into the direct validation of current computational lubrication models for hip replacements.

At first, a low-viscosity mineral oil SN 100 ($\eta_0 = 0.0332$ Pa s) was adopted to exclude the protein aggregation effect in synovial fluids and bovine serum solutions [14–17,21]. The satisfactory agreement between the computational and experimental averaged central film thickness (Fig. 5) indicated that for the given ball-in-socket configuration of hip replacements, the computational lubrication model could accurately predict the averaged central film thickness. Moreover, the agreement in the cross-sectional film profiles in the entraining and side leakage directions between the experiments and numerical analyses (Fig. 6) also supported the above statement. The disagreement in the positions of the maximum angular velocities and the maximum central film thicknesses of the numerical simulation and experiment was due to the well-known time lag caused by the squeeze-film action [10,36].

The small disagreements between the experiments and the numerical simulation in the cross-sectional film profiles of the low-viscosity lubricant case (Fig. 6) were mainly due to the effects of the surface roughness and the slightly different input conditions. When the transient central film thicknesses were measured, the average values of the film thicknesses within a 0.2 mm diameter circular area (Fig. 5) were adopted. Therefore, the positive and negative effects of the roughness were cancelled out and the experimentally measured average central film thicknesses were close to those of the numerical analysis. When the cross-sectional film profiles in the entraining (or the side leakage) direction were plotted, the values along one pixel in the entraining (or the side leakage) direction and 421 pixels in the perpendicular direction were extracted from the interferograms. Therefore, the differences

between the experiments and the numerical simulation became obvious for the cross-sectional film profiles (Fig. 6). The effect of the surface roughness can be clearly seen from the fluctuation of the experimentally measured cross-sectional film profiles. However, the surface roughness was not considered in the computational model due to excessively expensive computational costs to capture the surface roughness in the numerical simulation. Moreover, to achieve the analogous sinusoidal angular velocity (Fig. 2a), the pendulum was driven with slight manual assistance, which might introduce a slight impact on the input velocity and affect the accuracy of the measurement of the film thickness.

If the effect of the protein aggregation is not considered, both the bovine serum and synovial fluid are iso-viscous lubricants with very low viscosities [20,27] when the shear rate is greater than 1000 s^{-1} . The previous computational lubrication models have adopted such viscous properties for the bovine serum and synovial fluid [8,11,28,29,31,37]. Therefore, based on the above discussion for the low-viscosity mineral oil case, it is reasonable to believe that these numerical studies were accurate. However, in the study using the bovine serum solution as the lubricant, the film thicknesses predicted by the iso-viscous model were approximately five times smaller than the experimental measurements (Fig. 7), although the shear rates in the hip replacement were indeed larger than 1000 s^{-1} apart from a few time instants when the angular velocity tended to be zero (Fig. 10 (a)).

The disagreement in the film thickness between the experimental measurements and the theoretical lubrication analyses has been reported for the protein-containing lubricants, such as the bovine serum solutions [15]. A gel-like protein phase was found to form at the inlet of the lubricated contact area due to the aggregation of protein molecules [15]. At low speeds, when the gel-like protein phase was entrained into the contact, a high-viscosity film was formed. As the speed increased, the gel appeared to shear thin, producing much lower lubricant film thickness [15]. To consider this protein aggregation effect of the bovine serum solution, Myant et al. [15] proposed a relation between the effective viscosity and the entraining velocity ($\eta = k_1 U^{z_1}$) based on the Hooke's central film thickness equation and the measured central film thickness. However, in this study, this effective viscosity model did not accurately predict the central film thickness for the bovine serum solution case (Fig. 7). Several reasons may have contributed to the disagreement. First, the amplitude-decayed sinusoidal angular velocities reduced from 0.45 rad/s to 0 rad/s. Therefore, the corresponding entrainment velocities were 3.1 mm/s to zero. The equivalent viscosity would approach infinity when the entrainment velocity is zero if equation (2) is used to represent the viscosity (Fig. 10 (b)). This is not physically reasonable. Secondly, Hooke's central film thickness equation is only applicable for steady-state problems. Therefore, the transient effect caused by the oscillation of the pendulum was not considered in equation (2). In addition, a ball-in-socket configuration was modelled in this study, while a ball-on-disc test device was used in Myant et al.'s experiments [15]. The protein aggregation effect of the bovine serum or synovial fluid may play a different role in the ball-on-disc contact from that of the ball-in-socket contact. Therefore, the effective viscosity fitted from the ball-on-disc experiments may not be suitable for the lubrication simulation of hip replacements with a ball-in-socket geometry.

The newly proposed relation (equation (7)) between the viscosity and the entraining velocity followed the form of the Cross rheological model [35] but replaced the shear rate in the Cross rheological model using the entrainment velocity. Since the film thickness changed very slightly in one cycle and the variation of the shear rate was consistent with the velocity (Fig. 10 (a) and (c)), equation (7) was essentially similar to the Cross rheological model. Moreover, the effective viscosities calculated by equation (7) were higher for the lower entrainment velocities and lower for the higher lower entrainment velocities (Fig. 10 (c)). Thus, the protein aggregation effect described above was well represented by this new effective viscosity equation. Moreover, because the values of the parameters of equation (7) were derived from the full numerical solutions considering the transient effect and the realistic

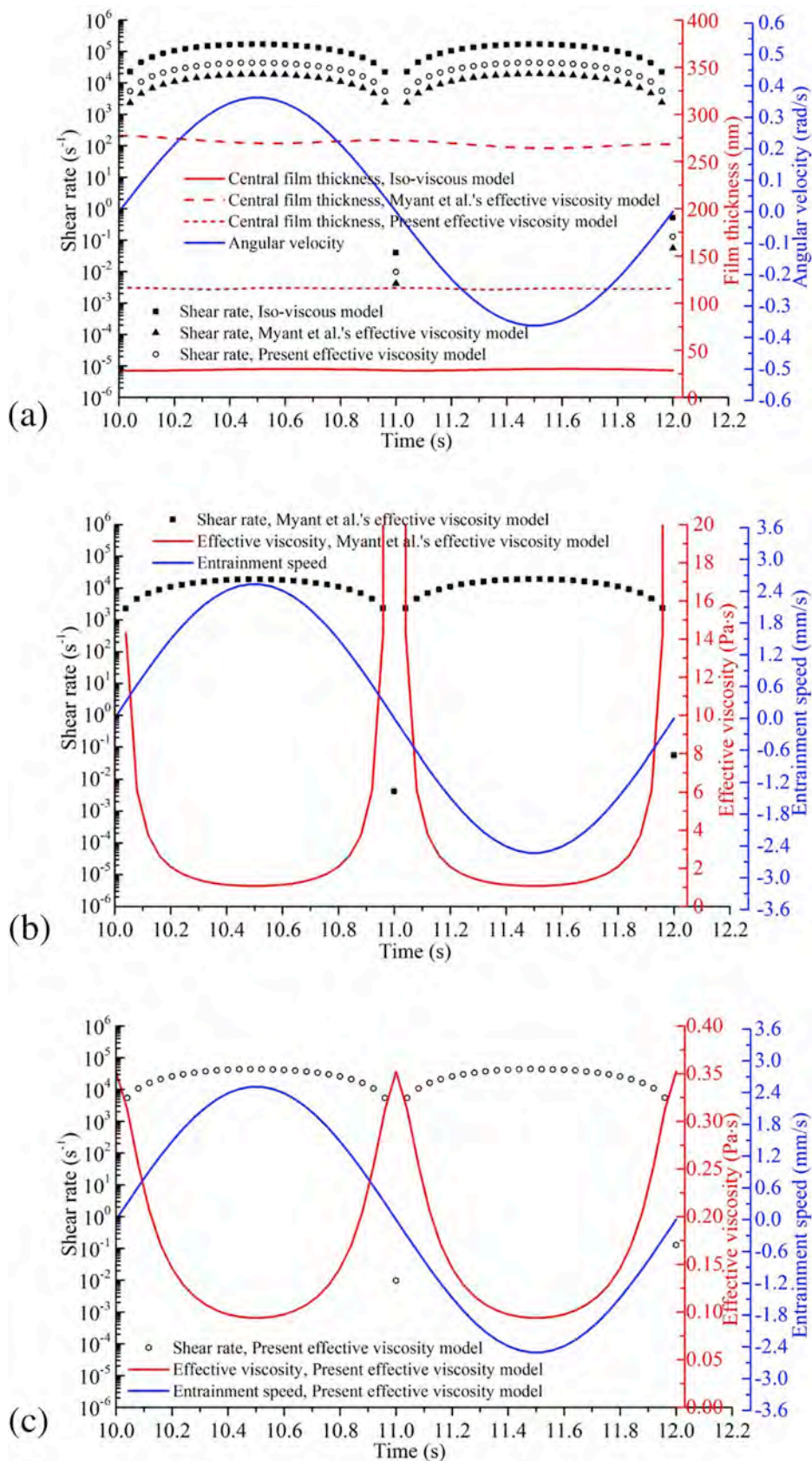


Fig. 10. The variation in the central film thickness and shear rate of the three viscosity models (the iso-viscous, the effective viscosity model proposed by Myant et al., and the effective viscosity model proposed in this study) with the angular velocity within one oscillation cycle ((a)). The variations in the entraining velocity, the shear rate, and the effective viscosity within one cycle of the effective viscosity models proposed by Myant et al. and this study ((b) and (c), respectively).

ball-in-socket geometry of hip replacements, these factors were also incorporated into the effective viscosity. Therefore, it is reasonable to believe that for bovine serum solution lubricants, this new effective viscosity equation can predict the transient lubrication film thickness of hip replacements more accurately.

Indeed, the central film thicknesses calculated using the new effective viscosity equation were much closer to the experimental measurements than those produced by the iso-viscous model and Myant et al.'s effective viscosity model (Figs. 7 and 9). Because only the effective viscosities of the first 3 s of the oscillation were used when the parameters in equation (7) were derived, the good agreement in the film thickness at the rest of time instants (from 3 s to 48 s) between the numerical analyses and the experimental measurements could be considered as the validation of the new effective viscosity equation. Moreover, the small difference (14%) between the numerical analyses and the experimental measurements could be improved by using more time instants to derive the parameters in equation (7).

Although the new effective viscosity equation was able to represent the higher viscosity lubricant caused by the gel-like protein phase, the real properties of the bovine serum and synovial fluid solution are more complicated than just a higher viscosity value. They usually tend to exhibit complex time-dependent film thickness behaviour [15], which is due to the particular properties of the bovine serum and synovial fluids solutions, such as viscoelasticity. In addition to the fluid film lubrication, a deposition of boundary film may also be formed on the contact surfaces of the hip replacements [38]. This boundary film appears to be nonhomogeneous and chaotic due to the complex multi-mode regimes of protein suspensions during sliding. Moreover, it has been observed that the gel-phase shows periodic characteristics when entrained into the contact area. The formed thick protein layer could be easily removed or disturbed by the scratches on the implant surface [15]. In addition to proteins, the bovine serum and synovial fluids also contain other compositions such as hyaluronic acid and phospholipids [21,39]. Therefore, although a new effective viscosity equation was proposed in this study, it is still an approximate description of the rheology of the bovine serum and synovial fluid solutions. To more accurately simulate the lubrication process of hip replacements, more sophisticated rheology models need to be developed to consider the above factors in future studies.

5. Conclusions

To validate the present full numerical lubrication models of hip replacements, the film thicknesses within the contact of a CoCr femoral head and a glass acetabular cup were numerically predicted by a computational model and experimentally measured by the optical interferometry method. A low-viscosity mineral-oil lubricant and a 25% bovine serum were used as the lubricants, respectively. Direct comparisons between the experimental measurements and numerical simulations were conducted for the film thickness. The main findings included:

- The current full numerical analyses for hip replacements could predict relatively accurate film thickness for the low-viscosity lubricant without macromolecular substances contained.
- The film thickness was not accurately predicted when both the iso-viscous model and the effective viscosity equation proposed by Myant et al. were used for the bovine serum solution.
- An new effective viscosity equation, incorporating the realistic geometry of hip replacements, transient effects, and the protein aggregation behaviour, was proposed for the bovine serum solution.

Declaration of competing interest

We are pleased to submit a manuscript titled "Towards the Direct Validation of Computational Lubrication Modelling of Hip Replacements" for your consideration as a research article. We declare that there is no conflict of interest in this article.

CRedit authorship contribution statement

Xianjiu Lu: Methodology, Software, Validation, Formal analysis, Investigation, Writing - original draft, Visualization. **David Nečas:** Methodology, Validation, Formal analysis, Investigation. **Qingen Meng:** Conceptualization, Formal analysis, Writing - review & editing, Supervision. **David Rebenda:** Methodology, Investigation. **Martin Vrbka:** Conceptualization, Project administration, Resources, Supervision, Funding acquisition. **Martin Hartl:** Resources, Funding acquisition. **Zhongmin Jin:** Conceptualization, Supervision, Project administration, Resources, Funding acquisition.

Acknowledgements

This study was carried out under the project LTAUSA17150 with financial support from the Ministry of Education, Youth and Sports of the Czech Republic. The research was also supported by National Natural Science Foundation of China [grant number 51323007].

References

- [1] Mattei L, Di Puccio F, et al. Lubrication and wear modelling of artificial hip joints: a review. *Tribol Int* 2011;44:532–49.
- [2] Liu F, Jin ZM, et al. Transient elastohydrodynamic lubrication analysis of a metal-on-metal hip implant under simulator-tested conditions. In: Proceedings CDROM of the sixth world congress on computational mechanics in conjunction with the second asian-pacific congress on computational mechanics, Beijing; 2004.
- [3] Dowson D. Elastohydrodynamic lubrication in 'soft-on-soft' natural synovial joints; 'hard-on-soft' cushion and 'hard-on-hard' metal-on-metal total joint replacements. Springer Netherlands; 2006. p. 297–308.
- [4] Jin ZM, Dowson D, et al. Analysis of fluid film lubrication in artificial hip joint replacements with surfaces of high elastic modulus. *Proc IME H J Eng Med* 1997; 211:247–56.
- [5] Meng QE, Liu F, et al. Contact mechanics and lubrication analyses of ceramic-on-metal total hip replacements. *Tribol Int* 2013;63:51–60.
- [6] Liu F, Jin ZM, et al. Importance of head diameter, clearance, and cup wall thickness in elastohydrodynamic lubrication analysis of metal-on-metal hip resurfacing prostheses. *Proc IME H J Eng Med* 2006;220:695–704.
- [7] Jalali-Vahid D, Jagatia M, et al. Prediction of lubricating film thickness in a ball-in-socket model with a soft lining representing human natural and artificial hip joints. *Proc IME J J Eng Tribol* 2001;215:363–72.
- [8] Liu F, Wang FC, et al. Steady-state elastohydrodynamic lubrication analysis of a metal-on-metal hip implant employing a metallic cup with an ultra-high molecular weight polyethylene backing. *Proc IME H J Eng Med* 2004;218:261–70.
- [9] Meng QE, Gao LM, et al. Contact mechanics and elastohydrodynamic lubrication in a novel metal-on-metal hip implant with an aspherical bearing surface. *J Biomech* 2010;43:849–57.
- [10] Meng QE. Elastohydrodynamic lubrication in metal-on-metal artificial hip joints with a spherical bearing surfaces and complex structures. PhD thesis. England: University of Leeds; 2010.
- [11] Dowson D, Hardaker C, et al. A hip joint simulator study of the performance of metal-on-metal joints. *J Arthroplasty* 2004;19:124–30.
- [12] Fan J, Myant CW, Underwood R, Cann PM, Hart A. Inlet protein aggregation: a new mechanism for lubricating film formation with model synovial fluids. *Proc IME H J Eng Med* 2011;225:696–709.
- [13] Mavraki A, Cann PM. Lubricating film thickness measurements with bovine serum. *Tribol Int* 2011;44:550–6.
- [14] Myant C, Underwood R, et al. Lubrication of metal-on-metal hip joints: the effect of protein content and load on film formation and wear. *J Mech Behav Biomed Mater* 2012;6:30–40.
- [15] Myant C, Cann P. In contact observation of model synovial fluid lubricating mechanisms. *Tribol Int* 2013;63:97–104.
- [16] Myant C, Cann P. On the matter of synovial fluid lubrication: implications for Metal-on-Metal hip tribology. *J Mech Behav Biomed Mater* 2014;34:338–48.
- [17] Myant CW, Cann P, et al. The effect of transient conditions on synovial fluid protein aggregation lubrication. *J Mech Behav Biomed Mater* 2014;34:349–57.
- [18] Vrbka M, Navrat T, et al. Study of film formation in bovine serum lubricated contacts under rolling/sliding conditions. *Proc IME J J Eng Tribol* 2013;227: 459–75.
- [19] Vrbka M, Krupka I, et al. In situ measurements of thin films in bovine serum lubricated contacts using optical interferometry. *Proc IME H J Eng Med* 2014;228: 149–58.
- [20] Mavraki A, Cann P. Lubricating film thickness measurements with bovine serum. *Tribol Int* 2011;44:550–6.
- [21] Fan J, Myant C, et al. Inlet protein aggregation: a new mechanism for lubricating film formation with model synovial fluids. *Proc IME H J Eng Med* 2011;225: 696–709.
- [22] Vrbka M, Nečas D, et al. Visualization of lubricating films between artificial head and cup with respect to real geometry. *Biotribology* 2015;1:61–5.

- [23] Nečas D, Vrbka M, et al. The effect of lubricant constituents on lubrication mechanisms in hip joint replacements. *J Mech Behav Biomed Mater* 2016;55: 295–307.
- [24] Nečas D, Vrbka M, et al. In situ observation of lubricant film formation in THR considering real conformity: the effect of diameter, clearance and material. *J Mech Behav Biomed Mater* 2017;69:66–74.
- [25] Essner A, Schmidig G, et al. The clinical relevance of hip joint simulator testing: in vitro and in vivo comparisons. *Wear* 2005;259:882–6.
- [26] Roelands C. Correlational aspects of the viscosity-temperature-pressure relationship of lubricating oils. Doctoral thesis. Technische Hogeschool te Delt; 1966.
- [27] Yao JQ, Laurent M, et al. The influences of lubricant and material on polymer/CoCr sliding friction. *Wear* 2003;255:780–4.
- [28] Liu F, Jin ZM, et al. Transient elastohydrodynamic lubrication analysis of metal-on-metal hip implant under simulated walking conditions. *J Biomech* 2006;39: 905–14.
- [29] Jin ZM, Dowson D. A full numerical analysis of hydrodynamic lubrication in artificial hip joint replacements constructed from hard materials. *Proc IME C J Mech Eng Sci* 1999;213:355–70.
- [30] Jagatia M, Jin ZM. Elastohydrodynamic lubrication analysis of metal-on-metal hip prostheses under steady state entraining motion. *Proc IME H J Eng Med* 2001;215: 531–41.
- [31] Meng QE, Gao LM, Liu F, et al. Transient elastohydrodynamic lubrication analysis of a novel metal-on-metal hip prosthesis with an aspherical acetabular bearing surface. *J Med Biomechanics* 2009;24:352–62.
- [32] Wang FC, Jin ZM. Prediction of elastic deformation of acetabular cups and femoral heads for lubrication analysis of artificial hip joints. *Proc IME J J Eng Tribol* 2004; 218:201–9.
- [33] Hartl M, Krupka I, et al. Thin film colorimetric interferometry. *Tribol Trans* 2001; 44:270–6.
- [34] Nečas D, Vrbka M, et al. In situ observation of lubricant film formation in THR considering real conformity: the effect of model synovial fluid composition. *Tribol Int* 2018;117:206–16.
- [35] Cross MM. Rheology of non-Newtonian fluids: a new flow equation for pseudoplastic systems. *J Colloid Sci* 1965;20:417–37.
- [36] Glovnea RP, Spikes HA. The influence of lubricant properties on EHD film thickness in variable speed conditions. *Tribol* 2003;43:401–8.
- [37] Gao L, Yang P, Dymond I, Fisher J, Jin Z. Effect of surface texturing on the elastohydrodynamic lubrication analysis of metal-on-metal hip implants. *Tribol Int* 2010;43:1851–60.
- [38] Malmsten M. Formulation of absorbed protein layers. *J Colloid Interface Sci* 1998; 20:186–99.
- [39] Cooke AF, Dowson D, Wright V. The rheology of synovial fluid and some potential synthetic lubricants for degenerate synovial joints. *Eng Med* 1978;7:66–72.

LUBRICATION OF KNEE JOINT REPLACEMENTS

The number of TKRs has been continuously increasing, while roughly two million knee surgeries are performed annually [144]. Moreover, an enormous increase of TKAs by 2050 is expected in the USA [145] and most probably also in other developed countries. Knee replacements usually exhibit a longer service life than hips. Based on the data available from registries, nearly 80% of implants survive for 25 years [9],[146]. Such longevity might be considered to be enough for most patients. However, it must be emphasized that the number of young patients undergoing THA has been increasing substantially [7], while young people are more likely to experience implant failure [147].

Although aseptic loosening as a sign of periprosthetic osteolysis has been still responsible for most of the reported failures [148], the reasons for revision have gradually changed since the introduction of HXLPE [136],[137]. While it is generally considered that HXLPE produces less wear than non-XLPE [149], the amount of wear particles is not always necessarily lower [150]. Besides, evident surface damage of retrieved implants was also observed in the case of HXLPEs [151],[152]. Finally, although some investigations reported decreased biological activity of HXLPE particles [153],[154], the reduced inflammatory and osteolytic potential remains uncertain [155],[156], while the fact that HXLPE produces a higher proportion of very small particles must be taken into account [157].

Although the incidence of TKA is comparable to THA, the number of studies exploring lubrication mechanisms in knee replacements is remarkably lower. Some numerical investigations suggest that the conclusions derived for hips may be transferred to knees. However, even though the used materials and wear damage mechanisms are comparable [151],[158],[159], there are evident contrasts in wear rates [160]. Moreover, the differences in design, kinematic, and loading parameters need to be considered. Furthermore, the gait cycle parameters were found to be one of the factors influencing the wear rate of the knee prosthesis [161]. To conclude, it is evident that TKR represents a unique system, which deserves greater attention of both numerical modelling and experimental investigations.

4.1 Numerical investigations

Up-to-date, only around ten numerical investigations focused on the lubrication of knee replacements have been published. The pilot studies were given by Tandon and Jaggi [162],[163] approximately forty years ago. Nevertheless, the numerical analyses were somewhat limited at that time in terms of geometry, kinematics, and load. The authors proposed an idealised model finding improved load carrying capacity with increasing viscoelastic parameter representing increased HA concentration in SF. Besides, it was found that a slip velocity within the joint has a substantial impact on its function. The EHL-based model for predicting transient film thickness in the knee implant with a compliant layer under simulated walking conditions was presented by Jin et al. [164]. The authors adopted a simplified ellipsoid-on-plane model considering circular, longitudinal, and transverse conjunctions (see Fig. 38). The results showed that the contact geometry has a considerable influence on fluid film formation. The maximum predicted film thickness was achieved for transverse conjunction. In that case, the semi-minor radius of the contact ellipse is aligned with the entrainment direction. Another advantage of this conjunction was in the elimination of contact starvation due to small stroke length. These findings were in qualitative agreement with the first experimental investigation described below. The authors also highlighted the overall positive role of increased contact conformity. The suggestion was later supported by Pascau et al. [165], who observed the benefit of conformity mainly during the early stance phase of the walking cycle when the implant operates in a mixed regime.

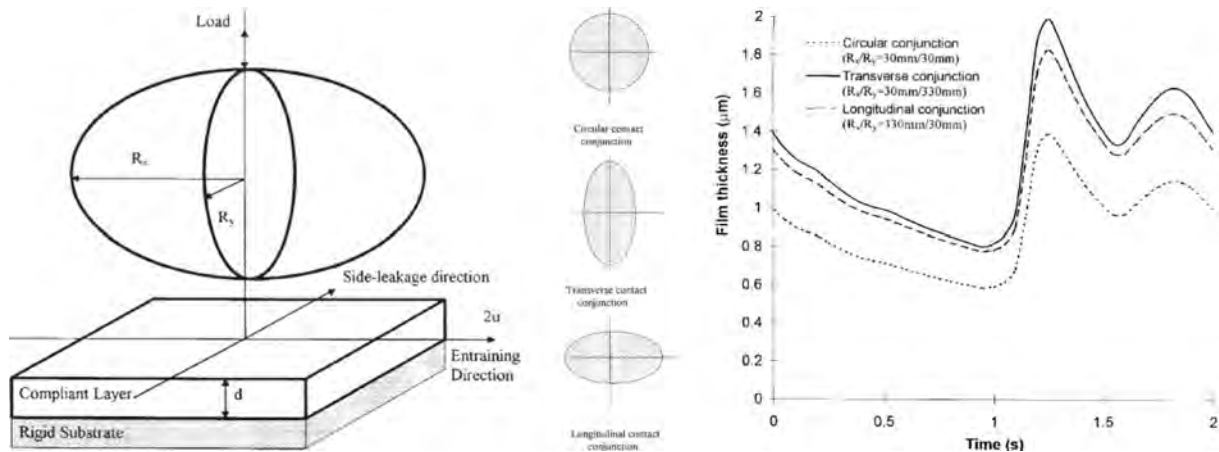


Figure 38: Ellipsoid-on-plane model (left); various considered contact conjunctions (middle); development of film thickness during the cycle (right). The figure was partially modified and reprinted based on [164].

Subsequently, Di Paolo and Berli [166] proposed a steady-state EHL numerical model based on a modified Reynolds equation, including non-Newtonian behaviour of the lubricant and simplified calculation of elastic deformations. The contact of the metal part and the compliant UHMWPE layer in cylinder-on-plane setup was investigated. The attention was focused on the effect of material properties towards enhanced lubrication. The simulation results showed that conventional PE is too rigid, disabling the formation of sufficient lubricant film protecting the contact surfaces. Thus, it is suggested that using a porous compliant layer instead of the standard

tibial component would positively impact the overall tribological performance, enhancing lubrication and lowering friction and wear. A further investigation simulated an oscillating rolling/sliding tribological test, considering the line contact of the two opposing cylinders from CoCr and UHMWPE [167]. Elasticity equation coupled with time-dependent Reynolds equation was solved using the MG method with full approximation and N-R approach for a highly nonlinear system solution. The simulation showed that the predicted film thickness is small throughout the oscillating cycle, indicating the prevalent mixed lubrication regime. Zero film was detected at the ends of the cycle, suggesting the presence of boundary lubrication. The authors further improved the proposed model, including non-Newtonian behaviour of the lubricant based on the Carreau model [168]. Various effects, such as material, load, kinematics, and fluid parameters, were investigated. In accordance with previous work [166], a positive impact of a softer material on film thickness was observed. An important implication of the paper is in the lower film thickness for non-Newtonian lubricant, limiting the analyses performed with Newtonian isoviscous fluids.

An improvement in numerical studies dealing with TKR is attributed to Su et al. [169],[170]. The authors introduced a complete time-dependent EHL analysis using the MG finite-difference approach for the Reynolds equation solution, coupled with the constrained column model for calculating elastic deformations. Physiological loading and motion conditions in terms of time-variable axial load, FE rotation, and anterior-posterior (AP) translation were considered. An ellipsoid-on-plane model with a finite thickness of the UHMWPE tibial layer was adopted. It was shown that the squeeze film action considerably affects the fluid film formation during the stance phase, while the entrainment velocity fundamentally affects the lubrication in the swing phase. In compliance with previous findings, it is concluded that specific design parameters may contribute to reduced pressure and enhanced lubrication conditions. Specifically, increased joint conformity combined with a thicker tibial inlay of lower elastic modulus was beneficial. Although the model substantially extended previous works, the simulation suffered from the Newtonian isoviscous lubricant. Therefore, a substantial contribution to the field was later achieved by Gao et al. [171], despite the paper was mainly focused on wear modelling of metal-on-UHMWPE pair. A more appropriate ball-in-socket model was developed while shear-thinning behaviour of the lubricant using a Cross model was involved. The authors analysed both knee compartments separately, while the respective forces and motions were applied. The simulation was running until stabilised wear was reached. After the running-in phase, a larger lubricated contact area was achieved, which led to improved lubrication associated with flattened pressure distribution and lower maximum pressure. The effect of surface texturing of the tibial component was also analysed in the study. While it was found that an appropriate texture design may improve the lateral condyle's performance, the influence was somewhat negative for the medial compartment.

4.2 Experimental investigations

While the number of numerical studies related to lubrication of TKRs is much lower than that of THRs, even fewer experimental papers were published yet. The pilot investigation performed

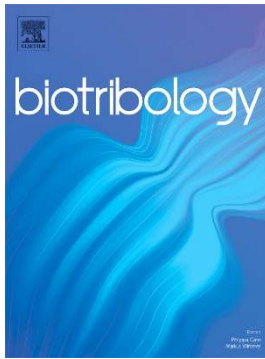
by Ohtsuki et al. [172] aimed at the measurement of surface separation in a simplified configuration between a metal ball and a conductive silicone rubber layer representing the tibial component. The film thickness of silicone oil was measured using an electrical resistance method. The lubrication ability of three different geometric conjunctions, i.e. circle, longitudinally long ellipse, and transversely long ellipse, was studied. The results revealed that the transverse geometry enhances surface separation, which was later confirmed by means of numerical modelling [164]. Later, Flannery et al. [58],[173] carried out a comprehensive tribological TKR assessment. Concerning lubrication, a protective function of proteins adsorbed on the surfaces led to a lower rate, despite a higher friction coefficient. Similar behaviour of solid-like adhered film was previously reported by Scholes et al. [56], who studied a unicondylar knee implant.

4.3 Author's contribution to the field

Based on the above overview, it may be seen that the knowledge of TKR lubrication is doubtlessly insufficient. Most of the numerical studies failed to include realistic rheological behaviour of the biological lubricants. Besides, only the sole experimental investigation focused on the measurement of film thickness was carried out. However, the authors employed the method exhibiting lower accuracy, while the experiments were realised in a simplified geometry, and the contact was lubricated by silicone oil instead of SF or BS. Concerning the implications related to the importance of contact conformity, measurements in real geometrical configurations should be of particular interest.

The author of the habilitation thesis published four papers introducing a complex investigation of lubrication mechanisms within TKR. The first study (i) is considered to be a pilot paper introducing a newly developed knee joint simulator allowing for direct in situ observation of TKR contact considering real contact conformity. The following study (ii) focused on the interaction of proteins in SF and its impact on knee lubrication. Besides, a detailed description of the contact zone migration throughout the cycle is presented. The third study (iii), which is the Part I of the investigation, was based on the use of multiple lubricants towards the detailed description of film formation, aiming at the role of specific SF constituents. The theoretical illustrative lubrication model was introduced based on the detailed experimental analysis. Furthermore, the differences in lubrication of the lateral and medial compartment were assessed. The effect of continuous load on the film thickness was also observed. The last paper (iv), representing Part II of the two-part study, introduced the development of the fully-coupled 3D model for soft-EHL contact solution based on the generalised Reynolds equation and FEM. The numerical data were compared with the experimental results published in Part I. Further, the influence of fluid rheology, geometry, and transient kinematic and loading effects are presented.

All the papers were published in peer-reviewed journals (one is published in Scopus database and the rest three are published in journals with IF in WoS). The list of the included papers is as follows:



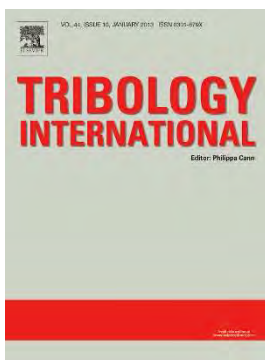
[174] Nečas, D., Sadecká, K., Vrbka, M., Gallo, J., Galandáková, A., Křupka, I., Hartl, M., 2019. Observation of lubrication mechanisms in knee replacement: A pilot study. Biotribology 17, 1-7.

Author's contribution (BUT): = 50%
Journal metrics (CiteScore₂₀₁₇): = 4.10
Citations (Google Scholar): = 2 (excl. self-citations)



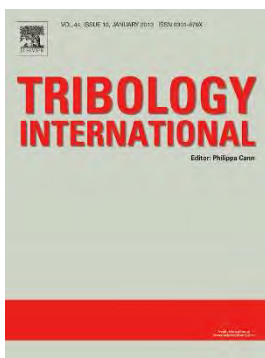
[175] Nečas, D., Sadecká, K., Vrbka, M., Galandáková, A., Wimmer, M.A., Gallo, J., Hartl, M., 2021. The effect of albumin and γ -globulin on synovial fluid lubrication: Implication for knee joint replacements. Journal of the Mechanical Behavior of Biomedical Materials 113, 104117.

Author's contribution (BUT): = 50%
Journal metrics (IF₂₀₁₉): = 3.37 (IF₂₀₂₁ is not yet available)
Citations (Google Scholar): = 0



[176] Nečas, D., Vrbka, M., Marian, M., Rothhammer, B., Tremmel, S., Wartzack, S., Galandáková, A., Gallo, J., Wimmer, M.A., Křupka, I., Hartl, M., 2021. Towards the understanding of lubrication mechanisms in total knee replacements – Part I: Experimental investigations. Tribology International 156, 106874.

Author's contribution (BUT): = 75%
Journal metrics (IF₂₀₁₉): = 4.27 (IF₂₀₂₁ is not yet available)
Citations (Google Scholar): = 0



[177] Marian, M., Orgeldinger, C., Rothhammer, B., Nečas, D., Vrbka, M., Křupka, I., Hartl, M., Wimmer, M.A., Tremmel, S., Wartzack, S., 2021. Towards the understanding of lubrication mechanisms in total knee replacements – Part II: Numerical modeling. Tribology International 156, 106809.

Author's contribution (BUT): = 80%
Journal metrics (IF₂₀₁₉): = 4.27 (IF₂₀₂₁ is not yet available)
Citations (Google Scholar): = 0

4.3.1 Observation of lubrication mechanisms in knee replacement: A pilot study

The first paper introduces a novel approach for the investigation of lubrication in TKR. A new knee simulator was developed, enabling to apply transient kinematic and loading conditions according to ISO standards. The contact is formed between the original CoCrMo femoral

component and the tibial insert of the actual geometry from PMMA. PMMA is used to enable direct optical observation of the contact. The insert is made by micro-machining based on the digital model obtained using reverse engineering by scanning the original UHMWPE insert and processing the digital model. The fluorescent measurement method is implemented to the simulator, while the used lubricants are fluorescently stained. Only the lateral compartment was observed in the first article.

The contact was lubricated by simple albumin and γ -globulin solutions and by the mixture of both proteins. As this was a pilot study, simplified conditions were applied, as shown in Fig. 39. While FE ranged from 0° to 58° as recommended by the standards, IE rotation and AP translation were disabled. The load varied between 270 N and 310 N, resulting in maximum contact pressure of 36 MPa, which corresponds to the physiological range. The applied load is generally lower than given by the norms for testing; however, the difference in mechanical properties of UHMWPE and PMMA needs to be taken into account. Therefore, the normal load was set based on the resulting pressure level. The test lasted three minutes at a lowered frequency of 0.5 Hz.

Simple solutions showed that albumin forms a much thicker lubricating layer; however, the film tends to decrease continuously after reaching the maximum. In contrast, γ -globulin layer was thinner but very stable, indicating the formation of a boundary protein film. When the mixtures were applied, it was found that the overall intensity of albumin protein decreased. Nevertheless, the film was stabilised, i.e. the decreasing tendency observed for the simple solution was no more present. Focusing on γ -globulin intensity when the mixture was applied, the film was slightly thicker, indicating a positive role of albumin on film formation. The contact was further observed during various phases of the cycle, revealing that the contact zone substantially migrates and that its shape is changed. This behaviour is attributed to the variable geometry (radii) of the compartment. The overall research scheme of the study is shown in Fig. 39.

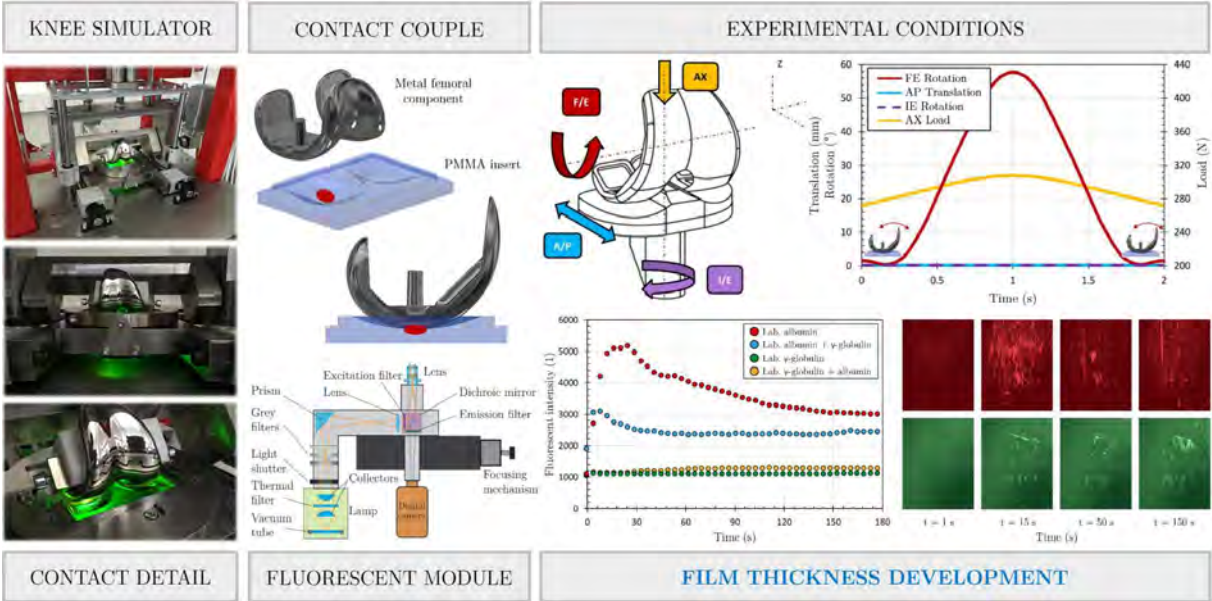


Figure 39: Research scheme of the study [174].

4.3.2 The Effect of Albumin and γ -globulin on Synovial Fluid Lubrication: Implication for Knee Joint Replacements

The subsequent paper aimed at a deeper understanding of the lubrication processes in TKR using the introduced experimental procedure. Greater attention was also paid to the analysis of contact migration during the cycle. Furthermore, the differences in the adsorbed film at the beginning and the end of the test were assessed. The contact was observed in the initial and maximally deflected FE position. Finally, the paper provided a detailed analysis of the potential limitations of the developed approach based on the use of PMMA insert, focusing on the issue of contact processes, surface roughness, wettability, or physical properties. Following the experience from the previous study, the simulator was further improved, allowing to increase the cycle frequency to 0.75 Hz. More complex SFs were applied (see Tab. 7), containing HA and PLs besides.

Lubricant no.	Albumin	γ -globulin	Hyaluronic acid	Phospholipids	Total concentration
Fluorescently labelled albumin					
1	24.9 mg/ml	–	–	–	24.9 mg/ml
2	24.9 mg/ml	6.1 mg/ml	–	–	31 mg/ml
3	24.9 mg/ml	6.1 mg/ml	1.49 mg/ml	0.34 mg/ml	32.83 mg/ml
Fluorescently labelled γ-globulin					
4	–	6.1 mg/ml	–	–	6.1 mg/ml
5	24.9 mg/ml	6.1 mg/ml	–	–	31 mg/ml
6	24.9 mg/ml	6.1 mg/ml	1.49 mg/ml	0.34 mg/ml	32.83 mg/ml
Fluorescently labelled albumin + γ-globulin					
7	24.9 mg/ml	6.1 mg/ml	1.49 mg/ml	0.34 mg/ml	32.83 mg/ml

Table 7: The summary of the applied test lubricants showing the combinations of labelled and non-labelled constituents [175].

The investigation showed clear interactions between SF constituents, confirming the implications obtained from the analysis of THRs. When focusing on albumin-based solutions, simple protein formed the thickest layer, while the addition of γ -globulin had a somewhat negative effect. However, HA and PLs addition was positive. Concerning γ -globulin behaviour, a similar tendency was observed, while HA and PLs had a stabilising impact. Throughout the cycle, the shape of the contact zone changes from a longitudinal, through a circle, to transverse conjunction. The time effect was also found to have a meaningful impact, since the amount of adsorbed proteins exhibited a continuous increase over time, as can be seen in Fig. 40.

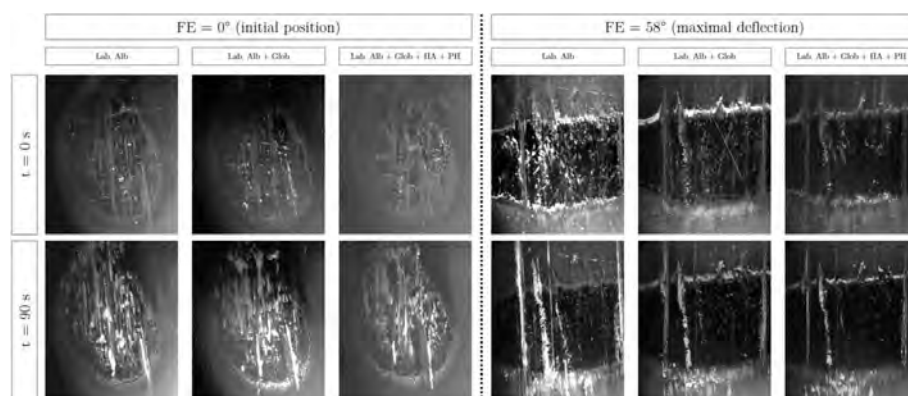


Figure 40: Fluorescent images of TKR contact taken at the beginning and the end of the test in two different FE positions for albumin-based solutions [175].

4.3.3 Towards the Understanding of Lubrication Mechanisms in Total Knee Replacements – Part I: Experimental Investigations

The last two papers in the field were published as the two-part study. Part I deals with a comprehensive experimental investigation. The detailed evaluation of the effect of lubricant composition and the load was carried out. The experiments were realised under ISO-recommended frequency of 1 Hz and realistic transient operating conditions. In addition to previous papers, both compartments were studied. The impact of interrupted loading on the lubricant film was further assessed.

The measurements were initially carried out under lubrication of low-viscosity mineral oil, allowing for direct comparison of the experimental data and predictions based on the numerical model developed within Part II. In this case, six different positions throughout the cycle were observed at both condyles. Subsequently, the same lubricants as in the case of hard-on-soft hip implants (see Tab. 5) were used to clarify the formation of the lubricating film, focusing on the role of specific constituents under transient conditions. In that phase of observation, attention was paid to the point of maximum load.

The results showed a very satisfactory qualitative agreement of empirical and numerical data. Regardless of the compartment, the results correlated for most of the observed locations, as is shown in Fig. 41. The compliance was considered as a proof of model/experiment reliability. The investigation of the role of the constituents revealed that γ -globulin forms a stable layer, which is reinforced by the presence of HA and PLs. On the contrary, simple albumin exhibited

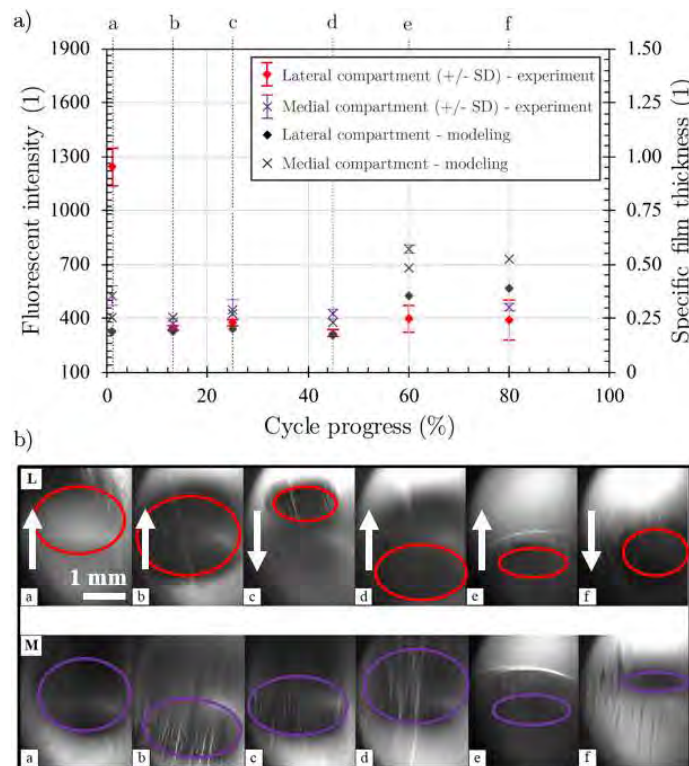


Figure 41: Comparison of experimental and predicted film thickness for the lateral and the medial compartment (a); respective contact images (b) [176].

limited adsorption ability. However, once the γ -globulin-based boundary film is formed, the albumin thickness increases, resulting in an increased overall tendency. Based on the experimental observation, a novel illustrative theoretical lubrication model was proposed in the study. When focusing on the behaviour of the medial and lateral compartment, it was found that the medial part suffers from worse lubrication conditions. This fact is attributed especially to the higher load. The finding corresponds with surgeons' observations during revision surgeries, confirming that the damage of the medial condyle of the tibial insert is usually more extensive.

Finally, the load-lasting effect was found to have a substantial impact on the film thickness. It was revealed that persisting load leads to thinning of the lubricant layer. Therefore, interrupted walking is recommended to enable film recovery, protecting the rubbing surfaces. The repetition test was finally carried out, finding overall excellent repeatability for both compartments and two different protein solutions. The proposed methodology is considered to be a handy tool for preclinical evaluation of knee implants. The fluorescent method enables examination of any material of the femoral component. The only limitation is in the necessity of a transparent counterface. The overall research scheme of the study is shown in Fig. 42.

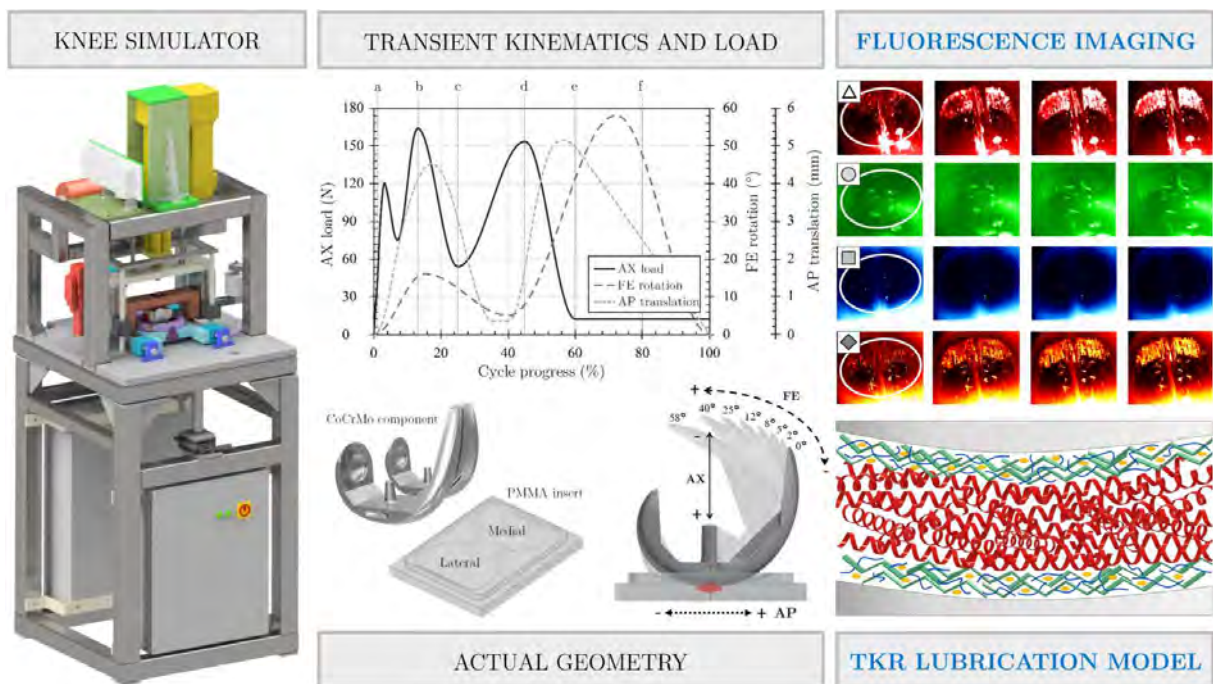


Figure 42: Research scheme of the study [176].

4.3.4 Towards the Understanding of Lubrication Mechanisms in Total Knee Replacements – Part II: Numerical Modeling

The second part of the study introduces a numerical model for predicting film thickness in TKR. The model is based on a full-system approach built upon FEM adopted to solve the soft-EHL problem. A three-dimensional and time-transient Reynolds equation were coupled with the elastic deformations of one equivalent body considering a ball-on-plane configuration. The velocity,

integral parameters, and thermal equations were coupled iteratively within the global solution scheme. Therefore, shear-thinning and thermal effects were also considered. Besides, cavitation effects were involved using a mass-converging algorithm, and mixed lubrication effects were captured via a load-sharing concept based on the Greenwood-Williamson model. The movements and loads depending on the radii of the model as a function of the FE angle represent the model inputs. Therefore, the developed model enables to include (i) non-Newtonian lubricant behaviour, (ii) SF viscosity, (iii) thermal effects, (iv) transient squeeze film effects, (v) implant geometry in terms of radius and thickness of the tibial insert in combination with (vi) relevant lubrication mechanisms. The model was applied to investigate the impact of various parameters, focusing on the prediction of contact pressure and film thickness.

The simulation showed that the medial compartment is exposed to higher contact pressure, resulting in smaller film thickness, suggesting the increased risk of surface asperity contact. The overall lubricant film decreased during the stance phase due to the combined action of geometry and load. In contrast, film formation in the swing phase was driven by geometry and kinematics. In general, turning points with zero speed substantially affected the lubrication performance. Therefore, it is concluded that especially the medial compartment may suffer from more extensive damage during the stance phase and reversing.

In addition to kinematics, geometry and load, the rheological properties of the SF had a considerable impact on film formation. This remark needs to be taken into account following the fact that the composition of SF of individual patients substantially differs. Therefore, the specific fluid composition may lead to diverse tribological conditions from full surface separation to predominant surface asperity contact, endangering the lifespan of the implant. It needs to be noted that the proposed model is based on the use of commercial FEM software. Since the guideline for the model implementation is provided per request, it is expected that the solution may support further development of implants, allowing for a quick and relevant assessment of the tribological performance including specific geometry and patient-specific factors. The overall research scheme of the study is shown in Fig. 43.

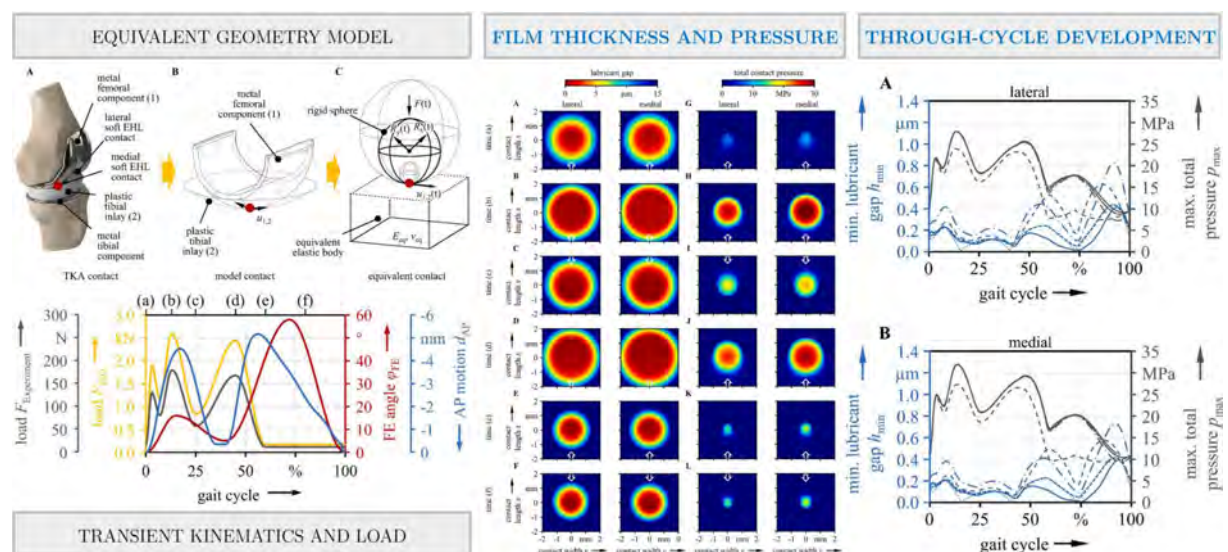


Figure 43: Research scheme of the study [177].



Observation of lubrication mechanisms in knee replacement: A pilot study

D. Nečas^{a,*}, K. Sadecká^a, M. Vrbka^a, J. Gallo^b, A. Galandáková^c, I. Křupka^a, M. Hartl^a

^a Faculty of Mechanical Engineering, Brno University of Technology, Czech Republic

^b Department of Orthopaedics, Faculty of Medicine and Dentistry, Palacky University Olomouc, University Hospital Olomouc, Czech Republic

^c Faculty of Medicine and Dentistry, Palacky University Olomouc, Czech Republic



ARTICLE INFO

Keywords:

Knee replacement

Lubrication

Proteins

Fluorescence

ABSTRACT

The present study introduces a unique experimental approach for in situ observation of lubricant film formation in knee joint replacements. A knee joint simulator was designed and equipped with optical module based on fluorescent optical method for film thickness observation. The contact between the femoral knee metal implant and real-shaped polymer insert mimicking actual contact nature is observed. The shape of the polymer insert was fabricated with respect to the shape of original polyethylene insert to ensure corresponding contact conformity. Simple solutions of albumin and γ -globulin proteins as well as its mixture were used while the film thickness was studied as a function of time considering simplified flexion/extension motion with variable load over the cycle. Adequate fluorescent markers were employed enabling to observe one particular protein during each measurement. The results showed a clear importance of the interaction of proteins since the mixtures showed different results compared to simple solutions. Especially considering albumin protein, its behaviour was substantially affected by adding γ -globulin. Moreover, a satisfactory compliance with previous findings related to hip joint lubrication in terms of the behaviour of both proteins was found. Finally, the motivation for future experimental work is highlighted.

1. Introduction

Total knee arthroplasty (TKA) has become a routine surgical technique for patients suffering from osteoarthritis. According to Health at a Glance: OECD Indicators report [1], 126 operations per hundred thousand inhabitants were performed in 2015. Considering the implant design, some new approaches have been proposed such as metal-free knee implant [2], oxinium knee implant [3], or post-cam design together with multilayer coating known as VEGA [4]. Nevertheless, despite the promising preliminary results, the implant consisting of metal tibial and knee component with polyethylene (PE) insert persists as the most common type of knee replacement [3].

When focusing on the durability of TKA, aseptic loosening, instability and prosthetic joint infection are recognized as the main reasons for reoperations [5,6]. Since aseptic loosening is associated with release of wear particles, it is apparent tribological processes substantially affect the condition of implant. Previously, the main attention of researchers was paid to the evaluation of wear rate and/or friction adopting both commercial and tailor-made simulators [7–11]. However, only a limited attention was paid to the lubrication mechanisms which play an important role as suggested in literature [12].

Following references dealing with lubrication of knee replacements

by means of numerical simulations were introduced [13–19]. The pilot study was given by Tandon and Jaggi [13] who proposed an idealized model considering the viscoelastic parameter of the lubricant to capture the increased load capacity caused by an increased concentration of hyaluronic acid (HA) in synovial fluid (SF). The study was subsequently extended by the same authors focusing on the calculation of wear rate, load capacity, and approaching time of the opposing surfaces [14]. It was found that the slip velocity plays an important role regarding the self-adjusting nature of the joint. Later, Jin et al. [15] simulated a walking cycle based on elastohydrodynamic lubrication (EHL) theory using simplified ellipsoid-on-plane numerical model. The authors predicted a transient lubricating film thickness in knee prostheses considering compliant layer between the implant surfaces. A substantial effect of contact geometry on fluid film lubrication was found while the maximum film thickness is expected when contact area of a transverse conjunction is maximized. A minimized risk of starvation due to small stroke is discussed as an another advantage. The published results were in a good qualitative agreement with the experimental investigation given by Ohtsuki et al. [16]. The authors investigated the contact of steel ball and tibial component represented by silicone rubber layer. Degree of separation based on the electrical resistance technique was measured; concluding that ability of fluid film formation was higher in

* Corresponding author.

E-mail address: david.necas@vut.cz (D. Nečas).

the case of transverse geometry compared to longitudinal one.

In a further numerical study given by Mongkolwongrojn et al. [17], a point contact was considered when predicting both film thickness and pressure distribution as a function of load, speed, material and lubricant properties. It was shown that the film thickness during the first cycle is always lower due to time required for film development. In the following cycles, the film is similar and dependent on loading and kinematic conditions related to human motion. Subsequently, Su et al. [18], performed time-dependent EHL analysis of knee implant considering transient loading and kinematic conditions respecting normal walking. As in some previous cases, ellipsoid-on-plane model was adopted. It was found that under the combined effect of squeeze-film and entraining action, the central film thickness decreases during the stance phase. On the contrary, during the swing phase, the film is kept relatively thick. Recently, Gao et al. [19] focused on the numerical prediction of wear and lubrication using ball-on-socket model. For the first time, the authors compared non-textured surface with micro-dimpled surface. Medial and lateral knee compartments were investigated finding that lateral compartment may benefit if the dimples are carefully designed; however, no advantage was found for medial compartment.

Apparently, there is very limited knowledge in terms of experimental investigation of lubrication in knee joint replacements. Nevertheless, some assumptions can be defined based on the lubrication of hip prosthesis, which have been extensively in recent years. In particular, it was found that contact conformity plays a key role while better compliance of the surfaces ensures better lubrication performance [20]. Later, focusing on the effect of constituents of SF, a clear effect of HA and HA and phospholipids was observed [21]. Focusing on the role of individual fluid components, fluorescent optical method was introduced and successfully validated examining the formation of albumin and γ -globulin lubricant film [22]. The method was recently adopted when investigating the lubrication mechanisms within hard-on-soft bearing surfaces [23]. As the results enabled clear explanation of film formation, the same method is used in the present study.

Based on the above references, it can be assumed that only a limited attention was paid to the lubrication of knee joint replacement. Most of the so far published studies are numerical, while some level of simplification in terms of geometry or lubricant behaviour is necessary in such case. The limitations of numerical simulations and the need of experimental validation was mentioned by Gao et al. [19]. Moreover, some effects such as protein adsorption or agglomeration cannot be considered in the models at all. Since the impact of lubrication on friction and wear is indisputable, the motivation of the performed study is to develop a methodology for in situ film thickness observation in knee replacement considering real geometry of rubbing surfaces.

2. Materials and Methods

The experiments were carried out using the knee joint simulator enabling to apply transient loading and kinematic conditions. In general, flexion/extension (F/E), anterior/posterior (A/P) translation, internal/external (I/E) rotation, and axial (AX) load can be controlled. Nevertheless, since this is a pilot study, simplified kinematic and loading conditions were applied, as is shown in Fig. 1. The F/E range was from 0° to 58° which corresponds to ISO 14243-3:2014 standard for wear testing of knee prosthesis while AX load varied from 270 N to 310 N. A/P translation as well as I/E rotation were fixed. The contact is realized between the real femoral knee implant component and transparent counterface insert enabling direct in situ observation. The optical module is mounted in an inverted arrangement and is composed of halogen illuminator, fluorescent microscope, high-speed camera, and PC. The model of the test device with the detail of the contact couple is displayed in Fig. 2. Photos of the contact zone illuminated by mercury lamp are shown in Fig. 3.

The contact bodies are represented by original CoCrMo femoral knee component (cruciate retaining implant, Zimmer Biomet) and the

insert made from transparent poly(methyl) methacrylate (PMMA). PMMA was chosen since its mechanical properties are relatively close to conventionally used PE. However, PE is not transparent so the direct observation of the contact is not possible. The shape of the PMMA insert corresponds to real PE tibial plateau. The original geometry was obtained using 3D optical scanning method [24]. Subsequently, the sample was manufactured by micro-chip machining technology using computer numerical control shape generator. Single point diamond turning (SPDT) method was applied enabling to reach the accuracy equal to fractions of nm. Surface topography was evaluated using 3D optical profilometer based on phase shifting interferometry. The R_a parameter of both the contact surfaces is similar varying from 6 nm (average value for PMMA insert) to 10 nm (for femoral knee component). The elastic modulus and Poisson's ratio of metal alloy and PMMA are as follows: $E_{\text{metal}} = 230 \text{ GPa}$, $\nu_{\text{metal}} = 0.28$; $E_{\text{PMMA}} = 4 \text{ GPa}$, $\nu_{\text{PMMA}} = 0.37$. It should be noted that elastic constants of ultra-high molecular weight polyethylene (UHMWPE) are approximately $E_{\text{UHMWPE}} = 700 \text{ MPa}$, $\nu_{\text{UHMWPE}} = 0.35$, respectively.

Due to the nature of PMMA which is poorly reflective and is not conductive, routine techniques such as optical interferometry [21] or electrical resistance method [16] could not be applied. Therefore, the fluorescent microscopy method was implemented [22]. The method was recently successfully validated when examining the lubrication mechanisms within hard-on-soft hip replacements where the same materials (metal vs. PMMA) were considered [23]. The evaluation of film thickness is based on the observation of fluorescent intensity as a function of time. It was previously proved in literature that the intensity is proportional to the layer of the lubricant [25]; therefore, the intensity is considered as a dimension-less film thickness. It means that the higher intensity corresponds to higher film thickness and vice versa. Therefore, based on the detected fluorescent emission, it is possible to assess the development of lubricant layer between the surfaces. Although the specific proteins were fluorescently stained, it is apparent that the proteins are uniformly distributed in the base fluid. It means that the whole fluid appear to be dyed. This is the reason why thickness of albumin/ γ -globulin layer throughout the observed zone could be detected. To determine the overall film thickness, both the proteins would have to be fluorescently stained at the same time.

It should be emphasized that the quantitative film thickness could not be evaluated due to some limitations discussed in a detail in previous study [23]. However, the particular value of film thickness is not decisive, as the laboratory investigation can hardly involve all the processes occurring within the body. Nevertheless, the trend of film thickness development as well as the understanding of the interaction of the SF constituents is of a great importance when clarifying the lubrication mechanisms between knee articulating surfaces.

To verify the designed methodology and to capture the mutual influence of SF constituents, various proteins solutions were used as the test lubricants. Initially, simple solutions of bovine serum albumin (A2153, Sigma-Aldrich) and γ -globulin from bovine blood (G5009, Sigma-Aldrich) were applied. The proteins were fluorescently stained in order to determine its role in film formation process. Albumin was stained by Rhodamine-B-isothiocyanate (283,924, Sigma-Aldrich) and γ -globulin was doped by Fluorescein-isothiocyanate (F7250, Sigma-Aldrich). The proteins were initially dissolved in phosphate-buffered saline (PBS). Subsequently, the proteins were mixed together. In each specific measurement, only one of the proteins was doped by corresponding fluorescent marker. This approach allows to determine the mutual interaction of the constituents enabling to determine the role of specific proteins in film formation process. The lubricants are summarized in Table 1. The overall volume of the test lubricant was 4 ml ensuring fully flooded conditions at the beginning of the test. To avoid any inaccuracies of film thickness development due to adsorbed protein film from the previous experiment, attention was paid to the cleaning procedure of the test samples. Before and after tests, the specimens were rinsed in water and washed by 1% solution of sodium dodecyl

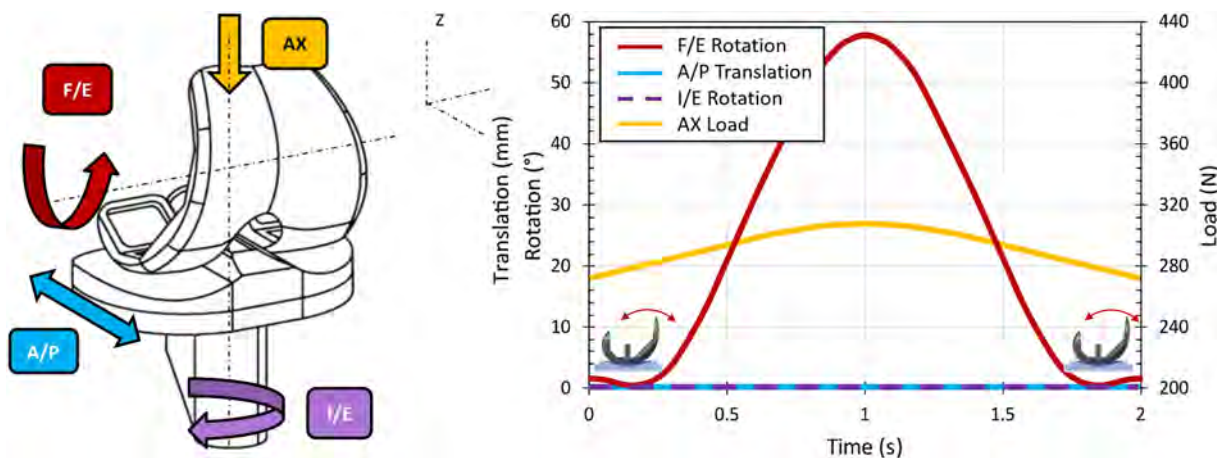


Fig. 1. A schematic illustration of the applied kinematic and loading conditions.

sulphate. Then, it was rinsed by deionized water, and washed in isopropyl alcohol.

To be able to compare the results of fluorescent intensity of two different components doped by different markers, normalization of the data had to be performed. This step is fundamental since it also eliminates the effects such as settings of light source, ambient light conditions or settings of fluorescent filters. The process of normalization is based on a simple division/multiplication. At the beginning of data analysis, the initial intensity is found for each measurement. To avoid any effect of the random variation of intensity, several tens of images within the first seconds of the test are analysed. Subsequently, independently of the performed test, the initial value is normalized to 1000. Therefore, the division/multiplication constant for each test is found. Then, all the rest of the data corresponding to the given measurement are divided/multiplied by the constant. This approach enables to compare the data independently of the used lubricant type or its concentration. The methodology was validated in our previous paper investigating hip replacement considering the same contact materials

(metal vs. PMMA) [23].

Since the simulator is newly developed and its function was not verified so far in terms of complex test with transient loading and kinematics, simple flexion-extension test was designed for the purpose of the present study. The PMMA insert was fixed in the simulator frame and the femoral component swung in the range from 0° (initial vertical position displayed in the bottom right corner of Fig. 2) to 58°. Frequency of the stroke was 0.5 Hz. The maximum applied load throughout the cycle was 310 N resulting to maximum contact pressure of approximately 36 MPa. With respect to standards for knee implant testing, the maximum load should be up to 2600 N. However, this is a peak value while the average load throughout the cycle is around 900 N. Assuming the simplified loading cycle employed within the present study, and noting that the elastic modulus of PMMA is around six times higher compared to UHMWPE, the resulting contact pressure should be similar considering metal-PMMA and metal-PE contact. Moreover, the presented data of maximum contact pressure are in accordance with expected pressures in knee replacement considering



Fig. 2. Model of the test device with the detail of the contact couple and optical module.

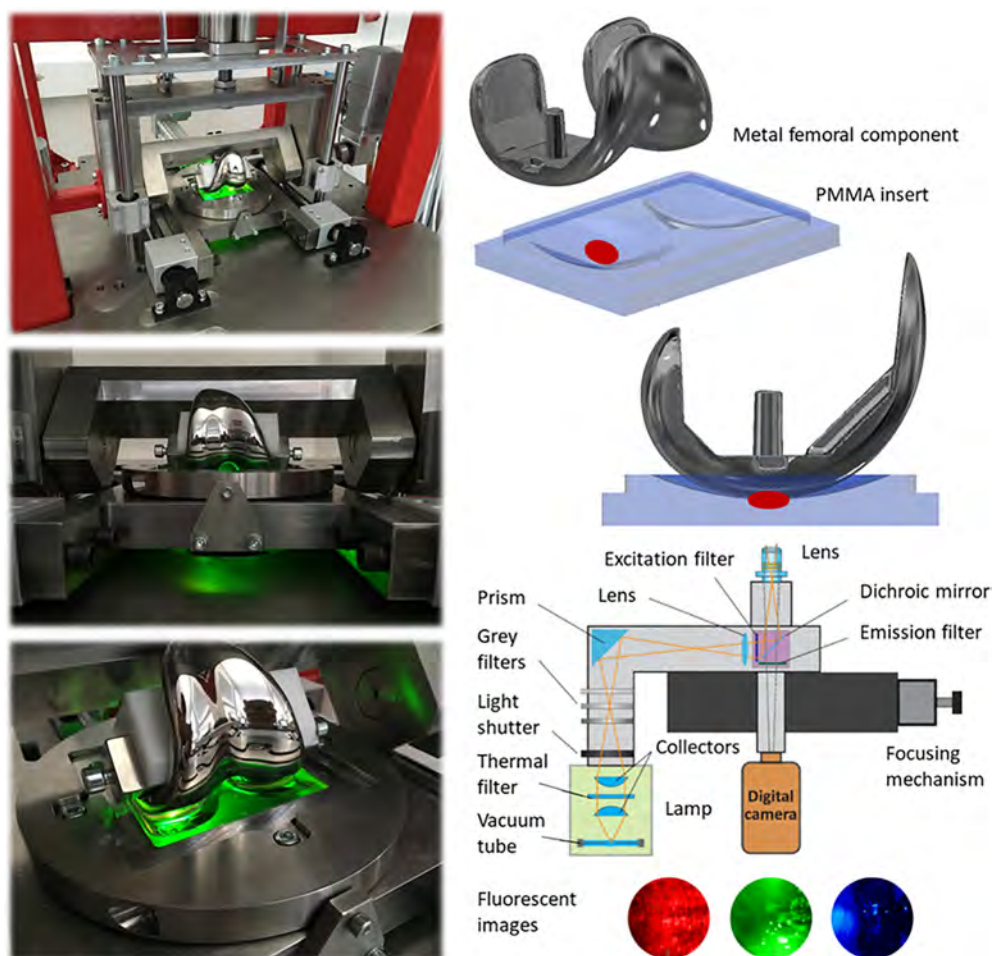


Fig. 3. Photo of the contact zone illuminated by mercury lamp. The red spot on the top right images indicate the observed zone where the film thickness is evaluated. (For interpretation of the references to colour in this figure legend, the reader is referred to the web version of this article.)

various references [26,27]. The contact area is an ellipse having the major and minor axis equal to 2.62 mm and 0.88 mm, respectively. The evaluated intensity is an average value over observed ellipse-shaped area depicted in Fig. 3 having length 2 mm and width 1.54 mm. The intensity is always evaluated in the zero position (when the position of the femoral component is vertical). The experiments were carried out under ambient temperature of 22 °C since it was shown in literature that an increase of lubricant temperature to 37 °C does not affect film formation [28].

3. Results and Discussion

The dimension-less film thickness was studied as a function of time. The corresponding fluorescence intensities for all the test lubricants considering lateral condyle are plotted in Fig. 4a. As can be seen, albumin film has a strongly increasing tendency during the first part of the experiment. Then, it continuously decreases and until the end of the

experiment. Almost identical behaviour of albumin film was previously observed even in the case of hip replacement [23]. When the fluorescently stained albumin was mixed with non-stained γ -globulin; surprisingly, the film became lower than that of pure albumin. The maximum film thickness was almost around half, while initial increase was followed by slight drop. However, contrary to pure albumin, the film formed by the mixture of the proteins showed much better lasting effect indicating better lubrication performance in long-term time interval. This phenomenon is very important. It should be emphasized that maximum film thickness in the case of few-minutes experiment is not as decisive parameter. Nevertheless, the ability of film formation over a long time is particularly important. The described behaviour supports our previous findings and suggestions highlighting the importance of the interaction of SF constituents in film formation process [21]. Moreover, it is expected that lower film thickness results in slightly higher friction which is in coincidence with our previous observation. Focusing on metal-polyethylene sliding test, it was found that a mixture

Table 1
Summary of the test lubricants.

Lubricant no.	Labelled constituent (concentration)	Non-labelled constituent (concentration)	Total concentration	Base fluid (total amount)
1	Albumin (24.9 mg/ml)	–	24.9 mg/ml	PBS (4 ml)
2	Albumin (24.9 mg/ml)	γ -globulin (6.1 mg/ml)	31 mg/ml	PBS (4 ml)
3	γ -globulin (6.1 mg/ml)	–	6.1 mg/ml	PBS (4 ml)
4	γ -globulin (6.1 mg/ml)	Albumin (24.9 mg/ml)	31 mg/ml	PBS (4 ml)

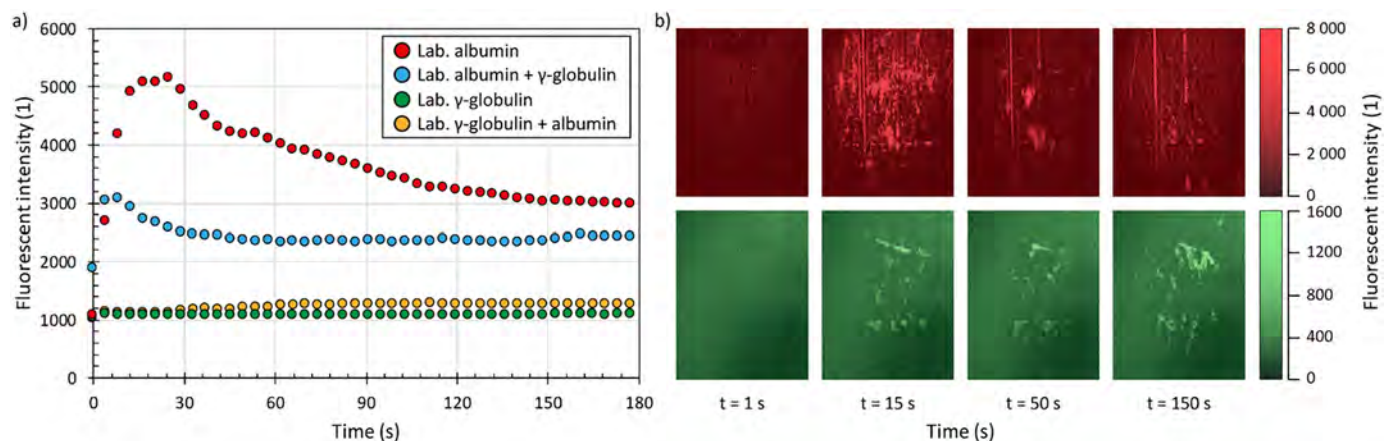


Fig. 4. a) Development of non-dimensional film thickness (fluorescent intensity) as a function of time for various test fluids; b) Images of the observed zone at defined time steps for albumin (red) and γ -globulin (green). (For interpretation of the references to colour in this figure legend, the reader is referred to the web version of this article.)

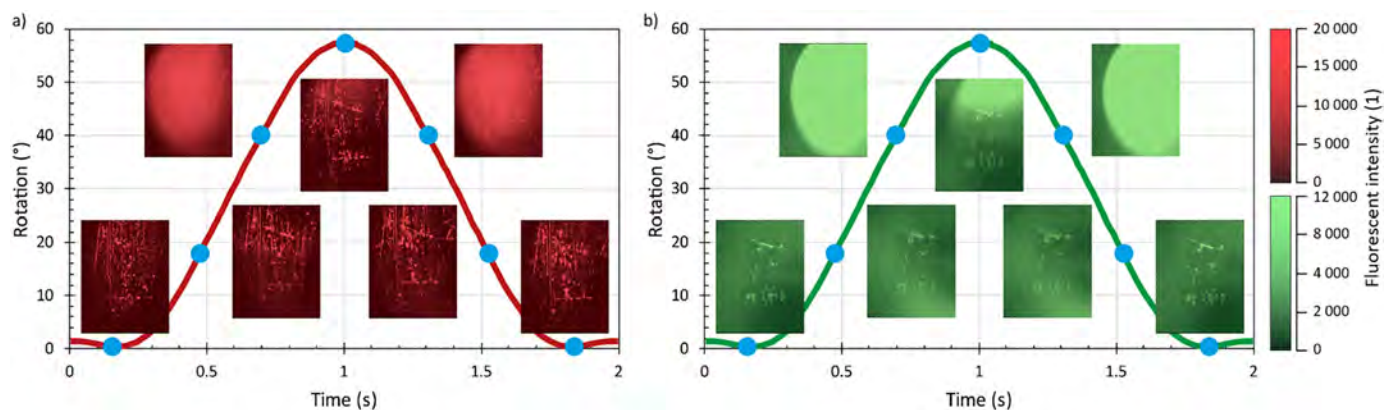


Fig. 5. Detail of the images of the observed part of the contact zone over the cycle: a) albumin; b) γ -globulin.

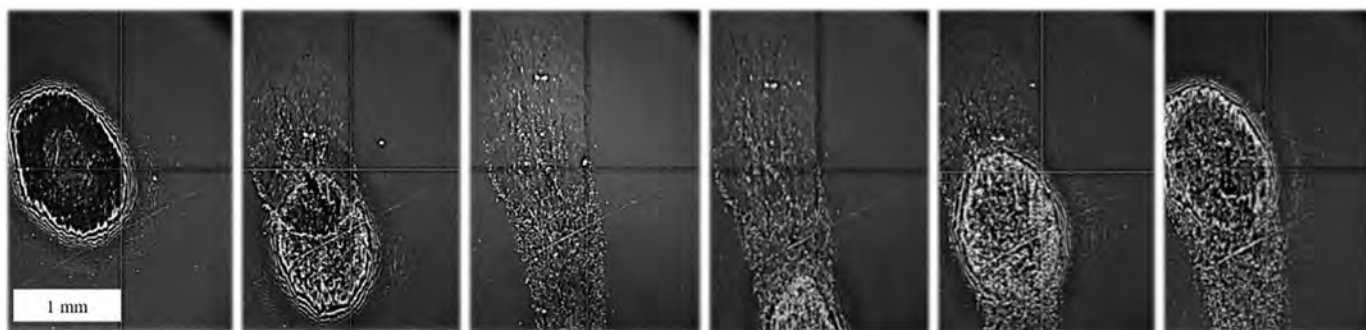


Fig. 6. Macroscopic observation of migrating contact zone.

of albumin and γ -globulin shows higher friction than simple protein solutions. In addition, the thickness of the adsorbed film was lower in the case of protein mixture which corresponds to current results [29].

Second set of experiments was performed with γ -globulin-based lubricants. Simple protein showed very limited lubrication ability while only a negligible increase of film thickness due to protein agglomerations could be observed. When albumin was added, the lubricant layer slightly increased (see Fig. 4a); nevertheless, the film was substantially lower than that of albumin-based model fluids (the thickness was less than half). This corresponds to findings related to lubrication of hard-on-soft hip implants [23]. However, in contrast to some previous observations, simple albumin formed thicker protein film compared to simple γ -globulin [21,30] which proves the importance of the contact

mechanics related to contact conformity (1) and soft nature of metal-on-PMMA contact (2).

The fluorescent images of the observed part of the contact zone for albumin and γ -globulin solutions are displayed in Fig. 4b. As can be seen, the appearance of the images corresponds well to the results of film thickness (Fig. 4a). In the case of albumin, rapid increase of intensity could be observed within the first 15 s. This is attributed to strong agglomeration of proteins at the early phase of the experiment. Subsequently, part of the proteins is removed/squeezed out from the contact, leading to thinning of the lubricant layer. In the later part of the experiment, small scratches can be observed on PMMA surface. Surprisingly, these scratches were not so substantial in the case of γ -globulin. This might be related to better lubricity of γ -globulin despite

the thinner lubricant film, ensuring lower coefficient of friction. This partially corresponds to previously published friction results [31]. As can be seen, only a limited protein formation can be observed in the case of γ -globulin solution. It should be emphasized that the fluorescent intensity plotted in Fig. 4a corresponds to average intensity over the whole observed zone. Therefore, it is evident that these limited localized protein clusters have quite limited impact on overall film thickness.

To be able to assess the recovery of the lubricant film during the swinging cycle, images of the contact zone over one cycle during 30th second (maximum albumin intensity) were taken. The illustrative images at various phases of F/E rotation are shown in Fig. 5. When focusing on the first and the last picture (the left and the right) along the cycle, it can be seen that the appearance of the contact zone at the beginning and the end of the cycle is very similar. This is an important verification regarding the methodology. Due to complicated geometry of the femoral implant, the contact migrates during the cycle. This can be clearly seen in terms of overexposed images. In that phase of F/E, the contact disappears for very short time outside the observed zone. However, in the subsequent back-swing, the contact returns to the initial position. The image corresponding to maximum deflection might be bit confusing; however, in that case, the contact area is the largest. Therefore, for a very short moment, the contact reaches the observed zone. This is the reason why only a small part of the image (when F/E = 60°) is overexposed.

The migrating contact zone shown in Fig. 6 is one of the limitations of the performed study. Microscopic images of the migrating contact were taken using no-magnification lens under transient load (maximum 400 N) to get better imagination about the contact motion over the cycle. Therefore, the camera holder mechanism will be redesigned in the future; thus enabling to observe the contact zone over the whole cycle. Thus, the development of film thickness in various phases of F/E will be evaluated. Another limitation is that we focused on lateral compartment when observing the lubricant film formation. However, it was pointed out in literature that in terms of wear, the behaviour of both lateral and medial compartments is different [19]; therefore, the future study should involve this suggestion and verify the findings in terms of lubrication. Further, it should be highlighted that the present study was focused mainly on the development of the knee joint simulator, experiment design, and methodology of evaluation of lubricant film formation. For this purpose, only simple and mixed protein solutions were employed to understand some fundamentals. Nevertheless, it was showed in the studies focused on hip joint lubrication that these simple solutions are not able to mimic the behaviour of complex model SF [21,23,28]. Therefore, more SF constituents have to be taken into account; e.g. HA and phospholipids, in particular.

Finally, relatively simple shape cycle was designed for this introductory study. Following the real joint kinematics and loading conditions, more complicated motion as well as more variable load over the cycle have to be taken into account. It is particularly complicated to confront the preliminary results coming from the performed study with literature dealing with knee replacements. The main reason is that so far there is only one experimental study while the authors used simplified geometry and different technique to determine the surface separation [16]. Other above-mentioned experimental works are mostly focused on wear and/or friction evaluation [8–12]. The references related to lubrication mechanisms are exclusively numerical [13,15,17–19]; while it can hardly involve the complexity of geometry; non-Newtonian behaviour of SF [30], or adsorption and agglomeration of proteins [23,32]. Therefore, further experimental investigation is necessary to be able to understand and clarify the lubrication mechanisms of knee implants in a more complex way.

4. Conclusion

The knee joint simulator enabling in situ observation of the contact

zone was introduced in the present study. The methodology based on fluorescent observation was employed while it was shown that the approach might help to significantly extend the knowledge about the lubrication of knee implants. Real geometry of rubbing surfaces was considered while a clear interaction of albumin and γ -globulin in terms of dimension-less film thickness was presented. The main goal of the present paper was to design and verify the method for lubricant film formation investigation in knee joint replacement. In particular, it was found that albumin layer is considerably thicker compared to γ -globulin. This is caused by higher concentration of albumin. In addition, it emphasizes the issue of contact mechanics since the results go partially against previous findings for hard-on-hard implants. However, it should be highlighted that maximum film thickness is not a decisive parameter as the function of replacement is a long term-process. Therefore the lasting effect of the lubricant (ability to form stable lubricating layer) was of a greater interest. Independently of the stained fluid component, it was found that mixture of the proteins exhibits better lubrication performance. This proves the importance of the interaction of the molecules contained in SF. The motivation for future study is to consider more complex model of SF together with transient kinematic and loading conditions with respect to various motion activities. In addition, the contact migration throughout the cycle will be issued and both the compartments should be considered into the analysis.

Acknowledgement

This research was carried out under the project LTAUSA17150 with financial support from the Ministry of Education, Youth and Sports of the Czech Republic. Further support was provided by Palacky University, Olomouc (RVO 61989592). The authors thank to V. Polnický for his help with simulator design and experimental setup.

References

- [1] OECD, Health at a Glance 2017: OECD Indicators, OECD Publishing, Paris, 2017.
- [2] E. Meier, K. Gelse, K. Trieb, M. Pachowsky, F.F. Hennig, A. Mauerer, First clinical study of a novel complete metal-free ceramic total knee replacement system, *J. Orthop. Surg. Res.* 11 (2016) 1–7.
- [3] C.J. Vertullo, P.L. Lewis, S. Graves, L. Kelly, M. Lorimer, P. Myers, Twelve-year outcomes of an oxinium total knee replacement compared with the same cobalt-chromium design, *J. Bone Joint Surg.* 99 (2017) 275–283.
- [4] D. Shervin, Anterior knee pain following primary total knee arthroplasty, *World J. Orthopedics.* 6 (2015) 795–803.
- [5] A. Postler, C. Lützner, F. Beyer, E. Tille, J. Lützner, Analysis of total knee arthroplasty revision causes, *BMC Musculoskelet. Disord.* 19 (2018), <https://doi.org/10.1186/s12891-018-1977-y>.
- [6] J. Gallo, S.B. Goodman, Y.T. Konttinen, M.A. Wimmer, M. Holinka, Osteolysis around total knee arthroplasty: a review of pathogenetic mechanisms, *Acta Biomater.* 9 (2013) 8046–8058.
- [7] J.P. Kretzer, J. Reinders, R. Sonntag, S. Hagmann, M. Streit, S. Jeager, et al., Wear in total knee arthroplasty—just a question of polyethylene? *Int. Orthop.* 38 (2014) 335–340.
- [8] J. Reinders, R. Sonntag, L. Vot, C. Gibney, M. Nowack, J.P. Kretzer, et al., Wear testing of moderate activities of daily living using in vivo measured knee joint loading, *PLoS One* 10 (2015), <https://doi.org/10.1371/journal.pone.0123155>.
- [9] A. Wang, A. Essner, C. Stark, J.H. Dumbleton, A biaxial line-contact wear machine for the evaluation of implant bearing materials for total knee joint replacement, *Wear* 225–229 (1999) 701–707.
- [10] A. Chyr, A.P. Sanders, B. Raeymaekers, A hybrid apparatus for friction and accelerated wear testing of total knee replacement bearing materials, *Wear* 308 (2013) 54–60.
- [11] T. Stewart, Z.M. Jin, J. Fisher, Friction of composite cushion bearings for total knee joint replacements under adverse lubrication conditions, *Proc. Inst. Mech. Eng. H J. Eng. Med.* 211 (2016) 451–465.
- [12] M. Flannery, E. Jones, C. Birkinshaw, Analysis of wear and friction of total knee replacements part II: Friction and lubrication as a function of wear, *Wear* 265 (2008) 1009–1016.
- [13] P.N. Tandon, S. Jaggi, A model for the lubrication mechanism in knee joint replacements, *Wear* 52 (1979) 275–284.
- [14] P.N. Tandon, S. Jaggi, Wear and lubrication in an artificial knee joint replacement, *Int. J. Mech. Sci.* 23 (1981) 413–422.
- [15] Z.M. Jin, D. Dowson, J. Fisher, N. Ohtsuki, T. Murakami, H. Higaki, et al., Prediction of transient lubricating film thickness in knee prostheses with compliant layers, *Proc. Inst. Mech. Eng. H J. Eng. Med.* 212 (2016) 157–164.
- [16] N. Ohtsuki, T. Murakami, S. Moriyama, H. Higaki, Influence of geometry of

- conjunction on elastohydrodynamic film formation in knee prostheses with compliant layer, *Elastohydrodynamics - '96 Fundamentals And Applications In Lubrication And Traction, Proceedings Of The 23Rd Leeds-Lyon Symposium On Tribology Held In The Institute Of Tribology, Department Of Mechanical Engineering, Elsevier, 1997*, pp. 349–359.
- [17] M. Mongkolwongrojn, K. Wongseedakaew, F.E. Kennedy, Transient elastohydrodynamic lubrication in artificial knee joint with non-Newtonian fluids, *Tribol. Int.* 43 (2010) 1017–1026.
- [18] Y. Su, P. Yang, Z. Fu, Z. Jin, C. Wang, Time-dependent elastohydrodynamic lubrication analysis of total knee replacement under walking conditions, *Computer Method. Biomec. Biomed. Eng.* 14 (2011) 539–548.
- [19] L. Gao, Z. Hua, R. Hewson, M.S. Andersen, Z. Jin, Elastohydrodynamic lubrication and wear modelling of the knee joint replacements with surface topography, *Biosurf. Biotribol.* 4 (2018) 18–23.
- [20] M. Vrbka, D. Nečas, M. Hartl, I. Křupka, F. Urban, J. Gallo, Visualization of lubricating films between artificial head and cup with respect to real geometry, *Biotribology*. 1-2 (2015) 61–65.
- [21] D. Nečas, M. Vrbka, D. Rebenda, J. Gallo, A. Galandáková, L. Wolfová, et al., In situ observation of lubricant film formation in THR considering real conformity: the effect of model synovial fluid composition, *Tribol. Int.* 117 (2018) 206–216.
- [22] D. Nečas, M. Vrbka, F. Urban, I. Křupka, M. Hartl, The effect of lubricant constituents on lubrication mechanisms in hip joint replacements, *J. Mech. Behav. Biomed. Mater.* 55 (2016) 295–307.
- [23] D. Nečas, M. Vrbka, A. Galandáková, I. Křupka, M. Hartl, On the observation of lubrication mechanisms within hip joint replacements. Part I: Hard-on-soft bearing pairs, *J. Mech. Behav. Biomed. Mater.* 89 (2019) 237–248.
- [24] M. Ranuša, J. Gallo, M. Vrbka, M. Hobza, D. Paloušek, I. Křupka, et al., Wear analysis of extracted polyethylene acetabular cups using a 3D optical scanner, *Tribol. Trans.* 60 (2016) 437–447.
- [25] A. Azushima, In situ 3D measurement of lubrication behavior at interface between tool and workpiece by direct fluorescence observation technique, *Wear* 260 (2006) 243–248.
- [26] Z.M. Jin, T. Stewart, D.D. Auger, D. Dowson, J. Fisher, Contact pressure prediction in total knee joint replacements Part 2: application to the design of total knee joint replacements, *Proc. Inst. Mech. Eng. H J. Eng. Med.* 209 (2016) 9–15.
- [27] A. Pascau, B. Guardia, J.A. Puertolas, E. Gómez-Barrena, Knee model of hydrodynamic lubrication during the gait cycle and the influence of prosthetic joint conformity, *J. Orthop. Sci.* 14 (2009) 68–75.
- [28] A. Mavraki, P.M. Cann, Lubricating film thickness measurements with bovine serum, *Tribol. Int.* 44 (2011) 550–556.
- [29] D. Nečas, Y. Sawae, T. Fujisawa, K. Nakashima, T. Morita, T. Yamaguchi, et al., The influence of proteins and speed on friction and adsorption of metal/UHMWPE contact pair, *Biotribology*. 11 (2017) 51–59.
- [30] C. Myant, R. Underwood, J. Fan, P.M. Cann, Lubrication of metal-on-metal hip joints: the effect of protein content and load on film formation and wear, *J. Mech. Behav. Biomed. Mater.* 6 (2012) 30–40.
- [31] D. Nečas, M. Vrbka, I. Křupka, M. Hartl, The effect of kinematic conditions and synovial fluid composition on the frictional behaviour of materials for artificial joints, *Mater.* 11 (2018).
- [32] M. Parkes, C. Myant, P.M. Cann, J.S.S. Wong, Synovial fluid lubrication: the effect of protein interactions on adsorbed and lubricating films, *Biotribology*. 1-2 (2015) 51–60.



Contents lists available at ScienceDirect

Journal of the Mechanical Behavior of Biomedical Materials

journal homepage: <http://www.elsevier.com/locate/jmbbm>

The effect of albumin and γ -globulin on synovial fluid lubrication: Implication for knee joint replacements

D. Nečas^{a,*}, K. Sadecká^a, M. Vrbka^a, A. Galandáková^b, M.A. Wimmer^c, J. Gallo^d, M. Hartl^a

^a Dept of Tribology, Faculty of Mechanical Engineering, Brno University of Technology, Czech Republic

^b Dept of Medical Chemistry and Biochemistry, Faculty of Medicine and Dentistry, Palacky University Olomouc, Czech Republic

^c Dept of Orthopedic Surgery, Rush University Medical Center, Chicago, IL, USA

^d Dept of Orthopaedics, Faculty of Medicine and Dentistry, Palacky University Olomouc, University Hospital Olomouc, Czech Republic

ARTICLE INFO

Keywords:

Knee joint replacement
Lubrication
Proteins
Fluorescence microscopy
Contact
Synovial fluid

ABSTRACT

Total knee arthroplasty has become a routine procedure for patients suffering from joint diseases. Although the number of operations continuously increases, a limited service-life of implants represents a persisting challenge for scientists. Understanding of lubrication may help to suitably explain tribological processes on the way to replacements that become durable well into the third decade of service. The aim of the present study is to assess the formation of protein lubricating film in the knee implant. A developed knee simulator was used to observe the contact of real femoral and transparent polymer tibial component using fluorescent microscopy. The contact was lubricated by various protein solutions with attention to the behaviour of albumin and γ -globulin. In order to suitably mimic a human synovial fluid, hyaluronic acid and phospholipids were subsequently added to the solutions. Further, the change in shape and the migration of the contact zone were studied. The results showed considerable appearance differences of the contact over the swing phase of the simplified gait cycle. Regarding film formation, a strong interaction of the various molecules of synovial fluid was observed. It was found that the thickness of the lubricating layer stabilizes within around 50 s. Throughout the contact zone, protein agglomerations were present and could be clearly visualised using the applied optical technique.

1. Introduction

Total knee arthroplasty (TKA) is recognized as an effective and well-established surgical treatment for patients suffering from a wide-range of diseases of the knee. In 2017, there were 135 knee replacements vs. 182 hip replacements per 100,000 capita in OECD countries (Health and Glance, 2019; OECD). It is expected that knee replacement numbers may overcome hips in less than ten years. In the US, the numbers for knees vs. hips flipped already in the early 2000's (Kurtz, 2005) and are presently three-to four-fold higher with expected further rapid growth by 2030 (Kurtz et al., 2007). Despite a rapid improvement of implant materials, younger patients, a more active lifestyle, and a longer lifetime expectancy require more durable joints. A limited longevity of the artificial joints requires revision surgery, representing a major drawback in quality of life for the patient. While it was clearly answered that most of the implants fail due to aseptic loosening as a consequence of osteolysis (Ding et al., 2012; Gallo et al., 2013; Schiffner et al., 2019), the mechanism of failure has been exposed to many debates of scientists

worldwide. Previously, wear of material due to articulation of the contacting surfaces was considered to be the driving aspect of failure (Rieker, 2016; Tandon and Jaggi, 1981). However, with the development of cross-linked polyethylene (X-PE), which is nowadays used as the material of choice for tibial inserts, a wear related failure scenario is less common. Actually, a recent study found that a significant number of implant failures is considered to be surgeon-related (Schroer et al., 2013). Despite these reports, which typically focus on the short term period, aseptic loosening due to wear may still prevail in the long term period (Gallo et al., 2013), particularly with implants that should last well into the third decade. Thus, a precise understanding of tribological performance is of paramount interest in order to minimize wear-related failures in the future. Apparently, wear and lubrication are related (Flannery et al., 2008). While several studies on wear and friction of total knee replacement have been published (Stewart et al., 1997; Chyr et al., 2013; Kretzer et al., 2014; Reinders et al., 2015), there is a limited knowledge about the underlying lubrication mechanisms.

The recent observations may be classified into two categories;

* Corresponding author.

E-mail address: david.necas@vut.cz (D. Nečas).

<https://doi.org/10.1016/j.jmbbm.2020.104117>

Received 2 April 2020; Received in revised form 31 August 2020; Accepted 24 September 2020

Available online 28 September 2020

1751-6161/© 2020 Elsevier Ltd. All rights reserved.

numerical simulations and experimental studies. Focusing on the numerical investigations, pilot papers were presented around forty years ago by Tandon and Jaggi (1979, 1981). The authors introduced an idealized model with consideration of increased load capacity due to the increased concentration of hyaluronic acid (HA) in a modelled synovial fluid (SF). The simulation was focused on the prediction of wear rate, load capacity and approaching time of the surfaces. The initial findings were extended nearly twenty years later. Di Paolo and Berli (2006) developed a steady state numerical model of knee implant considering non-Newtonian nature of SF. The main attention was paid to the effect of material parameters and potential introduction of porous tibial insert in order to improve lubrication conditions. The results showed that the commonly used PE is too rigid to allow for the formation of thick lubricating film to protect the rubbing surfaces. Moreover, it was suggested that the implementation of the insert made of porous elastic material would contribute to a thicker lubricating film, which would apparently have a positive effect on pressure, friction, and wear.

A later numerical simulation was focused on the prediction of film thickness and pressure distribution in knee replacement dependently on load, kinematics, material, and lubricant (Mongkolwongrojn et al., 2010). It was shown that the most significant difference in pressure and lubricating film occurs between the first two cycles. This was explained by the time required for lubricant film to be fully developed. During the subsequent steps, the film/pressure depends exclusively on the applied kinematic and loading conditions. Further findings were reported by Su et al. (2011, 2012) who provided a time-dependent elastohydrodynamic lubrication (EHL) analysis with respect to transient loading and kinematic conditions occurring during gait. The authors employed a simplified ellipsoid-on-plane geometrical model. It was pointed out that the film thickness tended to decrease during the stance phase while the swing phase led to a thicker film due to the combination of entraining action and squeeze film effect. A similar ellipsoid-on-plane model was presented also by Jin et al. (2016), who implemented the EHL theory when simulating a walking cycle. The authors predicted a real-time lubricant film thickness in the knee implant. Among others, a strong influence of joint geometry was observed. It was concluded that a thicker film thickness is expected when the contact area of a transverse conjunction is maximized. Following some limitations associated with a simplified geometrical model, Gao et al. (2018) developed an improved ball-on-socket configuration in order to predict wear and lubrication with respect to the surface conformity. The study investigated the potential benefit of surface texturing as well. The simulation was running until the steady-state wear rate was reached. After the running-in period, a larger lubricated area with flattened and more favourable pressure distribution could be observed. The authors also focused on the behaviour of both the medial and lateral compartments. While it was found that the lateral compartment may benefit from surface texturing, no positive effect of the dimples on lubrication and wear was observed for the medial meniscus.

All the above papers dealt with numerical modelling of tribological performance of knee implants, focusing, to some extent, on lubrication. Considering the experimental studies, only several papers have been published so far. The first investigation of lubrication was introduced by Ohtsuki et al. (1997) who focused on the measurement of degree of separation (lubricant film thickness) between the steel ball and the silicone rubber mimicking tibial component. The authors employed an electrical resistance technique showing that the ability to form a stable lubricant film was better in the case of transverse rather than longitudinal geometry. Scholes et al. (2006, 2007) carried out the in vivo simulation of the effect of loading and kinematic conditions on friction, lubrication, and wear of knee replacement. It was pronounced that the frictional behaviour is strongly affected by the presence of proteins adsorbed on the rubbing surfaces to create a solid-like film, thus preventing the rubbing surfaces against extensive wear. The authors also highlighted the necessity of the selection of suitable lubricants for further experimental investigations. Behaviour of polyurethane (PU)

unicondylar knee prostheses was observed in (Scholes et al., 2007) while it was shown that the metal-PU pair exhibits a significantly lower wear rate and improved lubrication performance compared to the conventional metal-PE pairs. The importance of lubrication regarding the wear of knee implant was also demonstrated by Kennedy et al. (2007). An oscillatory rolling/sliding contact composed of parallel metal and PE pucks lubricated by bovine serum (BS) was analysed. The experimental wear analysis was combined with numerical prediction of film thickness concluding that the thinnest film was detected in the area exhibiting the greatest wear rate. A comprehensive tribological description based on simulator testing was provided by Flannery et al. (2008a, 2008b) who extended the previous observations about the role of lubrication. In particular, it was shown that adsorbed proteins may lead to an increase in friction but to a lower wear rate due to protection of rubbing surfaces. The above papers indicate that lubrication apparently influences the performance of knee replacements. Thus, in order to design an optimal experimental approach, the nature of model lubricant has to be taken into account. Despite the similar rheology of BS and SF (Yao et al., 2003), a different friction was observed for these lubricants (Stevenson et al., 2019). In addition, the variance of SF composition of individual patients should be considered (Galandáková et al., 2016).

Following the above implications, we have recently introduced a novel experimental approach based on the combination of the knee simulator and fluorescent measurement method (Nečas et al., 2019a). A similar methodology was previously successfully adopted when exploring lubrication mechanisms within hard-on-soft hip implants (Nečas et al., 2019b). Regarding the knee simulator, the contact between the real femoral component and the real-shaped tibial insert made of transparent poly (methyl) methacrylate (PMMA) was observed using fluorescently stained protein solutions as the test lubricants. The pilot study has shown that the developed approach may lead to a detailed explanation of lubricant film formation in knee implants. Therefore, the aim of the present study is to understand the formation of lubricating film in the knee replacement, focusing on the role of individual proteins contained in SF. Moreover, a complex observation of the migration/deformation of the contact zone throughout the swinging cycle is presented.

2. Materials and methods

The experiments were performed using a developed knee joint simulator introduced in previous study (Nečas et al., 2019a). This device is composed of a rigid base frame and an exchangeable measurement module. A flexion/extension (FE) swinging arm is mounted on the plate enabling the internal/external (IE) rotation. The plate is fixed to a platform allowing for anterior/posterior (AP) translation. The axial load (AX) is applied through a vertically mounted spring. The simulator enables to apply the conditions corresponding to the walking cycle with respect to ISO-14243-3 standard. The contact area is observed via the optical measurement system based on fluorescent microscopy. A digital model of the simulator together with a detail of the knee implant module, the overview of fluorescent imaging, real photo of the illuminated contact, and the detail of the components can be seen in Fig. 1.

Observations of lubricant film formation are based on the use of mercury-lamp induced fluorescence (Nečas et al., 2016). Routine experimental techniques (e.g. optical interferometry, capacitance method) cannot be applied due to several limitations of the contact couple, such as limited conductivity and lack of light reflectivity. The optical system consists of mercury lamp, microscope, excitation and emission filters, dichroic mirror, lens, and sCMOS camera. The principle of the method is as follows. Initially, fluorescently stained proteins in the test lubricant are excited by the external light source. This phase is followed by the so-called excited-state lifetime during which the excited molecules exhibit energy dissipation allowing to emit light at a longer wavelength than excitation. It should be emphasized that chromium contained in the femoral component causes fluorescence quenching (Jie,

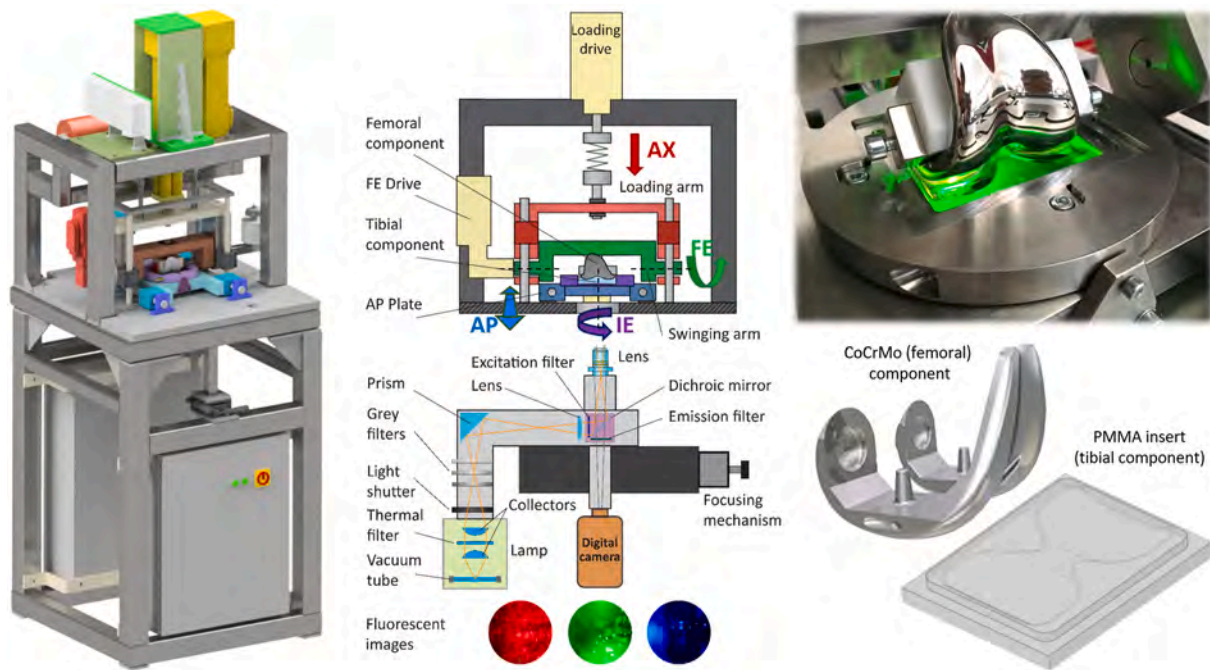


Fig. 1. Digital model of knee simulator (left); detail of measurement module and scheme of fluorescent microscopy (middle), photo of the illuminated contact (top right), and detail of the contact components (bottom right).

1998). This phenomenon can be hardly quantified. Therefore, the film thickness cannot be evaluated quantitatively. However, the fluorescent intensity is proportional to film thickness (Azushima, 2005) so the change of the lubricant film throughout the experiment can be expressed qualitatively, showing a dimensionless film thickness course over time.

The contact is composed of real femoral CoCrMo component (ZIMMER NexGen CR PC) articulating with a tibial insert (Fig. 1 bottom right). Focusing on the geometry of femoral part, it should be noted that the medial compartment exhibits a larger radius of curvature compared to the lateral one. The geometry was fully respected when designing the model of tibial insert. It was made based on the original PE insert geometry obtained with the use of 3D optical scanning (GOM ATOS Triple Scan) (Ranuša et al., 2016). A digital model was then processed, and the final product was fabricated by micro-chip machining technology from PMMA. This was chosen due to sufficient optical transparency and comparable mechanical properties to conventionally used PE, exhibiting relatively low hardness and toughness. The fabrication technology enabled us to achieve a very precise-shaped surface exhibiting a low surface roughness. A topography of the contact surfaces of both tested samples was evaluated with the use of 3D optical profiler based on phase shifting interferometry (Bruker Contour GT-X). In particular, the roughness of CoCrMo and PMMA components was around 55 nm and 40 nm, respectively.

Various model lubricants were used in order to clarify the role of proteins contained in SF. Phosphate-buffered saline (PBS) solution was used as a base liquid. The main attention was paid to the behaviour of bovine serum albumin (A2153, Sigma-Aldrich) and γ -globulin from bovine blood (G5009, Sigma-Aldrich), the content of which is significantly higher than that of other SF constituents (i.e. hyaluronic acid (HA) and phospholipids (PHs)). For fluorescent labelling, Rhodamine-Bisothiocyanate (283,924, Sigma-Aldrich) and Fluorescein-isothiocyanate (F7250, Sigma-Aldrich) were used. When examining mechanisms of synovial fluid lubrication, fluorescent labelling of the proteins is well-established procedure. Same technique was adopted in the previous studies (Murakami et al., 2009, 2011; Nakashima et al., 2005; Yarimitsu et al., 2007, Nečas et al., 2016, 2019a; 2019b). With respect to human SF, HA as well as PHs were consequently added to the protein solutions. A selection of proper lubricant as well as the content of

individual constituents are often discussed when testing joint implants. It should be noted that the designed fluid is based on the long-term analysis of SFs extracted from hundreds of patients during surgeries (primary, revision). As is apparent from the published data, there is a considerable variance in terms of both composition and viscosity of SF of various individuals (Galandáková et al., 2016). Therefore, the following composition of model SF was suggested which is believed to suitably fit an average osteoarthritic patient (patient expecting a knee replacement): albumin = 24.9 mg/ml, γ -globulin 6.1 mg/ml, HA = 1.49 mg/ml, and PHs = 0.34 mg/ml. The overall dose of lubricant used in each experiment was 4 ml, ensuring both the compartments to be fully flooded at the beginning of the test. Since the fluorescent microscopy enables to concentrate on one specific stained constituent, the experiments were repeated with more complex solutions; the albumin behaviour was observed during the first set while γ -globulin was detected during the second set of the tests. Initially, only a simple protein solution was used. Subsequently, the stained protein was mixed with another unstained protein. Then, unstained HA and PHs were added. A summary of the test lubricants is presented in Table 1. The reason why HA and PHs were not studied separately is that it was clearly shown that the simple HA has poor lubrication abilities (Nečas et al., 2018); moreover, PHs may not be fluorescently labelled using the employed labelling procedure. However, lubrication performance and interaction of HA and PHs should be of a greater interest in the upcoming study.

Although the simulator enables to apply transient axial load during the swinging cycle, simplified loading conditions were considered in order to clarify the role of individual proteins. The maximum applied load was set to around 270 N. This value is generally lower compared to that defined by the standards; however, the difference in material properties of the conventional PE and the used PMMA has to be taken into account. Elastic modulus and Poisson's ratios of the CoCrMo and PMMA component are as follows; $E_{\text{CoCrMo}} = 240$ GPa, $\mu_{\text{CoCrMo}} = 0.28$, $E_{\text{PMMA}} = 3$ GPa, and $\mu_{\text{PMMA}} = 0.37$. With respect to the geometry of the compartments, the results of applied load in contact pressure were between 25 and 30 MPa at FE = 0° (initial) position (see Fig. 2) which well corresponds to the previous studies (Di Paolo and Berli, 2006; Pascau et al., 2009; Mongkolwongrojn et al., 2010; Su et al., 2011, 2012). Finally, it should be emphasized that the above load value represents

Table 1
Overview of the used lubricants.

Lubricant no.	Albumin	γ -globulin	Hyaluronic acid	Phospholipids	Total concentration
Fluorescently labelled albumin					
1	24.9 mg/ml	–	–	–	24.9 mg/ml
2	24.9 mg/ml	6.1 mg/ml	–	–	31 mg/ml
3	24.9 mg/ml	6.1 mg/ml	1.49 mg/ml	0.34 mg/ml	32.83 mg/ml
Fluorescently labelled γ-globulin					
4	–	6.1 mg/ml	–	–	6.1 mg/ml
5	24.9 mg/ml	6.1 mg/ml	–	–	31 mg/ml
6	24.9 mg/ml	6.1 mg/ml	1.49 mg/ml	0.34 mg/ml	32.83 mg/ml
Fluorescently labelled albumin + γ-globulin					
7	24.9 mg/ml	6.1 mg/ml	1.49 mg/ml	0.34 mg/ml	32.83 mg/ml

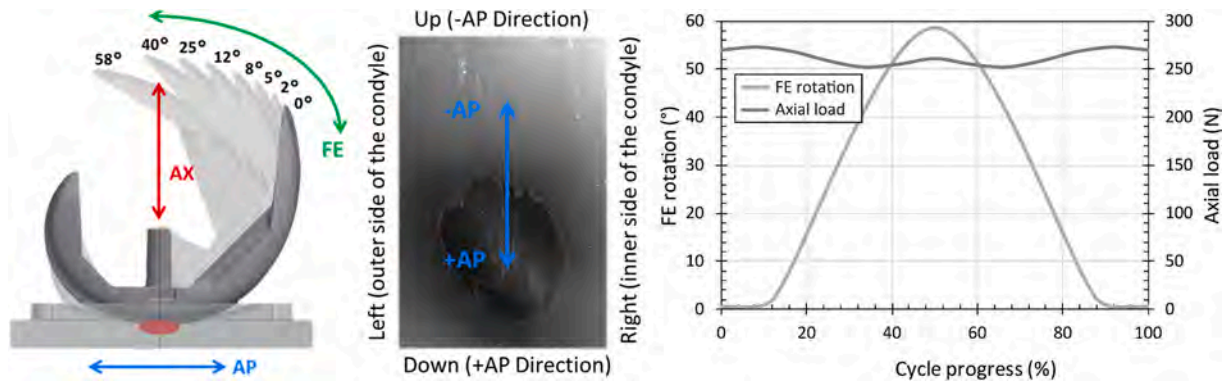


Fig. 2. Illustration of FE swing (left); orientation of the contact (middle); cycle description (right).

roughly an average load level throughout the standardized walking cycle. The overview of the model arrangement, orientation of the contact, and course of AX load and FE rotation can be seen in Fig. 2.

Prior to the experiments, the test specimens were carefully washed in 1% solution of sodium dodecyl sulphate, rinsed by distilled water and isopropyl alcohol. The components were then fixed to the simulator frame/swinging arm, and the tibial insert was flooded by the lubricant. Focusing on the specific tested kinematic conditions, a stroke frequency was set to 0.75 Hz while the FE swing ranged from 0° to 58° (Fig. 2). The dimensionless film thickness was studied in the initial position as a function of time for 3 min. The recorded images were processed while the average intensity of the square-shape area having the dimensions 1.2×1.2 mm and covering the majority of the contact zone (FE = 0°) was evaluated. It should be noted that the shape of the contact zone considerably changes over the cycle which is shown below. The albumin film was later observed also with the FE arm fully deflected (FE = 58°); in this case, the contact shape was totally different. All the experiments were carried out at ambient laboratory temperature since it is suggested that the elevated body temperature does not influence the formation of protein lubricant film (Mavraki and Cann, 2011).

3. Results

3.1. Observation of the contact zone

Assuming that the shape and size of the contact zone is continuously changing throughout the experiment, a detailed observation of the contact was carried out at the beginning of the study. The lateral compartment was of main interest while the images taken at the beginning and at the end of the test are shown in Fig. 3. It should be noted that during the natural motion, the knee bends in one direction, it never moves beyond the initial (FE = 0°) position. The instantaneous images were taken all along the FE swing at eight separate phases. As can be seen in Fig. 3, the contact at FE = 0° (still stand) is rather elliptic with a slightly larger minor axis along the direction of motion. Focusing

on the agglomeration of proteins, it is apparent that the proteins are formed along with the direction of motion while there is a limited protein film around the side edges of the zone. Soon after the beginning of motion (FE = 1°–3°), the contact becomes larger, exhibiting nearly a square-like shape. As can be seen, at the beginning of the experiment, the proteins are uniformly distributed (left images). With FE around 5°, the contact zone is quite large, having nearly a circular shape with a substantial number of proteins being dispersed throughout the contact. Moreover, there is no considerable difference between the beginning and the end of the test. Compared to previous phases, protein clusters are significantly smaller at the end of the test. The largest contact is observed when the FE rotation reaches approximately 8°. In this case, a clear transition in terms of visual appearance may be observed. In the remaining observed positions, the contact becomes ellipse-shaped with a significantly larger major axis perpendicular to the motion direction. At the same time, a substantial difference in protein behaviour was recorded. In earlier phases, from FE = 8°–12°, the proteins were agglomerated in the inner part of the contact; in later phases, a clear accumulation around the edge of the contact was observed.

3.2. Protein film formation

The subsequent set of experiments was carried out with albumin-based model lubricants. It should be emphasized that albumin was the only labelled constituent. Thus, the results show how the albumin behaviour is influenced by other SF molecules. The initial position (FE = 0°) was observed; the results are summarized in Fig. 4. The thickest film was observed for a simple albumin solution. When γ -globulin was added, the film was reduced to less than a half. On the contrary, adding of HA and PHs improved the lubricating film; however, the thickness of albumin film in complex fluid was still lower compared to that in the simple solution. The last experiment was performed with both albumin and γ -globulin to be fluorescently stained. The data (dark grey rhombus) represent the behaviour of complexly stained fluid. Apparently, a lower intensity is attributed to the emission re-absorption phenomenon when

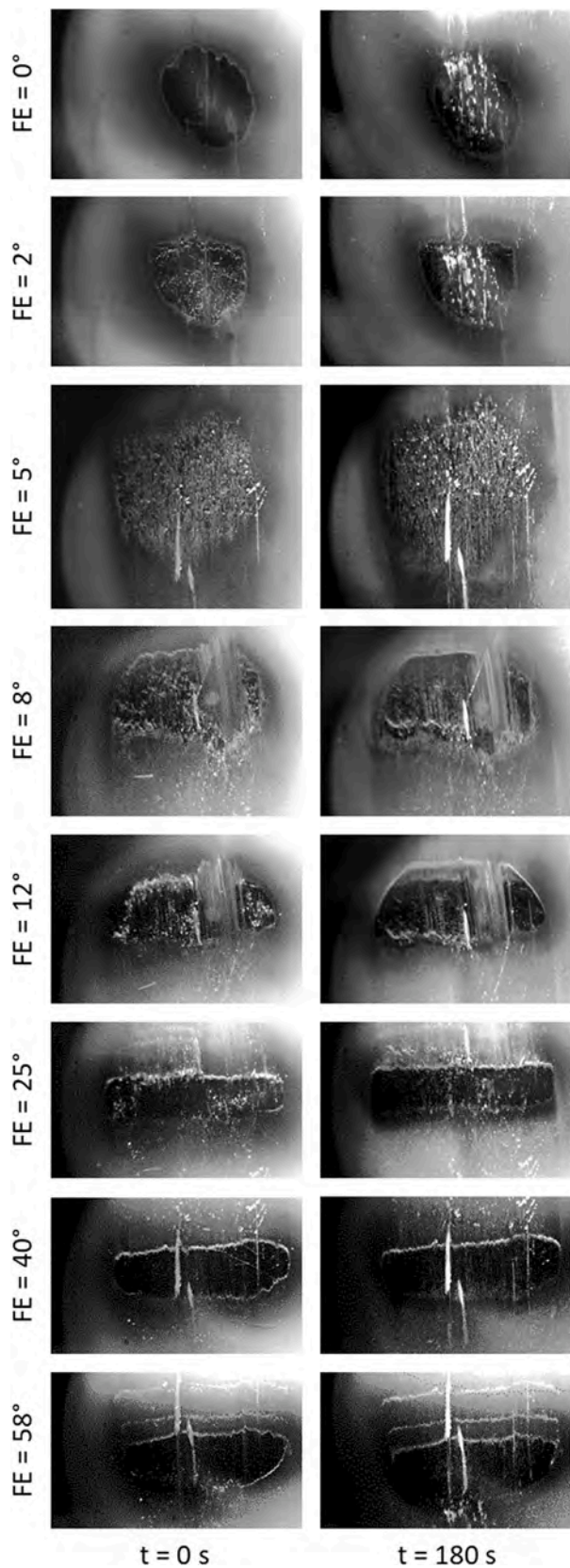


Fig. 3. Images of the contact zone taken over FE rotation at the beginning (left) and at the end (right) of the experiment; -AP direction (top); +AP direction (bottom).

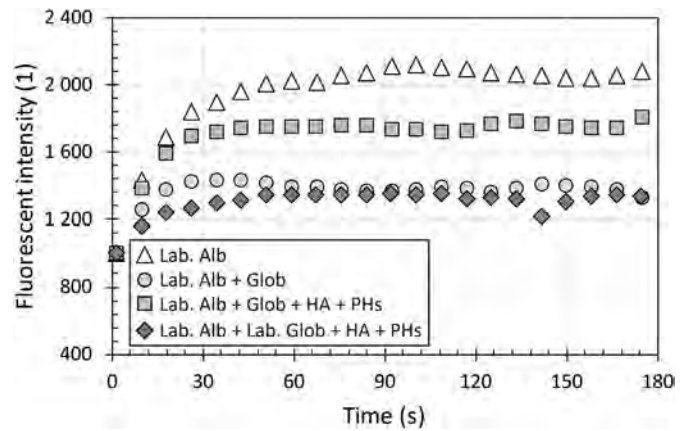


Fig. 4. Development of albumin-based film intensity (thickness) as a function of time (FE = 0°).

the emission of one fluorescent dye is partially consumed for the excitation of the second dye and vice versa (Hidrovic and Hart, 2001). The resulting intensity is lower than the expected one. Nevertheless, this experiment can confirm the trend of lubricant film development. Independently of the test lubricant, the mechanism of film formation was found to be very stable, exhibiting the initial increasing tendency of lubricant film lasting for 30–60 s with a subsequent stable phase observed for the rest of the experiment. Sudden slight fluctuations are attributed to the partial removals of protein agglomerations.

The development of film thickness for γ -globulin-based lubricants is presented in Fig. 5. The simple γ -globulin and the mixture with HA and PHs exhibit a comparable film thickness. In addition, the general increasing-stabilized behaviour is similar to that of albumin-based lubricants. While the simple γ -globulin forms a thinner layer compared to albumin, which is attributed to its lower concentration; with the complex fluid, the thickness of both specific proteins mixed together with HA and PHs is nearly the same (see the grey squares in Figs. 4 and 5). In contrary to the above results, a very unstable behaviour could be observed for the mixture of both proteins (light grey circles in Fig. 5). Qualitatively comparable results were observed when the experiment with this specific lubricant was repeated; it showed a limited ability of γ -globulin to form a stable layer when mixed only with albumin. In order to provide a clear comparison of the tested fluids, the results from Figs. 4 and 5 were merged to Fig. 6.

Later, the experiments were repeated while the camera was moved in order to enable the observation of the contact zone when the femoral component is maximally deflected according to ISO standard (FE = 58°). Some limitations of the methodology did not allow for imaging of the

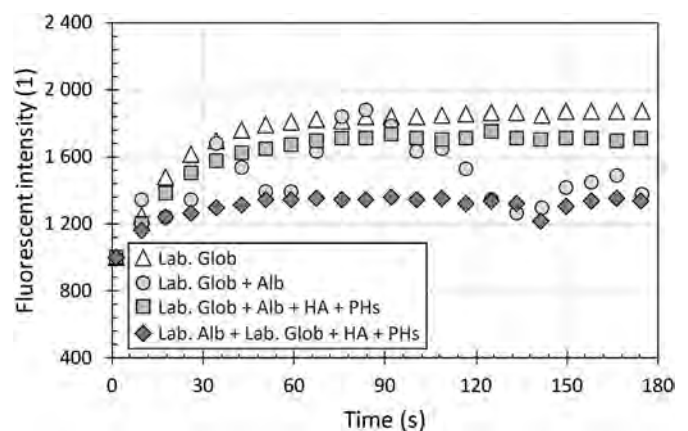


Fig. 5. Development of γ -globulin-based film intensity (thickness) as a function of time (FE = 0°).

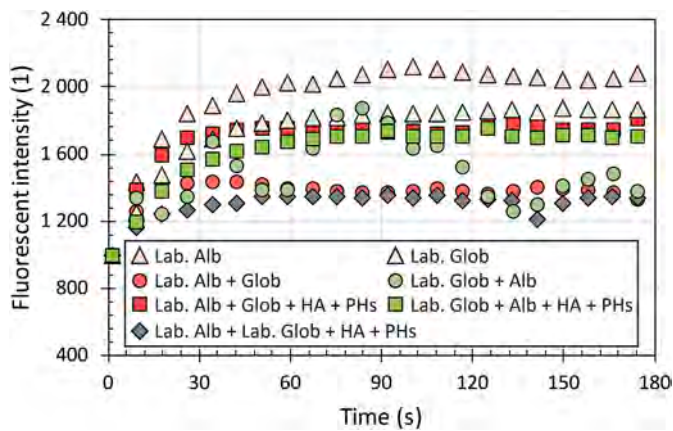


Fig. 6. Summary of results ($FE = 0^\circ$).

γ -globulin-based lubricants. This was especially due to adverse light conditions, probably due to reflection as a consequence of the increased curvature of the compartment in the location of the contact, together with generally lower intensity of the dye for staining the γ -globulin. Fig. 7 shows the results for albumin-based lubricants. Focusing on the scale of the vertical axis, not so considerable differences as in the case of the previous observations could be detected. Moreover, a complex fluid showed a reduction in the layer compared to the initial intensity. After a detailed analysis of the experiment record, it can be concluded that the film at this extreme point ($FE = 58^\circ$) is very unstable. The reader is referred to Fig. 3 showing a limited number of agglomerated proteins once the femoral component is rotated by more than 25° .

The images of the contact zone taken at the beginning of the experiment ($t = 0$ s) and after the film stabilization ($t = \text{approx. } 90$ s) for various albumin-based lubricants are shown in Fig. 8. Focusing on the initial ($FE = 0^\circ$) position, a clear increase of the adsorbed proteins together with their larger agglomerations can be observed for all the three lubricants. Considering the first cycle, it is evident that albumin forms bounded small clusters. These exhibit a tendency to be attracted close to the slight scratches of the insert oriented along the FE direction. However, it may be seen that the film is relatively uniformly distributed throughout the contact zone. After stabilization of film thickness, substantially larger and thicker protein clusters could be observed. The white colour indicates that the film is too thick, thus these localized spots are overexposed emitting a very high fluorescent intensity, indicating a thick layer of proteins. In contrary to the beginning of the test, the clusters also cover a considerably larger portion of the contact area. Regarding specific lubricant solutions, the images well illustrate the

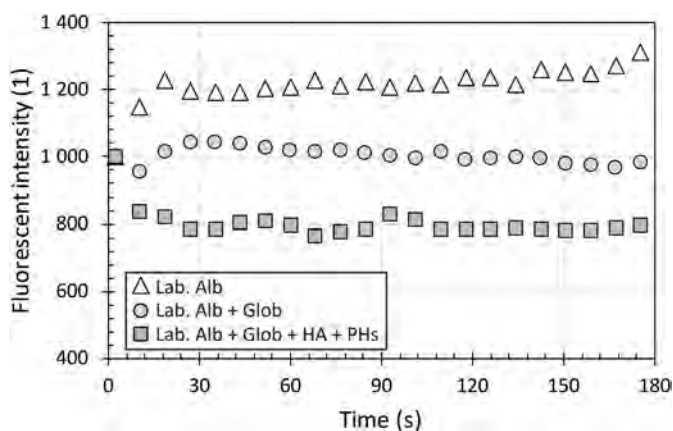


Fig. 7. Development of albumin-based film intensity (thickness) as a function of time ($FE = 58^\circ$).

above presented trends. It is evident that the simple albumin and the combination of albumin with HA and PHs form a more intense (i.e. thicker) layer, compared to the mixture of albumin and γ -globulin.

When the femoral component is fully deflected ($FE = 58^\circ$), the contact zone becomes wide and narrow, as shown in Fig. 3. Focusing on the formation of the film in the central part, there is an increased amount of albumin during the first operating cycle (see right part of Fig. 8). Further, as can be seen from the figure, the proteins tend to be grouped around the edge of the contact for all the tested fluids. Apparently, the constituents form tiny continuous clusters near the scratches as in the initial arrangement. At the later phase of the experiment, more pronounced agglomerations may be observed along the scratches. Based on the imaging of the contact, it may be concluded that the proteins tend to be formed in non-homogeneous locations. When confronting the images with the results presented in Fig. 7, the actual decrease of the number of proteins for the mixture may be seen.

4. Discussion

The information about development of film thickness inside the contact over the cycle is a fundamental parameter enabling to assess the lubrication performance of the knee replacement. However, the behaviour of the individual constituents is also of great importance. This is one of the apparent advantages of fluorescent microscopy technique. The ability to understand the formation of lubricating film in terms of individual components of SF is essential for complex understanding. Moreover, adsorption of the proteins potentially protecting the rubbing surfaces, thus lowering the wear rate (Scholes et al., 2007), may be better explained with the use of direct optical observations (Nečas et al., 2017). Focusing on the above presented results, the combined effect of the proteins without HA and PHs represents slightly misleading findings. When albumin was labelled, the addition of γ -globulin caused a rapid decrease in lubricating film. With the reversed solution (labelled γ -globulin with unlabelled albumin), the film was very unstable. Hence, the proteins influence each other's behaviour. In particular, it is assumed that the bonds between the proteins are stronger than those attracting the proteins to the surfaces. This leads to larger protein agglomerations, which was also observed in the case of hip replacements (Nečas et al., 2019c). In addition, larger clusters may be easily squeezed out of the contact, causing a decrease in lubricant film thickness. The importance of synergistic effect of SF constituents was pronounced in various references. The mutual interaction of various molecules is fundamental not only in the case of implant materials. It was shown by Nakashima et al. (2005) that combination of albumin and γ -globulin led to an improved wear resistance of hydrogel as a model of joint cartilage. Later, Yarimitsu et al. (2009) studied the formation of boundary lubricating layer on a glass substrate under static and rubbing conditions, finding that adsorption ability of HA is enhanced when mixed with γ -globulin under friction action. Finally, focusing on metal-PE interface, it was shown that the combined action of the proteins and PHs has a strong impact on wear behaviour of PE (Sawae and Murakami, 2001, Sawae et al., 2005, 2009). The authors highlighted that both the content and mutual ratio of the constituents play a role. Focusing on the combined effect of HA and PHs observed in the present study, it is apparent that the action is affected by the contact conditions. During the rolling phase of the experiment, HA and PHs had a positive stabilizing effect on lubricant film for the mixtures of the proteins (Figs. 4 and 5). However, in the later, sliding phase, addition of these constituents led to worse lubrication conditions (Fig. 7). Thus, the results indicate the sensitivity of the HA and PHs layer to a slip level which requires further investigation. To conclude, it is highly recommended to employ a complex model SF when performing biotribological analyses of artificial joints. When confronting the findings for hip and knee replacements, apparent differences are observed for simple protein solutions. While single proteins formed the thinnest film in the case of hips (Nečas et al., 2019b), a comparable thickness with complex fluid is reported in the present study

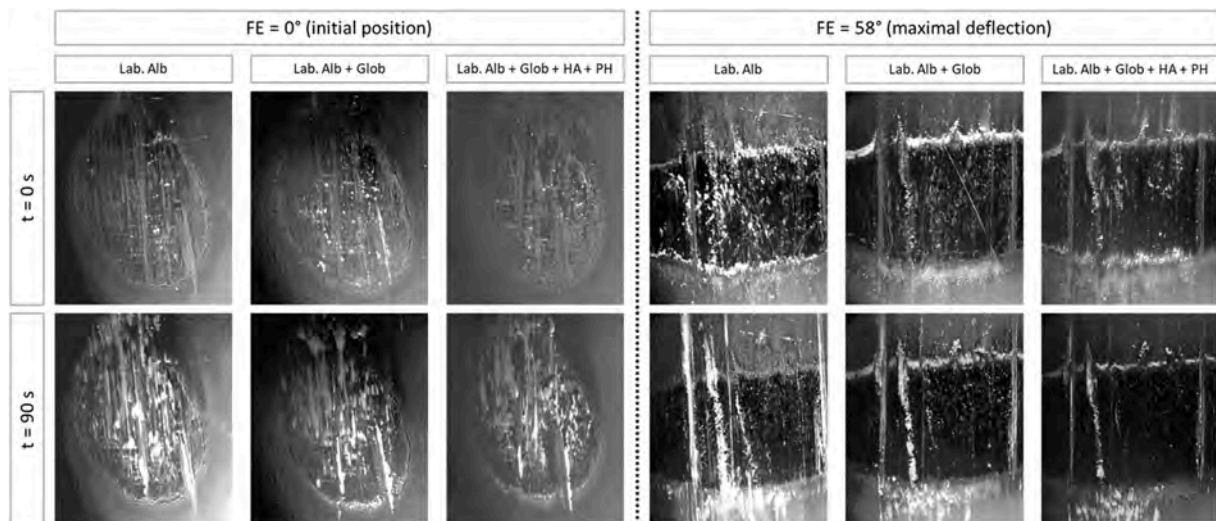


Fig. 8. Images of the contact zone at the initial and maximally deflected position for albumin-based solutions.

for knee implants. This finding supports an important role of geometry (conformity) and corresponding contact pressure. Therefore, simplified experimental configurations (e.g. ball-on-disc, pin-on-plate) will always suffer from this drawback.

Observations of protein film thickness are often exposed to debates regarding their repeatability. The reason is that the applied methodology is very demanding in terms of repeating the experiments due to (i) high costs associated with insert manufacturing and protein labelling, (ii) complicated and time-consuming experimental protocol, and (iii) complexity of behaviour of model SF. However, it should be noted that the repeatability was exposed to more doubts in the case of simplified ball-on-disc non-conformal configuration which was used previously (Mavraki and Cann, 2011; Nečas et al., 2016). When examining more conformal realistic arrangements such as ball-on-cup (hip implant) (Nečas et al., 2019b), or femoral-on-tibial (knee implant) (Nečas et al., 2019a), the repeatability became much better (Vrbka et al., 2015; Nečas et al., 2019a). Therefore, in order to propose a complex assessment of protein film behaviour, the experiments were conducted only once and repeated only in the case of unclear results. These were usually associated with hardware limitations, such as improper initial settings of the contact components or adverse light conditions. It must be emphasized that observations of film formation using the developed simulator together with the application of fluorescent method require a strong compliance with the defined laboratory protocol.

Regardless of the experience acquired from previous studies, an illustrative repeatability test was conducted in order to provide a comparison of results obtained from measurements realized in different days. The contact was lubricated by a simple albumin-based solution; the development of film thickness at $FE = 0^\circ$ position is shown in Fig. 9. As can be seen, almost identical results could be obtained. The maximum deviation in specific time steps was less than 4%. The purpose of this simple test is also to present an important issue of scaling. Fluorescent intensity is very sensitive and dependent on various factors, such as ambient light, intensity of light source, microscope filter, quenching due to presence of chromium (Jie, 1998), or fluorescent marker type (i.e. albumin labelled vs. γ -globulin labelled). Therefore, the intensity normalization has to be carried out in order to enable a mutual comparison of the results. The principle was explained in greater detail in our previous study (Nečas et al., 2019b). The point is that the average fluorescent intensity from one of the initial images is normalized to a given value (1000 in this specific case) by multiplication or division. The remaining intensity values are subsequently multiplied/divided by the given normalization constant. This approach enables to compare the data independently of the aforementioned side effects. The performed

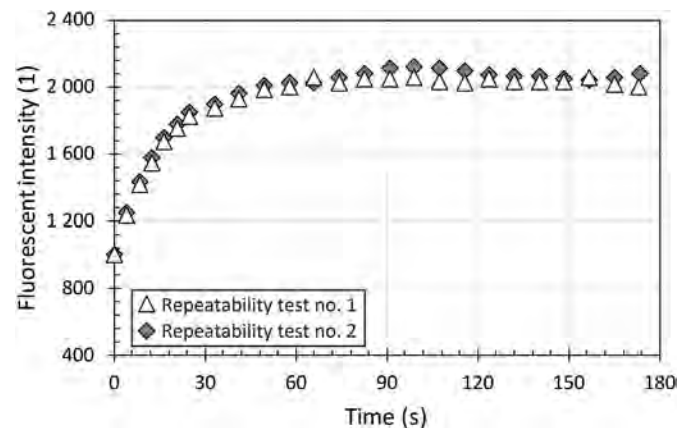


Fig. 9. Development of albumin protein film intensity (thickness) as a function of time – repeatability test ($FE = 0^\circ$).

sensitivity analysis showed that the selection of improper image for normalization may lead to a deviation of overall results by up to 20%. Therefore, it was suggested to use the first image once the cycle starts rather than the initial static image because the beginning of the cycle is associated with mutual alignment of the contact components. This phenomenon was apparently not observed for the hip implant where the ball precisely fits the cup during the arrangement (Nečas et al., 2019b). Therefore, the present study employed a calibration process based on the first image taken throughout swinging. Following the above explanation about the measurement principle, the images (Figs. 4–7 and 9) show a qualitative development of protein film while a double intensity at the end of the test corresponds to a double thickness of the initial lubricating film.

The limitations of the performed study and the motivation for further experimental investigation should be discussed. At first, the difference between the original PE and the used PMMA for tibial insert needs to be mentioned. PMMA exhibits about five-to six-times higher elastic modulus compared to PE which may affect formation of the lubricating film to some extent. However, the applied load was proportionally decreased in order to achieve contact pressure to be comparable with original material combination. Even that, it should be taken into account that the elastic deformations are smaller for PMMA due to higher elastic modulus under the same pressure conditions. If the size of the contact zone would be too small (e.g. fractions of millimetres typical for ball-on-

disc arrangements) and thus the pressure would be too high, the proteins couldn't easily enter the contact which would certainly affect film formation process. However, in the case of PMMA insert, the contact zone is large enough (3–6 mm) to enable full development of the film and passage of the proteins directly through the contact, as is illustrated in Fig. 3. Considering the potential differences, the issue of surface roughness should also be mentioned. As stated above, average roughness of CoCrMo and PMMA is around 55 nm and 40 nm, respectively. Roughness of the original PE insert is between 80 nm and 180 nm, dependently on the measurement location. However, it is expected that running-in articulation of compliant PE insert with rigid CoCrMo component may lead to further polishing of the insert, causing the roughness to be even closer to PMMA. Focusing on the surface properties, surface wettability has to be also taken into account. Both PE and PMMA are considered to be hydrophobic materials (Gong et al., 2016; Shahzadi et al., 2018). However, when focusing on the measurement of water contact angle (WCA), it was found that PE exhibits WCA to be 87° (Van Vrekhem et al., 2018) and PMMA showed WCA to be around 80° (Martínez-Pérez et al., 2020). Assuming that WCA equal to 90° represents the boundary between hydrophilicity and hydrophobicity, measurements of WCAs indicated that the surfaces of both the materials exhibit slightly hydrophilic behaviour. In order to confirm the reported findings, additional droplet test was carried out using the flat samples of PE and PMMA, focusing on WCA. Medical grade PE was used for fabrication of PE plate, while the surface roughness corresponded to the real knee insert. PMMA plate was manufactured from the same stock and processed in the same way as the employed PMMA insert. The droplet of water was applied through an electronic syringe pump enabling to control the amount of the supplied water. The gap between the tip of the syringe pump and the specimen was stable. The measurements were repeated three times for both the plates. It was found that average WCAs for PE and PMMA were $\theta_{PE} = 83.3^\circ$ and $\theta_{PMMA} = 79^\circ$, respectively. Very good repeatability was observed while WCAs ranged from 82° to 85° for PE and from 78° to 80° for PMMA (see Fig. 10). The obtained values are in good accordance with the above observations. Thus, it may be concluded that PE and PMMA exhibit similar surface properties. Finally, both PE and PMMA are thermoplastics and have comparable properties such as density, tensile strength, melting temperature, specific heat capacity, Vicat softening temperature or relative permittivity. Therefore, due to the necessity of one of the contact bodies to be transparent, it is assumed that PMMA is an appropriate representative of the polymer

insert material.

Further, as indicated above, only a simplified loading cycle was applied. Since Myant et al. (2014) showed that transient conditions substantially influence the behaviour of protein lubricating film, more complex operating conditions should be taken into account when assessing the lubrication performance. The use of simplified loading in the present paper is associated mainly with the complexity of the system. Measurement of friction or wear rate, using commercial simulators, is a routine procedure. However, a direct observation of the contact with respect to more complex conditions is a challenging task. Although, compared to the previous paper (Nečas et al., 2019a), the frequency of the stroke could be increased from 0.5 to 0.75 Hz, the application of transient load and motion was found to be hardly controlled at the same time and it requires further partial modification of the test rig. In addition, further increase of frequency up to 1 Hz would be helpful while it is suggested that a longer lasting cycle leads to a thinner lubricating film (Su et al., 2011). In general, it is strongly motivating to further improve the ability of the simulator as well as the experimental procedure when revealing mechanisms of film formation in the knee implant. Thus, the future study should respect not only the geometry, the fluid composition, and the contact pressure, but also real knee dynamics (kinematics and load).

The importance of proper operating conditions may be highlighted when comparing the results of the present and previous knee study (Nečas et al., 2019a). Although the previous paper concerned mainly with the description of methodology, some pilot data were also presented. The film behaviour was different, exhibiting an initial rapid increase with a subsequent decrease before the film was stabilized. This difference is attributed to a slip of the component over the contact area at the initial position throughout the experiment. Based on the preliminary study, the initial settings of the components were improved in order to allow for a slight shift in AP direction leading to a more continuous development of the lubricating film. Further, only the lateral compartment was observed while it was indicated in literature that the medial compartment may behave in a slightly different manner. In particular, more extensive wear together with larger maximum and smaller average film thickness was reported in the recent numerical study (Gao et al., 2018). However, on the contrary, experimental studies showed that the lateral compartment may suffer from greater friction (Scholes et al., 2006, 2007). Hence, the upcoming study should compare the behaviour of both compartments in order to clarify divergent findings reported by other authors.

Very promising is also the observation of film development throughout the individual cycles. Although the present study concentrated on the initial ($FE = 0^\circ$) and maximally deflected ($FE = 58^\circ$) position, a more detailed investigation into the swing can be highly appreciated for understanding of knee replacement lubrication function. Focusing on the contact conditions, the importance of slide-to-roll ratio (SRR) should be highlighted. When using simple ball-on-disc configuration, substantial effect of SRR on protein lubrication was observed previously (Mavraki and Cann, 2011; Vrbka et al., 2013; Nečas et al., 2016). However, in the case of current real-shaped model, it is very complicated to clearly assess the cycle by means of SRR. The base idea comes from the observation of the contact zone (see Fig. 3). Beyond $FE = 25^\circ$, only a limited protein formation may be observed for both the first and the last cycle. The suggested explanation of different mechanism of film formation is as follows. The femoral component rolls around the tibial insert during the first part of the cycle (movement along the negative AP direction, see Fig. 2) allowing for continuous formation of protein film; having reached the turning point, the femoral part starts to slide along the positive AP, thus removing the layer of the proteins from the insert surface. In order to determine the role of SRR in a detail, simplified geometrical arrangement (e.g. wheel-on-flat) enabling to control SRR over the cycle with respect to the real knee kinematics might help to explore the fundamentals of film formation. Moreover, the experiments performed with suitable Newtonian fluid (e.g. low viscosity

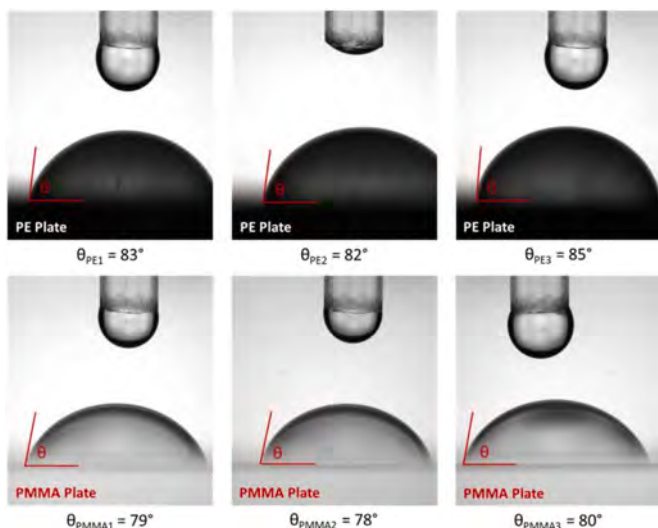


Fig. 10. Measurement of WCAs for PE (top) and PMMA (bottom) plate using water droplet test. Note: The difference in visual appearance is due to transparency of PMMA.

oil) may offer a better comparison with previous numerical investigations.

5. Conclusion

The present paper aimed at the behaviour of protein lubricating film in the knee joint replacement. A developed knee simulator was used to observe the contact of metal femoral and transparent polymer tibial component. The contact was lubricated by various model lubricants with attention being paid to the behaviour of fluorescently stained albumin and γ -globulin. The development of film thickness was observed with the use of fluorescent microscopy. The main findings are concluded as follows:

- The contact area within the knee implant is continuously changing throughout the walking cycle while its shape and size vary considerably. Focusing on the proteins, these exhibit a strong ability to be agglomerated near the scratches and edges of the contact. The protein layer is considerably thicker at the initial ($FE = 0^\circ$) position compared to the maximally deflected ($FE = 58^\circ$) position.
- Interaction of proteins plays an important role in lubrication of knee replacement while HA and PHs lead to a stabilizing behaviour ensuring a uniform distribution of the protein clusters over the contact area.
- Considering the differences compared to the hip implants, the essential effect of geometry has been highlighted; this may render simplified geometric configurations insignificant.
- Following the previous point, experimental investigations should be of greater interest when analysing the biotribological performance of the joint replacements in terms of the use of the lubricants exhibiting a comparable behaviour to those represented by human SF.

Further investigations should focus on (a) application of transient loading and kinematic conditions, (b) description of film thickness development throughout the individual loading cycles, (c) film formation as a function of SRR with respect to knee kinematics, (d) assessment of film thickness with the use Newtonian lubricant in order to validate previous numerical studies.

Author statement

D. Nečas: Conceptualization; Methodology; Formal analysis; Investigation; Writing - Original Draft; Writing - Review & Editing.

K. Sadecká: Formal analysis; Validation; Investigation; Writing - Original Draft.

M. Vrbka: Conceptualization; Data Curation; Writing - Original Draft; Writing - Review & Editing; Supervision.

A. Galandáková: Resources; Methodology; Investigation.

M.A. Wimmer: Supervision; Project administration; Funding acquisition; Writing - Original Draft.

J. Gallo: Supervision; Funding acquisition; Writing - Original Draft.

M. Hartl: Supervision; Project administration; Funding acquisition; Writing - Review & Editing.

Declaration of competing interest

The authors declare that they have no known competing financial interests or personal relationships that could have appeared to influence the work reported in this paper.

Acknowledgement

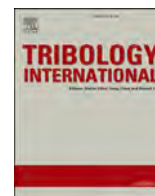
This study was carried out under the project LTAUSA17150 with financial support from the Ministry of Education, Youth and Sports of the Czech Republic. The research was also supported by the project CEITEC 2020 (LQ1601) with financial support from the Ministry of

Education, Youth and Sports of the Czech Republic under the National Sustainability Programme II and by RVO 61989592.

References

- Azushima, A., 2005. In lubro 3D measurement of oil film thickness at the interface between tool and workpiece in sheet drawing using a fluorescence microscope. *Tribol. Int.* 38, 105–112.
- Chyr, A., Sanders, A.P., Raeymaekers, B., 2013. A hybrid apparatus for friction and accelerated wear testing of total knee replacement bearing materials. *Wear* 308, 54–60.
- Di Paolo, J., Berli, M.E., 2006. Numerical analysis of the effects of material parameters on the lubrication mechanism for knee prosthesis. *Comput. Methods Biomech. Biomed. Eng.* 9, 79–89.
- Ding, Y., Qin, C.-qiang, Fu, Y.-ru, Xu, J., Huang, D.-sheng, 2012. In vitro comparison of the biological activity of alumina ceramic and titanium particles associated with aseptic loosening. *Biomed. Mater.* 7 <https://doi.org/10.1088/1748-6041/7/4/045019>.
- Flannery, M., McGloughlin, T., Jones, E., Birkinshaw, C., 2008. Analysis of wear and friction of total knee replacements: Part I. Wear assessment on a three station wear simulator. *Wear* 265, 999–1008.
- Flannery, M., Jones, E., Birkinshaw, C., 2008b. Analysis of wear and friction of total knee replacements: Part II: friction and lubrication as a function of wear. *Wear* 265, 1009–1016.
- Galandáková, A., Ulrichová, J., Langová, K., Hanáková, A., Vrbka, M., Hartl, M., Gallo, J., 2016. Characteristics of synovial fluid required for optimization of lubrication fluid for biotribological experiments. *J. Biomed. Mater. Res. B Appl. Biomater.* 105, 1422–1431.
- Gallo, J., Goodman, S.B., Kontinen, Y.T., Wimmer, M.A., Holinka, M., 2013. Osteolysis around total knee arthroplasty: a review of pathogenetic mechanisms. *Acta Biomater.* 9, 8046–8058.
- Gao, L., Hua, Z., Hewson, R., Andersen, M.S., Jin, Z., 2018. Elastohydrodynamic lubrication and wear modelling of the knee joint replacements with surface topography. *Biosurface and Biotribology* 4, 18–23.
- Gong, K., Qu, S., Liu, Y., Wang, J., Zhang, Y., Jiang, C., Shen, R., 2016. The mechanical and tribological properties of UHMWPE loaded ALN after mechanical activation for joint replacements. *Journal of the Mechanical Behavior of Biomedical Materials* 61, 334–344.
- Health at a Glance 2019, 2019. OECD. <https://doi.org/10.1787/4dd50c09-en>.
- Hidrovo, C.H., Hart, D.P., 2001. Emission reabsorption laser induced fluorescence (ERLIF) film thickness measurement. *Meas. Sci. Technol.* 12, 467–477.
- ISO 14243-3:2014, Implants for Surgery — Wear of Total Knee-Joint Prostheses — Part 3: Loading and Displacement Parameters for Wear-Testing Machines with Displacement Control and Corresponding Environmental Conditions for Test.
- Jie, N., 1998. Determination of chromium in waste-water and cast iron samples by fluorescence quenching of rhodamine 6G. *Talanta* 46, 215–219.
- Jin, Z.M., Dowson, D., Fisher, J., Ohtsuki, N., Murakami, T., Higaki, H., Moriyama, S., 2016. Prediction of transient lubricating film thickness in knee prostheses with compliant layers. *Proc. IME H J. Eng. Med.* 212, 157–164.
- Kennedy, F.E., Van Citters, D.W., Wongseedakaew, K., Mongkolwongrojn, M., 2007. Lubrication and wear of artificial knee joint materials in a Rolling/Sliding tribotester. *J. Tribol.* 129, 326–335.
- Kretzer, J.P., Reinders, J., Sonntag, R., Hagmann, S., Streit, M., Jeager, S., Moradi, B., 2014. Wear in total knee arthroplasty—just a question of polyethylene? *Int. Orthop.* 38, 335–340.
- Kurtz, S., 2005. Prevalence of primary and revision total hip and knee arthroplasty in the United States from 1990 through 2002. *J. Bone Joint Surg.* 87.
- Kurtz, S., Ong, K., Lau, E., Mowat, F., Halpern, M., 2007. Projections of primary and revision hip and knee arthroplasty in the United States from 2005 to 2030. *J. Bone Joint Surg.* 89, 780–785.
- Martínez-Pérez, A.I., Vera-Cárdenas, E.E., Luna-Bárceñas, G., Pérez-Robles, J.F., Mauricio-Sánchez, R.A., 2020. Characterization and sliding wear performance of PMMA reinforced with SiO₂ nanoparticles. *J. Thermoplast. Compos. Mater.* 33, 867–881.
- Mavraki, A., Cann, P.M., 2011. Lubricating film thickness measurements with bovine serum. *Tribol. Int.* 44, 550–556.
- Mongkolwongrojn, M., Wongseedakaew, K., Kennedy, F.E., 2010. Transient elastohydrodynamic lubrication in artificial knee joint with non-Newtonian fluids. *Tribol. Int.* 43, 1017–1026.
- Murakami, T., Nakashima, K., Sawae, Y., Sakai, N., Hosoda, N., 2009. Roles of adsorbed film and gel layer in hydration lubrication for articular cartilage. *Proc. IME J. J. Eng. Tribol.* 223, 287–295.
- Murakami, T., Nakashima, K., Yarimitsu, S., Sawae, Y., Sakai, N., 2011. Effectiveness of adsorbed film and gel layer in hydration lubrication as adaptive multimode lubrication mechanism for articular cartilage. *Proc. IME J. J. Eng. Tribol.* 225, 1174–1185.
- Myant, C.W., Cann, P., 2014. The effect of transient conditions on synovial fluid protein aggregation lubrication. *J. Mech. Behav. Biomed. Mater.* 34, 349–357.
- Nakashima, K., Sawae, Y., Murakami, T., 2005. Study on wear reduction mechanisms of artificial cartilage by synergistic protein boundary film formation. *JSME Int. J. Ser. C* 48, 555–561.
- Nečas, D., Vrbka, M., Urban, F., Krupka, I., Hartl, M., 2016. The effect of lubricant constituents on lubrication mechanisms in hip joint replacements. *J. Mech. Behav. Biomed. Mater.* 55, 295–307.

- Nečas, D., Vrbka, M., Urban, F., Gallo, J., Krupka, I., Hartl, M., 2017. In situ observation of lubricant film formation in THR considering real conformity: the effect of diameter, clearance and material. *J. Mech. Behav. Biomed. Mater.* 69, 66–74.
- Nečas, D., Vrbka, M., Rebenda, D., Gallo, J., Galandáková, A., Wolfová, L., Krupka, I., Hartl, M., 2018. In situ observation of lubricant film formation in THR considering real conformity: the effect of model synovial fluid composition. *Tribol. Int.* 117, 206–216.
- Nečas, D., Sadecká, K., Vrbka, M., Gallo, J., Galandáková, A., Krupka, I., Hartl, M., 2019a. Observation of lubrication mechanisms in knee replacement: a pilot study. *Biotribology* 17, 1–7.
- Nečas, D., Vrbka, M., Galandáková, A., Krupka, I., Hartl, M., 2019b. On the observation of lubrication mechanisms within hip joint replacements. Part I: hard-on-soft bearing pairs. *J. Mech. Behav. Biomed. Mater.* 89, 237–248.
- Nečas, D., Vrbka, M., Gallo, J., Krupka, I., Hartl, M., 2019c. On the observation of lubrication mechanisms within hip joint replacements. Part II: hard-on-hard bearing pairs. *J. Mech. Behav. Biomed. Mater.* 89, 249–259.
- Ohtsuki, N., Murakami, T., Moriyama, S., Higaki, H., 1997. Influence of geometry of conjunction on elastohydrodynamic film formation in knee prostheses with compliant layer. In: *Elastohydrodynamics - '96 Fundamentals and Applications in Lubrication and Traction*, Proceedings of the 23rd Leeds-Lyon Symposium on Tribology Held in the Institute of Tribology, Department of Mechanical Engineering, Tribology Series. Elsevier, pp. 349–359.
- Pascau, A., Guardia, B., Puertolas, J.A., Gómez-Barrena, E., 2009. Knee model of hydrodynamic lubrication during the gait cycle and the influence of prosthetic joint conformity. *J. Orthop. Sci.* 14, 68–75.
- Ranuša, M., Gallo, J., Vrbka, M., Hobza, M., Paloušek, D., Krupka, I., Hartl, M., 2016. Wear analysis of extracted polyethylene acetabular cups using a 3D optical scanner. *Tribol. Trans.* 1–11.
- Reinders, J., Sonntag, R., Vot, L., Gibney, C., Nowack, M., Kretzer, J.P., Zadpoor, A.A., 2015. Wear testing of moderate activities of daily living using in vivo measured knee joint loading. *PLoS One* 10.
- Rieker, C.B., 2016. Tribology of total hip arthroplasty prostheses. *EFORT Open Reviews* 1, 52–57.
- Sawae, Y., Murakami, T., 2001. Role of synovia in wear mechanism of UHMWPE. *Tribology in biomechanical systems. Sci. Appl.* 31–45.
- Sawae, Y., Murakami, T., Sawano, T., 2005. The influences of lipid and protein concentration on wear of ultra-high molecular weight polyethylene. In: *Life Cycle Tribology, Tribology and Interface Engineering Series*. Elsevier, pp. 171–177.
- Sawae, Y., Yamamoto, A., Murakami, T., 2008. Influence of protein and lipid concentration of the test lubricant on the wear of ultra high molecular weight polyethylene. *Tribol. Int.* 41, 648–656.
- Schiffner, E., Latz, D., Karbowski, A., Grassmann, J.P., Thelen, S., Windolf, J., Jungbluth, P., Schnependahl, J., 2019. Loosening of total knee arthroplasty – always aseptic? *J. Clin. Orthop. Trauma*. <https://doi.org/10.1016/j.jcot.2019.05.001>.
- Scholes, S.C., Unsworth, A., 2006. The effects of proteins on the friction and lubrication of artificial joints. *Proc. IME H J. Eng. Med.* 220, 687–693.
- Scholes, S.C., Unsworth, A., Jones, E., 2007. Polyurethane unicondylar knee prostheses: simulator wear tests and lubrication studies. *Phys. Med. Biol.* 52, 197–212.
- Schroer, W.C., Berend, K.R., Lombardi, A.V., Barnes, C.L., Bolognesi, M.P., Berend, M.E., Ritter, M.A., Nunley, R.M., 2013. Why are total knees failing today? Etiology of total knee revision in 2010 and 2011. *J. Arthroplasty* 28, 116–119.
- Shahzadi, I., Bashir, M., Bashir, S., Inayat, M.H., 2018. Thermally assisted coating of PVA for hydrophilic surface modification of PMMA microchannel for oil in water emulsion. In: 2018 15th International Bhurban Conference on Applied Sciences and Technology.
- Stevenson, H., Jaggard, M., Akhbari, P., Vaghela, U., Gupte, C., Cann, P., 2019. The role of denatured synovial fluid proteins in the lubrication of artificial joints. *Biotribology* 17, 49–63.
- Stewart, T., Jin, Z.M., Fisher, J., 1997. Friction of composite cushion bearings for total knee joint replacements under adverse lubrication conditions. *Proc. IME H J. Eng. Med.* 211, 451–465.
- Su, Y., Yang, P., Fu, Z., Jin, Z., Wang, C., 2011. Time-dependent elastohydrodynamic lubrication analysis of total knee replacement under walking conditions. *Comput. Methods Biomech. Biomed. Eng.* 14, 539–548.
- Su, Y., Fu, Z., Yang, P., Wang, C., 2012. A full numerical analysis of elastohydrodynamic lubrication in knee prosthesis under walking condition. *J. Mech. Med. Biol.* 10, 621–641.
- Tandon, P.N., Jaggi, S., 1979. A model for the lubrication mechanism in knee joint replacements. *Wear* 52, 275–284.
- Tandon, P.N., Jaggi, S., 1981. Wear and lubrication in an artificial knee joint replacement. *Int. J. Mech. Sci.* 23, 413–422.
- Van Vrekhem, S., Vloebergh, K., Asadian, M., Verbruggen, C., Declercq, H., Van Tongel, A., De Wilde, L., De Geyter, N., Morent, R., 2018. Improving the surface properties of an UHMWPE shoulder implant with an atmospheric pressure plasma jet. *Sci. Rep.* 8.
- Vrbka, M., Návrát, T., Krupka, I., Hartl, M., Šperka, P., Gallo, J., 2013. Study of film formation in bovine serum lubricated contacts under rolling/sliding conditions. *Proc. IME J. J. Eng. Tribol.* 227, 459–475.
- Vrbka, M., Nečas, D., Hartl, M., Krupka, I., Urban, F., Gallo, J., 2015. Visualization of lubricating films between artificial head and cup with respect to real geometry. *Biotribology* 1–2, 61–65.
- Yarimitsu, S., Nakashima, K., Sawae, Y., Murakami, T., 2007. Study on the mechanisms of wear reduction of artificial cartilage through in situ observation on forming protein boundary film. *Tribol. Online* 2, 114–119.
- Yarimitsu, S., Nakashima, K., Sawae, Y., Murakami, T., 2009. Influences of lubricant composition on forming boundary film composed of synovia constituents. *Tribol. Int.* 42, 1615–1623.
- Yao, J.Q., Laurent, M.P., Johnson, T.S., Blanchard, C.R., Crowninshield, R.D., 2003. The influences of lubricant and material on polymer/CoCr sliding friction. *Wear* 255, 780–784.



Towards the understanding of lubrication mechanisms in total knee replacements – Part I: Experimental investigations

David Nečas^{a,*}, Martin Vrbka^a, Max Marian^b, Benedict Rothhammer^b, Stephan Tremmel^c, Sandro Wartzack^b, Adéla Galandáková^d, Jiří Gallo^e, Markus A. Wimmer^f, Ivan Krupka^a, Martin Hartl^a

^a Department of Tribology, Faculty of Mechanical Engineering, Brno University of Technology, Technická 2896/2, 616 69, Brno, Czech Republic

^b Engineering Design, Friedrich-Alexander-Universität Erlangen-Nürnberg (FAU), Martensstr. 9, 910 58, Erlangen, Germany

^c Engineering Design and CAD, University of Bayreuth, Universitätsstr. 30, 95448, Bayreuth, Germany

^d Department of Medical Chemistry and Biochemistry, Faculty of Medicine and Dentistry, Palacky University Olomouc, Hněvotínská 3, 775 15, Olomouc, Czech Republic

^e Department of Orthopaedics, Faculty of Medicine and Dentistry, Palacky University Olomouc, University Hospital Olomouc, I. P. Pavlova 6, 775 20, Olomouc, Czech Republic

^f Department of Orthopedic Surgery, Rush University Medical Center, 1611 W. Harrison St., 60612, Chicago, IL, USA

ARTICLE INFO

Keywords:

Total knee replacement
Knee simulator
Fluorescent microscopy
Lubrication
Experiment

ABSTRACT

This contribution is aimed at the detailed understanding of lubrication mechanisms within total knee replacement. While Part I is focused on the experimental investigation, Part II deals with the development of a predictive numerical model. Here, a knee simulator was used for direct optical observation of the contacts between a metal femoral and a transparent polymer components. Transient dynamic conditions were applied. Mimicked synovial fluids with fluorescently labelled constituents were used as the test lubricants. The results showed that γ -globulin forms thin boundary lubricating film, being reinforced by the interaction of phospholipids and hyaluronic acid. Further development of lubricating film is attributed to albumin layering. Based on the results, a novel lubrication model of the knee implant is proposed.

1. Introduction

Surgery known as total knee arthroplasty (TKA) is bringing relief from pain and improving the knee function for up to 25 years after the surgery for the majority of patients [1,2]. The numbers of TKAs done world-wide continue to grow with a current rough estimation of about two million TKA surgeries performed annually [3,4]. Aseptic loosening in conjunction with periprosthetic osteolysis have been reported to be a leading long-term cause of TKA failure to date [5]. Osteolysis has been causally linked to wear of polyethylene surfaces. This pathogenic concept has been supported by isolation of a huge amounts of polyethylene particles in the periprosthetic tissues, histopathological examination of retrieved periprosthetic tissues, and a wide range of experimental studies [6]. Since the introduction of highly cross-linked polyethylene (HXLPE) in TKA, the reasons for revision of TKA have gradually changed in favor of alternative causes of TKA failure [7,8]. This change is a consequence of the increasing use of HXLPE that was initially reserved for applications in total hip arthroplasty (THA) [9].

While there is not information yet available, based on registry data roughly 80% of TKAs survive 25 years [10]. In order to increase the life span, more tribological fine tuning might be helpful.

Joint surface wear has been studied in both THA [11] and in TKA [12]. Despite the fact that the basic typology of material damage is very similar [13–16], there are obvious differences regarding wear rates [17]. Generally speaking, the wear performance of TKA depends on *in vivo* loading, design factors of the implant, and surgical and patient-specific factors. For example, polyethylene damage in a TKA may depend on gait characteristics [18] or the locking mechanism of the polyethylene insert in the metal tray [19]. Despite all the technological developments, the material characteristics of the implant play an important role [20].

Based on recent projections for the use of total joint replacement by 2050, there will be an enormous increase in the amount of TKA surgeries in the USA [21] and most likely worldwide. More and more, TKA is implanted in ever younger patients, which requires longer survival times of the implant. Although, HXLPE liners exhibit lower wear rate in comparison to non-XLPE [22], this may not always translate into fewer

* Corresponding author.

E-mail address: David.Necas@vut.cz (D. Nečas).

<https://doi.org/10.1016/j.triboint.2021.106874>

Received 14 October 2020; Received in revised form 27 December 2020; Accepted 8 January 2021

Available online 12 January 2021

0301-679X/© 2021 Elsevier Ltd. All rights reserved.

particles *in vivo* [23]. Also, a detectable surface damage of retrieved HXLPE liners from aseptically failed TKAs has been observed [13,24]. Finally, there is an uncertainty related to a reduced inflammatory and osteolytic potential of HXLPE particles [25,26], despite that some studies report their decreased specific biological activity [27,28]. Clearly, there is a higher proportion of smaller particles produced by HXLPE compared to non-XLPE [29]. Taken together, there is still room for further tribological improvements of TKA. In this context, it is vital to understand the individual biotribological situation and wear behavior in a particular TKA over time, and dependent on everyday activities. This includes the study of the formation and retention of lubricant films. Ideally, tribological testing should conform to ISO 14243 [30,31], which is an established standard for wear rate assessment of knee replacements [32]. The main motivation of using standardized conditions is in ability of comparison of the findings and data across various simulators, approaches and methodologies. Apparently, ISO is not able to cover all the clinical performance considering various activities or the effects such as sudden impacts. However, it should be noted that when revealing the fundamentals, the standards provide a suitable base which is frequently followed by researchers.

Assuming wear is considerably influenced by lubrication performance, and the efficiency of lubrication thus remarkably influences the implant lifetime [33], it must be emphasized that the lubrications mechanisms within TKA have not yet been sufficiently clarified. While few studies reported in literature deal with numerical simulation, see Part II [34], even less focus was on experimental investigation. A pilot study employed a technique based on resistivity measurement when detecting thickness of the lubricant layer in the contact between a metal ball and a conductive silicone rubber layer representing the tibial insert [35]. The contact was lubricated by silicone oils while the authors mostly focused on the influence of contact geometry. It was concluded that an ellipse-like contact with transversely elongated ellipse supported thicker films compared to a longitudinal ellipse or circle shaped contact. The importance of synovial fluid lubrication was later highlighted by Scholes et al. [36,37], who studied the influence of kinematics and loading conditions on biotribological performance of hip implants and a prototype of polyurethane (PU) unicompartmental knee replacement [36]. A prototype of PU knee implant was further investigated in terms of wear and lubrication in the subsequent paper [37]. Among others, the authors pointed out that the adsorbed proteins form solid-like films protecting the surfaces against extensive wear. The necessity of proper selection of the model lubricant was discussed as well. This statement is supported by later investigation provided by Bortel et al. [38]. The authors pointed out that often-employed calf serum may hardly mimic behavior of synovial fluid. The authors suggested model fluids containing proteins, hyaluronic acid (HA), phospholipids (PLs), and salts. It was concluded that proper composition of model fluid may provide clinically realistic friction and wear data when testing the prosthesis. Further investigation aimed at the detailed assessment of the influence albumin protein, which is dominant in both calf serum and synovial fluid, on wear of ultra-high molecular weight polyethylene (UHMWPE) [39]. It is suggested that conformational changes of albumin due to binding bilirubin contained in the fluid may lead to the formation of the bridges between UHMWPE and metal counterfaces, which eventually leads to elevated wear rate. The authors further found that these conformational changes may be prevented by the interaction of albumin with fatty acid. Nevertheless, it is assumed that albumin behavior has a substantial impact on wear processes within metal-PE implants. PE wear is further influenced by variations in constituent fractions [40], antimicrobial agents, polypeptides, or dilutive media [41]. The effect of dilutive media on wear of XLPE was studied by Guenther et al. [42]. The authors concluded that phosphate buffered saline should be a preferable media when differentiating the materials behavior maintaining the clinical relevance. Assuming that composition of synovial fluids of individuals substantially varies [43], laboratory investigation unnecessarily suffers from some uncertainty.

Lubrication mechanisms of knee implants were later investigated in more detail by Flannery et al. [44,45]. In particular, the combined role of protein adsorption was explored while the protective function of adsorbed layer was confirmed despite elevated friction level. These studies further highlighted the fundamental role of the lubricant nature when experimentally testing the knee replacements. Following the suggestions about the importance of lubrication, a knee simulator was developed for the ability of direct *in situ* observation of the contact between real-shaped knee implant components [46]. A pilot study introducing the general principle and methodology was recently followed by the study aimed at the behavior of the dominant proteins in model synovial fluid [47]. Using the simulator and fluorescent imaging, it is possible to observe the formation of the film containing key blood plasma proteins, HA and phospholipids PLs in appropriate concentrations. This approach has previously been employed successfully when the lubrication mechanisms within THA joints were studied [48,49]. The results for swing phase showed considerable differences in the contact appearance. With respect to the synovial film formation, a pronounced interplay between the different molecules was found. Thereby, the lubricant layer thickness stabilized within roughly 30–50 s for most of the lubricants with clear differences for specific test fluids. Protein agglomerations were present over the entire contact area and could be clearly detected. However, the study was mainly limited by the assumption of simplified loading and kinematic conditions that did not completely correspond to actual gait cycles, possibly affecting lubricant film formation process.

Based upon our preliminary work, it is apparent that lubrication mechanisms within TKA need to be further investigated. As presented above, most of the experimental studies used simplified geometries and/or inappropriate lubricant and/or experimental conditions. Thus, the main motivation of the present contribution was to experimentally assess the formation of the lubricating film, focusing on the specific synovial fluid constituents with respect to (i) implant geometry, (ii) actual fluid behavior, and (iii) loading and kinematic conditions during gait. Moreover, both the lateral and medial compartments were analyzed. In order to further investigate the mechanistic interactions of the synovial fluid constituents during lubrication, a sophisticated numerical model was employed that is presented in the Part II of the study [34].

2. Materials and methods

2.1. Knee joint apparatus, measurement method

The experiments were realized using a simulator, which enables the investigation of both THAs and TKAs with the use of the specific measurement modules. The machine was presented in more detail in a previous paper [47]. The tibial plateau was fixed in a frame performing motion in anterior/posterior (AP) direction and theoretically enabling application of internal/external (IE) rotation. The femoral component of the knee implant was fixed in a top swinging arm with controlled flexion/extension (FE) rotation and axial (AX) load. Thus, the real contact pairing was considered and the contact area was observed with the use of fluorescent optical module. To be able to observe specific contact locations on the lateral and medial compartments, the optical system was mounted on a movable platform enabling the microscope to be set to the specific position. Otherwise, such a complex observation could not be done due to large contact area migration along AP direction. The CAD model of the test device, the knee module and real appearance of illuminated test specimens are shown in Fig. 1.

Lubricant film formation was evaluated by means of mercury lamp-induced fluorescence. This method has been successfully utilized in various fields of tribology since the 1970s [50]. Although the method is frequently presented as a suitable technique for direct quantitative measurement of film thickness [51–53], it features some specific limitations disabling quantitative evaluation in this particular case. The

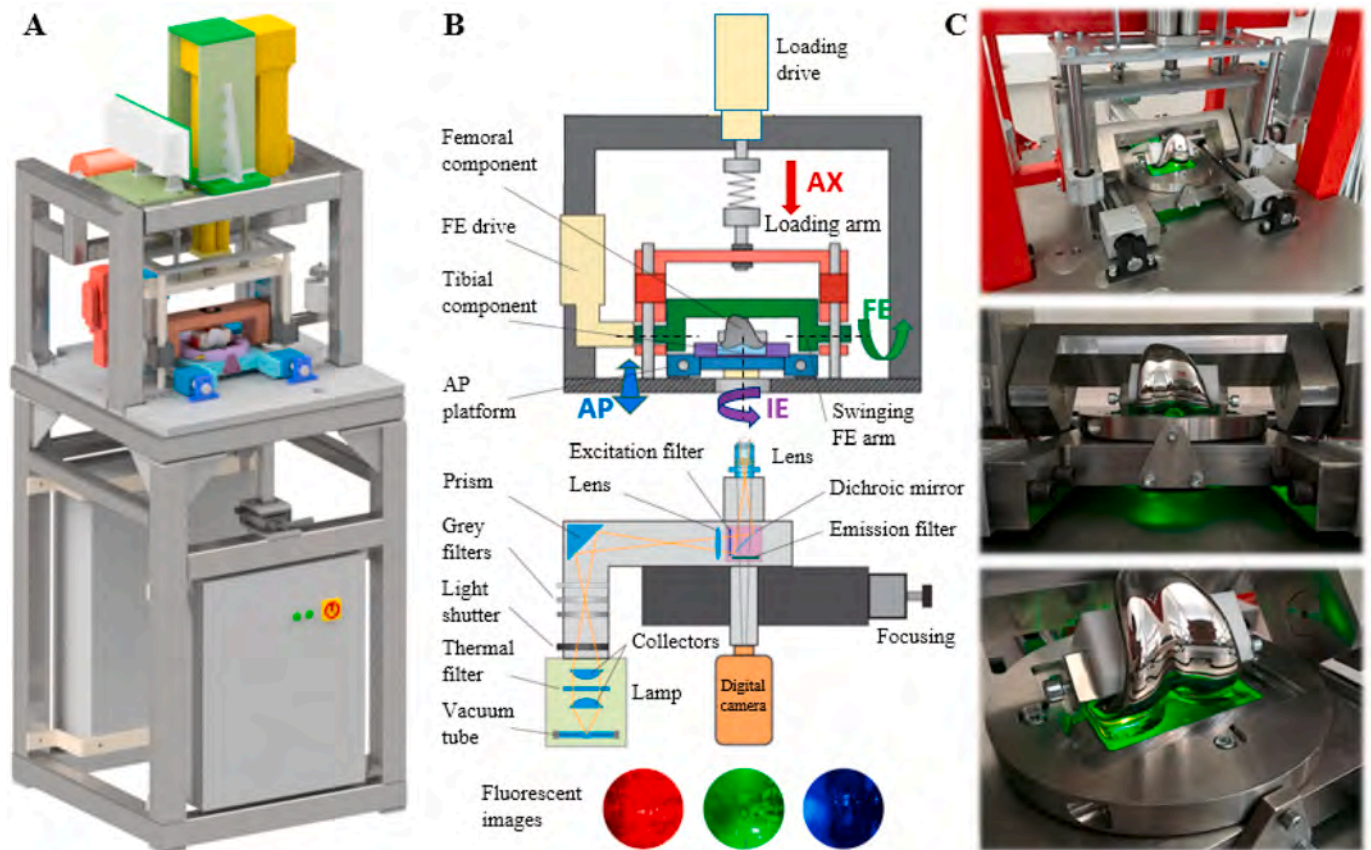


Fig. 1. (A) Knee test rig digital model. (B) Detailed measurement setup. (C) Real appearance of the contact couple under fluorescent illumination (partially edited based on [46,47]).

point is that the method is suitable especially for non-reflective materials, e.g. rubbers or polymers. However, the chromium contained in the original femoral component leads to a loss of fluorescent intensity, so-called quenching [54]. Moreover, undesired interference fringes arise since the surface is highly reflective, preventing accurate film thickness calibration [55]. Hence, the recorded intensity represents a dimensionless averaged thickness of the layer, allowing to explore general trends and differences between various model lubricants. This is valid due to the proportionality of lubricant layer thickness and emitted intensity [56]. This approach was recently validated upon investigation of hip implants [48].

2.2. Samples and lubricants

The contact of original femoral CoCrMo alloy and real-shaped polymer tibial knee components was observed. Tibial plateaus made from UHMWPE could not be used because of their non-transparent nature. Therefore, the original geometry of the insert was obtained using optical scanning and the model was subsequently fabricated by micro-chip machining from poly(methyl) methacrylate (PMMA). The motivation for usage of PMMA comes from similar surface nature compared to UHMWPE. In addition, this material is frequently employed in tribological testing of implants since it has been used as a bone cement, potentially being exposed to rubbing with joint components [57]. Prior to testing, the surface roughness was analyzed with a 3D optical profiler, revealing that the averaged values were comparable for both the tested components, being somewhere between 10 and 50 nm dependently on the location.

Considering the model lubricants, the present study was divided into two parts. At first, the authors concentrated on the comparison of the experimental approach with numerical modeling as presented in Part II

[34]. For this purpose, the contact was lubricated by pure mineral oil R834/80 (Paramo, Czech Republic) having a dynamic viscosity $\eta = 0.179$ Pa s at ambient temperature. Mineral oil is suitable not only because it can be clearly assessed for the numerical model, but also because it naturally emits fluorescence, so there is no need of fluorescent markers [58]. Both lateral and medial compartments were studied while instantaneous oil film intensity was taken at six positions of the contact corresponding to 0%, 14%, 25%, 45%, 60% and 80% of the applied gait cycle, as is illustrated in Fig. 2A. In order to show repeatability, the experiments were repeated three times on different days for both the compartments and all the locations.

Subsequently, the present study concentrated on the behavior of specific synovia constituents during film formation process. In that case, thirteen different lubricants of various complexity were used while various constituents were fluorescently stained. PBS represented a base medium. The initial experiments were carried out with labelled albumin from bovine serum (A2153, Sigma-Aldrich) based lubricants. A second set was carried out with the fluids containing stained bovine blood γ -globulin (G5009, Sigma-Aldrich). A third series was realized with labelled HA (Sodium Hyaluronate powder, Contipro). The details about fluorescent labelling may be found in the previous study [48]. Finally, a combined series was realized with the master model liquid, which contained all the three aforementioned constituents stained. The motivation of this test was to confirm the expected film formation based on the observation of individual constituents. PLs (P3556, Sigma-Aldrich) were also considered in this study. However, these were not stained due to very low concentration and very limited ability of staining using commercial products and established procedures. Despite the presence of specific constituents that was different in various lubricants, the concentration was kept constant to avoid any distraction due to fluid composition. Concentrations of albumin, γ -globulin, HA, and PLs were

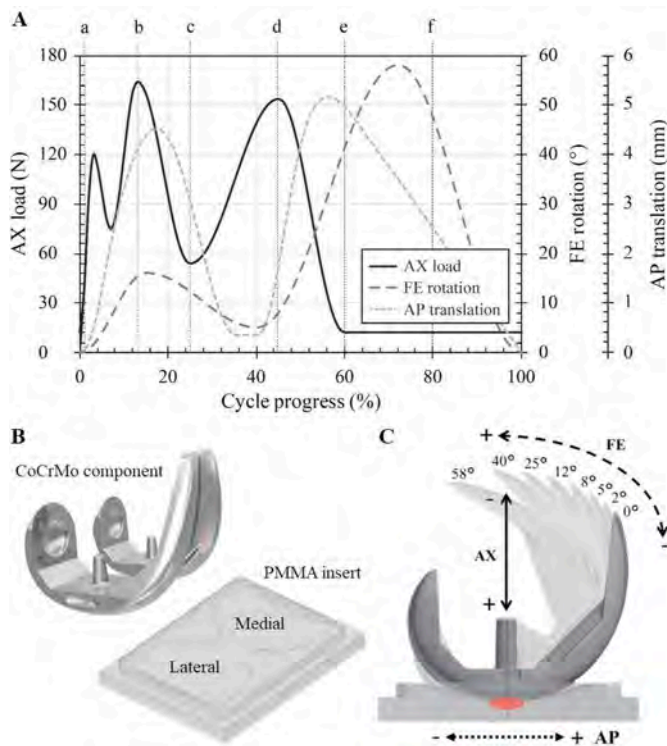


Fig. 2. (A) Course of AX load, FE rotation, AP translation. (B) Detail of the contact components. (C) Illustration of AX, FE, and AP with highlighted contact position.

24.9 mg per ml, 6.1 mg per ml, 1.49 mg per ml, and 0.34 mg per ml, respectively. This composition reflected the average composition of patients expecting TKA [43]. Both, the lateral and the medial compartments were investigated being lubricated by the artificial model fluids mimicking synovial fluid. However, the observation was done exclusively for maximal load, i.e. the load peak which occurs at 14% of the cycle (point (b), see Fig. 2A) due to the necessity to move the optical system when focusing on other positions and the excessive amounts of lubricant required. Repeatability of the system was studied using simple albumin and simple γ -globulin solutions, however, not with complex solutions because of the excessive amounts of lubricant required. Nevertheless, due to the superposition character of the study and due to the strict compliance with the laboratory protocol, we believe the generated data is representative. The information about the concentration of specific constituents together with the observed location is summarized in Table 1.

According to laboratory protocol, stained and non-stained constituents were prepared separately. Prior further use, these were stored frozen at $-22\text{ }^{\circ}\text{C}$. The solutions were then thawed naturally being exposed to ambient temperature for 1.5 h before the test started. After natural thawing under ambient temperature, stained and non-stained constituents were mixed together by mild shaking. After each experiment, the lubricant was discarded. Both the test specimens (femoral component, tibial insert) were carefully cleaned following the established protocol [48].

2.3. Experimental conditions

Since one of the goals of this study was to evaluate and visualize film formation under realistic transient loading and kinematic conditions, the parameters of the gait cycle were set following ISO 14243-3 standard [31] for AP translation and AX load. IE rotation was fixed as it varies in only a limited range throughout the cycle (0° – 5.2°). Following the mechanical properties of the components ($E_{\text{CoCrMo}} = 240\text{ GPa}$, $\nu_{\text{CoCrMo}} =$

Table 1

An overview of the test lubricants (partially modified based on [48]).

No.	Stained constituent	Non-stained constituent	Total concentration	Dynamic viscosity	Observed location
1.	Mineral oil	-	-	179 mPa s	a, b, c, d, e, f
2.	Albumin (24.9 mg/ml)	-	24.9 mg/ml	1.7 mPa s	b
3.	Albumin (24.9 mg/ml)	γ -globulin (6.1 mg/ml)	31 mg/ml	2 mPa s	b
4.	Albumin (24.9 mg/ml)	γ -globulin (6.1 mg/ml) HA (1.49 mg/ml)	32.49 mg/ml	3.2 mPa s	b
5.	Albumin (24.9 mg/ml)	γ -globulin (6.1 mg/ml) HA (1.49 mg/ml) PLs (0.34 mg/ml)	32.83 mg/ml	3.3 mPa s	b
6.	γ -globulin (6.1 mg/ml)	-	6.1 mg/ml	0.5 mPa s	b
7.	γ -globulin (6.1 mg/ml)	Albumin (24.9 mg/ml)	31 mg/ml	2 mPa s	b
8.	γ -globulin (6.1 mg/ml)	Albumin (24.9 mg/ml) HA (1.49 mg/ml) PLs (0.34 mg/ml)	32.49 mg/ml	3.2 mPa s	b
9.	γ -globulin (6.1 mg/ml)	Albumin (24.9 mg/ml) HA (1.49 mg/ml) PLs (0.34 mg/ml)	32.83 mg/ml	3.3 mPa s	b
10.	HA (1.49 mg/ml)	PLs (0.34 mg/ml)	1.83 mg/ml	2.2 mPa s	b
11.	HA (1.49 mg/ml)	Albumin (24.9 mg/ml) PLs (0.34 mg/ml)	26.73 mg/ml	3.2 mPa s	b
12.	HA (1.49 mg/ml)	γ -globulin (6.1 mg/ml) PLs (0.34 mg/ml)	7.93 mg/ml	3 mPa s	b
13.	HA (1.49 mg/ml)	Albumin (24.9 mg/ml) γ -globulin (6.1 mg/ml) PLs (0.34 mg/ml)	32.83 mg/ml	3.3 mPa s	b
14.	Albumin (24.9 mg/ml) γ -globulin (6.1 mg/ml) HA (1.49 mg/ml)	PLs (0.34 mg/ml)	32.83 mg/ml	3.3 mPa s	b

0.29, $E_{\text{PMMA}} = 3.5\text{ GPa}$, and $\nu_{\text{PMMA}} = 0.34$) the axial load was proportionally lowered (varying from 15 N to 175 N) compared to ISO standard in order to obtain a contact pressure at maximum load comparable to CoCrMo/UHMWPE contact pairing as UHMWPE has seven-fold lower elastic modulus than PMMA. Thus, the maximum pressure was between 25 and 35 MPa for lateral and medial compartment, respectively. These values are in accordance to those presented in Part II [34], as well as in other literature [59,60]. Range of FE rotation was between 0° (initial position) and 58° (maximally deflected position). AP translation ranged from 0 mm (initial position) to -5.2 mm (maximally shifted position).

The tests were performed at 1 Hz frequency and ambient temperature (23 °C–25 °C).

The plotted film thickness in results section represents an average value throughout the contact zone highlighted in the recorded images. The length of the tests was set to 30 s as it was previously shown to be adequate to clarify the interaction of the constituents and to get contact images of sufficient quality and resolution. At the end, an extra time test was conducted with complex model fluid no. 14. In that case, the experiment was run five times while 30 s were recorded within the first test. Then, the experiment was restarted, while the 30–60 s period was recorded. Thus the second test lasted 60 s, however, only 30 s were recorded. The same for interval 60–90 s, 90–120 s and 120–150 s, respectively. Therefore, the overall duration of the time test was 450 s. One of the benefits of this test is that continuity of the data is considered as a proof of measurement repeatability.

3. Results

3.1. Mineral oil

Initial tests were carried out using mineral oil enabling to compare the experimental measurement with the developed numerical model presented in Part II [34]. Both the lateral and the medial compartments were investigated while six specific locations throughout the cycle were observed (see Fig. 2A). Results of fluorescent intensity (experiment) and dimensionless specific film thickness (simulation), which represents overall lubricant gap height averaged over the contact domain of the respective compartment divided and scaled using the maximum value of the medial condyle [34], are displayed in Fig. 3A. Apparently, there is a good agreement of both approaches. Qualitatively, the measured data corresponded to those predicted by the model in most locations (b) to

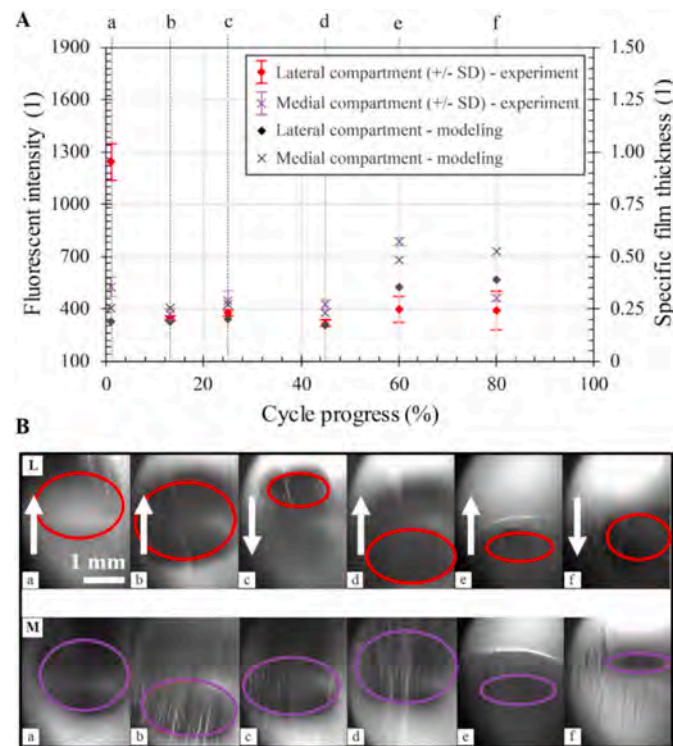


Fig. 3. (A) Oil film intensity for both the lateral and the medial compartments at specific locations throughout the cycle. (B) Fluorescent images with highlighted contact area for lateral (top) and medial (bottom) compartments at the locations. The white arrows in the top row of contact images (B) indicate lubricant inlet into the contact (upward/downward orientation is given by a combination of FE rotation and AP translation).

(f). The only considerable difference is observed at point (a) where AX load and AP translation exhibit a substantial transition at the same time, possibly leading to some fluctuations in experimental results. Further small disagreement may be identified for medial compartment between points (e) and (f). While simulation showed slight improvement of the lubricant layer in this phase, the experiment exhibited a drop of the film. This behavior is attributed to the fact that FE motion reaches the maximum between these points and the motion is being reversed which may lead to partial removal of the lubricant layer. This phenomenon may be hardly simulated. Further, the contact zone on medial condyle moves and changes its shape considerably between (e) and (f), as can be seen in Fig. 3B.

Focusing on the development of the film formation during the cycle, the lateral compartment exhibits sudden jump at the beginning of the experiment compared to medial one. During the rest of the cycle, the film thickness is quite comparable with the exception of point (e) where medial compartment showed enhanced film thickness. Qualitatively, this also agrees very well with the numerical study (see Fig. 3A). As is shown in Fig. 3A, the repeatability of the data was excellent for the medial condyle and standard deviations may be only hardly distinguished for most of the locations. In the case of the lateral compartment, a slight variance was observed at the beginning of the cycle, while this stage is associated with transition from maximal to minimal FE rotation together with swift from minimum to maximum AX load. Corresponding images of the observed areas with highlighted contact zones are presented in Fig. 3B. It should be noted that the sizes of the contact are not proportional to load in all the locations due to varying radii of the lateral and the medial compartments along sagittal and frontal axes. In some images, the contact area cannot be clearly recognized as these pictures are taken during the experiment. The positions and shapes of contact areas were determined based on the appearance of the static image taken at each specific phase. The differences of the contact areas underline the differences in the load of both the compartments due to geometry.

3.2. Albumin-based fluids

Further, an analysis of model synovial fluid lubricants was conducted. The first set of the tests was carried out with albumin-based lubricants. The results for lateral compartment are displayed in Fig. 4A. It is evident that addition of γ -globulin and HA did not enhance the film formation. However, when all the constituents including PLs were considered, the film was the thickest. Overall, similar tendency was observed for all the tested lubricants with initial gradual increase and stabilization after 15–20 s. An increase of film thickness can be clearly recognized when focusing on the contact images in Fig. 4C. In the figure, an interesting phenomenon leading to enhancement of the layer towards positive AP direction may be observed. This is associated with large protein clusters near the contact boundary. In the video of the test, it could be clearly observed that the femoral implant rolls up the lubricant in the direction of AP motion. Different behavior was observed for medial compartment (Fig. 4B). In that case, simple albumin and the mixture of the proteins showed a slight increase with subsequent decrease and stabilization. However, when HA and HA with PLs were added, the film dropped immediately after the beginning of the experiment. This was accompanied by the removal of the protein agglomerations out of the contact zone, as is apparent from Fig. 4D for time $t = 10$ s and later. Overall, a thicker lubricant layer was detected for lateral compartment, independently of the test lubricant.

3.3. γ -globulin-based fluids

Subsequent tests were realized using the lubricants on γ -globulin basis. The results of film intensities are shown in Fig. 5A and 5B. As can be seen, these fluids generally exhibited much thinner film compared to albumin solutions. The graphs contain the scaled details, showing that

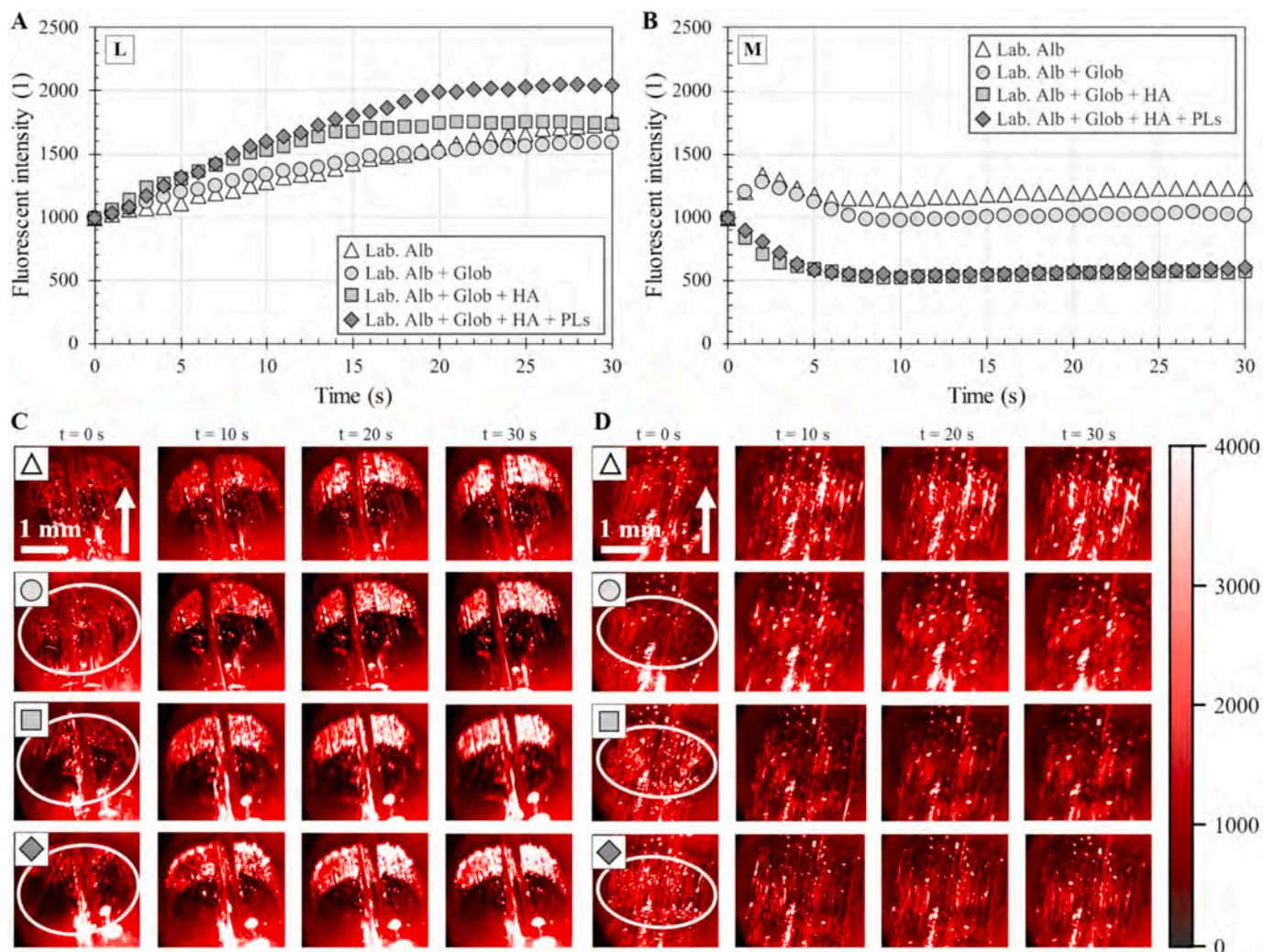


Fig. 4. (A) Evolution of albumin-based fluorescent intensity versus time for lateral and (B) medial compartment at point (b). (C) Fluorescent images for lateral and (D) medial compartment (the symbols in top left corner refer to the graphs above). The white arrows in the top left contact images (C), (D) indicate lubricant inlet into the contact.

the film gradually increased in the case of the lateral condyle (Fig. 5A). As for albumin solutions above, an increase of film is attributed to grouping of the proteins near contact boundary, as is displayed in Fig. 5C. Focusing on the medial compartment, very limited film formation was observed, as is displayed in Fig. 5B and 5D. Negligible fluctuations of the layer attributed to repeated entrapment and release of the proteins in and out the contact zone can be observed in Fig. 5D.

3.4. Hyaluronic acid-based fluids

HA is considered to be strongly supportive in terms of lubrication performance. Nevertheless, very limited ability to form stable lubricating layer of HA was recently observed for hip replacements [61]. In general, intensity of HA film is comparable to those for γ -globulin (Fig. 6A and 6B). Focusing on the lateral compartment, only the mixture of HA and albumin caused slight increase of HA layer. However, this can hardly be recognized on the contact images (Fig. 6C), indicating the effect was limited. In the case of the medial condyle (Fig. 6B and 6D) simple HA showed a continuous development, which corresponds to the contact images of the top row in Fig. 6D. When comparing both compartments, it is evident that HA shows a stronger tendency to be entrapped within medial compartment pointing on the sensitivity to load/contact pressure.

3.5. Complex solutions

Finally, results for three different complex solutions with labelled albumin, γ -globulin, and HA were compared to those for the liquid containing all the aforementioned constituents to be stained at the same time (master lubricant). This experiment is supposed to reveal the film formation mechanism by comparison of the trend for the master curve with the trends for the individual curves. As shown for lateral compartment (Fig. 7A and 7C), the overall tendency was in satisfactory compliance with the development of albumin-based complex fluid. This indicates a fundamental role of albumin in film formation process. The dominant presence of albumin can be clearly recognized when comparing top and bottom row of images in Fig. 7C. The lower intensity of the master curve compared to the albumin curve can be attributed to emission reabsorption, while the emitted intensity of the first fluorescent marker further excites another marker [62]. If the reabsorption would not take an action, the total fluorescent emission of the master curves would be higher. In preliminary tests dealing with the estimation of reabsorption level in a simplified ball-on-disc setup, it was found that combination of the markers used in the present study (Rhodamine-B-isothiocyanate and Fluorescein-isothiocyanate) led to a drop of intensity in the range from 25% to 40% for the expected thicknesses (several hundreds of nm to units of μm). Therefore, it is assumed that without the presence of this reabsorption phenomenon, the maximum intensity for

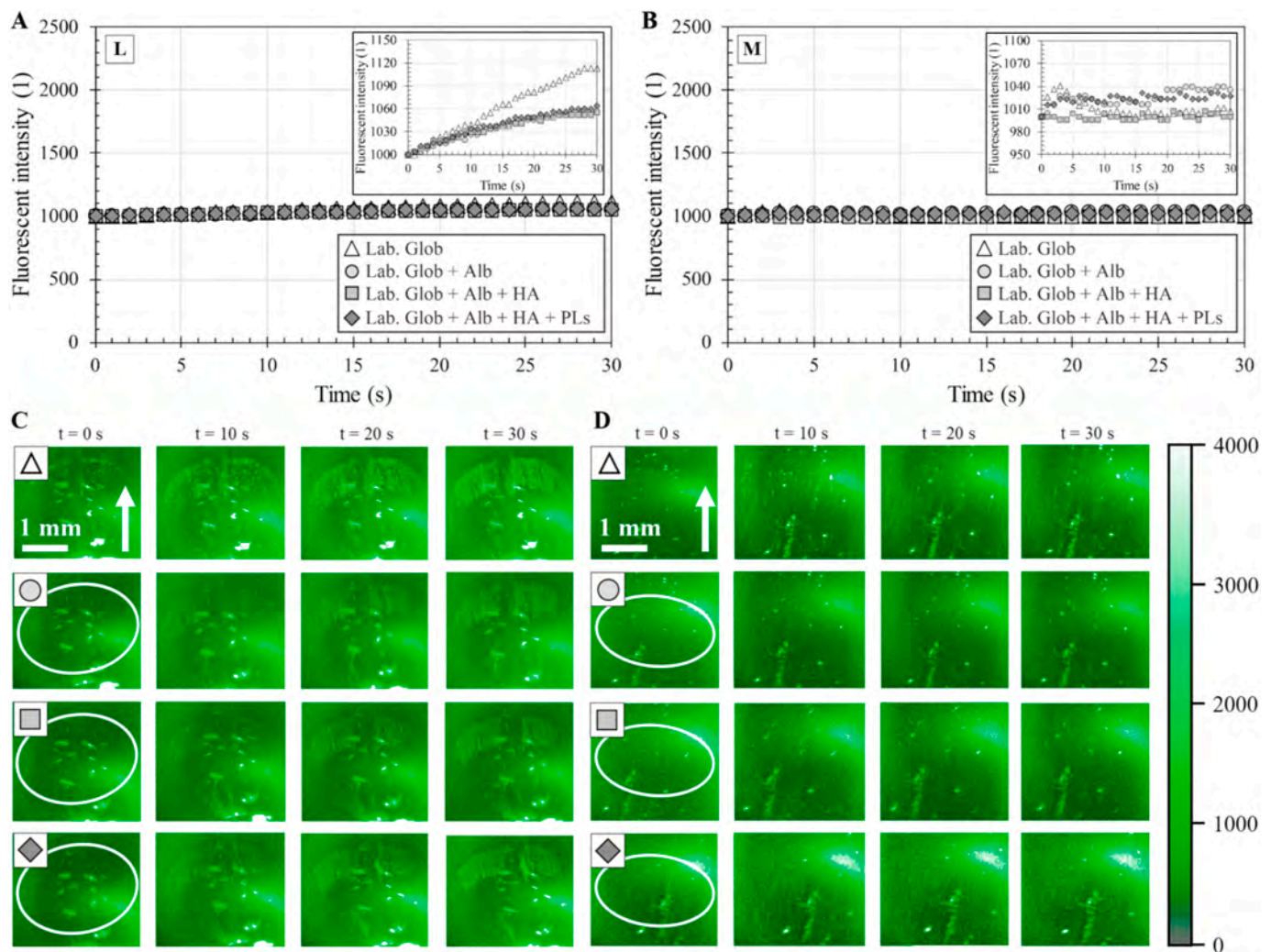


Fig. 5. (A) Evolution of γ -globulin-based lubricant film intensity versus time for lateral and (B) medial compartment at point (b). The details in top right corners are the same graphs with scaled y-axis. (C) Fluorescent images for lateral and (D) medial compartment (the symbols in top left corner refer to the graphs above). The white arrows in the top left contact images (C), (D) indicate lubricant inlet into the contact.

the lateral condyle (Fig. 7A) would be somewhere between 2200 and 2500. Regarding the medial compartment (Fig. 7B), the expected maximum intensity, if reabsorption could be eliminated, is in the range from 1200 to 1400.

Considering the medial compartment, the master curve is somewhere between albumin and other two curves for γ -globulin and HA based solutions. Thus, it can be estimated that the two constituents contribute to enhanced lubrication of the medial condyle despite the albumin drop. Nevertheless, the thickness of the lubricating layer is more than double for lateral compartment, indicating more favorable contact conditions, potentially positively affecting wear resistance.

In order to reveal the behavior of synovial fluid film in a longer time frame, cumulative tests were performed while only 30 s of the experiment were recorded as explained in section 2.3. Once the first test (30 s) finished, the contact was kept loaded for 5 min while neither FE rotation nor AP translation were applied. After the break, the experiment was restarted lasting 60 s while the 30–60 s period was recorded. This approach was repeated five times to get a cumulative data for 450 s of swinging. As there was no unloading phase, this experiment corresponded to an accumulation of a 30, 60, 90, 120, 150 s lasting walk and 5 min of still stand between the steps. As can be seen in Fig. 8A and 8B, the film increased during the first part of the test for lateral condyle. However, longer time led to the removal of the constituents out of the contact, decreasing the lubricating film which was stabilized eventually.

When analyzing the medial compartment, the lubricant layer exhibited a slight drop followed by an enhancement of the layer at the beginning of the experiment (Fig. 8A). The later phase was accompanied by quite stable behavior as can be seen for the contact shown in Fig. 8C.

4. Discussion

4.1. General discussion

The contribution focused on the assessment of lubrication mechanisms in TKA, focusing on the behavior of specific constituents contained in synovial liquid. The main benefits come from analyzing both the TKA separately and ability to distinguish dominant constituents of synovial fluid and to describe its mutual interactions. Concentrating on albumin protein, positive influence on lubricant film was observed when all the studied constituents were considered for the lateral compartment. On the contrary, opposite influence was reported for the medial condyle, indicating sensitivity of the layer on load. Albumin also showed a strong tendency to agglomerate, creating protein clusters. Focusing on γ -globulin solutions, these exhibited very thin lubricant layer for both the compartments. Despite the lower thickness, the layer was more stable and uniformly distributed over the contact with only localized agglomerations formed along AP direction. Similar behavior was also observed for HA which only hardly formed a stable lubricating layer.

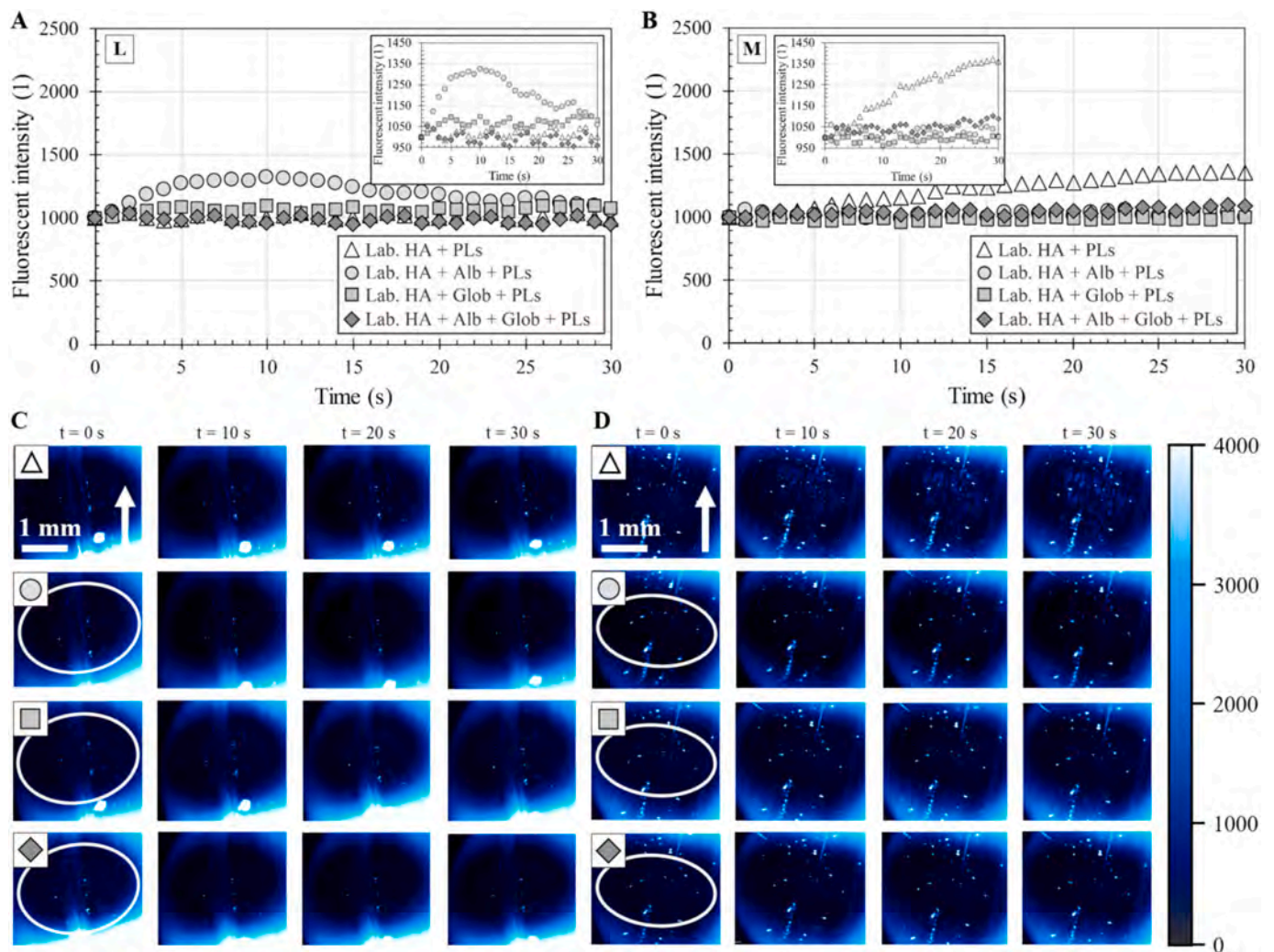


Fig. 6. (A) Evolution of HA-based fluid film intensity versus time for lateral and (B) medial compartment at point (b). The details in top right corners are the same graphs with scaled y-axis. (C) Fluorescent images for lateral and (D) medial compartment (the symbols in top left corner refer to the graphs above). The white arrows in the top left contact images (C), (D) indicate lubricant inlet into the contact.

To evaluate the lubrication mechanism, protein adsorption has to be taken into account. The ability of the proteins to adsorb on the rubbing surfaces is crucial in order to form boundary lubricating film. Protein adsorption on solid surfaces is a complex phenomenon combining hydrophobic, hydrogen-bonding, and electrostatic interactions [63]. Based on the literature, it is assumed that albumin and γ -globulin exhibit stronger adsorption to hydrophobic surfaces [64]. This is confirmed by the present observation. As PMMA is highly hydrophobic [65], the proteins tend to be adsorbed as can be clearly seen in contact images in Fig. 7C and 7D. Focusing on the specific proteins, its primary structure has to be taken into account. While albumin is dominantly presented in an α -helix form, γ -globulin has a β -sheet form. Based on recent observation, it is assumed that β -sheet exhibits a stronger adsorption onto rubbing surfaces while α -helix forms lubricating film of low shearing resistance, contributing to lower friction between the surfaces [66–68]. Stronger adsorption of γ -globulin is also expected for the femoral component of the TKA which is considered to be neither hydrophobic nor hydrophilic. Nevertheless, γ -globulin showed more pronounced connection to CoCr surface compared to albumin [69]. It must be emphasized that all the above information based on the particular investigations seem to be in accordance with the present observation.

Assuming the behavior of individual constituents in model synovial fluid, an illustrative lubrication model of the knee implant is proposed and is visualized in Fig. 9. It should be highlighted that the model is

based on the detailed observation of the video records of the experiment. It could not be established only based on the images of the contact zones presented in the paper. Thereby, we suggest that the relative motion of the opposing bodies leads to strong adsorption of thin, stable and uniform γ -globulin film on the contacting surfaces. This is supported by the clusters of γ -globulin which were found to move simultaneously with the movement of the femoral component, indicating adsorption to the metal surface. Further γ -globulin agglomerations remained at the same spot throughout the experiment which confirms the adsorption on the stationary PMMA insert. Moreover, referring to the video of the experiment, simple HA with PLs moved in a slightly chaotic way when examined alone despite the comparable intensity to γ -globulin (Fig. 5 versus Fig. 6). The film was apparently stabilized when γ -globulin was added to the fluid. This point is supported by Yarimitsu et al. [70], who observed improved HA adsorption when it was mixed together with γ -globulin. Very low ability of adsorption of sodium hyaluronate (salt form of hyaluronic acid) on polymer substrate was observed also by Serro et al. [33]. Therefore, it is assumed that γ -globulin layer is reinforced by the molecules of HA and PLs as it was discussed that HA exhibits substantially stronger interaction with γ -globulin compared to albumin [70] and it is well known that HA and PLs tend to interact. Thus, it is suggested that γ -globulin creates a boundary lubricating layer. However, because of β -sheet structure and structure of HA, internal adhesive forces within the layer are not sufficient to enable continuous

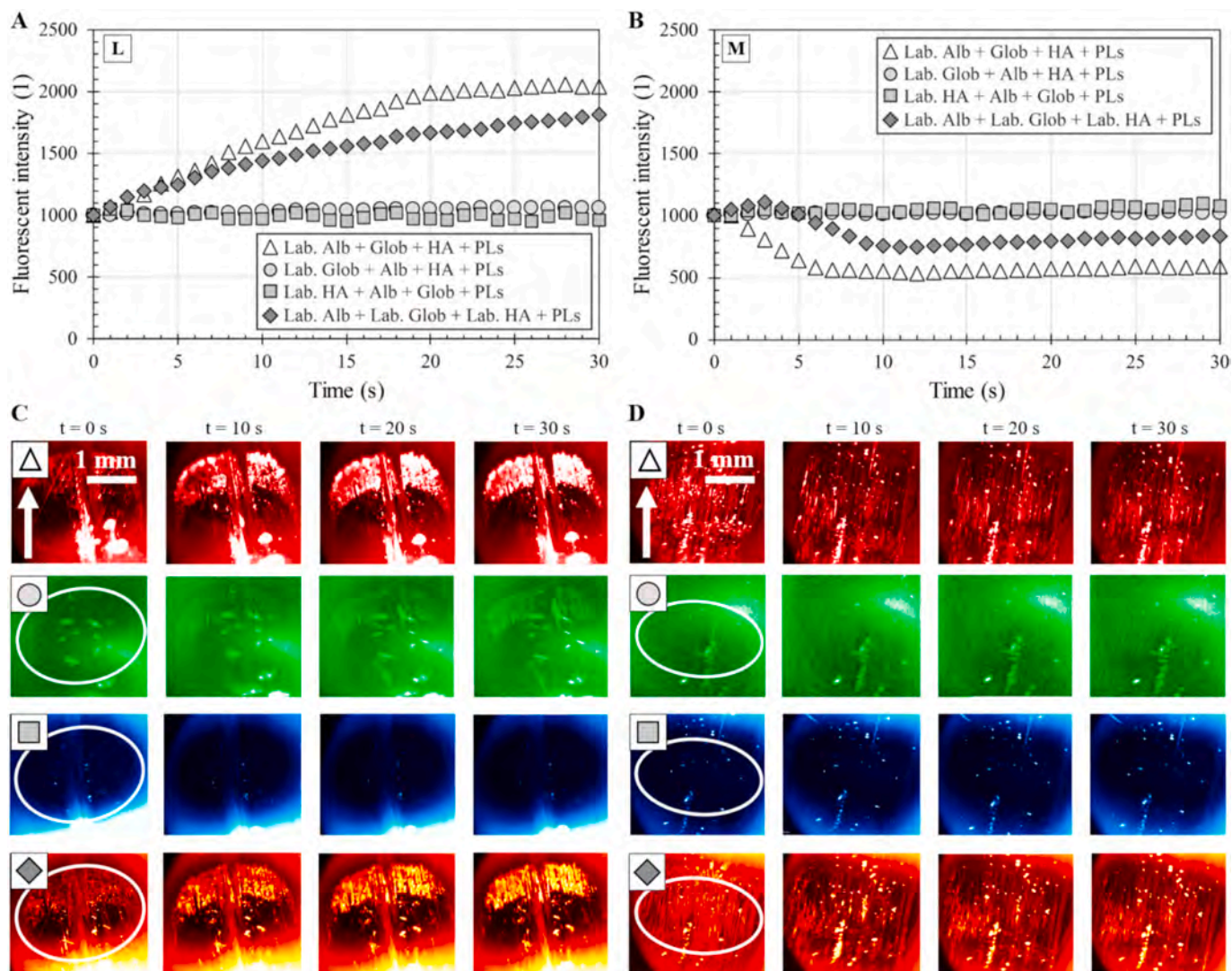


Fig. 7. (A) Evolution of complex fluorescent intensity versus time for various complex model fluids for lateral and (B) medial compartment. (C) Fluorescent images for lateral and (D) medial compartment (the symbols in top left corner refer to the graphs above). The white arrows in the top left contact images (C), (D) indicate lubricant inlet into the contact.

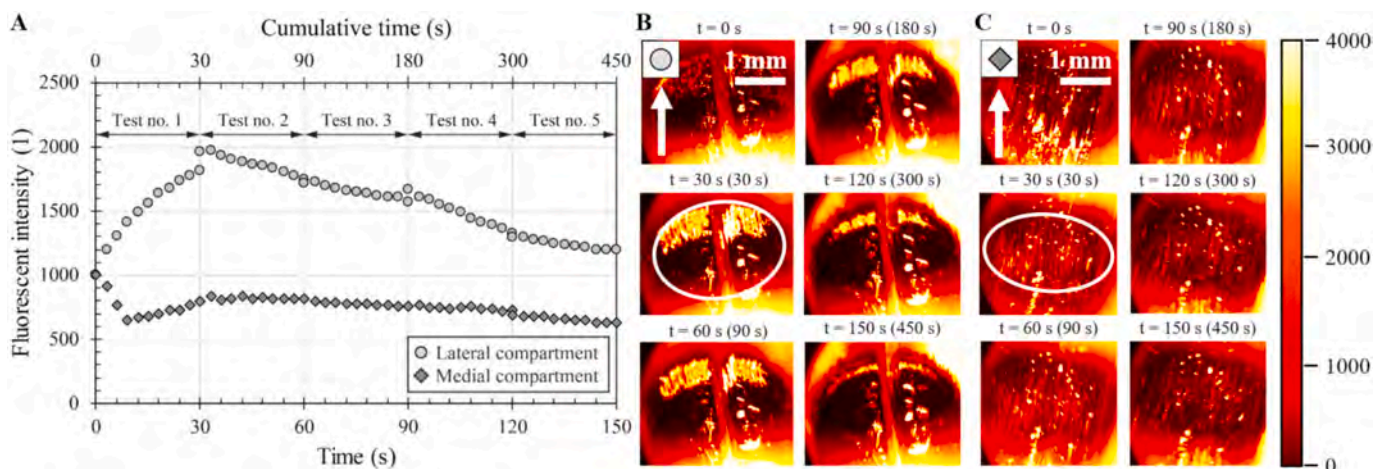


Fig. 8. (A) Time test - development of complex lubricant film intensity versus time for lateral and medial compartment. (B) Fluorescent images for lateral and (C) medial compartment (the symbols in top left corner refer to the graph (A)). The white arrows in the top left contact images (B), (C) indicate lubricant inlet into the contact.

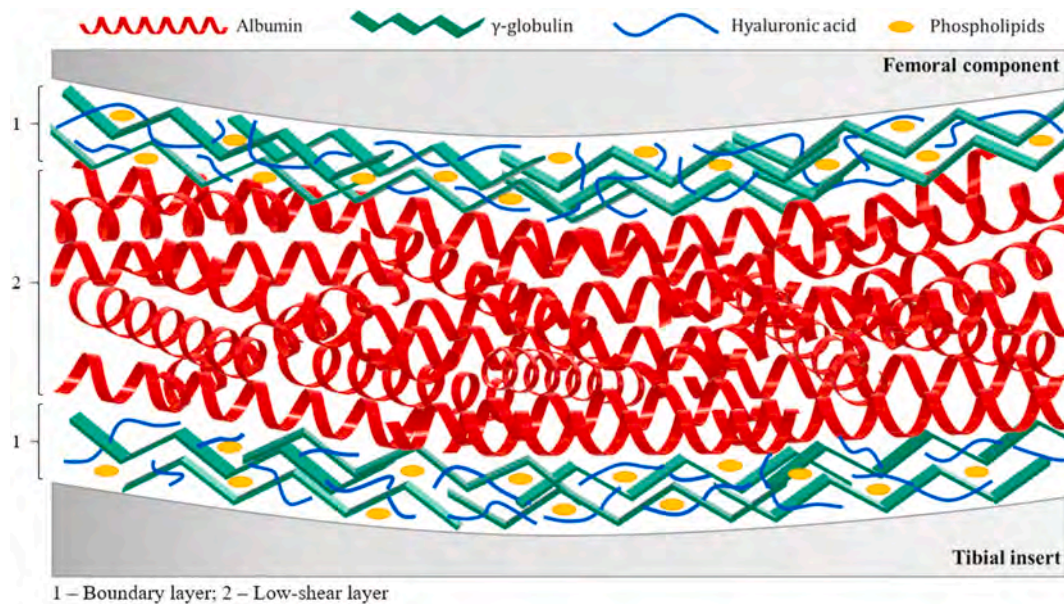


Fig. 9. Lubrication model of TKR.

growth of the layer. Hence, the further increase of film thickness is attributed exclusively to albumin which has a good ability to be attached to the boundary layer and its α -helix creates strong mutual bonds, enhancing the lubricating film. This mechanism is partially disrupted in the case of the medial compartment. In that case, the film formation is limited, indicating the importance and sensitivity of the film to the load. As described in chapter 2.3, the difference in contact pressure considering both the compartments is around 5–10 MPa which is equal to 15%–30% of the maximum load of the lateral compartment. While γ -globulin and HA seem to be resistive against the higher load (simple HA even increases, see Fig. 6B), the albumin layer is disrupted, leading to decrease of the lubricating film, as is shown in Fig. 4B. The film disruption is thus assumed to be related to (a) thinner unstable film at medial compartment and (b) increased portion of the applied load. Such a load difference apparently leads to worse lubrication conditions, which may contribute to a reduced service life of the medial compartment. Although it is well known that wear is influenced by more factors than only lubrication, it is suggested that insufficient lubrication contributes for elevated wear of the medial compartment, which is eventually responsible for shorter implant service life. This statement is supported by our clinical observation during revising surgeries, revealing the medial compartment to be generally more damaged compared to the lateral one. It also agrees with the findings reported in literature [71,72]. The assumption about the negative effect of elevated load at medial compartment is further supported by investigations of O'Brien et al. [73], who have shown that increasing contact pressure may result in increased XPE wear. The authors further pointed out at some limitations of simplified pin-on-disk testing, which highlights the importance of realistic geometry and applied conditions applied in the present study. Nevertheless, it should be noted that wear is influenced not only by lubrication and load. Other factors such as oxidation [13], position of the knee axis of rotation [74], or implant instability [75] have to be taken into account. Notwithstanding, lubrication seems to be an important contributing factor, which definitely cannot be neglected.

4.2. Data repeatability

Synovial fluid lubrication is considered to be very complex and sensitive to measurement methodology. Ideally, all the experiments should be repeated multiple times in order to enable a detailed statistical evaluation. However, the present study employed 14 different

lubricants, while the measurement repetition with all the fluids would unquestionably be very time and cost demanding. Regarding the fluid composition, this was designed to mimic diseased synovial fluid. Total protein concentration well corresponds to results published by Guenther et al. [76] (31 mg/ml versus 30 mg/ml), who analyzed samples of osteoarthritic and periprosthetic synovial fluid of forty patients. Further, the applied concentration of albumin is similar to those recommended in literature [38]; however, concentration of γ -globulin, HA is lower while concentration of PLs is higher. The designed composition is based on ongoing analysis of synovial fluids samples extracted during revision surgeries. Nevertheless, lower HA concentration does not need to be necessarily considered to have a negative effect since it was shown that the concentration of HA has not a substantial impact on wear of XPE [42]. Moreover, the concentration of HA (1.49 mg/ml) is nearly identical to those applied by DesJardins et al. [77], who performed rheological analysis of bovine serum mixed with 1.5 mg/ml of HA. The results indicated that the solution viscosity was not statistically different from those of synovial fluid taken during revision over a scope of shear rates corresponding to physiological conditions. Nevertheless, the lower viscosity of the applied lubricants (see Table 1) than reported in literature [38] is attributed mainly to lower concentration of HA and its lower molecular weight [78]. Referring to Fig. 3A, only a negligible variance of the results was observed for oil experiment which was repeated three times for all the investigated areas. Moreover, the authors recently published a number of studies dealing with lubrication of hip joints, establishing very strict laboratory protocols in order to eliminate external influences affecting the data. Nevertheless, four additional measurements were conducted with the use of simple protein (albumin, γ -globulin) solutions to demonstrate the repeatability.

As can be seen in Fig. 10A, there is a little variance for the lateral compartment while the difference of the end values is around 20%. This difference is attributed to normalization process, which is undertaken as the first step during data evaluation. Each experiment starts at a different intensity level. This is due to three dominant factors such as (i) type of fluorescent marker used, (ii) ambient light conditions, and (iii) intensity of light source (listed from the most to the least influencing factors). For the comparison of the individual experiments, initial value of fluorescent intensity is thus set to a specific chosen value (1000 in the case of our study) while all the rest intensities are multiplied/divided by the normalization constant. Normalization is based on a single image taken right after start of the test. Due to the high frame rate, a couple of

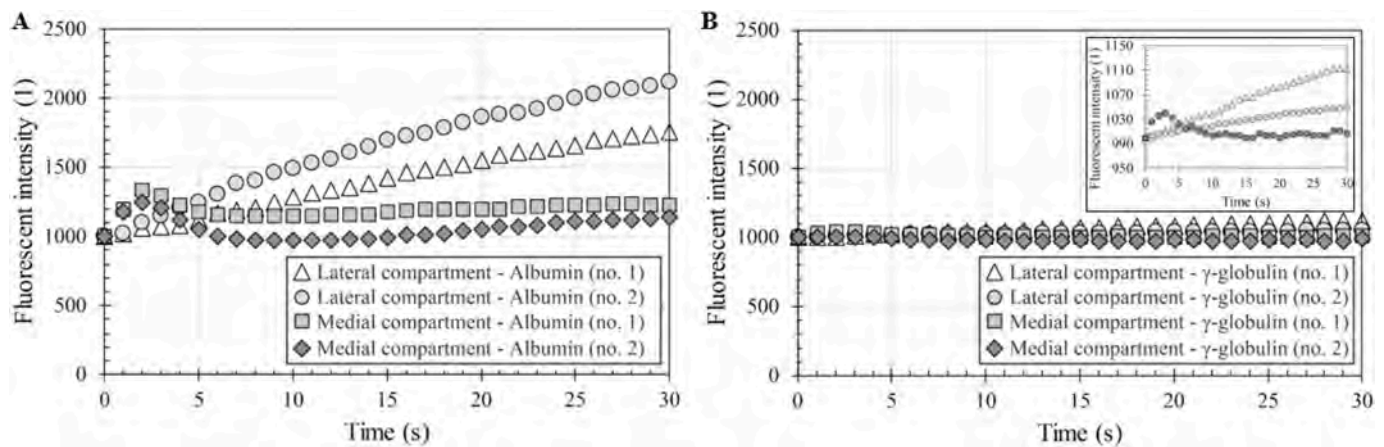


Fig. 10. (A) Illustration of data repeatability for albumin and γ -globulin solutions for lateral and (B) medial compartment. The detail in top right corner of Fig. 9B is the same graph with scaled y-axis.

images may be chosen to represent a calibration image. The first image is not necessarily always the best. Thus, the data in Fig. 9A for the lateral condyle represent two extreme values of normalization constants. Despite that, the agreement of the data is very satisfactory. Focusing on the medial compartment, the compliance of the data is even better. Similar behavior may be seen for γ -globulin solution (Fig. 10B). The lateral compartment exhibits some differences; however, the change of the intensity is nearly negligible focusing on the scaled y-axis. For the medial compartment, the data are nearly identical, overlapping each other.

Considerable proof of experimental repeatability also comes from Fig. 8. As it was described, the cumulative character of the diagram is based on repeating the tests lasting from 30 to 150 s while 30 s period was always recorded. The transition between the first and the second test for the lateral compartment was the only point where the data do not directly follow the previous curve. The explanation of higher emission right after start of the second test is that during the unrecorded period of the second test (0–30 s), the protein layer further increased. Further phases of the experiment revealed excellent continuity with the intensities at the beginnings of the individual experiments being almost identical with the intensities at the end of the previous test. This indicates that protein film at the lateral compartment increased for couple of tens of s after the motion starts with subsequent continuous thickness decrease. Considering the medial compartment, the film dropped at the beginning which was followed by a slight increase during the first 30 s (Fig. 10B). This behavior corresponds to observation displayed in Fig. 7B (grey rhomb data). With increasing time, the film continuously decreased while perfect continuity of each following test may be observed. Based on above, it is tempting to conclude that longer uninterrupted walking leads to deterioration of lubrication conditions within TKA, negatively affecting the service life of the implant. If proved by other experiments, an interrupted walking alternated with unloading phase enabling film recovery could be recommended in order to prolong the longevity of TKA. The issue of decreasing film thickness under interrupted loading can be considered as the main outcome of this experiment. The evidence of data repeatability is in very good agreement of the end and initial values of each subsequent measurement steps. As described, every recorded phase was preceded by time corresponding to the length of the previous test for what the experiment ran without recording. For example, during the third test, time range from 60 s to 90 s was recorded while the whole test lasted for 90 s. The fact that the results at the beginning of recorded phase of experiment no. 3 directly follows end values of experiment no. 2 indicate high level of measurement repeatability.

4.3. Limitations

The author admit couple of limitations of the performed study. At first, the used transparent PMMA insert may behave differently compare to conventional UHMWPE to some extent. This a difference is related to contact mechanics. In general, TKA is exposed to higher contact stress than THA due to variable geometry of the compartments and generally smaller contact area. Although the contact pressure achieved in this study corresponds to metal-UHMWPE pairs, the resulting contact area is smaller for metal-PMMA contact. This is due higher elastic modulus of PMMA driving the elastic deformation of the material. However, even in the case of PMMA, contact area in specific locations ranges from 2 to 5 mm, which is sufficient for the assessment of the formation of lubricant film. The differences of PMMA and UHMWPE are further discussed in the recent paper [47] and in Part II [34]. Further, IE rotation was fixed in the present study while lubricant film may be partially affected by this additional motion. However, based on the current observation, it is concluded that the formed film was stable even at the phases of the cycle when sliding occurred. Thus, it is expected that consideration of IE rotation might have some quantitative impact on the film thickness but not on qualitative character of film formation. Finally, some uncertainty can also be related to proteins and their interactions with biomaterial, or among themselves *in vivo*. In particular, the risk associated with conformational changes of albumin, potentially leading to increased wear reported in literature, needs to be considered [39]. Neither the contact pressure nor the expected temperature increase in the contact are high enough to cause change of the proteins structure. These effects are further studied in Part II [34]. Since model fluid with controlled composition was used, conformational changes due to interaction with other constituents (e.g. bilirubin) could not occur as well. Nevertheless, focusing on the real-environment conditions in human body, these processes definitely play a role. Further, the differences of synovial fluid composition [43] together with the action of antimicrobial agents, polypeptides [40] were not considered. However, these limitations are common to many *in vitro* studies. Some level on uncertainty may also arise from a limited amount of the applied lubricant (around 10 ml used for full flooding of the tibial insert) as it was reported that smaller volume of the fluid leads to higher degree of degradation [79]. Nevertheless, this is rather closely related to long-term wear tests as most of the experiments performed in the present study lasted couple minutes including test preparation.

5. Conclusion

The present contribution concentrated on the assessment of lubricant film formation within TKA. The tests were performed with the use of

knee test rig while the metal femoral component was in contact with the transparent polymer insert. The contact was observed using the fluorescent microscopy method. Transient dynamic conditions were applied. Initially, the contact was lubricated by mineral oil enabling to compare the experimental investigation with the developed numerical model which is presented in Part II [34]. Further experiments were realized using various lubricants, revealing the impact of specific synovial fluid constituents on evolution of film thickness during the gait cycle. The main conclusions are:

- Unique approach built on the direct optical monitoring of film formation in TKA was presented. Initial investigation considering mineral oil as the test lubricant revealed very good agreement of both experimental and numerical approaches [34].
- Based on the assessment of the behavior of albumin, γ -globulin, and HA in model synovial fluids of different degrees of complexity, a lubrication model for TKA was proposed.
- It is suggested that γ -globulin is strongly adsorbed to the substrate, creating a boundary lubricating layer which is reinforced by HA and PL molecules. Further enhancement of lubricant layer is due to layering of low-shear albumin layer.
- The medial condyle shows worse lubrication conditions which may potentially lead to shortening of service life of the TKA.
- Based on the observation of continuous decrease in film thickness, interrupted walking with rest periods may beneficially influence the film recovery. Resting periods may therefore be clinically important to improve implant longevity.

Credit author statement

D. Nečas, M. Vrbka and M. Marian conceived the idea. D. Nečas designed, performed and analyzed the experiments. A. Galandáková prepared the model fluids. D. Nečas, M. Marian, J. Gallo and M.A. Wimmer wrote the original draft of the manuscript. M. Hartl and I. Krupka supervised the study. All authors provided suggestions for the final discussions, reviewed, edited and read the manuscript as well as approved the final version.

Declaration of competing interest

The authors declare that they have no known competing financial interests or personal relationships that could have appeared to influence the work reported in this paper.

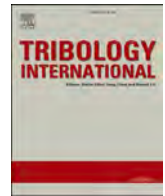
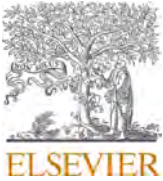
Acknowledgements

This work was supported by the Ministry of Education, Youth and Sports of the Czech Republic (LTAUSA17150) and RVO 61989592. M. Marian, B. Rothhammer, S. Tremmel and S. Wartzack greatly acknowledge the continuous support of Friedrich-Alexander-Universität Erlangen-Nürnberg (FAU), Germany. J. Gallo was supported by IGA_LF_2020_015. The authors thank to T. Sýkora who was involved in experimental study.

References

- [1] Cook R, Davidson P, Martin R. More than 80% of total knee replacements can last for 25 years. *BMJ* 2019;367:15680.
- [2] Ferket BS, Feldman Z, Zhou J, Oei EH, Bierma-Zeinstra SMA, Mazumdar M. Impact of total knee replacement practice: cost effectiveness analysis of data from the Osteoarthritis Initiative. *BMJ* 2017;356:1331–40.
- [3] Carr AJ, Robertsson O, Graves S, Price AJ, Arden NK, Judge A, et al. Knee replacement. *Lancet* 2012;379:1331–40.
- [4] Price AJ, Alvand A, Troelsen A, Katz JN, Hooper G, Gray A, et al. Knee replacement. *Lancet* 2018;392:1672–82.
- [5] Pietrzak J, Common H, Migaud H, Pasquier G, Girard J, Putman S. Have the frequency of and reasons for revision total knee arthroplasty changed since 2000? Comparison of two cohorts from the same hospital: 255 cases (2013–2016) and 68 cases (1991–1998). *J Orthop Traumatol: Surg Res* 2019;105:639–45.
- [6] Gallo J, Goodman SB, Kontinen YT, Wimmer MA, Holinka M. Osteolysis around total knee arthroplasty: a review of pathogenetic mechanisms. *Acta Biomater* 2013;9:8046–58.
- [7] Australian Orthopaedic Association National Joint Replacement Registry (AOANJRR). Hip, knee & shoulder arthroplasty: 2020 annual report. Adelaide: AOA; 2020. p. 1–474.
- [8] American Joint Replacement Registry (AJRR). Annual report. Rosemont, IL: American Academy of Orthopaedic Surgeons (AAOS), 2020; 2020.
- [9] Shi J, Zhu W, Liang S, Li H, Li S. Cross-linked versus conventional polyethylene for long-term clinical outcomes after total hip arthroplasty: a systematic review and meta-analysis. *J Invest Surg* 2019;1–11.
- [10] Evans JT, Walker RW, Evans JP, Blom AW, Sayers A, Whitehouse MR. How long does a knee replacement last? A systematic review and meta-analysis of case series and national registry reports with more than 15 years of follow-up. *Lancet* 2019;393:655–63.
- [11] McKellop HA. The lexicon of polyethylene wear in artificial joints. *Biomaterials* 2007;28:5049–57.
- [12] Knowlton CB, Bhutani P, Wimmer MA. Relationship of surface damage appearance and volumetric wear in retrieved TKR polyethylene liners. *J Biomed Mater Res B Appl Biomater* 2017;105:2053–9.
- [13] Spece H, Schachtner JT, MacDonald DW, Klein GR, Mont MA, Lee G-C, et al. Reasons for revision, oxidation, and damage mechanisms of retrieved vitamin E-stabilized highly crosslinked polyethylene in total knee arthroplasty. *J Arthroplasty* 2019;34:3088–93.
- [14] Fulin P, Slouf M, Krejčíková S, Nevorálová M, Sticha R, Pokorný D. Comparison of explanted UHMWPE hip replacement components of various manufacturers after 10 years in vivo. *Acta Chir Orthop Traumatol Cech* 2019;86:390–6.
- [15] Chakrabarty G, Vashishtha M, Leeder D. Polyethylene in knee arthroplasty: a review. *J Clin Orthop Trauma* 2015;6:108–12.
- [16] MacDonald DW, Higgs GB, Chen AF, Malkani AL, Mont MA, Kurtz SM. Oxidation, damage mechanisms, and reasons for revision of sequentially annealed highly crosslinked polyethylene in total knee arthroplasty. *J Arthroplasty* 2018;33:1235–41.
- [17] Pourzal R, Knowlton CB, Hall DJ, Laurent MP, Urban RM, Wimmer MA. How does wear rate compare in well-functioning total hip and knee replacements? A postmortem polyethylene liner study. *Clin Orthop Relat Res* 2016;474:1867–75.
- [18] Ngai V, Kunze J, Cip J, Laurent MP, Jacobs JJ, Wimmer MA. Backside wear of tibial polyethylene components is affected by gait pattern: a knee simulator study using rare earth tracer technology. *J Orthop Res* 2020.
- [19] Chen Z, Zhang J, Gao Y, Chen S, Zhang X, Jin Z. Effects of interference assembly of a tibial insert on the tibiofemoral contact mechanics in total knee replacement. *Proc IME H J Eng Med* 2019;233:948–53.
- [20] Mihalko WM, Haider H, Kurtz S, Marcolongo M, Urish K. New materials for hip and knee joint replacement: what's hip and what's in knee? *J Orthop Res* 2020.
- [21] Inacio MCS, Paxton EW, Graves SE, Namba RS, Nemes S. Projected increase in total knee arthroplasty in the United States – an alternative projection model. *Osteoarthritis Cartilage* 2017;25:1797–803.
- [22] Brown TS, Van Citters DW, Berry DJ, Abdel MP. The use of highly crosslinked polyethylene in total knee arthroplasty. *Bone Joint J* 2017;99-B:996–1002.
- [23] Orita K, Minoda Y, Sugama R, Ohta Y, Ueyama H, Takemura S, et al. Vitamin E-infused highly cross-linked polyethylene did not reduce the number of in vivo wear particles in total knee arthroplasty. *Bone Joint J* 2020;102-B:1527–34.
- [24] Liu T, Esposito C, Elpers M, Wright T. Surface damage is not reduced with highly crosslinked polyethylene tibial inserts at short-term. *Clin Orthop Relat Res* 2016;474:107–16.
- [25] Ilgen RL, Forsythe TM, Pike JW, Laurent MP, Blanchard CR. Highly crosslinked vs conventional polyethylene particles—an in vitro comparison of biologic activities. *J Arthroplasty* 2008;23:721–31.
- [26] Huang C-H, Lu Y-C, Chang T-K, Hsiao I-L, Su Y-C, Yeh S-T, et al. In vivo biological response to highly cross-linked and vitamin E-doped polyethylene-a particle-Induced osteolysis animal study. *J Biomed Mater Res B Appl Biomater* 2016;104:561–7.
- [27] Chen W, Bichara DA, Suhardi J, Sheng P, Muratoglu OK. Effects of vitamin E-diffused highly cross-linked UHMWPE particles on inflammation, apoptosis and immune response against *S. aureus*. *Biomaterials* 2017;143:46–56.
- [28] Baxter RM, MacDonald DW, Kurtz SM, Steinbeck MJ. Characteristics of highly cross-linked polyethylene wear debris in vivo. *J Biomed Mater Res B Appl Biomater* 2013.
- [29] Minoda Y, Kobayashi A, Sakawa A, Aihara M, Tada K, Sugama R, et al. Wear particle analysis of highly crosslinked polyethylene isolated from a failed total hip arthroplasty. *J Biomed Mater Res B Appl Biomater* 2008;86B:501–5.
- [30] ISO 14243-1. Implants for surgery — wear of total knee-joint prostheses - Part 1: loading and displacement parameters for wear-testing machines with load control and corresponding environmental conditions for test. 2009.
- [31] ISO 14243-3. Implants for surgery - wear of total knee-joint prostheses - Part 3: loading and displacement parameters for wear-testing machines with displacement control and corresponding environmental conditions for test. 2014.
- [32] Wang X-H, Zhang W, Song D-Y, Li H, Dong X, Zhang M, et al. The impact of variations in input directions according to ISO 14243 on wearing of knee prostheses. *PLoS One* 2018;13:e0206496.
- [33] Serro AP, Degiampietro K, Colaço R, Saramago B. Adsorption of albumin and sodium hyaluronate on UHMWPE: a QCM-D and AFM study. *Colloids Surf B Biointerfaces* 2010;78:1–7.
- [34] Marian M, Orgeldinger C, Rothhammer B, Nečas D, Vrbka M, Krupka I, et al. Towards the understanding of lubrication mechanisms in total knee replacements –

- Part II: numerical modeling. *Tribol. Int.* 2020;106809. <https://doi.org/10.1016/j.triboint.2020.106809>.
- [35] Ohtsuki N, Murakami T, Moriyama S, Higaki H. Influence of geometry of conjunction on elastohydrodynamic film formation in knee prostheses with compliant layer. *Elastohydrodynamics - '96 fundamentals and applications in lubrication and traction*. In: Proceedings of the 23rd Leeds-Lyon symposium on tribology held in the institute of tribology. Department of Mechanical Engineering, Elsevier; 1997. p. 349–59.
- [36] Scholes SC, Unsworth A. The effects of proteins on the friction and lubrication of artificial joints. *Proc IME H J Eng Med* 2006;220:687–93.
- [37] Scholes SC, Unsworth A, Jones E. Polyurethane unicondylar knee prostheses: simulator wear tests and lubrication studies. *Phys Med Biol* 2007;52:197–212.
- [38] Bortel E, Charbonnier B, Heuberger R. Development of a synthetic synovial fluid for tribological testing. *Lubricants* 2015;3:664–86.
- [39] Fullam S, He J, Scholl CS, Schmid TM, Wimmer MA. Competitive binding of bilirubin and fatty acid on serum albumin affects wear of UHMWPE. *Lubricants* 2020;8.
- [40] Brandt J-M, Charron K, Zhao L, MacDonald SJ, Medley JB. Calf serum constituent fractions influence polyethylene wear and microbial growth in knee simulator testing. *Proc IME H J Eng Med* 2012;226:427–40.
- [41] Brandt J-M, Mahmoud KK, Koval SF, MacDonald SJ, Medley JB. Antimicrobial agents and low-molecular weight polypeptides affect polyethylene wear in knee simulator testing. *Tribol Int* 2013;65:97–104.
- [42] Guenther LE, Turgeon TR, Bohm ER, Brandt J-M. The biochemical characteristics of wear testing lubricants affect polyethylene wear in orthopaedic pin-on-disc testing. *Proc IME H J Eng Med* 2015;229:77–90.
- [43] Galandáková A, Ulrichová J, Langová K, Hanáková A, Vrbka M, Hartl M, et al. Characteristics of synovial fluid required for optimization of lubrication fluid for biotribological experiments. *J Biomed Mater Res B Appl Biomater* 2017;105:1422–31.
- [44] Flannery M, McGloughlin T, Jones E, Birkinshaw C. Analysis of wear and friction of total knee replacements. *Wear* 2008;265:999–1008.
- [45] Flannery M, Jones E, Birkinshaw C. Analysis of wear and friction of total knee replacements part II: friction and lubrication as a function of wear. *Wear* 2008;265:1009–16.
- [46] Nečas D, Sadecká K, Vrbka M, Galandáková A, Krupka I, et al. Observation of lubrication mechanisms in knee replacement: a pilot study. *Biotribology* 2019;17:1–7.
- [47] Nečas D, Sadecká K, Vrbka M, Galandáková A, Wimmer MA, Gallo J, Hartl M. The effect of albumin and γ -globulin on synovial fluid lubrication: implication for knee joint replacements. *J Mech Behav Mater Biomed Mater* 2021;113:104117.
- [48] Nečas D, Vrbka M, Galandáková A, Krupka I, Hartl M. On the observation of lubrication mechanisms within hip joint replacements. Part I: hard-on-soft bearing pairs. *J Mech Behav Mater Biomed Mater* 2019;89:237–48.
- [49] Nečas D, Vrbka M, Gallo J, Krupka I, Hartl M. On the observation of lubrication mechanisms within hip joint replacements. Part II: hard-on-hard bearing pairs. *J Mech Behav Mater Biomed Mater* 2019;89:249–59.
- [50] Albahrani S, Philippon D, Vergne P, Bluet J. A review of in situ methodologies for studying elastohydrodynamic lubrication. *Proc IME J J Eng Tribol* 2015;230:86–110.
- [51] Myant C, Reddyhoff T, Spikes HA. Laser-induced fluorescence for film thickness mapping in pure sliding lubricated, compliant, contacts. *Tribol Int* 2010;43:1960–9.
- [52] Fowell MT, Myant C, Spikes HA, Kadiric A. A study of lubricant film thickness in compliant contacts of elastomeric seal materials using a laser induced fluorescence technique. *Tribol Int* 2014;80:76–89.
- [53] Nečas D, Jaroš T, Dockal K, Sperka P, Vrbka M, Krupka I, et al. The effect of kinematic conditions on film thickness in compliant lubricated contact. *J Tribol* 2018;140:051501.
- [54] Zhang L, Xu C, Li B. Simple and sensitive detection method for chromium(VI) in water using glutathione-capped CdTe quantum dots as fluorescent probes. *Microchimica Acta* 2009;166:61–8.
- [55] Sugimura J, Hashimoto M, Yamamoto Y. Study of elastohydrodynamic contacts with fluorescence microscope. In: Proceedings of the 26th Leeds-Lyon symposium on tribology. Elsevier; 2000. 609–317.
- [56] Azushima A. In situ 3D measurement of lubrication behavior at interface between tool and workpiece by direct fluorescence observation technique. *Wear* 2006;260:243–8.
- [57] Mischler S, Barril S, Landolt D. Fretting corrosion behaviour of Ti–6Al–4V/PMMA contact in simulated body fluid. *Tribol Mater Surface Interfac* 2013;3:16–23.
- [58] Ford RAJ, Foord CA. Laser-based fluorescence techniques for measuring thin liquid films. *Wear* 1978;51:289–97.
- [59] Pascau A, Guardia B, Puertolas JA, Gómez-Barrena E. Knee model of hydrodynamic lubrication during the gait cycle and the influence of prosthetic joint conformity. *J Orthop Sci* 2009;14:68–75.
- [60] Mongkolwongrojn M, Wongseedakaew K, Kennedy FE. Transient elastohydrodynamic lubrication in artificial knee joint with non-Newtonian fluids. *Tribol Int* 2010;43:1017–26.
- [61] Nečas D, Vrbka M, Rebenda D, Gallo J, Galandáková A, Wolfová L, et al. In situ observation of lubricant film formation in THR considering real conformity: the effect of model synovial fluid composition. *Tribol Int* 2018;117:206–16.
- [62] Hidrovo CH, Hart DP. Emission reabsorption laser induced fluorescence (ERLIF) film thickness measurement. *Meas Sci Technol* 2001;12:467–77.
- [63] Yan Y, Yang H, Su Y, Qiao L. Albumin adsorption on CoCrMo alloy surfaces. *Sci Rep* 2016;5.
- [64] Malmsten M. formation of adsorbed protein layers. *J Colloid Interface Sci* 1998;207:186–99.
- [65] Ko JS, Cho K, Han SW, Sung HK, Baek SW, Koh W-G, et al. Hydrophilic surface modification of poly(methyl methacrylate)-based ocular prostheses using poly (ethylene glycol) grafting. *Colloids Surf B Biointerfaces* 2017;158:287–94.
- [66] Nakashima K, Sawae Y, Murakami T. Study on wear reduction mechanisms of artificial cartilage by synergistic protein boundary film formation. *JSME Int J - Ser C* 2005;48:555–61.
- [67] Nakashima K, Sawae Y, Murakami T. Effect of conformational changes and differences of proteins on frictional properties of poly(vinyl alcohol) hydrogel. *Tribol Int* 2007;40:1423–7.
- [68] Nakashima K, Sawae Y, Murakami T. Influence of protein conformation on frictional properties of poly (vinyl alcohol) hydrogel for artificial cartilage. *Tribol Lett* 2007;26:145–51.
- [69] Duong C-T, Lee J-H, Cho Y, Nam J-S, Kim H-N, Lee S-S, et al. Effect of protein concentrations of bovine serum albumin and γ -globulin on the frictional response of a cobalt-chromium femoral head. *J Mater Sci Mater Med* 2012;23:1323–30.
- [70] Yarithitsu S, Nakashima K, Sawae Y, Murakami T. Influences of lubricant composition on forming boundary film composed of synovia constituents. *Tribol Int* 2009;42:1615–23.
- [71] Hirschmann MT, Becker R. *The unhappy total knee replacement*. Cham: Springer International Publishing; 2015.
- [72] Rad EM, Laurent MP, Knowlton CB, Lundberg HJ, Pourzal RR, Wimmer MA. Linear penetration as a surrogate measure for volumetric wear in TKR tibial inserts. Beyond the implant: retrieval analysis methods for implant surveillance, 100 Barr harbor drive. *ASTM International*; 2018. p. 75–92. Po Box C700, West Conshohocken, Pa 19428-2959.
- [73] O'Brien ST, Luo Y, Brandt J-M. In-vitro and in-silico investigations on the influence of contact pressure on cross-linked polyethylene wear in total knee replacements. *Wear* 2015;332–333:687–93.
- [74] Meng F, Jaeger S, Sonntag R, Schroeder S, Smith-Romanski S, Kretzer JP. How prosthetic design influences knee kinematics: a narrative review of tibiofemoral kinematics of healthy and joint-replaced knees. *Expet Rev Med Dev* 2019;16:119–33.
- [75] Lahuec C, Almouahed S, Arzel M, Gupta D, Hamitouche C, Jézéquel M, et al. A self-powered telemetry system to estimate the postoperative instability of a knee implant. *IEEE Trans Biomed Eng* 2011;58:822–5.
- [76] Guenther LE, Pyle BW, Turgeon TR, Bohm ER, Up Wyss, Schmidt TA, et al. Biochemical analyses of human osteoarthritic and periprosthetic synovial fluid. *Proc IME H J Eng Med* 2014;228:127–39.
- [77] DesJardins J, Aurora A, Tanner SL, Pace TB, Acampora KB, LaBerge M. Increased total knee arthroplasty ultra-high molecular weight polyethylene wear using a clinically relevant hyaluronic acid simulator lubricant. *Proc IME H J Eng Med* 2006;220:609–23.
- [78] Rebenda D, Vrbka M, Čípek P, Toropitsyn E, Nečas D, Pravda M, et al. On the dependence of rheology of hyaluronic acid solutions and frictional behavior of articular cartilage. *Materials* 2020;13.
- [79] Reinders J, Sonntag R, Kretzer JP. Synovial fluid replication in knee wear testing: an investigation of the fluid volume. *J Orthop Res* 2015;33:92–7.



Towards the understanding of lubrication mechanisms in total knee replacements – Part II: Numerical modeling

Max Marian^{a,*}, Christian Orgeldinger^a, Benedict Rothhammer^a, David Nečas^b, Martin Vrbka^b, Ivan Krupka^b, Martin Hartl^b, Markus A. Wimmer^c, Stephan Tremmel^d, Sandro Wartzack^a

^a Engineering Design, Friedrich-Alexander-Universität Erlangen-Nürnberg (FAU), Martensstr. 9, 91058, Erlangen, Germany

^b Department of Tribology, Faculty of Mechanical Engineering, Brno University of Technology, Technická 2896/2, 616 69, Brno, Czech Republic

^c Department of Orthopedic Surgery, Rush University Medical Center, 1611 W. Harrison St., 60612, Chicago, IL, USA

^d Engineering Design and CAD, University of Bayreuth, Universitätsstr. 30, 95448, Bayreuth, Germany

ARTICLE INFO

Keywords:

Total knee replacement
Synovial joint tribology
Soft-elastohydrodynamic lubrication
Finite element method

ABSTRACT

Total knee replacements are an effective surgical treatment to restore the function of the knee. For an adequate design, knowledge about stresses and lubrication conditions is vital. Part II proposes a fully-coupled transient 3D model for the soft elastohydrodynamically lubricated contact based upon the generalized Reynolds equation and Finite Element Method while Part I of this study focused on experimental observations. Within the scope of this contribution, a numerical model is presented and validated with experimental data. Good agreement between model predictions and experimental data was found. A strong influence of fluid and geometry assumptions and transient effects were found. Besides, it was demonstrated that the rheological synovial fluid properties have a decisive role in the tribological behavior.

1. Introduction

Total knee arthroplasty (TKA) is an effective surgical treatment against gonarthrosis and rheumatoid arthritis to restore the function of the knee and provide the patient with a pain-free, more mobile life [1]. Mostly, TKAs consist of a metallic femoral component rubbing against the bearing surface of the plastic tibial plateau [2]. For an adequate TKA design, fundamental knowledge about present deformations, contact pressures, stresses and lubrication conditions is vital. To evaluate the performance of TKA, tribological testing is usually carried out in model tests or physical joint simulators, which are associated with lengthy investigations, high costs and limited transferability [3]. This is also partly due to the lack of proper understanding about underlying lubrication mechanisms [4,5]. Appropriate numerical modeling might stimulate profound knowledge and accelerate the design and performance prediction of new and more reliable TKAs. Computational models based on Finite Element Method (FEM) have been widely developed in both joint scale and the musculoskeletal body scale to analyze contact stresses and stability of the knee implants subjected to complex dynamic activities [6–10]. In many of these studies lubrication was neglected or simplified [11] despite the occurrence of all lubrication regimes

(boundary, mixed and full-film lubrication [12–14]) with a well-known influence on wear performance [15]. This is mainly due to complicated geometries, multiple contacts and, most importantly, the complex multiphysical and multiscale character.

In general, (thermo-)elastohydrodynamically lubricated (TEHL) contacts are defined by a coupled response of the lubricant's hydrodynamics, the elastic deformation of the contacting bodies and the tribosystem's thermodynamics. In recent decades, the tribological characteristics of so called hard EHL contacts, such as those found, for example, in conventional gears [16], cam followers [17] or rolling bearings [18], have been intensively investigated by many authors utilizing sophisticated numerical models [19–22]. EHL contacts with at least one low-elastic-modulus material, e. g. elastomers, are usually referred to as soft-EHL contacts and are found for example in plastic gears [23], sealings [24], or in artificial joints [25]. In recent years, great progress has also been made in the simulation of synovial joints [26,27]. Especially for total hip replacements (THA), many lubrication phenomena in dependency of materials or the stress can be predicted very well, see for example Lu et al. [28] or Ruggiero et al. [29,30]. Considering the lubrication in TKAs, a more limited number of numerical studies can be found in literature. An early model of knee implants with

* Corresponding author.

E-mail address: marian@mfk.fau.de (M. Marian).

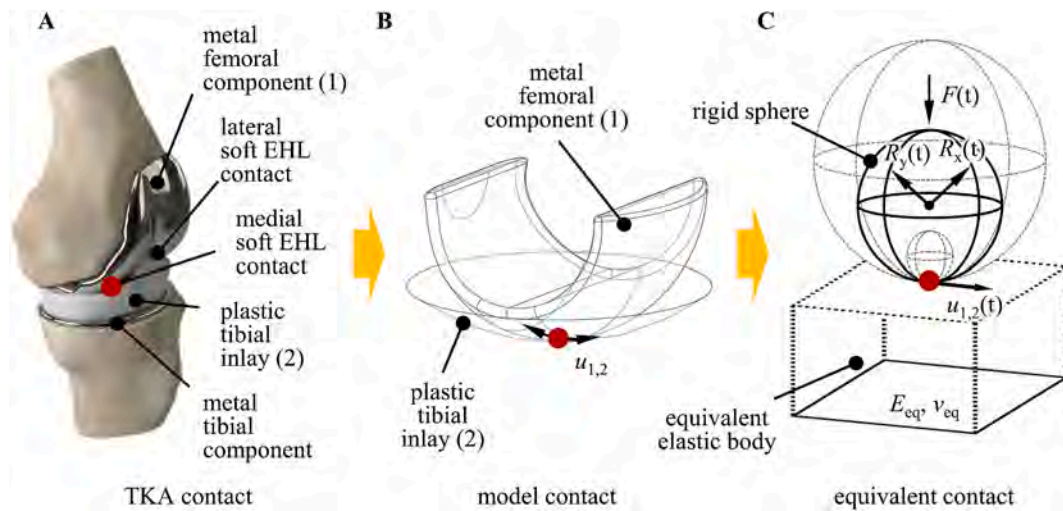


Fig. 1. (A) Contacts in total knee replacements and their simplification to (B) a model and to (C) an equivalent contact.

two described lubrication regions, the fluid flowing between a narrow gap of the knee joints and flowing into one porous surface material, was developed by Tandon and Jaggi [31]. Jin et al. [32] developed an EHL model based upon the superimposition method, considering a simplified ellipsoidal geometry and pure sliding only. Thereby, the contact area and fluid film thickness were predicted with various geometrical parameters under walking conditions. The TKA contact was also analyzed by Kennedy et al. [15] by adopting two cylindrical bodies to study an EHL line-contact with specified rolling-sliding motion while assuming constant load. Pascau et al. [33] evaluated the influence of prosthetic joint conformity on lubrication. However, both bearing surfaces were assumed to be rigid and hydrodynamic lubrication was considered only. Mongkolwongrojin et al. [34] presented transient EHL simulations in artificial knee joints with non-Newtonian fluids, limited by load and motion assumptions similar to Ref. [32]. Complete time-dependent EHL simulations of TKA based upon finite differences and a multigrid solver were performed by Su et al. [35]. Thereby, the elastic deformation was calculated by a constrained column model and Newtonian fluid behavior was assumed. Later, Gao et al. developed advanced wear models for lubricated artificial hip [36] and knee [37] joints in which an adapted Archard wear formula was coupled with lubrication parameters, derived from EHL modeling based upon the multigrid-method and fast Fourier transformation into spherical coordinates [38] under consideration of shear-thinning viscosity [39]. Again, simplifications regarding the geometry were made and none of the previous models was experimentally validated.

Summarizing, fundamental knowledge about lubrication conditions, contact pressures, deformations and stresses is crucial for TKA design. This requires numerical models that accurately and effectively describe geometries, loads and motions as well as all relevant material and fluid phenomena. These were neither covered in their entirety by models available in literature nor experimentally validated. Consequently, the objective of this study was to develop a holistic solution for the soft-EHL modeling of total knee arthroplasties. Thus, the influences of the modeling strategy and complexity as well as of different material and fluid properties on the tribological behavior are analyzed in detail within the scope of this contribution. Since appropriate validation of numerical simulations is a key factor in their successful utilization, this contribution also aims at the comparison with experimental data obtained in Part I [40] of this study. By providing guidelines for a validated FEM based implementation within commercial multiphysics software, the authors hope to stimulate the research in artificial synovial joint simulation, so that, hopefully, the research focus can be shifted even more on physical modeling instead of numerical aspects.

2. Materials and methods

In the following, the theory and governing equations for computing the soft-EHL contacts in total knee replacements based upon the so-called full-system FEM approach [41] are addressed step by step, taking into account realistic contact conditions, non-Newtonian fluid behavior, time-dependent squeeze effects, mass-conserving cavitation, linear elastic material behavior, mixed lubrication as well as thermal effects.

2.1. Material, kinematics and fluid properties

The contact conditions of TKAs are characterized by varying load, motion and geometries along the contact paths. The medial and lateral contact could each be interpreted as a transient model contact of two conformal sliding-rolling elements and subsequently further simplified to the contact between an elastic flat body with equivalent mechanical properties and a single rigid ball with variable radius, load and motion for each time step. The simplification from the TKA to a model contact and further to the equivalent point contact is illustrated in Fig. 1.

The geometry of the knee implant is mainly characterized by four radii, see Fig. 2, which are the radius of the femoral component (1) in medial-lateral (ML) direction $R_{1,ML}$ and in anterior-posterior (AP) direction $R_{1,AP}$ as well as the radius of the tibial component (2) in ML direction $R_{2,ML}$ and in AP direction $R_{2,AP}$ [42]. Within the scope of this study, the femoral AP radius varied in dependency of the FE angle ϕ_{FE} between 33 mm ($\phi_{FE} = 0^\circ$) and 24 mm ($\phi_{FE} = 58^\circ$) [35] while the other radii were considered constant, see Table 1. Within the scope of this

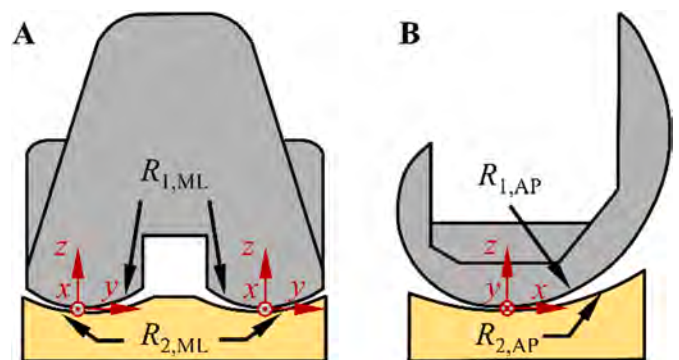


Fig. 2. Schematic geometry of femoral and tibial components in (A) ML and (B) AP direction.

Table 1
Geometry properties [40,42].

femoral radius in ML direction $R_{1,ML}$	18 mm
femoral radius in AP direction $R_{1,AP}$	24–33 mm
tibial radius in ML direction $R_{2,ML}$	21 mm
tibial radius in AP direction $R_{2,AP}$	45 mm

contribution, the influence of the assumption of variable or constant radius ($R_{1,AP} = 33$ mm) was also studied.

A cobalt-chromium-molybdenum cast alloy femoral component and two tibial inlay materials, namely polymethyl methacrylate (PMMA) as well as ultrahigh molecular weight polyethylene (UHMWPE), were studied within the scope of this contribution. These were chosen to match the experimental setup in Part I of this study [40] due to transparency and the possibility to use optical fluorescent measurement technique (PMMA) respectively because it is one of the most common material pairings for total knee replacements (UHMWPE). Mechanical and thermal properties are summarized in Table 2.

The kinematics were chosen based upon ISO14243-3 [43,44], see Fig. 3. Therefore, in accordance to the experimental setup in Part I [40], the load for the CoCrMo/PMMA-pairing was downscaled to approximate the contact pressure level of CoCrMo/UHMWPE. The load was assumed to be distributed by 40% and 60% to the lateral and the medial compartment, respectively. The dominant motion is flexion-extension (FE) of the femoral component, followed by AP displacement of the tibial component, resulting in a combination of sliding and rolling between the artificial bearing surfaces with changing slide-to-roll-ratio (SRR) and directional changes of the hydrodynamically effective sliding velocity. Tibial rotation was excluded within the scope of this study. The frequency of one gait cycle was 1 Hz and the validation with experimental data from Part I [40] was done for six characteristic positions (a) – (f) corresponding to 0%, 14%, 25%, 45%, 60% and 80% of the cycle.

The relative velocity of the femoral component was determined by

$$u_1(t) = \omega(t) \cdot R_{1,AP}, \quad (1)$$

whereas the one of the tibial component was defined as

$$u_2(t) = \frac{[d_{AP}(t) - d_{AP}(t - \Delta t)]}{\Delta t}, \quad (2)$$

where $\omega(t)$ was the angular velocity obtained by the FE angle $\phi_{FE}(t)$ of the femoral and $d_{AP}(t)$ the moving distance of the tibial component along the AP direction.

Generally, pressure, temperature or shear-rate distribution can have a significant influence on the lubricant’s properties, whereas changes in viscosity tend to have the largest impact on EHL contacts. Within the scope of this contribution, at first, pure mineral oil R834/80 was studied and compared with experimental data from Part I [40]. This was done because the rheological behavior of mineral oil is comparatively well known and the properties scatter less than that of synovial fluid, allowing to exclude this as potential influencing or distorting factors. Moreover, mineral oil naturally emits fluorescence without the addition of markers enabling the experimental observation of the fluid film formation. The density was modeled with dependency on pressure and

Table 2
Material properties [40].

	CoCrMo femoral (1)	PMMA tibial (2–1)	UHMWPE tibial (2–2)
Young’s modulus E_i	240 000 MPa	3500 MPa	660 MPa
Poisson’s ratio ν_i	0.29	0.34	0.46
density ρ_i	8280 kg/m ³	1180 kg/m ³	935 kg/m ³
heat conductivity λ_i	12.8 W/(m · K)	0.19 W/(m · K)	0.4 W/(m · K)
spec. heat capacity	452 J/(kg · K)	1500 J/(kg · K)	1900 J/(kg · K)
$c_{p,i}$			

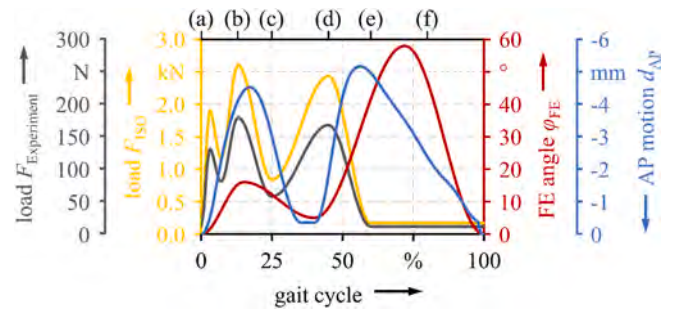


Fig. 3. Axial load, FE angle and AP motion according to Ref. [40] and ISO 14243-3 [43,44].

temperature following Dowson and Higginson [45]. For the viscosity, a pressure and temperature dependency according to Roelands [46] was modeled. Moreover, a modified Carreau-Yasuda model with two Newtonian plateaus in accordance with Bair [47] was used to describe the shear dependency. Relevant lubricant properties are summarized in Table 3.

Similarly, synovial fluid typically shows higher viscosity at lower and low viscosity at higher shear rates, doing a good job to prevent the cartilage from wear. However, the rheological behavior differs strongly between different individuals with healthy or diseased joints or its in vitro substitutes [48]. Here, three types of synovial fluid were examined, the parameters of which are listed in Table 4. In accordance to Ref. [37], the shear thinning behavior was modeled by a Cross model [49].

2.2. Hydrodynamics

Derived from the three-dimensional Navier-Stokes equations by considering reasonable assumptions for EHL contacts and no-slip boundary conditions, the velocity distribution in the lubricant film can be expressed by

$$u_x(x, z, t) = \frac{\partial p}{\partial x} \left(\int_0^z \frac{z}{\eta} dz - \frac{\int_0^h \frac{z}{\eta} dz}{\int_0^h \frac{1}{\eta} dz} \cdot \int_0^z \frac{1}{\eta} dz \right) + \frac{1}{\int_0^h \frac{1}{\eta} dz} \cdot (u_1 - u_2) \cdot \int_0^z \frac{1}{\eta} dz + u_2. \quad (3)$$

Inserting the velocity equations in the integral transient continuity

Table 3
Mineral oil properties [40,47].

base density ρ_0	898 kg/m ³
base viscosity η_0	0.179 Pa s
pressure coefficient α_p	2.3×10^{-8} Pa ⁻¹
Roelands coefficient β_η	0.06
critical shear stress G_c	4.8 kPa
limiting shear stress η_∞	0.59 η_0
Carreau parameter a_c	2.0
Carreau parameter n_c	0.62
thermal conductivity λ	0.15 W/(m · K)
specific heat capacity c_p	1675 J/(kg · K)

Table 4
Synovial fluid properties [37,40,48,50].

	healthy	diseased	artificial
base density ρ_0	1050 kg/m ³	1025 kg/m ³	1000 kg/m ³
base viscosity η_0	0.6 Pa s	0.2 Pa s	0.05 Pa s
plateau viscosity η_∞	0.3 Pa s	0.1 Pa s	0.002 Pa s
Cross parameter a_c	9.5 s	7.7 s	5.9 s
Cross parameter β_c	0.7	0.75	0.8
thermal conductivity λ	0.21 W/(m · K)	0.41 W/(m · K)	0.61 W/(m · K)
specific heat capacity c_p	3900 J/(kg · K)	4041 J/(kg · K)	4182 J/(kg · K)
intra-capsular pressure p_i	60 kPa	21 kPa	0 kPa

equation

$$\frac{\partial}{\partial x} \left(\int_0^h \rho \cdot u_x dz \right) + \frac{\partial}{\partial t} (\rho h) = 0 \quad (4)$$

results in the generalized Reynolds equation according to Yang and Wen [51] in slightly modified notation

$$\begin{aligned} \frac{\partial}{\partial x} \left[\left(\frac{\int_0^h \frac{z}{\eta} dz \cdot \int_0^h \rho \int_0^c \frac{1}{\eta} dz' dz}{\int_0^h \frac{1}{\eta} dz} - \int_0^h \rho \int_0^c \frac{z'}{\eta} dz' dz \right) \frac{\partial p}{\partial x} \right] + \frac{\partial}{\partial y} \left[\left(\frac{\int_0^h \frac{z}{\eta} dz \cdot \int_0^h \rho \int_0^c \frac{1}{\eta} dz' dz}{\int_0^h \frac{1}{\eta} dz} - \int_0^h \rho \int_0^c \frac{z'}{\eta} dz' dz \right) \frac{\partial p}{\partial y} \right] - \\ - \frac{\partial}{\partial x} \left[\frac{\int_0^h \rho \int_0^c \frac{1}{\eta} dz' dz}{\int_0^h \frac{1}{\eta} dz} (u_1 - u_2) + \int_0^h \rho dz \cdot u_2 \right] - \frac{\partial}{\partial t} \left(\int_0^h \rho dz \right) = 0, \end{aligned} \quad (5)$$

which was solved for the pressure p in a weak finite element form on the upper surface of the meshed body Ω_c . The first two (Poiseuille) terms described the influence of the pressure gradient, while the third (Couette) accounted for boundary velocities of the contacting bodies and the wedge shape of the lubricant gap. The last term reflected time-dependent squeeze effects. When non-Newtonian and thermal effects were not considered, the Reynolds equation [52] could be simplified to its original form

$$\frac{\partial}{\partial x} \left(\frac{\rho h^3}{12\eta} \frac{\partial p}{\partial x} \right) + \frac{\partial}{\partial y} \left(\frac{\rho h^3}{12\eta} \frac{\partial p}{\partial y} \right) - \frac{\partial}{\partial x} \left(\rho h \frac{(u_1 + u_2)}{2} \right) - \frac{\partial(\rho h)}{\partial t} = 0. \quad (6)$$

The Reynolds equation was complemented by Dirichlet boundary conditions ($p = p_i$, $\partial p / \partial x = \partial p / \partial y = 0$) at the contact's in- and outlet to match with the intracapsular pressure.

2.3. Cavitation

Cavitation effects were addressed by a mass-conserving algorithm as introduced by Marian et al. [53]. Therefore, density and viscosity were multiplied with the fractional film content

$$\rho = \theta(p) \cdot \rho_f, \quad \eta = \theta(p) \cdot \eta_f, \quad (7)$$

which was defined as the ratio of lubricant layer to gap height

$$\theta(p) = \frac{h_{liq}}{h} = e^{-\gamma(p) \cdot p^2}, \quad (8)$$

whereas $\gamma(p)$ is a penalty function that is 0 if $p < p_{cav}$. In any other case, $\gamma(p)$ equals to ξ , where ξ is a sufficiently high algebraic number. In accordance to Bartel [54], the thermal fluid properties were adjusted as follows:

$$\begin{aligned} c_p &= c_{p,gas} + \theta(p) \cdot (c_{p,f} - c_{p,gas}), \quad \lambda = \lambda_{gas} + \theta(p) \cdot (\lambda_f - \lambda_{gas}), \\ \beta &= \beta_{gas} + \theta(p) \cdot (\beta_f - \beta_{gas}). \end{aligned} \quad (9)$$

2.4. Contact mechanics

Based upon FEM, the elastic deformation of the equivalent body with equivalent Young's modulus and Poisson's ratio

$$E_{eq} = \frac{E_1^2 \cdot E_2 \cdot (1 + \nu_2)^2 + E_2^2 \cdot E_1 \cdot (1 + \nu_1)^2}{[E_1 \cdot (1 + \nu_2) + E_2 \cdot (1 + \nu_1)]^2}, \quad \nu_{eq} = \frac{E_1 \cdot \nu_2 \cdot (1 + \nu_2) + E_2 \cdot \nu_1 \cdot (1 + \nu_1)}{E_1 \cdot (1 + \nu_2) + E_2 \cdot (1 + \nu_1)} \quad (10)$$

was calculated by applying the linear elasticity equation and neglecting inertia effects and body forces

$$\nabla \cdot \sigma = 0, \quad \text{with } \sigma = C \cdot \varepsilon(U), \quad \delta(x, y, t) = |U_z(x, y, t)|. \quad (11)$$

Boundary conditions were zero displacement on the bottom and the total contact pressure p_t on the top of the calculation domain, which was employed as a normal stress. Free boundary conditions assuming zero normal and tangential stresses were applied to the remaining boundaries. Within the scope of this contribution, the influence of the consideration of the finite height of the tibial inlay was also analyzed ($h_{cub, infinite} = 60 \cdot b_{Hertz}$, $h_{cub, finite, PMMA} = 6.5 \text{ mm}$ [40], $h_{cub, finite, UHMWPE} = 10 \text{ mm}$ [35]).

2.5. Film thickness

The height of the separating fluid layer was described by the film thickness equation and consisted of the rigid body distance, the quadratic approximation of the undeformed geometry and the elastic deformation:

$$h(x, y, t) = h_0(t) + \frac{x^2}{2R_{eq,x}} + \frac{y^2}{2R_{eq,y}} + \delta(x, y, t). \quad (12)$$

2.6. Equilibrium of forces

The load balance equation ensured the equilibrium of forces between the applied load and the total contact pressure

$$F = \int_{\Omega_c} p_t(x, y, t) d\Omega_c = \int_{\Omega_c} [p(x, y, t) + p_a(x, y, t)] d\Omega_c, \quad (13)$$

whereas simultaneously occurring solid asperity contact and hydrodynamic pressure (mixed lubrication) was considered.

2.7. Mixed lubrication

Assuming linear elasticity and a Gaussian distribution, the asperity contact pressure was calculated by a statistical Greenwood-Williamson model, which was verified for soft-EHL contacts by Masjedi and Khonsari [55]. The implementation in MathWorks MATLAB followed Winkler et al. [18] and obtained solid asperity graphs were incorporated into the macro-scale TEHL model as interpolated functions.

2.8. Energy conservation

The temperature distribution in the fluid was described by the energy equation and heat sources due to lubricant shearing and compression

$$\rho c_p \left(\frac{\partial \theta}{\partial t} + u_x \frac{\partial \theta}{\partial x} \right) - \lambda \left(\frac{\partial^2 \theta}{\partial x^2} + \frac{\partial^2 \theta}{\partial y^2} + \frac{\partial^2 \theta}{\partial z^2} \right) - \eta \left[\left(\frac{\partial u_x}{\partial z} \right)^2 \right] - \beta_p \theta \left(\frac{\partial p}{\partial t} + u \frac{\partial p}{\partial x} \right) = 0, \quad (14)$$

while the energy equation of the contacting bodies was

$$\rho c_{p,i} \left(\frac{\partial \theta}{\partial t} + u_i \frac{\partial \theta}{\partial x} \right) - \lambda_i \left(\frac{\partial^2 \theta}{\partial x^2} + \frac{\partial^2 \theta}{\partial y^2} + \frac{\partial^2 \theta}{\partial z^2} \right) = 0. \quad (15)$$

The heat transitions between the solids and the lubricant were described by temperature and conductive heat flux continuity equations. Solids and lubricant entering the calculation domain were set to bulk temperature while no conductive heat flux was assumed for the respective properties leaving the domain.

2.9. Dimensionless parameters, stabilization and numerical procedure

For a good conditioning and a convenient numerical solution procedure of the highly non-linear system of equations with solution variables that differ by several orders of magnitude, the following variables were normalized on HERTZian or reference parameters:

$$\begin{aligned} X &= \frac{x}{b_{\text{HERTZ}}(t_{\text{ref}})}, Y = \frac{y}{b_{\text{HERTZ}}(t_{\text{ref}})}, Z_s = \frac{z}{b_{\text{HERTZ}}(t_{\text{ref}})}, Z_f = \frac{z}{h}, P = \frac{p}{p_{\text{HERTZ}}(t_{\text{ref}})}, \\ H &= \frac{h \cdot R_{\text{eq}}(t_{\text{ref}})}{b_{\text{HERTZ}}^2(t_{\text{ref}})}, \bar{\delta} = \frac{\delta \cdot R_{\text{eq}}(t_{\text{ref}})}{b_{\text{HERTZ}}^2(t_{\text{ref}})}, T = \frac{t \cdot u_m(t_{\text{ref}})}{b_{\text{HERTZ}}(t_{\text{ref}})}, \bar{\theta} = \frac{\theta}{\theta_0}, \bar{\rho} = \frac{\rho}{\rho_0}, \bar{\eta} = \frac{\eta}{\eta_0}, \\ C_u &= \frac{u_m(T)}{u_m(t_{\text{ref}})}, C_R = \frac{R_{\text{eq}}(T)}{R_{\text{eq}}(t_{\text{ref}})}, C_F = \frac{F(T)}{F(t_{\text{ref}})}. \end{aligned} \quad (16)$$

Here, the time step at 50% of the gait cycle was used as reference due to the comparably high load and velocity. More information on the dimensionless form of the governing equations and the normalization for transient operating conditions can be found elsewhere [56–58]. Isotropic diffusion [59] was utilized to accommodate numerical instabilities in the higher pressure region.

The numerical solution scheme is illustrated in Fig. 4A. After reading all required input variables and functions, initial values were determined based upon the Hertz theory. These were used to compute a starting solution for the deformation and thus the lubricant gap. In the next step, the fully-coupled steady-state isothermal Newtonian model was solved in the FEM-domain (P, H), see Fig. 4B. Therefore, a tetrahedral mesh with refinement in the contact center of the upper surface was applied. To reduce the computational effort, the symmetry of the contact was exploited. Without thermal or non-Newtonian effects, the time loop

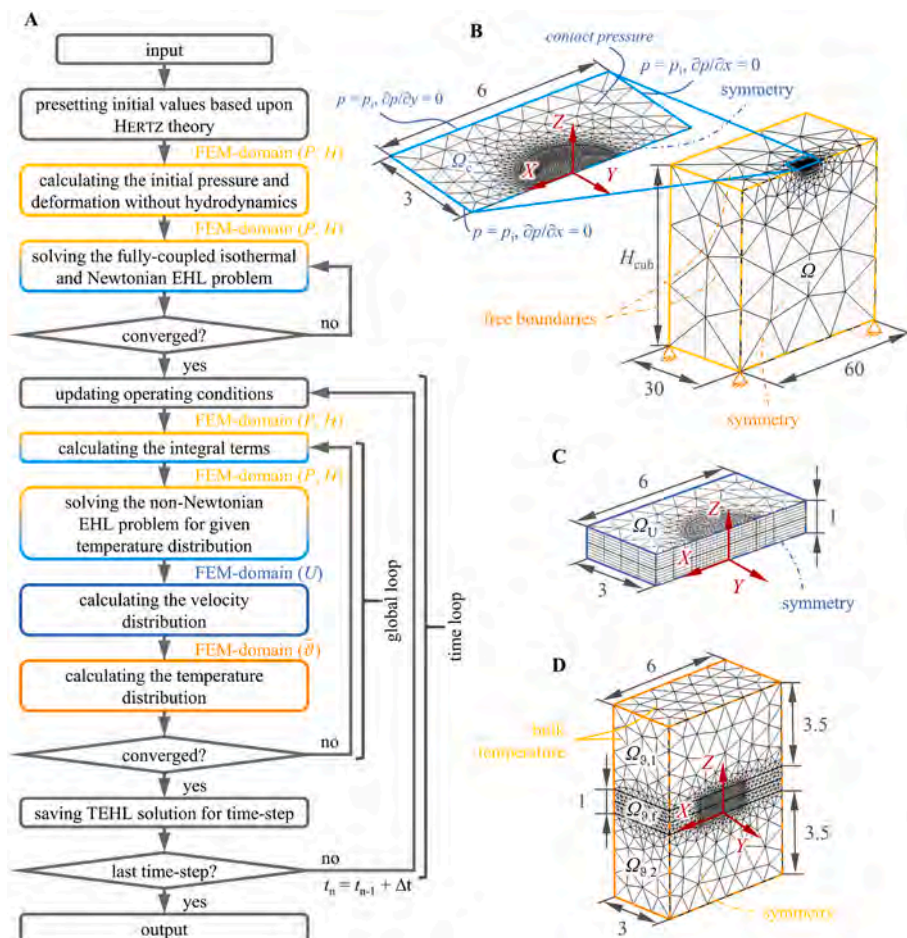


Fig. 4. (A) Numerical solution scheme and (B–D) utilized FEM-domains and boundary conditions.

would have been launched and repeated until the last time-step has been calculated. With their consideration, a sequential solver computed the integral terms of the generalized Reynolds equation followed by the fully coupled system of pressure and deformation in the FEM-domain (P , H) and finally the determination of the velocity distribution in the FEM-domain (U), see Fig. 4C. For the latter, a triangular mesh with regular distribution in gap direction was used. If thermal effects were considered, the last step of the sequential solver was the computation of the temperature distribution in the FEM-domain (ϑ) using a tetrahedral

mesh, see Fig. 4D. These steps were repeated until a converged solution for all solution variables was found. The coupling of the different FEM domains was done by linear extrusions. In the transient case, the time loop was launched and repeated until the last time-step was calculated. The coupling of two consecutive time-steps was realized by an implicit backward differentiation formula (BDF) scheme of second order [60]. More fundamental aspects about FEM on EHL contacts are given by Habchi [58] and for further information about the implementation in the software COMSOL MULTIPHYSICS, the interested reader is referred

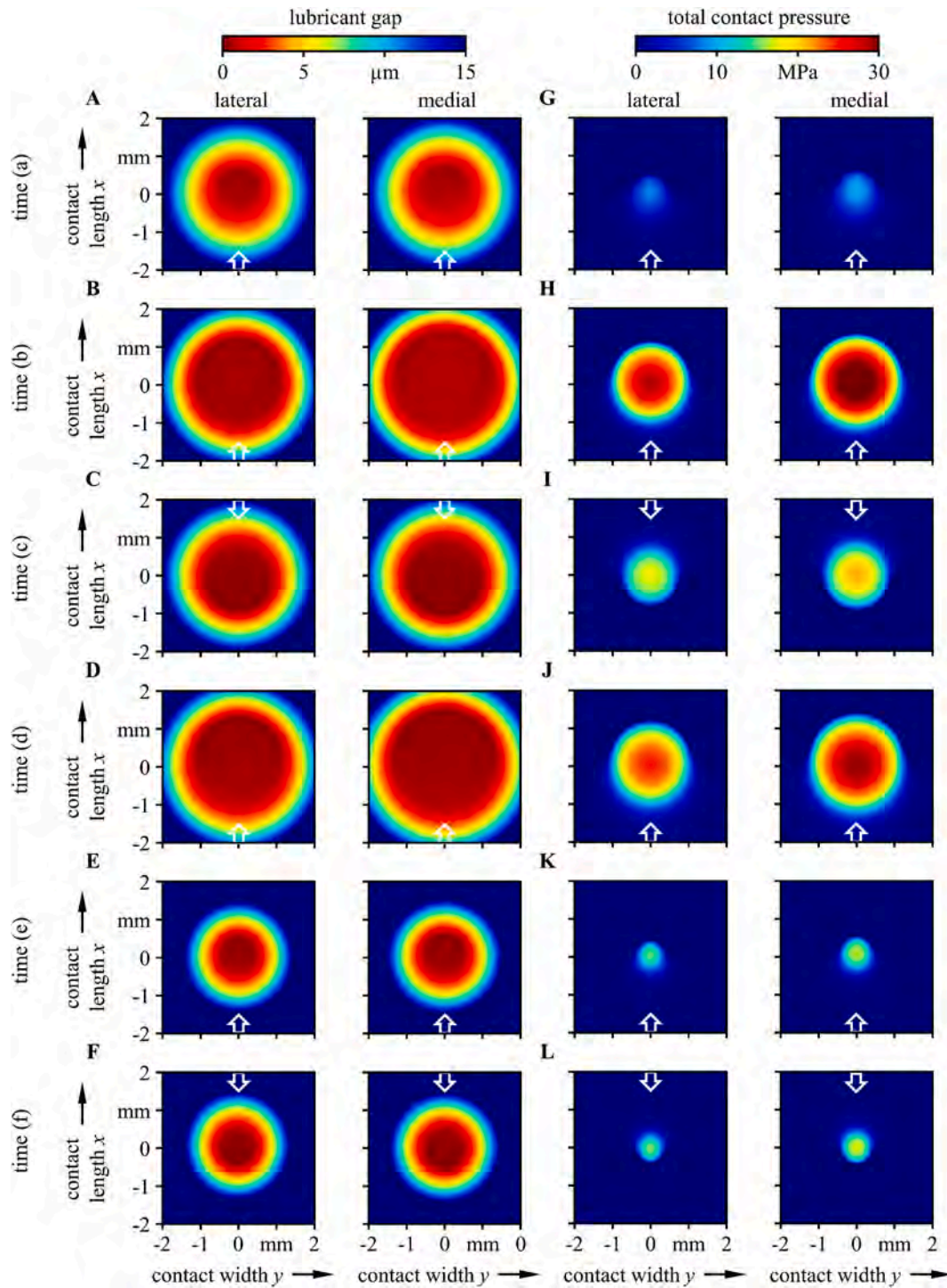


Fig. 5. (A–F) Simulated lubricant gap and (G–L) total pressure distribution for the lateral and medial compartment of the CoCrMo/PMMA-pairing and mineral oil lubrication at time steps (a) to (f). Scales are selected to properly visualize relevant effects, actually extrema are partially not mapped. The white arrows indicated the direction of lubricant drawing into the contact.

to Tan et al. [61] or Lohner et al. [62].

3. Results

In the following, numerical results on the CoCrMo/PMMA-pairing with mineral oil lubrication are first shown and compared with experimental results from Part I [40] to demonstrate the general validity of the numerical model. Subsequently, corresponding results for artificial synovial fluid lubrication as well as the influences due to the modeling complexity are presented. The aim is to indicate which effects and phenomena might be neglected and which have to be considered for balancing computation time and accuracy. Finally, the transfer to the CoCrMo/UHMWPE-pairing is conducted and the impact of synovial fluid properties on the tribological behavior is revealed to raise awareness to their decisive role and the necessity of appropriate rheological modeling.

3.1. Lubrication mechanisms and experimental validation (CoCrMo/PMMA, mineral oil lubrication)

The lubricant gap and total pressure distribution for the lateral and the medial compartment of the CoCrMo/PMMA-pairing under mineral oil lubrication as simulated are illustrated in Fig. 5A–L for the time steps (a) to (f) of the gait cycle. The direction in which the lubricant was drawn into the contact changed according to the kinematics and is indicated by white arrows. Both the condyles featured typical characteristics for soft-EHL point contacts [63] with significant elastic flattening of the contact center and an only very slightly horseshoe-shaped fluid film height with a minimum in the outlet region. Further, the pressure distribution showed no pronounced Petrusевич-spike and was similar to the one according to the Hertzian theory but rose earlier because of lubricant drawing into the contact. Comparing both compartments, the medial condyle experienced larger elastic deformations and featured higher contact pressures, which was due to the higher normal load proportion.

The evolution of the maximum pressure as depicted in Fig. 6A featured three clearly distinguishable peaks in the stance phase that apparently followed the normal force. This indicated that the hydrodynamic pressure was mainly generated by the load and the geometry and similar to the pressure under dry conditions. Furthermore, despite the lower load, a further pressure peak could be observed in the swing phase induced by the higher relative velocities. Therefore, hydrodynamic pressure partly exceeded those according to the dry Hertzian theory. Generally, the minimum film height tended to follow the pressure curve anti-cyclically and was further influenced by variations in the velocities. Despite entrainment speed was reduced to zero at the reversal points, the lubricant film did not break down due to squeeze film effects but showed three pronounced minima. Comparing both compartments, the minimum gap of the medial one was slightly lower.

The calculated specific film thickness, which was defined as the overall lubricant gap height averaged over the contact domain, is

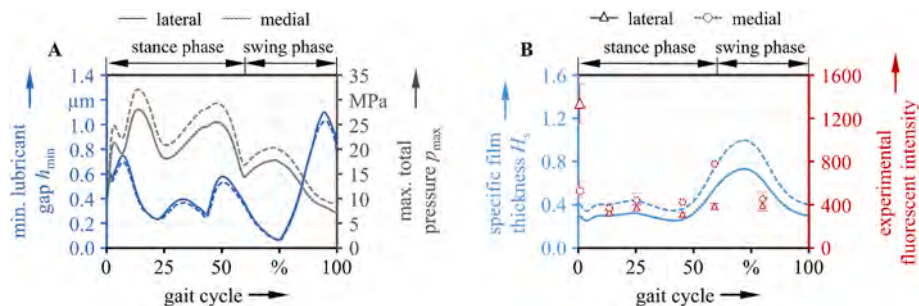


Fig. 6. (A) Minimum lubricant gap and maximum pressure over one gait cycle, (B) mean film height and comparison with experimental data at time steps a to f for the CoCrMo/PMMA-pairing and mineral oil lubrication.

plotted in Fig. 6B over the gait cycle and compared to experimental fluorescent intensity from Part I [40]. Apparently, the specific film height did not accurately follow the minimum lubricant gap and instead featured smaller values in the stance and higher ones in the swing phase. The fact that the medial compartment exhibited a larger specific film height despite higher load can be explained by the compressibility of mineral oil and the pressure dependence of density and viscosity. Generally, there was a strong correlation between the numerical prediction and the experimental validation for most locations, especially in the higher loaded stance phase. The only substantial difference was detected at point (a) where load and AP motion simultaneously exhibited a considerable change. Thus, observed differences as well as the slight discrepancies in the swing phase could be attributed to deviations in the stress collective assumptions compared to the real test conditions.

3.2. Influences of the modeling strategy (CoCrMo/PMMA, artificial synovial fluid lubrication)

Subsequently, corresponding results for lubrication with artificial synovial fluid as it is usually used for in vitro TKA testing are studied. Therefore, minimum fluid film height and maximum pressure are depicted in Fig. 7A for the lateral and in Fig. 7B for the medial compartment. Regarding the full model (continuous line), which considered thermal and non-Newtonian effects, variable femoral AP radius, finite tibial inlay as well as transient squeeze effects, the pressure was at a comparable level to that of mineral oil. However, the lubricant gap height was considerably smaller due to the lower viscosity of the synovial fluid. At the reversal points of entrainment velocity, the film height got so small that solid asperity contact became very likely, especially for the higher loaded medial compartment.

Furthermore, the influence of numerical modeling on simulation results is demonstrated. Therefore, calculations with (i) isothermal, (ii) Newtonian, (iii) constant femoral AP radius, (iv) infinite tibial inlay and (v) quasi-stationary assumptions were conducted. For this purpose, the averaged deviations of minimum film height and maximum pressure over the entire gait cycle from the full model are also summarized in Table 5. It was found that the pressure evolution was rather marginally affected by the modeling strategy. Only the neglect of the variable femoral AP radius led to a clear underestimation of pressure for both condyles, which was particularly pronounced in the swing phase. These observations were due to the larger possible elastic deformations respectively the larger elastically deformed contact area carrying the load. Regarding the fluid film height, rather moderate differences between the full thermal and the isothermal model could be observed. This was because fluid shearing and compression led to a maximum temperature rise of roughly 0.2 °C (lateral) or 0.3 °C (medial), only slightly affecting density and viscosity. Thus, thermal effects were not taken into account in the further investigations to reduce computational time and memory requirements. In contrast, the neglect of the non-Newtonian synovial fluid rheology had a major impact and led to a substantial

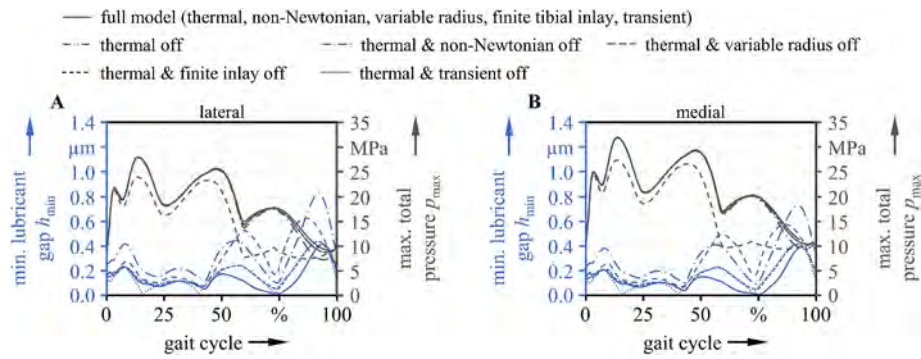


Fig. 7. Minimum lubricant gap and maximum pressure over one gait cycle (CoCrMo/PMMA-pairing and artificial synovial fluid lubrication) for different numerical modeling complexity in the (A) lateral and (B) medial compartment.

overestimation of the film formation. Particularly in areas with a higher velocity differences, i.e. in the swing phase, shear-thinning effects actually led to a lower lubricant gap. Similar to its influence on the pressure curve, the constant femoral AP radius also showed effects on the film height. The bigger elastically deformed contact area accordingly involved higher lubricant gaps. Finally, the disregard of time-dependent squeeze effects in the quasi-stationary approach led partly to an overestimation of the film formation, but also to a breakdown in the velocity reversal points.

3.3. Influences due to the synovial fluid (CoCrMo/UHMWPE)

Finally, results for the CoCrMo/UHMWPE pairing are demonstrated. Again, lubricant gap and total pressure distribution for the lateral and the medial compartment derived from the isothermal full model are illustrated in Fig. 8A–L for the time steps (a) to (f) of the gait cycle. The corresponding evolutions of minimum film height and maximum pressure are depicted in Fig. 9A and B. Evidently, the conditions that arose were basically similar to those of the CoCrMo/PMMA pairing with elastic flattening of the contact center, a slightly horseshoe-shaped lubricant gap and a minimum in the outlet region as well as a pressure distribution similar to Hertz with a slightly earlier increase in the contact inlet. The values obtained were also in a comparable range, although the lateral dimensions of the contact area with UHMWPE were obviously larger due to the higher load and the lower elastic modulus. Furthermore, the flattening was more distinct and the edges of the elastically deformed surface were sharper. Yet, the trend of the extreme values is also similar. In the stance phase, the maximum pressure profile reached slightly lower values than the PMMA, but also followed the external load and showed 3 pronounced peaks. Another peak could be detected at the reversal point of velocities in the swing phase. The fluid film height also revealed an analogous progression, i. e. was significantly lower in the stance compared to the swing phase and had clear minima at the reversal points. While only some difference in the pressure could be detected in the swing phase, it was found that the film height was particularly influenced by the synovial fluids investigated. The higher viscosity of healthy synovia led to a significantly enhanced separation of

Table 5

Averaged deviation of minimum lubricant film height and maximum pressure over the entire gait cycle when calculated with simplified models compared to the full model.

	mean deviation of min. lubricant gap		mean deviation of max. pressure	
	lateral	medial	lateral	medial
thermal off	+23.5%	+22.8%	-1.0%	-1.8%
thermal & non-Newtonian off	+126.6%	+122.8%	-3.2%	-3.1%
thermal & variable radius off	+102.0%	+102.5%	-20.9%	-20.7%
thermal & finite inlay off	+23.7%	+22.9%	-1.1%	-1.9%
thermal & transient off	-18.7%	+16.9%	-1.4%	-2.1%

the rubbing surfaces while thinner fluid resulted in up to a factor of 4 smaller lubricant gaps.

4. Discussion

The numerical FEM-based model presented within this contribution allowed a ‘numerical zoom’ into the contact area of both TKA compartments. Conducted studies focused on the prediction of fluid film formation with special emphasis on experimental validation and the influence of the modeling strategy as well as of the lubricant’s rheology.

4.1. Lubrication mechanisms

Fluid pressure and lubricant gap were defined by the coupled response to geometry and load. Thus, overall pressures were higher, and the film heights were tendentially during the stance phase. Good agreement between numerical results and experimental observations based upon fluorescent measurement from Part I [40] was observed. Fluid film formation was largely affected by the velocity reversal points ($u_m = 0$), where the constriction in the lubricant gap reached pronounced minima when contact in- and outlet changed sides. Yet, transient squeeze effects were able to prevent lubricant film collapsing to a large extent. These findings basically align well with other sophisticated numerical studies reported in literature [35,37].

4.2. Influences due to the modeling strategy

In some cases, however, simplifications in numerical modeling, geometry or kinematic assumptions led to minor or even major discrepancies in the calculated pressure or lubricant gap distribution and thus in predicted contact stresses. On the one hand, thermal effects could most likely be neglected due to the moderate heat generation (flash temperature) and the comparatively modest knowledge about temperature-dependent synovial fluid behavior. On the other hand, neglecting shear-thinning fluid characteristics or transient squeeze effects resulted in a significant overestimation of the fluid formation. Additionally, the consideration of the real geometry, which featured a radius varying over the FE angle, proved to be decisive for a realistic estimation of the pressure and lubricant gap height. In this respect, the model introduced significantly stands out from the studies published in the literature to date. Furthermore, the finite height of the tibial plateau showed only a subordinate role for the CoCrMo/PMMA pairing. However, as indicated by Su et al. [35], this could be more relevant for a CoCrMo/UHMWPE pairing due to the lower elastic modulus and induced larger deformation and stronger flattening of the contacting area.

4.3. Influences due to material and synovial fluid properties

In principle, similar fluid film formation mechanisms could be observed for both material pairings, which also supported the relevance

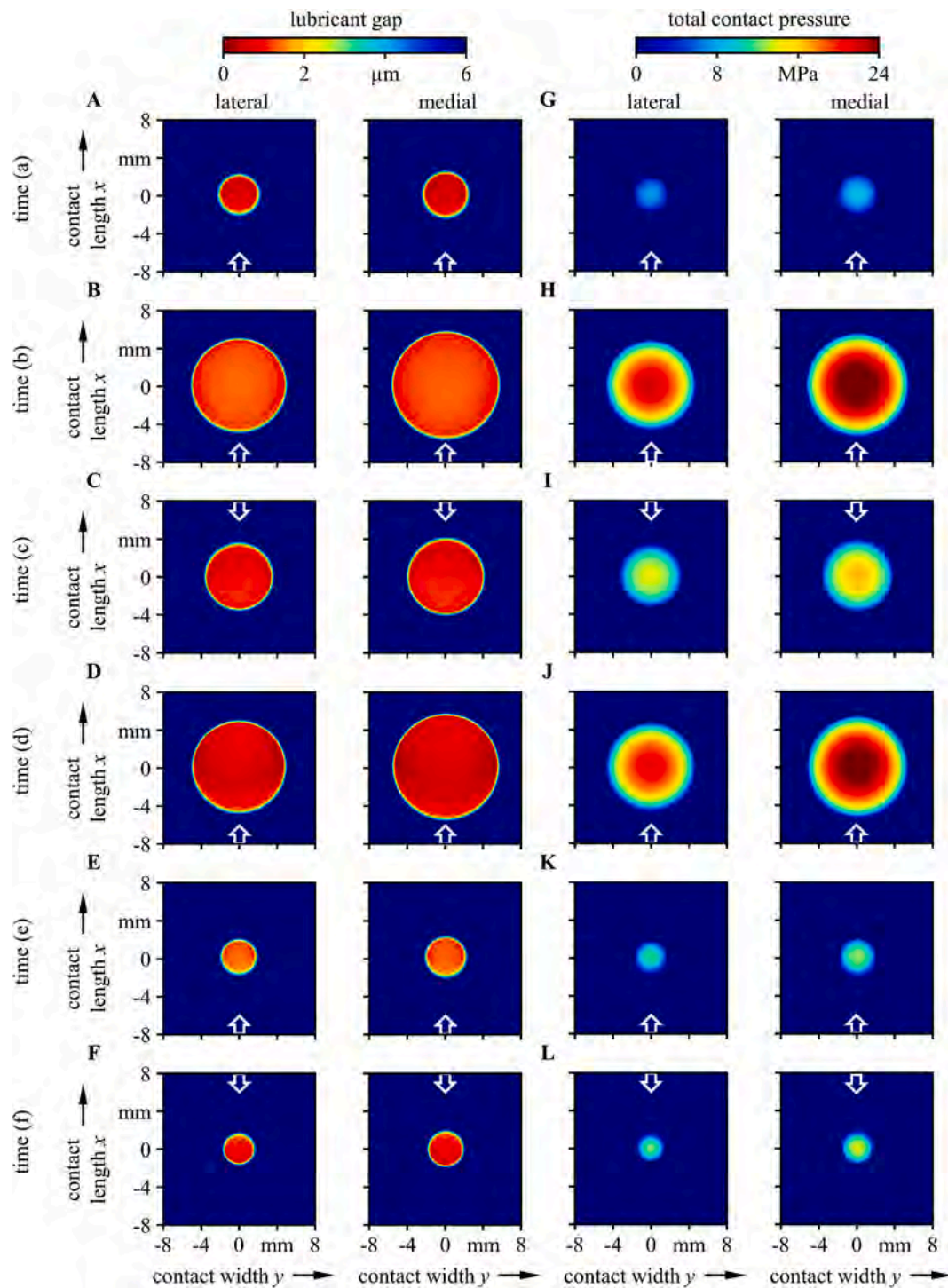


Fig. 8. (A–F) Simulated lubricant gap and (G–L) total pressure distribution for the lateral and medial compartment of the CoCrMo/UHMWPE-pairing and artificial synovial fluid lubrication at time steps (a) to (f). Scales are selected to properly visualize relevant effects, actually extrema are partially not mapped. The white arrows indicated the direction of lubricant drawing into the contact.

and validity of the experimental approach from Part I [40]. Finally, it could be shown that the fluid formation was largely influenced by the description of rheological properties and their dependence on the shear-rate. In addition, pressure and temperature induced effects are expected to play a role. Yet, these characteristics highly depend on the respective synovial fluid constituents [40] and vary greatly between different patients up to several orders of magnitude [48]. This implies that the individual tribological performance of TKA is largely affected by the fluid behavior and thus also strongly by the load and kinematics.

Therefore, a deeper understanding and more advanced analytical/numerical description of synovial fluid characteristics are crucial. Furthermore, similar to what has already been approached for total hip replacements [64], feeding the soft-EHL simulation of the TKA with preceding musculoskeletal biomechanical simulations might allow the consideration of more realistic load and motion spectra compared to the ISO [65,66]. Precise numerical modeling might finally allow the prediction of wear, the tailored design of optimized TKA macro-geometries or surface modifications, such as micro-textures or tribologically

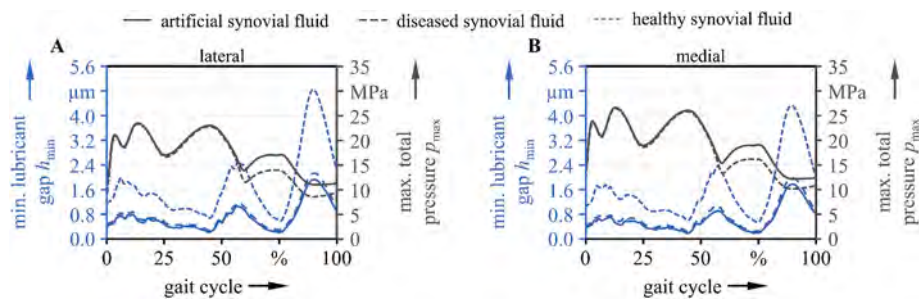


Fig. 9. Minimum lubricant gap and maximum pressure over one gait cycle (CoCrMo/UHMWPE pairing) in the (A) lateral and (B) medial compartment for different synovial fluid properties.

effective coatings.

4.4. Applicability and limitations

As is common and mandatory for numerical modeling, some assumptions and simplifications were made for the scope of this contribution. With regard to the mechanical properties of PMMA and UHMWPE, linear elastic material properties were considered. While this probably still adequately displayed the behavior of the former due to lower elastic deformations, the latter might be more accurately described by hyperelastic material characteristics [67]. Besides, although potential solid asperity contact was considered, the influence of the surface topography on the micro-hydrodynamics was neglected in the present study since the roughness was assumed to be isotropic. Basically, this could be incorporated either in a deterministic way or stochastically by flow-factors [68]. Although the viscosity of synovial fluid varies greatly from patient to patient, artificial model fluids used for in vitro testing of TKAs may be even thinner than assumed in this paper [48]. This was chosen in particular to ensure full film lubrication and to fit to the investigations in Part I [40]. However, even stronger mixed lubrication conditions may occur, which increases the relevance of surface topography and solid asperity contact. Further, IE rotation was fixed to match with the experimental setup in Part I [40] and because it is expected to have a subordinate impact on the qualitative character of film formation. However, this could be taken into account by an extended description of the kinematics with velocity components in x - and y -direction [18]. The investigation of the aforementioned influencing factors (hyperelastic material behavior, micro-hydrodynamics, IE rotation) on the tribological behavior of TKAs is subject of ongoing research. On top of that, the Reynolds differential equation applied to describe the fluid's hydrodynamics is subject to certain presumptions [69]. While these are generally met for the femur/tibial-contact in TKAs and mineral oil lubrication to a large extent, which was also substantiated by the experimental validation, certain discrepancies may occur due to a somewhat inhomogeneous composition of the synovial fluid. This again underlines the essential role of an adequate description of its rheological properties and emphasizes the need for further in-depth research.

5. Conclusions

The present study evaluated fluid film formation in TKAs. Numerical modeling was realized by means of FEM and fully coupling the lubricant's hydrodynamics represented by the generalized Reynolds equation with the elastic deformation of the rubbing surfaces while the energy equations were coupled within an iterative procedure. Thereby, realistic transient kinematics and loading conditions of the gait cycle were considered. Initially, the numerical prediction was experimentally validated for mineral oil lubrication by means of knee simulator and optical fluorescent measurement technique presented in Part I [40]. Further simulations were carried out to study the influence of the

modeling strategy and the role of synovial fluid properties on the film formation process. For the numerical studies conducted within the scope of this contribution, the main findings are summarized as follows:

- A unique approach to experimentally and numerically investigate the fluid film formation in TKAs was demonstrated. It appeared that the behavior can be adequately predicted by the simulation building upon commercial multiphysics FEM software solvers. In the future, it is estimated that this might stimulate and accelerate research in the field of synovial joint tribology, shifting the focus from numerics even more to physical modeling.
- The complexity of numerical modeling has a decisive effect on simulation results and thus on the prediction quality, especially for the fluid film height. Transient squeeze effects and shear-thinning fluid characteristics as well as realistic geometries, transient kinematics and loading conditions are vital.
- Comparing both condyles, the medial compartment was more heavily stressed and experienced higher pressures, smaller minimum film heights as well as higher probability for solid asperity contact. The overall lubricant gap was smaller in the stance phase, where load and geometry played a dominant role, whereas the swing phase was determined by geometry and kinematics. Generally, the fluid film formation was largely affected by reversal points of motion with zero entrainment speed, whereby the collapse of the lubrication film could be prevented by transient squeeze effects. Thus, it could be estimated that especially in the medial condyle, the stance phase and the turning points promote wear and are crucial for the TKA service life.
- Besides kinematics and loading, the individual rheological synovial fluid parameters have a decisive influence on the lubricant film formation. Due to the wide variation between different patients, this can also lead to diverse tribological behavior ranging from full separation of the rubbing surfaces over the whole gait cycle to strong solid asperity contact and associated wear mechanisms. In the future, such considerations on individual implant stresses might be included in TKA design and wear-protecting actions.

Authors contributions

M. Marian, B. Rothammer and D. Nečas conceived the idea. M. Marian and C. Orgeldinger designed, performed and analyzed the numerical studies. All authors provided suggestions for the final discussions. M. Marian, C. Orgeldinger, B. Rothammer and D. Nečas wrote the original draft of the manuscript. All authors have reviewed, edited and read the manuscript as well as approved the final version.

Declaration of competing interest

The authors declare that they have no known competing financial interests or personal relationships that could have appeared to influence the work reported in this paper.

Acknowledgements

M. Marian, B. Rothhammer, S. Tremmel and S. Wartzack greatly acknowledge the continuous support of Friedrich-Alexander-Universität Erlangen-Nürnberg (FAU), Germany. D. Nečas, M. Vrbka, I. Krupka and M. Hartl thank the Ministry of Education, Youth and Sports of the Czech Republic for the financial support (LTAUSA17150). The authors thank to T. Sýkora who was involved in experimental study.

References

- Seidlitz C, Kip M. Einführung in das Indikationsgebiet und Verfahren. In: Bleß H-H, Kip M, editors. *Weißbuch Gelenkersatz: Versorgungssituation bei endoprothetischen Hüft- und Knieoperationen in Deutschland*. Berlin, Heidelberg: Springer; 2017. p. 1–15.
- Flören M, Reichel H. *Implantate*. In: *Wirtz DC, editor. AE-Manual der Endoprothetik*. Heidelberg, Dordrecht, London, New York, NY: Springer; 2011. p. 57–71.
- Myant C, Underwood R, Fan J, Cann PM. Lubrication of metal-on-metal hip joints: the effect of protein content and load on film formation and wear. *J Mech Behav Biomed Mater* 2012;6:30–40. <https://doi.org/10.1016/j.jmbbm.2011.09.008>.
- Nečas D, Sadecká K, Vrbka M, Gallo J, Galandáková A, Krupka I, et al. Observation of lubrication mechanisms in knee replacement: a pilot study. *Biotribology* 2019; 17:1–7. <https://doi.org/10.1016/j.biotri.2019.02.001>.
- Nečas D, Sadecká K, Vrbka M, Galandáková A, Wimmer MA, Gallo J, et al. The effect of albumin and γ -globulin on synovial fluid lubrication: implication for knee joint replacements. *J Mech Behav Biomed Mater* 2020;113:104117. <https://doi.org/10.1016/j.jmbbm.2020.104117>.
- O'Brien ST, Luo Y, Brandt J-M. In-vitro and in-silico investigations on the influence of contact pressure on cross-linked polyethylene wear in total knee replacements. *Wear* 2015;332–333:687–93. <https://doi.org/10.1016/j.wear.2015.02.048>.
- Jin ZM, Zheng J, Li W, Zhou ZR. Tribology of medical devices. *Biosurface Biotribol* 2016;2(4):173–92. <https://doi.org/10.1016/j.bsbt.2016.12.001>.
- Penrose JMT, Holt GM, Beaugonin M, Hosi DR. Development of an accurate three-dimensional finite element knee model. *Comput Methods Biomech Biomed Eng* 2002;5(4):291–300. <https://doi.org/10.1080/1025584021000009724>.
- Donahue TLH, Hull ML, Rashid MM, Jacobs CR. A finite element model of the human knee joint for the study of tibio-femoral contact. *J Biomech Eng* 2002;124(3):273–80. <https://doi.org/10.1115/1.1470171>.
- O'Brien ST. *Computational wear simulations in total knee replacements with consideration for energy dissipation and colloid-mediated boundary lubrication* [PhD thesis]. Winnipeg, Canada: University of Manitoba; 2015.
- Fregly BJ, Sawyer WG, Harman MK, Banks SA. Computational wear prediction of a total knee replacement from in vivo kinematics. *J Biomech* 2005;38(2):305–14. <https://doi.org/10.1016/j.jbiomech.2004.02.013>.
- Auger DD, Dowson D, Fisher J. Cushion form bearings for total knee joint replacement. Part 2: wear and durability. *Proc Inst Mech Eng H* 1995;209(2): 83–91. https://doi.org/10.1243/PIME_PROC_1995_209_324_02.
- Auger DD, Dowson D, Fisher J. Cushion form bearings for total knee joint replacement. Part 1: design, friction and lubrication. *Proc Inst Mech Eng H* 1995; 209(2):73–81. https://doi.org/10.1243/PIME_PROC_1995_209_323_02.
- Murakami T, Ohtsuki N. Paper XII(iii) Lubricating film formation in knee prostheses under walking conditions. In: Dowson D, editor. *Fluid film lubrication—Osborne Reynolds centenary: proceedings of the 13th Leeds-Lyon symposium on tribology*, held in Bodington Hall. England: the University of Leeds; 1987. p. 387–92. 8–12 September 1986. Amsterdam, New York, New York, NY, U.S.A.: Elsevier for the Institute of Tribology, Leeds University and the Institut national des Sciences appliquées de Lyon; Distributors for the U.S. and Canada, Elsevier Science Pub. Co.
- Kennedy FE, van Citters DW, Wongseedakaew K, Mongkolwongrojn M. Lubrication and wear of artificial knee joint materials in a Rolling/Sliding tribotester. *J Tribol* 2007;129(2):326. <https://doi.org/10.1115/1.2464130>.
- Ziegltrum A, Lohner T, Stahl K. TEHL simulation on the influence of lubricants on the frictional losses of DLC coated gears. *Lubricants* 2018;6(1):17. <https://doi.org/10.3390/lubricants6010017>.
- Marian M, Tremmel S, Wartzack S. Microtextured surfaces in higher loaded rolling-sliding EHL line-contacts. *Tribol Int* 2018;127:420–32. <https://doi.org/10.1016/j.triboint.2018.06.024>.
- Winkler A, Marian M, Tremmel S, Wartzack S. Numerical modeling of wear in a thrust roller bearing under mixed elastohydrodynamic lubrication. *Lubricants* 2020;8(5):58. <https://doi.org/10.3390/lubricants8050058>.
- Venner CH, Lubrecht AA. *Multilevel methods in lubrication*. first ed. Amsterdam: Elsevier; 2000.
- Venner CH, Lubrecht AA. Multigrid techniques: a fast and efficient method for the numerical simulation of elastohydrodynamically lubricated point contact problems. *Proc IME J J Eng Tribol* 2000;214(1):43–62. <https://doi.org/10.1243/1350650001543007>.
- Hartinger M, Dumont M-L, Ioannides S, Gosman D, Spikes H. CFD modeling of a thermal and shear-thinning elastohydrodynamic line contact. *J Tribol* 2008;130(4):41503–4150316. <https://doi.org/10.1115/1.2958077>.
- Habchi W, Demirci I, Eyheramendy D, Morales-Espejel G, Vergne P. A finite element approach of thin film lubrication in circular EHD contacts. *Tribol Int* 2007; 40(10–12):1466–73. <https://doi.org/10.1016/j.triboint.2007.01.017>.
- Maier E, Ziegltrum A, Lohner T, Stahl K. Characterization of TEHL contacts of thermoplastic gears. *Forsch Ingenieurwes* 2017;81(2–3):317–24. <https://doi.org/10.1007/s10010-017-0230-4>.
- Nikas GK. Elastohydrodynamics and mechanics of rectangular elastomeric seals for reciprocating piston rods. *J Tribol Trans ASME* 2003;125(1):60–9. <https://doi.org/10.1115/1.1506316>.
- Duck FA. Acoustic properties of tissue at ultrasonic frequencies. In: Duck FA, editor. *Physical properties of tissue: a comprehensive reference book*. London: Academic Press; 1990. p. 73–135.
- Ruggiero A. Milestones in natural lubrication of synovial joints. *Front Mech Eng* 2020;6:657. <https://doi.org/10.3389/fmech.2020.00052>.
- Affatato S, Ruggiero A. A perspective on biotribology in arthroplasty: from in vitro toward the accurate in silico wear prediction. *Appl Sci* 2020;10(18):6312. <https://doi.org/10.3390/app10186312>.
- Lu X, Nečas D, Meng Q, Rebenda D, Vrbka M, Hartl M, et al. Towards the direct validation of computational lubrication modelling of hip replacements. *Tribol Int* 2020;146:106240. <https://doi.org/10.1016/j.triboint.2020.106240>.
- Ruggiero A, Sicilia A. Lubrication modeling and wear calculation in artificial hip joint during the gait. *Tribol Int* 2020;142:105993. <https://doi.org/10.1016/j.triboint.2019.105993>.
- Ruggiero A, Sicilia A, Affatato S. In silico total hip replacement wear testing in the framework of ISO 14242-3 accounting for mixed elasto-hydrodynamic lubrication effects. *Wear* 2020;460–461:203420. <https://doi.org/10.1016/j.wear.2020.203420>.
- Tandon PN, Jaggi S. A model for the lubrication mechanism in knee joint replacements. *Wear* 1979;52(2):275–84. [https://doi.org/10.1016/0043-1648\(79\)90068-1](https://doi.org/10.1016/0043-1648(79)90068-1).
- Jin ZM, Dowson D, Fisher J, Ohtsuki N, Murakami T, Higaki H, et al. Prediction of transient lubricating film thickness in knee prostheses with compliant layers. *Proc Inst Mech Eng H* 1998;212(3):157–64. <https://doi.org/10.1243/0954411981533935>.
- Pascou A, Guardia B, Puertolas JA, Gómez-Barrena E. Knee model of hydrodynamic lubrication during the gait cycle and the influence of prosthetic joint conformity. *J Orthop Sci* 2009;14(1):68–75. <https://doi.org/10.1007/s00776-008-1287-6>.
- Mongkolwongrojn M, Wongseedakaew K, Kennedy FE. Transient elastohydrodynamic lubrication in artificial knee joint with non-Newtonian fluids. *Tribol Int* 2010;43(5–6):1017–26. <https://doi.org/10.1016/j.triboint.2009.12.041>.
- Su Y, Fu Z, Yang P, Wang C. A full numerical analysis of elastohydrodynamically lubrication in knee prosthesis under walking condition. *J Mech Med Biol* 2010;10: 621–41. <https://doi.org/10.1142/S0219519410003605>. 04.
- Gao L, Dowson D, Hewson RW. Predictive wear modeling of the articulating metal-on-metal hip replacements. *J Biomed Mater Res B Appl Biomater* 2017;105(3): 497–506. <https://doi.org/10.1002/jbm.b.33568>.
- Gao L, Hua Z, Hewson R, Andersen MS, Jin Z. Elastohydrodynamic lubrication and wear modelling of the knee joint replacements with surface topography. *Biosurface Biotribol* 2018;4(1):18–23. <https://doi.org/10.1049/bsbt.2017.0003>.
- Gao L, Wang F, Yang P, Jin Z. Effect of 3D physiological loading and motion on elastohydrodynamic lubrication of metal-on-metal total hip replacements. *Med Eng Phys* 2009;31(6):720–9. <https://doi.org/10.1016/j.medengphys.2009.02.002>.
- Gao L, Dowson D, Hewson RW. A numerical study of non-Newtonian transient elastohydrodynamic lubrication of metal-on-metal hip prostheses. *Tribol Int* 2016; 93:486–94. <https://doi.org/10.1016/j.triboint.2015.03.003>.
- Nečas D, Vrbka M, Marian M, Rothhammer B, Tremmel S, Wartzack S, et al. Towards the understanding of lubrication mechanisms in total knee replacements – Part I: experimental investigation. *Tribol Int* 2021;106874. <https://doi.org/10.1016/j.triboint.2021.106874>.
- Habchi W, Eyheramendy D, Vergne P, Morales-Espejel G. A full-system Approach of the elastohydrodynamic line/point contact problem. *J Tribol* 2008;130(2). <https://doi.org/10.1115/1.2842246>. 021501/1-9.
- Martelli S, Pinksheva V, Visani A. Anatomical investigations on the knee by means of computer-dissection. *J Mech Med Biol* 2006;55–73. <https://doi.org/10.1142/S0219519406001820>. 06(01).
- Iso 14243-3:2014-11. Implants for surgery - wear of total knee-joint prostheses - Part 3: loading and displacement parameters for wear-testing machines with displacement control and corresponding environmental conditions for test.
- Iso 14243-1:2009-11. Implants for surgery - wear of total knee-joint prostheses - Part 1: loading and displacement parameters for wear-testing machines with load control and corresponding environmental conditions for test.
- Dowson D, Higginson GR. A numerical solution to the elasto-hydrodynamic problem. *J Mech Eng Sci* 1959;1(1):6–15. https://doi.org/10.1243/JMES_JOUR_1959_001_004_02.
- Sadeghi F, Sui PC. Thermal elastohydrodynamic lubrication of rolling/sliding contacts. *J Tribol* 1990;112(2):189–95. <https://doi.org/10.1115/1.2920241>.
- Bair S. *High-pressure rheology for quantitative elastohydrodynamics*. first ed. Amsterdam: Elsevier; 2007.
- Mazzucco D, McKinley G, Scott RD, Spector M. Rheology of joint fluid in total knee arthroplasty patients. *J Orthop Res* 2002;20(6):1157–63. [https://doi.org/10.1016/S0736-0266\(02\)00050-5](https://doi.org/10.1016/S0736-0266(02)00050-5).
- Cross MM. Rheology of non-Newtonian fluids: a new flow equation for pseudoplastic systems. *J Colloid Sci* 1965;20(5):417–37. [https://doi.org/10.1016/0095-8522\(65\)90022-X](https://doi.org/10.1016/0095-8522(65)90022-X).
- Moghadam MN, Abdel-Sayed P, Camine VM, Pioletti DP. Impact of synovial fluid flow on temperature regulation in knee cartilage. *J Biomech* 2015;48(2):370–4. <https://doi.org/10.1016/j.jbiomech.2014.11.008>.
- Yang P, Wen S. A generalized Reynolds equation for non-Newtonian thermal elastohydrodynamic lubrication. *J Tribol* 1990;112(4):631–6.

- [52] Reynolds O. On the theory of lubrication and its application to Mr. Beauchamp tower's experiments, including an experimental determination of the viscosity of olive oil. *Phil Trans Roy Soc Lond* 1886;177:157–234.
- [53] Marian M, Weschta M, Tremmel S, Wartzack S. Simulation of microtextured surfaces in starved EHL contacts using commercial FE software. *Matls. Perf. Charact.* 2017;6(2):165–81. <https://doi.org/10.1520/MPC20160010>.
- [54] Bartel D. *Simulation von Tribosystemen: Grundlagen und Anwendungen*. first ed. Wiesbaden: Vieweg+Teubner; 2010.
- [55] Masjedi M, Khonsari MM. Mixed lubrication of soft contacts: an engineering look. *Proc IMechE* 2017;231(2):263–73. <https://doi.org/10.1177/1350650116652286>.
- [56] Raisin J, Fillot N, Vergne P, Dureisseix D, Lacour V. Transient thermal elastohydrodynamic modeling of cam–follower systems: understanding performance. *Tribol Trans* 2016;59(4):720–32. <https://doi.org/10.1080/10402004.2015.1110865>.
- [57] Raisin J, Fillot N, Dureisseix D, Vergne P, Lacour V. Characteristic times in transient thermal elastohydrodynamic line contacts. *Tribol Int* 2015;82:472–83. <https://doi.org/10.1016/j.triboint.2014.02.022>.
- [58] Habchi W. *Finite element modeling of elastohydrodynamic lubrication problems*. Newark: John Wiley & Sons Incorporated; 2018.
- [59] Zienkiewicz OC, Taylor RL, Nithiarasu P. *The finite element method for fluid dynamics*. seventh ed. Oxford: Elsevier Butterworth-Heinemann; 2014.
- [60] Yang P, Wen S. The behavior of non-Newtonian thermal EHL film in line contacts at dynamic loads. *J Tribol* 1992;114(1):81. <https://doi.org/10.1115/1.2920872>.
- [61] Tan X, Goodyer CE, Jimack PK, Taylor RI, Walkley MA. Computational approaches for modelling elastohydrodynamic lubrication using multiphysics software. *Proc IME J J Eng Tribol* 2012;226(6):463–80. <https://doi.org/10.1177/1350650111428028>.
- [62] Lohner T, Ziegler A, Stemplinger J-P, Stahl K. Engineering software solution for thermal elastohydrodynamic lubrication using multiphysics software. *Adv Tribol* 2016;2016(2):1–13. <https://doi.org/10.1155/2016/6507203>.
- [63] Hamrock BJ, Schmid SR, Jacobson BO. *Fundamentals of fluid film lubrication*. second ed. New York: Dekker; 2004.
- [64] Ruggiero A, Merola M, Affatato S. Finite element simulations of hard-on-soft hip joint prosthesis accounting for dynamic loads calculated from a musculoskeletal model during walking. *Materials* 2018;11(4). <https://doi.org/10.3390/ma11040574>.
- [65] Affatato S, Ruggiero A. A critical analysis of TKR in vitro wear tests considering predicted knee joint loads. *Materials* 2019;12(10). <https://doi.org/10.3390/ma12101597>.
- [66] Zhang J, Chen Z, Wang L, Li D, Jin Z. A patient-specific wear prediction framework for an artificial knee joint with coupled musculoskeletal multibody-dynamics and finite element analysis. *Tribol Int* 2017;109:382–9. <https://doi.org/10.1016/j.triboint.2016.10.050>.
- [67] Kurtz SM. *UHMWPE biomaterials handbook: ultra high molecular weight polyethylene in total joint replacement and medical devices*. second ed. Amsterdam, Boston: Elsevier/Academic Press; 2009.
- [68] Patir N, Cheng HS. An average flow model for determining effects of three-dimensional roughness on partial hydrodynamic lubrication. *J Lubr Technol* 1978; 100(1):12–7. <https://doi.org/10.1115/1.3453103>.
- [69] Gohar R. *Elastohydrodynamics*. Chichester, New York [etc.]: E. Horwood; Halsted Press; op; 1988.

Nomenclature

a_c : Carreau parameter
 b_{Hertz} : Hertzian contact width
 $c_{p,i}$: specific heat capacity
 C : compliance matrix
 C_T : correction for transient load
 C_R : correction for transient radius
 C_v : correction for transient velocity
 d_{AP} : AP motion
 E_i : Young's modulus
 F : normal load
 G_c : critical shear stress
 h : lubricant gap
 h_0 : rigid body motion
 h_{cub} : tibial plateau height
 H_c : specific film thickness
 n_c : Carreau parameter
 p : hydrodynamic pressure
 p_c : asperity contact pressure
 p_{Hertz} : Hertzian contact pressure
 p_t : total contact pressure
 p_i : intracapsular pressure
 R_i : component's radius
 t : time
 U : displacement vector
 u_i : component's velocity
 u_{η_i} : entrainment velocity
 x, y, z : space coordinates
 α_c : Cross parameter
 α_p : pressure coefficient
 β_c : Cross parameter
 β_{η} : Roelands coefficient
 δ : elastic deformation
 ε : strain tensor
 η : viscosity
 η_0 : base viscosity
 η_{∞} : limiting shear stress
 θ : fractional film content
 θ_i : temperature
 λ_i : thermal conductivity
 ρ_0 : base density
 ρ_i : density
 σ : stress tensor
 ν : Poisson's ratio
 ϕ_{FE} : FE angle
 ω : angular velocity
 Ω : computational domain

CONCLUSIONS AND IMPLICATIONS FOR FURTHER RESEARCH

Total arthroplasty of the hip and knee joints represents the most effective way of returning patients suffering from severe OA and joint injuries to everyday life. It is evident that the numbers of THRs and TKRs have been continuously increasing while rapid growth is expected by 2050. Although the quality of the implants has been remarkably improved over the last decades, limited service life is considered as a persisting challenge. Furthermore, it needs to be assumed that even younger patients are indicated for THA or TKA. Thus, implant longevity is a crucial parameter. Since most reported failures are associated with wear-related issues, a detailed understanding of the tribological processes in artificial joints is essential.

Previously, most of the investigations dealt with the evaluation of the cumulative wear rate of real implant couples. However, such testing is both time- and cost-consuming. Moreover, it is noted that wear is just a consequence. The performance of the implant is driven by lubrication and associated friction processes. Two different approaches based on experimental measurements and computational modelling may be adopted to understand these processes better. Apparently, both ways have some advantages and disadvantages. While experimental investigations usually require some simplifications in terms of material, geometry, associated conformity, or kinematics and load, numerical modelling may hardly capture the realistic rheological behaviour of biological lubricants and does not allow for simulation of the adsorption effect. Therefore, it is doubtlessly worth to combine both approaches.

The habilitation thesis provides an insight into three related areas. Specifically, the friction of the joint replacements, lubrication of THRs, and lubrication of TKRs are discussed. The primary attention is paid to the detailed introduction of the current state of the art, highlighting the main findings and some limitations of the previous studies. At the end of each chapter, the author's contribution to the field is demonstrated through the respective journal papers. In total, twelve papers are presented in the thesis. All of them were published in peer-reviewed journals. Ten of the documents were issued in journals with IF (WoS database), and the rest two papers were published in journals with CiteScore (Scopus database).

Several previous papers employed the simplified pin-on-disc (-plate) and ball-on-disc (-plate) geometrical configurations when focusing on experimental investigations of the friction. Such an approach may indisputably contribute when understanding the fundamentals. However, less attention was focused to the interactions of SF constituents before, while some studies applied non-biological lubricants or simple protein solutions. Therefore, the author of the thesis published

two papers, while the first was focused on the effect of dominant proteins on the adsorbed film thickness and structure of the adsorbed layer. The second study aimed at the understanding of the protein interactions under a variety of experimental conditions, considering different model fluid compositions. Another group of analyses employs joint simulators allowing for studying real implant couples. Besides, the potential contribution of surface texturing on frictional behaviour has been underlined in recent years. Therefore, the author carried out the study focused on the effect of acetabular cup surface texturing on the friction coefficient when articulating with femoral heads of various materials. For this purpose, a pendulum hip joint simulator was used, allowing for the determination of friction based on the pendulum damping characteristic.

The chapter focused on the lubrication of hip replacements introduces numerical and experimental studies published within the last decades. While the computations provide quick initial information about the development of film thickness within the contact over the cycle, the neglecting of realistic rheology of biological fluids or even the full absence of lubricant is considered a substantial drawback. In contrast, most of the recent experimental investigations failed to mimic realistic surface conformity, which is indicated as one of the crucial parameters. Therefore, the author of the thesis published five papers in the field, considering the real compliance of rubbing surfaces in the ball-in-socket configuration using the pendulum simulator. Glass acetabular cup combined with metal and ceramic heads mimicked the behaviour of hard-on-hard bearing pairs. The effect of head material, nominal diameter, diametric clearance, and model SF composition could be assessed through film thickness measured using optical interferometry. Besides, the glass cup was replaced by the cup made from PMMA to mimic hard-on-soft pairs, enabling to describe the role of specific SF constituents using the fluorescent microscopy method. The last published paper is based on the direct comparison of the experimental and numerical data, introducing a novel velocity-viscosity relation, bringing perfect compliance of both approaches.

In contrast to THRs, only a low number of studies dealing with the lubrication of TKRs may be found. The main reason is in the complicated geometry. Concerning the numerical models, a simplified ellipsoid-on-flat model is usually adopted. However, each of the presented papers suffers from neglecting some parameters that may substantially impact film formation. Even fewer studies dealing with experimental evaluation were introduced. Thus, the author published four articles in the field. Three of the documents deal with direct in situ observation using a newly developed knee simulator, enabling to investigate the real geometry of TKR. The tibial insert sample was made from transparent polymer to mimic UHMWPE behaviour and allow in-contact observation. The investigations focused on describing the role of constituents, transient kinematic and loading conditions, and the performance of individual compartments. A theoretical model of the lubricating layer in TKR was proposed based on the gained knowledge. The last paper is aimed at the development of the predictive numerical model. All the essential factors, including non-Newtonian fluid nature, implant geometry, thermal effects, or respective lubrication mechanisms, are involved. Furthermore, the model is built upon the commercial FEM software, enabling fast implementation and easy modification of the inputs. As a result, the film thickness together with the pressure distribution throughout the cycle is provided.

The author of the habilitation thesis is particularly interested in experimental investigations of friction and lubrication mechanisms in THRs and TKRs. Thanks to cooperation with foreign research institutions, the author was also involved in the studies based on computational modelling. The combination of both approaches seems to be the best possible way to further develop artificial joints towards unlimited durability. The aim of the author is to continue with further improvement of experimental and numerical investigations in future. Specific attention will be paid to the suggested ways such as surface texturing or application of coatings. The author is also involved in the research focused on developing artificial cartilage to prevent the need for joint replacement. To conclude, biotribology of joint cartilage, natural and artificial joints offers a broad field of investigations. Moreover, research in this area is essential to help patients suffering from joint diseases and save substantial costs associated with medical treatment and surgeries.

REFERENCES

- [1] Tuan, R.S., Chen, A.F., Klatt, B.A., 2013. Cartilage Regeneration. *Journal of the American Academy of Orthopaedic Surgeons* 21, 303-311.
- [2] Onishi, K., Utturkar, A., Chang, E., Panush, R., Hata, J., Perret-Karimi, D., 2012. Osteoarthritis: A Critical Review. *Critical Reviews in Physical and Rehabilitation Medicine* 24, 251-264.
- [3] Bellamy, N., Campbell, J., Welch, V., Gee, T.L., Bourne, R., Wells, G.A., 2006. Viscosupplementation for the treatment of osteoarthritis of the knee. *Cochrane Database of Systematic Reviews* 19(2), CD005321.
- [4] Sayre, E.C., Li, L.C., Kopec, J.A., Esdaile, JM, Bar, S., Cibere, J., Boutron, I., 2010. The Effect of Disease Site (Knee, Hip, Hand, Foot, Lower Back or Neck) on Employment Reduction Due to Osteoarthritis. *PLoS ONE* 5(5), e10470.
- [5] OECD (2019), *Health at a Glance 2019: OECD Indicators*, OECD Publishing, Paris, <https://doi.org/10.1787/4dd50c09-en>.
- [6] Kurtz, S., Ong, K., Lau, E., Mowat, F., Halpern, M., 2007. Projections of Primary and Revision Hip and Knee Arthroplasty in the United States from 2005 to 2030. *The Journal of Bone & Joint Surgery* 89, 780-785.
- [7] Price, A.J., Alvand, A., Troelsen, A., Katz, J.N., Hooper, G., Gray, A., Carr, A., Beard, D., 2018. Knee replacement. *The Lancet* 392, 1672-1682.
- [8] Evans, J.T., Evans, J.P., Walker, R.W., Blom, A.W., Whitehouse, M.R., Sayers, A., 2019. How long does a hip replacement last? A systematic review and meta-analysis of case series and national registry reports with more than 15 years of follow-up. *The Lancet* 393, 647-654.
- [9] Cook, R., Davidson, P., Martin, R., 2019. More than 80% of total knee replacements can last for 25 years. *BMJ*.
- [10] Dattani, R., 2007. Femoral osteolysis following total hip replacement. *Postgraduate Medical Journal* 83, 312-316.
- [11] Gallo, J., Vaculova, J., Goodman, S.B., Konttinen, Y.T., Thyssen, J.P., 2014. Contributions of human tissue analysis to understanding the mechanisms of loosening and osteolysis in total hip replacement. *Acta Biomaterialia* 10, 2354-2366.
- [12] Gupta, S.K., Chu, A., Ranawat, A.S., Slamin, J., Ranawat, C.S., 2007. Review Article: Osteolysis After Total Knee Arthroplasty. *The Journal of Arthroplasty* 22, 787-799.

- [13] Gallo, J., Goodman, S.B., Konttinen, Y.T., Wimmer, M.A., Holinka, M., 2013. Osteolysis around total knee arthroplasty: A review of pathogenetic mechanisms. *Acta Biomaterialia* 9, 8046-8058.
- [14] Pajarinen, J., Jamsen, E., Konttinen, Y.T., Goodman, S.B., 2014. Innate Immune Reactions in Septic and Aseptic Osteolysis around Hip Implants. *Journal of Long-Term Effects of Medical Implants* 24, 283-296.
- [15] Du, Z., Zhu, Z., Wang, Y., 2018. The degree of peri-implant osteolysis induced by PEEK, CoCrMo, and HXLPE wear particles: a study based on a porous Ti6Al4V implant in a rabbit model. *Journal of Orthopaedic Surgery and Research* 13.
- [16] Ito, H., Kaneda, K., Yuhta, T., Nishimura, I., Yasuda, K., Matsuno, T., 2000. Reduction of polyethylene wear by concave dimples on the frictional surface in artificial hip joints. *The Journal of Arthroplasty* 15, 332-338.
- [17] Dowson, D., 2001. New joints for the Millennium: Wear control in total replacement hip joints. *Proceedings of the Institution of Mechanical Engineers, Part H: Journal of Engineering in Medicine* 215, 335-358.
- [18] Smith, S.L., Dowson, D., Goldsmith, A.A.J., 2001. The effect of femoral head diameter upon lubrication and wear of metal-on-metal total hip replacements. *Proceedings of the Institution of Mechanical Engineers, Part H: Journal of Engineering in Medicine* 215, 161-170.
- [19] Wang, A., Essner, A., Schmidig, G., 2004. The effects of lubricant composition on in vitro wear testing of polymeric acetabular components. *Journal of Biomedical Materials Research* 68B, 45-52.
- [20] Goldsmith, A.A.J., Dowson, D., Isaac, G.H., Lancaster, J.G., 2006. A comparative joint simulator study of the wear of metal-on-metal and alternative material combinations in hip replacements. *Proceedings of the Institution of Mechanical Engineers, Part H: Journal of Engineering in Medicine* 214, 39-47.
- [21] Knight, L.A., Pal, S., Coleman, J.C., Bronson, F., Haider, H., Levine, D.L., Taylor, M., Rullkoetter, P.J., 2007. Comparison of long-term numerical and experimental total knee replacement wear during simulated gait loading. *Journal of Biomechanics* 40, 1550-1558.
- [22] López-López, J.A., Humphriss, R.L., Beswick, A.D., Thom, H.H.Z., Hunt, L.P., Burston, A., Fawsitt, C.G., Hollingworth, W., Higgins, J.P.T., Welton, N.J., Blom, A.W., Marques, E.M.R., 2017. Choice of implant combinations in total hip replacement: systematic review and network meta-analysis. *BMJ* 359, j4651.
- [23] Robinson, P.G., Clement, N.D., Hamilton, D., Blyth, M.J.G., Haddad, F.S., Patton, J.T., 2019. A systematic review of robotic-assisted unicompartmental knee arthroplasty. *The Bone & Joint Journal* 101-B, 838-847.
- [24] Heisel, C., Silva, M., Schmalzried, T.P., 2003. Bearing surface options for total hip replacement in young patients. *The Journal of Bone and Joint Surgery-American Volume* 85, 1366-1379.
- [25] Brockett, C.L., Harper, P., Williams, S., Isaac, G.H., Dwyer-Joyce, R.S., Jin, Z., Fisher, J., 2008. The influence of clearance on friction, lubrication and squeaking in large diameter

- metal-on-metal hip replacements. *Journal of Materials Science: Materials in Medicine* 19, 1575-1579.
- [26] Chevillotte, C., Trousdale, R.T., An, K.-N., Padgett, D., Wright, T., 2012. Retrieval analysis of squeaking ceramic implants: Are there related specific features? *Orthopaedics & Traumatology: Surgery & Research* 98, 281-287.
- [27] Wu, G.-L., Zhu, W., Zhao, Y., Ma, Q., Weng, X.-S., 2016. Hip Squeaking after Ceramic-on-ceramic Total Hip Arthroplasty. *Chinese Medical Journal* 129, 1861-1866.
- [28] Damm, P., Dymke, J., Ackermann, R., Bender, A., Graichen, F., Halder, A., Beier, A., Bergmann, G., Zadpoor, A.A., 2013. Friction in Total Hip Joint Prosthesis Measured In Vivo during Walking. *PLoS ONE* 8.
- [29] Damm, P., Bender, A., Bergmann, G., Mukherjee, A., 2015. Postoperative Changes in In Vivo Measured Friction in Total Hip Joint Prosthesis during Walking. *PLOS ONE* 10.
- [30] Galandáková, A., Ulrichová, J., Langová, K., Hanáková, A., Vrbka, M., Hartl, M., Gallo, J., 2017. Characteristics of synovial fluid required for optimisation of lubrication fluid for biotribological experiments. *Journal of Biomedical Materials Research Part B: Applied Biomaterials* 105, 1422-1431.
- [31] ISO 14242-1: Implants for surgery - wear of total hip prostheses - Part 1: Loading and displacement parameters for wear-testing machines and corresponding environmental conditions for tests.
- [32] ISO 14243-1: Implants for surgery — wear of total knee-joint prostheses — Part 1: Loading and displacement parameters for wear-testing machines with load control and corresponding environmental conditions for test.
- [33] Sawae, Y., Murakami, T., Chen, J., 1998. Effect of synovia constituents on friction and wear of ultra-high molecular weight polyethylene sliding against prosthetic joint materials. *Wear* 216, 213-219.
- [34] Yao, J.Q., Laurent, M.P., Johnson, T.S., Blanchard, C.R., Crowninshield, R.D., 2003. The influences of lubricant and material on polymer/CoCr sliding friction. *Wear* 255, 780-784.
- [35] Widmer, M.R., Heuberger, M., Vörös, J., Spencer, N.D., 2001. Influence of polymer surface chemistry on frictional properties under protein-lubrication conditions: implications for hip-implant design. *Tribology Letters* 10, 111-116.
- [36] Heuberger, M.P., Widmer, M.R., Zobeley, E., Glockshuber, R., Spencer, N.D., 2005. Protein-mediated boundary lubrication in arthroplasty. *Biomaterials* 26, 1165-1173.
- [37] Yang, C.-B., Fang, H.-W., Liu, H.-L., Chang, C.-H., Hsieh, M.-C., Lee, W.-M., Huang, H.-T., 2006. Frictional characteristics of the tribological unfolding albumin for polyethylene and cartilage. *Chemical Physics Letters* 431, 380-384.
- [38] Gispert, M.P., Serro, A.P., Colaço, R., Saramago, B., 2006. Friction and wear mechanisms in hip prosthesis: Comparison of joint materials behaviour in several lubricants. *Wear* 260, 149-158.
- [39] Serro, A.P., Gispert, M.P., Martins, M.C.L., Brogueira, P., Colaço, R., Saramago, B., 2006. Adsorption of albumin on prosthetic materials: Implication for tribological behavior. *Journal of Biomedical Materials Research Part A* 78A, 581-589.

- [40] Crockett, R., Roba, M., Naka, M., Gasser, B., Delfosse, D., Frauchiger, V., Spencer, N.D., 2007. Friction, lubrication, and polymer transfer between UHMWPE and CoCrMo hip-implant materials: A fluorescence microscopy study. *Journal of Biomedical Materials Research Part A* 89A, 1011-1018.
- [41] Mishina, H., Kojima, M., 2008. Changes in human serum albumin on arthroplasty frictional surfaces. *Wear* 265, 655-663.
- [42] Chen, X.M., Jin, Z.M., Fisher, J., 2008. Effect of albumin adsorption on friction between artificial joint materials. *Proceedings of the Institution of Mechanical Engineers, Part J: Journal of Engineering Tribology* 222, 513-521.
- [43] Kanaga Karuppiah, K.S., Bruck, A.L., Sundararajan, S., Wang, J., Lin, Z., Xu, Z.-H., Li, X., 2008. Friction and wear behavior of ultra-high molecular weight polyethylene as a function of polymer crystallinity. *Acta Biomaterialia* 4, 1401-1410.
- [44] Mavraki, A., Cann, P.M., 2009. Friction and lubricant film thickness measurements on simulated synovial fluids. *Proceedings of the Institution of Mechanical Engineers, Part J: Journal of Engineering Tribology* 223, 325-335.
- [45] Duong, C.-T., Lee, J.-H., Cho, Y., Nam, J.-S., Kim, H.-N., Lee, S.-S., Park, S., 2012. Effect of protein concentrations of bovine serum albumin and γ -globulin on the frictional response of a cobalt-chromium femoral head. *Journal of Materials Science: Materials in Medicine* 23, 1323-1330.
- [46] Kobayashi, M., Koide, T., Hyon, S.-H., 2014. Tribological characteristics of polyethylene glycol (PEG) as a lubricant for wear resistance of ultra-high-molecular-weight polyethylene (UHMWPE) in artificial knee joint. *Journal of the Mechanical Behavior of Biomedical Materials* 38, 33-38.
- [47] Guezmil, M., Bensalah, W., Mezlini, S., 2016. Effect of bio-lubrication on the tribological behavior of UHMWPE against M30NW stainless steel. *Tribology International* 94, 550-559.
- [48] Guezmil, M., Bensalah, W., Mezlini, S., 2016. Tribological behavior of UHMWPE against TiAl6V4 and CoCr28Mo alloys under dry and lubricated conditions. *Journal of the Mechanical Behavior of Biomedical Materials* 63, 375-385.
- [49] Hall, R.M., Unsworth, A., Wroblewski, B.M., Burgess, I.C., 1994. Frictional characterisation of explanted Charnley hip prostheses. *Wear* 175, 159-166.
- [50] Scholes, S.C., Unsworth, A., Hall, R.M., Scott, R., 2000. The effects of material combination and lubricant on the friction of total hip prostheses. *Wear* 241, 209-213.
- [51] Scholes, S.C., Unsworth, A., 2000. Comparison of friction and lubrication of different hip prostheses. *Proceedings of the Institution of Mechanical Engineers, Part H: Journal of Engineering in Medicine* 214, 49-57.
- [52] Scholes, S.C., Unsworth, A., Goldsmith, A.A.J., 2000. A frictional study of total hip joint replacements. *Physics in Medicine and Biology* 45, 3721-3735.
- [53] Ash, H.E., Scholes, S.C., Unsworth, A., Jones, E., 2004. The effect of bone cement particles on the friction of polyethylene and polyurethane knee bearings. *Physics in Medicine and Biology* 49, 3413-3425.

- [54] Scholes, S.C., Unsworth, A., Blamey, J.M., Burges, I.C., Jones, E., Smith, N., 2005. Design aspects of compliant, soft layer bearings for an experimental hip prosthesis. *Proceedings of the Institution of Mechanical Engineers, Part H: Journal of Engineering in Medicine* 219, 79-87.
- [55] Smith, S.L., Ash, H.E., Unsworth, A., 2000. A tribological study of UHMWPE acetabular cups and polyurethane compliant layer acetabular cups. *Journal of Biomedical Materials Research* 53, 710-716.
- [56] Scholes, S.C., Unsworth, A., 2006. The Effects of Proteins on the Friction and Lubrication of Artificial Joints. *Proceedings of the Institution of Mechanical Engineers, Part H: Journal of Engineering in Medicine* 220, 687-693.
- [57] Scholes, S.C., Unsworth, A., Jones, E., 2007. Polyurethane unicondylar knee prostheses: simulator wear tests and lubrication studies. *Physics in Medicine and Biology* 52, 197-212.
- [58] Flannery, M., Jones, E., Birkinshaw, C., 2008. Analysis of wear and friction of total knee replacements part II: Friction and lubrication as a function of wear. *Wear* 265, 1009-1016.
- [59] Brockett, C., Williams, S., Jin, Z., Isaac, G., Fisher, J., 2007. Friction of total hip replacements with different bearings and loading conditions. *Journal of Biomedical Materials Research Part B: Applied Biomaterials* 81B, 508-515.
- [60] Bishop, N.E., Waldow, F., Morlock, M.M., 2008. Friction moments of large metal-on-metal hip joint bearings and other modern designs. *Medical Engineering & Physics* 30, 1057-1064.
- [61] Vrbka, M., Nečas, D., Bartošík, J., Hartl, M., Křupka, I., Galandáková, A., Gallo, J., 2015. *Acta chirurgiae orthopaedicae et traumatologiae Cechoslovaca* 82, 341-347.
- [62] O'Kelly, J., Unsworth, A., Dowson, D., Jobbins, B., Wright, V., 1977. Pendulum and simulator for studies of friction in hip joints. *Evaluation of artificial joints*, Edited by Dowson, D., Wright, V., Biological Engineering Society, London.
- [63] Choudhury, D., Vrbka, M., Mamat, A.B., Stavness, I., Roy, C.K., Mootanah, R., Krupka, I., 2017. The impact of surface and geometry on coefficient of friction of artificial hip joints. *Journal of the Mechanical Behavior of Biomedical Materials* 72, 192-199.
- [64] Kaddick, C., Malczan, M., Buechele, C., Hintner, M., Wimmer, M.A., 2015. On the Measurement of Three-Dimensional Taper Moments Due to Friction and Contact Load in Total Hip Replacement, in: *Modularity And Tapers In Total Joint Replacement Devices*. ASTM International, 100 Barr Harbor Drive, PO Box C700, West Conshohocken, PA 19428-2959, pp. 336-350.
- [65] Haider, H., Weisenburger, J.N., Garvin, K.L., 2016. Simultaneous measurement of friction and wear in hip simulators. *Proceedings of the Institution of Mechanical Engineers, Part H: Journal of Engineering in Medicine* 230, 373-388.
- [66] Sonntag, R., Braun, S., Al-Salehi, L., Reinders, J., Mueller, U., Kretzer, J.P., Williams, J.L., 2017. Three-dimensional friction measurement during hip simulation. *PLOS ONE* 12.
- [67] Nishimura, I., Yuhta, T., Ikubo, K., Shimooka, T., Murabayashi, S., Mltamura, Y., 1993. Modification of the Frictional Surfaces of Artificial Joints. *ASAIO Journal* 39, M762-M766.
- [68] Young, S.K., Lotito, M.A., Keller, T.S., 1998. Friction reduction in total joint arthroplasty. *Wear* 222, 29-37.

- [69] Kustandi, T.S., Choo, J.H., Low, H.Y., Sinha, S.K., 2010. Texturing of UHMWPE surface via NIL for low friction and wear properties. *Journal of Physics D: Applied Physics* 43.
- [70] Cho, M., Choi, H.-J., 2014. Optimization of Surface Texturing for Contact Between Steel and Ultrahigh Molecular Weight Polyethylene Under Boundary Lubrication. *Tribology Letters* 56, 409-422.
- [71] Roy, T., Choudhury, D., Ghosh, S., Bin Mamat, A., Pinguan-Murphy, B., 2015. Improved friction and wear performance of micro dimpled ceramic-on-ceramic interface for hip joint arthroplasty. *Ceramics International* 41, 681-690.
- [72] Borjali, A., Monson, K., Raeymaekers, B., 2018. Friction between a polyethylene pin and a microtextured CoCrMo disc, and its correlation to polyethylene wear, as a function of sliding velocity and contact pressure, in the context of metal-on-polyethylene prosthetic hip implants. *Tribology International* 127, 568-574.
- [73] Chyr, A., Qiu, M., Speltz, J.W., Jacobsen, R.L., Sanders, A.P., Raeymaekers, B., 2014. A patterned microtexture to reduce friction and increase longevity of prosthetic hip joints. *Wear* 315, 51-57.
- [74] Zhou, X., Galvin, A.L., Jin, Z., Yan, X., Fisher, J., 2012. The influence of concave dimples on the metallic counterface on the wear of ultra-high molecular weight polyethylene. *Proceedings of the Institution of Mechanical Engineers, Part J: Journal of Engineering Tribology* 226, 455-462.
- [75] Kanaga Karuppiah, K.S., Sundararajan, S., Xu, Z.-H., Li, X., 2006. The effect of protein adsorption on the friction behavior of ultra-high molecular weight polyethylene. *Tribology Letters* 22, 181-188.
- [76] Sawae, Y., Yamamoto, A., Murakami, T., 2008. Influence of protein and lipid concentration of the test lubricant on the wear of ultra high molecular weight polyethylene. *Tribology International* 41, 648-656.
- [77] Morillo, C., Sawae, Y., Murakami, T., 2010. Effect of bovine serum constituents on the surface of the tribological pair alumina/alumina nanocomposites for total hip replacement. *Tribology International* 43, 1158-1162.
- [78] Nečas, D., Sawae, Y., Fujisawa, T., Nakashima, K., Morita, T., Yamaguchi, T., Vrbka, M., Křupka, I., Hartl, M., 2017. The Influence of Proteins and Speed on Friction and Adsorption of Metal/UHMWPE Contact Pair. *Biotribology* 11, 51-59.
- [79] Nečas, D., Vrbka, M., Křupka, I., Hartl, M., 2018. The Effect of Kinematic Conditions and Synovial Fluid Composition on the Frictional Behaviour of Materials for Artificial Joints. *Materials* 11.
- [80] Nečas, D., Usami, H., Niimi, T., Sawae, Y., Křupka, I., Hartl, M., 2020. Running-in friction of hip joint replacements can be significantly reduced: The effect of surface-textured acetabular cup. *Friction* 8, 1137-1152.
- [81] Murakami, T., Yarimitsu, S., Nakashima, K., Sakai, N., Yamaguchi, T., Sawae, Y., Suzuki, A., 2015. Biphasic and boundary lubrication mechanisms in artificial hydrogel cartilage: A review. *Proceedings of the Institution of Mechanical Engineers, Part H: Journal of Engineering in Medicine* 229, 864-878.

- [82] Ma, L., Gaisinskaya-Kipnis, A., Kampf, N., Klein, J., 2015. Origins of hydration lubrication. *Nature Communications* 6.
- [83] Jahn, S., Seror, J., Klein, J., 2016. Lubrication of Articular Cartilage. *Annual Review of Biomedical Engineering* 18, 235-258.
- [84] Ruggiero, A., 2020. Milestones in Natural Lubrication of Synovial Joints. *Frontiers in Mechanical Engineering* 6.
- [85] Dowson, D., Jin, Z.-M., 2006. Metal-on-metal hip joint tribology. *Proceedings of the Institution of Mechanical Engineers, Part H: Journal of Engineering in Medicine* 220, 107-118.
- [86] Jin, Z.M., Stone, M., Ingham, E., Fisher, J., 2006. (v) Biotribology. *Current Orthopaedics* 20, 32-40.
- [87] Serro, A.P., Degiampietro, K., Colaço, R., Saramago, B., 2010. Adsorption of albumin and sodium hyaluronate on UHMWPE: A QCM-D and AFM study. *Colloids and Surfaces B: Biointerfaces* 78, 1-7.
- [88] Jin, Z.M., Dowson, D., Fisher, J., 1997. Analysis of fluid film lubrication in artificial hip joint replacements with surfaces of high elastic modulus. *Proceedings of the Institution of Mechanical Engineers, Part H: Journal of Engineering in Medicine* 211, 247-256.
- [89] Jin, Z.M., Dowson, D., 1999. A full numerical analysis of hydrodynamic lubrication in artificial hip joint replacements constructed from hard materials. *Proceedings of the Institution of Mechanical Engineers, Part C: Journal of Mechanical Engineering Science* 213, 355-370.
- [90] Udofia, I.J., Jin, Z.M., 2003. Elastohydrodynamic lubrication analysis of metal-on-metal hip-resurfacing prostheses. *Journal of Biomechanics* 36, 537-544.
- [91] Jagatia, M., Jalali-Vahid, D., Jin, Z.M., 2001. Elastohydrodynamic lubrication analysis of ultra-high molecular weight polyethylene hip joint replacements under squeeze-film motion. *Proceedings of the Institution of Mechanical Engineers, Part H: Journal of Engineering in Medicine* 215, 141-151.
- [92] Jin, Z.M., Heng, S.M., Ng, H.W., Auger, D.D., 1999. An axisymmetric contact model of ultra high molecular weight polyethylene cups against metallic femoral heads for artificial hip joint replacements. *Proceedings of the Institution of Mechanical Engineers, Part H: Journal of Engineering in Medicine* 213, 317-327.
- [93] Jagatia, M., Jin, Z.M., 2001. Elastohydrodynamic lubrication analysis of metal-on-metal hip prostheses under steady state entraining motion. *Proceedings of the Institution of Mechanical Engineers, Part H: Journal of Engineering in Medicine* 215, 531-541.
- [94] Hamrock, B.J., Dowson, D., 1978. Elastohydrodynamic Lubrication of Elliptical Contacts for Materials of Low Elastic Modulus I—Fully Flooded Conjunction. *Journal of Lubrication Technology* 100, 236-245.
- [95] Jalali-Vahid, D., Jin, Z.M., Dowson, D., 2003. Isoviscous elastohydrodynamic lubrication of circular point contacts with particular reference to metal-on-metal hip implants. *Proceedings of the Institution of Mechanical Engineers, Part J: Journal of Engineering Tribology* 217, 397-402.

- [96] Williams, S., Jalali-Vahid, D., Brockett, C., Jin, Z., Stone, M.H., Ingham, E., Fisher, J., 2006. Effect of swing phase load on metal-on-metal hip lubrication, friction and wear. *Journal of Biomechanics* 39, 2274-2281.
- [97] Jalali-Vahid, D., Jin, Z.M., Dowson, D., 2006. Effect of start-up conditions on elastohydrodynamic lubrication of metal-on-metal hip implants. *Proceedings of the Institution of Mechanical Engineers, Part J: Journal of Engineering Tribology* 220, 143-150.
- [98] Jalali-Vahid, D., Jagatia, M., Jin, Z.M., Dowson, D., 2000. Elastohydrodynamic lubrication analysis of UHMWPE hip joint replacements, in: *Thinning Films And Tribological Interfaces, Proceedings Of The 26Th Leeds-Lyon Symposium On Tribology, Tribology Series*. Elsevier, pp. 329-339.
- [99] Jalali-Vahid, D., Jagatia, M., Jin, Z.M., Dowson, D., 2001. Prediction of lubricating film thickness in a ball-in-socket model with a soft lining representing human natural and artificial hip joints. *Proceedings of the Institution of Mechanical Engineers, Part J: Journal of Engineering Tribology* 215, 363-372.
- [100] Jalali-Vahid, D., Jagatia, M., Jin, Z.M., Dowson, D., 2001. Prediction of lubricating film thickness in UHMWPE hip joint replacements. *Journal of Biomechanics* 34, 261-266.
- [101] Jalali-Vahid, D., Jin, Z.M., 2001. Transient elastohydrodynamic lubrication analysis of ultra-high molecular weight polyethylene hip joint replacements. *Proceedings of the Institution of Mechanical Engineers, Part C: Journal of Mechanical Engineering Science* 216, 409-420.
- [102] Jalali-Vahid, D., Jin, Z.M., Dowson, D., 2003. Elastohydrodynamic lubrication analysis of hip implants with ultra high molecular weight polyethylene cups under transient conditions. *Proceedings of the Institution of Mechanical Engineers, Part C: Journal of Mechanical Engineering Science* 217, 767-777.
- [103] Wang, F.C., Jin, Z.M., 2004. Prediction of elastic deformation of acetabular cups and femoral heads for lubrication analysis of artificial hip joints. *Proceedings of the Institution of Mechanical Engineers, Part J: Journal of Engineering Tribology* 218, 201-209.
- [104] Wang, F.C., Jin, Z.M., 2005. Elastohydrodynamic Lubrication Modeling of Artificial Hip Joints Under Steady-State Conditions. *Journal of Tribology* 127, 729-739.
- [105] Wang, F., Jin, Z., 2008. Transient Elastohydrodynamic Lubrication of Hip Joint Implants. *Journal of Tribology* 130.
- [106] Gao, L.M., Meng, Q.E., Wang, F.C., Yang, P.R., Jin, Z.M., 2007. Comparison of numerical methods for elastohydrodynamic lubrication analysis of metal-on-metal hip implants: Multi-grid verses Newton-Raphson. *Proceedings of the Institution of Mechanical Engineers, Part J: Journal of Engineering Tribology* 221, 133-140.
- [107] Gao, L., Wang, F., Yang, P., Jin, Z., 2009. Effect of 3D physiological loading and motion on elastohydrodynamic lubrication of metal-on-metal total hip replacements. *Medical Engineering & Physics* 31, 720-729.
- [108] Venner, C.H., Lubrecht, A.A., 2000. *Multilevel methods in lubrication*. Elsevier, Amsterdam.

- [109] Mattei, L., Piccigallo, B., Stadler, K., Ciulli, E., Di Puccio, F., 2009. EHL modeling of hip implants based on a ball-on-plane configuration. Ancona, Italy: AIMETA, 161–73.
- [110] Gao, L., Fisher, J., Jin, Z., 2011. Effect of walking patterns on the elastohydrodynamic lubrication of metal-on-metal total hip replacements. *Proceedings of the Institution of Mechanical Engineers, Part J: Journal of Engineering Tribology* 225, 515-525.
- [111] Meng, Q.E., Liu, F., Fisher, J., Jin, Z.M., 2010. Transient Elastohydrodynamic Lubrication Analysis of a Novel Metal-On-Metal Hip Prosthesis with a Non-Spherical Femoral Bearing Surface. *Proceedings of the Institution of Mechanical Engineers, Part H: Journal of Engineering in Medicine* 225, 25-37.
- [112] Meng, Q., Liu, F., Fisher, J., Jin, Z., 2013. Contact mechanics and lubrication analyses of ceramic-on-metal total hip replacements. *Tribology International* 63, 51-60.
- [113] Wang, W.-Z., Jin, Z.M., Dowson, D., Hu, Y.Z., 2008. A study of the effect of model geometry and lubricant rheology upon the elastohydrodynamic lubrication performance of metal-on-metal hip joints. *Proceedings of the Institution of Mechanical Engineers, Part J: Journal of Engineering Tribology* 222, 493-501.
- [114] Cooke, A.F., Dowson, D., Wright, V., 1978. The Rheology of Synovial Fluid and Some Potential Synthetic Lubricants for Degenerate Synovial Joints. *Engineering in Medicine* 7, 66-72.
- [115] Gao, L., Dowson, D., Hewson, R.W., 2016. A numerical study of non-Newtonian transient elastohydrodynamic lubrication of metal-on-metal hip prostheses. *Tribology International* 93, 486-494.
- [116] Allen, Q., Raeymaekers, B., 2020. Maximizing the Lubricant Film Thickness Between a Rigid Microtextured and a Smooth Deformable Surface in Relative Motion, Using a Soft Elasto-Hydrodynamic Lubrication Model. *Journal of Tribology* 142.
- [117] Allen, Q., Raeymaekers, B., 2021. The Effect of Texture Floor Profile on the Lubricant Film Thickness in a Textured Hard-On-Soft Bearing With Relevance to Prosthetic Hip Implants. *Journal of Tribology* 143.
- [118] Albahrani, S.M.B., Philippon, D., Vergne, P., Bluet, J.M., 2015. A review of in situ methodologies for studying elastohydrodynamic lubrication. *Proceedings of the Institution of Mechanical Engineers, Part J: Journal of Engineering Tribology* 230, 86-110.
- [119] Dowson, D., McNie, C.M., Goldsmith, A.A.J., 2000. Direct experimental evidence of lubrication in a metal-on-metal total hip replacement tested in a joint simulator. *Proceedings of the Institution of Mechanical Engineers, Part C: Journal of Mechanical Engineering Science* 214, 75-86.
- [120] Smith, S.L., Dowson, D., Goldsmith, A.A.J., Valizadeh, R., Colligon, J.S., 2001. Direct evidence of lubrication in ceramic-on-ceramic total hip replacements. *Proceedings of the Institution of Mechanical Engineers, Part C: Journal of Mechanical Engineering Science* 215, 265-268.
- [121] Smith, S.L., Dowson, D., Goldsmith, A.A.J., 2001. The effect of diametral clearance, motion and loading cycles upon lubrication of metal-on-metal total hip replacements.

- Proceedings of the Institution of Mechanical Engineers, Part C: Journal of Mechanical Engineering Science 215, 1-5.
- [122] Parkes, M., Myant, C., Cann, P.M., Wong, J.S.S., 2014. The effect of buffer solution choice on protein adsorption and lubrication. *Tribology International* 72, 108-117.
- [123] Mavraki, A., Cann, P.M., 2011. Lubricating film thickness measurements with bovine serum. *Tribology International* 44, 550-556.
- [124] Fan, J., Myant, C.W., Underwood, R., Cann, P.M., Hart, A., 2011. Inlet protein aggregation: a new mechanism for lubricating film formation with model synovial fluids. *Proceedings of the Institution of Mechanical Engineers, Part H: Journal of Engineering in Medicine* 225, 696-709.
- [125] Myant, C., Underwood, R., Fan, J., Cann, P.M., 2012. Lubrication of metal-on-metal hip joints: The effect of protein content and load on film formation and wear. *Journal of the Mechanical Behavior of Biomedical Materials* 6, 30-40.
- [126] Myant, C., Cann, P., 2013. In contact observation of model synovial fluid lubricating mechanisms. *Tribology International* 63, 97-104.
- [127] Myant, C.W., Cann, P., 2014. The effect of transient conditions on synovial fluid protein aggregation lubrication. *Journal of the Mechanical Behavior of Biomedical Materials* 34, 349-357.
- [128] Myant, C., Cann, P., 2014. On the matter of synovial fluid lubrication: Implications for Metal-on-Metal hip tribology. *Journal of the Mechanical Behavior of Biomedical Materials* 34, 338-348.
- [129] Vrbka, M., Návrat, T., Křupka, I., Hartl, M., Šperka, P., Gallo, J., 2013. Study of film formation in bovine serum lubricated contacts under rolling/sliding conditions. *Proceedings of the Institution of Mechanical Engineers, Part J: Journal of Engineering Tribology* 227, 459-475.
- [130] Parkes, M., Myant, C., Cann, P.M., Wong, J.S.S., 2015. Synovial Fluid Lubrication: The Effect of Protein Interactions on Adsorbed and Lubricating Films. *Biotribology* 1-2, 51-60.
- [131] Vrbka, M., Křupka, I., Hartl, M., Návrat, T., Gallo, J., Galandáková, A., 2014. In situ measurements of thin films in bovine serum lubricated contacts using optical interferometry. *Proceedings of the Institution of Mechanical Engineers, Part H: Journal of Engineering in Medicine* 228, 149-158.
- [132] Vrbka, M., Nečas, D., Hartl, M., Křupka, I., Urban, F., Gallo, J., 2015. Visualization of lubricating films between artificial head and cup with respect to real geometry. *Biotribology* 1-2, 61-65.
- [133] Choudhury, D., Rebenda, D., Sasaki, S., Hekrle, P., Vrbka, M., Zou, M., 2018. Enhanced lubricant film formation through micro-dimpled hard-on-hard artificial hip joint: An in-situ observation of dimple shape effects. *Journal of the Mechanical Behavior of Biomedical Materials* 81, 120-129.
- [134] Nečas, D., Vrbka, M., Urban, F., Křupka, I., Hartl, M., 2016. The effect of lubricant constituents on lubrication mechanisms in hip joint replacements. *Journal of the Mechanical Behavior of Biomedical Materials* 55, 295-307.

- [135] Nečas, D., Vrbka, M., Křupka, I., Hartl, M., Galandáková, A., 2016. Lubrication within hip replacements – Implication for ceramic-on-hard bearing couples. *Journal of the Mechanical Behavior of Biomedical Materials* 61, 371-383.
- [136] Australian Orthopaedic Association National Joint Replacement Registry (AOANJRR). Hip, Knee & Shoulder Arthroplasty: 2020 Annual Report, Adelaide; AOA, 2020: 1-474.
- [137] American Joint Replacement Registry (AJRR): 2020 Annual Report. Rosemont, IL: American Academy of Orthopaedic Surgeons (AAOS), 2020.
- [138] National Joint Registry for England, Wales, Northern Ireland, the Isle of Man and the States of Guernsey. 17th Annual Report 2020
- [139] Nečas, D., Vrbka, M., Urban, F., Gallo, J., Křupka, I., Hartl, M., 2017. In situ observation of lubricant film formation in THR considering real conformity: The effect of diameter, clearance and material. *Journal of the Mechanical Behavior of Biomedical Materials* 69, 66-74.
- [140] Nečas, D., Vrbka, M., Rebenda, D., Gallo, J., Galandáková, A., Wolfová, L., Křupka, I., Hartl, M., 2018. In situ observation of lubricant film formation in THR considering real conformity: The effect of model synovial fluid composition. *Tribology International* 117, 206-216.
- [141] Nečas, D., Vrbka, M., Galandáková, A., Křupka, I., Hartl, M., 2019. On the observation of lubrication mechanisms within hip joint replacements. Part I: Hard-on-soft bearing pairs. *Journal of the Mechanical Behavior of Biomedical Materials* 89, 237-248.
- [142] Nečas, D., Vrbka, M., Gallo, J., Křupka, I., Hartl, M., 2019. On the observation of lubrication mechanisms within hip joint replacements. Part II: Hard-on-hard bearing pairs. *Journal of the Mechanical Behavior of Biomedical Materials* 89, 249-259.
- [143] Lu, X., Nečas, D., Meng, Q., Rebenda, D., Vrbka, M., Hartl, M., Jin, Z., 2020. Towards the direct validation of computational lubrication modelling of hip replacements. *Tribology International* 146.
- [144] Carr, A.J., Robertsson, O., Graves, S., Price, A.J., Arden, N.K., Judge, A., Beard, D.J., 2012. Knee replacement. *The Lancet* 379, 1331-1340.
- [145] Inacio, M.C.S., Paxton, E.W., Graves, S.E., Namba, R.S., Nemes, S., 2017. Projected increase in total knee arthroplasty in the United States – an alternative projection model. *Osteoarthritis and Cartilage* 25, 1797-1803.
- [146] Evans, J.T., Walker, R.W., Evans, J.P., Blom, A.W., Sayers, A., Whitehouse, M.R., 2019. How long does a knee replacement last? A systematic review and meta-analysis of case series and national registry reports with more than 15 years of follow-up. *The Lancet* 393, 655-663.
- [147] Julin, J., Jämsen, E., Puolakka, T., Konttinen, Y.T., Moilanen, T., 2010. Younger age increases the risk of early prosthesis failure following primary total knee replacement for osteoarthritis. *Acta Orthopaedica* 81, 413-419.
- [148] Dyrhovden, G.S., Lygre, S.H.L., Badawy, M., Gøthesen, Ø., Furnes, O., 2017. Have the Causes of Revision for Total and Unicompartmental Knee Arthroplasties Changed During the Past Two Decades? *Clinical Orthopaedics & Related Research* 475, 1874-1886.

- [149] Lachiewicz, P.F., Geyer, M.R., 2011. The Use of Highly Cross-linked Polyethylene in Total Knee Arthroplasty. *American Academy of Orthopaedic Surgeon* 19, 143-151.
- [150] Orita, K., Minoda, Y., Sugama, R., Ohta, Y., Ueyama, H., Takemura, S., Nakamura, H., 2020. Vitamin E-infused highly cross-linked polyethylene did not reduce the number of in vivo wear particles in total knee arthroplasty. *The Bone & Joint Journal* 102-B, 1527-1534.
- [151] Spece, H., Schachtner, J.T., MacDonald, D.W., Klein, G.R., Mont, M.A., Lee, G.-C., Kurtz, S.M., 2019. Reasons for Revision, Oxidation, and Damage Mechanisms of Retrieved Vitamin E-Stabilized Highly Crosslinked Polyethylene in Total Knee Arthroplasty. *The Journal of Arthroplasty* 34, 3088-3093.
- [152] Liu, T., Esposito, C., Elpers, M., Wright, T., 2016. Surface Damage Is Not Reduced With Highly Crosslinked Polyethylene Tibial Inserts at Short-term. *Clinical Orthopaedics & Related Research* 474, 107-116.
- [153] Baxter, R.M., MacDonald, D.W., Kurtz, S.M., Steinbeck, M.J., 2013. Characteristics of highly cross-linked polyethylene wear debris in vivo. *Journal of Biomedical Materials Research Part B: Applied Biomaterials*.
- [154] Chen, W., Bichara, D.A., Suhardi, J., Sheng, P., Muratoglu, O.K., 2017. Effects of vitamin E-diffused highly cross-linked UHMWPE particles on inflammation, apoptosis and immune response against *S. aureus*. *Biomaterials* 143, 46-56.
- [155] Illgen, R.L., Forsythe, T.M., Pike, J.W., Laurent, M.P., Blanchard, C.R., 2008. Highly Crosslinked vs Conventional Polyethylene Particles—An In Vitro Comparison of Biologic Activities. *The Journal of Arthroplasty* 23, 721-731.
- [156] Huang, C.-H., Lu, Y.-C., Chang, T.-K., Hsiao, I.-L., Su, Y.-C., Yeh, S.-T., Fang, H.-W., Huang, C.-H., 2016. In vivo biological response to highly cross-linked and vitamin e-doped polyethylene-a particle-Induced osteolysis animal study. *Journal of Biomedical Materials Research Part B: Applied Biomaterials* 104, 561-567.
- [157] Minoda, Y., Kobayashi, A., Sakawa, A., Aihara, M., Tada, K., Sugama, R., Iwakiri, K., Ohashi, H., Takaoka, K., 2008. Wear particle analysis of highly crosslinked polyethylene isolated from a failed total hip arthroplasty. *Journal of Biomedical Materials Research Part B: Applied Biomaterials* 86B, 501-505.
- [158] Fulin, P., Slouf, M., Krejcikova, S., Nevoralova, M., Sticha, R., Pokorny, D., 2019. Comparison of explanted uhmwpe hip replacement components of various manufacturers after 10 years in vivo. *Acta Chir Orthop Traumatol Cech* 86, 390-396.
- [159] MacDonald, D.W., Higgs, G.B., Chen, A.F., Malkani, A.L., Mont, M.A., Kurtz, S.M., 2018. Oxidation, Damage Mechanisms, and Reasons for Revision of Sequentially Annealed Highly Crosslinked Polyethylene in Total Knee Arthroplasty. *The Journal of Arthroplasty* 33, 1235-1241.
- [160] Pourzal, R., Knowlton, C.B., Hall, D.J., Laurent, M.P., Urban, R.M., Wimmer, M.A., 2016. How Does Wear Rate Compare in Well-functioning Total Hip and Knee Replacements? A Postmortem Polyethylene Liner Study. *Clinical Orthopaedics & Related Research* 474, 1867-1875.

- [161] Ngai, V., Kunze, J., Cip, J., Laurent, M.P., Jacobs, J.J., Wimmer, M.A., 2020. Backside wear of tibial polyethylene components is affected by gait pattern: A knee simulator study using rare earth tracer technology. *Journal of Orthopaedic Research* 38, 1607-1616.
- [162] Tandon, P.N., Jaggi, S., 1979. A model for the lubrication mechanism in knee joint replacements. *Wear* 52, 275-284.
- [163] Tandon, P.N., Jaggi, S., 1981. Wear and lubrication in an artificial knee joint replacement. *International Journal of Mechanical Sciences* 23, 413-422.
- [164] Jin, Z.M., Dowson, D., Fisher, J., Ohtsuki, N., Murakami, T., Higaki, H., Moriyama, S., 1998. Prediction of transient lubricating film thickness in knee prostheses with compliant layers. *Proceedings of the Institution of Mechanical Engineers, Part H: Journal of Engineering in Medicine* 212, 157-164.
- [165] Pascau, A., Guardia, B., Puertolas, J.A., Gómez-Barrena, E., 2009. Knee model of hydrodynamic lubrication during the gait cycle and the influence of prosthetic joint conformity. *Journal of Orthopaedic Science* 14, 68-75.
- [166] Di Paolo, J., Berli, M.E., 2006. Numerical analysis of the effects of material parameters on the lubrication mechanism for knee prosthesis. *Computer Methods in Biomechanics and Biomedical Engineering* 9, 79-89.
- [167] Kennedy, F.E., Van Citters, D.W., Wongseedakaew, K., Mongkolwongrojn, M., 2007. Lubrication and Wear of Artificial Knee Joint Materials in a Rolling/Sliding Tribotester. *Journal of Tribology* 129, 326-335.
- [168] Mongkolwongrojn, M., Wongseedakaew, K., Kennedy, F.E., 2010. Transient elastohydrodynamic lubrication in artificial knee joint with non-Newtonian fluids. *Tribology International* 43, 1017-1026.
- [169] Su, Y., Fu, Z., Yang, P., Wang, C., 2012. A full numerical analysis of elastohydrodynamic lubrication in knee prosthesis under walking condition. *Journal of Mechanics in Medicine and Biology* 10, 621-641.
- [170] Su, Y., Yang, P., Fu, Z., Jin, Z., Wang, C., 2011. Time-dependent elastohydrodynamic lubrication analysis of total knee replacement under walking conditions. *Computer Methods in Biomechanics and Biomedical Engineering* 14, 539-548.
- [171] Gao, L., Hua, Z., Hewson, R., Andersen, M.S., Jin, Z., 2018. Elastohydrodynamic lubrication and wear modelling of the knee joint replacements with surface topography. *Biosurface and Biotribology* 4, 18-23.
- [172] Ohtsuki, N., Murakami, T., Moriyama, S., Higaki, H., 1997. Influence of Geometry of Conjunction on Elastohydrodynamic Film Formation in Knee Prostheses with Compliant Layer, in: *Elastohydrodynamics - '96 Fundamentals And Applications In Lubrication And Traction*, Proceedings Of The 23Rd Leeds-Lyon Symposium On Tribology Held In The Institute Of Tribology, Department Of Mechanical Engineering, Tribology Series. Elsevier, pp. 349-359.
- [173] Flannery, M., McGloughlin, T., Jones, E., Birkinshaw, C., 2008. Analysis of wear and friction of total knee replacements. *Wear* 265, 999-1008.

- [174] Nečas, D., Sadecká, K., Vrbka, M., Gallo, J., Galandáková, A., Křupka, I., Hartl, M., 2019. Observation of lubrication mechanisms in knee replacement: A pilot study. *Biotribology* 17, 1-7.
- [175] Nečas, D., Sadecká, K., Vrbka, M., Galandáková, A., Wimmer, M.A., Gallo, J., Hartl, M., 2021. The effect of albumin and γ -globulin on synovial fluid lubrication: Implication for knee joint replacements. *Journal of the Mechanical Behavior of Biomedical Materials* 113, 104117.
- [176] Nečas, D., Vrbka, M., Marian, M., Rothhammer, B., Tremmel, S., Wartzack, S., Galandáková, A., Gallo, J., Wimmer, M.A., Křupka, I., Hartl, M., 2021. Towards the understanding of lubrication mechanisms in total knee replacements – Part I: Experimental investigations. *Tribology International* 156, 106874.
- [177] Marian, M., Orgeldinger, C., Rothhammer, B., Nečas, D., Vrbka, M., Křupka, I., Hartl, M., Wimmer, M.A., Tremmel, S., Wartzack, S., 2020. Towards the understanding of lubrication mechanisms in total knee replacements – Part II: Numerical modeling. *Tribology International* 156, 106809.

LIST OF FIGURES

Figure 1: The detail of total hip and total knee joint replacement.	13
Figure 2: Viscosities of various lubricants (left) and corresponding friction coefficients in UHMWPE-on-CoCr configuration (right). The figure was partially modified and reprinted based on [34].	16
Figure 3: Left: A molecular model of boundary protein film for various natures of polymer surfaces. (N) – native protein structure, (D) – a form of the irreversibly denatured protein, μ – coefficient of friction [36]. Right: A hypothesis adsorption model of folded and unfolded albumin onto hydrophobic polymer surface [37].....	17
Figure 4: Fluorescent images of transferred UHMWPE film on CoCrMo surface after friction test. Coefficient of friction corresponding to the left and right image was 0.06 and 0.11, respectively [40].	18
Figure 5: A scheme of pin-on-disc tribometer (left); results of friction coefficient for various material combinations lubricated by albumin solution (right top) and PBS (right bottom). The figure was partially modified and reprinted based on [41].....	19
Figure 6: Frictional behaviour of various material combinations under lubrication by BCS as a function of sliding speed [42].	20
Figure 7: Ball-on-disc test device for friction measurements (left); results of friction coefficients in steel-on-steel configuration considering protein solutions in different buffers (right). The figure was partially modified and reprinted based on [44].....	21
Figure 8: Stribeck curves for PU and PE knee tibial component articulating with CoCrMo femoral part lubricated by a mixture of water and bone cement particles [53].....	23
Figure 9: Resulting friction coefficients in various experiment stages for two tested pairs lubricated by different solutions. The figure was partially modified and reprinted based on [58].	24
Figure 10: Scheme of the simulator central part (left, middle); applied conditions (right). The figure was partially modified and reprinted based on [60].....	25
Figure 11: Hip joint simulator with a 6-DOF load cell (left); results of friction coefficient – Test 1 (right top); results of friction coefficient – Test 2 (right bottom). The figure was partially modified and reprinted based on [65].	27
Figure 12: Model of the hip joint simulator (left); frictional torque moments for individual pairs (right A); peak resulting moments (right B). The figure was partially modified and reprinted based on [66].	27

Figure 13: Left: various area densities (a, b) and various depths of the pores (c, d). Right: the sleeve around the dimple edge (a), dimple profile after polishing (b). The figure was partially modified and reprinted based on [70].	29
Figure 14. The designed patterns of surface texturing and the dimple profiles (left); respective friction coefficients for HXLPE pin (right). The figure was partially modified and reprinted based on [72].	29
Figure 15. Designed parameters and patterns of the textures (left); respective friction coefficients for various patterns and loads (right). The figure was partially modified and reprinted based on [73].	30
Figure 16: Results of friction coefficient (top) and adsorbed film thickness (bottom) for various protein solutions in the reciprocating pin-on-plate test under lower (left) and higher (right) sliding speed. The figure was partially modified and reprinted based on [78].	33
Figure 17: Research scheme of the study [78].	34
Figure 18: Research scheme of the study [79].	35
Figure 19: Results of friction coefficients for various material combinations lubricated by PBS and model SF. The figure was partially modified and reprinted based on [80].	36
Figure 20: Research scheme of the study [80].	37
Figure 21: Simplification of the geometry of THR and TKR often adopted in numerical simulations.	78
Figure 22: The effect of femoral head radius, radial clearance, UHMWPE cup thickness, and UHMWPE cup elastic modulus on predicted minimum film thickness using the ball-in-socket model. The figure was partially modified and reprinted based on [100].	79
Figure 23: The variation of minimum, central, and average film thickness under the walking cycle; vertical load and FE motion (left); 3D load and motion (right) [107].	80
Figure 24: Central (a), minimum (b) film thickness and pressure distribution (c) for CoM pair considering the effect of the head radius (left) and radial clearance (middle); prediction of the parameters for CoC, CoM, and MoM pairs (right). The figure was partially modified and reprinted based on [112].	81
Figure 25: Results of the film thickness of BS (left) and protein solutions in various buffers (right) in ball-on-disc configuration measured by optical interferometry. The figure was partially modified and reprinted based on [44].	84
Figure 26: The scheme of modified ball-on-disc tribometer for direct observation of the contact lubricated by BS using optical interferometry method [123].	84
Figure 27: Images of the contact zones at various speeds (left); detail of the aggregated inlet phase of proteins (middle); dependence of inlet phase length and the film thickness (right). The figure was partially modified and reprinted based on [126].	85

Figure 28: A set of the interferograms illustrating the passage of the protein film through the contact for metal (a) and ceramic (b) femoral head under positive sliding conditions [129].	86
Figure 29: Modification of ball-on-disc tribometer towards improved compliance of the contact conditions mimicking THR [131].	87
Figure 30: Various shapes of textures made on the metal femoral heads (left); respective film thickness measured by optical interferometry (right) [133].	88
Figure 31: Time-dependence of film thickness for the metal femoral head at lower (a) and higher (b) speed under positive sliding conditions in ball-on-disc configuration; fluorescent images of the contact zone (c). The figure was partially modified and reprinted based on [134].	89
Figure 32: Research scheme of the study [139].	92
Figure 33: Development of film thickness for various model lubricants (a); respective contact images (b) [140].	93
Figure 34: Development of film thickness for simple solutions of albumin, γ -globulin, and HA (a); respective contact images (b) [140].	94
Figure 35: Research scheme of the study [141].	96
Figure 36: Repeatability test performed with three SFs of different composition. The figure was partially modified and reprinted based on [142].	97
Figure 37: Comparison of the central film thickness based on the experimental measurement and predictive numerical model. Isoviscous and literature-based effective viscosity model (left); the novel velocity-effective viscosity equation (right). The figure was partially modified and reprinted based on [143].	98
Figure 38: Ellipsoid-on-plane model (left); various considered contact conjunctions (middle); development of film thickness during the cycle (right). The figure was partially modified and reprinted based on [164].	156
Figure 39: Research scheme of the study [174].	160
Figure 40: Fluorescent images of TKR contact taken at the beginning and the end of the test in two different FE positions for albumin-based solutions [175].	161
Figure 41: Comparison of experimental and predicted film thickness for the lateral and the medial compartment (a); respective contact images (b) [176].	162
Figure 42: Research scheme of the study [176].	163
Figure 43: Research scheme of the study [177].	164

LIST OF TABLES

Table 1: Detailed description of the tested THR pairs [59].....	25
Table 2: Summary of the tested THR couples [139].....	92
Table 3: The summary of the applied test lubricants [140].....	93
Table 4: The summary of the performed experiments [140].....	93
Table 5: The summary of the applied test lubricants showing the combinations of labelled and non-labelled constituents [141].	95
Table 6: Comparison of hard-on-soft and hard-on-hard bearing couples [142].....	96
Table 7: The summary of the applied test lubricants showing the combinations of labelled and non-labelled constituents [175].	161

LIST OF ABBREVIATIONS

AA	Abduction–adduction
AFM	Atomic force microscopy
AP	Anterior-posterior
BCS	Bovine calf serum
BS	Bovine serum
BSA	Bovine serum albumin
BSF	Bovine synovial fluid
BUT	Brno University of Technology
CMC	Carboxymethyl cellulose
CNC	Computer numerical control
CoC	Ceramic-on-ceramic
CoP	Ceramic-on-polyethylene
DI	Deionized water
DOF	Degree of freedom
EHL	Elastohydrodynamic lubrication
FE	Flexion-extension
FEM	Finite element method
HA	Hyaluronic acid
HBSS	Hanks’ balanced salt solution
HSA	Human serum albumin
HXLPE	Highly cross-linked polyethylene
IE	Internal-external
IF	Impact factor
LST	Laser surface texturing
MG	Multigrid
MLMI	Multi-level multi-integration
MoM	Metal-on-metal
MoP	Metal-on-polyethylene
N-R	Newton-Raphson
OA	Osteoarthritis
PAL	Protein aggregation lubrication
PBS	Phosphate-buffered saline
PE	Polyethylene
PHs	Phospholipids
PLs	Phospholipids
PMMA	Poly(methyl methacrylate)
PU	Polyurethane
RS	Ringer’s solution

SF	Synovial fluid
SFFT	Spherical fast Fourier transformation
SRR	Slide-to-roll ratio
THA	Total hip arthroplasty
THR	Total hip replacement
TKA	Total knee arthroplasty
TKR	Total knee replacement
Tris	2-amino-2-(hydroxymethyl)-1,3-propanediol
UHMWPE	Ultra-high molecular weight polyethylene
VS	Viscosupplementation
WoS	Web of Science